

Page is intentionally blank.

Program and Abstracts

2014

Atomic, Molecular, and Optical Sciences
Research Meeting

Bolger Conference Center
Potomac, Maryland
October 26–29, 2014

Chemical Sciences, Geosciences, and Biosciences Division
Office of Basic Energy Sciences
Office of Science
U.S. Department of Energy

Cover Graphics: The titles of the abstracts for this year's meeting were used as the input for the Wordle cover art. The font is Vigo.

The research grants and contracts described in this document are supported by the U.S. DOE Office of Science, Office of Basic Energy Sciences, Chemical Sciences, Geosciences and Biosciences Division

Page is intentionally blank.

FOREWARD

This volume summarizes the 34th annual Research Meeting of the Atomic, Molecular and Optical Sciences (AMOS) Program sponsored by the U. S. Department of Energy (DOE), Office of Basic Energy Sciences (BES), and comprises descriptions of the current research sponsored by the AMOS program. The participants of this meeting include the DOE laboratory and university principal investigators (PIs) within the BES AMOS Program. The purpose is to facilitate scientific interchange among the PIs and to promote a sense of program identity.

The BES/AMOS program is vigorous and innovative, and enjoys strong support within the Department of Energy. This is due entirely to our scientists, the outstanding research they perform, and the relevance of this research to DOE missions. The AMOS community continues to explore new scientific frontiers relevant to the DOE mission and the strategic challenges facing our nation and the world.

We are deeply indebted to the members of the scientific community who have contributed their valuable time toward the review of proposals and programs, either by mail review of grant applications, panel reviews, or on-site reviews of our multi-PI programs. These thorough and thoughtful reviews are central to the continued vitality of the AMOS program.

We are privileged to serve in the management of this research program. In performing these tasks, we learn from the achievements and share the excitement of the research of the scientists and students whose work is summarized in the abstracts published on the following pages.

Many thanks to the staff of the Oak Ridge Institute for Science and Education (ORISE), in particular Connie Lansdon and Tim Ledford, and to the Bolger Conference Center for assisting with the meeting. We also thank Diane Marceau, Robin Felder, and Michaelena Kyler-Leon in the Chemical Sciences, Geosciences, and Biosciences Division for their indispensable behind-the-scenes efforts in support of the BES/AMOS program.

Tom Settersten (Detailee)
Jeffrey L. Krause
Chemical Sciences, Geosciences, and Biosciences Division
Office of Basic Energy Sciences
Office of Science
US Department of Energy

Page is intentionally blank.

Agenda

Page is intentionally blank.

2014 Meeting of the Atomic, Molecular and Optical Sciences Program
Office of Basic Energy Sciences
U. S. Department of Energy

Bolger Center, Potomac, Maryland, October 26–29, 2014

Sunday, October 26

3:00 – 6:00 pm **** Registration ****
6:00 pm **** Reception (No Host, Pony Express Bar & Grill) ****
6:30 pm **** Dinner (Osgood's Restaurant) ****

Monday, October 27

7:30 am **** Breakfast (Osgood's Restaurant) ****

All presentations held in Stained Glass Hall

8:15 am *Welcome and Introductory Remarks*
Jeff Krause, BES/DOE

Session I Chair: **Linda Young**, Argonne National Laboratory

8:30 am *PULSE Attosecond and High Field Science*
Phil Bucksbaum, SLAC National Accelerator Laboratory

9:00 am *Spatial-Temporal Imaging During Chemical Reactions*
Lou DiMauro, Ohio State University

9:30 am *Using Strong Optical Fields to Manipulate and Probe Coherent Molecular Dynamics*
Bob Jones, University of Virginia

10:00 am **** Break ****

10:30 am *Atomic and Molecular Physics in Strong Fields*
Shih-I Chu, University of Kansas

11:00 am *High Intensity Femtosecond XUV Pulse Interactions with Atomic Clusters*
Todd Ditmire, University of Texas at Austin

11:30 am *Dynamics of Atomic Soft X-ray Laser Plasma Amplifiers*
Jorge Rocca, Colorado State University

12:00 pm **** Lunch ****

1:00 – 4:00 pm Free/Discussion Time

- Session II** Chair: **Victor Klimov**, Los Alamos National Laboratory
- 4:00 pm *Ultrafast Processes in Strong Laser Fields in Nanostructured Systems*
Mark Stockman, Georgia State University
- 4:30 pm *Nonlinear Materials Spectroscopies Probed by Ultrafast X-rays*
Keith Nelson, MIT
- 5:00 pm *Monitoring Quantum Hydrodynamics and Interfacial Charge-Transfer Dynamics with Ultrafast X-ray Tools*
Oliver Gessner, Lawrence Berkeley National Laboratory
- 5:30 pm *Imaging and Controlling the Nuclear and Electronic Motion in Atoms, Molecules and Nanostructures with Ultrashort XUV and IR Pulses: from Femto to Attosecond Timescales and Back*
Uwe Thumm, Kansas State University
- 6:00 pm ***** Reception (No Host, Pony Express Bar & Grill) *****
- 6:30 pm ***** Dinner (Osgood's Restaurant) *****

Tuesday, October 28

- 7:30 am ***** Breakfast (Osgood's Restaurant) *****

- Session III** Chair: **Wen Li**, Wayne State University
- 8:30 am *Photon and Electron Driven Non-Born-Oppenheimer Dynamics in Polyatomic Molecules*
Ali Belkacem, Lawrence Berkeley National Laboratory
- 9:00 am *Control of Molecular Dynamics: Algorithms for Design and Implementation*
Hersch Rabitz, Princeton University
- 9:30 am *Theory of Atomic Collisions and Dynamics*
Joe Macek, University of Tennessee
- 10:00 am ***** Break *****
- 10:30 am *Atoms and Ions Interacting with Particles and Fields*
Francis Robicheaux, Purdue University
- 11:00 am *Transient Absorption and Reshaping of Ultrafast Radiation*
Ken Schafer, Louisiana State University
- 11:30 am *Tracking Chemical Dynamics with Synchrotron X-ray Spectroscopy*
Anne Marie March, Argonne National Laboratory
- 12:00 pm ***** Lunch (Osgood's Restaurant) *****
- 1:00 – 4:00 pm Free/Discussion Time

- Session IV** Chair: **Berny Schlegel**, Wayne State University
- 4:00 pm *Applications of the Complex Kohn Method: Probing Core-Hole Localization in Polyatomic Molecules and Extensions to $(e/2e)$ with Polyatomic Targets*
Tom Rescigno, Lawrence Berkeley National Laboratory
- 4:30 pm *Probing Electron-Molecule Scattering Using One-Photon Ionization to High Harmonic Generation*
Robert Lucchese, Texas A&M University
- 5:00 pm *Collective Coulomb Excitations and Reaction Imaging*
Jim Feagin, California State University, Fullerton
- 5:30 pm *Angular Distributions in Polyatomic Dissociative Electron Attachment and Molecular Frame Photoionization*
Ann Orel, NSF/University of California, Davis
- 6:00 pm ***** Reception (No Host, Pony Express Bar & Grill) *****
- 6:30 pm ***** Dinner (Osgood's Restaurant) *****

Wednesday, October 29

- 7:30 am ***** Breakfast (Osgood's Restaurant) *****
- Session V** Chair: **Shambhu Ghimire**, SLAC National Accelerator Laboratory
- 8:30 am *Stimulated Attosecond X-ray Raman Spectroscopy of Charge and Energy Transfer in Molecules*
Shaul Mukamel, University of California, Irvine
- 9:00 am *Applications of Laser Streaking to XFELs*
Gilles Doumy, Argonne National Laboratory
- 9:30 am *Electronic Rearrangement and Nuclear Dynamics After Inner-Shell Photoionization*
Artem Rudenko, Kansas State University
- 10:00 am ***** Break *****
- 10:30 am *Decay Dynamics Following Two-Photon Inner-Shell Absorption in Ne, Xe and XeF₂*
Bertold Krässig, Argonne National Laboratory
- 11:00 am *Structure from Fleeting Illumination of Faint Spinning Objects in Flight*
Abbas Ourmazd, University of Wisconsin, Milwaukee
- 11:30 am *Closing Remarks*
Jeff Krause, BES/DOE
- 11:45 am ***** Lunch (Osgood's Restaurant) *****
- 1:00 pm Discussion
- 3:00 pm Adjourn

Page is intentionally blank.

Table of Contents

Page is intentionally blank.

TABLE OF CONTENTS

Forward	iii
Agenda	v
Table of Contents	xi

Laboratory Research Summaries (by Institution)

Argonne National Laboratory

<i>AMO Physics at Argonne National Laboratory</i>	1
Intense X-ray Physics	
<i>Laser Streaking at LCLS</i> Gilles Doumy	2
<i>Double K-Hole Spectroscopy in Neon with High-Intensity X-rays from the LCLS</i> Bertold Krässig	3
<i>Understanding Inner-Shell Dynamics with Intense, Femtosecond XFEL Pulses</i> Steve Southworth	4
<i>Theoretical Tracking of Resonance-Enhanced Multiple Ionization Pathways in XFEL Pulses</i> Linda Young	5
<i>Modeling of Intense X-ray Laser Damage in Biomolecules and Nanomaterials</i> Linda Young	6
<i>Theoretical Tracking of Radiation Damage Dynamics of Diamond by High-Brilliance X-ray Pulses in Nanosecond/Mesocale Regime</i> Linda Young	7
X-ray Probes of Molecular Dynamics	
<i>Ligand Substitution and Competing Mechanisms</i> Anne Marie March	8
<i>Investigating Electronic Excitation in ZnO Nanoparticles Using Time-Resolved X-ray Absorption and Emission Spectroscopy</i> Anne Marie March	9
<i>Studying the Structural and Electronic Configurations During Photocatalytic Activation of O₂ at a Diiron(II) Complex</i> Anne Marie March	10
<i>Development of X-ray Emission Spectrometers</i> Anne Marie March	10
<i>Molecular Response to X-ray Absorption and Vacancy Cascades</i> Bob Dunford	11

<i>Short Pulse X-ray Beamline at the Advanced Photon Source</i>	
Linda Young	12
Optical Control and X-ray Imaging of Nanoparticles	
<i>Optical Trapping of Metal Nanoparticles</i>	
Norbert Scherer	12
<i>Optical Control of Metal Nanowires and Single-Particle X-ray Diffraction</i>	
Norbert Scherer	13
J.R. Macdonald Laboratory	
<i>J.R. Macdonald Laboratory Overview</i>	17
<i>Structure and Dynamics of Atoms, Ions, Molecules, and Surfaces: Molecular Dynamics with Ion and Laser Beams</i>	
Itzik Ben-Itzhak	19
<i>Strong-Field Dynamics of Few-Body Atomic and Molecular Systems</i>	
Brett Esry	23
<i>Ultrafast Processes in Aligned Molecules</i>	
Vinod Kumarappan	27
<i>Strong Field Rescattering Physics and Attosecond Physics</i>	
Chii-Dong Lin	31
<i>Electronic Rearrangement and Nuclear Dynamics in Inner-Shell and Strong Field Ionization</i>	
Artem Rudenko	35
<i>Structure and Dynamics of Atoms, Ions, Molecules and Surfaces</i>	
Uwe Thumm	39
<i>Strong-Field Time-Dependent Spectroscopy</i>	
Carlos Trallero	43
Lawrence Berkeley National Laboratory	
<i>Atomic, Molecular and Optical Sciences at LBNL</i>	47
<i>Inner-Shell Photoionization and Dissociative Electron Attachment to Small Molecules</i>	
Ali Belkacem, Daniel Slaughter, and Thorsten Weber	48
<i>Electron-Atom and Electron-Molecule Collision Processes</i>	
Tom Rescigno, Dan Haxton, and Bill McCurdy	53
<i>Ultrafast X-ray Science Laboratory</i>	57
<i>Attosecond Atomic and Molecular Science</i>	
Steve Leone and Dan Neumark	57

<i>Non-Born-Oppenheimer Dynamics and Nonlinear Interaction of Femtosecond X-rays with Atoms and Molecules</i>	
Ali Belkacem and Thorsten Weber	59
<i>Soft X-ray High Harmonic Generation and Applications in Chemical Physics</i>	
Oliver Gessner, Steve Leone, and Dan Neumark	61
<i>Ultrafast X-ray Studies of Condensed Phase Molecular Dynamics</i>	
Robert Schoenlein	63
<i>Theory and Computation</i>	
Martin Head-Gordon, Dan Haxton, and Bill McCurdy	64
<i>Early Career: Ultrafast X-ray Studies of Intramolecular and Interfacial Charge Migration</i>	
Oliver Gessner	71
<i>Early Career: The Multiconfiguration Time-Dependent Hartree-Fock Method for Interactions of Molecules with Ultrafast X-Ray and Strong Laser Pulses</i>	
Dan Haxton	75

Los Alamos National Laboratory

<i>Engineered Electronic and Magnetic Interactions in Nanocrystal Quantum Dots</i>	
Victor Klimov	79

SLAC National Accelerator Laboratory

<i>PULSE Ultrafast Chemical Science Program</i>	83
<i>ATO: Attoscience</i>	
Phil Bucksbaum and Markus Gühr	87
<i>NLX: Ultrafast X-ray Optical Science and Strong Field Control</i>	
David Reis and Shambhu Ghimire	91
<i>NPI: Non-Periodic Imaging</i>	
Claudiu Stan	95
<i>SFA: Strong-Field Laser Matter Interactions</i>	
Phil Bucksbaum	99
<i>SPC: Solution Phase Chemical Dynamics</i>	
Kelly Gaffney	103
<i>UTS: Ultrafast Theory and Simulation</i>	
Todd Martínez	107
<i>Early Career: Understanding Photochemistry using Extreme Ultraviolet and Soft X-ray Time Resolved Spectroscopy</i>	
Markus Gühr	111
<i>Early Career: Strongly-Driven Attosecond Electron Dynamics in Periodic Media</i>	
Shambhu Ghimire	115

University Research Summaries (by PI)

<i>Tracing and Controlling Ultrafast Dynamics in Molecules</i>	121
Andreas Becker	
<i>Probing Complexity using the LCLS and the ALS</i>	125
Nora Berrah	
<i>Ultrafast Electron Diffraction from Aligned Molecules</i>	129
Martin Centurion	
<i>Atomic and Molecular Physics in Strong Fields</i>	133
Shih-I Chu	
<i>Formation of Ultracold Molecules</i>	137
Robin Côté	
<i>Optical Two-Dimensional Spectroscopy of Disordered Semiconductor Quantum Wells and Quantum Dots</i>	141
Steve Cundiff	
<i>Understanding and Controlling Strong-Field Laser Interactions with Polyatomic Molecules</i>	145
Marcos Dantus	
<i>Production and Trapping of Ultracold Polar Molecules</i>	149
Dave DeMille	
<i>Spatial-Temporal Imaging During Chemical Reactions</i>	153
Lou DiMauro, Pierre Agostini, and Terry Miller	
<i>Attosecond and Ultra-Fast X-ray Science</i>	157
Lou DiMauro and Pierre Agostini	
<i>High Intensity Femtosecond XUV Pulse Interactions with Atomic Clusters</i>	161
Todd Ditmire	
<i>Electron Correlation in Strong Radiation Fields</i>	165
Joe Eberly	
<i>Image Reconstruction Algorithms</i>	169
Veit Elser	
<i>Collective Coulomb Excitations and Reaction Imaging</i>	173
Jim Feagin	
<i>Transient Absorption and Reshaping of Ultrafast Radiation</i>	177
Mette Gaarde, and Ken Schafer	
<i>Studies of Autoionizing States Relevant to Dielectronic Recombination</i>	181
Tom Gallagher	
<i>Experiments in Ultracold Collisions and Ultracold Molecules</i>	185
Phil Gould	

<i>Physics of Correlated Systems</i>	
Chris Greene	189
<i>Using Strong Optical Fields to Manipulate and Probe Coherent Molecular Dynamics</i>	
Bob Jones	193
<i>Molecular Dynamics Probed by Coherent Soft X-rays</i>	
Henry Kapteyn and Margaret Murnane	197
<i>Imaging Multi-particle Atomic and Molecular Dynamics</i>	
Allen Landers	201
<i>Exploiting Non-equilibrium Charge Dynamics in Polyatomic Molecules to Steer Chemical Reactions</i>	
Wen Li, Raphael Levine, Henry Kapteyn, H. Bernhard Schlegel, Françoise Remacle, and Margaret Murnane	205
<i>Probing Electron-Molecule Scattering with HHG: Theory and Experiment</i>	
Robert Lucchese and Erwin Poliakoff	211
<i>Properties of Actinide Ions from Measurements of Rydberg Ion Fine Structure</i>	
Steve Lundeen	215
<i>Theory of Atomic Collisions and Dynamics</i>	
Joe Macek	219
<i>Photoabsorption by Free and Confined Atoms and Ions</i>	
Steve Manson	223
<i>Electron-Driven Processes in Polyatomic Molecules</i>	
Vince McKoy	227
<i>Electron/Photon Interactions with Atoms/Ions</i>	
Alfred Msezane	231
<i>Theory and Simulations of Nonlinear X-ray Spectroscopy of Molecules</i>	
Shaul Mukamel	235
<i>Nonlinear Photoacoustic Spectroscopies Probed by Ultrafast X-rays</i>	
Keith Nelson and Margaret Murnane	239
<i>Electron and Photon Excitation and Dissociation of Molecules</i>	
Ann Orel	243
<i>Low-Energy Electron Interactions with Complex Molecules and Biological Targets</i>	
Thom Orlando	245
<i>Structure from Fleeting Illumination of Faint Spinning Objects in Flight</i>	
Abbas Ourmazd	249
<i>Control of Molecular Dynamics: Algorithms for Design and Implementation</i>	
Herschel Rabitz and Tak-San Ho	253
<i>Atoms and Ions Interacting with Particles and Fields</i>	
Francis Robicheaux	257

<i>Generation of Bright Soft X-ray Laser Beams</i>	
Jorge Rocca	261
<i>Spatial Frequency X-ray Heterodyne Imaging and Ultrafast Nanochemistry</i>	
Christoph Rose-Petruck	265
<i>Time-Resolved High Harmonic Spectroscopy: A Coherently Enhanced Probe of Charge Migration</i>	
Kenneth Schafer, Mette Gaarde, Kenneth Lopata, Louis DiMauro, Pierre Agostini, Robert Jones	269
<i>Strong-Field Control in Complex Systems</i>	
Tamar Seideman	271
<i>Inelastic X-ray Scattering under Extreme and Transitional Conditions</i>	
Jerry Seidler	275
<i>Dynamics of Few-Body Atomic Processes</i>	
Tony Starace	279
<i>Femtosecond and Attosecond Laser-Pulse Energy Transformation and Concentration in Nanostructured Systems</i>	
Mark Stockman	283
<i>Laser-Produced Coherent X-ray Sources</i>	
Don Umstadter	287
<i>Combining High Level Ab Initio Calculations with Laser Control of Molecular Dynamics</i>	
Tom Weinacht and Spiridoula Matsika	291
<i>New Scientific Frontiers with Ultracold Molecules</i>	
Jun Ye	295
Participants	297

Laboratory Research Summaries
(by institution)

Page is intentionally blank.

AMO Physics at Argonne National Laboratory

Gilles Doumy, Robert Dunford, Elliot Kanter, Bertold Krässig,
Anne Marie March, Steve Southworth, Linda Young
X-ray Science Division
Argonne National Laboratory, Argonne, IL 60439
gdoumy@aps.anl.gov, dunford@anl.gov, kanter@anl.gov, kraessig@anl.gov
amarch@anl.gov, southworth@anl.gov, young@anl.gov

Norbert Scherer
Chemistry Department
University of Chicago, Chicago, IL 60637
nfschere@uchicago.edu

1 OVERVIEW

The Argonne AMO physics program is focused on quantitative understanding of x-ray interactions and inner-shell processes from the weak-field limit explored at the Advanced Photon Source (APS) to the strong-field regime accessible at the Linac Coherent Light Source (LCLS). Single-photon x-ray processes can be dramatically altered in the presence of strong optical fields, and we exploit ultrafast x-ray sources to study these effects. The use of tunable, polarized x rays to probe strong-field processes *in situ* can lead to new physical insights and quantitative structural information not accessible by other techniques. Theory is a key component of our program by predicting phenomena that motivate experiments and by simulating and interpreting measured results.

The intense femtosecond x-ray pulses generated at the LCLS and SACLA XFELs are used to study multiple-photon ionization and inner-shell decay dynamics in gas-phase atoms and molecules and to study the photochemical dynamics of solvated molecules. Theory and advanced computational platforms are used to simulate the interactions of intense, ultrafast x-ray pulses with atoms, molecules, clusters, and nanoparticles. The APS remains our primary source of intense, tunable, polarized x rays for time-resolved laser-pump/x-ray-probe experiments of chemical dynamics and for x-ray and inner-shell interactions with gas-phase atoms and molecules. We continually seek to enhance and exploit instrumentation and techniques that increase understanding of x-ray and strong-field phenomena. To exploit the full x-ray flux available at the APS, we have developed high-repetition-rate laser systems for pump-probe experiments at MHz pulse rates. This capability enables measurements of laser-induced, transient electronic and atomic structures with high sensitivity.

Optical lasers can trap, orient, and order nanoparticles, providing a new route towards manipulation and assembly of nanomaterials. Advanced techniques to optically trap nanoparticles and measure their spectroscopic properties and interactions are being developed in the laboratory of Professor Norbert Scherer at the University of Chicago. We are also exploiting that expertise to develop optical traps for x-ray diffraction and coherent imaging of nanoparticles at the APS.

2 INTENSE X-RAY PHYSICS

Laser streaking at LCLS

(G. Doumy, A. L. Cavalieri,¹ L. F. DiMauro,² M. Meyer,³ W. Helml,⁴ R. Coffee,⁵ and other collaborators)

X-ray free electron lasers are capable of producing very intense and short x-ray pulses ranging from a few fs up to a few tens of femtoseconds. Those sources have already revolutionized the field of ultrafast time resolved x-ray science, in spite of the current lack of exact determination of the pulse duration characteristics. Any measuring scheme is rendered even more challenging by the SASE mode of operation (Self Amplified Spontaneous Emission), which makes a purely chaotic source. Ultimately, a single shot measurement of every shot is required to get a full characterization of the source properties.

Our large collaboration has been using the technique known as laser streaking to get a handle on those pulse properties. The temporal characteristics are transposed to electron wave-packets produced during ionization of a gas target. The simultaneous presence of a strong laser field (operating in the visible, IR or THz region) modifies the energy spectrum of those electrons' wave-packets in a deterministic way. It is then possible to extract from the measured final energy distribution some of the properties of the x-ray pulses.

Attempts at measuring the temporal profile of XFEL pulses have been complicated by the unavoidable timing jitter that exists between the XFEL and the strong laser field, as well as the limitations of the streaking method which requires that the pulse duration be less than half of the laser period. An elegant solution uses THz sources to produce the streaking effect. The long period (150 to 300 fs) allows for both capturing the whole range of pulse durations and controlling for jitter variations on the order of 100–150 fs, which represent the routine synchronization performances at XFELs. However, obtaining time resolution sufficient to identify the expected substructure of SASE pulses remained elusive mostly due to the limited energy resolution of the photoelectron energy measurements.

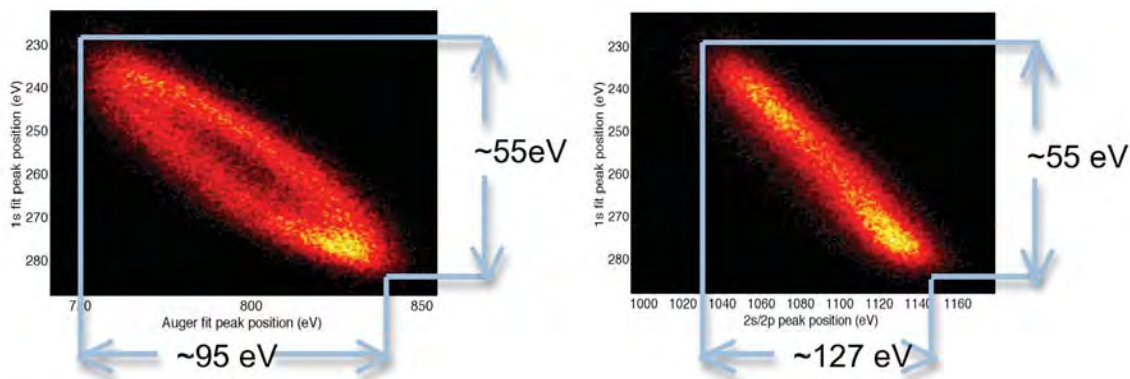


Figure 1: Correlation plots of the center of mass of neon Auger electrons (left) and valence photoelectrons (right) against the core hole photoelectron. The elliptical shape on the left is due to the delay introduced by the hole lifetime (2.7 fs), which means that the two families of electrons are experiencing a different streaking field.

Going further with the streaking measurements requires using shorter wavelengths, and thus shorter laser periods. This does mean that the jitter has to be handled separately. We have followed two main approaches:

- 1 - Measure the jitter independently from the streaking measurement. State of the art methods

using transient absorption of a continuum laser pulse through x-ray excited SiN membranes are now able to pinpoint with femtosecond precision the arrival time of the x-ray pulse related to the optical laser. This ensures that a precise knowledge of the strength of the streaking field is available, which is crucial for successful reconstruction. One such measurement was attempted at LCLS in June, 2014 using 6 μm wavelength laser pulses stretched to a few picoseconds to facilitate even more retrieval of the streaking conditions.

2 - Eliminate the jitter by measuring both a reference signal and the signal of interest at the same time, in the same streaking conditions. The reference signal is produced by the instantaneous photoionization, while one can study even delayed processes such as Auger decay. The hope is that one could then be able to not only get access to the x ray pulse durations, but more importantly be able to follow in the time domain the subsequent processes following the photoionization event. Technical issues hampered the first attempt in 2013, but still demonstrated the power of the combined measurement. The method is illustrated in Fig. 1, plotting the center of mass of the streaking spectra of both photoelectrons and Auger electrons in Neon atoms ionized by 1 keV x-ray photons that clearly exposes the fact that the core hole lifetime imposes a delay between the ionization and the decay channel, such that the electrons are not exposed to the same streaking strength. Therefore, Auger electrons appear to have a lower or higher energy than if they had been emitted at the same time as the photoelectrons, depending on the slope of the streaking laser vector potential, and present an elliptical shape in the correlation map with photoelectrons. This effect will in fact be used to further reduce the uncertainty in the streaking field strength in a future LCLS beam time in February, 2015.

Double *K*-hole spectroscopy in neon with high-intensity x rays from the LCLS

(B. Krässig, E. P. Kanter, G. Doumy, A. M. March, S. H. Southworth, L. Young)

Double *K*-hole formation, mediated by electron-electron correlation, occurs in a fraction of *K*-shell ionization events. The ratio of double to single *K*-hole production in single photon absorption in neon is 0.3% [44]. The decay of the double-core excited states leads to characteristic “hypersatellite” lines in the fluorescence and Auger emission spectra which are shifted up in energy due to the higher binding energy of the doubly core excited state. A double core hole state can also be created by sequential photoabsorption events in an atom that occur within the lifetime span of the core excitation (2.4 fs for neon). The multiphoton absorption conditions are met with focused ultrashort x-ray pulses from the Linac Coherent Light Source (LCLS) and the increased production of hypersatellite Auger electrons was observed during the first user experiment at LCLS [41]. The fraction of double-to-single core hole creation in an atom depends nonlinearly on the intensity of the x-ray field. What is observed experimentally in an accumulated spectrum is an average over the focal area and for average intensity of the chaotic temporary pulse structure of the self-amplified spontaneous emission (SASE) x-ray pulses from the LCLS. Nevertheless, in this manner we were able to record complete high-resolution Auger *KK-KLL* hypersatellite spectra of neon with better contrast to the background signal of *K-LL* emission and consequently shorter accumulation times than in single-photon absorption measurements at storage ring light sources. The hypersatellite spectra were measured with different x-ray pulse lengths and at angles of 0° , 54.6° , and 90° relative to the x-ray polarization. We found that the cleanest spectra were obtained for the shortest possible x-ray bunch durations (~ 3 fs) and at a spectrometer angle of 90° relative to the x-ray polarization direction. At longer pulse lengths, multi-photon absorption leads to further core ionization of the decay products and Auger structures from higher charge states that complicate the assignment of the *KK-KLL* transitions. At the photon energy of the measurements, 1050 eV, weak photoelectron structures broadened by the x-ray bandwidth, correlation satellites associated with $2s$ and $2p$ valence ionization, underlie the spectral region of interest for the *KK-KLL* hypersatellites. At

90° from the polarization direction the photosatellite signal is suppressed due to their respective angular distribution. Because of the low background signal it is possible to obtain the level width of the KK double core hole state from fitting a Voigt profile to the experimental data recorded at 90° and judging the KK level width from the Lorentzian tails of the line profile rather than from the full width at half maximum, which is dominated by the temporal resolution of the Time-of-Flight spectrometer. The measured Auger hypersatellite line positions and intensities are sensitive to many-electron interactions in the initial and final states and are compared with available theoretical calculations [45, 46].

Understanding inner-shell dynamics with intense, femtosecond XFEL pulses

(A. Picón, C. S. Lehmann, S. H. Southworth, G. Doumy, P. J. Ho, E. P. Kanter, B. Krässig, A. M. March, D. Moonshiram, L. Young, S. T. Pratt,⁶ C. Bostedt,⁵ A. Rudenko,⁷ D. Rolles⁷, R. Wehlitz,⁸ L. Cheng,⁹ J. F. Stanton,⁹ and other collaborators)

The advent of XFELs and the concept of “diffract before destroy” for biomolecular coherent imaging [42] have created a significant need to understand molecular core-hole dynamics as it is responsible for radiation damage. It is informative to study core-hole decays in XeF_2 , because measurements can be compared with corresponding core-hole decays in atomic Xe, and accurate atomic ionization codes are available. Theory and calculational methods for inner-shell processes in molecules are far less developed. We first studied K -shell core-hole decays in Xe and XeF_2 using hard x rays at the Advanced Photon Source [5]. We have recorded new, more detailed data using APS x rays, and the status of that work is discussed later in this report.

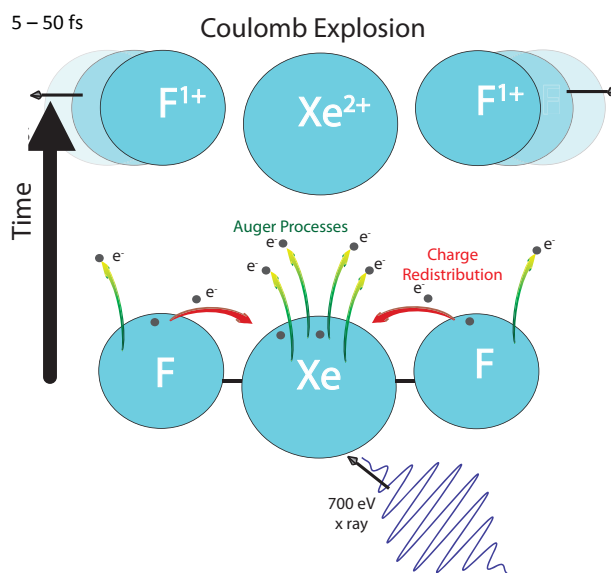


Figure 2: Illustration of inner-shell decay dynamics of XeF_2 . Absorption of a 700-eV photon ejects a Xe 3d electron and initiates a core-hole decay process with the ejection of several Auger electrons. While the first decay step remains localized on Xe, subsequent decays involve delocalized valence electrons and charge is redistributed to the F atoms. The molecular ion then Coulomb explodes. Ion yields were measured as a function of photon energy using synchrotron x rays. The time dependence of the process was then explored using x-ray-pump/x-ray-probe measurements at the LCLS.

Core-hole decay in molecules is a complex process that occurs on the time scale of a few fs to tens of fs. The processes of electronic Auger transitions, charge redistribution, and Coulomb explosion

occur concurrently. For example, ion fragment kinetic energies are typically smaller than expected based on the Coulomb energy that would be stored in the molecular ion at the neutral ground-state geometry, because the atomic ions begin moving apart while Auger transitions proceed and charge is increasing and distributing on the atomic sites. We noted the complexity of molecular core-hole decay in our earlier experiments on XeF_2 compared with atomic calculations [5]. The recent capability at LCLS of generating two-color, femtosecond x-ray pulses with controlled delay over $\sim 5\text{--}50$ fs [43] prompted us to conduct a pump-probe experiment to explore the time dependence of core-hole decays in XeF_2 . The process is illustrated in Fig. 2. Absorption of an x ray with energy near 700 eV ejects a Xe 3d electron and triggers the core-hole decay. The initial hole and first decay step involve electrons localized on the Xe site, but subsequent decays involve delocalized valence electrons so charge is distributed to the F sites. The molecular ion Coulomb explodes into energetic fragments. The F 1s electrons have similar ionization energies as Xe 3d. We exploited the two-color capability at LCLS to attempt to pump Xe 3d and probe F 1s, which we term “hetero-site-specific” pump-probe spectroscopy. Ion coincidence data were recorded with a “reaction microscope” that will provide momentum-resolved images of the decay dynamics. Data were recorded at low hit rates to reduce random coincidences. A few data sets were recorded at selected pump and probe energies with delays of 5, 25, and 50 fs. The data analysis procedures are well known but challenging to implement. In addition to the two-color pump-probe measurements, ion fragmentation of XeF_2 was also measured using single ~ 100 fs pulses with variable fluence to span the single-to-multiple photoionization regimes.

In preparation for the LCLS experiments, ion yield branching ratios and photoionization cross sections of Xe and XeF_2 were measured over the 650–740 eV range at Wisconsin’s Synchrotron Radiation Center. This energy range encompasses the ionization thresholds and near-edge regions of Xe $3d_{5/2}$, Xe $3d_{3/2}$, and F 1s electrons. Particularly interesting are strong resonant features in the XeF_2 data from excitation of the lowest unoccupied molecular orbital (LUMO). The theorists in our collaboration used Equation of Motion Coupled Cluster calculations to predict the resonant energies and oscillator strengths. Those results are being prepared for publication. The synchrotron measurements and corresponding calculations were very useful in planning and conducting the LCLS experiments. Additional theoretical work is in progress to incorporate inner-shell transitions in molecular quantum chemical codes.

Theoretical tracking of resonance-enhanced multiple ionization pathways in XFEL pulses

(P. J. Ho, C. Bostedt,⁵ S. Schorb,⁵ and L. Young)

We present an extended Monte Carlo rate equation (MCRE) approach to examine the inner-shell ionization dynamics of atoms in an intense x-ray free-electron laser (XFEL) pulse. In addition to photoionization, Auger decay and fluorescence processes, we include bound-to-bound transitions in the rate equation calculations. Using an efficient computational scheme, we account for “hidden resonances” unveiled during the course of an XFEL pulse. For Ar, the number of possible electron configurations is increased ~ 10 billion-fold over that required under non-resonant conditions. We investigated the complex ionization dynamics of Ar atoms exposed to an 480-eV XFEL pulse, where production of ions above charge-state 10^+ is not allowed via direct one-photon ionization. We found that resonance-enhanced x-ray multiple ionization (REXMI) pathways play a dominant role in producing these nominally inaccessible charge states. Our calculated results agree with the measured Ar ion yield and pulse-duration dependence [38]. A report on this work is submitted for publication [33]. The MCRE method enables theoretical exploration of the complex dynamics of resonant high-intensity x-ray processes and will be applied to other atomic systems that have been or will be studied at XFELs.

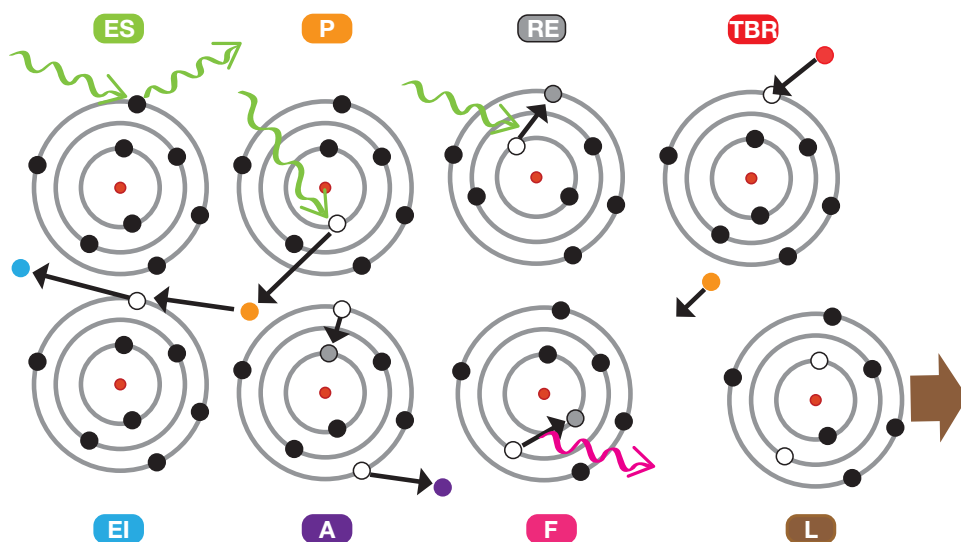


Figure 3: Primary and secondary electronic processes important to consider in interactions of XFEL pulses with matter: elastic x-ray scattering (ES), photoionization (P), resonant excitation (RE), three-body electron-ion recombination (TBR), electron-impact ionization (EI), Auger decay (A), fluorescence (F), and lattice dynamics (L).

Modeling of intense x-ray laser damage in biomolecules and nanomaterials

(P. J. Ho, C. Knight,¹⁰ and L. Young)

X-ray free-electron laser (XFEL) pulses, such as those available at the Linac Coherent Light Source (LCLS) and Spring-8 Angstrom Compact Free Electron Laser (SACLA) facilities, provide extraordinary spatial resolution and elemental specificity. When coupled with femtosecond pulse durations, these intense x-ray pulses enable the generation of real-time movies that can follow key ultrafast processes during chemical reactions in liquids, advanced materials, and biological systems. As new technologies are utilized, such as multi-bend achromats (MBA) planned in the upgrade of the Advanced Photon Source, the resulting new frontiers in x-ray pump-probe experiments will significantly advance imaging and the study of dynamical processes of materials with reduced data collection times. To fully exploit the dual advance in the achievable spatial and temporal resolution with XFEL pulses, it is critical to fully understand the fundamental interactions of these intense x-ray pulses with large molecules and materials in order to overcome the practical limitations of these experiments (e.g. radiation damage via inner-shell ionization). A thorough understanding of XFEL pulse-mediated electronic transitions and the ensuing response of the atomistic environment serves not only to clarify the interpretation of images produced by coherent x-ray scattering, but also guide the design of new, unique experiments and light source facilities. The work proposed here is an important step forward in understanding high-brightness, high-energy, coherent x-ray laser pulses and their interactions with materials, supporting the DOE mission to extend the scientific and technological strengths of the U.S.

The main objective of this project is to understand the fundamental mechanisms of radiation damage induced by high-intensity x-ray laser pulses in nanostructures, doped rare-gas clusters, and a polypeptide, which serves as a model protein. The challenges associated with tracking the motion of particles and evolution of electronic configurations are addressed with a novel Monte-Carlo/Molecular-Dynamics simulation algorithm (see Fig. 3) implemented in a highly parallelized

simulation code. The molecular dynamics algorithm [39] is used to propagate classical particle trajectories forward in time and the quantum nature of interactions with an XFEL pulse is accounted for by a Monte Carlo method to calculate probabilities of electronic transitions. The combination of this novel simulation method, which has been significantly extended by some of the PIs, with leadership computational resources will facilitate the efficient investigation of the truly multiscale nature of these complicated processes. All three systems considered are equally important in their own right and are representative of the wide range of experiments ongoing at current light facilities and those expected to come online or upgraded in the near future. The comparison of the results from these simulations with experimental characterization of the same systems will aid in the further development of the applied methodology, interpretation of experimental findings, and ultimately advancing the field of ultrafast x-ray science.

To carry out the above theoretical investigation, we have submitted an INCITE proposal to request about 300 million computation hours on Mira, a new 10-petaflops high performance computing resource at (Advanced Leadership Computing Facility) ALCF, over a period of two years. The award will be announced at the end of November 2014 and the resource will be available in January 2015.

Theoretical tracking of radiation damage dynamics of diamond by high-brilliance x-ray pulses in nanosecond/mesocale regime

(P. J. Ho, C. Knight,¹⁰ L. Young, K.-J. Kim, Y. Shvydko, S. Stoupin)

Even though our proposed x-ray radiation damage simulations with biomolecules and nanomaterials are focused on physics in femtosecond XFEL pulses, the results from these simulations will guide us to further extend the simulation methodology to track the radiation damage of matter in the nanosecond/mesoscale regime. This regime will be of interest to the science endeavors enabled by not only the current APS pulses, but also the future x-ray sources at APS enabled by the new technology of multi-bend achromats (MBA) to deliver high-brightness, picosecond coherent x-rays. Understanding the radiation damage by these future APS pulses is crucial as these pulses have the potential to facilitate significant advances in imaging and the study of dynamical processes of materials with reduced data collection times. Here, we propose to investigate radiation damage dynamics initiated by a sequence of picosecond hard x-ray pulses (~ 10 keV) in diamond out to the sub-microsecond timescale and mesoscopic length scale, eventually micron-sized systems, at the level of atoms and electrons. Our atomistic method is based on our recently developed hybrid MC/MD method which extends the treatment of Jurek *et al.* [40] by including information on electronic configurations.

The challenge of this investigation lies in tracking the actions of a large number of particles (electrons and nuclei) for hundreds of nanoseconds. There are more than a trillion particles in a micron-sized diamond system, and an atomistic view of their x-ray response will allow us to trace the emergence and relaxation of correlated particle dynamics of various length scales and potentially spatial inhomogeneity of particle distribution due to anisotropic electron emission. On the other hand, in a time domain computation, we need to capture the phase transition or relaxation in the bulk, which might take nanoseconds or longer, and resolve the ultrafast electronic transitions initiated by x-ray pulses, which can occur on a subfemtosecond timescale. To further complicate the situation, tracking the interaction of 10-keV electrons generated from the hard x-ray pulses with surrounding electrons/atoms/ions will require attosecond time resolution since these electrons can travel more than 0.5 \AA in an attosecond. It is clear that reaching the 100-ns time regime with a constant attosecond time step integration scheme is impractical, since 10^{14} simulation steps would be required. Thus, developing efficient schemes for multiscale computation both in space and time are crucial. The success of this theoretical effort is expected to be useful for the design of

diamond-based x-ray instruments, like the X-ray free-electron oscillator (XFEL), by being able to compute physical observables that can be directly compared with the measurements from planned experiments at APS led by Kwang-Je Kim, Yury Shvydko and Stanislav Stoupin.

In the coming months, we will investigate the effectiveness of the Tersoff potential in characterizing the timescale and length scales of the correlated electronic/atomic response in various relaxation processes and phase transitions, including graphitization. Analysis will be conducted to understand the roles of electron-hole pairs in initiating large-scale phase transitions in diamond after x-ray exposure. Our goal is to efficiently track the dynamics of these systems up to tens of nanoseconds. To do this, we will test the effectiveness of an adaptive time resolution propagation scheme by comparing the results with those obtained from a constant time step integration scheme. In addition, we will examine the possibility of incorporating coarse-grained modeling with adaptive resolution in these hybrid MC/MD simulations. We will test the effectiveness of this mixed-resolution model on smaller systems with a few electron-hole pairs generated from x-ray pulses. The results from the coarse-grained calculations will be compared directly with those from the full atomistic calculations.

Plans are currently aimed at adapting as necessary these mixed-resolution simulation methods to the leadership computing resources available at ALCF. We have recently been awarded 360,000 core hours on the high-performance computing cluster at the Center of Nanomaterials (CNM) at Argonne to carry out these studies on diamond. The results from each of these proposed theoretical efforts will then provide a direct roadmap to model mesoscale/nanosecond response of diamond nanostructures exposed to x-ray pulses.

3 X-RAY PROBES OF MOLECULAR DYNAMICS

Ligand substitution and competing mechanisms

(A. M. March, G. Doumy, S. H. Southworth, E. P. Kanter, L. Young, T. Assefa,³ Z. Németh,¹¹ D. Szemes,¹¹ A. Bordage,¹¹ C. Bressler,³ G. Vankó,¹¹ W. Gawelda,³ M. Ochmann,¹ N. Huse¹)

We are continuing studies on ligand substitution in liquid phase systems, tackling the case where competing mechanisms are present. We have studied two solvated transition metal complexes and have demonstrated our ability to separate the different contributions.

The first sample is the model system $[\text{Fe}(\text{II})(\text{CN})_6]^{4-}$ (ferrocyanide) in an aqueous solution, studied after laser excitation using x-ray absorption spectroscopy (XAS) and x-ray emission spectroscopy (XES). We studied the system with 10 ps laser pulses at 355 nm, where the photoexcited state is believed to evolve into the pentacyano-aquo complex $[\text{Fe}(\text{II})(\text{CN})_5\text{H}_2\text{O}]^{3-}$ via ligand dissociation, and also at 266 nm where the excited state can also lead to photo-injection of an electron into the solvent, concomitant to the oxidation state change of the iron center, yielding $[\text{Fe}(\text{III})(\text{CN})_6]^{3-}$. Previously, we collected XANES data and XES $K\beta_{1,3}$ (1s-3p) at both wavelengths as well as EXAFS data at 355 nm with good statistics. Initial analysis of the XANES and XES data indicated that the spectra at 266 nm excitation are due to the presence of both $[\text{Fe}(\text{II})(\text{CN})_5\text{H}_2\text{O}]^{3-}$ and $[\text{Fe}(\text{III})(\text{CN})_6]^{3-}$. By comparison of the spectra at the two excitation wavelengths, we were able to quantify the contributions from each species and thus reconstruct the absorption spectrum of the pentacyano-aquo complex intermediate. Further analysis has suggested that the reconstructed pentacyano-aquo spectrum contains contributions from pentacyanide, which lacks the water ligand. Continuing to take advantage of our high-repetition-rate pump-probe setup at APS 7ID-D, we performed additional measurements tracking the time dependence of particular spectral features following laser excitation in order to confirm our hypothesis that both $[\text{Fe}(\text{II})(\text{CN})_5\text{H}_2\text{O}]^{3-}$ and $[\text{Fe}(\text{II})(\text{CN})_5]^{3-}$ were present. Also, we carried out theoretical XANES simulations for the proposed species involved. The simulations and delay measurements are also suggesting that in-

deed both $[\text{Fe(II)(CN)}_5\text{H}_2\text{O}]^{3-}$ and $[\text{Fe(II)(CN)}_5]^{3-}$ are present 120 ps after laser excitation and that $[\text{Fe(II)(CN)}_5]^{3-}$ converts to $[\text{Fe(II)(CN)}_5\text{H}_2\text{O}]^{3-}$ within 4.6 ns. The measurements demonstrate the ability of synchrotron x-ray measurements to capture transient states, in this case the $[\text{Fe(II)(CN)}_5]^{3-}$ species formed after dissociation of the CN^- ligand and before the association of an H_2O . Analysis of the EXAFS data continues at attempting to determine the structure of both the $[\text{Fe(II)(CN)}_5]^{3-}$ and $[\text{Fe(II)(CN)}_5\text{H}_2\text{O}]^{3-}$ species, as well as quantifying the relative weights of the two products.

These successful observations at the Advanced Photon Source motivated a follow up experiment using an XFEL in order to track the processes on a faster time scale (on the order of a picosecond), and thus be able to answer the question as to whether the pentacyanide product is a necessary intermediary in the ligand substitution process. A combination of techniques was used in June, 2014 at SACLA/Spring8, with both hard x-ray spectroscopies (absorption and $K\beta$ emission) as well as x-ray diffuse scattering as another tool capable of yielding transient structures, especially as EXAFS is not viable at an XFEL yet. First indications during the experiment are confirming the attribution of spectroscopic features to the products we were considering, as well as presenting some fast, picosecond decay behavior of the purported pentacyanide transient that has yet to be explained.

The second sample is $[\text{Mn(CO)}_5]_2$ (dimanganese decacarbonyl) solvated in isopropanol. Along with being an important reagent in organic synthesis, $[\text{Mn(CO)}_5]_2$ is an important model system in the photochemistry of metal-metal bonds. From ultrafast visible and infrared spectroscopy, it is known that upon photoexcitation two dissociation channels open up: 1) the photodetachment of one of the CO ligands producing $\text{Mn}_2(\text{CO})_9$ and 2) the formation of two identical radicals in their doublet ground state, Mn(CO)_5 , which remain stable in solution until nongeminate recombination occurs. The individual yields are wavelength dependent, and for wavelengths >300 nm the Mn-Mn cleavage is strongly favored. Using 266 nm and 355 nm optical pump wavelengths, we would expect to deal with both photoproducts in different weights. The aim is to unambiguously determine the quantum yields that can then be used as the input needed to extract the transient structures of both species.

Investigating electronic excitation in ZnO nanoparticles using time-resolved x-ray absorption and emission spectroscopy

(A. M. March, G. Doumy, S. H. Southworth, E. P. Kanter, L. Young, W. Gawelda,³ J. Szlachentko,¹² C. Milne¹²)

Collaborating with researchers from the Paul Scherrer Institute, we have explored the photo-generated electron relaxation times in ZnO nanoparticles using our high-repetition-rate pump-probe setup at APS 7ID-D and a von Hamos x-ray emission spectrometer. ZnO shares several characteristics with TiO_2 , the most widely used photocatalyst. Namely, both have a wide band gap, which is located at similar positions with respect to the normal hydrogen electrode zero potential, and both materials are able to adsorb water and CO_2 , making them good candidates to perform artificial photosynthesis. However, ZnO photocatalytic performance is drastically lower than that obtained with TiO_2 for reasons not yet understood. Charge carrier lifetime has been highlighted as a possible explanation for the low reaction quantum yields. Charge dynamics often occur in a time regime spanning from fs to ns, as measured with TiO_2 , whereas chemical transformations often involve several steps that span up to ms or even longer. Therefore, reaction is only attained when there is an overlap between charge dynamics and chemical transformation time scales, i.e., the probability to use free carriers in a chemical transformation diminishes with the decrease of their lifetime. Based on this premise, the study of photo-generated electron relaxation times will bring insight into ZnO charge dynamics and determine if the fast recombination is the prime reason for

ZnO low chemical reactivity. We collected $K\alpha$, $K\beta$ and valence-to-core x-ray emission spectra as well as resonant inelastic x-ray scattering (RIXS) data ~ 100 ps after UV (355 nm) excitation. This allowed us to establish the efficiency of the photoexcitation of the ZnO nanoparticles in solution and estimate the number of available electrons for photocatalysis. The RIXS/XES data should establish the relaxation pathways of the excited electrons back to the valence band, and potentially identify changes between long-lived (catalytically active) and short-lived (catalytically inactive) electronic states. Further analysis is underway. The high quality data obtained at the APS has motivated pursuing the study of this process on faster time scales after the laser excitation, using an XFEL to provide subpicosecond resolution. A proposal was accepted at SACLA, and experiments will happen in November, 2014.

Studying the structural and electronic configurations during photocatalytic activation of O_2 at a diiron(II) complex

(D. Moonshiram, C. S. Lehmann, A. Picón, A. M. March, G. Doumy, S. H. Southworth)

Several mono and carboxylate-bridged diiron nuclear enzymes are critical in activating dioxygen in various biological processes such as DNA synthesis, hydrocarbon metabolism and cell proliferation [47]. Iron-containing enzymes such as cytochrome P450, peroxidases, catalases and methane monooxygenase (MMO) have been shown to activate dioxygen by using two electrons and protons to produce iron (IV) oxo intermediates [48, 49, 50]. The remarkable efficiency of these enzymes is often attributed to the formation of these iron(IV) cations which serve as active oxidants in enzymatic reactions and are able to attack the C-H bonds of a wide range of hydrocarbon substrates [51]. It is widely postulated that ferryl-oxo species are key intermediates in the mechanism of cytochrome P450 and MMO. However due to the complexity of the protein environments in biological iron enzymatic systems [47], monitoring the structural changes occurring during dioxygen activation is a complex undertaking. This project serves to study the light driven activation of a well characterized artificial analogue of an diiron MMO enzyme, (μ -peroxo) (μ -carboxylato) diiron(III) complex, $[Fe_2(\mu-O_2)(N-EtHPTB)(\mu-PhCO_2)]^{2+}$ in a chromophore/diiron complex assembled unit. Such types of assemblies provide new avenues for study of catalytic reaction mechanisms. They are promising examples of artificial molecular systems leading to dioxygen activation as visible light is efficiently absorbed at the chromophore, and light energy is in turn converted into a chemical potential via an electron relay through charge accumulation processes at the iron metal center. Formation of high valent iron peroxo species have been shown by UV-Vis, EPR and Resonance Raman spectroscopy as well as X-ray spectroscopic analysis. We are using tunable APS x-rays for x-ray absorption near-edge spectroscopy (XANES), extended x-ray absorption fine structure spectroscopy (EXAFS), and x-ray emission spectroscopy (XES) to characterize these systems. Recent XANES and EXAFS measurements revealed formation of an iron peroxo species with different coordination number and formation of a peroxo bridge.

Development of x-ray emission spectrometers

(A. M. March, G. Doumy, S. H. Southworth, D. Moonshiram, L. Young, X. Shi, D. Casa, X. Huang, E. Kasman, A. Kastengren)

X-ray emission spectroscopy (XES) is a powerful tool for studying molecular dynamics. By probing the occupied electronic states, XES is complementary to x-ray absorption spectroscopy (XAS) that only probes unoccupied states. A major challenge to full utilization of this technique is the fact that the signal level for XES is substantially lower than for XAS. As an example, during our recent XES measurements on aqueous ferrocyanide given an incident flux rate of 5×10^{10} x-ray photons per second, the detected rate at the peak of the $K\beta$ emission spectrum was 9 photons/second while that at the K -edge of the absorption spectrum was 2×10^4 photons/second.

Even though the use of high repetition rate lasers has enabled successful use of the XES technique in time resolved measurements, this had been limited to looking at the $K\alpha$, $K\beta$ and 1s-2p resonant x-ray emission (RIXS/RXES) [7, 16]. To be sensitive to the chemical changes happening after photoexcitation, the even weaker Valence-to-Core emission needs to be collected, which requires the development of more efficient detection without loss of resolution.

Collaborating with x-ray crystal experts at the APS, we are exploring two promising designs, contrasting with the use of spherically bent crystal analyzers in a Rowland circle geometry where the distance between the source and the crystal is the result of a compromise between collection solid angle and resolution. The first option uses the well-established von Hamos geometry where cylindrically bent crystals are used. In the flat direction a large bandwidth is dispersed onto a 1D or 2D detector, while in the other direction the collection efficiency is improved. This scheme is particularly attractive for time resolved measurements because systematics can be easily removed by collecting the full spectrum at the same time. The second option represents a challenging technical extension of the Rowland circle geometry of the scanning spectrometer. The idea is to create a crystal that approximates the Johansson geometry where the Rowland circle radius is half that of the Bragg planes. This so-called Wittry geometry allows increasing the solid angle without compromising energy resolution. The substrates needed to press crystal strips into a stepped Wittry geometry have been fabricated, and the crystal dicing procedure is being developed. A full comparison of the different analyzer geometries will be attempted in real conditions at the APS in November, 2014. To further increase collection solid angles, several analyzer crystals can be used simultaneously with 1D and 2D detectors. Our goal is to make XES a viable technique for time-resolved studies.

Molecular response to x-ray absorption and vacancy cascades

(R. W. Dunford, E. P. Kanter, S. H. Southworth, B. Krässig, G. Doumy)

Analysis is continuing on recent experiments to explore molecular response following x-ray photoionization at the Advanced Photon Source. We focus on molecules which contain a heavy component such as Xe, I, or Br. In these experiments, we measure the cascade decays following deep inner-shell ionization of the heavy atom and measure breakup modes and kinetic energy release (KER). In earlier work [5], we observed molecular effects in vacancy cascades of the molecule XeF₂. Our method was to compare the total charge produced in atomic Xe to that produced in XeF₂ following K -shell ionization of Xe. This work showed evidence that the total charge produced in the XeF₂ molecule was larger than that produced in the isolated Xe atom and led to theoretical work in which the cascade decay from Xe following K -shell ionization was simulated, taking into account Auger and Coster-Kronig rates, fluorescence rates, and shake-off branching ratios. It was found that the appearance of 5p electrons signals the time scale for participation of the molecular orbitals and when ionization of F atoms is expected. The results of this analysis indicated that the F atoms participate in the decay cascade during the fragmentation process and this lowers the kinetic energy release (KER) in comparison to a model in which the KER is estimated based on the ground state Xe-F intermolecular distance. This reduction in KER is in qualitative agreement with experimental observations [5].

To further explore these issues experimentally, we built an improved apparatus with a position-sensitive ion detector which allows a complete reconstruction of each ion fragmentation event. This apparatus has been used in a series of experiments; first doing a more detailed study of the XeF₂ molecule and then moving on to other species such as IBr, and CH₂BrI. For IBr, K -shell holes can be created in either the Br atom at 13 keV or on the I atom at 33 keV. These data allow us to study these molecules for two different excitation modes and compare with theoretical calculations based on atomic theory. We used similar techniques to study the molecule CH₂BrI to explore the

effect of changing the separation between the I and Br atoms in a molecule.

One of the challenges to the analysis of these data is that the highly charged ions produced in these experiments have large cross sections for electron pickup in the target or from background gas in the chamber. The effects of this charge exchange can be seen in the molecular data as well as the data from atomic Xe. These effects distort the observed ion distributions following photoionization and add additional ions (from background gas) unrelated to the ions from the molecular breakup we are studying. A further complication is the variation of detection efficiency with charge state and atomic/molecular species. To understand these issues and be able to make corrections and more reliably estimate uncertainties, we have developed a Monte-Carlo code to model these experiments. The code accounts for the cross sections for charge exchange of the different species on the background gas and the variation of detection efficiency of the different ions as a function of their charge states. The code allows us to explore the distortions caused by these effects starting with different initial conditions such as idealized breakup modes based on theory. The code can be expanded to include other imperfections of the apparatus and will be useful in the design of future experiments, as one can choose experimental conditions that minimize the distortions caused by systematic effects.

Short pulse x-ray beamline at the Advanced Photon Source

(R. Reininger, E. M. Dufresne, M. Borland, M. Beno, L. Young, P. G. Evans⁸)

Experimental facilities for picosecond X-ray spectroscopy and scattering based on RF deflection of stored electron beams face a series of optical design challenges. Beamlines designed around such a source enable time-resolved diffraction, spectroscopy and imaging studies in chemical, condensed matter and nanoscale materials science using few-picosecond-duration pulses possessing the stability, high repetition rate and spectral range of synchrotron light sources. The RF-deflected, chirped electron beam produces a vertical fan of undulator radiation with a correlation between angle and time. The duration of the x-ray pulses delivered to experiments is selected by a vertical aperture. In addition to the radiation at the fundamental photon energy in the central cone, the undulator also emits the same photon energy in concentric rings around the central cone, which can potentially compromise the time resolution of experiments. A detailed analysis of this issue was performed for the proposed SPXSS beamline for the Advanced Photon Source. An optical design that minimizes the contamination of off-axis radiation and provides variable x-ray pulse duration in the few to tens of picosecond regime was done. A paper was published on this work [29].

4 OPTICAL CONTROL AND X-RAY IMAGING OF NANOPARTICLES

Optical trapping of metal nanoparticles

(U. Manna,¹³ Z. Yan,¹³ N. F. Scherer¹³)

We have developed new optical trapping methods [36] and investigated the interactions of photonically interacting metal nanoparticles [37]. The new trapping method uses a force that can be created in optical trapping configurations due to phase gradients that arise naturally (or can be tailored) in shaped and focused optical beams. Figure 4 from Ref. [36] shows the scheme and also characterization of the optical phase gradient in an optical line trap. The images in Fig. 4a show identical intensity profiles but oppositely signed phase gradients that in turn drive nano particles toward the edges. Figure 4b shows the measured intensity and phase profiles for line traps of various widths. The number of phase profiles is doubled in color-coded pairs with + and - phase gradients. The forces that result from the phase gradients is 1-fold larger in these line traps as the force from the intensity gradient. We expect that this will be useful for future optical trapping configurations for x-ray diffraction experiments. The work described in Ref. [37] is to quantify the

electrodynamic interactions amongst arrays of metal nanoparticles by way of a dipolar interaction that occurs on intermediate length scales, leading to forces between the particles known as optical binding. We expect to be able to use these forces to create aligned arrays of metal nanoparticles that will be of interest in future x-ray diffraction experiments.

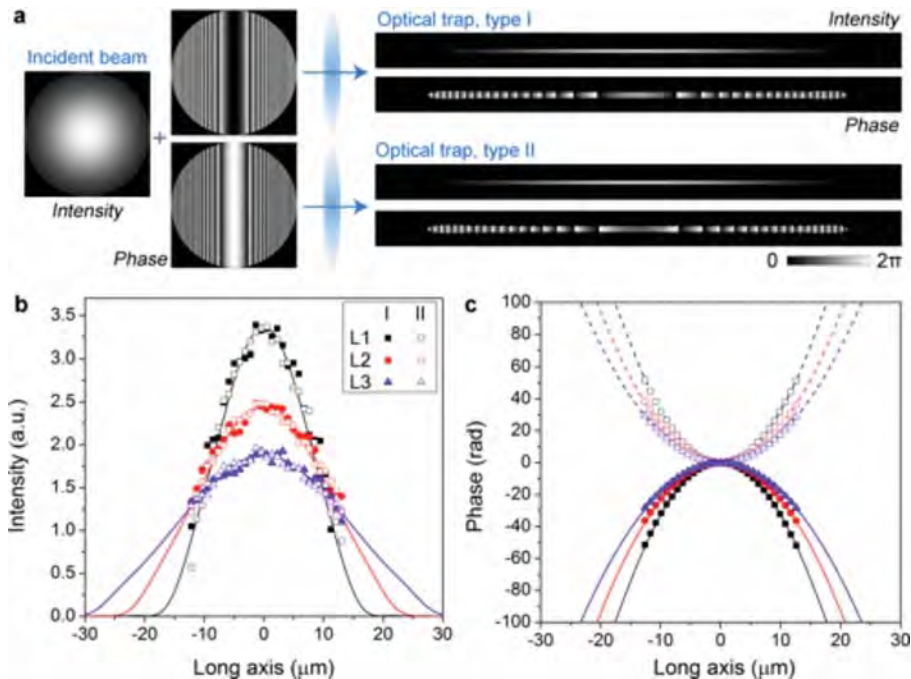


Figure 4: (a) Optical beam, phase profiles programmed onto a 2D spatial light modulator (SLM) and the resulting calculated intensity and phase profiles. (b) Measurements of the intensity and phase profiles of line traps of various widths. Both + and - phase profiles (that have the same intensity profiles) are generated and measured using a Shack-Hartmann wavefront sensor.

Optical control of metal nanowires and single-particle x-ray diffraction

(Y. Gao, N. F. Scherer,¹³ M. Pelton,¹⁴ J. Guest,¹⁵ U. Manna,¹³ R. Harder, N. Phillips,¹⁶ S. H. Southworth and collaborators)

We have built a compact optical-trapping apparatus which is capable of operating at the APS beamlines. The apparatus was assembled and tested in the optics lab of the AMO group. It includes a spatial light modulator (SLM), which is able to shape the phase of optical fields and create multiple traps as needed. In order to cancel out radiation pressure and enhance the stability of the trap, the apparatus utilized a dual-beam, counter-propagating design. In comparison with the interferometric Bessel-beam trap [8, 9, 27], the counter-propagating trap does not require the extended focal spot generated by a Bessel-beam, providing more flexibility in creating and aligning multiple optical traps.

We have tested the apparatus at the APS beamline 34-ID-C during the beamtime in August, 2014. We optically trapped and aligned $\sim 3 \mu\text{m}$ zinc oxide (ZnO) nanorods and observed the (001) Bragg peak from the unfocused coherent x-ray beam at 34-ID. In order to simplify aligning the nanorods, we only used a single-beam trap in this experiment. The laser beam was shaped by the SLM to create a double-focus trap, which is able to hold the nanorods stably in 2-D. Then the particles were trapped against the inner-surface of the sample holder (quartz capillary tube). By

modifying the phase mask displayed on the SLM, we rotated the trapped nanorod to the Bragg diffraction angle and successfully observed the Bragg peak.

Next year we will aim to observe coherent diffraction images from the optically trapped particles. According to the result of the first beamtime, we are going to make several improvements on the current apparatus. To be specific, we will modify the setup of the sample holder, add motorized stages into the apparatus, and synthesize/purchase more nanoparticles with different shapes and materials. These will reduce the time spent on sample preparation, and allow us to remotely control the optical trap while collecting diffraction images.

The second beamtime has been allocated during 2014-3 on beamline 34-ID-C. This beamtime will be devoted to testing the improved apparatus and determining optimum conditions and techniques for recording coherent diffraction images. The third beamtime will be allocated during either 2015-1 or 2015-2.

5 Affiliations of collaborators

¹Center for Free-Electron Laser Science, DESY, Hamburg, Germany

²Ohio State University, Columbus, OH

³European XFEL, Hamburg, Germany

⁴MPQ, Garching, Munich, Germany

⁵Linac Coherent Light Source, SLAC National Accelerator Laboratory, Menlo Park, CA

⁶Chemical Sciences & Engineering Division, Argonne National Laboratory, Argonne, IL

⁷Kansas State University, Manhattan, KS

⁸University of Wisconsin, Madison, WI

⁹The University of Texas at Austin, Austin, TX

¹⁰Argonne Leadership Computing Facility, Argonne National Laboratory, Argonne, IL

¹¹Wigner Research Centre for Physics, Hungarian Academy Sciences, Budapest, Hungary

¹²Paul Scherrer Institute, Villigen, Switzerland

¹³University of Chicago, Chicago, IL

¹⁴University of Maryland, Baltimore County, MD

¹⁵Center for Nanoscale Materials, Argonne National Laboratory, Argonne, IL

¹⁶La Trobe University, Melbourne, Victoria, Australia

References

Publications 2012–2014

- [1] M. Meyer, P. Radcliffe, T. Tschentscher, J. T. Costello, A. L. Cavalieri, I. Grguras, A. R. Maier, R. Kienberger, J. Bozek, C. Bostedt, S. Schorb, R. Coffee, M. Messerschmidt, C. Roedig, E. Sistrunk, L. F. Di Mauro, G. Doumy, K. Ueda, S. Wada, S. Düsterer, A. K. Kazansky, and N. M. Kabachnik, “Angle-resolved electron spectroscopy of laser-assisted Auger decay induced by a few-femtosecond x-ray pulse,” *Phys. Rev. Lett.* **108**, 063007 (2012).
- [2] C. Buth, J.-C. Liu, M. H. Chen, J. P. Cryan, L. Fang, J. M. Glowina, M. Hoener, R. N. Coffee, and N. Berrah, “Ultrafast absorption of intense x rays by nitrogen molecules,” *J. Chem. Phys.* **136**, 214310 (2012).
- [3] M. C. Kohler, C. Müller, C. Buth, A. B. Voitkiv, K. Z. Hatsagortsyan, J. Ullrich, T. Pfeiffer, C. H. Keitel, “Electron correlation and interference effects in strong-field processes,” in *Multiphoton Processes and Attosecond Physics*, K. Yamanouchi and K. Midorikawa, Springer Proceedings in Physics **125**, Springer, Berlin, 2012.
- [4] S. M. Cavaletto, C. Buth, Z. Harman, E. P. Kanter, S. H. Southworth, L. Young, and C. H. Keitel, “Resonance fluorescence in ultrafast and intense x-ray free-electron-laser pulses,” *Phys. Rev. A* **86**, 033402 (2012).
- [5] R. W. Dunford, S. H. Southworth, D. Ray, E. P. Kanter, B. Krässig, L. Young, D. A. Arms, E. M. Dufresne, D. A. Walko, O. Vendrell, S.-K. Son, and R. Santra, “Evidence for interatomic Coulombic decay in Xe *K*-shell-vacancy decay of XeF₂,” *Phys. Rev. A* **86**, 033401 (2012).
- [6] L. Fang, T. Osipov, B. Murphy, F. Tarantelli, E. Kukk, J. Cryan, P. H. Bucksbaum, R. N. Coffee, M. Chen, C. Buth, and N. Berrah, “Multiphoton ionization as a clock to reveal molecular dynamics with intense short x-ray free electron laser pulses,” *Phys. Rev. Lett.* **109**, 263001 (2012).

- [7] K. Haldrup, G. Vankó, W. Gawelda, A. Galler, G. Doumy, A. M. March, E. P. Kanter, A. Bordage, A. Dohn, T. B. van Driel, K. S. Kjaer, H. T. Lemke, S. E. Canton, J. Uhlig, V. Sundström, L. Young, S. H. Southworth, M. M. Nielsen, and C. Bressler, “Guest-host interactions investigated by time-resolved x-ray spectroscopies and scattering at MHz rates: solvation dynamics and photoinduced spin transition in aqueous $[\text{Fe}(\text{bipy})_3]^{2+}$,” *J. Phys. Chem. A* **116**, 9878 (2012).
- [8] Z. Yan, J. E. Jureller, J. Sweet, M. J. Guffey, M. Pelton, and N. F. Scherer, “Three-dimensional optical trapping and manipulation of single silver nanowires,” *Nano Lett.* **12**, 5155 (2012).
- [9] Z. Yan, J. Sweet, J. E. Jureller, M. J. Guffey, M. Pelton, and N. F. Scherer, “Controlling the position and orientation of single silver nanowires on a surface using structured optical fields,” *ACS Nano* **6**, 8144 (2012).
- [10] B. Krässig, E. P. Kanter, S. H. Southworth, L. Young, R. Wehlitz, B. A. deHarak, and N. L. S. Martin, “Dipole-quadrupole interference spectroscopy: the observation of an autoionizing $\text{He } ^1D$ Rydberg series,” *Phys. Rev. A* **86**, 053408 (2012).
- [11] L. Young, “A comb in the extreme ultraviolet,” *Nature* **482**, 45 (2012).
- [12] S. Stoupin, A. M. March, H. Wen, D. A. Walko, Y. Li, E. M. Dufresne, S. A. Stepanov, K.-J. Kim, Yu. V. Shvyd'ko, V. D. Blank, and S. A. Terentyev, “Direct observation of dynamics of thermal expansion using pump-probe high-energy-resolution x-ray diffraction,” *Phys. Rev. B* **86** 054301 (2012).
- [13] W. Becker, X. J. Liu, P. J. Ho, and J. H. Eberly, “Theories of photoelectron correlation in laser-driven multiple atomic ionization,” *Rev. Mod. Phys.* **84**, 1011 (2012).
- [14] B. Adams, M. Borland, L. X. Chen, P. Chupas, N. Dashdorj, G. Doumy, E. Dufresne, S. Durbin, H. Drr, P. Evans, T. Graber, R. Henning, E. P. Kanter, D. Keavney, C. Kurtz, Y. Li, A. M. March, K. Moffat, A. Nassiri, S. H. Southworth, V. Srajer, D. M. Tiede, D. Walko, J. Wang, H. Wen, L. Young, X. Zhang, and A. Zholents, “X-ray capabilities on the picosecond timescale at the Advanced Photon Source,” *Synch. Rad. News* **25**, 6 (2012).
- [15] B. W. Adams, C. Buth, S. M. Cavaletto, J. Evers, Z. Harman, C. H. Keitel, A. Pálffy, A. Picón, R. Röhlberger, Y. Rostovtsev, and K. Tamasaku, “X-ray quantum optics,” *J. Mod. Opt.* **60**, 2 (2013).
- [16] G. Vankó, A. Bordage, P. Glatzel, E. Gallo, M. Rovezzi, W. Gawelda, A. Galler, C. Bressler, G. Doumy, A. M. March, E. P. Kanter, L. Young, S. H. Southworth, S. E. Canton, J. Uhlig, V. Sundström, K. Haldrup, T. Brandt van Driel, M. M. Nielsen, K. S. Kjaer, and H. T. Lemke, “Spin-state studies with XES and RIXS: From static to ultrafast,” *J. Electron. Spectrosc. Relat. Phenom.* **188**, 166 (2013).
- [17] A. Picón, C. Buth, G. Doumy, B. Krässig, L. Young, and S. H. Southworth, “Optical control of resonant Auger processes,” *Phys. Rev. A* **87**, 013432 (2013).
- [18] C. Buth, F. He, J. Ullrich, C. H. Keitel, and K. Z. Hatsagortsyan, “Attosecond pulses at kiloelectronvolt photon energies from high-order harmonic generation with core electrons,” *Phys. Rev. A*, in press (2013).
- [19] R. Reininger, E. M. Dufresne, M. Borland, M. A. Beno, L. Young, K.-J. Kim, and P. G. Evans, “Optical design of the short pulse x-ray imaging and microscopy time-angle correlated diffraction beamline at the Advanced Photon Source,” *Rev. Sci. Instrum.* **84**, 053013 (2013).
- [20] R. Reininger, D. Keavney, M. Borland and L. Young, “Optical design of the Short Pulse Soft X-Ray Spectroscopy beamline at the Advanced Photon Source, *J. Synch. Rad.* **20**, 654 (2013).
- [21] “SPX First Experiments,” Contributors: D. Reis, A. Lindenberg, M. Trigo, M. DeCamp, C. Milne, A. M. March, G. Doumy, M. Borland, D. Keavney, R. Reininger, L. X. Chen, W.-S. Lee, Z. X. Shen, H. Ihee, J. Kim, K. Moffat, V. Srajer, R. Henning. Contacts: L. Young and P. Evans.
- [22] “Preliminary Expected Performance Characteristics of an APS Multi-Bend Achromat Lattice, M. Borland for the APS Upgrade team.
- [23] A. Picón, P. J. Ho, G. Doumy, and S. H. Southworth, “Optically-dressed resonant Auger processes induced by high-intensity x rays,” *New J. Phys.* **15**, 083057 (2013).
- [24] C. Hernández-García, A. Picón, J. San Román, and L. Plaja, “Attosecond extreme ultraviolet vortices from high-order harmonic generation,” *Phys. Rev. Lett.* **111**, 083602 (2013).
- [25] C. Bostedt, J.D. Bozek, P.H. Bucksbaum, R.N. Coffee, J.B. Hastings, Y. Huang, R.W. Lee, S. Schorb, J.N. Corlett, P. Denes, P. Emma, R.W. Falcone, R.W. Schoenlein, G. Doumy, E. Kanter, B. Krässig, S. Southworth, L. Young, L. Fang, M. Hoener, N. Berrah, C. Roedig, L.F. DiMauro, “Ultra-fast and ultra-intense x-ray sciences: first results from the Linac Coherent Light Source free-electron laser,” *J. Phys. B* **46**, 1 (2013).
- [26] T. Osipov, L. Fang, B. Murphy, F. Tarantelli, E. R. Hosler, E. Kukk, J. D. Bozek, C. Bostedt, E. P. Kanter, and N. Berrah, “Sequential multiple ionization and fragmentation of SF_6 induced by an intense free electron laser pulse,” *J. Phys. B* **46**, 164032 (2013).
- [27] Z. Yan, Y. Bao, U. Manna, R. A. Shah, N. F. Scherer, “Enhancing nano particle electrostatics with gold nanoplate mirrors, Supporting Information,” *Nano Lett.* **14**, 2436 (2014).
- [28] L. Young, “Ultraintense X-ray interactions at the Linac Coherent Light Source,” Chapter 15, 529-556. In *Attosecond and XUV Physics*, Editors: Thomas Schultz and Marc Vrakking, Wiley (2014).
- [29] R. Reininger, E. M. Dufresne, M. Borland, M. Beno, L. Young, P. G. Evans, “A short-pulse X-ray beamline for spectroscopy and scattering,” *J. Synchrotron Rad.* **21**, 1194 (2014).

- [30] L. Young, "Understanding ultraintense x-ray interactions with matter," *Advances in Chemical Physics*, Volume 157: Proceedings of the 240 Conference: Science's Great Challenges, First Edition, p. 183, editor: Aaron R. Dinner, in press (2015).
- [31] C. Bressler, W. Gawelda, A. Galler, M. M. Nielsen, V. Sundström, G. Doumy, A. M. March, S. H. Southworth, L. Young, and G. Vankó, "Solvation dynamics monitored by combined X-ray spectroscopies and scattering: photoinduced spin transition in aqueous $[\text{Fe}(\text{bpy})_3]^{2+}$," *Faraday Discuss.*, DOI: 10.1039/c4fd00097h (2014).
- [32] Y. Pushkar, D. Moonshiram, V. Purohit, L. Yan, and I. Alperovich, "Spectroscopic analysis of catalytic water oxidation by $[\text{Ru}^{II}(\text{bpy})(\text{tpy})\text{H}_2\text{O}]^{2+}$ suggests that $\text{Ru}^V=\text{O}$ is not a rate-limiting intermediate," *J. Am. Chem. Soc.* **136**, 11938 (2014).
- [33] P. J. Ho, C. Bostedt, S. Schorb, and L. Young, "Theoretical tracking of resonance-enhanced multiple ionization pathways in XFEL pulses," submitted (2014).
- [34] G. Vankó *et al.*, "Detailed characterization of a nanosecond-lived excited state: X-ray and theoretical investigation of the quintet state in photoexcited $[\text{Fe}(\text{terpy})_2]^{2+}$," in preparation (2014).
- [35] A. M. March *et al.*, "Valence-to-core x-ray emission spectroscopy for tracking chemical dynamics in solutions," in preparation (2014).
- [36] Z. Yan, M. Sajjin, N. F. Scherer, "Tailoring nano particle dynamics with optical phase," in preparation (2014).
- [37] U. Manna, Z. Yan, Y. Bao, J. Jureller, N. F. Scherer, "Meso-scale dipolar interactions in synthetic photonic metal nanoparticle lattices," in preparation (2014).

Other cited references

- [38] S. Schorb, D. Rupp, M. L. Swiggers, R. N. Coffee, M. Messerschmidt, G. Williams, J. D. Bozek, S.-I. Wada, O. Kornilov, T. Möller, and C. Bostedt, "Size-dependent ultrafast ionization dynamics of nanoscale samples in intense femtosecond x-ray free-electron-laser pulses," *Phys. Rev. Lett.* **108**, 233401 (2012).
- [39] S. Plimpton, "Fast parallel algorithms for short-range molecular dynamics," *J. Comp. Phys.* **117**, 1 (1995).
- [40] Z. Jurek, G. Faigel, and M. Tegze, "Dynamics in a cluster under the influence of intense femtosecond hard X-ray pulses," *Eur. Phys. J. D* **29**, 217 (2004).
- [41] L. Young, E. P. Kanter, B. Krässig, Y. Li, A. M. March, S. T. Pratt, R. Santra, S. H. Southworth, N. Rohringer, L. F. DiMauro, G. Doumy, C. A. Roedig, N. Berrah, L. Fang, M. Hoener, P. H. Bucksbaum, J. P. Cryan, S. Ghimire, J. M. Glowina, D. A. Reis, J. D. Bozek, C. Bostedt, and M. Messerschmidt, "Femtosecond electronic response of atoms to ultra-intense x-rays," *Nature* **466**, 56 (2010).
- [42] R. Neutze, R. Wouts, D. van der Spoel, E. Weckert, and J. Hajdu, "Potential for bimolecular imaging with femtosecond x-ray pulses," *Nature* **406**, 752 (2000).
- [43] A. A. Lutman, R. Coffee, Y. Ding, Z. Huang, J. Krzywinski, T. Maxwell, M. Messerschmidt, and H.-D. Nuhn, "Experimental demonstration of femtosecond two-color x-ray free-electron lasers," *Phys. Rev. Lett.* **110**, 134801 (2013).
- [44] S. H. Southworth, E. P. Kanter, B. Krässig, L. Young, G. B. Armen, J. C. Levin, D. L. Ederer, and M. H. Chen, "Double K -shell photoionization of neon," *Phys. Rev. A* **67**, 062712 (2003).
- [45] M. H. Chen, "Auger transition rates and fluorescence yields for the double- K -hole state," *Phys. Rev. A* **44**, 239 (1991).
- [46] Y. Liu, J. Zeng, J. Yuan, "Auger energies, branching ratios, widths and x-ray rates of double K -vacancy states of Ne^{2+} : a close-coupling calculation," *J. Phys. B* **46**, 145002 (2013).
- [47] L. H. Do, T. Hayashi, P. Moenne-Loccoz, and S. J. Lippard, "Carboxylate as the protonation site in (peroxo) diiron(III) model complexes of soluble methane monooxygenase and related diiron proteins," *J. Am. Chem. Soc.* **132**, 1273 (2010).
- [48] H. Kotani, T. Suenobu, Y.-M. Lee, W. Nam, and S. Fukuzumi, "Photocatalytic generation of non-heme oxo-iron(IV) complex with water as an oxygen source," *J. Am. Chem. Soc.* **133**, 3249 (2011).
- [49] Q. J. Lawrence, "The road to non-heme oxoferryls and beyond," *Acc. Chem. Res.* **40**, 493 (2007).
- [50] S. Fukuzumi, T. Kishi, H. Kotani, Y.-M. Lee, and W. Nam, "Highly efficient photocatalytic oxygenation reactions using water as an oxygen source," *Nat. Chem.* **3**, 38 (2010).
- [51] C. Krebs, D. G. Fujimori, C. T. Walsh, and J. M. Bollinger, "Non-heme Fe(IV)-oxo intermediates," *Acc. Chem. Res.* **40**, 484 (2007).

J.R. Macdonald Laboratory Overview

The J.R. Macdonald Laboratory focuses on the interaction of intense laser pulses with matter for the purpose of understanding and even controlling the resulting ultrafast dynamics. The timescales involved range from attoseconds, necessary for studying electronic motion in matter, to femtoseconds and picoseconds for molecular vibration and rotation, respectively. We continue to harness the multi-timescale expertise within the Lab to further our progress in both understanding and control. The synergy afforded by the close interaction of theory and experiment within the Lab serves as a significant multiplier for this effort. To achieve our goals, we are advancing theoretical modeling and computational approaches as well as experimental techniques, for example by taking advantage of our expertise in particle imaging techniques (such as COLTRIMS, VMI, MDI, etc.).

Most of our research projects are associated with one of two themes: “Attosecond Physics” and “Control”. These themes serve as broad outlines only, as the boundary between them is not always well defined. A few examples from each are briefly mentioned below, while further details are provided in the individual abstracts of the PIs: I. Ben-Itzhak, B.D. Esry, V. Kumarappan, C.D. Lin, A. Rudenko, U. Thumm, and C.A. Trallero.

Attosecond physics: Attosecond science is motivated by the idea of observing electronic motion in atoms and molecules on its natural timescale. Light pulses whose duration approaches this timescale are a necessary component of this work, and our ability to produce such pulses has continued to improve. In addition to studies of electronic motion, attosecond-scale pulses can also serve as very precise triggers or probes of the femtosecond-scale nuclear motion in molecules. Moreover, the underlying high-harmonic generation (HHG) mechanism, used to create attosecond pulses, provides essential information about the target and has been the focus of some of our theoretical and experimental studies. Theoretical work from the Lab has shown, for instance, that optimizing the waveform of the driving infrared pulse can improve HHG by orders of magnitude. To that end, we continue to develop an intense light synthesizer. High harmonics from aligned molecules have also been used to experimentally uncover information about the orbitals involved in the process. Our ability to align molecules has also enabled molecular-frame studies of ionization and fragmentation, as well as studies of rotational and electronic wave packets in molecules. Pump-probe measurements using EUV-pump pulses to initiate molecular dynamics in ions have recently been extended to neutral molecules.

Control: Methods for controlling the motion of heavy particles in small molecules continue to be developed. Theoretically, our work has shown that carrier-envelope phase (CEP) effects, two-color control, and the physics of overlapping attosecond pulse trains and infrared pulses all arise from interference between different multiphoton pathways and can be treated with the same analytical framework. To further demonstrate this formulation, we have conducted extensive measurements of the CEP dependence of D^* production in strong-field dissociation of D_2 . We have used techniques such as the Discrete Fourier Transform to extract quantitative information from these measurements, such as the difference in photon number between interfering pathways, which allows us to detect the presence of higher order effects. Work in the Lab has also led to the imaging of structural rearrangement in small polyatomic molecules and a theoretical treatment of nuclear dynamics imaging. Related work on charge migration following inner-shell ionization by

X-rays has been conducted at the LCLS. Significant steps to improve impulsive alignment of symmetric, and even asymmetric, top molecules have also been made in the Lab.

In addition to our laser-related research, we have conducted some studies using our low-energy ECR ion source in collaboration with visiting scientists, specifically the group of S. Lundeen. We also have very productive collaborations in our laser research, such as with E. Wells from Augustana Collage and E. Poliakoff from Louisiana State University.

Like the visitors benefiting from the use of our facilities, we pursue several outside collaborations at other facilities and with other groups (*e.g.*, ALS, Århus, FLASH, University of Frankfurt, University of Jena, LBNL, LCLS, Max-Planck Institutes for Quantum Optics and Kernphysik, Ohio State University, Texas A&M, Tokyo, Weizmann Institute, and others).

On the personnel side, we have hired Dr. Daniel Rolles from FLASH, Germany, as an Assistant Professor to fill the vacancy created in our group by the departure of Matthias Kling. Also, while Itzik Ben-Itzhak was on sabbatical during 2013–2014, Brett Esry served as Interim Director of the Lab with significant help from the Associate Director for Lab Operations, Kevin Carnes.

Finally, it is worth mentioning the ongoing changes in the Lab. Before we took delivery of our DOE-funded PULSAR laser (10–20 kHz, 790 nm, 2 mJ/pulse, ~21 fs FWHM, CEP stable), now in regular operation and producing published results, the university funded renovation of one of our old experimental rooms in anticipation of future laser use. That space is now occupied by a new laser system, funded in large part by an NSF-MRI grant, which has been operating since the spring. This 1 kHz laser system, HITS, features high-power pulses at tunable long wavelengths and can be CEP locked over extended periods of time.

Combining the experimental and theoretical expertise within the Lab with the capabilities becoming available with the new laser facilities continues to produce exciting physics. Some of this physics was on display last November, 2013, when we co-hosted (with ITAMP) an ultrafast dynamics workshop that took place here at the university.

**Structure and Dynamics of Atoms, Ions, Molecules, and Surfaces:
Molecular Dynamics with Ion and Laser Beams**

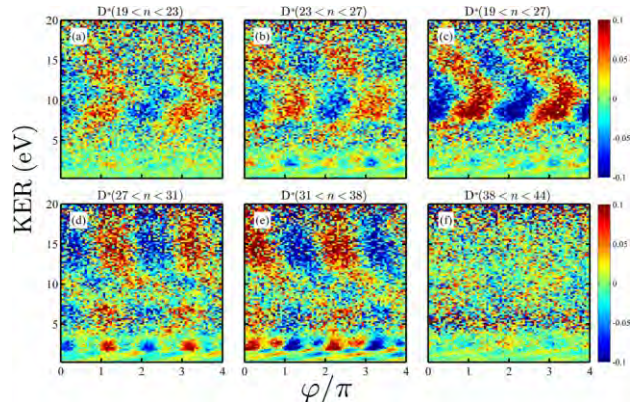
*Itzik Ben-Itzhak, J. R. Macdonald Laboratory, Kansas State University
Manhattan, KS 66506; ibi@phys.ksu.edu*

Scope: *The goal of this part of the JRML program is to study and control molecular dynamics under the influence of ultrashort intense laser pulses or the swift Coulomb field of ions. To this end we typically use molecular ion beams as the subject of our studies and have a close collaboration between theory and experiment.ⁱ Examples of our recent work are given below.*

Carrier-envelope phase (CEP) control over molecular dynamicsⁱⁱ, *Nora G. Kling, M. Zohrabi, B. Berry, Travis Severt, Bethany Jochim, U. Ablikim, Nora G. Kling, K.J. Betsch, K.D. Carnes, S. Zeng, F. Anis, Y. Wang, B.D. Esry, and I. Ben-Itzhak* – The phase between the carrier and the pulse envelope has been used in recent years to control, for example, photoionization (Refs. [1,2] and Pub. 8,19,24) and molecular dissociation (Refs. [3-4] and Pubs. 16,20,28). In the latter case, studies have focused mainly on spatial asymmetries along the laser polarization – a symmetry broken by the CEP, ϕ , in broadband pulses (e.g. Fourier Transform Limited (FTL) pulses approaching single cycle). Taking advantage of technology advancements – CEP-tagging [2,5] of sub 5 fs FTL pulses from our 10 kHz PULSAR laser – we were able to perform first-of-a-kind CEP-dependence measurements on a thin ion-beam target (Ref. [6] and Pub. 20). Specifically, we have measured the CEP dependence of H_2^+ dissociation, a one electron system that can be solved nearly exactly, and state-of-the-art calculations by Esry’s group compare well with the measurements (Pub. 20). Presently, we are exploring the CEP dependence of the branching ratio in HD^+ dissociation, i.e. preference for $H+D^+$ over H^++D , and we plan to extend these studies to more complex systems.

In addition to the work on the benchmark molecular ion, H_2^+ , mentioned above, we explored the CEP dependence of D^* formation upon dissociation of D_2 in intense broadband laser pulses (i.e., a bandwidth sufficient to support a sub 5fs FTL pulse). The production of D^* fragments, i.e. $D(nl)$ with $n \gg 1$, has been attributed to the “frustrated tunneling ionization” mechanism [6], vanishes for circular polarization [6] and decreases rapidly with increasing ellipticity (Pub. 4). The high- and low-kinetic energy release (KER) D^* fragments are associated with D^+ and D fragments, respectively [6]. With its high density of Rydberg states, this process is practically impossible to treat from first principles, making it an excellent test of the general predictions of the photon-phase CEP formalism of Esry’s group since they require no computation. We were able to measure the predicted [7,8] periodic oscillations in total yield and spatial asymmetry, i.e. D^* ejection one way or the other along the laser polarization, and extract meaningful information about the interfering paths responsible for the observed oscillations with CEP (see, Refs. [7,8] and the abstract of B.D. Esry).

Figure 1. The asymmetry of $D(nl)$ -fragment production from D_2 breakup in 5 fs, FTL, 8×10^{14} W/cm², linearly polarized laser pulses. Each panel shows the CEP and KER dependence for a subset of n -states as labeled on the panel (adapted from Mohammad Zohrabi PhD thesis, Kansas State University 2014).

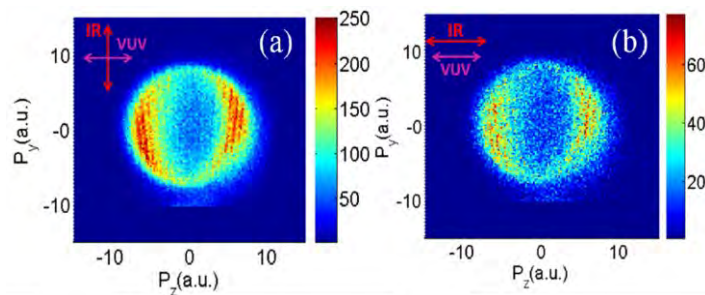


The CEP-dependence of $D(nl)$ fragment production has been measured employing field-ionization techniques for specific small groups of excited Rydberg states. Both asymmetry and total yield dependence on CEP changes from one subset of quantum states to the other, as shown in Fig. 1 for the asymmetry parameter.

VUV-pump – IR-probe studies of D_2 dissociation, *Wei Cao, C. Lewis Cocke, and Itzik Ben-Itzhak* – We have developed a table top VUV light source, which possesses both time resolution (100 fs) and energy resolution (<200 meV), to investigate molecular fragmentation processes. By combining the VUV with a delayed IR pulse, the onset of a previously unobserved dissociative ionization (DI) pathway is demonstrated in D_2 molecules. One uncommon signature of this process is that it does not follow the polarization direction of the strong IR field but rather the weaker VUV, as shown in Fig. 2 (The momentum images were generated by employing the COLTRIMS technique to measure both ions and electrons from the fragmentation process).

The fragmentation mechanism proposed to explain these observations involves excitation of the molecule by the VUV pulse followed by predissociation into two atomic fragments, one of which is in an excited state. The excited atom is later ionized by the synchronized IR-probe pulse. By adjusting the VUV-IR delay, the predissociation yield has been altered allowing the retrieval of the associated lifetime, which was determined to be about one picosecond. This emphasizes the necessity of a short temporal width of the VUV pulse. By varying the VUV photon energy from 16.95 eV to 17.45 eV, the DI process transits from a single dominant pathway to two distinguishable competing pathways. This highlights the significance of the spectral resolution of the VUV pulse for launching different DI mechanisms. This doubly-sensitive dependence of the DI process, namely the delay dependence and photon energy dependence, reveals the significance of compromise between the temporal and energy resolution of the initiator pulse in a photochemical-reaction study. We plan to extend this experimental approach, offering the possibility of time-resolved and channel-resolved studies, to more complex molecules.

Figure 2. Dissociative ionization data of D_2 by 16.95 eV photons as the pump pulse. The D^+ momentum distribution with the IR polarization (a) parallel and (b) perpendicular to the VUV polarization (adapted from Wei Cao PhD thesis, Kansas State University 2014).



Laser induced dissociation of molecular dications beam targets, *Travis Severt, Bethany Jochim, M. Zohrabi, B. Gaire, B. Berry, U. Ablikim, Nora G. Kling, K.J. Betsch, K.D. Carnes, F. Anis, B.D. Esry, and I. Ben-Itzhak* – We have continued our studies of the dissociation of metastable molecular dications introduced into the laser focus as a few keV beam. These molecular ions provide unique opportunities, like a vibrationally cold CO^{2+} beam [10]. We explored the dissociation of NO^{2+} in a strong laser field and have experimental evidence for the important role of transitions driven by the permanent dipole of the molecule, which are supported by calculations guided by Brett Esry. In another example, we observed a “pump-

dump” like process leading to the dissociation of CS^{2+} without absorbing energy from the field. We plan to complete these studies and extend them to other molecular ions of interest.

Future plans: We will continue to probe molecular-ion beams in a strong laser field, specifically exploring challenging two-color, pump-probe and CEP-dependence experiments. We will carry on our studies of more complex systems, including triatomic and simple polyatomic molecules.

References:

1. G.G. Paulus *et al.*, Nature (London) **414**, 182 (2001)
2. N.G. Johnson *et al.*, Phys. Rev. A **83**, 013412 (2011)
3. M.F. Kling *et al.*, Science **312**, 246 (2006)
4. M. Kremer *et al.*, Phys. Rev. Lett. **103**, 213003 (2009)
5. T. Rathje *et al.*, J. Phys. B **45**, 074003 (2012)
6. T. Rathje *et al.*, Phys. Rev. Lett. **111**, 093002 (2013)
7. B. Manschwetus *et al.*, Phys. Rev. Lett. **102**, 113002 (2009)
8. V. Roudnev and B.D. Esry, Phys. Rev. Lett. **99**, 220406 (2007)
9. J.J. Hua and B.D. Esry, J. Phys. B **42**, 085601 (2009)
10. J. McKenna *et al.*, Phys. Rev. A **81**, 061401(R) (2010)

Publications of DOE sponsored research in the last 3 years:

29. “[Thick-lens velocity-map imaging spectrometer with high resolution for high-energy charged particles](#)”, N.G. Kling, D. Paul, A. Gura, G. Laurent, S. De, H. Li, Z. Wang, B. Ahn, C.H. Kim, T.K. Kim, I.V. Litvinyuk, C.L. Cocke, I. Ben-Itzhak, D. Kim, and M.F. Kling, Journal of Instrumentation **9**, P05005 (2014)
28. “[Subfemtosecond steering of hydrocarbon deprotonation through superposition of vibrational modes](#)”, A.S. Alnaser, M. Kübel, R. Siemering, B. Bergues, Nora G. Kling, K.J. Betsch, Y. Deng, J. Schmidt, Z.A. Alahmed, A.M. Azzeer, J. Ullrich, I. Ben-Itzhak, R. Moshhammer, U. Kleineberg, F. Krausz, R. de Vivie-Riedle, and M.F. Kling, Nature Communications **5**, 3800 (2014)
27. “[Multielectron effects in strong-field dissociative ionization of molecules](#)”, X. Gong, M. Kunitski, K.J. Betsch, Q. Song, L.Ph.H. Schmidt, T. Jahnke, Nora G. Kling, O. Herrwerth, B. Bergues, A. Senfleben, J. Ullrich, R. Moshhammer, G.G. Paulus, I. Ben-Itzhak, M. Lezius, M.F. Kling, H. Zeng, R.R. Jones, and J. Wu, Phys. Rev. A **89**, 043429 (2014)
26. “[Hydrogen and fluorine migration in photo-double-ionization of 1,1-difluoroethylene \(1,1-C₂H₂F₂\) near and above threshold](#)”, B. Gaire, I. Bocharova, F.P. Sturm, N. Gehrken, J. Rist, H. Sann, M. Kunitski, J. Williams, M.S. Schöffler, T. Jahnke, B. Berry, M. Zohrabi, M. Keiling, A. Moradmand, A.L. Landers, A. Belkacem, R. Dörner, I. Ben-Itzhak, and Th. Weber, Phys. Rev. A **89**, 043423 (2014)
25. “[Attosecond Control of electron emission from atoms](#)”, G. Laurent, W. Cao, I. Ben-Itzhak, and C.L. Cocke, Journal of Physics: Conference Series **488**, 012008 (2014) – ICPEAC 2013 proceedings – invited talk
24. “[Non-sequential double ionization of Ar: from the single- to the many-cycle regime](#)”, M. Kübel, K.J. Betsch, Nora G. Kling, A.S. Alnaser, J. Schmidt, U. Kleineberg, Y. Deng, I. Ben-Itzhak, G.G. Paulus, T. Pfeifer, J. Ullrich, R. Moshhammer, M.F. Kling, and B. Bergues, New J. Phys. **16**, 033008 (2014)
23. “[Elucidating isotopic effects in intense ultrafast laser-driven D₂H⁺ fragmentation](#)”, A.M. Sayler, J. McKenna, B. Gaire, Nora G. Johnson, K.D. Carnes, B.D. Esry, and I. Ben-Itzhak, J. Phys. B: At. Mol. Opt. Phys. **47**, 031001 (2014) – Fast Track Communication – IOP Select (see also [LabTalk](#))
22. “[Photo-double-ionization of ethylene and acetylene near threshold](#)”, B. Gaire, S.Y. Lee, D. J. Haxton, P.M. Pelz, I. Bocharova, F.P. Sturm, N. Gehrken, M. Honig, M. Pitzer, D. Metz, H-K. Kim, M. Schöffler, R. Dörner, H. Gassert, S. Zeller, J. Voigtsberger, W. Cao, M. Zohrabi, J. Williams, A. Gatton, D. Reedy, C. Nook, Thomas Müller, A.L. Landers, C.L. Cocke, I. Ben-Itzhak, T. Jahnke, A. Belkacem, and Th. Weber, Phys. Rev. A **89**, 013403 (2014) – Editors’ suggestion
21. “[Adaptive strong-field control of chemical dynamics guided by three-dimensional momentum imaging](#)”, E. Wells, C.E. Rallis, M. Zohrabi, R. Siemering, B. Jochim, P.R. Andrews, U. Ablikim, B. Gaire, S. De, K.D. Carnes, B. Bergues, R. de Vivie-Riedle, M.F. Kling, and I. Ben-Itzhak, Nature Communications **4**, 2895 (2013)
20. “[Carrier-envelope phase control over pathway interference in strong-field dissociation of H₂⁺](#)”, Nora G. Kling, K.J. Betsch, M. Zohrabi, S. Zeng, F. Anis, U. Ablikim, Bethany Jochim, Z. Wang, M. Kübel, M.F. Kling, K.D. Carnes, B.D. Esry, and I. Ben-Itzhak, Phys. Rev. Lett. **111**, 163004 (2013)
19. “[Nonsequential double ionization of N₂ in a near-single-cycle laser pulse](#)”, M. Kübel, Nora G. Kling, K.J. Betsch, N. Camus, A. Kaldun, U. Kleineberg, I. Ben-Itzhak, R.R. Jones, G.G. Paulus, T. Pfeifer, J. Ullrich, R. Moshhammer, M.F. Kling, and B. Bergues, Phys. Rev. A **88**, 023418 (2013)
18. “[Attosecond pulse characterization](#)”, G. Laurent, W. Cao, I. Ben-Itzhak, and C.L. Cocke, Opt. Exp. **21**, 16914 (2013)

17. [“Charge asymmetric dissociation of CO⁺ molecular ion beams induced by strong laser fields”](#), Nora G. Kling, J. McKenna, A.M. Sayler, B. Gaire, M. Zohrabi, U. Ablikim, K.D. Carnes, and I. Ben-Itzhak, *Phys. Rev. A* **87**, 013418 (2013)
16. [“Controlled directional ion emission from several fragmentation channels of CO driven by a few-cycle laser field”](#), K.J. Betsch, Nora G. Johnson, B. Bergues, M. Kübel, O. Herrwerth, A. Senfleben, I. Ben-Itzhak, G.G. Paulus, R. Moshhammer, J. Ullrich, M.F. Kling, and R.R. Jones, *Phys. Rev. A* **86**, 063403 (2012)
15. [“Frustrated tunneling ionization during strong-field fragmentation of D₃⁺”](#), J. McKenna, A.M. Sayler, B. Gaire, Nora G. Johnson, B.D. Esry, K.D. Carnes, and I. Ben-Itzhak, *New J. Phys.* **14**, 103029 (2012)
14. [“Quantum control of photodissociation by manipulation of bond softening”](#), Adi Natan, Uri Lev, Vaibhav S. Prabhudesai, Barry D. Bruner, Daniel Strasser, Dirk Schwalm, Itzik Ben-Itzhak, Oded Heber, Daniel Zajfman, and Yaron Silberberg, *Phys. Rev. A* **86**, 043418 (2012)
13. [“Measurements of intense ultrafast laser-driven D₃⁺ dynamics”](#), A.M. Sayler, J. McKenna, B. Gaire, Nora G. Johnson, K.D. Carnes, and I. Ben-Itzhak, *Phys. Rev. A* **86**, 033425 (2012)
12. [“Fragmentation of molecular-ion beams in intense ultrashort laser pulses”](#), Itzik Ben-Itzhak, *Fragmentation Processes - Topics in Atomic and Molecular Physics*, edited by Colm T. Whelan (Cambridge University Press, 2013) p. 72 – *Invited*
11. [“Attosecond control of orbital parity mix interferences and the relative phase of even and odd harmonics in an attosecond pulse train”](#), G. Laurent, W. Cao, H. Li, Z. Wang, I. Ben-Itzhak, and C. L. Cocke, *Phys. Rev. Lett.* **109**, 083001 (2012)
10. [“Study of asymmetric electron emission in two-color ionization of helium \(XUV-IR\)”](#), G. Laurent, W. Cao, I. Ben-Itzhak, and C.L. Cocke, in *Multiphoton Processes and Attosecond Physics* (Proceedings of the 12th International Conference on Multiphoton Processes (ICOMP12) and the 3rd International Conference on Attosecond Physics, edited by K. Yamanouchi and K. Midorikawa, Springer Proceedings in Physics, Vol. **125** (2012) p. 173
9. [“Tracing nuclear-wave-packet dynamics in singly and doubly charged states of N₂ and O₂ with XUV-pump–XUV-probe experiments”](#), M. Magrakvelidze, O. Herrwerth, Y.H. Jiang, A. Rudenko, M. Kurka, L. Foucar, K.U. Kühnel, M. Kübel, Nora G. Johnson, C.D. Schröter, S. Düsterer, R. Treusch, M. Lezius, I. Ben-Itzhak, R. Moshhammer, J. Ullrich, M.F. Kling, and U. Thumm, *Phys. Rev. A* **86**, 013415 (2012)
8. [“Attosecond tracing of correlated electron-emission in nonsequential double ionization”](#), B. Bergues, M. Kübel, N.G. Johnson, B. Fischer, N. Camus, K.J. Betsch, O. Herrwerth, A. Senfleben, A.M. Sayler, T. Rathje, I. Ben-Itzhak, R.R. Jones, G.G. Paulus, F. Krausz, R. Moshhammer, J. Ullrich, and M.F. Kling, *Nature Communications* **3**, 813 (2012)
7. [“Spectral splitting and quantum path study of high-harmonic generation from a semi-infinite gas cell”](#), W. Cao, G. Laurent, Cheng Jin, H. Li, Z. Wang, C.D. Lin, I. Ben-Itzhak, and C.L. Cocke, *J. Phys. B: At. Mol. Opt. Phys.* **45**, 074014 (2012)
6. [“Dynamics of D₃⁺ slow dissociation induced by intense ultrashort laser pulses”](#), B. Gaire, J. McKenna, M. Zohrabi, K.D. Carnes, B.D. Esry, and I. Ben-Itzhak, *Phys. Rev. A* **85**, 023419 (2012)
5. [“Controlling strong-field fragmentation of H₂⁺ by temporal effects with few-cycle laser pulses”](#), J. McKenna, F. Anis, A.M. Sayler, B. Gaire, Nora G. Johnson, E. Parke, K.D. Carnes, B.D. Esry, and I. Ben-Itzhak, *Phys. Rev. A* **85**, 023405 (2012)
4. [“Frustrated tunneling ionization during laser-induced D₂ fragmentation: Detection of excited metastable D^{*} atoms”](#), J. McKenna, S. Zeng, J.J. Hua, A.M. Sayler, M. Zohrabi, Nora G. Johnson, B. Gaire, K.D. Carnes, B.D. Esry, and I. Ben-Itzhak, *Phys. Rev. A* **84**, 043425 (2011)
3. [“Dynamic modification of the fragmentation of autoionizing states of O₂⁺⁺”](#), W. Cao, G. Laurent, S. De, M. Schöffler, T. Jahnke, A.S. Alnaser, I.A. Bocharova, C. Stuck, D. Ray, M.F. Kling, I. Ben-Itzhak, Th. Weber, A.L. Landers, A. Belkacem, R. Dörner, A.E. Orel, T.N. Rescigno, and C.L. Cocke, *Phys. Rev. A* **84**, 053406 (2011)
2. [“Effect of linear chirp on strong field photodissociation of H₂⁺⁺”](#), Vaibhav S. Prabhudesai, Uri Lev, Oded Heber, Daniel Strasser, Dirk Schwalm, Daniel Zajfman, Adi Natan, Barry D. Bruner, Yaron Silberberg, and Itzik Ben-Itzhak, *Journal of Korean Physical Society* **59**, 2890 (2011)
1. [“Following dynamic nuclear wave packets in N₂, O₂ and CO with few-cycle infrared pulses”](#), S. De, M. Magrakvelidze, I.A. Bocharova, D. Ray, W. Cao, I. Znakovskaya, H. Li, Z. Wang, G. Laurent, U. Thumm, M.F. Kling, I.V. Litvinyuk, I. Ben-Itzhak, and C.L. Cocke, *Phys. Rev. A* **84**, 043410 (2011)

ⁱ In addition to the close collaboration with the theory group of *Brett Esry*, some of our studies are done in collaboration with *Lew Cocke*, *Matthias Kling*'s group, *C.W. Fehrenbach*, and others

ⁱⁱ *Z. Wang*, *M. Kübel*, *M.F. Kling* contributed to the *CEP H₂⁺* project

Strong-field dynamics of few-body atomic and molecular systems

B.D. Esry

J. R. Macdonald Laboratory, Kansas State University, Manhattan, KS 66506

esry@phys.ksu.edu

Program Scope

A main component of my program is to quantitatively understand the behavior of simple benchmark systems in ultrashort, intense laser pulses. As we gain this understanding, we will work to transfer it to more complicated systems. The other main component of my program is to develop novel analytical and numerical tools to more efficiently and more generally treat these systems and to provide rigorous, self-consistent pictures within which their non-perturbative dynamics can be understood. The ultimate goal is to uncover the simplest picture that can explain the most—ideally, without heavy computation being necessary.

Few- and many-cycle carrier-envelope phase effects in strong-field fragmentation

Recent progress

One of our ongoing efforts shows that carrier-envelope phase (CEP) effects, two-color control, and the physics of overlapping attosecond pulse trains and infrared pulses are all manifestations of multi-color control and can all be rigorously treated with exactly the same analytical framework [1–3]. In particular, our formulation shows that these effects arise from interference between different multiphoton pathways.

Briefly, this interpretation follows from the observation that the Hamiltonian—and thus the time-dependent wave function—is periodic in the CEP φ . This permits the Fourier decomposition

$$\Psi(t) = \sum_n e^{in\varphi} \psi_n(t) \quad (1)$$

in which n counts the net number of photons in much the same way as in the Floquet representation, leading to the interpretation of ψ_n as the n -photon channel function. Using Eq. (1), the CEP dependence of any observable can be formally evaluated. For instance, the photofragment momentum distribution is

$$\frac{\partial^2 P}{\partial E \partial \theta_k} = \sum_{n,n'} e^{i(n-n')\varphi} \langle \psi_{n'} | \psi_{\mathbf{k}}^{(-)} \rangle \langle \psi_{\mathbf{k}}^{(-)} | \psi_n \rangle. \quad (2)$$

From this equation, the normalized CEP-induced spatial asymmetry,

$$\mathcal{A} = \frac{P_{\text{up}} - P_{\text{down}}}{P_{\text{up}} + P_{\text{down}}},$$

can be evaluated analytically. Defining P_{up} (P_{down}) to be the probability of \mathbf{k} lying in the upper (lower) hemisphere relative to the linearly polarized laser pulse, the numerator and denominator of \mathcal{A} can be simplified to

$$P_{\text{up}} - P_{\text{down}} = 4\text{Re} \sum_{\substack{n \text{ even} \\ n' \text{ odd}}} e^{i(n-n')\varphi} \langle \psi_{n'} | \psi_{\mathbf{k}}^{(-)} \rangle \langle \psi_{\mathbf{k}}^{(-)} | \psi_n \rangle$$

$$P_{\text{up}} + P_{\text{down}} = 4\text{Re} \sum_{\substack{n, n' \text{ even} \\ n, n' \text{ odd}}} e^{i(n-n')\varphi} \langle \psi_{n'} | \psi_{\mathbf{k}}^{(-)} \rangle \langle \psi_{\mathbf{k}}^{(-)} | \psi_n \rangle.$$

While the CEP dependence in \mathcal{A} is now explicit, all of the details of the strong-field dynamics and the target structure are contained in the amplitudes $\langle \psi_{\mathbf{k}}^{(-)} | \psi_n \rangle$. These equations show that \mathcal{A} will have only odd frequencies, that the yield $P_{\text{up}} + P_{\text{down}}$ will have only even frequencies, and that CEP effects in both cases require the overlap of different n -photon peaks $|\langle \psi_{\mathbf{k}}^{(-)} | \psi_n \rangle|^2$ —*i.e.* the interference of different multiphoton pathways.

One motivation for pursuing this general formulation of CEP effects is the inadequacy of the usual picture based on the spatial asymmetry of the electric field (often used to explain, for instance, CEP effects for photoelectrons) for understanding CEP effects in dissociation. Besides correctly predicting many features of CEP-dependent observables for all currently available experiments—including atomic and molecular targets as well as nanoparticles—our formulation provides a prediction not obviously possible with the field picture: CEP effects for a many-cycle laser pulse.

In particular, since the CEP effects above depend on the overlap of the n -photon peaks, our photon-phase representation shows that it is the bandwidth of the laser pulse that is important rather than the pulse length. This follows from the fact that the widths of the n -photon peaks scale with the pulse bandwidth (at least in a lowest-order perturbation theory sense). Consequently, a many-cycle pulse may still show CEP effects so long as it has a bandwidth comparable to the photon energy. Such pulses are necessarily chirped, but one can show that all of the above expressions for the CEP dependence still hold *exactly* in the presence of any higher order contribution to the laser field's phase.

To test this prediction, we solved the time-dependent Schrödinger equation as a function of pulse length, keeping the bandwidth fixed by including the lowest-order chirp. We considered both atomic and molecular systems, verifying the prediction in all

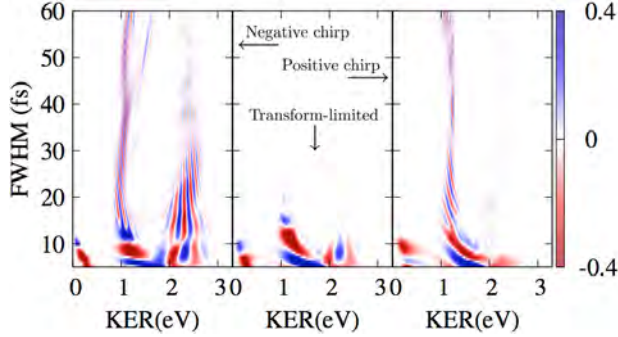


Figure 1: Theoretical calculation of \mathcal{A} for $\text{H}_2^+ + n\omega \rightarrow p + \text{H}$ as a function of pulse length for three different chirping scenarios. The bandwidth was held fixed at 5 fs in all cases. The central wavelength is 800 nm, the intensity is 4×10^{13} W/cm², $\varphi = 0$, and a small cutoff of 10^{-3} was added to the denominator of \mathcal{A} to prevent emphasizing tiny signals.

cases. A typical example for \mathcal{A} is shown in Fig. 1. Note that the maximum of $|\mathcal{A}|$ is only weakly dependent on the pulse length, although its dependence on the energy is sensitive to the chirp [4]. Having gained greater confidence in our prediction, the experimental group of I. Ben-Itzhak took on the challenge of experimentally verifying it. The resulting confirmation is shown in Fig. 2. They show observable asymmetry for pulses nearly 10 cycles long.

In related work, my group provided theoretical support for the first measurements of CEP-induced asymmetry in H_2^+ dissociation [P8,P10]. A long follow-up paper providing greater theoretical analysis is in progress. In particular, we want to understand why the measured asymmetry was larger than predicted. All of the averages needed to compare theory with experiment had already been done, leaving two main possibilities: (i) the greater intensity used in

Rigorous retrieval of photon pathway information from strong-field experiments

Recent Progress

The photon-phase expansion of the wave function in Eq. (1) provides an unambiguous way to define the n -photon contributions—even in a strong field and even for short pulses. This definition applies to the “tunneling” regime just as well as it does to the “multiphoton” regime. In fact, if one has solved the time-dependent Schrödinger equation for several φ , then a Fourier transform will provide the n -photon channel function ψ_n . Figure 3 gives an example for hydrogen in the multiphoton regime, showing that this procedure produces the results one would expect.

Another implication of the photon-phase representation of the observables—Eq. (2), for example—is that they, too, can be Fourier-transformed to retrieve information about the photon channels. In this case,

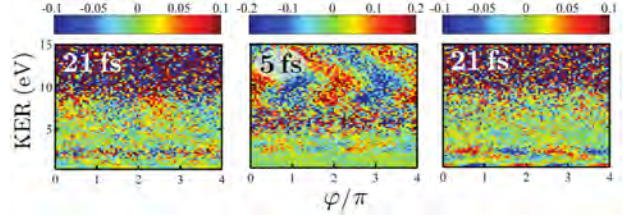


Figure 2: Experimental measurement of the normalized asymmetry for many-cycle laser pulses. D^* fragments resulting from strong-field dissociation of D_2 were measured. The pulses for each panel have a bandwidth corresponding to a 5-fs, transform-limited pulse: left is negatively chirped, middle is transform limited, and right is positively chirped. The pulses were centered at 800 nm with a peak intensity of 1.8×10^{13} W/cm². (From I. Ben-Itzhak’s group.)

the experiment and (ii) the deviation of the experimental pulse from the Gaussian assumed in the calculation. In Pub. [P8], we had already included the experimental power spectrum, but not the spectral phase. Preliminary calculations including the full measured laser pulse suggests that the pre-pulses present in the experiment are playing a role in enhancing \mathcal{A} in ways similar to those we proposed in Pub. [P5]. It may thus turn out that some of the CEP-induced asymmetries that have been presented in the literature owe their magnitude not only to short pulses, but also to substantial pre-pulses.

Future plans

We will continue to apply our photon-phase formulation and explore its implications, especially as a means to make predictions without having to solve the time-dependent Schrödinger equation. We will also work to explicitly incorporate the chirp and other higher order contributions to the laser’s phase into the analytic expressions for observables.

however, it is not ψ_n itself that is retrieved, but rather the sum over all possible paths with a given photon difference, $\Delta n = n - n'$:

$$\frac{\partial^2 P}{\partial E \partial \theta_k} = \sum_{\Delta n} e^{i\Delta n \varphi} \left(\sum_n \langle \psi_n | \psi_{\mathbf{k}}^{(-)} \rangle \langle \psi_{\mathbf{k}}^{(-)} | \psi_{n+\Delta n} \rangle \right).$$

The Fourier transform in φ of a measured spectrum thus provides the quantity in parentheses above. And, although this seems to give only rather gross information about the system, the energy can be used to greatly reduce the number of pathways likely contributing. With this approach, it is thus possible to rigorously extract information from experiments about the photon pathways that interfere to produce a particular CEP effect—even when there are no clear photon peaks.

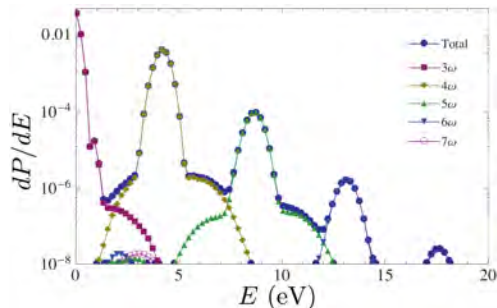


Figure 3: Hydrogen atom ATI spectra of individual photon channels. The laser parameters are $\omega=4.5$ eV, $\tau_{\text{FWHM}}=5$ fs (~ 6 cycles), $I_0=2.0 \times 10^{13}$ W/cm², and $\varphi=0$. The Keldysh parameter is 6.9.

Working with the experimental groups of I. Ben-Itzhak and V. Kumarappan from JRML, we have been able to test these ideas. Figures 4 and 5 show the CEP-dependent spatial asymmetry of D^{*} fragments from strong-field dissociation of D₂ and the CEP-dependent high-harmonic spectrum from NO, respectively. We have derived photon-phase expressions for both observables and can now begin to use them to glean greater physical insight from these results. Note that the Fourier transform in each case is consistent with these expressions and that they show high frequency contributions—a result not easily predicted from the usual electric-field-based picture.

Future Plans

We will pursue this approach further to see what can be learned about the strong-field processes involved. In particular, we would like to get more specific channel information from the experimental ob-

Adiabatic hyperspherical treatment of H₂

Recent Progress

Despite all that we know about calculating molecular properties, the theoretical treatment of molecular ionization remains a challenge—especially within the context of strong-field physics. While the Born-Oppenheimer approximation can, in principle, still be used, there are practical issues in its implementation and its interpretation. In particular, once energies above the lowest ionization threshold are reached, the shape of the molecular potentials generally depend strongly on the boundary conditions used to solve the electronic problem.

To try to address at least some of these problems, we have carried out an adiabatic hyperspherical analysis of H₂. The adiabatic hyperspherical representation produces adiabatic potentials as a function of the hyperradius R (R measures the overall size of the system) [5]. It thus has the advantage of including all possible breakup channels— $\text{H}_2 + n\omega \rightarrow \text{H}(n) + \text{H}(n)$,

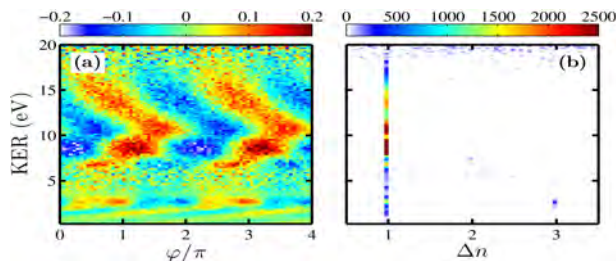


Figure 4: (Left) CEP-dependent normalized spatial asymmetry \mathcal{A} of D^{*} fragments from D₂ dissociation in a 8×10^{13} -W/cm², 5-fs, 800-nm laser pulse. (Right) Fourier transform showing the odd frequencies expected from the photon-phase analysis. (From I. Ben-Itzhak's group.)

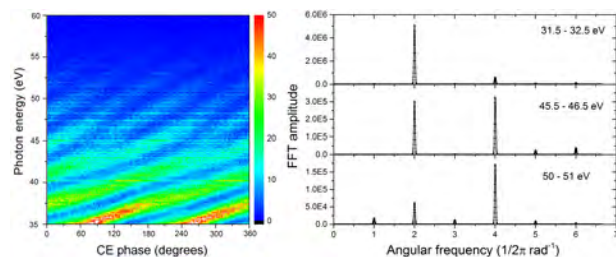


Figure 5: (Left) CEP-dependent high-harmonic spectrum for NO in a 7×10^{14} -W/cm², 6-fs, 800-nm laser pulse. (Right) Fourier transforms of select energy regions showing the even frequencies expected from the photon-phase analysis. (Preliminary results from V. Kumarappan's group.)

servables. It might be possible, for instance, to Fourier transform the CEP-dependence of the full momentum distribution to extract individual amplitudes $\langle \psi_{\mathbf{k}}^{(-)} | \psi_n \rangle$. Other approaches to differentiate the channels will also be pursued.

$\text{H}(n) + p + e^-$, $\text{H}^- + p$, and $\text{H}_2^+ + e^-$ —and treating them on an equal footing. Ionization is thus naturally included as are doubly-excited states.

Since we wanted to explore the value of this representation for molecules, our first study allows only one-dimensional motion of each of the particles. One-dimensional H₂ already has all of the types of channels of interest, and a full, three-dimensional calculation would have unduly diverted our attention from the physics. Figure 6 shows our adiabatic hyperspherical potentials. Note that all of the physics of the system is displayed concisely within this plot. Of course, the potentials are relatively dense, but we have made substantial progress in identifying various families of potential curves.

Future Plans

There is still much to understand about the adiabatic hyperspherical representation for H₂, including whether it is ultimately a useful approach. We be-

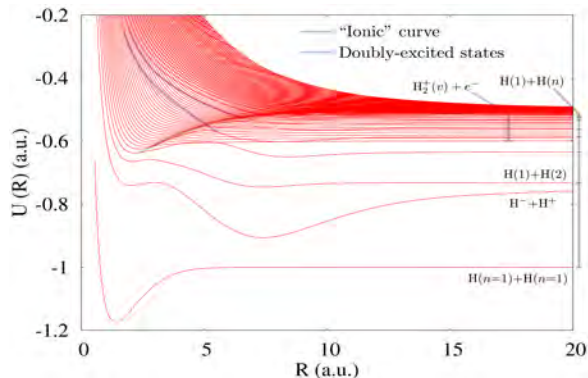


Figure 6: Adiabatic hyperspherical potentials for one-dimensional H_2 in the electron-singlet, nuclear-singlet, even-parity symmetry. The model was designed to exactly reproduce the lowest H_2 and H_2^+ Born-Oppenheimer potentials.

lieve, however, that it will provide useful insights, especially about ionization and the exchange of energy between the nuclei and electrons via their correlated motion.

Publications of DOE-sponsored research in the last 3 years

- [P11] “Elucidating isotopic effects in intense ultrafast laser-driven D_2H^+ fragmentation,” A.M. Sayler, J. McKenna, B. Gaire, N.G. Kling, K.D. Carnes, B.D. Esry, and I. Ben-Itzhak, *J. Phys. B* **47**, 031001(FTC) (2014).
- [P10] “Carrier-envelope phase control over pathway interference in strong-field dissociation of H_2^+ ,” N.G. Kling, K.J. Betsch, M. Zohrabi, S. Zeng, F. Anis, U. Ablikim, B. Jochim, Z. Wang, M. Kübel, M.F. Kling, K.D. Carnes, B.D. Esry, and I. Ben-Itzhak, *Phys. Rev. Lett.* **111**, 163004 (2013).
- [P9] “Electron-nuclear energy sharing in above-threshold multiphoton dissociative ionization of H_2 ,” J. Wu, M. Kumitski, M. Pitzer, F. Trinter, L.Ph.H. Schmidt, T. Jahnke, M. Magrakvelidze, C.B. Madsen, L.B. Madsen, U. Thumm, and R. Dörner, *Phys. Rev. Lett.* **111**, 023002 (2013). Although my name does not appear, C.B. Madsen was a postdoc in my group.
- [P8] “Coherent control at its most fundamental: CEP-dependent electron localization in photodissociation of a H_2^+ molecular ion beam target,” T. Rathje, A. M. Sayler, S. Zeng, P. Wustelt, H. Figger, B.D. Esry, and G.G. Paulus, *Phys. Rev. Lett.* **111**, 093002 (2013).
- [P7] “Frustrated tunnelling ionization during strong-field fragmentation of D_3^+ ,” J. McKenna, A.M. Sayler, B. Gaire, N.G. Kling, B.D. Esry, K.D. Carnes, and I. Ben-Itzhak, *New J. Phys.* **14**, 103029 (2012).
- [P6] “Multiphoton above threshold effects in strong-field fragmentation,” C.B. Madsen, F. Anis, L.B. Madsen, and B.D. Esry, *Phys. Rev. Lett.* **109**, 163003 (2012).
- [P5] “Enhancing the intense field control of molecular fragmentation,” F. Anis and B.D. Esry, *Phys. Rev. Lett.* **109**, 133001 (2012).
- [P4] “Multiphoton dissociation of HeH^+ below the $He^+(1s)+H(1s)$ threshold,” D. Ursrey, F. Anis and B.D. Esry, *Phys. Rev. A* **85**, 023429 (2012).
- [P3] “Dynamics of D_2^+ slow dissociation induced by intense ultrashort laser pulses,” B. Gaire, J. McKenna, M. Zohrabi, K.D. Carnes, B.D. Esry, and I. Ben-Itzhak, *Phys. Rev. A* **85**, 023419 (2012).
- [P2] “Controlling strong-field fragmentation of H_2^+ by temporal effects with few-cycle laser pulses,” J. McKenna, F. Anis, A.M. Sayler, B. Gaire, N.G. Johnson, E. Parke, K.D. Carnes, B.D. Esry, and I. Ben-Itzhak, *Phys. Rev. A* **85**, 023405 (2012).
- [P1] “Frustrated tunneling ionization during laser-induced D_2 fragmentation: detection of excited metastable D^* atoms,” J. McKenna, S. Zeng, J.J. Hua, A.M. Sayler, M. Zohrabi, N.G. Johnson, B. Gaire, K.D. Carnes, B.D. Esry, and I. Ben-Itzhak, *Phys. Rev. A* **84**, 043425 (2011).

References

- [1] V. Roudnev and B. D. Esry, “General theory of carrier-envelope phase effects,” *Phys. Rev. Lett.* **99**, 220406 (2007).
- [2] J. J. Hua and B. D. Esry, “The role of mass in the carrier-envelope phase effect for H_2^+ dissociation,” *J. Phys. B* **42**, 085601 (2009).
- [3] J. V. Hernández and B. D. Esry, “Attosecond pulse trains as multi-color coherent control,” ArXiv:0911.2693.
- [4] E. A. Pronin, A. F. Starace, and L.-Y. Peng, “Perturbation-theory analysis of ionization by a chirped few-cycle attosecond pulse,” *Phys. Rev. A* **84**, 013417 (2011).
- [5] C. H. Greene, “Adiabatic hyperspherical treatment of the H_2^+ molecule,” *Phys. Rev. A* **26**, 2974 (1982).

Ultrafast Processes in Aligned Molecules

Vinod Kumarappan

James R. Macdonald Laboratory, Department of Physics
 Kansas State University, Manhattan, KS 66506
vinod@phys.ksu.edu

Program Scope

The goal of this program is to improve molecular alignment methods, especially for asymmetric top molecules, and to then use well-aligned molecules for further experiments in ultrafast molecular physics. We use multiple pulse sequences for 1D alignment and orientation and for 3D alignment of molecules. The angle-dependent physics we study includes strong-field ionization and fragmentation, high harmonic generation and carrier-envelope-phase-dependent processes in few-cycle laser pulses.

Recent progress

Single-shot f-2f measurements correlated to stereo-ATI CEP meter:

(*X. Ren, A. Vajdi, V. Makhija, and, C. Trallero and V. Kumarappan*)

When the duration of ultrashort pulses approaches a few cycles, the phase difference between the peak of the envelop of the pulse and the peak of the carrier (the carrier-envelope phase or CEP) becomes an important pulse parameter. While stabilizing this phase is essential for generating attosecond pulses, many experiments that study the role of CEP can be performed by determining the phase for each laser shot and then tagging single-shot measurements with the phase. While a stereo-ATI (above-threshold ionization) phase meter [1] has been used for this purpose [2], the phase meter is a relatively large and expensive addition to the actual experiment. We tested whether an f-2f spectrometer operating in single-shot mode with a fast CMOS camera as the detector—a much simpler and cheaper system than the stereo-ATI phase meter—can be used for phase-tagging. Instead of broadening the laser output in sapphire to cover a full octave for the f-2f spectrometer, we directly used the output from the gas-filled capillary that is compressed to produce the few-cycle pulse. The two systems were synchronized and the correlation between the measured phases was characterized. The results are shown in Fig. 1; the relative error between the two measurements is comparable the quality of CEP stabilization typically available with chirped pulse amplified systems. One known source of error is the coupling of pointing instability to the phase measurement in the f-2f. An improved version that solves this problem is under construction. The correlation measurement was done with the 10-kHz-repetition-rate PULSAR laser (only one in every ten shots was characterized), but the f-2f will be used extensively with the 2-kHz KLS and the 1-kHz HITS lasers. Fig. 1 in the contribution from C. Trallero shows the CEP stability of the HITS laser as measured by this spectrometer.

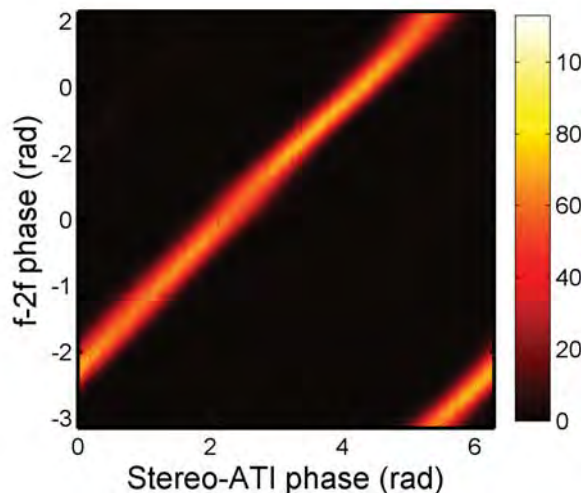


Figure 1: The distribution of synchronized measurements of the CEP using a single-shot f-2f spectrometer and a stereo ATI phase meter. A total of six million laser shots were monitored. The standard deviation of the difference between the two phases was 220 mrad.

Phase-tagged high-order harmonic spectroscopy:

(*A. Vajdi, V. Makhija, and V. Kumarappan*)

By using a high-speed imaging system (CMOS camera viewing a microchannel plate detector with a fast phosphor) to measure the high-order harmonics produced by a \sim two-cycle laser pulse and a stereo-ATI phase meter to synchronously record the CEP of the laser system, we can now measure CEP-tagged HHG spectra. The CEP dependence of HHG in atoms has been studied extensively with CEP-stabilized lasers and is essential for attosecond pulse generation. Figure 2 shows harmonic spectra from argon; measurements from NO are shown in the contribution from Brett Esry in the context of his general theoretical framework for understanding CEP dependent effects. The single-shot f-2f spectrometer described previously was developed after these measurements, but has now been adapted for this purpose. In the context of molecular alignment, we plan to study the effect of CEP on HHG spectra in the vicinity of shape resonances and Cooper minima, and in the presence of multi-orbital contributions.

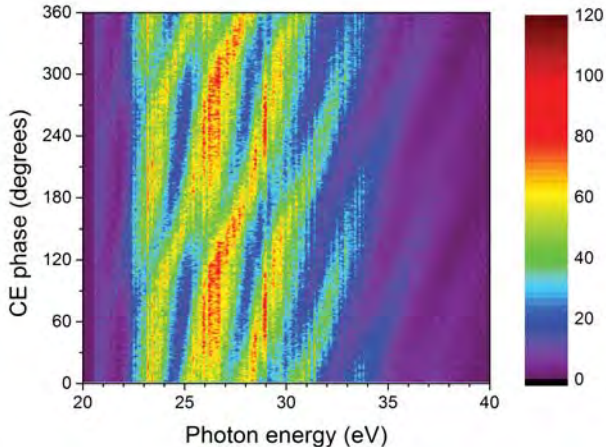


Figure 2: HHG spectrum from argon measured with single-shot phase tagging of few-cycle laser pulses.

Molecular frame measurements using rotational wavepackets:

(*V. Makhija, X. Ren and V. Kumarappan*)

While the alignment of linear molecules has found extensive use in ultrafast molecular physics, the same cannot be said of asymmetric top molecules. The reasons are not only the complex dynamics on laser-driven rotational wave packets in asymmetric tops but also the difficulty in characterizing the molecular axis distribution. In general, one dimensional alignment is not sufficient for molecular frame measurements with asymmetric tops. It is well-understood—but does not seem to be widely appreciated—that even a linearly polarized laser pulse excites rotational motion that involves two Euler angles (the polar angle θ and the body frame azimuthal angle χ) [3]. For a linearly polarized probe pulse, a molecular frame measurement should resolve the dependence on these two angles which determine the direction of the laser polarization in the molecular frame. We have been able to extract this 2D angle dependence of ethylene ionization and fragment yields by choosing a Wigner function basis to write the relevant function and obtaining the values of the coefficients by fitting long and high-resolution scans of the delay-dependent yields of the respective ions. This procedure also provides best-fit values for the pump (alignment) laser parameters as well the rotational temperature of the gas, thus determining the time evolution of the molecular axes and obviating the need for a separate measurement to characterize the degree of alignment.

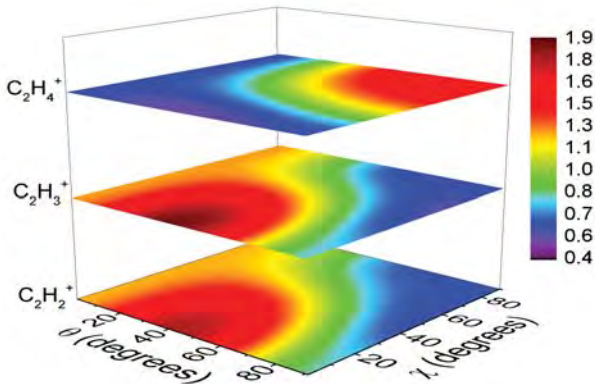


Figure 3: Extracted angle-dependent yields of three ions from ethylene. Ionization from the HOMO leads to the stable molecular ion, while ionization from HOMO-1 and HOMO-2 results in the two fragments.

Figure 3 shows angle-dependent yields of the molecular ion and two fragment ions with one and two hydrogens removed, respectively, by a probe pulse at 2.5×10^{14} W/cm² peak intensity. According to SFA calculations by A.-T. Le, the molecular ion yield is consistent with ionization from the HOMO of the

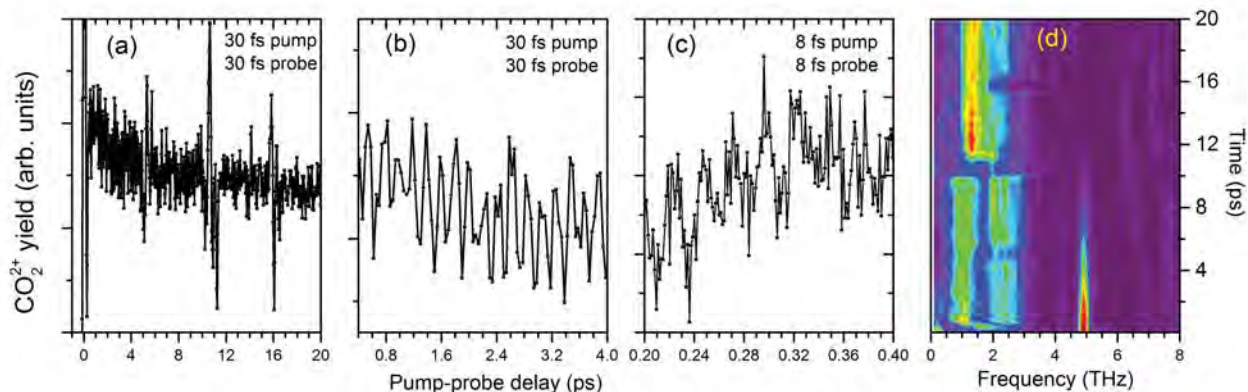


Figure 4: Pump-probe delay-dependent yield of CO_2^+ on three different time scales in two different experiments. (a) Rotational revivals are seen at multiples of 5.5 ps, which is $1/8^{\text{th}}$ of the full rotation period of both CO_2 and CO_2^+ . (b) Detail from (a) showing 200 fs oscillation that correspond to a spin-orbit wave packet in the \tilde{X} state of CO_2^+ . (c) An independent measurement with higher time resolution shows a vibrational wave packet (period 27 fs). This measurement also exhibits the spin-orbit oscillation (not shown). (d) A sliding-window Fourier transform of the data in (a) shows the decay of the spin-orbit coherence in roughly $1/8^{\text{th}}$ of the rotational period.

molecules; the molecular ion is stable in the ground electronic state (\tilde{X}^2B_{3u}) of the cation. The appearance threshold of the two fragment ions is known to be correlated to ionization to the \tilde{A}^2B_{3g} and \tilde{B}^2A_g states. The extracted angle dependence is consistent with the SFA expectation for ionization to these two states. The fragmentation process is known to be slow enough that momentum imaging cannot be used to determine this angle dependence. Neither 3D alignment nor momentum imaging can be used to determine the full angle dependence of ionization to the stable ground electronic state of the molecular ion: the former does not allow independent control of the angle χ and the latter fails because the momentum of stable ion does not carry any information about the orientation of the molecule. Thus, our rotational wave packet technique affords us a unique perspective on molecular processes in asymmetric top molecules.

Multi-scale wavepackets CO_2^+ :

(V. Makhija, A. Rudenko and V. Kumarappan)

In collaboration with Artem Rudenko, we measured the dynamics of rotational and electronic wavepackets in CO_2^+ . A 30-fs pulse was used to singly ionize jet-cooled CO_2 molecules in a velocity map imaging spectrometer. The wavepacket launched in the ionic state was monitored by a subsequent probe pulse which further ionized the CO_2^+ to CO_2^{2+} . The yield of this dication was measured as a function of pump-probe delay and is shown in Fig 4(a). Apart from the fractional rotational revivals (the full rotational period is 44 ps), a ~ 200 fs oscillation is seen for the first ~ 5 ps or so (Fig 4(b)). An earlier measurement by Rudenko *et al.* with 8 fs pulses for both pump and probe also shows a 27 fs oscillation (Fig 4(c)), which is not seen in current measurements because both the pump and the probe pulses are too long. Fourier transformation of the delay-dependent data allows us to identify the main frequencies: the ~ 200 -fs oscillation corresponds to the spin-orbit splitting in the \tilde{X} state, the ~ 27 fs oscillation consists of vibrational motion in the \tilde{B} and \tilde{C} states, and the peaks at the sub-multiples of 44 ps period correspond to rotational motion of the cation. A sliding window Fourier transform of the 30-fs data (Fig 4(d)) shows that the spin-orbit wave packet decays by the first $1/8^{\text{th}}$ revival of the rotation wave packet. This decay is likely to be a consequence of the coupling to rotational motion by a mechanism similar to the one suggested for neutral NO by Kraus *et al.* [4]. These measurements indicate that complex wavepackets are launched in the singly charged molecular ion, but a complete theoretical understanding is lacking at this point.

Molecular alignment for ultrafast electron diffraction:

(J. Yang, V. Makhija, V. Kumarappan and Martin Centurion)

A collaboration with Martin Centurion resulted in a numerical demonstration of a scheme to measure

the 3D structure of trifluorotoluene, an asymmetric top molecule, using gas-phase electron diffraction. We calculated the molecular axis distributions necessary to test the method. These results show that a realistic degree of alignment can be sufficient for structure retrieval.

Outlook and Plans

We believe that extracting angle information from rotational wave packets is a powerful new tool. The measurements shown here can be extended to more complex observables. Preliminary experiments to measure delay-dependent correlation maps for fragment ions, which should reveal the angle dependence of individual channels rather than ions, and photoion and photoelectron momentum distributions have been carried out. If successful, the photoelectron measurements will provide us access to molecular frame photoelectron angular distributions for asymmetric tops.

The single-shot imaging system (at 1 kHz) that was initially developed for VMI spectrometer has now been adapted to HHG measurements and f-2f spectrometers. With the f-2f camera synchronized with the VMI or HHG camera, we can now study CEP-dependent phenomena in multiple observables. Of particular interest are waveform-controlled processes in aligned molecules, including recollision-induced fragmentation and electron localization.

The HITS laser has opened up new options, including strong adiabatic alignment and access to few-cycle pulses at longer wavelengths. This combination will be used for HHG from strongly aligned molecules, including full 3D alignment with using the “hold and spin” method [5]. While the presence of the alignment pulse poses challenges, the degree of alignment in adiabatic fields can be substantially larger than is possible with impulsive techniques.

Publications from DOE-funded research:

- [P1] V. Makhija, X. Ren, V. Kumarappan, “*Metric for three-dimensional alignment of molecules*”, Physical Review A 85, 033425 (2012).
- [P2] X. Ren, V. Makhija, V. Kumarappan, “*Measurement of field-free alignment of jet-cooled molecules by nonresonant femtosecond degenerate four-wave mixing*”, Physical Review A 85, 033405 (2012).
- [P3] X. Ren, V. Makhija, A.-T. Le, J. Troß, S. Mondal, C. Jin, C. Trallero and V. Kumarappan, “*Shape Resonance and Cooper Minimum in High Harmonic Generation from Strongly Aligned Nitrogen*”, In CLEO: 2013, JTh2A.11. San Jose, California: Optical Society of America, 2013.
- [P4] X. Ren, V. Makhija, A.-T. Le, J. Troß, S. Mondal, C. Jin, V. Kumarappan and C. Trallero-Herrero, “*Measuring the angle-dependent photoionization cross section of nitrogen using high-harmonic generation*”, Physical Review A 88, 043421 (2013).
- [P5] X. Ren, V. Makhija, V. Kumarappan, “*Multipulse Three-Dimensional Alignment of Asymmetric Top Molecules*”, Physical Review Letters 112, 173602 (2014).
- [P6] X. Ren, V. Makhija, H. Li, M. F. Kling, V. Kumarappan, “*Alignment-assisted field-free orientation of rotationally cold CO molecules*”, Physical Review A 90, 013419 (2014).
- [P7] J. Yang, V. Makhija, V. Kumarappan, M. Centurion, “*Reconstruction of three-dimensional molecular structure from diffraction of laser-aligned molecules*”, Structural Dynamics 1, 044101 (2014).

References:

- [1] T. Wittmann, B. Horvath, W. Helml, M. G. Schatzel, X. Gu, A. L. Cavalieri, G. G. Paulus and R. Kienberger, Nat. Phys. **5**, 357 (2009).
- [2] N. G. Johnson *et al.* Phys. Rev. A **83**, 013412 (2011).
- [3] E. Peronne, M. D. Poulsen, C. Z. Bisgaard, H. Stapelfeldt and T. Seideman, Phys. Rev. Lett. **91**, 043003 (2003).
- [4] P. M. Kraus, S. B. Zhang, A. Gijsbertsen, R. R. Lucchese, N. Rohringer and H. J. Wörner, Phys. Rev. Lett. **111**, 243005 (2013).
- [5] S. S. Viftrup, V. Kumarappan, S. Trippel, H. Stapelfeldt, E. Hamilton and T. Seideman, Phys. Rev. Lett. **99**, 143602 (2007).

Strong field rescattering physics and attosecond physics

C. D. Lin

J. R. Macdonald Laboratory, Kansas State University
 Manhattan, KS 66506
 e-mail: cdlin@phys.ksu.edu

Program Scope:

We investigate the interaction of ultrafast intense laser pulses, and of attosecond pulses, with atoms and molecules. Most notable accomplishments in the past year are: (1) Waveform synthesis for optimizing high-order harmonic generation; (2) Imaging polyatomic molecules using laser-induced electron diffraction; (3) Wavelength scaling of returning electron wave packets with mid-infrared lasers. (4) Benchmark attosecond pulses characterization. Additional results and plans for the coming year will be summarized.

Introduction

When an atom or molecule is exposed to an intense infrared laser pulse, an electron which was released earlier may be driven back by the laser field to recollide with the parent ion. The recollision of electrons with the ion can be described by the quantitative rescattering theory (QRS) established in 2009 under this program. The QRS theory has been the backbone of our theoretical tools for studying rescattering phenomena in strong field physics. Below are specific progress made in the last year.

1. Waveform synthesis for optimizing high-order harmonic generation

Recent progress

Bright, coherent light sources over a broad electromagnetic spectrum are always in great demand for physical sciences. Today such sources are available only at large synchrotron and free-electron X-ray lasers facilities. Through high-order harmonics generation (HHG), a broadband coherent light can be generated with intense infrared and mid-infrared lasers, but conversion efficiency of HHG is quite small. To enhance HHG yields so far most of the experimental effort is to optimize phase-matching conditions. In this program we study how to optimize HHG yields at the atomic level by manipulating the waveform of the laser pulse through synthesis of two- or three-color fields. Our simulations have shown that enhancement of the HHG yields by two-order of magnitude without increase of laser power. The optimized waveform also enhances HHG from the so-called short-trajectory electrons, thus additional enhancement is achieved after propagation in the gas medium. The first results of this work were published in Nature Communications, see Ref. A3 below.

Our studies have shown that harmonic yields can be significantly enhanced by mixing a small amount of its third harmonic. In subsequent studies we investigated the optimal fundamental wavelength for a given target (neon or helium) to reach a given cutoff energy and maximal harmonic yield. Such results are important in future applications of realizing table-top light sources based on the HHG. This work has been submitted for publication (Ref. B1 below).

Ongoing projects and future plan

A number of laboratories are now perfecting waveform synthesis method for enhancing harmonic generation. Further studies in this area will depend on how stable the phases in the lasers can be controlled. In the meanwhile, we are studying the performance of harmonic generation inside a waveguide. Inside a waveguide, the laser intensity can be maintained nearly constant. Since our synthesized waves also favor harmonics generated via short-trajectory electrons, we found another order of enhancement in the propagated harmonics in a waveguide as compared to generation in a gas

cell. By identifying the optimal pressure in the waveguide, this method allows additional knob to enhance harmonic generation.

Another area that we have been looking at is whether we can selectively enhance harmonics only in a certain energy region. With two- or three-color fields, this requires that the pulses be chirped. At the single-atom level, we have shown that one or two harmonics can be selectively enhanced with great contrast. Further investigations are needed but it may be possible to optimize the generation of a certain range of harmonics by proper maneuver of the whole waveform of a laser pulse. This would remove the need of filters in eliminating undesired harmonics in applications. Clearly tailored waveform optimization for maximal HHG yields would be the most important application of coherent control.

2. Laser-induced electron diffraction from aligned polyatomic molecules

Recent progress

In our earlier study [Xu et al., Phys. Rev. A82, 033403 (2010)] we have established the condition for laser-induced electron diffraction (LIED) for self-imaging interatomic separations of a molecule with mid-infrared lasers. The first proof-of-principle experiment was reported in 2012 [Blaga et al, Nature 483, 194 (2012)] for diatomic molecules. LIED has now been extended to aligned polyatomic molecules. Here we collaborated with the experimental group of Biegert et al in Barcelona. Using 160 kHz, 3.1 μ m laser and COLTRIM, they have been able to generate high-energy photoelectron spectra of acetylene (C₂H₂). By analyzing photoelectron spectra in coincidence with the C₂H₂⁺ fragment channel, we were able to retrieve the C-C and C-H bond lengths that are in good agreement with the known equilibrium distances. This work has been submitted for publication now [Ref. B2]. In addition, in collaboration with Dr. Junliang Xu and DiMauro's group, an alternative procedure for extracting molecular structure has been proposed, by taking advantage of the broadband nature of the returning electron wave packet. This method has the advantage of not relying on the knowledge of orientation/alignment dependence of the tunneling ionization rate of the molecule. This work has been published recently [Ref. A2].

Ongoing projects and future plan

The recent success of LIED from aligned polyatomic molecules motivates us to place greater emphasis in developing better tools for retrieving molecular structures from aligned complex molecules. Since the number of parameters to be retrieved will increase quickly for a complex molecule, a more powerful and direct method is needed. We are in the process of extending established methods used by X-ray and electron diffraction communities to LIED. Since in LIED backscattered electrons are measured while in X-ray and electron diffraction the signals are detected in the forward directions, suitable modifications are needed.

3. Benchmarking methods of attosecond pulses characterization

Recent progress and future plan

Attosecond pulses are now being generated in many laboratories worldwide, but the methods of characterizing such short pulses in the time domain have never been carefully scrutinized. Existing methods for characterizing attosecond pulses all rely on laser-dressed photoionization where photoelectron momentum distribution along the polarization direction is measured vs the time delay between the two pulses. Methods such as FROG-CRAB and PROOF for characterizing attosecond pulses are based on the strong field approximation (SFA) for describing laser-dressed photoionization. It is well-known that SFA fails to describe photoelectron momentum spectra since SFA does not account for atomic structure. An extension of PROOF based on the 2nd-order perturbation theory, called iPROOF [Laurent et al, Opt. Exp. 21, 16914 (2013)] has been proposed. This theory is more accurate in general, but the approximation used in the evaluation of the 2nd-order matrix elements renders the method less reliable as well. In this

project, we aimed at improving iPROOF by evaluating the 2nd order matrix elements accurately. We generated photoelectron spectra by solving time-dependent Schrodinger equation with known attosecond pulses. Following the “ ω - modulation” of the time delay spectra, we retrieve the attosecond pulse to compare with the known input pulse. Our result shows the need of including atomic structure in the PROOF method, but the correction included using the iPROOF is inadequate. Our tests so far have been focused on asec pulses with energies below 100 eV. Extension of the method to asec pulses toward water window region will be pursued in the coming grant period.

4. Wavelength scaling of harmonic generation by mid-infrared lasers

Recent progress

Understanding the wavelength scaling of HHG is very important as harmonics reaching sub- to few-keV region are being generated. Since the cutoff harmonic energy increases as λ^2 , reaching higher photon energy is not difficult with longer wavelength driving lasers. However, how the harmonic yield scales with λ ? While there have been a number of such studies previously, the scaling has been addressed for a given fixed photon energy range, thus leaving out the high-energy part of the harmonic spectrum as the wavelength is increased. In this work, we show that the returning electron wave packet for harmonic generation (in the context of QRS) converges to a universal limit for a laser wavelength above about $3\mu\text{m}$, and the results are consistent among the different methods: numerical solution of the time-dependent Schrodinger equation, the strong field approximation, the quantum orbits theory. Our study also considers contributions of HHG from short vs long trajectory electrons and how they survive the propagation in the medium. No further plan on this project except that we are preparing a tutorial article on this topic for Journal of Physics B: Atomic, Molecular and Optical Physics.

Several other works listed in the publication list are not discussed here.

Publications

A. Published and accepted papers (10 papers from 2012 not listed)

A1. A.T. Le, Hui Wei, Cheng Jin, Vu Ngoc Tuoc, Toru Morishita and C. D. Lin, “Universality of returning electron wave packet in high-order harmonic generation with mid-infrared laser pulses”, Phys. Rev. Lett. 113, 033001 (2014).

A2. Junliang Xu, Cosmin Blaga, K. K. Zhang, Y. H. Lai, C. D. Lin, T. Miller, P. A. Agostini and L. F. DiMauro, “ Diffraction using laser-driver broadband electron wave packets”, Nature. Communications. 5, 5635 (2014).

A3. Cheng Jin , Guoli Wang, Hui Wei, Anh-Thu Le, C. D. Lin , “Waveforms for Optimal sub-keV High-Order Harmonics with Synthesized Two- or Three-Color Laser Fields”, Nature Commun, 5, 4003 (2014).

A4. Wei-Chun Chu, Toru Morishita, and C. D. Lin, “Probing dipole-forbidden autoionizing states by isolated attosecond pulses”, Phys. Rev. A89, 033427 (2014).

A5. Wei-Chun Chu, Toru Morishita and C. D. Lin, ” Probing and controlling autoionization dynamics with attosecond light pulses in a strong dressing laser field”, Chin. J. Phys. 52, 301 (2014).

A6. Qianguang Li, Xiao-Min Tong, Toru Morishita, Hui Wei, and C. D. Lin, “Fine structures in the intensity dependence of excitation and ionization probabilities of hydrogen atom in intense 800 nm laser pulses”, *Phys. Rev. A* 89, 023421 (2014).

A7. A. T. Le, R. R. Lucchese and C. D. Lin, “high harmonic generation from molecular isomers with mid-infrared intense laser pulses”, *Phys. Rev. A* 88, 021402 (2013)

A8. Toru Morishita and C. D. Lin, “Photoelectron spectra and high Rydberg states of lithium generated by intense lasers in the over-the-barrier ionization regime”, *Phys. Rev. A* 87, 063405 (2013).

A9. A.-T. Le, R. R. Lucchese and C. D. Lin, “Quantitative rescattering theory of high-order harmonic generation for polyatomic molecules”, *Phys. Rev. A* 87, 063406 (2013).

A10. C. D. Lin and Wei-Chun Chu, “Controlling atomic line shapes”, *Science*, 340, 694 (2013)

A11. Wei-Chun Chu and C. D. Lin, “Probing and controlling the autoionization dynamics with attosecond light pulses”, in *Progress in Ultrafast Intense Laser science IX*. Ed K. Yamanouchi and K. Midorikawa, Springer 2013.

A12. Wei-Chun Chu and C. D. Lin, “ Absorption and emission of single attosecond light pulses in an autoionizing gaseous medium dressed by a time-delayed control field”, *Phys. Rev. A* 87, 013415 (2013)

A13. M. C. H. Wong, A.-T. Le, A. F. Alharbi, A. E. Boguslavskiy, R. R. Lucchese, J.-P. Brichta, C. D. Lin, and V. R. Bhardwaj, “High harmonic spectroscopy of the Cooper Minimum in Molecules”, *Phys. Rev. Lett.* 110, 033006 (2013)

B. Papers submitted for Publications

B1. Cheng Jin, Guoli Wang, A. T. Le and C. D. Lin, “Route to Optimal Generation of keV High-Order Harmonics with Synthesized Two-Color Laser Fields”, submitted to *Scientific Reports*.

B2. Michael Pullen, Benjamin Wolter, Anh-Thu Le, Matthias Baudisch, Michaël Hemmer, Arne Senftleben, Claus Dieter Schröter, Joachim Ullrich, Robert Moshhammer, C. D. Lin, and Jens Biegert, “ Imaging aligned polyatomic molecules with laser-induced electron diffraction“, Submitted to *Science*.

B3. Xu Wang, Cheng Jin, and C. D. Lin, Coherent control of high harmonic generation using waveform-synthesized chirped laser fields, submitted to *Phys. Rev. A*.

B4. Qianguang Li, Xiao-Min Tong , Toru Morishita , Cheng Jin , Hui Wei , and C. D. Lin, “Rydberg states in strong field ionization of hydrogen by 800, 1200 and 1600 nm lasers”, to be published in *J. Phys. B*.

B5. M. Reduzzi, W.-C. Chu, C. Feng, A. Dubrouil, F. Calegari, F. Frassetto, L. Poletto, M. Nisoli, C.-D. Lin, G. Sansone, “Attosecond control of quantum beating in electronic molecular wave packets”, submitted to *New J. Phys.*

Electronic Rearrangement and Nuclear Dynamics in Inner-Shell and Strong Field Ionization

Artem Rudenko

J. R. Macdonald Laboratory, Department of Physics, Kansas State University, Manhattan, KS 66506

rudenko@phys.ksu.edu

Program scope: The main goals of this research are (i) to understand basic physics of (non-linear) light-matter interactions in a broad span of wavelengths, from terahertz and infrared (IR) to XUV and X-ray domains, and (ii) to apply the knowledge gained for real-time imaging of ultrafast photo-induced reactions. These goals are being pursued using both, lab-based laser and high-harmonic sources, and external free-electron laser facilities.

Recent progress:

1. Imaging charge transfer in molecules upon inner-shell photoabsorption (in collaboration with D. Rolles)

The development of high-intensity, short-pulsed XUV and x-ray radiation sources promises revolutionary new techniques in diverse scientific fields, among others nurturing the vision of dynamic imaging of matter with angstrom spatial and femtosecond (or even sub-femtosecond) temporal resolution. In particular, the start-up of the first hard X-ray free-electron laser (FEL), the Linac Coherent Light Source (LCLS) triggered a variety of imaging experiments on small molecules, clusters, nanocrystals, isolated bio- and nanoparticles or He microdroplets [1-5, P1,11,12]. The basic prerequisite for designing these experiments is understanding the response of individual atoms, and tracing electronic and nuclear dynamics in the vicinity of the atom that absorbed X-ray photon(s), i.e., understanding basic mechanisms of local radiation damage [6,7]. Pursuing this goal, we have recently performed a series of experiments comparing multiphoton multiple ionization of isolated atoms and similar atoms in molecular systems by intense soft X-ray (1.5-2 keV) radiation. In these experiments we found evidences that intermediate resonant excitations are crucial for our understanding of extremely high charge states observed at certain wavelengths [P2,4,16], and observed the signatures of efficient ultrafast charge redistribution from the absorbing atom to its neighbours in molecular systems [P5-7]. As a next step, we applied the technique of coincident ion momentum imaging to study the mechanisms of this charge rearrangement, in particular, electron transfer, in time-resolved pump-probe experiments. An example of such a measurement performed at the LCLS [P13] is illustrated in Fig 1. Here, we used 800 nm fs laser to dissociate the iodomethane molecule (CH_3I), which was subsequently ionized by 1500 eV LCLS pulses at different separations between the iodine atom (ion) and the methyl group. We use channel-selective ion momentum spectroscopy to recalculate the internuclear distance for different fragmentation channels. Since the X-rays are absorbed almost exclusively by

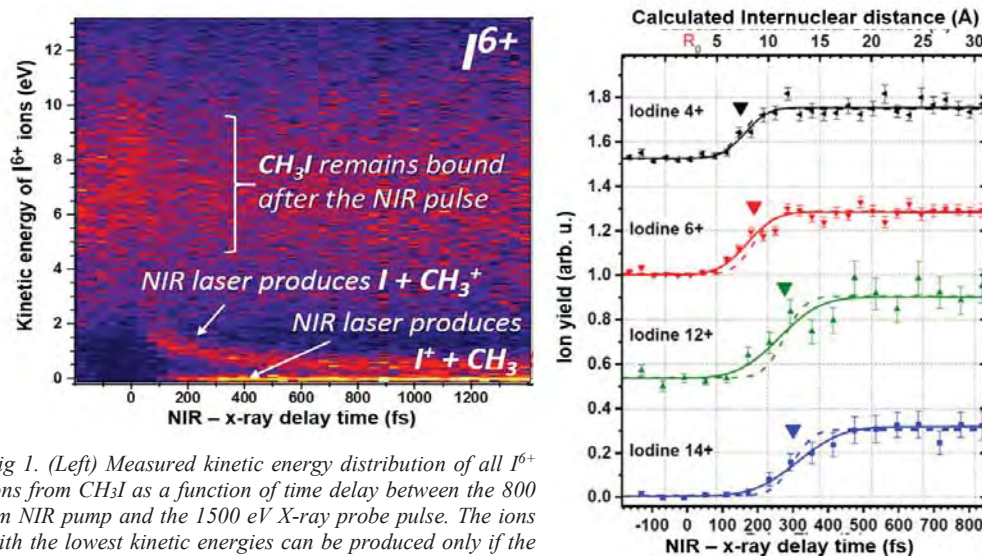


Fig 1. (Left) Measured kinetic energy distribution of all I^{6+} ions from CH_3I as a function of time delay between the 800 nm NIR pump and the 1500 eV X-ray probe pulse. The ions with the lowest kinetic energies can be produced only if the methyl group remains neutral after both pulses. (Right):

Yields of different iodine charge states in this lowest-energy channel as a function of pump-probe delay. The solid lines show fits to the data. The triangles indicate critical distances beyond which the charge transfer is forbidden within the classical over-the-barrier model [8,9]. The dashed lines depict the predictions of this model convolved with the experimental temporal resolution (~ 110 fs). Figure adapted from [P13].

the 3d shell of the iodine fragment, by measuring the charge at the methyl side, we can map the distance-dependent electron transfer probability. We observe signatures of electron transfer for distances up to 20 Å and show that a realistic estimate of its effective spatial range can be obtained from a classical over-the-barrier model developed earlier for ion-atom collisions [8,9]. Recently we applied the same experimental approach to study electronic rearrangement after iodine 4d ionization of I₂ molecules in NIR-XUV [P14] and XUV-XUV [P15] pump-probe experiments at the Free-Electron Laser at Hamburg (FLASH), and showed that the results can be understood within the framework of the same over-the barrier model.

Further developments in this direction include internuclear-distance resolved Auger electron spectroscopy in dissociating molecules at LCLS (first results for CH₃I and CH₃F obtained in L649 experiment are currently being analysed), and lab-based experiments on I 4d shell of iodine-containing molecules with a HHG source. A 10 kHz setup based on the KMLabs eXtreme Ultraviolet Ultrafast Source, which has recently been commissioned at the JRML, covers ~ 40-90 eV photon energy range and opens the way to ion-electron coincidence experiments on charge transfer with considerably improved time resolution. We also plan to use this setup for time-resolved experiments on Interatomic Coulombic Decay following our recent proof-of-principle measurement at FLASH [P8].

2. First AMO experiments with ultra-intense hard X-rays at LCLS (in collaboration with D. Rolles and Argonne National Lab group)

Since XFEL imaging experiments mentioned above ideally require angstrom wavelengths and extreme intensities ($> 10^{20}$ W/cm²) to reach atomic resolution, there is a strong need to extend basic experiments on individual atom / small molecule response and radiation damage mechanisms into this parameter regime. Recently we have accomplished first steps in this direction by studying ionization of rare gas atoms and small polyatomic molecules by ultra-intense X-ray radiation at 5-8 keV photon energy range. The experiments were performed using the nanofocus of the coherent imaging beamline (CXI) at LCLS. Focusing few mJ, 40 fs hard X-ray LCLS pulses to a spot size less than 250 nm in diameter, we were able to reach the intensities exceeding 10^{20} W/cm², unprecedented for this photon energy range. Under these conditions we were able to strip all electrons from argon atoms, all but two 1s electrons from krypton, and reached the record 48+ charge state for xenon ionization at 8.3 keV. Although the highest charge states is reached at the highest photon energy (8.3 keV), the wavelength dependence of the spectra shows significant overall enhancement in the production of charge states from Xe³⁰⁺ to Xe⁴⁰⁺ at the intermediate photon energies (~ 6.5 keV). Comparing the data with the simulation based on the XATOM model of R. Santra's group [10], we conclude that the simple sequential ionization picture [6,10] needs to be modified to include resonant excitations to explain the obtained results, although the effect of the intermediate resonances is not as extreme as in the soft X-ray regime [P2,5,16].

Following the approach we developed earlier for the XUV and the soft-X-ray domains, we compared the ionization of isolated xenon atoms and iodine atoms embedded into molecular systems, and obtained first experimental results on ultrafast charge rearrangement in small and medium-size molecules. In contrast to our results in the soft X-ray regime [P6,7,13], the presence of molecular partners does not significantly reduce the highest charge state observed for high-Z elements in small systems: we observed I⁴⁷⁺ ions from iodomethane (CH₃I) at 8.3 keV (compared to Xe⁴⁸⁺). The most likely reason for this is a limited amount of electrons available from the neighbouring atoms, and very large photon density allowing for further ionization of partially neutralized iodine. However, for larger molecules like iodobenzene (C₆H₅I), the maximum charge state observed is ~ I³⁰⁺, indicating that the charge transfer from the neighbouring atoms still plays an important role if enough electrons are present. Analyses of ion-ion coincident data and kinetic energy distributions for different final states is currently underway for both above-mentioned molecules.

Furthermore, in order to reveal the effect of the spectral shape of the X-ray pulses on X-ray induced multiphoton ionization and fragmentation, we compared the results obtained with the regular LCLS pulses generated by the self-amplified spontaneous emission scheme and with the self-seeded X-ray pulses [11]. We expect the effect of self-seeding to influence ion charge state distributions for atoms and to result in increased Coulomb explosion energies for molecules.

3. Imaging and control of light-induced proton migration in small polyatomic molecules.

This part of the program aims at real time imaging and control of prototypical photo-induced structural rearrangement reactions (isomerization, hydrogen migration, bond formation, H₂ / H₃ elimination etc.). Following up on our proof-of-principle measurements on XUV-induced isomerization in C₂H₂ cation [9,10,P9], we performed first experiments aimed to control the hydrogen migration processes induced by femtosecond laser pulses at JRML. As illustrated in Fig. 2, the pathways of this simplest prototype isomerization reactions in C₂H₂ and C₂H₄ ionic states can be readily modified by simply adjusting the duration / chirp of femtosecond laser pulses. Here, we applied ion-ion coincident momentum spectroscopy to map different Coulomb explosion pathways: symmetric breakup (top) and isomerization channel (bottom). Whereas for the acetylene/vinylidene transformation the evolution of the kinetic energy release (KER) spectra with increasing pulse duration most

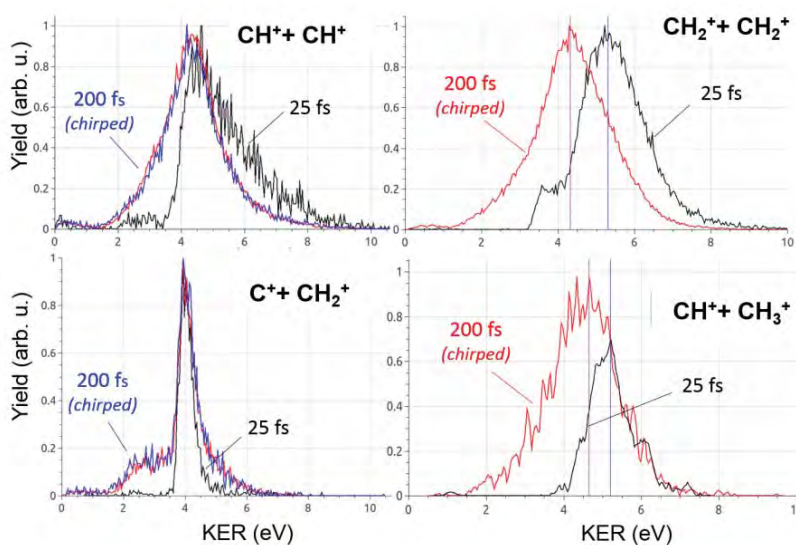


Fig. 2. Kinetic energy release (KER) spectra of symmetric breakup (top) and isomerization (bottom) channels in acetylene (left) and ethylene (right) fragmentation by 800 nm $2 \times 10^{14} \text{ W/cm}^2$ laser pulses with different pulse durations. Whereas the symmetric channel in both molecules yields lower KER fragments for longer pulses reflecting the stretching of the molecular bond within the pulse, the isomerization channel reveals more complicated behavior reflecting the change of the dominant proton migration mechanism.

likely reflects the opening of the isomerization in the intermediate (cationic) state [11] and the field-induced lowering of the isomerization barrier in the doubly charged final state [12] (for high- and low-energy part of the distribution, respectively), the origin of the low-energy shift of the ethylene isomerization KER (which is also accompanied by a factor of 3 increase in the isomerization yield) remains unclear. Next steps for this part of the program will include two-colour pump-probe experiments on hydrogen migration, structural rearrangement and elimination reactions in these and somewhat larger hydrocarbons, and time-resolved imaging of ionization-induced ro-vibrational and electronic wave packets in simple molecules.

References

- [1] M.M. Seibert et al., *Nature* 470, 78 (2011).
- [2] H.N. Chapman et al., *Nature* 470, 73 (2011).
- [3] T. Gorkhover et al., *Phys. Rev. Lett.* 108, 245005 (2012).
- [4] D. Loh et al., *Nature* 486, 513 (2012).
- [5] L. Gomes et al., *Science* 345 906 (2014).
- [6] L. Young et al., *Nature* 466, 56 (2010).
- [7] M. Hoener et al., *Phys. Rev. Lett.* 104, 253002 (2010).
- [8] H. Ryufuku, K. Sasaki, and T. Watanabe, *Phys. Rev. A* 21, 745-750 (1980).
- [9] A. Niehaus, *J. Phys. B: At. Mol. Opt. Phys.* 19, 2925-2937 (1986).
- [11] J. Amann et al., *Nature Photonics* 6 693 (2012).
- [10]. S.K. Son and R. Santra, *Phys. Rev. A* 85 063415 (2012).
- [9] Y. H. Jiang, A. Rudenko, O. Herrwerth et al., *Phys. Rev. Lett.* 105, 263002 (2010).
- [10] J. Ullrich, A. Rudenko and R. Moshhammer, *Annu. Rev. Phys. Chem.* 63, 635 (2012).
- [11] H. Ibrahim et al., *Nature Communications*, 5, 4422 (2014).
- [12] E. Wells et al., *Nature Communications*, 4, 2895 (2013).

Publications from the DOE-funded research (in the last 3 years):

- [P1] "Single-particle structure determination by correlations of snapshot X-ray diffraction patterns", D. Starodub, A. Aquila, S. Bajt, M. Barthelmess, A. Barty, C. Bostedt, J. D. Bozek, N. Coppola, R.B. Doak, S.W. Epp, B. Erk, L. Foucar, L. Gumprecht, C.Y. Hampton, A. Hartmann, R. Hartmann, P. Holl, S. Kassemeyer, N. Kimmel, H. Laksmono, M. Liang, N. D. Loh, L. Lomb, A. V. Martin, K. Nass, C. Reich, D. Rolles, B. Rudek, A. Rudenko, J. Schulz, R. L. Shoeman, R.G. Sierra, H. Soltau, J. Steinbrener, F. Stellato, S. Stern, G. Weidenspointner, M. Frank, J. Ullrich, L. Strüder, I. Schlichting, H. N. Chapman, J.C.H. Spence, M. J. Bogan, *Nature Communications*, 3 1276 (2012).
- [P2] "Ultra-efficient ionization of heavy atoms by intense X-Rays", B. Rudek, S.-K. Son, L. M. Foucar, S. W. Epp, B. Erk, R. Hartmann, M. Adolph, R. Andritschke, A. Aquila, N. Berrah, C. Bostedt, J. Bozek, N. Coppola, F. Filsinger, H. Gorke, T. Gorkhover, H. Graafsma, L. Gumprecht, A. Hartmann, G. Hauser, S. Herrmann, H. Hirsemann, P. Holl, A. Hömke, L. Journel, C. Kaiser, N. Kimmel, F. Krasniqi, K.-U. Kühnel, M. Matysek, M. Messerschmidt, D. Miesner, T. Möller, R. Moshhammer, K. Nagaya, B. Nilsson, G. Potdevin, D. Pietschner, C. Reich, D. Rupp, G. Schaller, I. Schlichting, C. Schmidt, F. Schopper, S. Schorb, C.-D. Schröter, J. Schulz, M. Simon, H. Soltau, L. Strüder, K. Ueda, G. Weidenspointner, R. Santra, J. Ullrich, A. Rudenko, and D. Rolles, *Nature Photonics*, 6 858 (2012).
- [P3] "Tracing nuclear-wave-packet dynamics in singly and doubly charged states of N₂ and O₂ with XUV-pump – XUV-probe experiments", M. Magrakvelidze, O. Herrwerth, Y.H. Jiang, A. Rudenko, M. Kurka, L. Foucar, K.U. Kühnel, M. Kübel, Nora G. Johnson, C.D. Schröter, S. Düsterer, R. Treusch, M. Lezius, I. Ben-Itzhak, R. Moshhammer, J. Ullrich, M.F. Kling, and U. Thumm, *Phys. Rev. A*, 86, 013415 (2012).

- [P4] “Resonance-enhanced multiple ionization of krypton at an x-ray free-electron laser”, B. Rudek, D. Rolles, S.-K. Son, L. Foucar, B. Erk, S.W. Epp, R. Boll, D. Anielski, C. Bostedt, S. Schorb, R. Coffee, J. Bozek, S. Trippel, T. Marchenko, M. Simon, L. Christensen, S. De, S. Wada, K. Ueda, I. Schlichting, R. Santra, J. Ullrich and A. Rudenko, *Phys. Rev. A.*, 87, 023413 (2013).
- [P5] “Strong-field interactions at EUV and X-ray wavelengths”, A. Rudenko, Chapter 15 in “Attosecond and Free-Electron Laser Physics”, T. Schultz and M.J.J. Vrakking, Editors, Wiley (2013).
- [P6] “Ultrafast charge rearrangement and nuclear dynamics upon inner-shell multiple ionization of small polyatomic molecules”, B. Erk, D. Rolles, L. Foucar, B. Rudek, S.W. Epp, M. Cryle, C. Bostedt, S. Schorb, J. Bozek, A. Rouzee, T. Marchenko, M. Simon, F. Filsinger, L. Christensen, S. De, S. Trippel, J. Küpper, H. Stapelfeldt, S. Wada, K. Ueda, M. Swiggers, M. Messerschmidt, C.D. Schröter, R. Moshhammer, I. Schlichting, J. Ullrich and A. Rudenko, *Phys. Rev. Lett.*, 110, 053003 (2013).
- [P7] “Inner-shell multiple ionization of polyatomic molecules with an intense x-ray free-electron laser studied by coincident ion momentum imaging”, B. Erk, D. Rolles, L. Foucar, B. Rudek, S.W. Epp, M. Cryle, C. Bostedt, S. Schorb, J. Bozek, A. Rouzee, A. Hundertmark, T. Marchenko, M. Simon, F. Filsinger, L. Christensen, S. De, S. Trippel, J. Küpper, H. Stapelfeldt, S. Wada, K. Ueda, M. Swiggers, M. Messerschmidt, C. D. Schröter, R. Moshhammer, I. Schlichting, J. Ullrich and A. Rudenko, *J. Phys. B: At. Mol. Opt. Phys.*, 46, 164031 (2013).
- [P8] “Time-Resolved Measurement of Interatomic Coulombic Decay in Ne³⁺”, K. Schnorr, A. Senftleben, M. Kurka, A. Rudenko, L. Foucar, G. Schmid, A. Broska, T. Pfeifer, K. Meyer, D. Anielski, R. Boll, D. Rolles, M. Kübel, M.F. Kling, Y.H. Jiang, S. Mondal, T. Tachibana, K. Ueda, T. Marchenko, M. Simon, G. Brenner, R. Treusch, S. Scheit, V. Averbukh, J. Ullrich, C.D. Schröter, R. Moshhammer, *Phys. Rev. Lett.*, 111, 093402 (2013).
- [P9] “Ultrafast dynamics in acetylene clocked in a femtosecond XUV stopwatch”, Y H Jiang, A. Senftleben, M. Kurka, A. Rudenko, L. Foucar, O. Herrwerth, M. F. Kling, M. Lezius, J. V. Tilborg, A. Belkacem, K. Ueda, D. Rolles, R. Treusch, Y. Z. Zhang, Y. F. Liu, C. D. Schröter, J. Ullrich and R. Moshhammer, *J. Phys. B: At. Mol. Opt. Phys.*, 46 164027 (2013).
- [P10] “Femtosecond photoelectron diffraction on laser-aligned molecules: Towards time-resolved imaging of molecular structure”, R. Boll, D. Anielski, C. Bostedt, J. D. Bozek, L. Christensen, R. Coffee, S. De, P. Decleva, S. W. Epp, B. Erk, L. Foucar, F. Krasniqi, J. Küpper, A. Rouzee, B. Rudek, A. Rudenko, S. Schorb, H. Stapelfeldt, M. Stener, S. Stern, S. Techert, S. Trippel, M.J.J. Vrakking, J. Ullrich and D. Rolles, *Phys. Rev. A.*, 8, 061402(R) (2013).
- [P11] “X-Ray diffraction from isolated and strongly aligned gas-phase molecules with a free-electron laser”, J. Küpper, S. Stern, L. Holmegaard, F. Filsinger, A. Rouzee, D. Rolles, A. Rudenko, P. Johnsson, A. V. Martin, M. Adolph, A. Aquila, S. Bajt, A. Barty, C. Bostedt, J. D. Bozek, C. Caleman, R. Coffee, N. Coppola, T. Delmas, S. Epp, B. Erk, L. Foucar, Tais Gorkhover, L. Gumprecht, A. Hartmann, R. Hartmann, G. Hauser, P. Holl, A. Homke, N. Kimmel, F. Krasniqi, K.-U. Kühnel, J. Maurer, M. Messerschmidt, R. Moshhammer, C. Reich, B. Rudek, R. Santra, I. Schlichting, C. Schmidt, S. Schorb, J. Schulz, H. Soltau, L. Strueder, T. Jan, M. J. J. Vrakking, G. Weidenspointner, T. A. White, C. Wunderer, G. Meijer, J. Ullrich, H. Stapelfeldt and H. N. Chapman, *Phys. Rev. Lett.*, 112, 083002 (2014).
- [P12] “Towards atomic resolution diffractive imaging of isolated molecules with X-ray free-electron lasers”, S. Stern, L. Holmegaard, F. Filsinger, A. Rouzee, A. Rudenko, P. Johnsson, A. V. Martin, A. Barty, C. Bostedt, J. Bozek, R. Coffee, S. Epp, B. Erk, L. Foucar, L. Gumprecht, N. Hartmann, N. Kimmel, K.-U. Kühnel, J. Maurer, M. Messerschmidt, B. Rudek, D. Starodub, J. Thøgersen, G. Weidenspointner, T. A. White, H. Stapelfeldt, D. Rolles, H. N. Chapman and J. Küpper, *Faraday Discussions*, 171, DOI: 10.1039/c4fd00028e (2014).
- [P13] “Imaging charge transfer in iodomethane upon x-ray photoabsorption”, B. Erk, R. Boll, S. Trippel, D. Anielski, L. Foucar, B. Rudek, S.W. Epp, R. Coffee, S. Carron, S. Schorb, K.R. Ferguson, M. Swiggers, J.D. Bozek, M. Simon, T. Marchenko, J. Küpper, I. Schlichting, J. Ullrich, C. Bostedt, D. Rolles, A. Rudenko, *Science* 345, 288 (2014).
- [P14] “Multiple ionization and fragmentation dynamics of molecular iodine studied in IR-XUV pump-probe experiments”, K. Schnorr, A. Senftleben, G. Schmid, A. Rudenko, M. Kurka, K. Meyer, L. Foucar, M. Kübel, M.F. Kling, Y.H. Jiang, S. Düsterer, R. Treusch, C. D. Schröter, J. Ullrich, T. Pfeifer, R. Moshhammer, *Faraday Discussions*, 171, DOI: 10.1039/c4fd00031e (2014).
- [P15] “Electron Rearrangement Dynamics in Dissociating I₂ⁿ⁺ Molecules Accessed by Extreme Ultraviolet Pump-Probe Experiments”, K. Schnorr, A. Senftleben, M. Kurka, A. Rudenko, G. Schmid, T. Pfeifer, K. Meyer, M. Kübel, M.F. Kling, Y.H. Jiang, R. Treusch, S. Düsterer, B. Siemer, M. Wöstmann, H. Zacharias, R. Mitzner, T. J. M. Zouros, J. Ullrich, C. D. Schröter and R. Moshhammer, *Physical Review Letters*, 113, 073001 (2014).
- [P16] “Probing ultrafast electronic and molecular dynamics with free-electron lasers”, L. Fang, T. Osipov, B.F. Murphy, A. Rudenko, D. Rolles, V.S. Petrovic, C. Bostedt, J.D. Bozek, P.H. Bucksbaum, N. Berrah, *J. Phys. B: At. Mol. Opt. Phys.*, 47, 124006 (2014).
- [P17] “Femtosecond x-ray photoelectron diffraction on gas-phase dibromobenzene molecules”; D. Rolles, R. Boll, M. Adolph, A. Aquila, C. Bostedt, J.D. Bozek, H.N. Chapman, R. Coffee, N. Coppola, P. Decleva, T. Delmas, S.W. Epp, B. Erk, F. Filsinger, L. Foucar, L. Gumprecht, A. Hömke, T. Gorkhover, L. Holmegaard, P. Johnsson, C. Kaiser, F. Krasniqi, K.-U. Kühnel, J. Maurer, M. Messerschmidt, R. Moshhammer, W. Quevedo, I. Rajkovic, A. Rouzee, B. Rudek, I. Schlichting, C. Schmidt, S. Schorb, C.D. Schröter, J. Schulz, H. Stapelfeldt, M. Stener, S. Stern, S. Techert, J. Thøgersen, M.J.J. Vrakking, A. Rudenko, J. Kupper, J. Ullrich, *J. Phys. B: At. Mol. Opt. Phys.*, 47, 124035 (2014).
- [P18] “Imaging molecular structure through femtosecond photoelectron diffraction on aligned and oriented gas-phase molecules”, R. Boll, A. Rouzee, M. Adolf, D. Anielski, A. Aquila, S. Bari, C. Bomme, C. Bostedt, J. D. Bozek, H.N. Chapman, L. Christensen, R. Coffee, N. Coppola, S. De, P. Decleva, S. W. Epp, B. Erk, F. Filsinger, L. Foucar, T. Gorkhover, L. Gumprecht, A. Homke, L. Holmegaard, P. Johnsson, J.S. Kienitz, T. Kierspel, F. Krasniqi, K.-U. Kühnel, J. Maurer, M. Messerschmidt, R. Moshhammer, N.L.M. Müller, B. Rudek, E. Saveliev, I. Schlichting, C. Schmidt, F. Scholz, S. Schorb, J. Schulz, J. Seltmann, M. Stener, S. Stern, S. Techert, J. Thøgersen, S. Trippel, J. Viehhaus, M.J.J. Vrakking, H. Stapelfeldt, J. Küpper, J. Ullrich, A. Rudenko, and D. Rolles, *Faraday Discussions*, 171, DOI: 10.1039/c4fd00037d (2014).

Structure and Dynamics of Atoms, Ions, Molecules and Surfaces

Uwe Thumm

J.R. Macdonald Laboratory, Kansas State University, Manhattan, KS 66506, thumm@phys.ksu.edu

A. Laser-assisted XUV double ionization of He

Project scope: To examine - with atomic resolution in time - correlation effects, photoexcitation, and photoemission mechanisms during the single ionization and double ionization (DI) of He atoms exposed to intense short XUV and IR pulses.

Recent progress: We validated our new FE-DVR code for the time-propagated *ab-initio* calculation of single and double excitation and ionization of He by comparing conditional angular distributions (CADs=DI yield for one electron being detected at a fixed angle) for single-XUV-photon DI with published experimental and theoretical data for coplanar emission at equal [1] and non-equal [2] energy sharing (Fig.1).

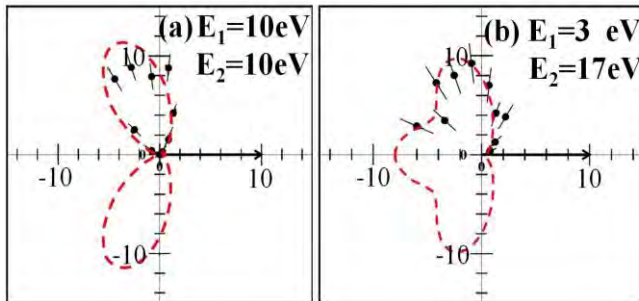


Fig.1: CADs in $\text{beV}^{-1} \text{sr}^{-2}$ for emission of one electron (black arrows) along the linearly polarized electric field of a 99 eV, 10^{14} W/cm^2 , 0.5 fs XUV pulse. E_1 and E_2 are the approximate asymptotic energies of the emitted electrons. The black dots with error bars are experimental results [R1]. The red dashed lines are our calculated results. (a) Equal energy sharing. (b) Unequal energy sharing.

We next calculated CADs and mutual angle distributions (MADs=DI yields as a function of the angle between the emitted electrons), comparing N_{XUV} -photon DI with and without the presence of a short IR pulse (for $N_{\text{XUV}}=1,2,3$) as a function of the energy-sharing $\varepsilon = E_i/(E_1+E_2)$, $i=1,2$, and pulse length τ of the XUV (Fig.2). Our results indicate that the assisting IR pulse promotes side-by-side emission (both electrons are emitted in almost the same direction along the polarization axis of the linearly polarized XUV and IR pulses) and enables back-to-back emission (electrons are emitted in the opposite directions) for equal [1] and a large range of unequal [2] energy sharings ε . We further observed that the assistance of the IR laser field adds characteristic side-bands to and tends to split photoemission peaks in joint energy distributions, joint angular distributions (JADs = DI yield as a function of the two electron's emission angles) and CADs [1,2]. In addition, by analyzing calculated CADs, we found that back-to-back emission is rather robust with regard to changes in ε and τ , while for emission into the same hemisphere DI yields and angular distributions are sensitive to both parameters (insets in Fig.2).

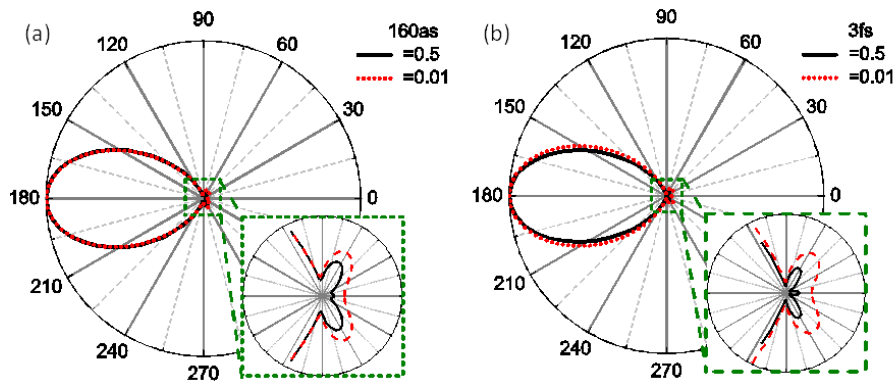


Fig.2: Normalized CADs for two-photon DI of He, where one electron is detected to the right and along the linear polarization of 50 eV, 10^{14} W/cm^2 pulses. Numerical results for equal ($\varepsilon=0.5$) and very unequal ($\varepsilon=0.01$) energy sharing and (a) XUV pulse lengths of $\tau=160 \text{ as}$ and (b) $\tau=3 \text{ fs}$.

Future plans: (i) We intend to extend these studies to variable delays between ultrashort XUV and IR pulses in order to examine the range of operation and to resolve in time DI by various (sequential, non-sequential) emission mechanisms. We further plan to apply our FE-DVR code [1] to (ii) calculate time-resolved IR Stark

shifts for He, for comparison with recent and emerging transient absorption measurements, and (iii) search for ideal laser parameters for the observation, with sub-IR-cycle resolution, of IR level shifts in delay-dependent single and non-sequential double-ionization probabilities. At a later stage, we envision (iv) extending this code to compute, *ab-initio*, the laser-dressed autoionization of He and to compare with results obtained within our technically simple heuristic model for the decay of laser-coupled autoionizing states [3,4].

B. Complementary imaging of the nuclear dynamics in laser-excited diatomic molecular ions in the time and frequency domains

Project scope: To develop conceptual, analytical, and numerical tools to (i) predict the effects of strong IR-laser, XUV, and X-ray fields on the bound and free electronic and nuclear dynamics in small molecules and (ii) image their laser-controlled nuclear and electronic dynamics.

Recent progress: Based on quantum-dynamical simulations, we studied the bound and dissociative nuclear motion of vibrationally excited diatomic molecular ions in the time and frequency domains [5]. While time-domain kinetic-energy-release spectra (KERS) [6-9] display oscillation periods, revival times, and nuclear-probability-density evolutions (Fig. 3a), quantum-beat (QB) imaging (i.e., harmonic analysis of KERS or nuclear probability densities) in the frequency domain [10-12] complements time-domain investigations of the nuclear dynamics by revealing (i) QB frequencies and the nodal structure of vibrational states within a given adiabatic molecular potential curve (Fig. 3b) and (ii) laser-electric-field-dressed molecular potential curves [5,12]. QB frequencies (wave-packet oscillation periods) and revival times are characteristics that indicate which adiabatic states of a photo-excited diatomic molecular ion are transiently. Identifying the corresponding potential curves by the combined analysis of experimentally-measured KERS in the time and frequency domains, in comparison with simulated KERS, thus provides a promising tool for analyzing nuclear dynamics in molecules and for identifying nuclear dissociation (and reaction) pathways [5,10,11].

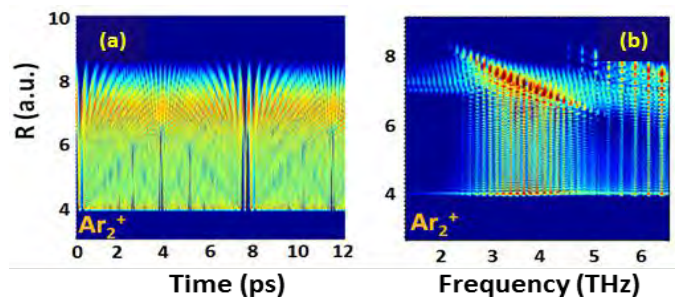


Fig.3: (a) Probability density and (b) corresponding power (or QB) spectrum (logarithmic color scale) for the external-field-free propagation of nuclear vibrational wave packets in the $^2\Sigma_u^+$ adiabatic electronic state of Ar_2^+ .

Due to the weak binding of noble-gas dimer cations and their small number of relevant electronic states, noble-gas dimers are distinct targets for modeling the nuclear dissociation dynamics, allowing for the scrutiny of details such as the (i) existence and importance of transient bond-hardening (BH) states in field-dressed molecular potential curves, (ii) growing influence of fine-structure effects, and (iii) progressive classical character of the nuclear dynamics for noble-gas dimers of increasing molecular mass [6,7] (Fig. 4).

To identify states that are relevant in the dissociation dynamics of (diatomic) molecules, we composed a scheme in which wave-packet propagation calculations are first performed separately for individual adiabatic potential curves, allowing for the selection of relevant adiabatic electronic states by identifying characteristic features (such as revival times, oscillation periods, and quantum-beat frequencies) that the simulated time- and frequency-domain spectra have in common with measured KER spectra [5,10,11]. Next, after selecting the closest matches to the measured spectra, more complex calculations are undertaken, including the dipole coupling of these preselected states in the laser pulses. The QB imaging technique also allows for the direct mapping of adiabatic nuclear potential curves. It furthermore provides the distribution of stationary states that superimpose to form the nuclear (ro-)vibration wave packet that is launched by the molecular ionization in the pump pulse. This technique, in principle, can be used to deduce the internuclear-distance-dependent nuclear wave functions (up to an overall phase) from KER spectra (still awaiting experimental verification) [5,12].

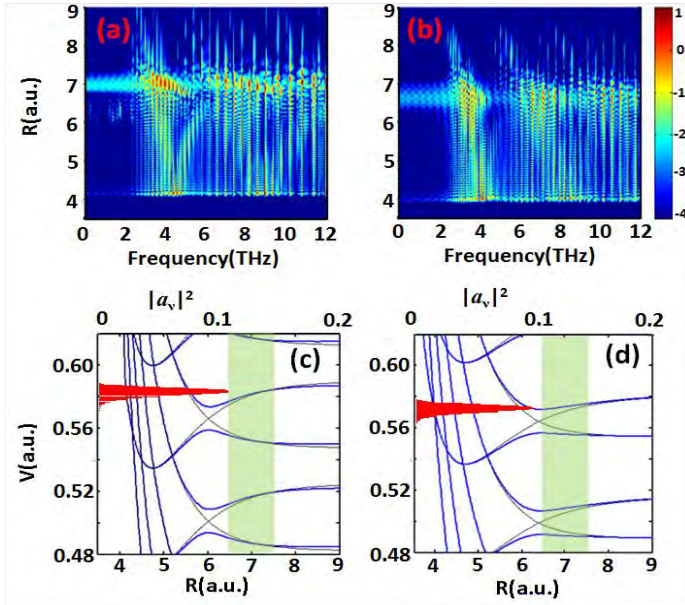


Fig. 4: (a,b) QB spectra (logarithmic color scale) and (c,d) corresponding field-dressed potential curves for Ar_2^+ in 80 fs, 10^{12} W/cm 2 , 1400 nm probe laser pulses, based on dipole-coupled (a) $^2\Sigma_u^+$ and $^2\Sigma_g^+$ potential curves, not including fine-structure splitting, and (b) $I(1/2)_u$ and $II(1/2)_g$ potential curves, including fine-structure splitting. Field-dressed potential curves (thick blue lines) and field-free (c) $^2\Sigma_u^+$ and $^2\Sigma_g^+$ and (d) $I(1/2)_u$ and $II(1/2)_g$ adiabatic potential curves (thin black lines). Green-shaded areas indicate the Franck-Condon (FC) region. Red horizontal lines indicate the FC probabilities $|a_v|^2$ at the corresponding stationary vibrational-state energies. The one-photon BH well is more prominent in the $^2\Sigma_u^+$ and $^2\Sigma_g^+$ than in the $I(1/2)_u$ and $II(1/2)_g$ adiabatic states.

Future plans: We plan to (i) refine the simultaneous analysis of measured and simulated KER spectra in both, time and energy domains in order to better understand the rotational-vibrational nuclear dynamics following the ionization of diatomic molecules by short laser, XUV, and X-ray pulses and to (ii) apply this method to larger molecules with spectrally isolated reaction coordinates (e.g., the $\text{CH}_3\text{-I}$ stretch mode in iodomethane [R2]).

C. Time-resolved photoelectron (PE) spectroscopy

Project scope: To numerically model and understand IR-streaked [13] (and IR side-banded [14]) XUV PE emission and Auger decay in pump-probe experiments with atoms, molecules, and more complex targets.

Recent progress: We calculated and analyzed PE spectra and relative time delays for laser-assisted photoemission by single attosecond XUV pulses from valence-band (VB) and 2p core levels (CLs) of a Mg(0001) surface within a quantum-mechanical model. Comparing the time-dependent dispersion of photoelectron wave packets for VB band CL emission, we found striking differences in their dependence on the electron mean-free path (MFP) in the solid, screening of the streaking laser field, and chirp of the attosecond pulse. The relative photoemission delay between VB and 2p PEs we found to be sensitive to the electron MFP and screening of the streaking laser field inside the solid. Our model [15,16] is able to reproduce measured [R3] streaked PE spectra and photoemission time delays.

Motivated by recent experiments with Mg-covered W(110) surfaces [R4], we calculated, analyzed, and reproduced the dependence of streaked photoemission spectra on the Mg film-thickness D . We found the relative streaking time delay between electrons emitted from the 4f CL band of W(110) and CB of the Mg/W(110) system to depend sensitively on D and on our modeling of the effective potentials at the Mg-W interface [17].

Future plans: We intend to further improve our modeling of (i) photoemission from atoms and molecules and (ii) the transport of photo-released electrons inside complex targets. We will collaborate with experimental groups to explore the feasibility of and ideal parameters for the observation of dielectric response (plasmonic) effects during and after the XUV-pulse-triggered release of PEs from metal surfaces and nanoparticles [13,16].

Publications and manuscripts acknowledging DOE support addressed in this abstract

- [1] *Laser-assisted XUV few-photon double ionization of helium: joint angular distributions*, A. Liu and U. Thumm, Phys. Rev. A **89**, 063423 (2014).
- [2] *Laser-assisted XUV few-photon double ionization of helium: energy-sharing dependence of joint angular distributions*, A. Liu and U. Thumm, Phys. Rev. A, in preparation.
- [3] *Attosecond time-resolved autoionization of argon*, H. Wang, M. Chini, S. Chen, C.-H. Zhang, F. He, Y. Cheng, Y. Wu, U. Thumm, Z. Chang, Phys. Rev. Lett. **105**, 143002 (2010).

- [4] *Attosecond probing of instantaneous AC Stark shifts in helium atoms*, F. He, C. Ruiz, A. Becker, U. Thumm, J. Phys. B **44**, 211001 (fast track comm., 2011).
- [5] *Complementary Imaging of the Nuclear Dynamics in Laser-Excited Diatomic Molecular Ions in the Time and Frequency Domains*, M. Magrakvelidze, A. Kramer, K. Bartschat, U. Thumm, J. Phys. B **47**, 124003 (2014), see also LabTalk contribution <http://iopscience.iop.org/0953-4075/labtalk-article/57443>.
- [6] *Steering the nuclear motion in singly ionized argon dimers with mutually detuned laser pulses*, J. Wu, M. Magrakvelidze, A. Vredenberg, L. Ph. H. Schmidt, T. Jahnke, A. Czasch, R. Dörner, U. Thumm, Phys. Rev. Lett. **110**, 033005 (2013).
- [7] *Dissociation dynamics of noble-gas dimers in intense two-color IR laser fields*, M. Magrakvelidze and U. Thumm, Phys. Rev. A **88**, 013413 (2013).
- [8] *Tracing nuclear wave packet dynamics in singly and doubly charge states of N_2 and O_2 with XUV pump – XUV probe experiments*, M. Magrakvelidze, O. Herrwerth, Y.H. Jiang, A. Rudenko, M. Kurka, L. Foucar, K.U. Kühnel, M. Kübel, N. G. Johnson, C.D. Schröter, S. Düsterer, R. Treusch, M. Lezius, C.L. Cocke, I. Ben-Itzhak, R. Moshhammer, J. Ullrich, M. F. Kling, U. Thumm, Phys. Rev. A **86**, 013415 (2012).
- [9] *Laser-controlled vibrational heating and cooling of oriented H_2^+ molecules*, T. Niederhausen, U. Thumm, F. Martin, J. Phys. B **45**, 105602 (2012).
- [10] *Dissociation dynamics of diatomic molecules in intense laser fields: a scheme for selecting relevant molecular potential curves*, M. Magrakvelidze, C. Aikens, U. Thumm, Phys. Rev. A **86**, 023402 (2012).
- [11] *Following dynamic nuclear wave packets in N_2 , O_2 and CO with few-cycle infrared pulses*, S. De, M. Magrakvelidze, I. Bocharova, D. Ray, W. Cao, I. Znakovskaya, H. Li, Z. Wang, G. Laurent, U. Thumm, M. F. Kling, I. V. Litvinyuk, I. Ben-Itzhak, C. L. Cocke, Phys. Rev. A **84**, 043410 (2011).
- [12] *Time-series analysis of vibrational nuclear wave packet dynamics in D_2^+* , U. Thumm, T. Niederhausen, B. Feuerstein, Phys. Rev. A **77**, 063401 (2008).
- [13] *Attosecond Physics: attosecond streaking spectroscopy of atoms and solids*, U. Thumm, Q. Liao, E. M. Bothschafter, F. Süßmann, M. F. Kling, R. Kienberger, Handbook of Photonics (Wiley), in print.
- [14] *Laser-assisted photoemission from adsorbate-covered metal surfaces: time-resolved core-hole relaxation dynamics from sideband profiles*, C.-H. Zhang and U. Thumm, Phys. Rev. A **80**, 032902 (2009).
- [15] *Attosecond time-resolved photoelectron dispersion and photoemission time delays*, Q. Liao and U. Thumm, Phys. Rev. Lett. **112**, 023602 (2014).
- [16] *Initial-state, mean-free-path, and skin-depth dependence of attosecond time-resolved IR-streaked XUV photoemission from single-crystal magnesium*, Q. Liao and U. Thumm, Phys. Rev. A **89**, 033849 (2014).
- [17] *Film-thickness dependent attosecond time-resolved photoemission from adsorbate-covered surfaces*, Q. Liao and U. Thumm, Phys. Rev. Lett., in preparation.

Other recent publications and manuscripts acknowledging DOE support (2012-14)

- *Attosecond science – What will it take to observe processes in real time*, S. R. Leone, C. W. McCurdy, J. Burgdörfer, L. Cederbaum, Z. Chang, N. Dudovich, J. Feist, C. Greene, M. Ivanov, R. Kienberger, U. Keller, M. Kling, Z.-H. Loh, T. Pfeifer, A. Pfeiffer, R. Santra, K. Schafer, A. Stolow, U. Thumm, M. Vrakking, Nature Photonics **8**, 162 (2014).
- *Understanding the role of phase in chemical bond breaking with coincidence angular streaking*, J. Wu, M. Magrakvelidze, L. Ph. H. Schmidt, M. Kunitski, T. Pfeifer, M. Schöffler, M. Pitzer, M. Richter, S. Voss, H. Sann, H. Kim, J. Lower, T. Jahnke, A. Czasch, U. Thumm, R. Dörner, Nat. Commun. **4**, 2177 (July 2013).
- *Electron-nuclear energy sharing in above-threshold multiphoton dissociative ionization of H_2* , J. Wu, M. Kunitski, M. Pitzer, F. Trinter, L. Ph. H. Schmidt, T. Jahnke, M. Magrakvelidze, C. B. Madsen, L. B. Madsen, U. Thumm, R. Dörner, Phys. Rev. Lett. **111**, 023002 (2013).
- *H formation by electron capture in collision of H with an Al(100) surface*, B. Obreshkov and U. Thumm, Phys. Rev. A **87**, 022903 (2013).
- *Attosecond time-resolved photoelectron spectroscopy of surfaces*, Uwe Thumm and Chang-hua Zhang, invited paper, Light at extreme intensities (Szeged, HU 2011), AIP Conf. Proc **1462**, 57 (2012).

References: [R1] H. Bräuning *et al.*, J. Phys. B **31**, 5149 (1998). [R2] B. Erk *et al.*, Science **345**, 288 (2014). [R3] S. Neppl *et al.*, Phys. Rev. Lett. **109**, 087401 (2012). [R4] S. Neppl *et al.*, to be published.

Strong-Field Time-Dependent Spectroscopy

Carlos A. Trallero

J. R. Macdonald Laboratory, Kansas State University, Manhattan, KS 66506
trallero@phys.ksu.edu

Scope

The main scope of my research is to measure time dependent molecular structure with ultrafast time resolution. As a complement of this goal I'm developing novel ultrafast optical sources.

1 Optics development

1.1 HITS: A Terawatt class CEP stable laser system

The newly acquired high intensity tunable source (HITS) laser started installation at the JRML in April 2014. In August 2014 the laser met or surpassed all required specifications which are,

- 20 mJ of energy per pulse,
- 1KHz repetition rate,
- 25 fs pulse duration (FWHM of the intensity),
- noise on the intensity of the third harmonic less than 1% over one hour,
- CEP RMS noise less than 220 mrad over an hour and 320 mrad over 14 hours, measured as single shot.

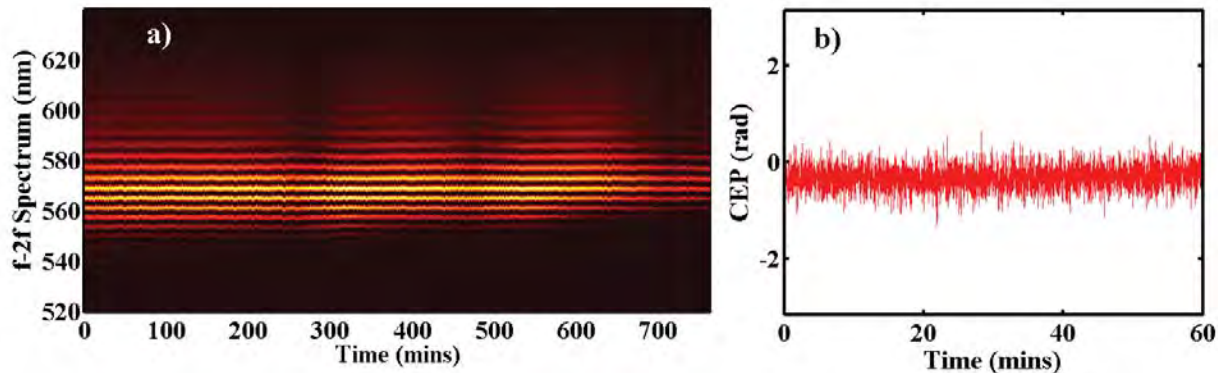


Figure 1: a) Single shot f-2f spectra measuring the CEP after the second stage amplification of HITS. RMS deviations in the CEP over the 750 minutes is 320 mrad. b) Single shot phase calculated from the first 60 minutes of the spectrum in a). RMS deviation of the CEP is 220 mrad over this hour.

The laser was purchased from KMLabs through an NSF-MRI grant in 2011. It is to date one of the highest energy-per-pulse CEP stable systems worldwide. Figure 1 a) shows single shot spectra after an f-2f interferometer used to measure the CEP. The length of the scan is over 750 minutes! The system could stay CEP locked longer, it was artificially stopped once this scan was over. The CEP is calculated from the spectrum shown in Fig. 1 a) by calculating a fast Fourier transform and retrieving the phase of the first frequency component for each point. The phase, calculated as a function of time in this manner is shown in Fig. 1 b) for an interval of 1 hour of the first 100 minutes in a). The CEP RMS deviation for the entire 750 minutes is 320 mrad, CEP RMS deviation for the 60 min subset is of 220 mrad. Again both measurements are single shot. We need to point out that the environment for this scans was not controlled. Parts of the CEP development was done jointly between KMLabs and the JRML.

The laser is used to pump a high energy, white-light-seeded high energy optical parametric amplifier (HE-OPA) with 18 mJ of the 20 mJ available from HITS, producing a maximum of 6 mJ of energy in the

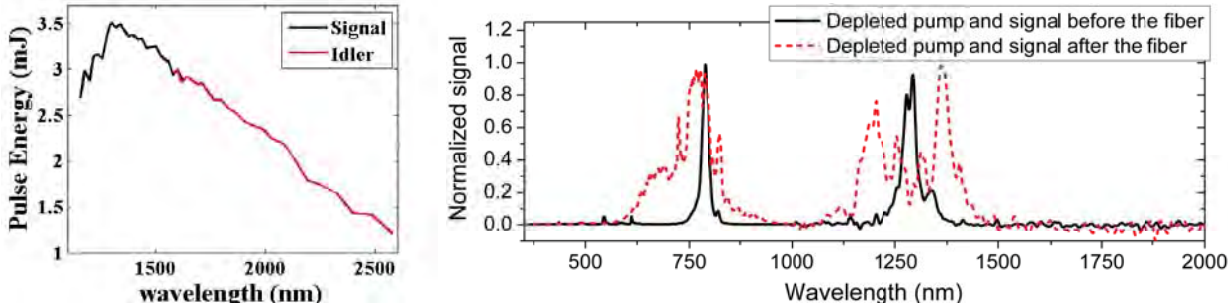


Figure 2: a) Energy per pulse in the signal (black) and idler (red) out of the HE-OPA as a function of wavelength. The maximum total energy is 6 mJ (signal + idler), b) Simultaneous broadening of the signal and depleted pump after SPM. Pulse durations, as measured by a SHG-FROG are 6.5 fs for the depleted pump and 15 fs for the signal (1300 nm).

signal plus idler. The energy per pulse of the signal and idler out of the HE-OPA measured as a function of wavelength is shown in Fig. 2. It should be noted that even at the extremes of the of tuning curve (1100 nm for the signal and 2550 nm for the idler) the energy per pulse is still in excess of 1 mJ at 1KHz repetition rate. Thus this HE-OPA is perfectly suited for strong field physics experiments in a wide range of wavelengths.

1.2 Steps towards an intense light synthesizer

We are interested in developing synthesized light fields with intensities high enough to drive multiphoton processes in atoms and molecules. Our approach starts with the HE-OPA and it’s capability of generating intense pulses in a broad range of wavelengths. The next step is to broaden all the main frequency components (signal, idler and 800 nm pump) using self phase modulation (SPM). Because the HE-OPA is white-light-seeded and pumped with a CEP stable source, the phase between all pulses is preserved.

We have succeeded in generating a continuous spectra from 320 nm to 2500 nm by broadening each component independently, reaching a total energy of 2.3 mJ. To improve the stability of the synthesized pulses and also the overall efficiency of the system we try to use the depleted pump (DP) emerging from the HE-OPA. Such beam is usually discarded because of the low-quality spatial profile. However, we recently demonstrated that the DP can be used simultaneously with the signal to generate few cycle pulses. SPM is done by propagating both beams through a 1 m hollow core fiber and Fig. 2 b) shows the spectrum after broadening. After the fiber both beams are separated with a dichroic mirror. Pulse durations are measured using a second harmonic generation frequency resolved optical gating (SHG-FROG) yielding durations of 6.5 fs for the DP and 15 fs for the signal. The additional advantage of using the DP for synthesis is that it has the same optical path as the signal and idler and there is no need to use additional delay lines.

2 Phase matching and multiorbital contributions to HHG.

in collaboration with A.-T Le, V. Kumarappan, R. Lucchese and E. Poliakkoff

In this area we continue making advances on using higher order harmonic generation (HHG) as a spectroscopic tool to extract the photoionization dipole moment in molecular systems.

2.1 SF₆

We now have complimentary theoretical simulations on the generation of harmonics from SF₆. These simulations show that the observed harmonics in SF₆ are generated from different orbitals. In particular, the theoretically calculated HHG yield from the HOMO ($1t_{1g}$) of SF₆, exhibits a peak centered on H23 (36 eV). This behavior is attributed to the strong shape resonance present in the $1t_{1g}$ photoionization cross section. Symmetry resolved analysis shows that the resonance has a t_{2u} nature and enhances the HHG spectra near H23. This observation is in qualitative agreement with features of the experimental HHG yield, in which a peak is noted in the energy region of H21 to H29, but is centered on H23 at optimal phase matching conditions. The impact of the resonance is made clearer by comparing the long trajectory data to the short trajectory data. The resonant enhancement in the harmonic envelope is present in the spectra containing

long trajectories and missing or significantly diminished in the spectra limited to short trajectories. The resonance behaves as a "trapping" of the electron after it has returned to the ion. Shape resonant trapping has an associated lifetime related to the Heisenberg uncertainty principle. Shape resonances typically have an energetic width between 2 and 5 eV, which translates into a typical lifetime of 65 to 165 as. The period of the laser, by contrast, is approximately 2.5 fs. The duration of the short trajectory is less than the half cycle of the laser pulse which prevents a population buildup. In contrast, long trajectories are temporally longer than the half cycle of the laser pulse, allowing a rapid population buildup in the energy region of a resonance.

In conclusion, we observe a set of maxima and minima in SF6 that are very stable to macroscopic conditions. Because these structures are resilient to a wide variety of intensities and macroscopic conditions, we have established that they are a result of the dipole moment in the recombination step. By comparing our position and intensity dependent data for Ar with existing cross section data we were able to determine an ideal set of experimental conditions for spectroscopic studies of SF6 using HHG. For both Ar and SF6 we observe large blue detuning when comparing HHG spectra to experimental or theoretical cross sections. However, the HHG spectra for Ar reported here matches very closely experimentally measured ionization cross sections

2.2 N_2

We perform an angle dependent measurement of the harmonic yield at the time of the full revival in the time dependent non-adiabatic alignment trace of N_2 . This correspond to a peak in the HHG signal at 17.04 ps. At this time, molecules are preferentially aligned parallel to the harmonic generating field when the pump polarization is parallel to the probe beam. We choose this time delay as a fixed delay and change the angle between the pump pulses and the probe pulse. In doing so, we acquire an angle dependent harmonic yield.

To understand the angular and time dependent harmonic structure, we compare the photoionization cross section (PICS) of the HOMO, HOMO-1 to the harmonic yield as a function of angle in Fig. 3. In the figure, PICS for HOMO and HOMO-1 are represented in dotted and dashed line respectively, while the harmonic yield is in solid. For low order harmonics we expect to observe a maximum in the harmonic yield and PICS at 0° . The harmonics shown here have a minimum at 0° because of the Cooper minimum in the PICS at these energies. The Cooper minimum has a maximum at an angle $\sim 45^\circ$ but this minimum doesn't explain however the local maximum in H35 to H41 at 90° . To explain the angular distribution of H39 and H41 we need to take a closer look at the PICS of HOMO-1 at energies corresponding to H35-H41. These cross sections show that the HOMO-1 has a maximum at 90° relative to the molecular axis that matches relatively well the measured harmonics. The harmonic yield at 0° won't go to zero because the measured harmonics are generated from a superposition of both the HOMO and HOMO-1 states and our current measurement doesn't provide access to the relative contributions from these states.

We should point out that while previous measurements show strong evidence of the HOMO-1 contribution when using only perpendicular pump and probe in the delay scans, we can see a clear contribution in our angle scans with parallel polarizations. Additionally, it has been proposed that HOMO-1 contributions are observed only in the cutoff harmonics at high intensities, we used relatively low peak intensities of 190 TW/cm^2 . Instead, we have strong evidence that selectivity from HOMO and HOMO-1 contributions can be controlled almost purely by selecting a proper phase matching condition.

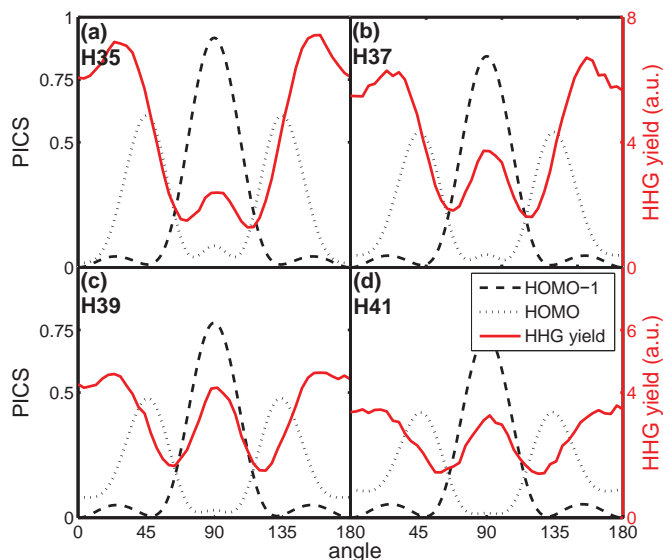


Figure 3: A comparison between the experimental angle scans at the full revival of 17.04ps and theoretical calculations of the photoionization cross sections of HOMO and HOMO-1. The cross section is normalized to 1, while the experimental data is normalized to the isotropic harmonic yield.

3 Interferometric studies with higher order harmonic generation

in collaboration with V. Kumarappan

One of the main benefits of using HHG as a spectroscopic tool is the possibility of providing heterodyne measurements. Therefore, one of our goals is to extract, not only the absolute value of the photoionization dipole moment but also its phase. We make use of an interferometric setup to extract the phase of different harmonics relative to a reference. In particular, we attempt to extract the phase of each harmonic as a function of molecular alignment angle relative to an unaligned sample. Experimentally, we generate harmonics from two sources that are close to each other but without overlap. The experimental setup is shown in Fig. 4. Harmonics emerging from each focus position interfere in the far field (the detector plane) creating an interference pattern similar to the one shown in the figure. We then rotate the molecular alignment angle by changing the polarization of the pump beam in S2 and record the interference pattern as a function of angle. Afterwards, we perform a Fourier transform of the interference pattern for each harmonic. The phase of the first Fourier component is the relative phase between harmonic emerging from S1 and S2.

As a check we first performed measurements in N₂. In this case, the delay between the pump and probe in S2 was 8.2 ps, the delay at which we reach maximum alignment. Our observation shows a fairly good agreement between our measured phase and the alignment-averaged theoretically calculated phase.

We also performed several scans around the first J-type revival in C₂H₄, corresponding to a delay between pump and probe of 7 to 12 ps. The absolute harmonic yield (harmonics 9, 11 and 15) is shown in Fig. 5 a), measured when only source S2 is present. We then allow S1 to propagate and generate the harmonic-dependent interference pattern. From the interference pattern we extract the harmonic and angle dependent relative phase. The results are shown in Fig. 5 b) as a function of delay.

We are currently working on improving our experimental setup and comparing it to theoretical calculations.

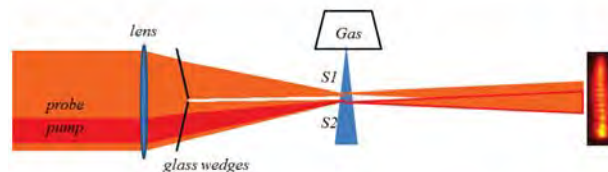


Figure 4: Interferometric HHG setup. S1 is a source of unaligned harmonics while S2 is source of harmonics that are aligned. Harmonics emerging from S1 and S2 overlap in the far field creating an interference pattern.

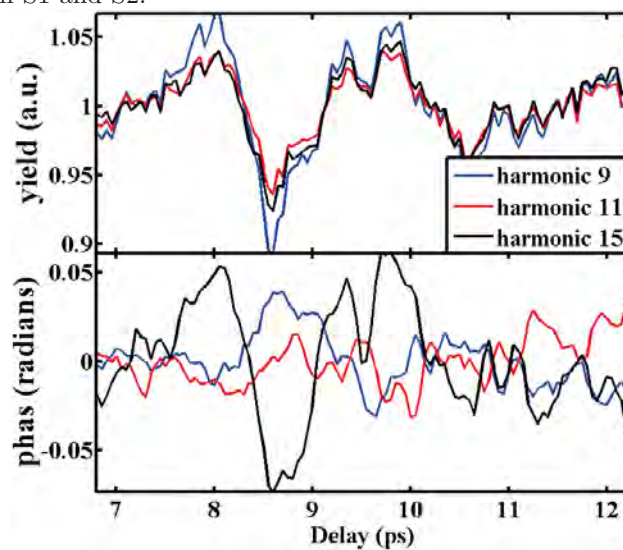


Figure 5: a) Yield of harmonics 9, 11 and 15 as a function of delay for C₂H₄. b) Relative phase between the aligned and unaligned ensembles for the same harmonics. Delay values are between 7 and 12 ps, centering around the J-type revival.

DOE Supported Publications

- Ren, X., Makhija, V., Le, A.-T., Tro, J., Mondal, S., Jin, C., Trallero-Herrero, C., Measuring the angle-dependent photoionization cross section of nitrogen using high-harmonic generation. *Physical Review A*, **88**, 043421, (2013).
- Summers, A., Ramm, A., Kling, M. F., Flanders, B. N., and Trallero-Herrero, C. A., Optical damage threshold of single-crystalline gold nanowires with ultrafast pulses. *Optics Express*, **22**, 4235 (2014).
- Wilson, D., Ren, X., Trallero-Herrero, C., Simultaneous broadening of the depleted pump and signal from an optical parametric amplifier. *CLEO: 2014, STh4E.5*, (2014).

Atomic, Molecular and Optical Sciences at LBNL

Ali Belkacem, Daniel J. Haxton, Clyde W. McCurdy, Thomas N. Rescigno, Daniel Slaughter and Thorsten Weber

Chemical Sciences Division, Lawrence Berkeley National Laboratory, Berkeley, CA 94720
Email: abelkacem@lbl.gov, djhaxton@lbl.gov, cwmcurdy@lbl.gov, tnrescigno@lbl.gov,
dsslaughter@lbl.gov, tweber@lbl.gov

Objective and Scope

The AMOS program at LBNL is aimed at understanding the structure and dynamics of atoms and molecules using photons and electrons as probes. The experimental and theoretical efforts are strongly linked and are designed to work together to break new ground and provide basic knowledge that is central to the programmatic goals of the Department of Energy as formulated in the “*Grand Challenges*”. The current emphasis of the program is in three major areas with important connections and overlap: inner-shell photo-ionization and multiple-ionization of atoms and small molecules; low-energy electron impact and dissociative electron attachment of molecules; and time-resolved studies of atomic processes using a combination of femtosecond x-rays and femtosecond laser pulses. This latter part of the program is folded in the overall research program in the Ultrafast X-ray Science Laboratory (UXSL).

The experimental component at the Advanced Light Source makes use of the Cold Target Recoil Ion Momentum Spectrometer (COLTRIMS) to advance the description of the final states and mechanisms of the production of these final states in collisions among photons, electrons and molecules. Parallel to this experimental effort, the theory component of the program focuses on the development of new methods for solving multiple photo-ionization of atoms and molecules. This dual approach is key to break new ground and provide a new understanding how electronic energy channels into nuclear motion and chemical energy in polyatomic molecules as well as unravel unambiguously electron correlation effects in multi-electron processes.

Inner-Shell Photoionization and Dissociative Electron Attachment to Small Molecules

Ali Belkacem, Daniel Slaughter, and Thorsten Weber

Chemical Sciences Division, Lawrence Berkeley National Laboratory, Berkeley, CA 94720

Email: abelkacem@lbl.gov, dsslaught@lbl.gov, tweber@lbl.gov

Objective and Scope: This experimental subtask is focused on studying photon and electron impact ionization, excitation and dissociation of small molecules and atoms. The first part of this project deals with the interaction of X-rays with atoms and simple molecules by seeking new insight into atomic and molecular dynamics and electron correlation effects. The second part of this project deals with the interaction of low-energy electrons with small molecules with particular emphasis on Dissociative Electron Attachment (DEA). Both studies are strongly linked to our AMO theoretical studies by C.W. McCurdy, D. Haxton and T.N. Rescigno. Both experimental studies (photon and electron impact) make use of the powerful COLd Target Ion Momentum Spectroscopy (COLTRIMS) method to achieve a high level of completeness in the measurements.

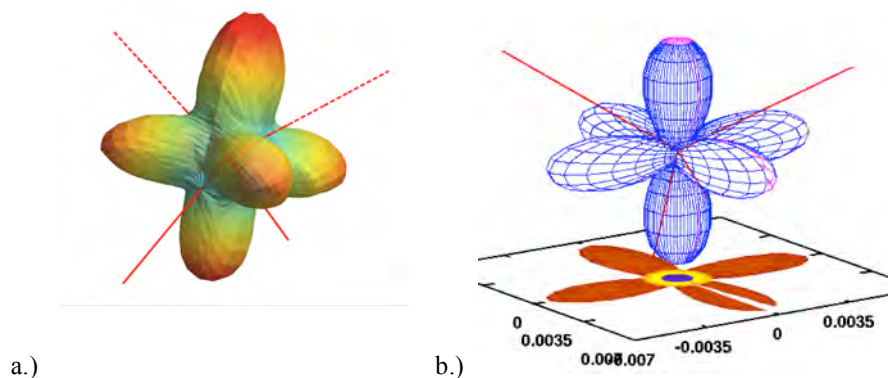
Inter Coulombic decay (ICD) and dissociation of small dimers.

Applying our COLTRIMS scheme at the ALS to nitrogen and carbon monoxide dimers we could experimentally verify for the first time how energy between molecules can be transferred (10x) more efficiently (resonantly) on an atomic level and ultrafast time scale in a theoretically predicted so called Resonant Auger ICD (RA-ICD). In this scheme an incoming photon resonantly excites one core nitrogen (or carbon monoxide) molecule locally in a molecular (N_2)₂ (or (CO)₂) dimer. A subsequent spectator Auger decay takes place, i.e. an innershell electron fills the vacancy and emits an Auger electron while the left behind molecular ion in the small cluster is still in an excited state. When this excited state decays it exchanges a virtual photon with the neighboring molecule that has enough energy to ionize the neutral end of the dimer after which the dimer falls apart which represents the terminal ICD step. The process was identified and isolated using electron-ion energy correlation maps and angle correlation patterns of the Auger electron with respect to the dimer axis. This also showed that the ICD between the dimer constituents happened faster than the dissociation (<20fs) of one end of the dimer, the latter process likely leaving the neighboring molecule unharmed. On the other hand, resonant-Auger ICD (RA-ICD) could be used to induce selected atoms in a cancerous environment to emit electrons with tunable energies to specifically target and break certain molecules. This explains how destructive localized excitation and ionization can multiply in a molecular compound (and cells in the long run) after irradiation with monochromatic X-rays. This work was published in Nature.

Structural imaging and anti-imaging of molecular bonds

Imaging molecular structure is a critical challenge in chemical physics because the ability to visualize real-time changes in future pump-probe experiments has the potential to ultimately film chemical reactions on their natural time scales. In a joint collaboration with C.W. McCurdy, C.S. Trevisan, and T.N. Rescigno we recently performed experimental measurements and theoretical calculations for the photoionization of CH₄ at the carbon K-edge. The measurements performed with our COLTRIMS method at the ALS combined with the complex Kohn variational calculations of the photoelectron in the molecular frame demonstrated the surprising result that the low energy photoelectrons (~4eV) effectively image the molecular tetrahedral structure by emerging along the bond axes. In these experiments we were able for the first time to create 3d-molecular frame photoelectron angular distributions (3d-MFPADs). In this scheme the K-shell

ionization is followed by a subsequent single or even double Auger decay which results in two or sometimes three fragment ions necessary to deduce the molecular orientation in three dimensions at the time of photo ionization. The triple and quadruple coincidences between the photo electron and the recoiling ions were analyzed to extract and distinguish the breakup channels in PhotoIon-PhotoIon COincidence spectra (PIPICO and TriPICO in case of the double Auger decay) and to generate momentum correlation plots which ultimately were transformed into 3d-MFPADs for selected regions of the KER. But do electron angular distributions always follow the shape of the molecule? We extended our scheme to a more complex molecule but with the same geometry, i.e. tetrafluoromethane (CF_4). In this molecule the hydrogen bonds are replaced by the strongest bindings in organic chemistry. The theoretical prediction and modeling of the K-shell ionization of CF_4 near threshold hinted towards the opposite trend, i.e. an emission of electrons perpendicular to the fluorine bonds due to their polar covalent nature which essentially attracts the majority of electrons to the very electronegative fluorine atoms resulting in partial charges. In this ongoing project we were able to prove the “anti-imaging” effect, i.e. we probed the local electron density at the fluorine atoms and found the photo electrons ($\sim 4\text{eV}$) to be emitted perpendicular to the fluorine bonds (see figure).



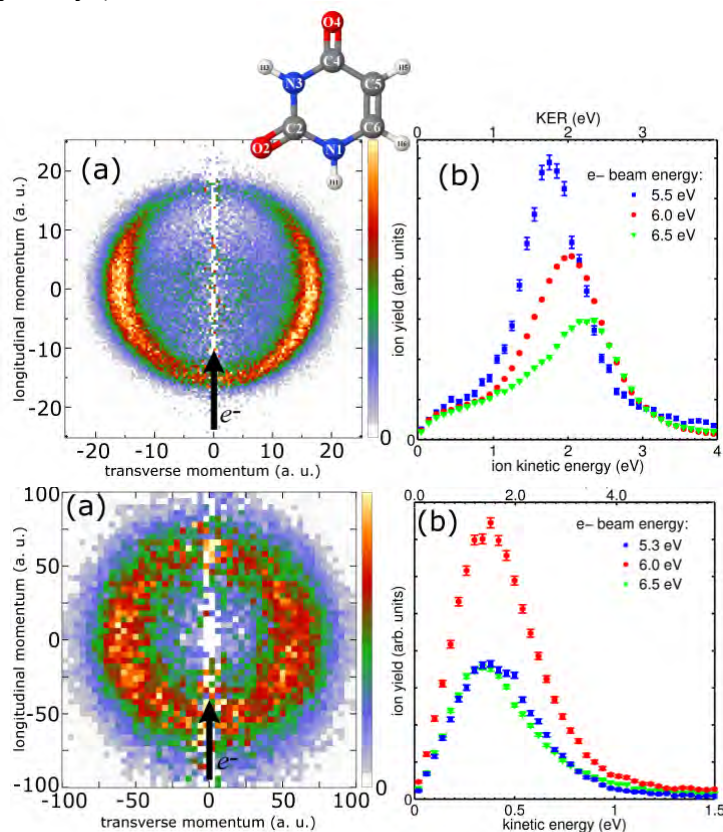
a.) experiment: 3d-MFPAD for ($\sim 4\text{eV}$) photo electrons of CF_4 after C(1s) K-shell ionization with eV (linear polarized). The red lines indicate the orientation of the emitted fluorines. b) theory: photo electron angular distribution for 3.27eV (C.W. McCurdy, C. Trevisan).

Dissociative electron attachment dynamics of uracil:

Fragmentation of the molecules found in DNA by low-energy electrons is highly relevant to a more complete understanding of radiation damage in living tissue, which is known to proceed primarily through DEA of secondary electrons that are produced with a high abundance ($\sim 4 \times 10^4$ per MeV of deposited energy) by primary ionizing radiation and by chemical reactions involving radicals such as OH that are also produced in DEA reactions. We have measured 3-dimensional ion momentum distributions following DEA to the nucleobase uracil. This was made possible by the development of a compact molecular oven that produces an effusive molecular beam from low – vapor pressure targets. The oven is capable of heating solid and liquid samples to above 600K, allowing the density and clustering properties of the effusive vapor target to be precisely controlled.

DEA at the three low-energy π^* shape resonances of uracil dissociate exclusively by the loss of neutral hydrogen, while several higher-energy (possibly doubly-excited) resonances in the 5-10 eV electron energy range produce a multitude of ion fragments that are consistent with multiple bond-breaking and substantial rearrangement that is much less likely to be repairable in nature, for example by proton transfer from the aqueous environment.

Our measured ion momentum distributions from the dissociation channels resulting from one of these resonances in uracil, at 6 eV electron attachment energy, suggest at least two different characteristic post - electron attachment dynamics. In the case of H^- and $\text{C}_3\text{H}_3\text{N}_2\text{O}^-$, the latter corresponding to loss of neutral H and CO (or possibly HCO), we observe a narrow ion kinetic energy peak that is a signature of large kinetic energy release (see Figure). Several other fragmentation channels are observed with isotropic ion momentum distributions of varying widths, all peaked at zero kinetic energy. The momentum spectra indicate that the final state products of these dissociation channels are highly vibrationally excited. This work was done in an ongoing collaboration with Vincent McKoy and Carl Winstead (Cal Tech) and Yoshiro Azuma (Sophia University, Tokyo).



Momentum and kinetic energy distributions of H^- and $\text{C}_3\text{H}_3\text{N}_2\text{O}^-$ fragments following dissociative electron attachment at around electron impact energies near 6 eV

Dissociative electron attachment dynamics to Pyrimidine and Pyrazine:

DEA resonances involving doubly-excited anions present an enormous theoretical challenge in terms of accurately describing the electronic structure by *ab initio* methods due to highly-correlated electron dynamics. These challenges are magnified in relatively large multi-electron systems such as the nucleobases and many other biologically relevant molecules. It is therefore desirable to understand more about the dissociation dynamics of singly-excited anion shape resonances that are ubiquitous in aromatic compounds. We recently targeted the diazines pyrimidine and pyrazine toward this purpose, as they are relatively well-known by electron-scattering theory and experiments to have shape resonances with energies up to 4.5 eV that might be stable enough with respect to autodetachment that they also participate in DEA. It is

noteworthy that no experimental data exist to date in the literature that have measured DEA products for diazines.

In the first experimental measurements of DEA to diazines, we did not find any ion fragments from either pyrazine or pyrimidine at the predicted shape resonance energies below 5 eV. Nevertheless we did discover many dissociation channels at the slightly higher electron attachment energies of 5-7 eV, that contrast remarkably with the similarly structured uracil molecule. As in uracil, multiple bond-breaking occurs, resulting in CN^- , $\text{C}_2\text{H}_2\text{N}^-$ and $\text{C}_3\text{N}_2\text{H}_3^-$ and H^- from each of these diazines. Remarkably, every one of these fragmentation channels exhibits a very small kinetic energy release and therefore the available energy is effectively channeled into vibrational excitation. This finding is likely to be crucial in our future investigations of DEA to nucleobases.

Future Plans

We plan to continue application of the COLTRIMS approach to achieve complete descriptions of single photon double ionization to polyatomic molecules studying dissociation dynamics, ionization mechanisms and structural imaging. In particular we will investigate more complex systems such as C_4H_8 , C_3H_6 and C_3H_4 and $\text{C}_2\text{H}_2\text{F}_2$. The latter molecule nicely combines the two imaging and “anti-imaging” hydrogen and fluorine bonds. We plan to continue our on-going work using our Dissociative Electron Attachment modified-COLTRIMS to study DEA to uracil and pyrazine. This latter work is being done in close collaboration with Vincent McKoy from the theory side.

Recent Publications (2012-2014)

1. Adaniya H., Slaughter D.S., Osipov T. Weber T., Belkacem A., “A momentum imaging microscope for dissociative electron attachment”, *Rev. Scient. Inst.* **83** (2012) 023106.
2. J.B. Williams, C.S. Trevisan, M.S. Schoffler, T. Jahnke, I. Bocharova, H. Kim, B. Ulrich, R. Wallauer, F. Sturm, T. N. Rescigno, A. Belkacem, R. Dorner, Th. Weber, C.W. McCurdy, A. L. Landers, “Imaging polyatomic molecules in three dimensions using molecular frame photoelectron angular distributions”, *Phys. Rev. Lett.* **108** (2012) 233002.
3. F. Robicheaux, M.P. Jones, M. Schoeffler, T. Jahnke, K. Kreidi, J. Titze, C. Stuck, R. Doerner, A. Belkacem, Th. Weber and A.L. Landers, “Calculated and measured angular correlation between photoelectrons and Auger electrons from K-shell ionization “, *J. Phys. B: At. Mol. Opt. Phys.*, **45**, (2012), 175001.
4. F. Trinter, L.Ph.H. Schmidt, T. Jahnke, M.S. Schöffler, O. Jagutzki, A. Czasch, J. Lower, T. A. Isaev, R. Berger, A.L. Landers, Th. Weber, R. Dörner, H. Schmidt-Böcking , Multi fragment vector correlation imaging: A search for hidden dynamical symmetries in many-particle molecular fragmentation processes, *Molecular Physics*, Vol. 110, Nos. 15-16, (2012), 1863-1872
5. J.B. Williams, C.S. Trevisan, M.S. Schoeffler, T. Jahnke, I. Bocharova, H. Kim, B. Ulrich, R. Wallauer, F. Sturm, T.N. Rescigno, A. Belkacem, R. Doerner, Th. Weber, C.W. McCurdy, and A.L. Landers, Probing the Dynamics of Dissociation of Methane Following Core Ionization Using Three-Dimensional Molecular Frame Photoelectron Angular Distributions, *J. Phys. B: At. Mol. Opt. Phys.*, **45**, (2012), 194003
6. D.S. Slaughter, D.J. Haxton, H. Adaniya, T. Weber, T.N. Rescigno, C.W. McCurdy, and A. Belkacem, Ion momentum imaging of dissociative electron attachment dynamics in methanol *Phys. Rev. A*, **87**, (2013), 052711
7. M.S. Schoeffler, C. Stuck, M. Waitz, F. Trinter, T. Jahnke, U. Lenz, M. Jones, A. Belkacem, A. Landers, C. L. Cocke, J. Colgan, A. Kheifets, I. Bray, H. Schmidt-Boecking, R. Doerner, and Th. Weber, Ejection of quasi free electron pairs from the helium atom ground state by a single Photon, *Phys. Rev. Lett.*, **111**, (2012), 013003
8. F. Trinter, M. Schoeffler, H.K. Kim, F. Sturm, K. Cole, N. Neumann, A. Vredenburg, J. Williams, I. Bocharova, R. Guillemin , M. Simon , A. Belkacem, A. Landers, Th. Weber, H. Schmidt-Boecking, R. Doerner, and T. Jahnke, Resonant Auger decay driven intermolecular Coulombic decay as a tool for site-selective creation of low energy electrons in biological system, to be published in *Nature*

9. A. Moradmand, D.S. Slaughter, D.J. Haxton, T.N. Rescigno, C.W. McCurdy, Th. Weber, S. Matsika, A.L. Landers, A. Belkacem, and M. Fogle, Dissociative electron attachment to carbon dioxide via the 2P_u shape resonance, accepted for publication in *Phys. Rev. A*, 88, (2013)
10. B. Gaire, D.J. Haxton, P. Braun, S.Y. Lee, I. Bocharova, F.P. Sturm, N. Gehrken, M. Honig, M. Pitzer, D. Metz, H-K. Kim, T. Jahnke, H. Gassert, S. Zeller, J. Voigtsberger, W. Cao, M. Zohrabi, J. Williams, A. Gatton, D. Reedy, C. Nook, Th. Mueller, A. Landers, C. L. Cocke, I. Ben-Itzhak, R. Doerner, A. Belkacem, and Th. Weber, Photo double ionization of ethylene and acetylene near threshold, Draft to be submitted to *Phys. Rev. A*, (2013)
11. Gaire, D.J. Haxton, P. Braun, S.Y. Lee, I. Bocharova, F.P. Sturm, N. Gehrken, M. Honig, M. Pitzer, D. Metz, H-K. Kim, T. Jahnke, H. Gassert, S. Zeller, J. Voigtsberger, W. Cao, M. Zohrabi, J. Williams, A. Gatton, D. Reedy, C. Nook, Th. Mueller, A. Landers, C. L. Cocke, I. Ben-Itzhak, R. Doerner, A. Belkacem, and Th. Weber, Hydrogen and Fluorine migration in the photo double ionization of 1,1-difluoroethylene ($C_2H_2F_2$) near threshold Draft to be submitted to *Phys. Rev. A*, (2013)
12. D.S. Slaughter, D.J. Haxton, H. Adaniya, T. Weber, T.N. Rescigno, C.W. McCurdy, and A. Belkacem, Ion momentum imaging of dissociative electron attachment dynamics in methanol *Phys. Rev. A*, 87, (2013), 052711
13. M.S. Schoeffler, C. Stuck, M. Waitz, F. Trinter, T. Jahnke, U. Lenz, M. Jones, A. Belkacem, A. Landers, C. L. Cocke, J. Colgan, A. Kheifets, I. Bray, H. Schmidt-Boecking, R. Doerner, and Th. Weber, Ejection of quasi free electron pairs from the helium atom ground state by a single Photon, *Phys. Rev. Lett.*, 111, (2013), 013003
14. A. Moradmand, D.S. Slaughter, D.J. Haxton, T.N. Rescigno, C.W. McCurdy, Th. Weber, S. Matsika, A.L. Landers, A. Belkacem, and M. Fogle, Dissociative electron attachment to carbon dioxide via the 2P_u shape resonance, accepted for publication in *Phys. Rev. A*, 88, (2013)
15. B. Gaire, D.J. Haxton, P. Braun, S.Y. Lee, I. Bocharova, F.P. Sturm, N. Gehrken, M. Honig, M. Pitzer, D. Metz, H-K. Kim, T. Jahnke, H. Gassert, S. Zeller, J. Voigtsberger, W. Cao, M. Zohrabi, J. Williams, A. Gatton, D. Reedy, C. Nook, Th. Mueller, A. Landers, C. L. Cocke, I. Ben-Itzhak, R. Doerner, A. Belkacem, and Th. Weber, "Photo double ionization of ethylene and acetylene near threshold", *Phys. Rev. A*, **2014**, 89, 013403, Featured under "Editors' Suggestion"
16. B. Gaire, D.J. Haxton, P. Braun, S.Y. Lee, I. Bocharova, F.P. Sturm, N. Gehrken, M. Honig, M. Pitzer, D. Metz, H-K. Kim, T. Jahnke, H. Gassert, S. Zeller, J. Voigtsberger, W. Cao, M. Zohrabi, J. Williams, A. Gatton, D. Reedy, C. Nook, Th. Mueller, A. Landers, C. L. Cocke, I. Ben-Itzhak, R. Doerner, A. Belkacem, and Th. Weber, "Hydrogen and fluorine migration in the photo double ionization of 1,1-difluoroethylene ($C_2H_2F_2$) near threshold", *Phys. Rev. A*, **89**, (2014), 043423
17. F. Trinter, M. Schoeffler, H.K. Kim, F. Sturm, K. Cole, N. Neumann, A. Vredenburg, J. Williams, I. Bocharova, R. Guillemin, M. Simon, A. Belkacem, A. Landers, Th. Weber, H. Schmidt-Boecking, R. Doerner, and T. Jahnke, "Resonant Auger decay driven intermolecular Coulombic decay as a tool for site-selective creation of low energy electrons in biological systems", *Nature*, Vol. 505, (2013), 664 - 666
18. A. Menssen, J.B. Williams, B. Gaire, A.S. Gatton, F. Trinter, A. Kuhlins, J. Sator, M. Zohrabi, B. Berry, M. Schoeffler, A. Belkacem, I. Ben-Itzak, A. Landers, R. Doerner and Th. Weber, "Probing electron density in CF_4 using core level photo electrons", draft to be submitted to *Phys. Rev. Lett.*, 2014

Electron-Atom and Electron-Molecule Collision Processes

T. N. Rescigno, D. J. Haxton and C. W. McCurdy

Chemical Sciences, Lawrence Berkeley National Laboratory, Berkeley, CA 94720

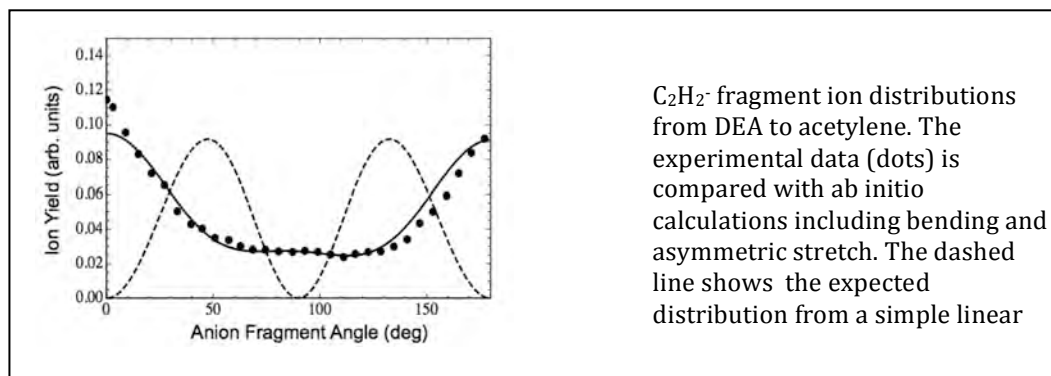
trescigno@lbl.gov, djhaxton@lbl.gov, cwmccurdy@lbl.gov

Program Scope: This project seeks to develop theoretical and computational methods for treating electron processes that are important in electron-driven chemistry and physics and that are currently beyond the grasp of first principles methods, either because of the complexity of the targets or the intrinsic complexity of the processes themselves. A major focus is the development of new methods for solving multiple photoionization and electron-impact ionization of atoms and molecules. New methods are also being developed and applied for treating low-energy electron collisions with polyatomic molecules and clusters. A state-of-the-art approach is used to treat multidimensional nuclear dynamics in polyatomic systems during resonant electron collisions and predict channeling of electronic energy into vibrational excitation and dissociation.

Recent Progress and Future Plans:

Dissociative Electron Attachment

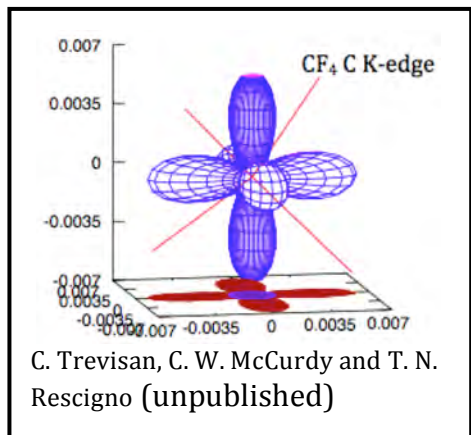
Dissociative electron attachment (DEA) plays an important role in radiation therapy, waste remediation, nanofabrication and in the chemistry of planetary atmospheres. Its fundamental importance in electron-driven chemistry provides an impetus for understanding the mechanism of DEA. Our earlier studies of DEA to water, CO₂ (ref. 12) and methanol (ref. 8) have shown that the topology of the transient anion surfaces relevant to DEA can be quite complicated, with conical intersections between shape resonances, Feshbach resonances and virtual states that can play a role in the dissociation dynamics. We have found that with polyatomic targets, studies of the total dissociation cross sections can belie the complexity of the dissociation dynamics, which is only revealed in angular distribution of the product anions. This is the case with acetylene where our joint experimental/theoretical study (ref. 17) done in collaboration with Prof. A. E. Orel and the group at Auburn confirmed that a non-axial recoil mechanism involving cis- and trans-bending, as well as asymmetric stretch, combined with *ab initio* computations of the entrance amplitude faithfully reproduced the measured angular distributions.



We are undertaking a similar study of DEA to CF₄. Preliminary calculations show that DEA in the 6-9 eV region is the result of overlapping negative ion shape resonances of A1 and T2 symmetry which correlate with different product ion channels – F⁻ + CF₃ and F + CF₃⁻. The complicated angular dependence that is observed may result from a conical intersection involving these anion states.

Molecular-Frame Photoelectron Angular Distributions (MFPADS)

Our unexpected discovery that, for the class of molecules containing a single heavy atom and several hydrogen's atoms (CH_4 , H_2O , NH_3 - refs. 2-4), the K-shell MFPADS at relatively low photoelectron energies, when averaged over all photon polarization directions, effectively image the geometry of the molecule is a simple reflection of the fact that core-level MFPADS are extraordinarily sensitive to nuclear geometry (refs. 5,7,10).



We have since found that the situation with molecules containing more than one central heavy atom can be more complicated, with multiple scattering effects leading to additional structure in the MFPADS. The origin of these imaging effects is still not well understood. For example, in work carried out in collaboration with Prof. Cynthia Trevisan of California Maritime Academy, we have found that carbon 1s ionization from CF_4 produces an MFPAD that actually *anti-images* the molecule, that is, the electron is

preferentially ejected in directions between the CF bonds, producing a six-lobed octahedral figure. These results raise a number of interesting questions. What if the molecule contains a heavy atom with a mixture of hydrogen and other heavy atoms bonded to them? In a collaborative study with Cynthia Trevisan and the experimental AMO group in Frankfurt, we have initiated calculations on carbon 1s MFPADS for the series of fluorinated hydrocarbons, CH_3F , CH_2F_2 and CHF_3 , to see if the combined effects of imaging and anti-imaging persist. Another interesting aspect of core-hole ionization we wish to examine concerns core-electron ejection from molecules with two or more equivalent heavy atoms, like acetylene (HCCH). These calculations will be undertaken with a view toward guiding and interpreting ongoing and planned experiments at the ALS searching for evidence of the localization of core holes.

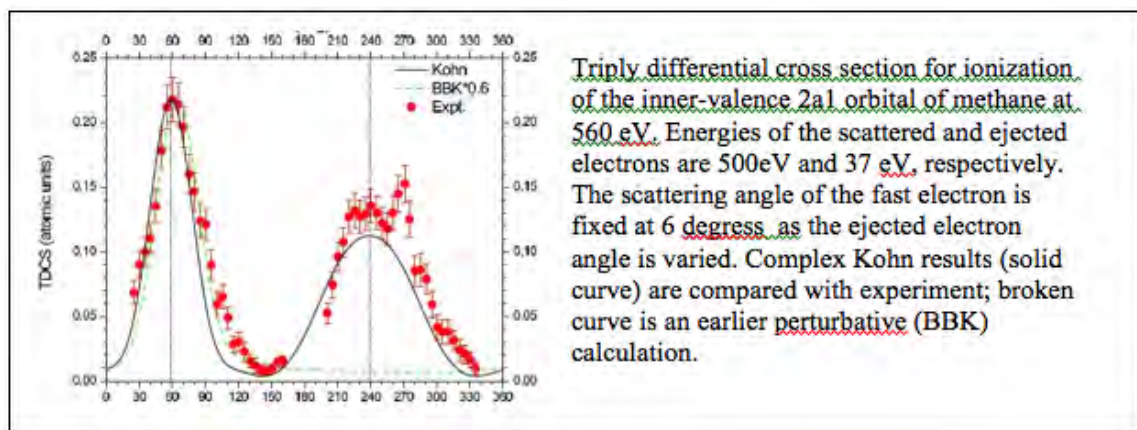
Photo-Double Ionization of Complex Targets

Single-photon double ionization (DPI) is an exquisitely sensitive probe of electron correlation. For the simplest atomic and molecular targets, advanced, grid-based, non-perturbative methods have produced essentially exact results. To overcome the computational obstacles involved in applying such methods to more complex molecular targets, we developed an expanded frozen-core treatment which produces an effective 2-electron problem which we found to give surprisingly accurate differential DPI cross sections for neon and argon (ref. 6). We have taken the first steps in extending this treatment to molecular targets. To avoid single-center expansions, which are prohibitively slow for complex molecules, we are developing a new hybrid approach that uses multi-centered basis functions in the restricted region of coordinate space spanned by the frozen molecular orbital's, combined with a grid-based, exterior complex scaled finite-element DVR radial basis in the exterior region. The associated angular functions for high l -values are then only needed in the first few elements close to the target region. In collaboration with Prof. Frank Yip of California Maritime Academy, we have taken the first step of demonstrating an efficient construction of one-electron molecular ion continuum functions which will be needed as the testing functions in a DPI calculation. Our planned efforts will be directed at carrying out the first calculations of DPI on O_2 and N_2 with the specific goal of exploring the possible signature of an effect yet to be addressed, either theoretically or experimentally – that of inter- versus intra-shell correlation.

Molecular ($e/2e$) at High Impact Energy

Most of the theoretical work on computing fully differential cross sections for electron impact ionization of molecules with more complex targets than H_2 has been carried out using perturbative treatments, for both scattered and ejected electrons, with simplifying assumptions such as the use of spherically averaged interaction potentials. The complex Kohn approach to

($e/2e$) at high-energy electron impact which we developed and successfully applied to the case of water (ref. 13) allows us to treat the slow, ejected electron in ($e/2e$) processes without simplifying approximations, under the assumption that the fast incident and scattered electrons can be treated in the first Born approximation. We have completed and published a similar study on methane (ref. 16). Methane has triply degenerate (t_2) occupied orbitals and therefore a coupled-channel treatment was required to produce accurate results. From our studies to date we have found that the recoil peak in the triple differential cross sections is usually more difficult to accurately describe than the binary peak. This is especially true when the ionization involves a delocalized valence orbital. Since the recoil peak corresponds classically to a collision where the ejected electron is scattered by the nucleus before exiting the molecular field, such collisions are more sensitive to details of the molecular target wave function. We plan to examine the sensitivity of the recoil region to the use of more elaborate correlated wave functions which can be



accommodated in the complex Kohn approach. We will also examine more complex processes such as molecular excitation/ionization, which are generally beyond the scope of simple perturbative methods.

New Complex Kohn Methodology

Our complex Kohn suite of codes, which we rely on for electron-molecule, electron-ion, molecular photoionization and high-energy ($e/2e$) calculations, is presently interfaced to the MESA (Molecular Electronic Structure Applications) package, a legacy code developed in the 1980's. While quite flexible, it had been restricted in terms of the number of basis functions, configurations and, consequently, the size of molecular targets it could handle, being written in Fortran77 for single processor machines whose memory was small by present standards. In collaboration with Prof. Robert Lucchese of Texas A&M University, we have made two major improvements to the MESA and complex Kohn codes. We now have new versions of the codes that compile under GFORTRAN and use 8-bit integer array addressing, effectively eliminating the restrictions on the number of basis functions that can be used and more than tripling the limit on the number of configurations. The new codes have been used in coupled-channel studies of SF_6 photoionization (ref. 14) and multi-photon ionization of NO_2 (ref. 15). We have also implemented a configuration contraction scheme that makes it possible to eliminate the occurrence of pseudo-resonances that can appear in close-coupling expansions when correlated target states are used. Our study of dissociative excitation of H_2O (ref. 9), as well as ongoing studies of methanol excitation, made use of this new capability.

With a view toward treating electron-molecule collision processes, including electron correlation effects, on systems that are significantly larger than can be studied currently, we have initiated, also in collaboration with Prof. Lucchese, the development of a new *numerical* complex Kohn method designed to run optimally on distributed memory parallel platforms, using from 32 to 512 processors depending on the size of the problem. The idea will be to replace the analytic basis functions currently used with numerical grid-based functions, in combination with complex continuum functions, as part of an iterative solution of the complex Kohn equations using an iterative Krylov subspace method with orthogonalization to solve the linear equations. In addition to opening a path to calculations on much larger molecules, the new method will allow us to drop approximations such as separable exchange, which are fundamentally linked to the old methodology.

Publications (2012-2014):

1. F. L. Yip, A. Palacios, C. W. McCurdy, T. N. Rescigno and F. Martín, “Time-dependent formalism of double ionization of multielectron atomic targets”, *Chem. Phys.* **414**, 112 (2013).
2. J. B. Williams, C. S. Trevisan, M. S. Schöffler, T. Jahnke, I. Bocharova, H. Kim, B. Ulrich, R. Wallauer, F. Sturm, T. N. Rescigno, A. Belkacem, R. Dörner, Th. Weber, C. W. McCurdy and A. L. Landers, “Imaging Polyatomic Molecules in Three Dimensions using Molecular Frame Photoelectron Angular Distributions”, *Phys. Rev. Lett.* **108**, 233002 (2012).
3. J. B. Williams, C. S. Trevisan, M. S. Schöffler, T. Jahnke, I. Bocharova, H. Kim, B. Ulrich, R. Wallauer, F. Sturm, T. N. Rescigno, A. Belkacem, R. Dörner, Th. Weber, C. W. McCurdy and A. L. Landers, “Probing the Dynamics of Dissociation of Methane Following Core Ionization Using Three-Dimensional Molecular Frame Photoelectron Angular Distributions”, *J. Phys. B* **45**, 194003 (2012).
4. C. S. Trevisan, C. W. McCurdy and T. N. Rescigno, “Imaging Molecular Shapes with Molecular Frame Photoelectron Angular Distributions from Core Hole Ionization”, *J. Phys. B* **45**, 194002 (2012).
5. T. N. Rescigno, N. Douguet and A. E. Orel, “Imaging Molecular Isomerization Using Molecular-Frame Photoelectron Angular Distributions”, *J. Phys. B* **45**, 194001 (2012).
6. F. L. Yip, T. N. Rescigno, C. W. McCurdy and F. Martín, “Fully Differential Single-Photon Double Ionization of Neon and Argon”, *Phys. Rev. Lett.* **110**, 173001 (2013).
7. N. Douguet, T. N. Rescigno and A. E. Orel, “Time-resolved molecular-frame photoelectron angular distributions: Snapshots of acetylene-vinylidene cationic isomerisation”, *Phys. Rev. A* **86**, 013425 (2013).
8. D. S. Slaughter, D. J. Haxton, H. Adaniya, T. Weber, T. N. Rescigno, C. W. McCurdy and A. Belkacem, “Ion-momentum imaging of resonant dissociative-electron-attachment dynamics in methanol”, *Phys. Rev. A* **87**, 052711 (2013).
9. T. N. Rescigno and A. E. Orel, “A Theoretical Study of Excitation of the Low-Lying Electronic States of Water by Electron Impact”, *Phys. Rev. A* **88**, 012703 (2013).
10. N. Douguet, T. N. Rescigno and A. E. Orel, “Carbon K-shell molecular-frame photoelectron angular distribution in the photoisomerization of neutral ethylene”, *Phys. Rev. A* **88**, 013425 (2013).
11. D. J. Haxton, “Breakup of H_2^+ by Photon Impact”, *Phys. Rev. A* **88**, 013415 (2013).
12. A. Moradmand, D. S. Slaughter, D. J. Haxton, T. N. Rescigno, C. W. McCurdy, Th. Weber, S. Matsika, A. L. Landers, A. Belkacem, and M. Fogle, “Dissociative electron attachment to carbon dioxide via the $^2\Pi_u$ shape resonance”, *Phys. Rev. A* **88**, 032703 (2013).
13. Chih-Yuan Lin, C. W. McCurdy and T. N. Rescigno, “Complex Kohn Approach to Molecular Ionization by High-Energy Electrons: Application to H_2O ”, *Phys. Rev. A* **89**, 012703 (2014).
14. J. Jose, R. R. Lucchese and T. N. Rescigno, “Interchannel coupling effects in the valence photoionization of SF_6 ”, *J. Chem. Phys.* **140**, 204305 (2014).
15. S. M. Poullain, C. Elkharrat, W. B. Li, K. Veyrinas, J. C. Houver, C. Cornaggia, T. N. Rescigno, R. K. Lucchese and D. Doweck, “Recoil frame photoemission in multiphoton ionization of small polyatomic molecules: photodynamics of NO_2 probed by 400 nm fs pulses”, *J. Phys. B* **47**, 124024 (2014).
16. Chih-Yuan Lin, C. W. McCurdy and T. N. Rescigno, “Theoretical study of $(e/2e)$ from outer- and inner-valence orbitals of CH_4 : A complex Kohn treatment” *Phys. Rev. A* **89**, 052718 (2014).
17. M. Fogle, D. J. Haxton, A. L. Landers, A. E. Orel and T. N. Rescigno, “Ion-momentum imaging of dissociative electron attachment dynamics in acetylene”, *Phys. Rev. A* (submitted).

Ultrafast X-ray Science Laboratory

C. William McCurdy (Director), Ali Belkacem, Oliver Gessner, Dan Haxton, Martin Head-Gordon, Stephen Leone, Daniel Neumark, Robert W. Schoenlein, Thorsten Weber

Chemical Sciences, Lawrence Berkeley National Laboratory, Berkeley, CA 94720

CWMcCurdy@lbl.gov, ABelkacem@lbl.gov, OGessner@lbl.gov, DJHaxton@lbl.gov, MHead-Gordon@lbl.gov, SRLeone@lbl.gov, DMNeumark@lbl.gov, RWSchoenlein@lbl.gov, TWeber@lbl.gov

Program Scope: This program exploits the use of short X-ray and XUV pulses to provide basic knowledge of ultrafast dynamics of photo-excited atoms and molecules from the natural time scale of electron motion to the time scale of the chemical transformations. There are five subtasks in the UXSL effort, reflecting the essential strategy of attacking these problems using an approach that applies an entire arsenal of ultrafast experimental and theoretical methodology spanning time scales from attoseconds to picoseconds to the study of systems that include atoms and molecules in the gas phase, clusters, nanodroplets and condensed phase transition-metal complexes.

Recent Progress and Future Plans:

1. Attosecond atomic and molecular science -- *Stephen Leone and Daniel Neumark*

The UXSL attosecond dynamics subtask strives to use the unique ability to generate isolated attosecond pulses to directly study electronic processes, such as autoionization and electronic coherences, in atoms and small molecules. In this effort, high harmonic generation and double optical gating are used to produce isolated attosecond pulses in the energy range of 15 to 80 eV. The attosecond pulses are used in combination with a time-delayed perturbative near-infrared (NIR) pulse to measure laser-induced changes in the absorption of a target gas. Recent work has used Sn filters to spectrally limit the attosecond pulses to 18-24 eV, resulting in pulse durations of about 400 as.

In addition to the fast timescales that can be accessible with attosecond pulses, the extremely broad bandwidth of the attosecond pulse allows simultaneous excitation of multiple states. Recent experimental work in neon uses transient absorption spectroscopy to observe a coherent superposition of Rydberg states below the first ionization potential of neon. In this work, the attosecond pulse prepares the coherent superposition. Then, the NIR pulse interrogates the initial excitation by perturbing the induced polarization at varying time delay. The NIR pulse causes long-lived Rydberg states to switch from Lorentzian to Fano lineshapes [Ott *et al.*, *Science* **340**, 716 (2013)] as seen in the inset in figure 1(a). Quantum beating is observed as a modulation in the absorption of various states as a function of NIR-attosecond pulse time delay. This beating is very prominent in the spin orbit split *3d* features, which has a period of 40 fs, corresponding the energy difference of 0.1 eV between the two states. Extensive work in conjunction with the theory groups of Ken Schafer and Mette Gaarde from LSU has provided an understanding of the mechanism of this beating. However, the relative strengths of the observed beating in the *3d* states is not correctly captured by either a simple depletion-

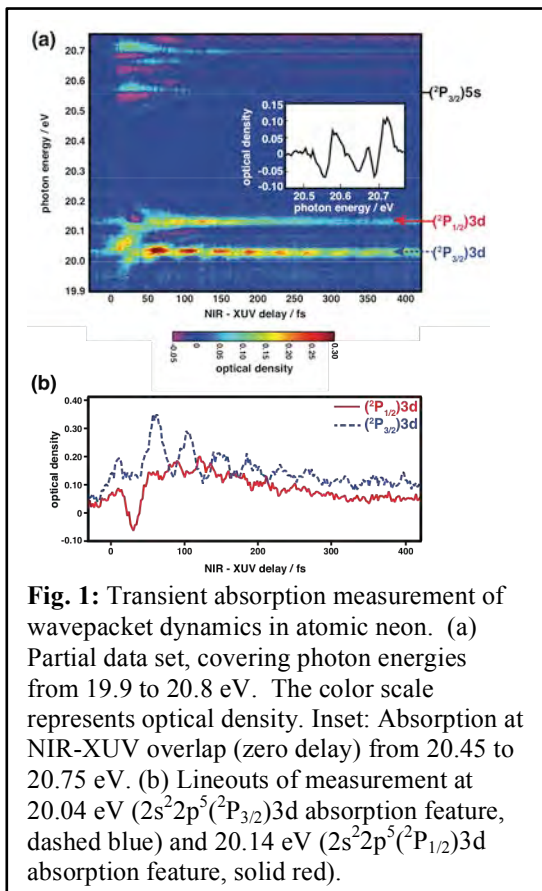


Fig. 1: Transient absorption measurement of wavepacket dynamics in atomic neon. (a) Partial data set, covering photon energies from 19.9 to 20.8 eV. The color scale represents optical density. Inset: Absorption at NIR-XUV overlap (zero delay) from 20.45 to 20.75 eV. (b) Lineouts of measurement at 20.04 eV ($2s^22p^5(^1P_{3/2})3d$ absorption feature, dashed blue) and 20.14 eV ($2s^22p^5(^1P_{1/2})3d$ absorption feature, solid red).

only model, which assumes population is removed from one or the other state in the superposition, or a more complicated coupling model, in which some population is transferred between the two $3d$ states by coupling through an intermediate $2p$ state. Approximate agreement between experiment and theory is attained only by considering the variable spectrum of the NIR pulse and admitting some uncertainty in the dipole coupling between various states in the calculations. Schafer *et al.* have shown theoretically in helium that sub-cycle features can be observed that reveal, through the slope of their interference fringes, the coupling parameters between various states [Chen *et al.*, Phys. Rev. A **87**, 033408 (2013)]. Observation of these subcycle features in neon would offer a clearer picture of the electronic interactions that play a role in the detection of quantum beats.

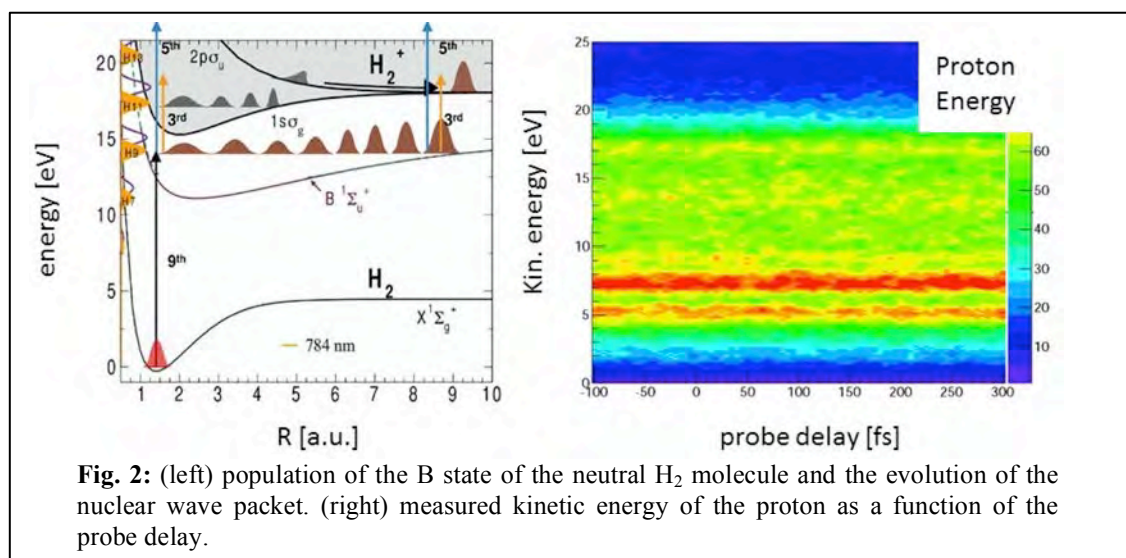
In pursuit of this goal, much effort has been invested to improve the laser pulse characteristics. New chirped mirrors supporting a broader bandwidth have been

installed, shortening the probing NIR pulse duration from 12 fs to 7 fs. The carrier envelope phase (CE phase) locking electronics were upgraded, improving the phase jitter over time to 150 as. An electron time-of-flight spectrometer was added to the apparatus to optimize the attosecond pulses and CE phase control. A new interferometer is currently being tested to improve the NIR focus quality and allow the intensity to be increased by at least a factor of two. Finally, since previous work on autoionizing resonances in xenon revealed the importance of isolating the line center of absorption features to correctly extract the lifetime of the state, a new grating was installed, improving the spectral resolution by a factor of two, to 8 meV at 20 eV.

Future work will focus on expanding the complexity of target systems to small molecules such as HBr and HF. The HBr experiments will apply the experimental expertise gained from the xenon lifetime measurements to directly measure the lifetimes of autoionizing $3d$ core-excited states located around 75 eV. This experiment will provide an opportunity to examine electron-correlation driven processes that linewidth-derived lifetime measurements cannot access because of the numerous broadening mechanisms that come into play in the study of molecular species. The HF experiments will track electronic wavepackets generated by exciting electronic states located at energies from 15 to 18 eV, where some members of the electronic superposition are decaying on a few femtosecond timescale due to autoionization.

2. Non-Born-Oppenheimer dynamics and non-linear interaction of femtosecond X-rays with atoms and molecules -- *Ali Belkacem and Thorsten Weber*

This subtask of the UXSL is focused on using two-color Extreme Ultraviolet (XUV) pump and XUV probe to study non-Born-Oppenheimer dynamics in polyatomic molecules as well as non-linear X-ray processes. Higher-order harmonic generation has reached intensities high enough as to induce multiphoton ionization processes. This past year we focused on major laser upgrades and laboratory development. We commissioned our newly constructed reaction microscope (MISTERS) endstation at the 50Hz HHG



laser beamline which we recently equipped with an attenuation gas cell and energy filter element. High harmonics were generated, selected and overlapped in three dimensions with our supersonic gas-jet, and analyzed while first recoiling ions were imaged in the momentum spectrometer. We established photo effect measurements on Helium atoms as suitable procedures to calibrate our ion detection scheme. Subsequently, first two-color test experiments on molecules were performed on H_2 and C_2H_4 measuring ion momenta. The hydrogen molecules with its known dynamics serve as a benchmark for testing the setup and its capabilities. Pump pulses with 4.6 to 14 eV and probe pulses with 4.6 and 7.7 eV were chosen. While populating the B state of the neutral H_2 molecule we try to observe the evolving wave packet by recording the H_2^+ and H^+ signal and look for changes in the KER of the proton as shown in Fig 2.

For ethylene we compared two photon processes generated from pump-probe schemes using 8eV only with 8 and 14 eV light pulses shown in Fig. 3. In the latter we were able to break the C=C bond and found a preferred emission of the CH_2^+ fragments along the polarization direction while fragments from higher-order excitation showed an isotropic distribution. We could confirm a distinct sharp KER peak at zero seen in our VMI experiments before; its origin remains unknown at this point. Both experiments and their analysis are ongoing.

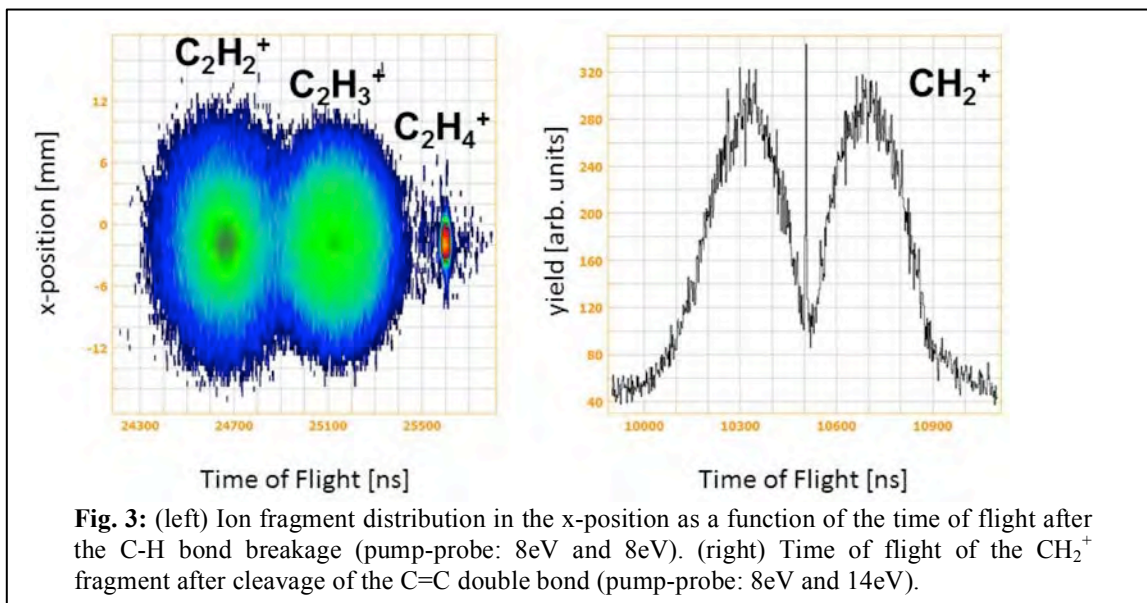


Fig. 3: (left) Ion fragment distribution in the x-position as a function of the time of flight after the C-H bond breakage (pump-probe: 8eV and 8eV). (right) Time of flight of the CH_2^+ fragment after cleavage of the C=C double bond (pump-probe: 8eV and 14eV).

Parallel to the upgrade of the low repetition high harmonic system we commissioned a new state-of-the-art laser system (30 mJ, 1 kHz and 25fs) in an adjacent laboratory. A similar high harmonic generation scheme to the 50 Hz was constructed and commissioned. This latter system produces routinely in excess of 10^9 photons per harmonic at 1-kHz making it a one-of-a-kind source of high-intensity and high repetition rate XUV photons. In addition to ion fragmentation pathways, we will attempt photoelectron spectroscopy in the molecular frame. We used this new high repetition rate intense high harmonic source to study CO_2 .

UV-driven ultrafast dynamics in carbon dioxide: Despite extensive studies of the vacuum ultraviolet photolysis of CO_2 our understanding of its photochemistry still presents a major challenge. This challenge is due to a very complicated manifold of

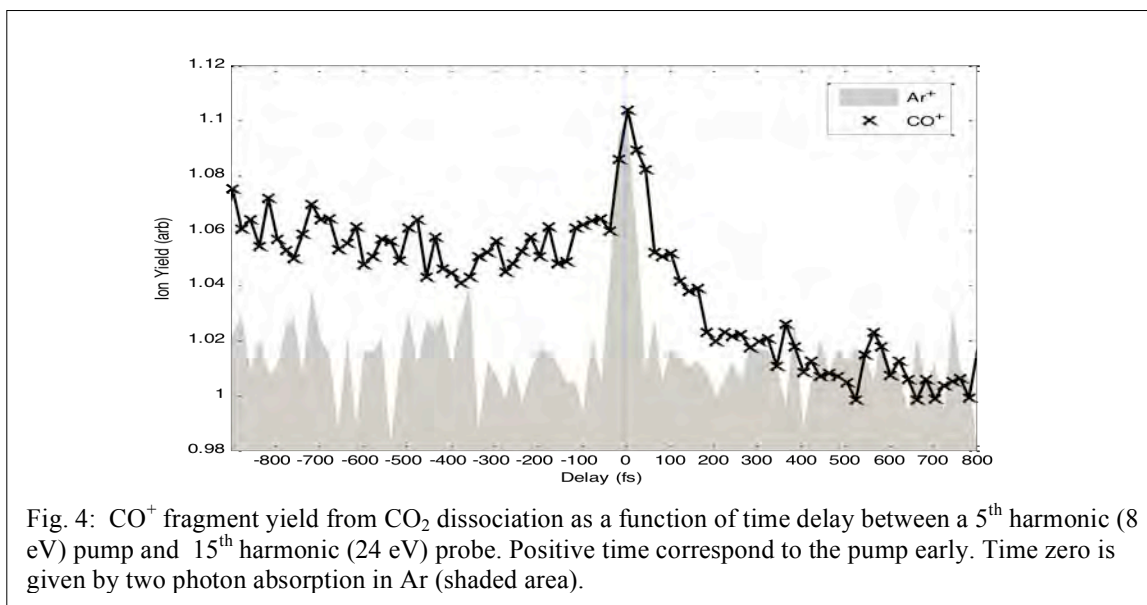


Fig. 4: CO^+ fragment yield from CO_2 dissociation as a function of time delay between a 5th harmonic (8 eV) pump and 15th harmonic (24 eV) probe. Positive time correspond to the pump early. Time zero is given by two photon absorption in Ar (shaded area).

excited-states for this prototypical three-atom molecule. In the 6-9 eV energy range there are two weak bands corresponding to photon driven electronic transition between the $^1\Sigma_g^+$ ground-state of CO₂ and the group of ($^1\Pi_g$, $^1\Sigma_u^-$, $^1\Delta_u$ and $^1\Sigma_g^+$) excited-states. A remarkable aspect is that all these transitions accessible in the energy of interest for us are dipole forbidden. It is shown in a recent theoretical work that bending vibration vibronically induces the electronic transition. In the 8 eV energy region the spectrum is irregular and diffuse. Recent theoretical study showed that the primary reason of the irregularities of level spacing and diffusiveness are non-adiabatic interactions. These interactions are numerous and strong and render questionable the quality of the familiar Born-Oppenheimer and Franck-Condon approximations. It is well established that photo-excitation of CO₂ in this energy leads to two asymptotic channels that leave the oxygen fragment in a singlet (1D) and triplet (3P) state. The latter is a result of singlet-triplet interstate crossing since it does not correlate directly to the excited-states populated in the Franck-Condon region. Using our XUV pump-probe capability we excited gas phase CO₂ molecules with the 5th harmonic (8 eV) and probed the excited state dynamics as a function of time delay with a 15th harmonic (24 eV) probe. Fig. 4 shows the production of CO⁺ fragments as a function of pump-probe delay. It is quite remarkable that we are able to excite a substantial fraction of the target (several % effects) despite the weak transition due the “dark” nature of these states. The 15th harmonic is energetic enough to break the CO bond in the cationic state producing directly CO⁺ or O⁺ fragments. We observe a long decay time when the 5th pump precedes the 15th probe. The 15th harmonic probe can also ionize CO and O fragments at the asymptotic times. Fig. YY shows that the dissociation of CO₂ takes over 300 fs to reach asymptotic limits, much longer than the case of C₂H₄ reported last year. This is an indication that dissociation of CO₂ involves a very rich dynamics prior to dissociation as suggested by the topology of the energy surfaces calculated by recent theoretical calculations. This work is being written for publication.

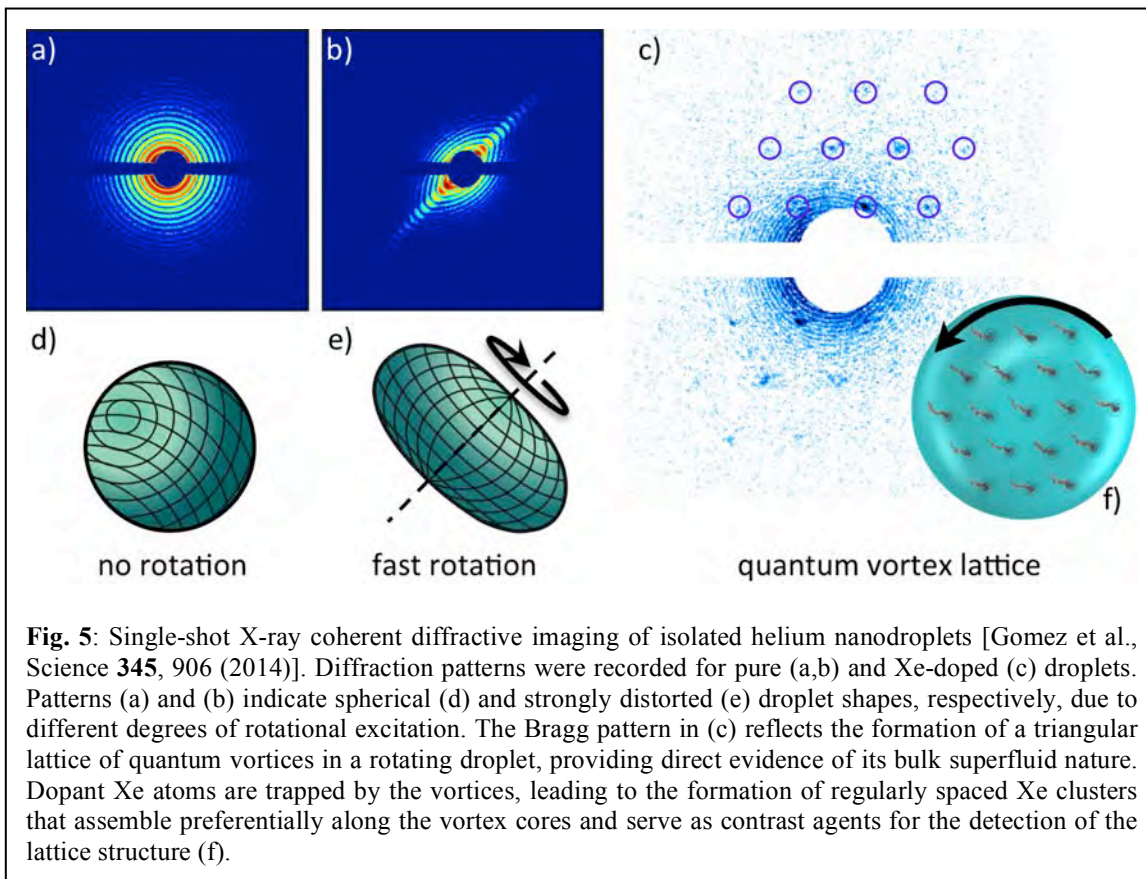
3. Soft X-ray high harmonic generation and applications in chemical physics --

Oliver Gessner, Stephen Leone and Daniel Neumark

The chemical dynamics project concentrates on fundamental dynamics in molecules and clusters, which are studied by ultrafast X-ray spectroscopy and imaging techniques. Laboratory based experiments using high-order harmonic generation (HHG) light sources are complemented by studies at the Linac Coherent Light Source (LCLS) and the FERMI free electron laser. Experimental techniques include time-resolved photoelectron spectroscopy, electron- and ion-imaging, transient XUV absorption spectroscopy, and femtosecond coherent diffractive imaging.

A recent highlight of the project is the first detection of quantum vortex lattices in rotating helium nanodroplets by X-ray coherent diffractive imaging (Fig. 5). Isolated pure and Xe-doped nanodroplets were imaged by single X-ray ($h\nu=1.5$ keV) pulses of the LCLS AMO instrument, giving access to the droplet shapes (Fig. 1 a,b,d,e) and vorticities (Fig. 1c,f). Vortices are imaged by doping the droplets with Xe atoms, which are attracted to the vortex cores, where they cluster and act as contrast agents for the detection of the elusive quantum phenomenon. The studies provide the first definitive evidence for the bulk superfluid nature of helium nanodroplets and demonstrate vorticities that are at least

five orders of magnitude higher than in any previous experiment on superfluid helium. The shapes of the fastest spinning droplets confirm an about fifty year old prediction that liquid droplets that lack viscosity retain their axisymmetric shapes at rotational speeds well beyond the stability limits of classical, viscous droplets.



Most recently, the LCLS-based cluster imaging studies were extended by a femtosecond time-resolved X-ray-pump/X-ray-probe experiment on Xe and mixed Xe/He clusters using the newly installed LAMP chamber in combination with the latest, undulator-based LCLS double-pulse generation scheme. A preliminary analysis of the data indicates that the experiment is capable of tracing the intense X-ray induced disintegration dynamics of pure Xe clusters. For hybrid Xe/He core-shell systems, indications for charge transfer between the ionized Xe core and the surrounding He shell have been detected, potentially providing new benchmarks for the use of superfluid helium as a tamper layer in so-called diffract-and-destroy experiments.

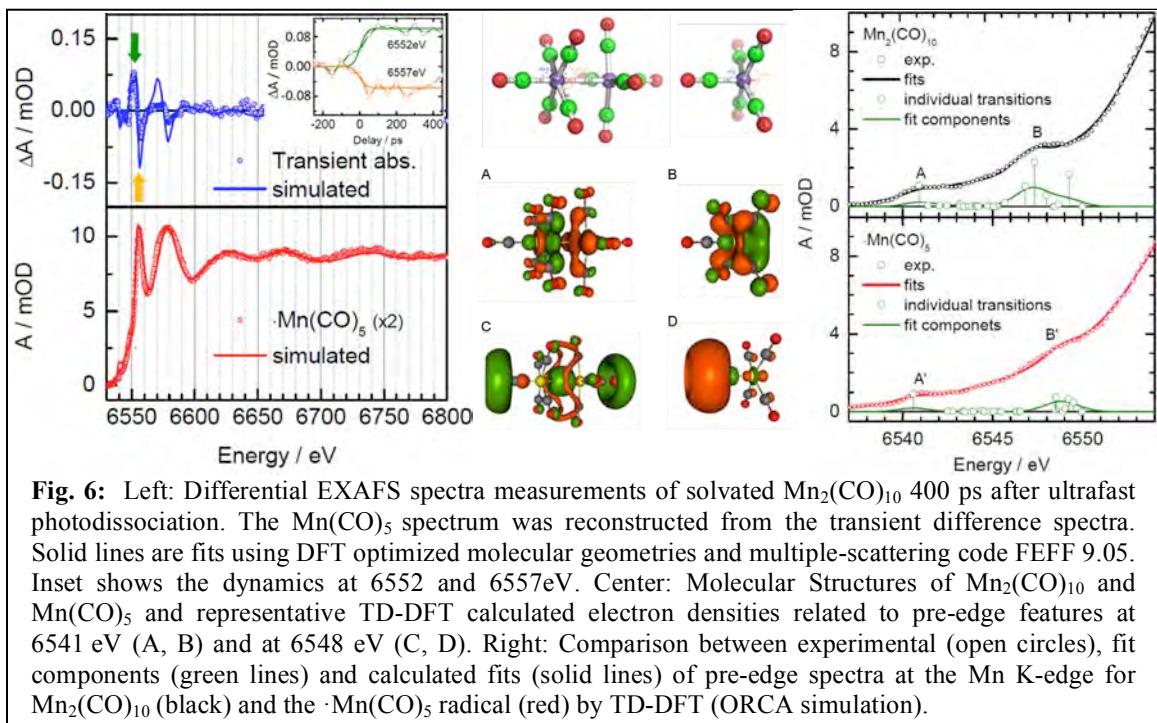
Laboratory-based femtosecond XUV photoelectron spectroscopy experiments on the relaxation dynamics of electronically excited helium nanodroplets have been extended by a UV probing scheme that reveals previously inaccessible spectroscopic features. In particular, a long-standing hypothesis suggesting an efficient interband transition from states associated with the $n=3,4$ Rydberg manifold to those associated with $n=2$ Rydberg excitations has been directly confirmed. Surprisingly, though, this transition proceeds on an ~ 300 fs time scale, almost an order of magnitude faster than previously believed and is

succeeded by continued intraband relaxation within the $n=2$ manifold. The results are corroborated by femtosecond photoelectron spectroscopy data recorded at the FERMI free electron laser after excitation into the 2p Rydberg band. The results clearly illustrate both intraband relaxation within the 2p band and interband relaxation to the 2s band on timescales commensurate with the laboratory-based data. Efforts are underway to unravel the underlying physics with the aid of *ab initio* based molecular dynamics simulations.

4. Ultrafast X-ray Studies of Condensed Phase Molecular Dynamics – Robert W. Schoenlein

The objective of this UXSL subtask is to advance our understanding of solution-phase molecular dynamics using ultrafast X-rays as time-resolved probes of the evolving electronic and atomic structure of solvated molecules. Time-resolved XANES provide detailed information about dynamics of the valence charge structure, while time-dependent EXAFS provides information about changes in the local atomic structure. X-ray measurements thereby reveal important new information about reactions including: charge transfer processes, changes in oxidation states, formation/dissolution of bonds, and conformational changes. This subtask exploits two time-resolved picosecond X-ray beamlines at the ALS (0.2 to 10 keV), beamline 11-ID at APS, and ultrafast capabilities at the LCLS X-ray laser, complemented by ultrafast optical spectroscopy studies.

One area of present focus is on solvated transition-metal complexes exhibiting strong coupling between molecular structure, charge transfer, and electronic properties arising from the ligand field. These include transition-metal polypyridyl compounds, metal-porphyrins, metal-carbonyls, and bridged heteronuclear metal-metal compounds. Understanding the fundamental dynamics in these classes of compounds is relevant for solar energy conversion schemes, photo-catalysis, and related processes.



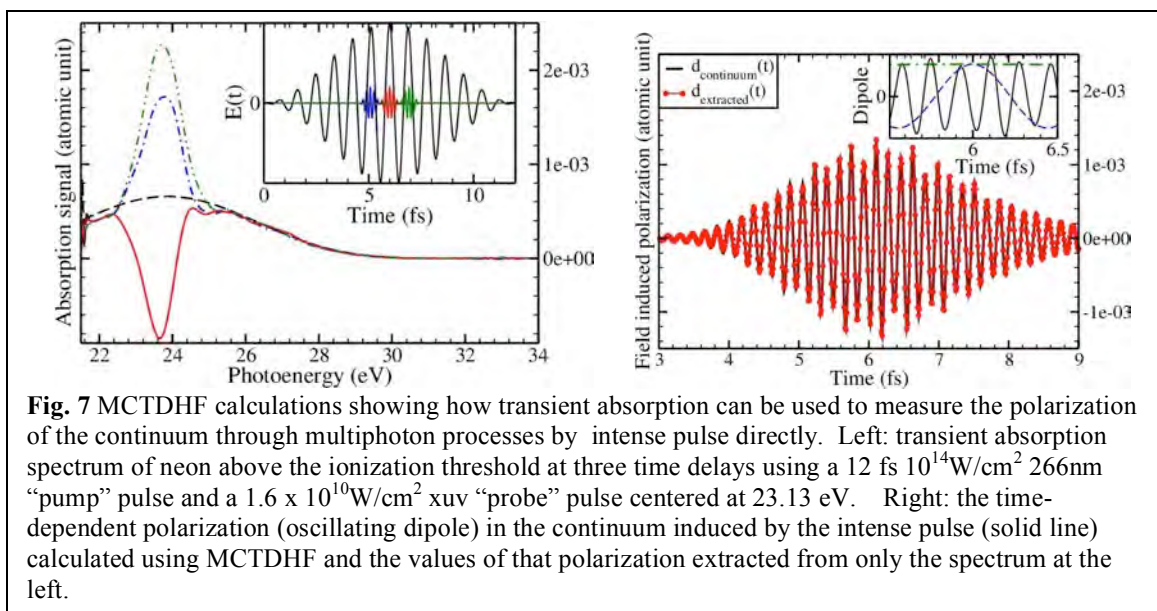
Photodissociation dynamics in metal-metal bonded carbonyl dimers: This year we have completed the first time-resolved XANES and EXAFS spectroscopy studies of the transient electronic and molecular structure of bimetallic $\text{Mn}_2(\text{CO})_{10}$ following photodissociation. $\text{Mn}_2(\text{CO})_{10}$ is one of the simplest binuclear metal carbonyl complexes and is a prototype for understanding solution photolysis of organometallic compounds with metal-metal bonds.

Transient differential Mn K-edge spectra of $\text{Mn}_2(\text{CO})_{10}$ are compared with simulations based *ab-initio* multiple scattering calculations and reveal surprisingly small structural modifications upon formation of the $\bullet\text{Mn}(\text{CO})_5$ radicals. These remain 5-fold coordinated C_{4v} structures, nearly exactly half the $\text{Mn}_2(\text{CO})_{10}$ parent, with slight increases in Mn-C bond distances and $\text{C}_{\text{ax}}\text{-Mn-C}_{\text{eq}}$ bond angles. However, modification of the local electronic charge distribution is significant. The spectral changes reflect altered hybridization of metal-3*d*, -4*p*, and ligand-2*p* orbitals, and the loss of inter-ligand interaction accompanied by the spin transition associated with radical formation.

Charge-transfer Dynamics in Ru-polypyridine Complexes: We have initiated new studies of the photochromic Ru-complex $[\text{Ru}(\text{bpy})_2(\text{pyESO})]^{2+}$ which exhibits photo-driven isomerization that is predicted to be mediated by conical intersections. Time-resolved XAS at the Ru L-edge and S K-edges (ALS BL6.0.1) provide complimentary views of the isomerization dynamics, and yield the first experimental evidence of a metal-centered intermediate state. We are conducting related studies of the “light-switch” compound $[\text{Ru}(\text{bpy})_2(\text{dppp2})]^{2+}$ which exhibits photo-induced charge-transfer processes that are poorly understood, and yet are central for solar energy conversion (e.g. dye sensitized solar cells) and photo-catalysis. Time-resolved XAS at the Ru L-edge provides a quantitative understanding of the charge transfer dynamics, transient electronic structures, and the solvent role in photo-excited complexes with dppz and dppp2 ligands. One important question to be addressed is the relative time-scale of both the triplet-state interconversion (which can be tuned over an order of magnitude via solvent stabilization) and the associated recovery of the ground state. Future studies in Ru-based light-harvesting complexes will focus on molecular structure via EXAFS at the Ru K-edge, and a “ligand-view” of the charge dynamics via time-resolved XANES at the N K-edge.

5. Theory and computation -- Martin Head-Gordon, Dan Haxton and C. William McCurdy

This part of the program focuses on the theoretical description of the next generation of ultrafast XUV and X-ray experiments. To that end, we have completed an entirely new implementation of the Multiconfiguration Time-dependent Hartree Fock (MCTDHF) method with “all electrons active” based on finite-element grids in prolate spheroidal coordinates to represent the time-dependent orbitals.

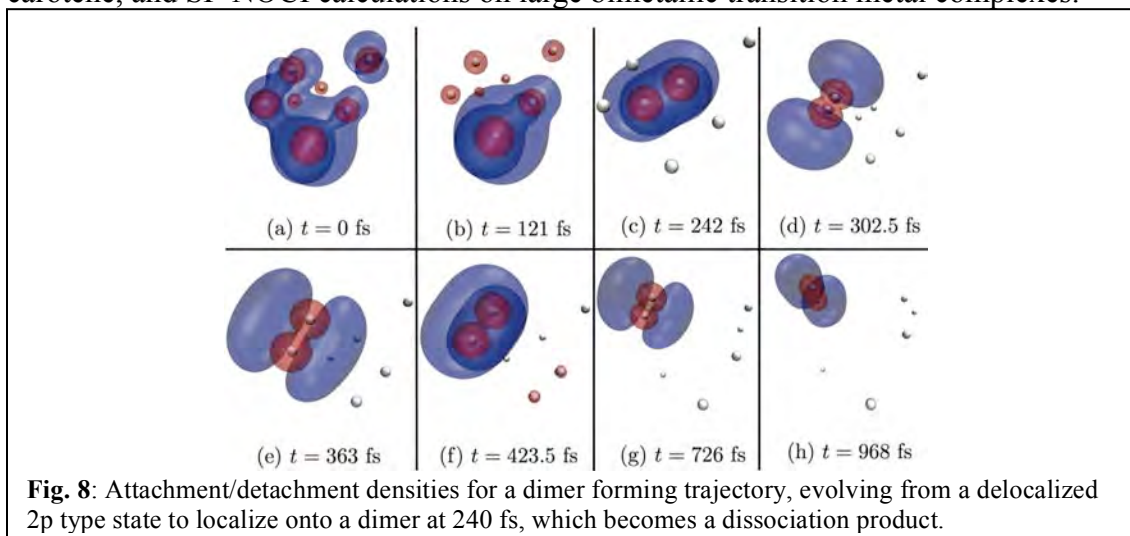


The method treats general diatomics including for the combination of (1) a rigorous representation of the ionization continuum via the method of exterior complex coordinate scaling, (2) an all-electrons-active treatment in which excitations are allowed from all orbitals and all orbitals are time dependent, and (3) the possibility of treating nuclear motion in diatomics on the same footing as electronic motion. This capability has opened the door to the complete *ab initio* simulation of both many-electron atoms and many-electron diatomic molecules in short, intense XUV and X-ray pulses. We have applied this computational capability to study the transfer of population between valence states of the lithium atom and NO molecule via core excited autoionizing states far above the ground state using pulse sequences planned proposed for stimulated X-ray Raman spectroscopy.

In Fig. 7 displays the elements of a newly-proposed scheme for the measurement of the polarization of atoms and molecules above the ionization threshold induced by intense IR or visible laser pulses using transient absorption methods. MCTDHF calculations on several systems have revealed that the polarizations (time-dependent dipole) at frequencies above the ionization threshold induced by a combination of an intense visible or IR pulse, and a sub-femtosecond XUV pulse are additive over a wide range of intensities and time delays. That fact allows us to use only the transient absorption spectra for three time delays of the XUV pulse relative to the intense pump pulse and a knowledge of the characteristics of the pulses themselves to extract the polarization due to only the pump pulse. This measurement technique is predicted to be robust under realistic experimental conditions and uncertainty in the transient absorption spectrum.

The crucial photochemical events in processes ranging from vision to light-harvesting to light emission involve ultrafast processes that involve multiple excited states, including multi-electron excited states. Experiments provide one window on the relevant states while first principles computations offers another, complementary, view. We have been making progress on the development of viable methods to calculate multielectron excited

states, using new complete active space spin-flipping ideas, and non-orthogonal configuration interaction, and, most recently, the two combined. These methods have the ability to be applied to large systems, as exemplified by NOCI calculations on beta carotene, and SF-NOCI calculations on large bimetallic transition metal complexes.



We completed *ab initio* trajectory studies that explore post-electronic excitation dynamics of small helium clusters, as a simulation counterpart to UXSL experiments. The dynamics typically show dramatic cluster fragmentation, including a small fraction of dimers (a sample trajectory is shown in Fig. 8). Additionally, the development of local excited state methods that are capable of treating much larger cluster sizes than standard algorithms is approaching production capability.

UXSL Publications, by Subtask (2012-2014)

1. S. Chen, M. J. Bell, A. R. Beck, H. Mashiko, M. Wu, A. N. Pfeiffer, M. B. Gaarde, D. M. Neumark, S. R. Leone, and K. J. Schafer, "Light-induced states in attosecond transient absorption spectra of laser-dressed helium." *Phys. Rev. A* **86**, 6 (2012).
2. M. J. Bell, A. R. Beck, H. Mashiko, D. M. Neumark, and S. R. Leone, "Intensity dependence of light induced states in transient absorption of laser dressed helium measured with isolated attosecond pulses." *J. Mod. Opt.* **60**, 1506 (2013).
3. A. N. Pfeiffer, M. J. Bell, A. R. Beck, H. Mashiko, D. M. Neumark, and S. R. Leone, "Alternating absorption features during attosecond pulse propagation in a laser-controlled gaseous medium." *Phys. Rev. A* **88**, 051402(R) (2013).
4. H. Mashiko, M. J. Bell, A. R. Beck, D. M. Neumark, and S. R. Leone, "Frequency Tunable Attosecond Apparatus." in *Progress in Ultrafast Intense Laser Science X*, K. Yamanouchi, G. Paulus, D. Mathur, eds., Springer Science+Business Media, Inc. (2014).
5. B. Bernhardt, A. R. Beck, X. Li, E. R. Warrick, M. J. Bell, D. J. Haxton, C. W. McCurdy, D. M. Neumark, and S. R. Leone, "High-spectral-resolution attosecond absorption spectroscopy of autoionization in xenon." *Phys. Rev. A* **89**, 023408 (2014).
6. A.R. Beck, B. Bernhardt, E.R. Warrick, M. Wu, S. Chen, M. Gaarde, K. Schafer, D.M. Neumark, and S.R. Leone, "Attosecond transient absorption probing of electronic superpositions of bound states in neon: detection of quantum beats." *New J. Phys.*, *submitted* (2014).

7. Allison T.K., Tao H., Glover W.J., Wright T., Stooke A.M., Khurmi C., van Tilborg J., Liu Y., Falcone R.W., Martinez T.J., Belkacem A., “Ultrafast internal conversion in ethylene. II. Mechanisms and pathways for quenching and hydrogen elimination”, *Jour. Chem. Phys.* **136**, 124317 (2012).
8. Cryan, J.P., Glowonia J.M., Andreasson J., Belkacem A., Berrah N., Blaga C.I., Bostedt C., Bozek J., Cherepkov N.A., Dimauro L.F., Fang L., Gessner O., Guhr M., Hajdu J., Hertlein M.P., Hoener M., Korlinov O., Marangos J.P., March A.M., McFarland B.K., Merdji H., Messerschmidt M., Petrovic V.S., Raman C., Ray D., Reis D.A., Semenov S.K., Trigo M., White J.L., White W., Young L., Bucksbaum P.H., Coffee R.N., “Molecular frame Auger electron spectrum from N₂”, *Jour. Phys. B – At. Mol. Opt. Phys.* **45**, 055601 (2012).
9. Y. Jiang, A. Senftleben, M. Kurka, A. Rudenko, L. Foucar, O. Herrwerth, M. Kling, M. Lezius, J. Tilborg, A. Belkacem, K. Ueda, D. Rolles, R. Treusch, Y. Zhang, Y. Liu, C. Schroeter, J. Ullrich and R. Moshhammer, “Ultrafast dynamics in acetylene clocked in a femtosecond XUV stopwatch”, *Journal of Physics B*, **46**, 164027 (2013).
10. Oliver Bünermann, Oleg Kornilov, Stephen R. Leone, Daniel M. Neumark, and Oliver Gessner, “Femtosecond Extreme Ultraviolet Ion Imaging of Ultrafast Dynamics in Electronically Excited Helium Nanodroplets”, *IEEE J. Sel. Top. Quantum Electron.* **18**, 308 (2012).
11. J. P. Cryan, J. M. Glowonia, J. Andreasson, A. Belkacem, N. Berrah, C. I. Blaga, C. Bostedt, J. Bozek, N. A. Cherepkov, L. F. DiMauro, L. Fang, O. Gessner, M. Gühr, J. Hajdu, M. P. Hertlein, M. Hoener, O. Kornilov, J. P. Marangos, A. M. March, B. K. McFarland, H. Merdji, M. Messerschmidt, V. Petrovic, C. Raman, D. Ray, D. Reis, S. K. Semenov, M. Trigo, J. White, W. White, L. Young, P. H. Bucksbaum, and R. N. Coffee, “Molecular Frame Auger Electron Energy Spectrum from N₂”, *J. Phys. B: At. Mol. Opt. Phys.* **45**, 055601 (2012).
12. Fabian Weise, Daniel M. Neumark, Stephen R. Leone, and Oliver Gessner, “Differential Near-Edge Coherent Diffractive Imaging for Element-Specific Contrast Enhancement in Ultrafast Imaging Applications”, *Opt. Express* **20**, 26167 (2012).
13. Oliver Bünermann, Oleg Kornilov, Daniel J. Haxton, Stephen R. Leone, Daniel M. Neumark, and Oliver Gessner, “Ultrafast Probing of Ejection Dynamics of Rydberg Atoms and Molecular Fragments from Electronically Excited Helium Nanodroplets”, *J. Chem. Phys.*, **137**, 214302 (2012).
14. Ming-Fu Lin, Adrian N. Pfeiffer, Daniel M. Neumark, Stephen R. Leone, and Oliver Gessner, “Strong-Field induced XUV Transmission and Autler-Townes Multiplet Splitting in $4d^{1}6p$ Core-excited Xe studied by Femtosecond XUV Transient Absorption Spectroscopy”, *J. Chem. Phys.* **137**, 244305 (2012).
15. Olga Smirnova and Oliver Gessner, “Attosecond Spectroscopy”, *Chem. Phys.* **414**, 1 (2013).
16. Andrey Shavorskiy, Amy Cordones, Josh Vura-Weis, Katrin Siefertmann, Daniel Slaughter, Felix Sturm, Fabian Weise, Matthew Strader, Hana Cho, Ming-Fu Lin, Camila Bacellar, Champak Khurmi, Marcus Hertlein, Jinghua Guo, Hendrik Bluhm, Tolek Tyliczszak, David Prendergast, Giacomo Coslovich, Joseph Robinson, Robert Kaindl, Robert W. Schoenlein, Ali Belkacem, Thorsten Weber, Daniel M. Neumark, Stephen R. Leone, Dennis Nordlund, Hirohito Ogasawara, Anders R. Nilsson, Oleg Krupin, Joshua J. Turner, William F. Schlotter, Michael R. Holmes, Philip A. Heimann, Marc Messerschmidt, Michael P. Minitti, Martin Beye, Sheraz Gul, Jin Zhang, Nils Huse, and Oliver Gessner, “Time-Resolved X-Ray Photoelectron Spectroscopy Techniques for Real-Time Studies of Interfacial Charge Transfer Dynamics”, *Application of Accelerators in Research and Industry*, AIP Conf. Proc. **1525**, 475 (2013).
17. Ming-Fu Lin, Daniel M. Neumark, Oliver Gessner, and Stephen R. Leone, “Ionization and Dissociation Dynamics of Vinyl Bromide Probed by Femtosecond Extreme Ultraviolet Transient Absorption Spectroscopy”, *J. Chem. Phys.* **140**, 064311 (2014).
18. Kristina D. Closser, Oliver Gessner, and Martin Head-Gordon, “Simulations of the dissociation of small helium clusters with ab initio molecular dynamics in electronically excited states”, *J. Chem. Phys.* **140**, 134306 (2014).

19. K. R. Siefertmann, C. D. Pemmaraju, S. Nepl, A. Shavorskiy, A. A. Cordones, J. Vura-Weis, D. S. Slaughter, F. P. Sturm, F. Weise, H. Bluhm, M. L. Strader, H. Cho, M.-F. Lin, C. Bacellar, C. Khurmi, J. Guo, G. Coslovich, J. S. Robinson, R. A. Kaindl, R. W. Schoenlein, A. Belkacem, D. M. Neumark, S. R. Leone, D. Nordlund, H. Ogasawara, O. Krupin, J. J. Turner, W. F. Schlotter, M. R. Holmes, M. Messerschmidt, M. P. Minitti, S. Gul, J. Z. Zhang, N. Huse, D. Prendergast, and O. Gessner, "Atomic Scale Perspective of Ultrafast Charge Transfer at a Dye-Semiconductor Interface", *J. Phys. Chem. Lett.* **5**, 2753 (2014).
20. Luis F. Gomez, Ken R. Ferguson, James P. Cryan, Camila Bacellar, Rico Mayro P. Tanyag, Curtis Jones, Sebastian Schorb, Denis Anielski, Ali Belkacem, Charles Bernando, Rebecca Boll, John Bozek, Sebastian Carron, Gang Chen, Tjark Delmas, Lars Englert, Sascha W. Epp, Benjamin Erk, Lutz Foucar, Robert Hartmann, Alexander Hexemer, Martin Huth, Justin Kwok, Stephen R. Leone, Jonathan H.S. Ma, Filipe R. N. C. Maia, Erik Malmerberg, Stefano Marchesini, Daniel M. Neumark, Billy Poon, James Prell, Daniel Rolles, Benedikt Rudek, Artem Rudenko, Martin Seifrid, Katrin R. Siefertmann, Felix P. Sturm, Michele Swiggers, Joachim Ullrich, Fabian Weise, Petrus Zwart, Christoph Bostedt, Oliver Gessner, Andrey F. Vilesov, "Shapes and Vorticities of Superfluid Helium Nanodroplets", *Science* **345**, 906 (2014).
21. Andrey Shavorskiy, Stefan Nepl, Daniel S. Slaughter, James P. Cryan, Katrin R. Siefertmann, Fabian Weise, Ming-Fu Lin, Camila Bacellar, Michael P. Ziemkiewicz, Ioannis Zegkinoglou, Matthew W. Fraund, Champak Khurmi, Marcus P. Hertlein, Travis W. Wright, Nils Huse, Robert W. Schoenlein, Tolek Tylliszczak, Giacomo Coslovich, Joseph Robinson, Robert A. Kaindl, Bruce S. Rude, Andreas Ölsner, Sven Mähl, Hendrik Bluhm, and Oliver Gessner, "Sub-Nanosecond Time-Resolved Ambient-Pressure X-ray Photoelectron Spectroscopy Setup for Pulsed and Constant Wave X-ray Light Sources", *Rev. Sci. Instrum.* **85**, 093102 (2014).
22. Stefan Nepl, Andrey Shavorskiy, Ioannis Zegkinoglou, Matthew Fraund, Daniel S. Slaughter, Tyler Troy, Michael P. Ziemkiewicz, Musahid Ahmed, Sheraz Gul, Bruce Rude, Jin Z. Zhang, Anton S. Tremsin, Per-Anders Glans, Yi-Sheng Liu, Cheng Hao Wu, Jinghua Guo, Miquel Salmeron, Hendrik Bluhm, and Oliver Gessner, "Capturing interfacial photo-electrochemical dynamics with picosecond time-resolved X-ray photoelectron spectroscopy", *Faraday Discuss., Advance Article* (2014), DOI: 10.1039/C4FD00036F.
23. S. Nepl, Y.-S. Liu, C.-H. Wu, A. Shavorskiy, I. Zegkinoglou, T. Troy, D. S. Slaughter, M. Ahmed, A. S. Tremsin, J.-H. Guo, P.-A. Glans, M. Salmeron, H. Bluhm, and O. Gessner, "Toward Ultrafast In Situ X-Ray Studies of Interfacial Photoelectrochemistry", in *Ultrafast Phenomena XIX*, Kaoru Yamanouchi, Steven Cundiff, Regina de Vivie-Riedle, Makoto Kuwata-Gonokami, Louis DiMauro, Eds., Springer, *submitted* (2014).
24. Michael P. Ziemkiewicz, Camila Bacellar, Katrin Siefertmann, Stephen R. Leone, Daniel M. Neumark, and Oliver Gessner, "Femtosecond time-resolved XUV + UV photoelectron imaging of pure helium nanodroplets", *J. Chem. Phys.*, *submitted* (2014).
25. H. Cho, M.L. Strader, K. Hong, L. Jamula, E.M. Gullikson, T.K. Kim, F.M.F. de Groot, J.K. McCusker, R.W. Schoenlein, and N. Huse, "Ligand-field symmetry effects in Fe(II) polypyridyl compounds probed by transient X-ray absorption spectroscopy," *Faraday Discuss.* **157**, 463-474 (2012).
26. B.E. Van Kuiken, N. Huse, H. Cho, M.L. Strader, M.S. Lynch, R.W. Schoenlein, and M. Khalil, "Probing the electronic structure of a photoexcited solar cell dye with transient X-ray absorption spectroscopy," *J. Phys. Chem. Lett.*, **3**, 1695-1700 (2012).
27. B. Van Kuiken, M. Valiev, S. Daifuku, C. Bannan, M. Strader, H. Cho, N. Huse, R. Schoenlein, N. Govind, M. Khalil, "Simulating Ru L₃-edge X-ray Absorption Spectroscopy with Time-Dependent Density Functional Theory: Model Complexes and Electron Localization in Mixed-Valence Metal Dimers," *J. Phys. Chem. A*, **117**, 4444-4454 (2013).
28. D. J. Haxton, K. V. Lawler and C. W. McCurdy, "Single photoionization of Be and HF using the multiconfiguration time-dependent Hartree-Fock method," *Phys. Rev. A* **86**, 013406 (2012).

29. X. Li, C. W. McCurdy and D. J. Haxton, "Population transfer between valence states via core-hole states using ultrafast pulses: the limitations of adiabatic passage," *Phys. Rev. A* **89**, 031404(R) 2014.
30. D. J. Haxton and C. W. McCurdy, "Ultrafast population transfer among valence levels of a molecule with X-ray pulses," *Phys. Rev. Letts.* (*submitted to Physical Review A*).
31. E. Luppi and M. Head-Gordon, "Computation of high harmonic generation spectra of H₂ and N₂ due to intense laser pulses using quantum chemistry methods and time-dependent density functional theory," *Mol. Phys.* **110**, 909-923 (2012).
32. P.M. Zimmerman, C.B. Musgrave, and M. Head-Gordon, "A Correlated Electron View of Singlet Fission", *Acc. Chem. Res.* **46**, 1339-1347 (2013).
33. E. Luppi and M. Head-Gordon, "The role of Rydberg and continuum levels in computing high harmonic generation spectra of the hydrogen atom using time-dependent configuration interaction", *J. Chem. Phys.* **139**, 164121 (2013).
34. E.J. Sundstrom and M. Head-Gordon, "Non-Orthogonal Configuration Interaction for the Calculation of Multi-electron Excited States", *J. Chem. Phys.* **140**, 114103 (2014).
35. K. D. Closser, O. Gessner, and M. Head-Gordon, "Ab initio molecular dynamics simulations of the photodissociation of small helium clusters", *J. Chem. Phys.* **140**, 134306 (2014).
36. D. Zuev, T.-C. Jagau, K.B. Bravaya, E. Epifanovsky, Y. Shao, E. Sundstrom, M. Head-Gordon and A.I. Krylov, "Complex absorbing potentials within EOM-CC family of methods: Theory, implementation, and benchmarks", *J. Chem. Phys.* **141**, 024102 (2014).
37. N.J. Mayhall, P.R. Horn, E.J. Sundstrom, and M. Head-Gordon, "Spin-flip non-orthogonal configuration interaction: A variational and almost black-box method for describing strongly correlated electrons", *PCCP* (submitted, June, 2014).

Page is intentionally blank.

Early Career: Ultrafast X-ray Studies of Intramolecular and Interfacial Charge Migration

Oliver Gessner

Chemical Sciences Division, Lawrence Berkeley National Laboratory, Berkeley, CA 94720

OGessner@lbl.gov

Program Scope: Interfacial electronic dynamics are key processes in many emerging technologies aimed at providing scalable, low-cost options for photovoltaic and photocatalytic solar energy conversion. This program is focused at developing and applying time-domain X-ray spectroscopy and imaging techniques to enable an atomic-scale understanding of the fundamental mechanisms underlying interfacial photoelectrochemical performance. In particular, ultrafast dynamics at molecule-semiconductor and liquid-semiconductor interfaces are studied by time-resolved X-ray photoelectron spectroscopy (TRXPS) and time-resolved X-ray absorption spectroscopy (TRXAS) techniques, which are deployed at the Linac Coherent Light Source (LCLS) and the Advanced Light Source (ALS). They are complemented by the development of laboratory-based time-resolved near-edge coherent diffractive imaging (CDI) techniques driven by femtosecond high-harmonic generation (HHG) light sources.

Recent Progress and Future Plans: In a concerted effort of femtosecond TRXPS measurements at the LCLS and constrained density functional theory (CDFT) calculations, an interfacial charge-transfer state has been identified as the intermediate electronic configuration that precedes free charge carrier generation upon photoexcitation

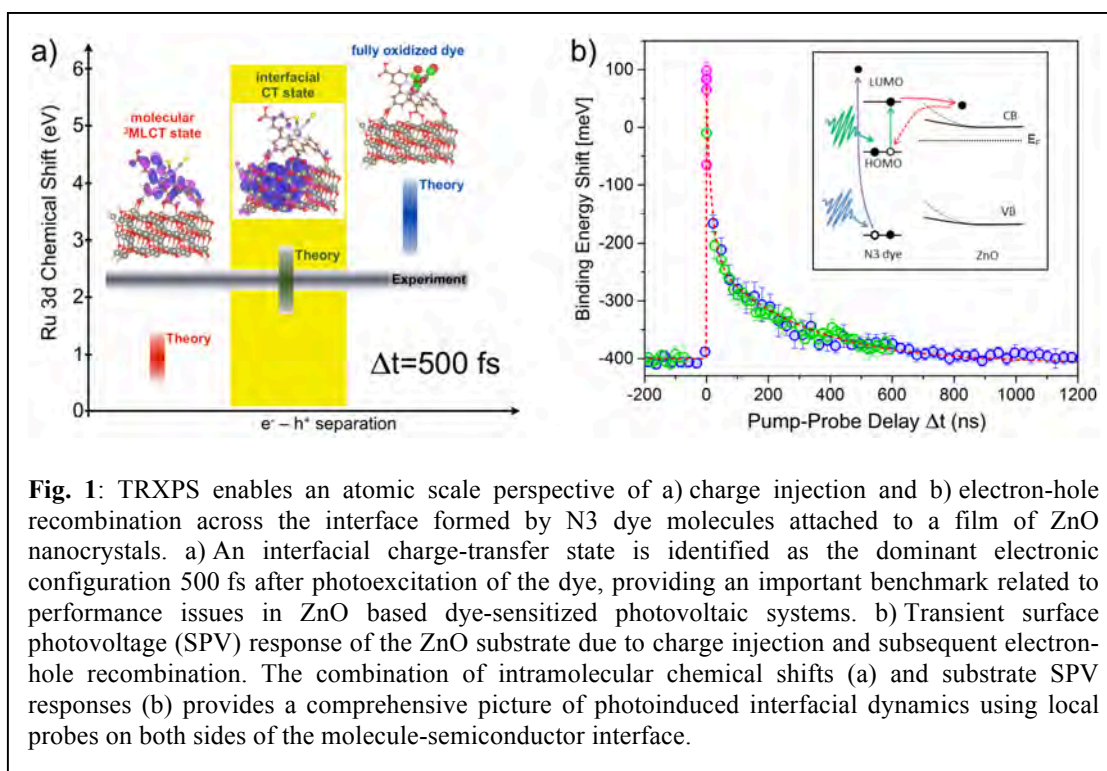


Fig. 1: TRXPS enables an atomic scale perspective of a) charge injection and b) electron-hole recombination across the interface formed by N3 dye molecules attached to a film of ZnO nanocrystals. a) An interfacial charge-transfer state is identified as the dominant electronic configuration 500 fs after photoexcitation of the dye, providing an important benchmark related to performance issues in ZnO based dye-sensitized photovoltaic systems. b) Transient surface photovoltage (SPV) response of the ZnO substrate due to charge injection and subsequent electron-hole recombination. The combination of intramolecular chemical shifts (a) and substrate SPV responses (b) provides a comprehensive picture of photoinduced interfacial dynamics using local probes on both sides of the molecule-semiconductor interface.

of a film of ZnO nanocrystals sensitized with N3 dye molecules (Fig. 1a). The results provide an important benchmark for the long-standing quest to identify the fundamental mechanisms underlying the performance differences of TiO₂- and ZnO-based hybrid molecule-semiconductor systems for photoinduced charge generation. Overlapping spectroscopic features from neutral and ionized dye molecules as well as potential interfacial states pose a significant challenge to distinguish different proposed scenarios with conventional time-domain techniques. In contrast, the element-specificity of TRXPS provides a site-selective view of the interfacial charge transfer process from the viewpoint of the Ru metal center of the dye. The measured chemical shift of the Ru 3d photoline within the critical first picosecond after photoexcitation of the dye is compared to a series of CDFT calculations describing ranges of expected chemical shifts for different transient electronic configurations (Fig. 1a). The analysis provides strong support for the temporary retention of the electron in an interfacial complex in which the negative charge has already departed from the molecular dye but still resides in immediate proximity within the semiconductor substrate.

The LCLS based femtosecond time-resolved experiments are complemented by picosecond time-resolved experiments at the ALS. A novel TRXPS technique has been developed that, principally, does not require a specific beamline, provides an electron bunch-length limited temporal resolution of ~ 70 ps (FWHM), and can be applied in all operating modes of the ALS (2-bunch and multi-bunch) while making use of a large fraction of the total ALS X-ray flux. The new capability has been employed to characterize the transient surface photovoltage (SPV) response of a nanoporous N3-sensitized ZnO semiconductor substrate due to photoinduced interfacial charge-injection and recombination dynamics (Fig. 1b). While time-resolved SPV measurements have been used in the past to study electronic dynamics in semiconductors after direct, above band-gap excitation, to the best of our knowledge this is the first time that charge-injection across a molecule-semiconductor interface is probed with this method. The measurements demonstrate a substantial SPV response of the sintered nanocrystal film and provide direct insight into the dynamics induced in the electron acceptor of the dye-semiconductor interface. The relaxation dynamics are multi-exponential with at least two contributing time scales on the order of ~ 80 ps and ~ 2.3 ns. Both similarities and pointed differences of the dynamics compared to those in above band-gap excited semiconductors are observed. Efforts are underway to gain a microscopic understanding of the origins of these results. The combination of transient chemical shifts in the molecular photoemission lines and the simultaneously recorded transient SPV response of the semiconductor substrate provide previously unattainable, complementary viewpoints of the interfacial electron dynamics from both sides of the interface. In a next step, the new technique will be used to identify contributions from different moieties of the molecular dye to the charge injection process and to gain a deeper understanding of the surface and/or trap states within the molecule-semiconductor system that may contribute to the charge transfer dynamics.

A new *in situ* TRXAS technique has been developed at the ALS to study interfacial electron dynamics in photoelectrochemical devices under application-like conditions. Similar to the new TRXPS setup, the TRXAS technique can be employed in all operating

modes of the ALS with bunch-length limited time-resolution (~ 70 ps FWHM). First *in operando* TRXAS spectra have been recorded for a photoelectrochemical cell based on a thin film hematite ($\alpha\text{-Fe}_2\text{O}_3$) working electrode exposed to an aqueous NaOH electrolyte. A series of experiments is scheduled to probe the nature and dynamics of interfacial hole states, which facilitate the electrochemical activity of the liquid-hematite interface.

Publications

1. Olga Smirnova and Oliver Gessner, "Attosecond Spectroscopy", Chem. Phys. **414**, 1 (2013).
2. Andrey Shavorskiy, Amy Cordones, Josh Vura-Weis, Katrin Siefermann, Daniel Slaughter, Felix Sturm, Fabian Weise, Matthew Strader, Hana Cho, Ming-Fu Lin, Camila Bacellar, Champak Khurmi, Marcus Hertlein, Jinghua Guo, Hendrik Bluhm, Tolek Tylliszczak, David Prendergast, Giacomo Coslovich, Joseph Robinson, Robert A. Kaindl, Robert W. Schoenlein, Ali Belkacem, Thorsten Weber, Daniel M. Neumark, Stephen R. Leone, Dennis Nordlund, Hirohito Ogasawara, Anders R. Nilsson, Oleg Krupin, Joshua J. Turner, William F. Schlotter, Michael R. Holmes, Philip A. Heimann, Marc Messerschmidt, Michael P. Minitti, Martin Beye, Sheraz Gul, Jin Z. Zhang, Nils Huse, and Oliver Gessner, "Time-Resolved X-Ray Photoelectron Spectroscopy Techniques for Real-Time Studies of Interfacial Charge Transfer Dynamics", Application of Accelerators in Research and Industry, AIP Conf. Proc. **1525**, 475 (2013).
3. K. R. Siefermann, C. D. Pemmaraju, S. Neppel, A. Shavorskiy, A. A. Cordones, J. Vura-Weis, D. S. Slaughter, F. P. Sturm, F. Weise, H. Bluhm, M. L. Strader, H. Cho, M.-F. Lin, C. Bacellar, C. Khurmi, J. Guo, G. Coslovich, J. S. Robinson, R. A. Kaindl, R. W. Schoenlein, A. Belkacem, D. M. Neumark, S. R. Leone, D. Nordlund, H. Ogasawara, O. Krupin, J. J. Turner, W. F. Schlotter, M. R. Holmes, M. Messerschmidt, M. P. Minitti, S. Gul, J. Z. Zhang, N. Huse, D. Prendergast, and O. Gessner, "Atomic Scale Perspective of Ultrafast Charge Transfer at a Dye-Semiconductor Interface", J. Phys. Chem. Lett. **5**, 2753 (2014).
4. Andrey Shavorskiy, Stefan Neppel, Daniel S. Slaughter, James P. Cryan, Katrin R. Siefermann, Fabian Weise, Ming-Fu Lin, Camila Bacellar, Michael P. Ziemkiewicz, Ioannis Zegkinoglou, Matthew W. Fraund, Champak Khurmi, Marcus P. Hertlein, Travis W. Wright, Nils Huse, Robert W. Schoenlein, Tolek Tylliszczak, Giacomo Coslovich, Joseph Robinson, Robert A. Kaindl, Bruce S. Rude, Andreas Ölsner, Sven Mähl, Hendrik Bluhm, and Oliver Gessner, "Sub-Nanosecond Time-Resolved Ambient-Pressure X-ray Photoelectron Spectroscopy Setup for Pulsed and Constant Wave X-ray Light Sources", Rev. Sci. Instrum. **85**, 093102 (2014).
5. Stefan Neppel, Andrey Shavorskiy, Ioannis Zegkinoglou, Matthew Fraund, Daniel S. Slaughter, Tyler Troy, Michael P. Ziemkiewicz, Musahid Ahmed, Sheraz Gul, Bruce Rude, Jin Z. Zhang, Anton S. Tremsin, Per-Anders Glans, Yi-Sheng Liu, Cheng Hao Wu, Jinghua Guo, Miquel Salmeron, Hendrik Bluhm, and Oliver Gessner, "Capturing interfacial photo-electrochemical dynamics with picosecond time-resolved X-ray photoelectron spectroscopy", Faraday Discuss., Advance Article (2014), DOI: 10.1039/C4FD00036F.
6. S. Neppel, Y.-S. Liu, C.-H. Wu, A. Shavorskiy, I. Zegkinoglou, T. Troy, D. S. Slaughter, M. Ahmed, A. S. Tremsin, J.-H. Guo, P.-A. Glans, M. Salmeron, H. Bluhm, and O. Gessner, "Toward Ultrafast In Situ X-Ray Studies of Interfacial Photoelectrochemistry", in Ultrafast Phenomena XIX, Kaoru Yamanouchi, Steven Cundiff, Regina de Vivie-Riedle, Makoto Kuwata-Gonokami, Louis DiMauro, Eds., Springer, submitted (2014).

Page is intentionally blank.

Early Career Project: The Multiconfiguration Time-Dependent Hartree-Fock Method for Interactions of Molecules with Ultrafast X-Ray and Strong Laser Pulses

Daniel J. Haxton
 Lawrence Berkeley National Laboratory MS2R0100
 1 Cyclotron Road, MS 2R0100
 Berkeley, CA 94720
 djhaxton@lbl.gov

Program scope / definition

This project is based upon a computer code for solving the nonrelativistic Schrodinger equation for a small molecule, subject to arbitrarily strong laser fields, nonperturbatively. It is ab initio and includes correlated wave functions. The code was begun before the start of this project. It presently treats atoms and diatomic molecules, with an initial implementation of fully nonadiabatic motion in the internuclear degree of freedom.

The final goal of the project is a fully ab initio nonadiabatic treatment of polyatomic molecules, electronic and nuclear degrees of freedom.

Several applications of the method will be pursued, making use of the capabilities already implemented, and as additional capabilities are added.

Recent progress

1) The Cartesian sinc basis treatment for polyatomics has been implemented in a simple version of the code, for electrons only (no nuclear motion yet).

Our understanding of the underlying method is evolving. We have not yet submitted a paper describing the sinc basis function treatment. As of last year, significant progress had been made in arriving at a workable method to calculate two-electron integrals. However there are aspects of this method that we have understood more fully only recently. It seems now that the way we calculate the two-electron matrix elements is unnecessarily complicated. It appears now that our method for two electron matrix elements can be summarized as follows: We perform a resolution of the identity, approximating densities, which are sums of products of sinc functions, as sums of sinc functions, via $\text{sinc}(x) \text{sinc}(x + n\pi) \approx \delta_{0n} \text{sinc}(x)$; otherwise, we do business as usual. The paper needs to be re-phrased along these lines and then will be submitted.

New postdoc Chen Zhang will be working on the sinc DVR for polyatomics. We have not resolved two issues. 1) We wish to stretch and scale the Cartesian grid. We have expressions derived for this that we have yet to attempt to use. 2) The method should produce no corrugation in the energy of a state calculated as a function of position. At present, it is not working as it should and does produce corrugation.

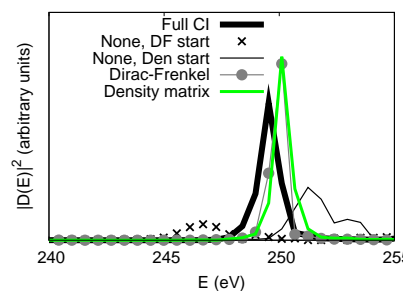
It appears that we can achieve double zeta accuracy with Neon using a grid spacing of about 0.05 bohr. We can use about 100 sinc functions on a side, for a total of one million primitive basis functions, before the storage necessary for the two-electron integrals becomes prohibitive. While this will allow interesting calculations, we would like to be able to use a finer grid. Dr Zhang is pursuing the use of contact operators, as used in effective theory in nuclear structure, for instance, for this purpose.

2) An implementation allowing restricted configuration spaces – that is, not full configuration interaction, spaces like those used in quantum chemistry like configuration interaction with singles and doubles (CISD) – is necessary in order to make the method scalable to bigger molecules. One way of doing this (in which the one electron density matrix is kept block diagonal) was already done before the project. I have also now programmed and understood the other, variational way to do it, arguably the best way, using the variational principle from which the rest of the equations are derived.

The paper on this subject, which I indicated was near submission last year, is not yet submitted. Last year I did not understand the underlying concepts and had produced a method that worked, but that I had not accurately characterized. The paper is now almost completely done, and I understand everything completely. It truly will be submitted soon.

The subject is fascinating on its own, regardless of its significance to the problem of making MCTDHF work for a large molecule. The main issue is that for some parameterized wave functions, two variational principles are equivalent, and for others, they are inequivalent. The principles are the McLachlan variational principle, which minimizes the norm of the error of the derivative with respect to time, and the Lagrangian variational principle, which conserves energy for time-independent Hamiltonians. When these are equivalent, they are collectively referred to as the Dirac-Frenkel variational principle. I believe I am the first one to understand how these principles become different within MCTDHF for restricted configuration spaces. This issue has been swept under the rug by prior authors. The upcoming paper should be regarded as the first time the MCTDHF equations have actually been explicitly completed for the general case.

To the right I show Fourier transforms of a dipole moment induced in Be near a 1s transition. One can see that the Dirac-Frenkel and Density matrix treatments of restricted configuration spaces give a peak that is similar to the Full CI result. The calculations done with restricted configuration spaces but using the Full CI equations – the “dumb” way – are labeled “None” and differ significantly from Full CI.



Below I show a table of energies, in Hartree, before and after a pulse, for a restricted configuration space in which the Lagrangian and McLachlan variational principles become equivalent. One can see that the Lagrangian principle, which is derived by considering the energy, calculates the work done by the pulse (the change in energy) to within one part in 100,000, relative to Full CI; the “dumb way” has an error of one

part in 20. These results, in particular, convince me that I have correctly implemented these variational principles. I have found that I may make an ad hoc combination of the two principles, which is more numerically stable than either alone.

	Start	Finish	Change
Full CI	-61.275139	-60.611515	0.663624
Lagrangian	-61.275135	-60.611508	0.663627
McLachlan	-61.275135	-60.611208	0.663927
Combination	-61.275135	-60.611330	0.663805
None	-61.275135	-60.645813	0.629322

3) The paper on stimulated X-ray Raman within the NO molecule that we submitted last year was rejected from PRL. We have spent a good amount of this year addressing the issues raised by the referee. At the time of writing (Sept 15 2014) there are still some calculations to finish before this paper is finally accepted. It will appear in Phys Rev A.

4) The code has been completely rewritten. It went from 40,000 to 19,500 lines of code, maintaining the same capabilities, but doing everything right and without redundancy. There are now different executable files for different coordinate systems. Coordinate system dependent routines are collected and compiled separately into separate archive files; separate versions of the code are then linked for each different archive file. This work was necessary before hiring a postdoc to begin work on the project.

The code is still written in Fortran; in 2015 I plan to convert it to C++.

Future plans

1) Dr. Zhang is working on deriving the Hamiltonian using modified prolate coordinates. Once this is finished, we will begin to use the nonadiabatic capability of the code. We will proceed to study processes like light induced conical intersections as described in the proposal.

The other applications that will be pursued include

- 2) An extensive study of NO, and stimulated X ray Raman transitions in other molecules
- 3) Control of x ray processes in strong fields
- 4) Nonadiabatic processes in strong fields

Page is intentionally blank.

Engineered Electronic and Magnetic Interactions in Nanocrystal Quantum Dots

Victor I. Klimov

Chemistry Division, C-PCS, MS-J567, Los Alamos National Laboratory
Los Alamos, New Mexico 87545, klimov@lanl.gov, <http://quantumdot.lanl.gov>

1. Program Scope

Chemically synthesized semiconductor nanocrystals (NCs), known also as nanocrystal quantum dots (QDs), have been extensively studied as both a test bed for exploring the physics of strong quantum confinement as well as a highly flexible materials platform for the realization of a new generation of solution-processed optical, electronic and optoelectronic devices. Due to readily size-tunable emission, colloidal NCs are especially attractive for applications in light-emitting diode (LED) displays, solid-state lighting, lasing, and single-photon sources. It is universally recognized that the realization of these and other prospective applications of NCs requires a detailed understanding of carrier-carrier interactions in these structures, as they have a strong effect on both recombination dynamics of charge carriers and spectral properties of emitted light. A unifying theme of this project is fundamental physics of electronic and magnetic interactions involving strongly confined carriers/spins with focus on control of these interactions via size/shape manipulation, doping/heterostructuring, and “interface engineering.” Our goals in this project include: the development of high-efficiency NC-based LEDs free from detrimental effects of Auger recombination such as efficiency “roll-off” at high currents; realization of electrically pumped single-NC light sources; the achievement of NC lasing under continuous-wave excitation; and demonstration of ferromagnetic behavior in optically-active NCs doped with magnetic impurities.

2. Recent Progress

During the past year, our work has focused on improving our understanding on nonradiative Auger recombination in QDs and devising new methods for its suppression, as well as on elucidation of the effect of Auger decay on

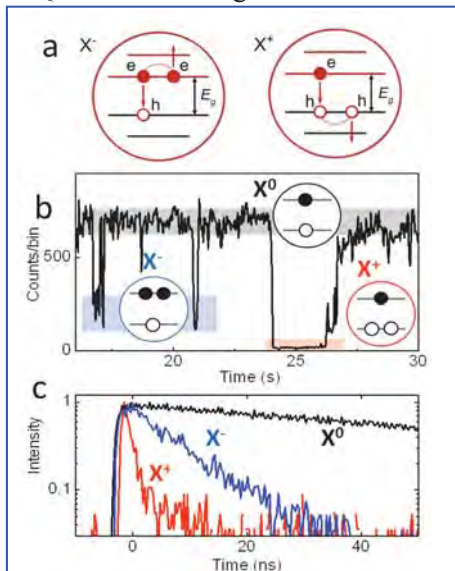


Figure 1. (a) Auger decay of a negative (left) vs. positive (right) trion. (b) PL intensity trajectory for the single CdSe/CdS QD (1.5 nm core radius, 5.5 nm shell thickness). (c) Neutral exciton (X⁰), and negative (X⁻) and positive (X⁺) trion dynamics extracted from periods of, respectively, high, intermediate and low emissivities.

the performance of QD-LEDs. Three specific areas of our research were: (1) the relationship between Auger recombination rates of charged and neutral multi-carrier states, (2) control of Auger recombination via “interface engineering,” and (3) the effect of Auger recombination on efficiency roll-off of QD-LEDs.

2.1 Auger decay of positive vs. negative trions in relation to biexciton Auger recombination. Previous studies of Auger decay have mostly focused on charge-neutral multiexcitons, such as biexcitons, triexcitons, etc. Auger dynamics of charged species have been less thoroughly investigated partially due to difficulties in controlling the degree of charging. To fill this gap, during the past project period we have conducted detailed studies of charged excitons applying a variety of ensemble and single-dot techniques.

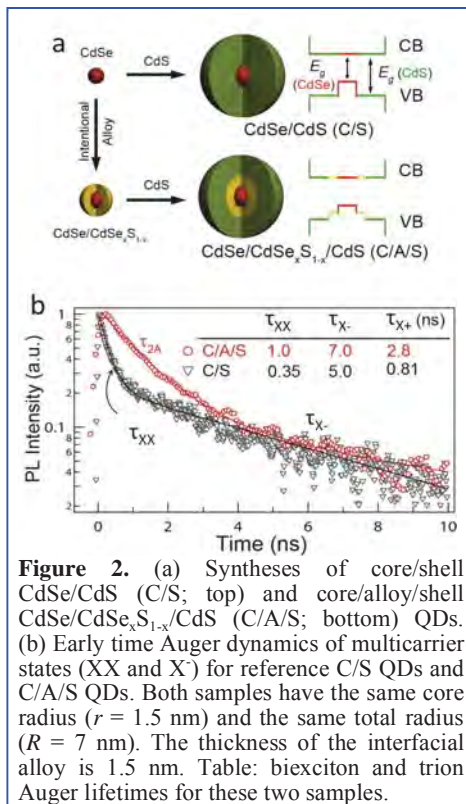
The simplest charged state is a trion, comprising a neutral exciton and either an extra electron (negative trion, X⁻) or an extra hole (positive trion, X⁺); Fig. 1a. In idealized structures with identical conduction and valence bands, the Auger lifetimes of negative (τ_{X^-}) and positive (τ_{X^+}) trions are equal to each other, and further, are four times longer than the neutral biexciton (XX) Auger lifetime. Indeed, based on “statistical” arguments, biexciton Auger decay can be described as a superposition of two independent positive-trion- and negative-trion-like pathways (Fig. 1a), implying that its rate can be presented as $1/\tau_{XX} = 2(1/\tau_{X^-} + 1/\tau_{X^+})$, which leads to $\tau_{X^-} = \tau_{X^+} = 4\tau_{XX}$ if we assume that $\tau_{X^-} = \tau_{X^+}$.

Our recent studies of trion recombination using ultrafast cathodoluminescence, however, indicated that the measured trion and biexciton lifetimes are not necessarily related by a factor of 4, suggesting that τ_{X^-} may not always equal to τ_{X^+} . In order to evaluate τ_{X^+} and τ_{X^-} and their relation to the biexciton time constant, we have

conducted independent measurements of τ_{XX} , τ_{X^+} and τ_{X^-} using single-dot spectroscopic methods applied to thick-shell CdSe/CdS QDs. In these studies we used a Hanbury Brown and Twiss setup in which the photoluminescence (PL) was split between two equivalent channels and detected with two single-photon avalanche photodiodes coupled to a time-correlated single-photon counting (TCSPC) module. By utilizing a multichannel, time-tagged, time-resolved mode we simultaneously recorded a PL intensity trajectory, PL decay dynamics of both single excitons and biexcitons, and the second-order intensity correlation function.

An example of these measurements is displayed in Fig. 1b. The intensity trajectory shows high, intermediate, and low intensity levels, associated respectively with a neutral exciton (X^0), X^- and X^+ trions. By analyzing PL photon arrival times for each intensity level, we derived the lifetimes of these three species (Fig. 1c). Further, by picking the second PL photon detected during a given excitation cycle, we measured the biexciton lifetime. Thus, using this method we were able to obtain four time constants (τ_X , τ_{XX} , τ_{X^+} , and τ_{X^-}) simultaneously from a single measurement. For the CdSe/CdS QD shown in Fig. 1c, this measurement yields $\tau_{X^-} = 9.1$ ns and $\tau_{X^+} = 1.5$ ns, indicating a large ~ 6 -fold difference between negative and positive trion lifetimes. This disparity can be explained by two factors. One is the high density of valence-band states common of II-VI semiconductors, which favors the X^+ pathways by making it easier to meet the energy conservation requirement for Auger processes involving re-excitation of a hole (Fig 1a, right). The second factor relates to a much greater degree of confinement experienced by the hole in the CdSe/CdS QDs (confined to the QD core) vs. the electron (delocalized over the entire QD), which further enhances the rate of the X^+ Auger channel.

Interestingly, despite a large disparity between the τ_{X^-} and τ_{X^+} time constants, they still can be used to accurately predict the biexciton lifetime. For example, based on the measured X^- and X^+ dynamics in Fig. 1c, the expected value of τ_{XX} is 0.64 ns, which is in close correspondence with the result of direct measurements (0.72 ns). This relationship between trion and biexciton lifetimes was systematically observed for all studied core/shell samples, indicating that independent of exact values for τ_{X^-} and τ_{X^+} the XX decay can be always be described in terms of two parallel X^+ and X^- channels. In CdSe/CdS-based systems, it is dominated by the X^+ pathway (that is, $\tau_{XX} \approx \tau_{X^+}/2$), suggesting that the suppression of biexciton Auger recombination requires primarily the suppression of the X^+ decay. Based on this finding, in our work on Auger-rate engineering (see next section) we have focused on manipulating the rate of positive trion decay.



2.2 Suppression of Auger recombination via “interface engineering.”

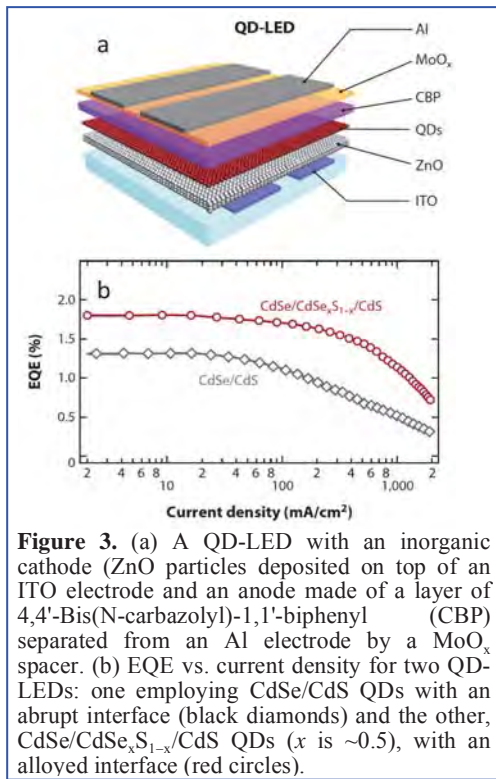
In monocomponent QDs, the Auger recombination time scales linearly with particle volume (sometimes referred to as a V -scaling). Follow-up studies conducted within the present project have shown that V -scaling is a universal trend observed for a large number of QD compositions. Calculations by Cragg & Efros (*Nano Lett.* **10**, 313, 2010) suggest that in addition to QD size, the shape of the confinement potential also has a significant effect on Auger decay rate, as it influences the matrix element of the Auger transition. Specifically, these calculations have demonstrated that by *smoothing* the confinement potential (by going, e.g., from a sharp step-like potential to a smooth parabolic profile) one can achieve orders-of-magnitude reduction in the rate of Auger decay.

The correlation between unintentional interfacial alloying and suppression of biexciton Auger recombination in CdSe/CdS QDs with a varied shell thickness (Garcia-Santamaria, et al., *Nano Lett.* **11**, 687, 2011) provided strong indication that the shape of the confinement does play an important role in Auger recombination. In this project, we have directly addressed this problem by studying carrier dynamics in core/shell CdSe/CdS QDs with a well-defined CdSe_xS_{1-x} alloy layer incorporated between the core and the shell. These studies were enabled by a novel synthesis that allowed for a much faster growth of a thick CdS shell compared to the more traditional successive ionic layer adsorption and reaction (SILAR) method; this was essential for avoiding unintentional alloying at the CdSe/CdS interface. Using this

method we synthesized structures with two distinct interfaces: one with a sharp core-shell boundary (C/S QDs) and the other with a $\text{CdSe}_x\text{S}_{1-x}$ alloy layer incorporated between the core and the shell (C/A/S QDs; see Fig. 2a). Grading of the core/shell interface affects primarily the hole confinement potential, and therefore, is expected to influence the X^+ Auger recombination pathway that is dominant in these structures (see previous section).

Side-by-side studies of the spectroscopic properties of these QDs indicated that the incorporation of an interfacial alloy layer did not have any appreciable effect on single-exciton properties, but strongly affected biexciton dynamics (Fig. 2b). Specifically, we observed a considerable lengthening of τ_{XX} accompanied by an increase in the biexciton emission efficiency. These observations were consistent with significant suppression of Auger recombination arising from smoothing of the confinement potential. These findings demonstrate the large potential of a new approach of *interface engineering* for manipulating the rate of Auger decay and perhaps other Auger-type processes such as Auger ionization and carrier multiplication.

2.3 Effect of Auger recombination on performance of QD-LEDs. To evaluate the practical benefits of interface engineering we have conducted side-by-side comparison of the performance of LEDs fabricated from CdSe/CdS



QDs with a sharp core/shell interface to those made using similar QDs but with an intermediate $\text{CdSe}_{0.5}\text{S}_{0.5}$ alloy layer. In our LEDs we apply a so-called inverted architecture in which the QD active layer is sandwiched between an inorganic ZnO electron transport layer and an organic hole transport layer based on conjugated molecules (Fig. 3a). This architecture has been shown previously to produce low turn-on voltage (\approx QD band gap), high external quantum efficiencies (EQEs) at practical brightness ($100 - 1000 \text{ cd/m}^2$) and good operational stability (half lifetime ~ 500 hr). By analyzing carrier dynamics directly within the QD active layer we detect a considerable degree of QD charging with extra electrons as a result of spontaneous charge injection from the cathode, which occurs due to energetic proximity of the QD conduction-band level to the Fermi level of ZnO. The presence of extra carriers in the QD results in activation of nonradiative Auger decay, which greatly reduces LED efficiency especially at large driving currents leading to EQE roll-off (known also as *droop*). By comparing LEDs fabricated from alloyed QDs to those made of QDs with a sharp core/shell interface we observe a considerable improvement in performance for alloyed structures which is a direct consequence of suppression of Auger recombination. In addition to a ca. two-fold improvement in the absolute EQE, the use of alloyed QDs pushed the onset of EQE roll-off to three-fold higher current density (Fig. 3b). This work provides convincing evidence that the efficiency roll-off in QD-LEDs originates from Auger recombination rather than field-induced separation between electrons and holes; further, it demonstrates a practical solution to this problem involving the use of “interface-engineered” QDs with suppressed Auger recombination.

3. Future Plans

In our future work we will continue exploitation “interface engineering” for achieving a more complete suppression of Auger decay. Specifically, we will develop and study structures in which not only a hole (as in our existing QDs) but also an electron experiences a graded confinement potential which should allow us to suppress Auger decay channels involving re-excitation of either an electron or a hole (known, respectively, as negative- and positive-trion pathways). We will also explore the type-II energy alignment of electronic states in heterostructured QDs for controlling conduction-to-valence band coupling as a means for suppressing Auger decay. We plan to extend our work on Auger decay engineering to new compositions, including III-V semiconductors (e.g., InP and InSb) as well as I-III-VI $_2$ materials such as CuInS_2 and CuInSe_2 . These will allow us to access near-infrared (near-IR) spectral energies relevant to telecommunications and should also facilitate

applications in real-life technologies by eliminating concerns associated with the toxicity of Cd-containing materials.

In addition to ensemble spectroscopic methods, the newly developed structures will be studied using single-NC techniques, which will allow us to characterize heterogeneities in single- and multiexciton properties in relation to structural parameters of the samples. Our previous studies on this topic focused on elucidating the mechanisms for PL intermittency, and the effect of Auger recombination or a proximal metal nanostructure on statistical properties of emitted light. We have also demonstrated a new mechanism for photon antibunching using a dynamic hole-blockade in core/shell NCs with exceptionally thick shells, termed by us “dot-in-bulk” (DiB) NCs.

In our future studies, we will apply the developed methodology for characterizing single/multiexciton dynamics as well as statistical properties of emitted light in novel engineered NCs including those with emission in the near-infrared (IR). The results of these studies will help optimize NC fabrication procedures for a more complete and uniform suppression of Auger decay. In our work on single-photon emitters, we will explore the use of the hole-blockade phenomenon for demonstrating strong photon antibunching at both visible and IR energies. We will begin this work using optical excitation and eventually extend it to the regime of electrical charge injection by adapting previously reported QD-LED architectures.

The newly developed NCs will be incorporated into proof-of-principle device structures including LEDs and light-emitting field-effect transistors. Evaluation of device performance conducted in parallel with spectroscopic studies of QDs directly within the devices will help us better understand their operational principles as well as the impact of various physical processes (e.g., Auger recombination) on their output characteristics (e.g., efficiency, brightness, “turn-on” bias, etc.). The feedback from these studies will be used to optimize the structural parameters of the NCs for specific applications.

4. Publications (2012 - 2014)

1. J. Lim, B. G. Jeong, M. Park, J. K. Kim, J. M. Pietryga, Y.-S. Park, V. I. Klimov, C. Lee, D.C. Lee, W.K. Bae, *Influence of shell thickness on the performance of light emitting devices based on CdSe/Zn_{1-x}Cd_xS core/shell quantum dots*, Adv. Mater., in press (2014)
2. Y.-S. Park, W. K. Bae, J. M. Pietryga, V. I. Klimov, *Auger recombination of biexcitons and negative and positive trions in individual quantum dots*, ACS Nano **8**, 7288 (2014).
3. S. Brovelli, W. K. Bae, F. Meinardi, M. Lorenzon, C. Galland, V. I. Klimov, *Electrochemical control of two-color emission from colloidal dot-in-bulk nanocrystals*, Nano Lett. **5**, 3855 (2014).
4. V. I. Klimov, *Multicarrier interactions in semiconductor nanocrystals in relation to the phenomena of Auger recombination and carrier multiplication*, Annu. Rev. Condens. Matter Phys. **5**, 13.1 (2014).
5. S. Brovelli, W. K. Bae, C. Galland, U. Giovanella, F. Meinardi, V. I. Klimov, *Dual-color electroluminescence from dot-in-bulk nanocrystals*, Nano Lett. **14**, 486 (2014).
6. Y.-S. Park, W. K. Bae, L. A. Padilha, J. M. Pietryga, V. I. Klimov, *Effect of the core/shell interface on Auger recombination evaluated by single-quantum dot spectroscopy*, Nano Lett. **13**, 396 (2013)
7. W. K. Bae, S. Brovelli, V. I. Klimov, *Spectroscopic insights into the performance of quantum dot light-emitting diodes*, MRS Bulletin **38**, 721 (2013).
8. C. Galland, S. Brovelli, W.K. Bae, L.A. Padilha, F. Meinardi, V.I. Klimov, *Dynamic hole blockade yields two-color quantum and classical light from ‘dot-in-bulk’ nanocrystals*, Nano Lett. **13**, 321 (2013)
9. L.A. Padilha, W.K. Bae, V.I. Klimov, J.M. Pietryga, R.D. Schaller, *Response of semiconductor nanocrystals to extremely energetic excitation*, Nano Lett. **13**, 925 (2013).
10. Y.-S. Park, Y. Ghosh, Y. Chen, A. Piryatinski, P. Xu, N. H. Mack, H. -L. Wang, V. I. Klimov, J. A. Hollingsworth, H. Htoon, *Super-Poissonian statistics of photon emission from single core/shell nanocrystals coupled to metal nanostructures*, Phys. Rev. Lett. **110**, 117401 (2013).
11. A. Pandey, S. Brovelli, R. Viswanatha, J.M. Pietryga, V. I. Klimov, S. A. Crooker, *Long-lived photoinduced magnetization in copper doped ZnSe–CdSe core-shell nanocrystals*, Nature Nanotech. **7**, 792 (2012).
12. S. Brovelli, C. Galland, R. Viswanatha, V. I. Klimov, *Tuning radiative recombination in Cu-doped nanocrystals via electrochemical control of surface trapping*, Nano Lett. **12**, 4327 (2012).
13. B. N. Pal, Y. Ghosh, S. Brovelli, R. Laocharoensuk, V. I. Klimov, Jennifer Hollingsworth, H. Htoon, *“Giant” CdSe/CdS core/shell nanocrystal quantum dots as efficient electroluminescent materials: Strong influence of shell thickness on light-emitting diode performance*, Nano Lett. **12**, 331 (2012).

PULSE Ultrafast Chemical Science Program

Philip Bucksbaum (spokesperson), David Reis, Kelly Gaffney, Markus Guehr, Claudiu Stan, Shambhu Ghimire, and Todd Martinez

Chemical Science Division, SLAC National Accelerator Laboratory, Menlo Park, CA

Science objectives: The PULSE Ultrafast Chemical Science Program at SLAC focuses on ultrafast chemical physics research enabled by LCLS, the world's first hard x-ray free-electron laser. Our overarching goal is to establish research at SLAC that makes optimal use of LCLS and LCLS-II for fundamental discoveries and new insights in ultrafast science. The on-site presence of LCLS with its facilitating connections to our research is one of two distinguishing advantages of this program within the AMOS portfolio. Our other advantage is our close connection to Stanford University maintained through the **Stanford PULSE Institute**. These help to keep us competitive on a national and international level.

Current and future progress: Specific progress of individual research tasks will be laid out in separate abstracts. Our success depends on the cooperative and collaborative synergy made possible by our coordination and co-location in the PULSE Institute at SLAC. There are three cross-cutting themes of our center:

- **Imaging on the nanoscale in space and the femtoscale or attoscale in time.** Microscopy at its most essential level in both space and time is paramount to the BES mission to control matter. Non-periodic nano-structures and ultrafast timescales dominate the workings of biology and chemistry. To understand and control function we therefore must first observe structure and motion on these scales.

X-ray FELs are revolutionary x-ray sources for investigations on the nanoscale, and our largest theme is devoted to developing science using coherent x-ray imaging techniques at this and other x-ray free electron lasers. This work includes nanocrystal imaging on the few-Angstrom scale; nonperiodic imaging of single biomolecules; cell imaging; and imaging of aerosols.

Imaging of still smaller structures such as small molecules use other techniques, such as particle fragment velocity maps, and electron holography. Here we are exploring fundamental energy-relevant processes such as photo-induced isomerization, dissociation, and x-ray damage, using optical and x-ray probes, and a combination of linear and nonlinear spectroscopic methods.

Time scale measurements are a particular challenge at the femtosecond scale, but this is where chemistry happens and therefore we devote much of our effort to this range. Simple- "pump-probe" spectroscopy at visible and infrared wavelengths must be extended to the soft and hard x-ray range, and to new sources such as FELs.

- **Light conversion chemistry.** Light from the sun is the primary source of energy on earth, and so we are exploring its conversion to electron motion and then to chemical bonds. Some molecules are particularly adept at this conversion and we would like to understand how they work. For example, we are especially interested in the process of photocatalysis within coordination complexes and similar materials.

Energy conversion is initiated by charge separation, and we know that the charge distribution of the electron and hole, as well as the presence of low energy ligand field excited states greatly influence the lifetime of optically generated charge transfer excited states. Still, the detailed mechanism for the excited state quenching remains unclear. New methods of linear and nonlinear spectroscopy, and especially x-ray spectroscopy involving short-pulse FEL's, can help provide the answer.

An equally important problem is the protection of some chemical bonds, particularly in biology, from destruction in the presence of ultraviolet sunlight. Photoprotection is also an ultrafast process involving charge transfer, and so these new techniques such as ultrafast x-ray absorption and Auger emission can show how critical bonds are protected.

The incorporation of theory within this program is critical for rapid progress in light conversion chemistry. The theory group helps us to focus our efforts in areas of greatest impact.

• **The eV scale in time, space, and field strength.** This is the fundamental scale that determines structure and dynamics of electrons in molecules, and motivates advances in sub-femtosecond time-resolution and Angstrom spatial resolution in theory and experiments. To achieve an adequate view of the molecular realm with at this level, we must interrogate atoms with fields comparable to Coulomb binding fields, and on time scales set by the electronic energy splittings in atoms.

One method to reach this scale is through high harmonic generation. We plan to extend our use of this technique to higher energies and with greater control over the target molecule, to interrogate the detailed motion of the electrons. We are particularly interested in coupled motion of multiple electrons, that goes beyond the “single active electron” approximation that has dominated thinking about strong field laser-atom physics. New theoretical approaches are also required for this, and we are tackling these as well.

LCLS is a source which is also capable of sub-femtosecond or few femtosecond pulses, and these have the unique property of wavelengths short enough to reach the most deeply bound electrons in first and second row atoms. Through the use of novel methods such as low bunch charge, double-slotted spoilers, strong laser fields, and novel data sorting methods, as well as future methods such as self-seeding, we will incorporate LCLS fully as a tool for sub-femtosecond spectroscopy.

Management structure: This research program is managed within the the Chemical Sciences Division, SLAC Photon Sciences Directorate. The current Division Director is Jens Norkov. Major changes in the organization at SLAC in the past year include a new Director and Associate Laboratory Director.

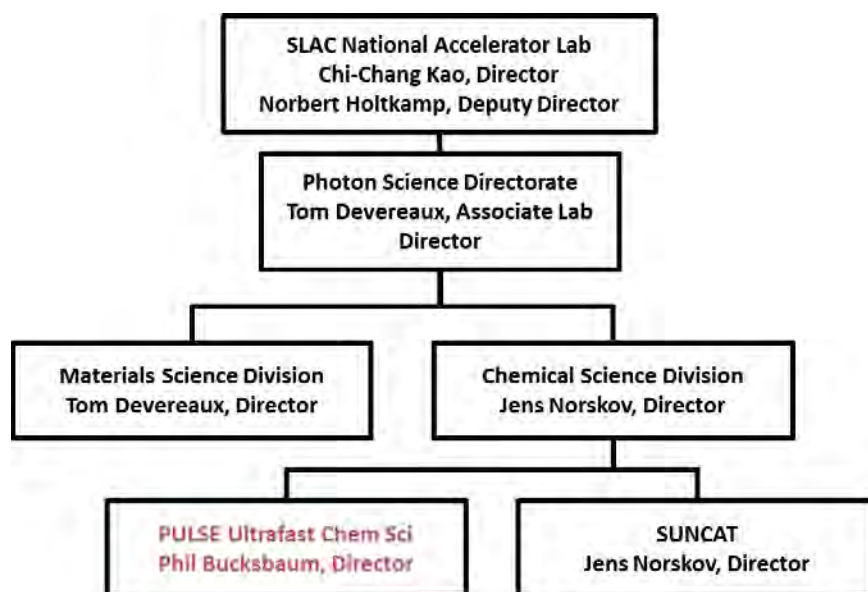


Figure 1: Partial organization chart for SLAC, showing the relation of the PULSE Ultrafast Chemical Science Program to other units with close research ties.

The Ultrafast Chemical Science program is the primary source of research funds and SLAC salary for six Principal Investigator and one Acting PI, who are responsible for proposing and carrying out this science:

Professor Philip Bucksbaum, AMO Physics, Program Spokesperson;
 Associate Professor David Reis, Nonlinear x-ray science, Deputy Spokesperson;
 Assistant Professor Kelly Gaffney, Physical Chemistry;
 Professor Todd Martinez, theory;

Professor Tony Heinz, ultrafast physics;
Senior Research Scientist Dr. Markus Guehr, AMO science.

In addition to these six, we also have a Senior Staff Scientist, Dr. Shambhu Ghimire, who recently received a DOE Early Career within the AMOS program, and we have a program in nonperiodic imaging and bioscience that is presently led by Staff Scientist Claudiu Stan as Acting PI. Dr. Kelly Gaffney has recently become the director of SSRL, but remains the leader of his AMOS program in solution phase chemistry, although there is an active search for a physical chemist to take over the PI responsibilities.

Subtasks: These key personnel are responsible for subtasks, which represent different areas of expertise:

1. UTS: Ultrafast Theory and Simulation (Martinez)
2. ATO: Attoscience (Bucksbaum, Guehr)
3. SPC: Ultrafast Chemistry (Gaffney)
4. NPI: Non-periodic X-ray Imaging (Stan, acting, with oversight from Bucksbaum and Gaffney)
5. SFA: Strong Field AMO Physics (Bucksbaum)
6. NLX: Strong-Field and Nonlinear X-ray Optical Science (Reis)
7. Low Dimensional Systems (Heinz, new program in 2014, no abstract this year)
8. Ultrafast X-ray Spectroscopy (Guehr, Early Career ending 2015)
9. Attosecond X-ray Photonics (Ghimire, Early Career starting 2014)

The broad backgrounds of our PIs provide needed synergy for effective collaborations in cross-disciplinary projects.

Support operations (finance, HR, safety, purchasing, travel) are directed by the Photon Science Associate Laboratory Director and the Chemical Sciences Director and their staff. They provide oversight and delegate the work to appropriate offices in the SLAC Operations Directorate or to the staff of the Stanford PULSE Institute.

Connections to other units within the SLAC organizational structure: Close collaborations are maintained with the Science R&D Division within the LCLS Directorate; the Materials Science Division (SIMES) within the Photon Science Directorate; SSRL; and the SUNCAT Center within our own Chemical Sciences Division, as shown in figure 1. Our colocation with these facilities and research organizations at SLAC greatly aids collaboration.

Other important connections: The PIs have many separate affiliations with other Stanford University research and academic units: Most especially, all members of this program are members of the Stanford PULSE Institute. In addition, several are affiliated with the SIMES Institute, Bio-X, the Ginzton Laboratory, and the Departments of Chemistry, Physics, and Applied Physics.

Laser Research Coordination: Within the past year we have helped to start to organize a new coordinated laser research activity at SLAC and Stanford, in order to make more effective use of some of our state-of-the-art capabilities, both within DOE and in the larger international community. This activity has acquired special significance as plans for LCLS-II move forward, since this upgrade will benefit greatly from close coordination between laser-based research and x-ray science.

We also have collaborative connections to other outside research labs, including DESY, the Lawrence Berkeley Laboratory, the Advanced Photon Source at Argonne Laboratory, the Center for Free Electron Lasers (CFEL) in Hamburg, and BES funded groups at the University of Michigan, the Ohio State University, the University of Connecticut, LSU, and Northwestern University.

Connections to LCLS: The transfer of knowledge and expertise to and from LCLS is extremely fluid and critical to our success. Much of our research creates benefits for LCLS by providing new research

methods and research results, and in addition there are several more direct transfers of our research product to help LCLS:

- In 2014, the PULSE Institute has taken as new members two LCLS staff scientists: Ryan Coffee and Christoph Bostedt. They will both continue to have user support duties and be managed through LCLS, but will spend 25% of their effort building in-house science in PULSE. We anticipate that this will encourage even closer collaboration between scientists in the Photon Science and LCLS Directorates at SLAC, and that these individuals will help us build our science portfolio in the future in AMOS and the larger Chemical Sciences Division of DOE.
- Some of our graduate students provide user support through the LCLS laser group and various end station groups, and receive salary supplements for this work.
- We have assisted in the development of timing tools currently in use at LCLS.
- Some of our postdocs and students have transferred to permanent staff positions at LCLS.
- We connect LCLS to the Stanford PULSE Institute, since all of our staff are members of PULSE, and LCLS Director Jo Stohr is a member of PULSE as well. PULSE assists LCLS in several direct ways:
 - PULSE has helped LCLS to institute a Graduate Fellowship program, and PULSE manages LCLS graduate student campus appointments.
 - PULSE conducts an annual Ultrafast X-ray Summer School to train students and postdocs about LCLS science opportunities.

Productivity metrics. Individual subtasks list their recent publications with their abstracts. We track approximate aggregate statistics for the PULSE Institute, with the assistance of data bases such as Google Scholar. AMOS programs account for more than half of this activity. Since January 2013 PULSE PIs have approximately 157 publications, 99 of which are in refereed journals. There are 14,500 citations to PULSE co-authored articles that have been published since 2009. Our institute-wide “H-index” for articles since 2009 is 59. 241 of these articles have more than ten citations, which means we have nearly 50 of these “high impact” publications per year in PULSE.

Advisory committee. The Ultrafast Chemical Science program receives valuable external advice from the External Advisory Board of the Stanford PULSE Institute. This board of advisors serves the PULSE Institute Director and meets annually. It reports to the PULSE Director and to the Stanford Dean of Research. The reports have also been forwarded to the SLAC Director, the ALD for Photon Science, and to the SLAC Science Policy Committee at their request.

Educational programs and outreach activities. We have an extremely active outreach and visitors program through our affiliation with the Stanford PULSE Institute. PULSE maintains a Stanford-funded visitors program, a website (ultrafast.stanford.edu) as well as an annual Ultrafast X-ray Summer Session. This session, which was founded by the PIs of this program in 2006, continues to be a main mechanism for expanding the research community interested in using x-ray free electron lasers for their research. It receives support from Stanford, and also from BES through the AMOS program in the CSGB Division as well as the x-ray and neutron scattering program in the Materials Science Division. The session now alternates between Europe and SLAC. Our 2014 session at SLAC was a great success. In 2016 the session will return to Stanford.

ATO: Attoscience

Principle Investigator: Philip H. Bucksbaum; **Co-PI:** Markus Guehr; **Grad students:** Limor Spector, Song Wang, Julien Devin. **Undergrads:** Ian Tenney, Rex Garland. **Collaborators:** PULSE Institute, especially Shungo Miyabe, Todd Martinez, Adi Natan.

Objective and Scope:

We seek to observe and control sub-femtosecond electron dynamics in atoms and small molecules. Our discovery that multiple electron orbitals can contribute to HHG in molecules is now employed to investigate electronic structural symmetries and subfemtosecond dynamics in field-ionized molecules. Strong sub-femtosecond pulses are ideal for exploring electron dynamics in molecules.

Recent Progress:**Transient Impulsive Giant Electronic Raman (TIGER) processes with attosecond pulses:**

Resonant Raman excitation, whether by HHG laser pulses or soft x-rays from LCLS-II, should be a means to study electron dynamics in molecules. However, experiments must contend with background ionization: Frequencies high enough to reach resonant core-valence transitions will ionize all occupied orbitals as well, and therefore core excitation leads to rapid autoionization or Auger ionization, foiling the attempt to excite an electronic wave packet in the neutral molecule. New calculations in collaboration with Miyabe show that attosecond pulses will induce a stimulated process, Transient Impulsive Giant Electronic Raman (TIGER) scattering, which can overwhelm autoionization. Calculations are performed for atomic sodium, but the principal is valid for many molecular systems. This approach opens the path for high fidelity multidimensional spectroscopy with attosecond pulses from HHG or FELs.

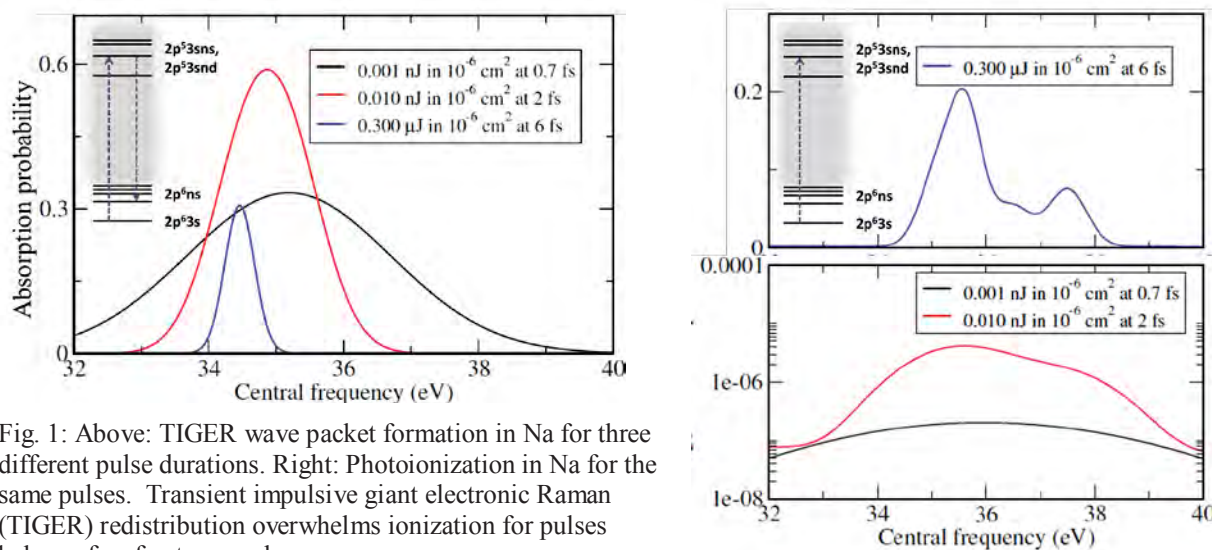


Fig. 1: Above: TIGER wave packet formation in Na for three different pulse durations. Right: Photoionization in Na for the same pulses. Transient impulsive giant electronic Raman (TIGER) redistribution overwhelms ionization for pulses below a few femtoseconds.

Vibrational and Rotational Symmetry probes of harmonics in asymmetric molecules.

(Collaboration with T. Seideman, A. Saenz, and T. Martinez) Last year we reported on our work in asymmetric tops, which showed (1) a new method to obtain molecular frame information by component decomposition of the coherent tumbling of a molecular ensemble following impulsive rotational excitation; and (2) the use of this method led to our discovery of inner orbital contributions to HHG in SO₂. This has been followed up by studies of impulsive vibrational excitation in the

molecule. These new studies show that HHG is strongly influenced by coherent vibrations in the molecule. Limor Spector graduated and Julien Devlin has taken over this study, which we hope to provide new insights about high harmonics.

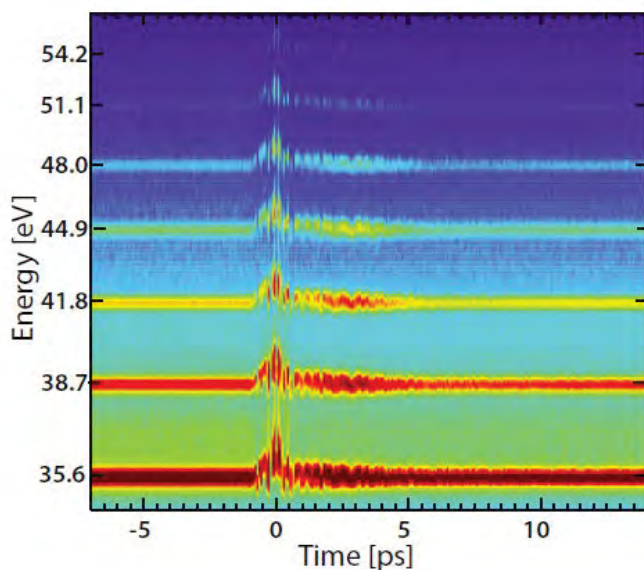


Fig. 2: An infrared pulse at $t=0$ drives impulsive vibrational Raman redistribution in sulfur dioxide, which is probed by using the target as a source of high harmonics. The molecular vibrations in SO_2 can be seen in energy as well as in amplitude of the harmonics. Both the impulsive excitation laser and the HHG laser are s-polarized.

HHG in oriented water. High harmonic generation in water is complicated by the low mass of the protons, which can move significantly during the 0.5 to 1.5 femtoseconds that elapse between field ionization and inelastic recombination. Proton motion can be driven by the displacement of the neutral and cationic potential energy surface minima. For example, removal of an electron from the (HOMO-1) $3a_1$ orbital which screens the protons from each other can result in rapid straightening of the bent molecule. On the other hand, removal of an electron from the (HOMO) $1b_1$ orbital, with its electron node in the molecular plane, does not change the atomic screening significantly and so HHG from this orbital is not expected to drive motion in the molecule. To study these effects we need to orient the molecule. The standard molecular alignment technique, transient rotational Raman scattering, does not work because of water's low induced polarizability; but impulsive THz excitation works well. Therefore we have constructed a tiled array of photoconducting switches to drive intense THz fields in an ensemble of H_2O in the target region of our HHG source apparatus. The design and construction has employed a collaboration with a Stanford undergraduate, Rex Garland.

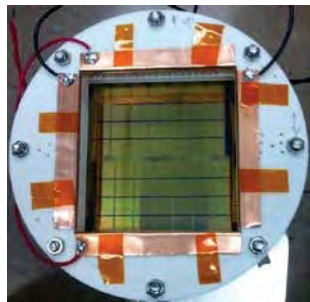


Fig. 3: Four inch phased array antenna THz source, developed by Rex Garland. The tiles are 1 cm interdigitated conductors with 10 micron spacings on a polished GaAs substrate.

Future projects:

Isolated attosecond pulses for TIGER redistribution and nonlinear spectroscopy: The new project underway in our lab is the design, construction, and testing of a source of isolated attosecond pulses, to be

used in transient impulsive excitation studies such as the TIGER redistribution described above. This will require consolidation of equipment and space into a new shared facility in the PULSE institute that can be used for attoscience as well as strong field and chemical studies. Our current plans are to build a 1 terrawatt driver for HHG, and to implement optical gating methods to create isolated attosecond pulses.

THz orientation of water and other asymmetric top molecules: We intend to continue our studies of oriented molecules for HHG, and would like to extend the orientation methods to larger molecules, and to clusters. These studies will involve collaborations with the NPI and the Theory subtasks, as well as SFA.

HHG in vibrating molecules: The few observations that have been made of HHG in coherently vibrating molecules tend to show dramatic dependence of the HHG spectrum on the vibrations. We would like to study this in some select molecules to attempt to understand the connection. This is particularly interesting because of the possibility to get new insights into the ultrafast induced couplings between electronic and ionic degrees of freedom in molecules. The work will involve close collaboration with theory as well.

Connecting our work to LCLS and LCLS-II: We are actively engaged in planning research that could be aided by the capabilities of LCLS-II, which will be a soft x-ray FEL with repetition rates as high as a MHz.

Publications:

- Berrah, Nora, and Philip H. Bucksbaum. "The Ultimate X-Ray Machine." *Scientific American* 310, no. 1 (December 17, 2013): 64–71. doi:10.1038/scientificamerican0114-64.
- Bucksbaum, Philip. "Molecular Dissociation Dynamics Driven by Strong-Field Multiple Ionization." *Bulletin of the American Physical Society* 59 (2014).
- Bucksbaum, Philip H. "Ultrafast Quantum Control in Atoms and Molecules." In *Ultrafast Nonlinear Optics*, edited by Robert Thomson, Christopher Leburn, and Derryck Reid, 105–28. Scottish Graduate Series. Springer International Publishing, 2013. http://dx.doi.org/10.1007/978-3-319-00017-6_5.
- Bucksbaum, Philip H., Joseph Farrell, Limor Spector, Brian McFarland, Song Wang, and Markus Guehr. "High Harmonic Probes of Inner Electron Sub-Cycle Dynamics in Molecules." LTu5H.1. OSA, 2012. doi:10.1364/LS.2012.LTu5H.1.
- Bucksbaum, Philip, Thomas Möller, and Kiyoshi Ueda. "Frontiers of Free-Electron Laser Science." *Journal of Physics B: Atomic, Molecular and Optical Physics* 46, no. 16 (August 1, 2013): 160201. doi:10.1088/0953-4075/46/16/160201.
- Fang, L., M. Hoener, O. Gessner, F. Tarantelli, S. T. Pratt, O. Kornilov, C. Buth, et al. "Double Core-Hole Production in N₂: Beating the Auger Clock." *Physical Review Letters* 105, no. 8 (August 2010). doi:10.1103/PhysRevLett.105.083005.
- Farrell, Joe, Brian McFarland, Nora Berrah, C. Bostedt, John Bozek, Phil Bucksbaum, Ryan Coffee, et al. "Ultrafast X-Ray Probe of Nucleobase Photoprotection," QW1F.4. OSA, 2012. doi:10.1364/QELS.2012.QW1F.4.
- Farrell, Joe, Brian K. McFarland, Limor S. Spector, Philip H. Bucksbaum, and Markus Guehr. "Isotope Effect in the High Harmonics of Water," QMC4. OSA, 2011. doi:10.1364/QELS.2011.QMC4.
- Farrell, Joseph P., Simon Petretti, J. Foerster, Brian K. McFarland, Limor S. Spector, Y. V. Vanne, P. Decleva, Philip H. Bucksbaum, Alejandro Saenz, and Markus Guehr. "Ionic State Superposition in the Strong Field Ionization of Water," LWF1. OSA, 2011. doi:10.1364/LS.2011.LWF1.
- Farrell, Joseph P., Simon Petretti, Johann Förster, Brian K. McFarland, Limor S. Spector, Yulian V. Vanne, Piero Decleva, Philip H. Bucksbaum, Alejandro Saenz, and Markus Gühr. "Strong Field Ionization to Multiple Electronic States in Water." *Physical Review Letters* 107, no. 8 (August 2011). doi:10.1103/PhysRevLett.107.083001.
- Farrell, J. P., L. S. Spector, B. K. McFarland, P. H. Bucksbaum, M. Gühr, M. B. Gaarde, and K. J.

- Schafer. “Influence of Phase Matching on the Cooper Minimum in Ar High-Order Harmonic Spectra.” *Physical Review A* 83, no. 2 (February 2011). doi:10.1103/PhysRevA.83.023420.
- Guehr, Markus, Brian McFarland, Joseph Farrell, Shungo Miyabe, Francesco Tarantelli, Alejandro Aguilar, Nora Berrah, et al. “Delayed Ultrafast X-Ray Induced Auger Probing,” LW5H.3. OSA, 2013. doi:10.1364/LS.2013.LW5H.3.
- McFarland, B K, N Berrah, C Bostedt, J Bozek, P H Bucksbaum, J C Castagna, R N Coffee, et al. “Experimental Strategies for Optical Pump – Soft X-Ray Probe Experiments at the LCLS.” *Journal of Physics: Conference Series* 488, no. 1 (April 10, 2014): 012015. doi:10.1088/1742-6596/488/1/012015.
- McFarland, B. K., J. P. Farrell, N. Berrah, C. Bostedt, J. Bozek, P.H. Bucksbaum, R. Coffee, et al. “Probing Nucleobase Photoprotection with Soft X-Rays.” Edited by M. Chergui, A. Taylor, S. Cundiff, R. de Vivie-Riedle, and K. Yamagouchi. *EPJ Web of Conferences* 41 (2013): 07004. doi:10.1051/epjconf/20134107004.
- McFarland, B. K., J. P. Farrell, S. Miyabe, F. Tarantelli, A. Aguilar, N. Berrah, C. Bostedt, et al. “Ultrafast X-Ray Auger Probing of Photoexcited Molecular Dynamics.” *Nature Communications* 5 (June 23, 2014). doi:10.1038/ncomms5235.
- McFarland, BK, JP Farrell, S Miyabe, F Tarantelli, A Aguilar, N Berrah, C Bostedt, J Bozek, PH Bucksbaum, and JC Castagna. “Delayed Ultrafast X-Ray Auger Probing (DUXAP) of Nucleobase Ultraviolet Photoprotection.” *arXiv Preprint arXiv:1301.3104*, 2013.
- McFarland, Brian, Joseph Farrell, Nora Berrah, Christoph Bostedt, John Bozek, Philip H. Bucksbaum, Ryan Coffee, et al. “Ultrafast Nucleobase Photoprotection Probed by Soft X-Rays,” LTu2H.1. OSA, 2012. doi:10.1364/LS.2012.LTu2H.1.
- Spector, Limor S., Maxim Artamonov, Shungo Miyabe, Todd Martinez, Tamar Seideman, Markus Guehr, and Philip H. Bucksbaum. “Axis-Dependence of Molecular High Harmonic Emission in Three Dimensions.” *Nature Communications* 5 (February 7, 2014). doi:10.1038/ncomms4190.
- Spector, Limor S, Maxim Artamonov, Shungo Miyabe, Todd Martinez, Tamar Seideman, Markus Guehr, and Philip H Bucksbaum. “Orientational Decomposition of Molecular High Harmonic Emission in Three Dimensions.” *arXiv Preprint arXiv:1207.2517*, 2012.
- Spector, Limor S., Joseph P. Farrell, Brian K. McFarland, Philip H. Bucksbaum, Mette B. Gaarde, Kenneth J. Schafer, and Markus Guehr. “Influence of Phase Matching of the Cooper Minimum in Argon High Harmonic Spectra,” QMF4. OSA, 2011. doi:10.1364/QELS.2011.QMF4.
- Spector, Limor S, Todd Martinez, Maxim Artamonov, Tamar Seideman, Philip H Bucksbaum, Markus Guehr, and Shungo Miyabe. “Quantified Angular Contributions for High Harmonic Emission of Molecules in Three Dimensions.” *Nature Communications* 5, no. arXiv: 1207.2517 (2012): 3190.
- Spector, Limor S, Shungo Miyabe, Alvaro Magana, Simon Petretti, Piero Decleva, Todd Martinez, Alejandro Saenz, Markus Guehr, and Philip H Bucksbaum. “Multiple Orbital Contributions to Molecular High-Harmonic Generation in an Asymmetric Top.” *arXiv Preprint arXiv:1308.3733*, 2013.
- Spector, Limor, Song Wang, Joe Farrell, Brian McFarland, Markus Guehr, Phil Bucksbaum, Maxim Artamonov, and Tamar Seideman. “Field-Free Asymmetric Top Alignment and Rotational Revivals Using High Harmonic Generation,” AW3J.3. OSA, 2012. doi:10.1364/CLEO_AT.2012.AW3J.3.

NLX: Ultrafast X-ray Optical Science and Strong Field Control

David A. Reis*, Shambhu Ghimire

Stanford PULSE Institute
SLAC National Accelerator Laboratory, MS 59
2575 Sand Hill Rd.
Menlo Park, CA 94025

[*dreis@slac.stanford.edu](mailto:dreis@slac.stanford.edu)

Program Scope:

The goal of this subtask in the Ultrafast Chemical Sciences FWP at SLAC is to understand and control the fundamental processes that occur during the interaction of ultrafast and ultra-strong electromagnetic fields with dense matter. We are particularly interested in exploration of fundamental light-matter interactions involving ultrafast optical, coherent and nonlinear phenomena in the x-ray regime and extreme nonlinear optics involving the attosecond electron response in solids.

Progress Report

Over the past few years we have focused our effort in two major areas: (1) long-wavelength strong-field interactions in periodic media, including a detailed comparison of both the above and below threshold high order harmonic generation in gas and solid phase argon and (2) exploration of fundamental x-ray nonlinear optics including phase matched second harmonic generation, nonlinear Compton scattering and two-photon inner-shell absorption.

On the first front, we have previously shown that crystalline HHG differs from nonperiodic atomic and molecular HHG in several key ways, including linear scaling of the cutoff with field, relative insensitivity to elliptical polarization, odd only or odd and even harmonics depending on symmetry. We also predicted that the energy of the high harmonic cutoff would be insensitive to wavelength. This work has motivated renewed theoretical and experimental interest in strong-field effects in solids, including a substantial debate over whether the HHG process is periodic media driven primarily by intra or inter-band transitions. We are making significant progress in understanding the process better in both strongly bonded bulk insulators and weakly bonded rare gas solids. For example, we have shown in the wide-band gap insulator MgO that we can produce harmonics well into the XUV, exceeding the maximum energy difference between valence and conduction bands. Unlike MgO, solid Ar is a van der Waals crystal and thus much better approximates a periodic array of isolated atoms. Here we are focusing on a direct comparison of gas and solid-phase harmonics, including intensity, wavelength and polarization scaling. We have shown, for instance, that over a range of intensities, that higher harmonics can be produced in the solid. However, we have also seen strong thickness dependence for both the above and below-gap harmonics that is indicative of complex propagation effects involving the interference of multiple generation mechanisms.

On the second front, we continue our campaign to study nonlinear coherent x-ray processes in the hard x-ray regime (both resonant and non-resonant). This has been made possible by the unprecedented peak-brightness of x-ray free electron lasers such as the LCLS at SLAC and more recently the SACLA free electron laser in Japan which allows for focused intensities in excess of 10^{20} W/cm² and thus fields in excess of kilovolts/Å. Since the field reverses sign on a sub-attosecond time-scale and the subsequent ponderomotive energy is negligible compared to the photon energy, high-field and nonlinear processes in the hard x-ray regime operate in a very different regime than ordinary optics. Nonetheless, these processes are observable on current FELs and our ability to exploit them will be important for LCLS-II. Under DOE funding, we have observed the first phase-matched x-ray second harmonic generation (in diamond at 10^{16} W/cm²) in collaboration with Sharon Shwartz and Steve Harris; x-ray optical sum frequency generation, in collaboration with Ernie Glover; and we have led experiments in which we have observed two-photon Compton scattering (in beryllium at 10^{19} – 10^{20} W/cm²) and below threshold two-photon inner shell absorption in the hard x-ray regime (Zr 1s). In the Compton experiment, we discovered an anomalously large red-shift in scattered photons (i.e. the energy of the outgoing photon is substantially smaller than kinematically allowed for a free-electron process from a single electron). While in the 2-photon absorption experiment, the cross-section appears consistent with simple Z-scaling laws. We have carried out first experiments on resonant second harmonic generation with Sharon Shwartz, although no signal has been observed to date.

The next three years: In the short run, we are finishing the experiments and analysis on the solid-Ar experiments, working on the theory of nonlinear Compton scattering in solids and the final analysis of the Zr paper. Future experiments on HHG in this sub-task are aimed at wavelength and band-gap scaling and separating microscopic from macroscopic effects in the generation process. As appropriate, we will collaborate with Ghimire's new efforts on characterization of the atto-chirp and imaging of attosecond electron dynamics through time-resolved photo-emission which is funded under his early career proposal. We will also embark on a complementary effort to image the attosecond electron dynamics with atomic-scale resolution using non-perturbative x-ray optical wave-mixing in periodic solids under conditions of HHG. There we have worked out a novel geometry that simultaneously achieves phase and group velocity matching conditions over the entire comb of side-bands. We also intend to explore how periodicity affects the nonlinearities in the x-ray regime, for example by looking at phase matched third harmonic generation and the possibility of self-focusing and self phase modulation.

References to publications of DOE sponsored research

2014

- [1] S. Ghimire, G. Ndabashimiye, A. DiChiara, E. Sistrunk, M. Stockman, P. Agostini, L. DiMauro, and D. A. Reis, Strong-field and attosecond physics in solids, Accepted J. Phys. B. 2014.
- [2] J. Goodfellow, M. Fuchs, D. Daranciang, S. Ghimire, F. Chen, H. Loos, D. A. Reis, A. S. Fisher, and A. M. Lindenberg. Below gap optical absorption in gaas driven by intense, single-cycle coherent transition radiation. *Optics Express*, 22(14):17423–17429, 2014.
- [3] S. Shwartz, M. Fuchs, J. B. Hastings, Y. Inubushi, T. Ishikawa, T. Katayama, D. A. Reis, T. Sato, K. Tono, M. Yabashi, S. Yudovich, and S. E. Harris. X-ray second harmonic generation. *Phys. Rev. Lett.*, 112:163901, 2014.
- [4] G. Ndabashimiye, S. Ghimire, and D. Reis. High harmonic mixing in solid argon. *Bulletin of the American Physical Society*, 59, P5.00005 DAMOP, 2014.

2013

- [1] M. Trigo, M. Fuchs, J. Chen, M. P. Jiang, M. Cammarata, S. Fahy, D. M. Fritz, K. Gaffney, S. Ghimire, A. Higginbotham, S. L. Johnson, M. E. Kozina, J. Larsson, H. Lemke, A. M. Lindenberg, G. Ndabashimiye, F. Quirin, K. Sokolowski-Tinten, C. Uher, G. Wang, J. S. Wark, D. Zhu, and D. A. Reis. Fourier-transform inelastic x-ray scattering from time- and momentum-dependent phonon-phonon correlations. *Nat Phys*, 9(12):790–794, 12 2013. [Ghimire contribution]
- [2] S. Shwartz, M. Fuchs, J. B. Hastings, Y. Inubushi, D. A. Reis, M. Yabashi, and S. E. Harris. Second harmonic generation at x-ray wavelengths. In *Nonlinear Optics*. Optical Society of America, 2013.
- [3] A. D. DiChiara, S. Ghimire, D. A. Reis, L. F. DiMauro, and P. Agostini. Strong-field and attosecond physics with mid-infrared lasers. In *Attosecond Physics*, pages 81–98. Springer, 2013.
- [4] G. Ndabashimiye, S. Ghimire, D. Reis, and D. Nicholson. Measurement of coherence lengths of below threshold harmonics in solid argon. In *CLEO: 2013*, page QW1A.7. Optical Society of America, 2013.
- [5] T. Glover, D. Fritz, M. Cammarata, T. Allison, S. Coh, J. Feldkamp, H. Lemke, D. Zhu, Y. Feng, R. Coffee, M. Fuchs, S. Ghimire, J. Chen, S. Shwartz, D. Reis, S. Harris, and J. Hastings. X-ray / optical sum frequency generation. In *2013 Conference on Lasers and Electro-Optics (CLEO 2013)*.

2012

- [1] S. Ghimire, A. D. DiChiara, E. Sistrunk, G. Ndabashimiye, U. B. Szafruga, A. Mohammad, P. Agostini, L. F. DiMauro, and D. A. Reis. Generation and propagation of high-order harmonics in crystals. *Physical Review A*, 85:043836, 2012.
- [2] T. E. Glover, D. M. Fritz, M. Cammarata, T. K. Allison, S. Coh, J. M. Feldkamp, H. Lemke, D. Zhu, Y. Feng, R. N. Coffee, M. Fuchs, S. Ghimire, J. Chen,

- S. Shwartz, D. A. Reis, S. E. Harris, and J. B. Hastings. X-ray and optical wave mixing. *Nature*, 488(7413):603–608, 08 2012.
- [3] J. P. Cryan, J. M. Glowina, J. Andreasson, A. Belkacem, N. Berrah, C. I. Blaga, C. Bostedt, J. Bozek, N. A. Cherepkov, L. F. DiMauro, L. Fang, O. Gessner, M. Gühr, J. Hajdu, M. P. Hertlein, M. Hoener, O. Kornilov, J. P. Marangos, A. M. March, B. K. McFarland, H. Merdji, M. Messerschmidt, V. S. Petrović, C. Raman, D. Ray, D. A. Reis, S. K. Semenov, M. Trigo, J. L. White, W. White, L. Young, P. H. Bucksbaum, and R. N. Coffee. Molecular frame auger electron energy spectrum from n 2. *Journal of Physics B: Atomic, Molecular and Optical Physics*, 45(5):055601, 2012.
- [4] D. Reis. Strong-field nonperturbative effects in solids. In *42nd Annual Meeting of the APS Division of Atomic, Molecular and Optical Physics*, volume 56, page T4.00001, 2012.
- [5] S. Ghimire, G. Ndabashimiye, and D. A. Reis. High-order harmonic generation in solid argon. In *CLEO: QELS-Fundamental Science*, page QW1F.1. Optical Society of America, 2012.
- [6] F. Krasniqi, Y.-P. Zhong, D. A. Reis, M. Scholz, R. Hartmann, A. Hartmann, D. Rolles, A. Rudenko, S. W. Epp, L. Foucar, M. Trigo, M. Fuchs, D. M. Fritz, M. Cammarata, D. Zhu, H. Lemke, M. Braune, M. Ilchen, J. Larsson, S. Techert, L. Strüder, I. Schlichting, and J. Ullrich. Resonant x-ray emission spectroscopy with free electron lasers: Nonequilibrium electron dynamics in highly excited polar semiconductors. In *Research in Optical Sciences*, page IW1D.2. Optical Society of America, 2012.

NPI: Non-Periodic Imaging

Claudiu A. Stan, Raymond G. Sierra, Hartawan Laksmono, Hasan Demirci
 Stanford PULSE Institute for Ultrafast Energy Science
 SLAC National Accelerator Laboratory, Menlo Park, CA 94025
 Email: cstan@slac.stanford.edu

PROGRAM SCOPE

The main goal of the Non-Periodic Imaging Task of the Ultrafast Chemical Science field work proposal is the determination of the dynamics and structure of matter that cannot be investigated with standard atomic-resolution techniques—disordered and biological systems, and materials undergoing fast structural transformations—taking advantage of the brilliance, time resolution, and coherence of X-ray free-electron laser (XFEL) light sources such as the Linac Coherent Light Source (LCLS) at SLAC. To realize the full potential of XFELs for these tasks, it is critical (i) to identify important scientific systems and processes that can be investigated with X-ray lasers, and (ii) to develop a range of new techniques that are necessary for these experiments. The NPI group works in both areas, supporting DOE's mission of understanding and controlling matter through in-house science and the development of techniques useful to the XFEL user community.

Our recent work focuses on developing femtosecond X-ray scattering methods at LCLS to investigate two classes of phenomena whose atomic-scale dynamics are invisible to other scattering methods: the structure and phase transitions of water, and structural changes in biological macromolecules. The work on phase transitions addresses primarily aspects of the nucleation of ice from deeply super-cooled water, such as anomalies in nucleation kinetics revealed by LCLS experiments. We are developing methods for determining the structural dynamics induced by chemical binding to macromolecular receptors, through serial femtosecond crystallography (SFX) of small crystals in which binding is practically instantaneous on the timescale of macromolecule dynamics. We are also developing techniques and instrumentation for XFEL experiments, both in-lab and at LCLS endstations. A new research direction in the past year focuses on investigating the effects of strong X-ray pulses of liquids; these effects limit the data acquisition rate in XFEL experiments, but could be used to trigger phase transitions for future LCLS studies.

This program's near-term goals include analysis of data collected in recent experiments, determining the crystalline structure of metastable dendritic ice formed during the freezing of supercooled water, solving time-resolved protein structures at atomic resolution using SFX at LCLS, and development of sample delivery and optical imaging systems at LCLS.

RECENT PROGRESS

Our group's activities focused on developing and running experiments at SLAC's X-ray facilities, Linac Coherent Light Source (LCLS), and the Stanford Synchrotron Radiation Lightsource (SSRL). In FY 13–14 we led 1 LCLS and 2 SSRL experiments, were major collaborators in 6 LCLS experiments and in-house experiments, and contributed to 3 LCLS experiments. We are scheduled to lead 3 LCLS beamtimes and be major collaborators in 4 LCLS experiments in the upcoming run 11. The research conducted at LCLS led to 7 published and 2 submitted papers in the last year. The work described below represents a selection of work performed during FY 14 in which our lab had a leading role.

Anomalous behavior of homogenous ice nucleation in “no-man's land”. An important class of experiments performed at LCLS investigates the structure and properties of water in short-lived metastable states. We participated in a study that investigated the structure of bulk liquid water in drops that were supercooled further than was previously possible (Sellberg 2014), into a “no-man's land” range of temperatures where conventional X-ray scattering methods are not possible due to rapid ice nucleation and crystallization, but single-shot XFEL experiments can access statistically improbable liquid drops at temperatures below the homogenous nucleation temperature.

The ice nucleation kinetics can also be evaluated from this experiment, and our group led the investigation and interpretation of homogenous ice nucleation rates (Laksmono *et al.*, submitted). Ice nucleation rates were evaluated down to 227 K (5 K below previous measurements), in a range of temperatures where water properties are expected to change rapidly. We observed a slower rate of increase with decreasing temperature than extrapolations based on previous measurements. This can be explained by a rapid decrease in water's diffusivity, which is consistent with the

proposed “fragile-to-strong” transition anomaly in water, and suggests that ice nucleation kinetics and the anomalous physical properties of supercooled water are intimately related.

Microflows induced by XFEL pulses at LCLS.

We have investigated, using time-resolved imaging, the effect of focused X-ray pulses on micron-sized drops and jets at LCLS (Stan *et al.*, in preparation). These experiments surveyed most of the liquid injection systems used at LCLS—drops, Rayleigh jets, gas-dynamic virtual nozzles (GDVN), and lipidic cubic phase injectors (LCP)—and revealed that the explosions caused by X-rays in liquids caused effects that last much longer and range much further than in solid targets. For experiments that use liquids for sample delivery, this is a form of X-ray damage that limits the data acquisition rate depending on the injection method and parameters; while all methods are suitable for LCLS, only a few of them will be compatible with the European XFEL and LCLS-II.

These experiments uncovered a new problem: what is the response of an unenclosed liquid after the deposition of a large amount of energy through X-rays? We found that explosions induce several distinct phases of flow, some of them not observed before. Figure 1 illustrates part of this flow sequence in a Rayleigh jet, in which vapor from the explosion pushes liquid from the jet ends into conical water films. These flow phenomena are long-term consequences of “instantaneous” deposition of energy through X-rays, and provide a signature of the mechanisms of intense energy conversion and propagation in liquid matter. Starting from scaling laws characteristic to matter under extreme conditions and to instantaneous energy release, we are developing analytical models that explain the explosion-driven growth of the gap in jets, and also the kinematic effects of explosions on drops.

Time-resolved macromolecular SFX crystallography. One of our major goals is to study the molecular dynamics of antibiotic and substrate binding to wild-type and mutant ribosomes by using SFX. In order to achieve this, initial SFX diffraction data was collected from empty 30S ribosomal subunit microcrystals during the March 2013 screening beamtime at the CXI endstation of LCLS (Demirci 2013). We have two pending LCLS proposals for data collection from antibiotic-bound 30S and 50S ribosomal subunit crystals during the next LCLS run. Additional supporting time-resolved 30S-antibiotic SAXS experiments will be carried out at the SSRL beamline 4.2 with the help of Dr. Thomas Weiss. In collaboration with Joseph Puglisi’s laboratory at Stanford, we collected synchrotron X-ray diffraction data of novel decoding complexes of ribosome crystals at beamline 12-2 of SSRL containing antibiotics (Demirci *et al.*, in preparation).

We participated in several collaborative serial femtosecond crystallography experiments at LCLS that required either the low-consumption electrospun jet that we developed for SFX (Sierra 2012), or monitoring of sample delivery through high-speed imaging. These collaborations included the study of the photosystem II membrane protein complex (Kern 2014, Kupitz 2014) aimed at elucidating the molecular mechanisms involved in photosynthesis.

Instrumentation development at LCLS. In the past year, we have collaborated closely with the coherent X-ray imaging (CXI) endstation at LCLS to develop instruments and methods for CXI’s users. We designed and built a

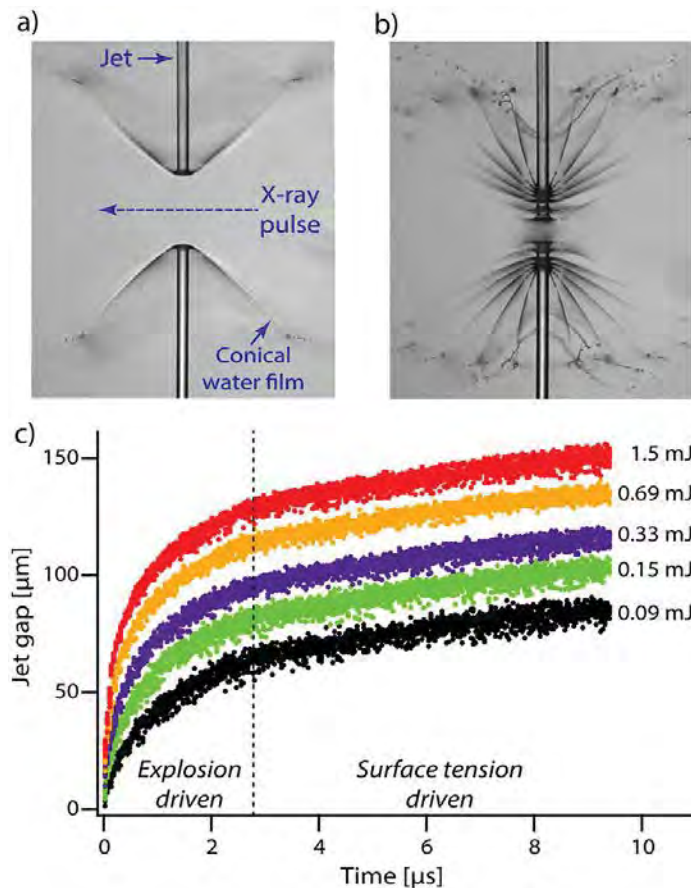


Fig. 3 a) A 20- μm water jet, 3 μs after absorption of a X-ray pulse focused to 1 μm . The gas from the explosion pushes the liquid from the jet into a thin film. b) Overlaid images of the jet at 75 ns, 235 ns, and 1, 2, 3, 4 and 5 μs . c) Jet gap growth. During the explosion-driven phase the gap grows logarithmically with time, and the gap size at the end of this phase scales logarithmically with the pulse energy. These dependencies show that the expansion of water vaporized by the X-ray pulse is approximately self-similar.

high-resolution optical imaging system at CXI, initially used for the jet explosion project and now available to user experiments. We have also developed our electrospun injector to be easily compatible with CXI experiments; this version of the injector was already used in two crystal screening beamtimes. In addition, we have demonstrated new XFEL techniques during LCLS beamtimes at CXI: high-speed optical imaging, simultaneous optical imaging and X-ray diffraction, a new triggering scheme for efficient surveys of dynamic phenomena, and drop synchronization to LCLS pulses at 120 Hz.

In-house instrumentation development. We continued to develop our in-house microcrystal growth facility for higher capacity and more versatility. Screening at SSRL beamline 12-2 confirmed the high quality of the ribosome crystals produced in our lab for future SFX studies. To prepare more complex LCLS experiments in the future, we are currently building a vacuum test chamber that will allow the simulation of the endstation environment in our lab.

FUTURE PLANS

The structure of metastable ice formed under atmospheric-relevant conditions. Recent research suggests that a significant fraction of the ice produced in the atmosphere might be the metastable cubic phase of ice, rather than the stable hexagonal ice. Understanding how cubic ice forms is important for the modeling of atmospheric processes; a significant proportion of cubic ice in the Earth's atmosphere would change how clouds form from atmospheric water vapor. Previous X-ray diffraction experiments showed that rapidly frozen water droplets produced in the lab have a partially cubic ice structure, but did not have the temporal resolution necessary to investigate the structure of the ice most susceptible to a metastable structure—ice dendrites formed in supercooled water at microsecond timescales and micron length scales. We have been awarded a LCLS beamtime during Run 10 to determine the structure of dendritic ice, in which we will use simultaneous optical imaging to select from a population of drops freezing in vacuum the small fraction that are in the early stages of freezing when probed by XFEL pulses.

Structural dynamics of enzymatic reactions. We have two scheduled screening beamtimes at the CXI endstation in November 2014. During these beamtimes we plan to collect preliminary SFX diffraction data from 70S ribosome decoding complexes and HIV reverse transcriptase elongation complexes to better understand the molecular mechanisms of peptide bond formation and HIV infection at a physiologically more relevant temperature. The third screening beamtime at the XPP endstation of LCLS is scheduled in December, and we plan to collect femtosecond diffraction data from extremely radiation-damage sensitive, antibiotic-resistant mutant ribosome crystals on a grid-based fixed target goniometer setup.

In parallel with the development and testing of ribosome crystal systems, we are developing a coaxial mixing device that will be integrated in our electrospun injector. The mixing device will be used to deliver the antibiotics and substrates to crystals shortly before sample injection for SFX.

Sample delivery for XFEL experiments. Drying and freezing due to rapid evaporation of liquids in vacuum affect several sample delivery systems used at XFEL facilities: our electrospun jet, the LCP injector, and drop-on-demand injectors. We have been awarded a screening beamtime to demonstrate in-vacuum hydration for our electrospun jet, by localized introduction of pure water vapor near the jet-XFEL interaction region.

Producing water at extreme negative pressures with XFEL pulses. Liquids are unstable at negative pressures, and it is very difficult to stretch them to deeply metastable states whose study would contribute significantly to the understanding of the phase diagrams of liquid matter. Our drop explosion experiments indicate that we can use focused XFEL pulses to stretch water, and analysis of the data suggests that it is possible to generate transient negative pressures exceeding the lowest pressures previously produced in water. We submitted an LCLS proposal to generate negative pressures in water drops, and to measure the stability limit beyond which water ruptures. We are also evaluating designs for X-ray pump-probe experiments at LCLS to investigate the structure of water at negative pressures.

COLLABORATIONS: This work was done with colleagues from SLAC, LCLS, Stanford, LLNL, Uppsala, LBNL, Arizona State University, Max Planck Biomedical Heidelberg, CFEL@DESY, Brown University and others.

PUBLICATIONS WHICH NPI WAS PRIMARY AUTHOR

- Bogan, M. J. (2011). "Ultrafast X-ray Lasers Illuminate Airborne Nanoparticle Morphology." *MRS Proceedings* **1349**, mrs11-1349-dd1307-1305, doi:10.1557/opl.2011.1405.
- Bogan, M. J., *et al.* (2012). "Apparatus and method for nanoflow serial femtosecond x-ray protein nanocrystallography", provisional patent.
- Demirci, H., *et al.* (2013). "Serial femtosecond X-ray diffraction of 30S ribosomal subunit microcrystals in liquid suspension at ambient temperature using an X-ray free-electron laser." *Acta Crystallog.* **F69**, 1066.
- Laksmono, H. *et al.* (2014). "Anomalous behavior of the homogeneous ice nucleation rate in 'No-man's land.'", submitted to *Proc. Natl. Acad. Sci. USA*.
- Loh, N. D., *et al.* (2010). "Cryptotomography: reconstructing 3D Fourier intensities from randomly oriented single-shot diffraction patterns." *Phys. Rev. Lett.* **104**, 225501.
- Loh, N. D., *et al.* (2012a). "Profiling structured beams using injected aerosols." *Proc. SPIE* **8504**, 850403.
- Loh, N. D., *et al.* (2012b). "Fractal morphology, imaging and mass spectrometry of single aerosol particles in flight." *Nature* **486**, 513.
- Loh, N. D., *et al.* (2013). "Sensing the wavefront of x-ray free-electron lasers using aerosol spheres." *Opt. Express* **21**, 12385.
- Pedersoli, E., *et al.* (2013). "Mesoscale morphology of airborne core-shell nanoparticle clusters: x-ray laser coherent diffraction imaging." *J. Phys. B At. Mol. Opt. Phys.* **46**, 164033.
- Sierra, R. G., *et al.* (2012). "Nanoflow electrospinning serial femtosecond crystallography." *Acta Crystallog.* **D68**, 1584.
- Starodub, D., *et al.* (2012). "Single-particle structure determination by correlations of snapshot X-ray diffraction patterns" *Nat. Commun.* **3**, 1276.

SELECTED PUBLICATIONS IN WHICH NPI WAS A MAJOR COLLABORATOR

- Alonso-Mori, R., *et al.* (2012). "Energy-dispersive X-ray emission spectroscopy using an X-ray free-electron laser in a shot-by-shot mode." *Proc. Natl. Acad. Sci. USA* **109**, 19103.
- Aquila, A., *et al.* (2012). "Time-resolved protein nanocrystallography using an X-ray free-electron laser." *Opt. Express* **20**, 2706.
- Barty, A., *et al.* (2011). "Self-terminating diffraction gates femtosecond X-ray nanocrystallography measurements." *Nat. Photonics* **6**, 35.
- Boutet, S., *et al.* (2012). "High-resolution protein structure determination by serial femtosecond crystallography." *Science* **337**, 362.
- Chapman, H., *et al.* (2011). "Femtosecond X-ray protein nanocrystallography." *Nature* **470**, 73.
- Ekeberg, T., *et al.* (2012). "Three-dimensional structure determination with an X-ray laser." *Doctoral thesis preprint*, Uppsala Universitet.
- Frank, M., *et al.* (2011). "Single-particle aerosol mass spectrometry (SPAMS) for high-throughput and rapid analysis of biological aerosols and single cells." In *Rapid Characterization of Microorganisms by Mass Spectrometry*. Demirev, American Chemical Society, pp161-166.
- Hattne, J., *et al.* (2014). "Accurate macromolecular structures using minimal measurements from X-ray free-electron lasers." *Nat. Methods* **11**, 545.
- Johansson, L. C., *et al.* (2012). "Lipidic phase membrane protein serial femtosecond crystallography." *Nat. Methods* **9**, 263.
- Kassemeyer, S., *et al.* (2012). "Femtosecond free-electron laser x-ray diffraction data sets for algorithm development." *Opt. Express* **20**, 4149.
- Kern, J., *et al.* (2012). "Room temperature femtosecond X-ray diffraction of photosystem II microcrystals." *Proc. Natl. Acad. Sci. USA* **109**, 9721.
- Kern, J., *et al.* (2014). "Methods development for diffraction and spectroscopy studies of metalloenzymes at X-ray free-electron lasers." *Phil. Trans. R. Soc. B* **369**, 20130590
- Kern, J., *et al.* (2014). "Taking snapshots of photosynthetic water oxidation using femtosecond X-ray diffraction and spectroscopy." *Nat. Comm.* **5**, 4371.
- Koopmann, R., *et al.* (2012). "In vivo protein crystallization opens new routes in structural biology." *Nat. Methods* **9**, 259.
- Kupitz, C., *et al.* (2014). "Serial time-resolved crystallography of photosystem II using a femtosecond X-ray laser." *Nature* **513**, 261.
- Lomb, L., *et al.* (2011). "Radiation damage in protein serial femtosecond crystallography using an x-ray free-electron laser." *Phys. Rev. B* **84**, 214111.
- Martin, A. V., *et al.* (2011). "Single particle imaging with soft x-rays at the Linac Coherent Light Source." *Proc. SPIE* **8078**, 807809.
- Martin, A. V., *et al.* (2012a). "Femtosecond dark-field imaging with an X-ray free electron laser." *Opt. Express* **20**, 13501.
- Martin, A. V., *et al.* (2012b). "Noise-robust coherent diffractive imaging with a single diffraction pattern." *Opt. Express* **20**, 16650.
- Mitzner, R., *et al.* (2013). "L-Edge X-ray Absorption Spectroscopy of Dilute Systems Relevant to Metalloproteins Using an X-ray Free-Electron Laser." *J. Phys. Chem. Lett.* **4**, 3641.
- Pedersoli, E., *et al.* (2011). "Multipurpose modular experimental station for the DiProI beamline of Fermi@Elettra free electron laser." *Rev. Sci. Instrum.* **82**, 043711.
- Saldin, D. K., *et al.* (2011). "New light on disordered ensembles: ab-initio structure determination of one particle from scattering fluctuations of many copies." *Phys. Rev. Lett.* **106**, 115501.
- Schreck, S., *et al.* (2014). "Reabsorption of soft-x-ray emission at high x-ray free-electron laser fluences." *Phys. Rev. Lett.*, accepted.
- Seibert, M. M., *et al.* (2011). "Single mimivirus particles intercepted and imaged with an X-ray laser" *Nature* **470**, 78.
- Sellberg, J. A., *et al.* (2014). "Ultrafast X-ray probing of water structure below the homogenous ice nucleation temperature" *Nature*, **510**, 381.
- Sellberg, J. A., *et al.* (2014). "X-ray Emission Spectroscopy of Bulk Liquid Water in 'No-man's Land'", submitted to *J. Chem. Phys.*.
- Yoon, C. H., *et al.* (2011). "Unsupervised classification of single-particle X-ray diffraction snapshots by spectral clustering." *Opt. Express* **19**, 16542.

SFA: Strong-field laser mater interactions

PI: P. Bucksbaum; Research Associate: Adi Natan; Staff Scientist: Ryan Coffee;
 Graduate Students: Matthew Ware, Lucas Zipp, Andrei Kamalov
 PULSE Ultrafast Chemical Science Program, SLAC National Accelerator Laboratory, Menlo
 Park, CA 94025. Email: phb@slac.stanford.edu

Program Scope: The SFA program studies *short wavelength strong field interactions* in small molecules and atoms. We explore the transient impulsive regime of bound electron dynamics in strongly driven molecules. On a sub-picosecond time scale we have studied transient impulsive rotational Raman scattering, which is important for molecular alignment and is also displays quantum localization behavior as an archetype for a quantum kicked rotor. The 10-100 femtosecond time scale is the regime of strongly driven Born-Oppenheimer dynamics, which includes wave packets interacting with and around conical interesections in molecules, as well as light-induced conical intersections that can control intramolecular motion and contribute to Berry's phase or other phenomena associated with separation of time scales among the protons, electrons, and heavier nuclei. We also study X-ray-molecule interactions, which involve dynamics on the 0.1-10 femtosecond scale of electron-electron interactions. Here we have studied the competition between proton migration and Auger relaxation in x-ray-ionized molecules at LCLS. Finally on the shortest time scale studied, 10-100 attoseconds, we observe the temporal dynamics of above-threshold ionization. This could be an important area of study at future high repetition rate soft x-ray FELs such as LCLS-II. Progress has been made in all of these areas.

Recent Progress and Future Work:

Attosecond dynamics in above-threshold ionization: Attosecond delays in photoemission from atoms and molecules have been observed in several recent studies through the interference of short ionizing pulses of extreme ultraviolet (XUV) radiation with an infrared (IR) reference. Such phase measurement techniques allow the observation of ultrafast dynamics during photoionization. We have now extended these methods to ATI in an intense laser field by measuring the relative phase of different ATI peaks in a manner that is analogous to the XUV single photon phase measurements that employ RABBITT or the attosecond streak camera.

This is multi-path interference of adjacent ATI peaks by a weak probe field at *half* the frequency. Sideband peaks appear due to absorption or emission of a single probe photon from adjacent ATI levels (Fig. 2a). The outgoing photoelectron has no parity due to mixing of quantum pathways with even and odd ATI orders. Therefore each sideband asymmetry oscillates with the relative optical phase, similar to the modulation of sideband peaks in RABBITT and the oscillations from interference of even and odd harmonics. Phase shifts in the modulation probe the phase delays in ATI, which are found to be greatly affected by non-perturbative processes.

Future work: will expand these observations to incorporate more detailed treatment of the delay of different symmetry states using the rich angular information measured, understanding the origin of these delays, and studying different regimes of strong-field ionization in systems of increasing complexities.

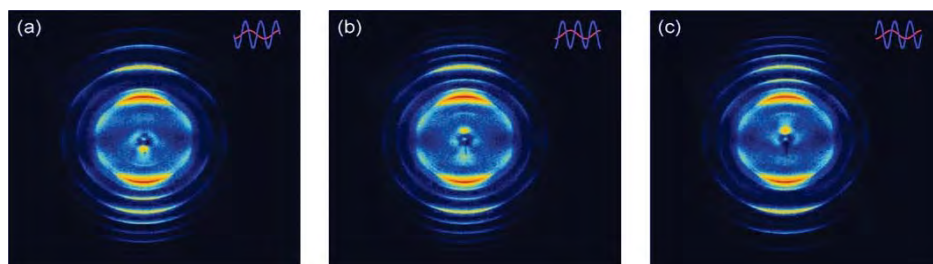


Fig. 1 (a-c): Electron VMI at relative phase delay $\phi = 0, \pi/2,$ and π show the phase-dependent shifts in the ATI distribution

Dynamical localization of angular momentum in non-periodically kicked quantum rotors Molecular alignment is a useful tool for studies of molecules in the body-centered frame. Studies of field-free alignment following multiple nonresonant impulses have been particularly useful because they can lead to high degree of alignment while minimizing undesirable background processes such as ionization. Substantial literature exists on the alignment of linear molecules after the application of a multi-pulse trains with uniform pulse separation, but there have not been investigations using multi-pulse sequences with non-uniform time separation.

We have found evidence supporting Anderson-type dynamical localization of angular momentum in the periodically kicked quantum linear rotor by studying the population alignment of ^{14}N caused by pulse trains with uniform or non-uniform spacings between individual pulses. We find that the population alignment, a measure of the rotor's rotational energy, exhibits resistance to change when the excitation train is periodic. We also show the angular momentum can break out and experiences rapid growth for disordered, non-periodic pulse trains. This could point to methods to control molecular alignment in ultrafast experiments utilizing lasers or x-ray lasers in the future.

Light-induced conical intersections: Conical intersections (CI) are natural degeneracies between Born-Oppenheimer surfaces in the spectrum of molecules that have three or more atoms. CIs facilitate non-radiative energy transfer between electronic states, and play an important role in molecular dynamics. **Light induced conical intersections** (LICI) are degeneracies in the light-induced dressed state basis of the Born-Oppenheimer surfaces. Unlike ordinary CIs, the LICIs can be realized even in diatomic molecules, because the laser polarization adds an additional degree of freedom. We have found evidence for wave packet diffraction around a LICI in H_2^+ undergoing dissociation in strong fields. The topological singularity that characterizes the LICI creates interference fringes in the angular distribution of energy-selected dissociation fragments. We have developed a full 3d simulation and calculated these interference patterns. We are developing theoretical tools that will help us understand the role of Berry's phase and the non-adiabatic coupling terms in the dynamics.

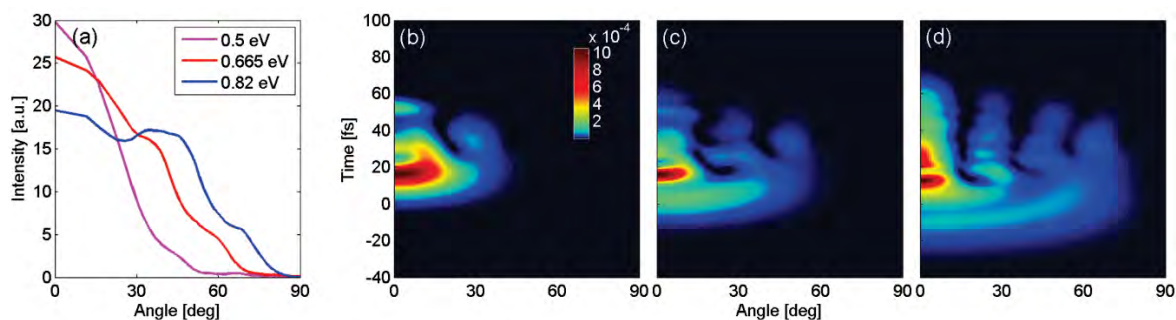


Fig. 2 (a) Measured dissociation yield vs Angle of H_2^+ reveal modulations at different angles for vibration levels $v=7,8,9$. The calculated disassociation probability as function of time and angle for molecules that were initialized in the (b) 7th, (c) 8th and (d) 9th vibrational eigen-states with, in the ground rotational state. Peak intensity of pulse happens at $t = 0$ fs.

Future work: Our results point the way to further quantum control studies, including Berry's Phase studies in these systems.

Ultrafast x-ray driven proton migration We have collaborated with another program in the PULSE Institute to study fast proton migration dynamics in x-ray-ionized acetylene at LCLS. A carbon atom in acetylene HCCH undergoes K-shell ionization, which induces proton motion to form vinylidene CCHH , and at the same time leads to dication formation via Auger decay. These

processes are detected by a second ionization event after a variable time delay. This allows us to study the interplay between proton motion and Auger relaxation in the molecule.

We have seen that proton migration begins with a few femtoseconds following K-shell ionization. **Future work:** In the future we believe it is possible to map out the electronic states responsible for the isomerization

References

1. Berrah, N. and P. H. Bucksbaum (2013). *Scientific American* **310**(1): 64-71.
2. Bostedt, C., J. Bozek, P. Bucksbaum, R. Coffee, J. Hastings, Z. Huang, R. Lee, S. Schorb, J. Corlett and P. Denes (2013). *Journal of Physics B: Atomic, Molecular and Optical Physics* **46**(16): 164003.
3. Bucksbaum, P. (2012). "Atomic and molecular physics at the lcls x-ray laser." *Mexican Optics and Photonics Meeting*.
4. Bucksbaum, P. (2014). "Molecular dissociation dynamics driven by strong-field multiple ionization." *Bulletin of the American Physical Society* **59**.
5. Bucksbaum, P. and J. Glowonia (2013). *EPJ Web of Conferences* **57**: 04001.
6. Bucksbaum, P., T. Möller and K. Ueda (2012). *Journal of Physics B: Atomic, Molecular and Optical Physics* **45**(16): 160101.
7. Bucksbaum, P. H. (2011). "Observing structure and motion in molecules with ultrafast strong field and short wavelength laser radiation." ANL (Argonne National Laboratory (ANL), Argonne, IL (United States)).
8. Bucksbaum, P. H. (2013). *Ultrafast nonlinear optics*, Springer: 105-128.
9. Bucksbaum, P. H., R. Coffee and N. Berrah (2011). *Advances in Atomic Molecular and Optical Physics* **60**: 239-289.
10. Cryan, J., J. Glowonia, J. Andreasson, A. Belkacem, N. Berrah, C. Blaga, C. Bostedt, J. Bozek, N. Cherepkov and L. DiMauro (2012). *Journal of Physics B: Atomic, Molecular and Optical Physics* **45**(5): 055601.
11. Cryan, J., J. Glowonia, N. Cherepkov, P. Bucksbaum and R. Coffee (2011) *Bulletin of the American Physical Society* **56**.
12. Cryan, J. P., J. M. Glowonia, D. W. Broege, Y. Ma and P. H. Bucksbaum (2011). *Physical Review X* **1**(1): 011002.
13. Doumy, G., C. Roedig, S.-K. Son, C. I. Blaga, A. DiChiara, R. Santra, N. Berrah, C. Bostedt, J. Bozek and P. Bucksbaum (2011). *Physical Review Letters* **106**(8): 083002.
14. Fang, L., T. Osipov, B. Murphy, A. Rudenko, D. Rolles, V. Petrovic, C. Bostedt, J. Bozek, P. Bucksbaum and N. Berrah (2014). *Journal of Physics B: Atomic, Molecular and Optical Physics* **47**(12): 124006.
15. Fang, L., T. Osipov, B. Murphy, F. Tarantelli, E. Kukk, J. Cryan, M. Glowonia, P. Bucksbaum, R. Coffee and M. Chen (2012). *Physical Review Letters* **109**(26): 263001.
16. Farrell, J., B. McFarland, N. Berrah, C. Bostedt, J. Bozek, P. Bucksbaum, R. Coffee, J. Cryan, L. Fang and R. Feifel (2012). *Quantum Electronics and Laser Science Conference*, Optical Society of America.
17. Fung, R., J. Glowonia, J. Cryan, A. Natan, P. Bucksbaum and A. Ourmazd (2012). *Signal* **1**: i2.
18. Glowonia, J. M., A. Ourmazd, R. Fung, J. Cryan, A. Natan, R. Coffee and P. Bucksbaum (2012). *Quantum Electronics and Laser Science Conference*, Optical Society of America.
19. Glowonia, J. M., A. Ourmazd, R. Fung, J. Cryan, A. Natan, R. Coffee and P. Bucksbaum (2012). "Sub-cycle strong-field influences in x-ray photoionization." *Quantum Electronics and Laser Science Conference*, Optical Society of America.
20. Kanter, E., B. Krässig, Y. Li, A. March, P. Ho, N. Rohringer, R. Santra, S. Southworth, L. DiMauro and G. Doumy (2011). *Physical Review Letters* **107**(23): 233001.

21. Li, H., L.-J. Chen, H. P. H. Cheng, J. May, S. Smith, K. Muehlig, J. C. Frisch, A. R. Fry, F. X. Kärtner and P. H. Bucksbaum (2013). *CLEO: Applications and Technology*, Optical Society of America.
22. McFarland, B., N. Berrah, C. Bostedt, J. Bozek, P. Bucksbaum, J. Castagna, R. Coffee, J. Cryan, L. Fang and J. Farrell (2014). *Journal of Physics: Conference Series* **488**: 012015.
23. McFarland, B., J. Farrell, N. Berrah, C. Bostedt, J. Bozek, P. Bucksbaum, R. Coffee, J. Cryan, L. Fang and R. Feifel (2013). *EPJ Web of Conferences* **41**, 07004 (2013) **41**: 07004.
24. McFarland, B., J. Farrell, N. Berrah, C. Bostedt, J. Bozek, P. Bucksbaum, R. Coffee, J. Cryan, L. Fang and R. Feifel (2013). *EPJ Web of Conferences* **41**, 07004 (2013) **41**: 07004.
25. McFarland, B., J. Farrell, N. Berrah, C. Bostedt, J. Bozek, P. H. Bucksbaum, R. Coffee, J. Cryan, L. Fang and R. Feifel (2012). *Laser Science*, Optical Society of America.
26. Natan, A., M. R. Ware and P. H. Bucksbaum (2014). *International Conference on Ultrafast Phenomena*, Optical Society of America.
27. Natan, A., M. R. Ware and P. H. Bucksbaum (2014). *CLEO: QELS_Fundamental Science*, Optical Society of America.
28. Petrovic, V., S. Schorb, J. Kim, J. White, J. Cryan, J. M. Glowonia, L. Zipp, D. Broege, S. Miyabe and H. Tao (2013). *ABSTRACTS OF PAPERS OF THE AMERICAN CHEMICAL SOCIETY*, AMER CHEMICAL SOC 1155 16TH ST, NW, WASHINGTON, DC 20036 USA.
29. Petrovic, V. S., S. Schorb, J. Kim, J. White, J. P. Cryan, J. M. Glowonia, L. Zipp, D. Broege, S. Miyabe and H. Tao (2012) *arXiv preprint arXiv:1212.3728*.
30. Petrovic, V. S., S. Schorb, J. Kim, J. White, J. P. Cryan, J. M. Glowonia, L. Zipp, D. Broege, S. Miyabe and H. Tao (2013). *The Journal of chemical physics* **139**(18): 184309.
31. Petrović, V. S., M. Siano, J. L. White, N. Berrah, C. Bostedt, J. D. Bozek, D. Broege, M. Chalfin, R. N. Coffee and J. Cryan (2012). *Physical Review Letters* **108**(25): 253006.
32. Roedig, C., G. Doumy, S.-K. Son, C. Blaga, A. DiChiara, R. Santra, N. Berrah, C. Bostedt, J. Bozek and P. H. Bucksbaum (2011). *Laser Science*, Optical Society of America.
33. Zipp, L., A. Natan and P. Bucksbaum (2014). *Bulletin of the American Physical Society* **59**.
34. Zipp, L., A. Natan and P. H. Bucksbaum (2014). *CLEO: QELS_Fundamental Science*, Optical Society of America.

Solution Phase Chemical Dynamics, Kelly Gaffney PI

Program Scope: Understanding how molecular properties dictate the non-equilibrium dynamics of molecular excited states represents a critical step towards a better utilization of light triggered molecular phenomena. Our work's emphasis on solution phase dynamics and more complex molecular systems complements the small molecule, gas phase chemical dynamics efforts in the *Ultrafast Chemistry* field work proposal at the SLAC National Accelerator Laboratory.

The development of the LCLS, an ultrafast x-ray free electron laser, presents a tremendous opportunity to harness the advantages of x-ray scattering and spectroscopy to investigate chemical dynamics (Kunnus 2012; Kunnus 2013; Lemke 2013; Zhang 2014). X-ray methods provide a novel approach to distinguishing electronic and nuclear dynamics in time resolved measurements, a central challenge in experimental studies of chemical dynamics. We complement these ultrafast x-ray studies with time resolved vibrational spectroscopy (Jha 2011; Jha 2012; Zhang 2012; Zhang 2012) and steady state x-ray resonant inelastic x-ray scattering (Meyer 2010). Our current research focuses on the non-adiabatic dynamics of charge transfer excitations, primarily in, but not limited to, transition metal coordination compounds.

Recent Progress and Future Plans

Tracking excited state charge and spin dynamics in iron coordination complexes: For transition metal containing molecular complexes, excited state electron transfer and spin crossover represent key phenomena for characterization and ideally control. Poly-pyridal iron complexes, such as $[\text{Fe}(2,2'\text{-bipyridine})_3]^{2+}$, provide archetypical coordination complexes where the excited state charge and spin dynamics involved in spin crossover have long been a source of interest and controversy. While experimental evidence supporting the ultrafast time scale for excited state charge and spin dynamics in these iron complexes has been accumulating, the spin crossover mechanism remains unclear. Mechanistic understanding has proven difficult because the generally complex electronic structure of coordination compounds make unambiguous theoretical and experimental studies of these chemical dynamics challenging. Most critically, robust determination of the ultrafast spin dynamics has been impeded by the indirect sensitivity of optical spectroscopy to spin dynamics, and the flux limitations of ultrafast x-ray sources.

We have used femtosecond resolution Fe K-edge XANES (Lemke 2013) and $\text{K}\beta$ x-ray fluorescence (Zhang 2014) to study the ultrafast charge and spin dynamics of $[\text{Fe}(2,2'\text{-bipyridine})_3]^{2+}$ induced by metal to ligand charge transfer (MLCT) excitation. These measurements demonstrate the ability of x-ray fluorescence to robustly track the charge and spin dynamics of an electronically excited molecule. Our initial measurements demonstrate spin crossover in $[\text{Fe}(2,2'\text{-bipyridine})_3]^{2+}$ occurs step wise from both a spin and electron transfer perspective. At this point we have a firm handle of the electronic states involved in spin crossover and the transition rates between these states.

Controlling excited state internal conversion and intersystem crossing in 3d coordination complexes with ligand engineering: Our present work focuses of two objectives: (1) understanding how ligand modifications, such as ligand substitution, influence the interaction between charge transfer and ligand field excited states and (2) determining the vibrational coordinates that govern the non-adiabatic electronic transitions involved in internal conversion and intersystem crossing. We are currently working on three classes of coordination complex to address these questions.

- (1) A series of mixed ligand complexes involving both 2,2'-bipyridine and cyanide ligands. Here we have proven with a combination of femtosecond resolution iron hard x-ray fluorescence and femtosecond UV-visible spectroscopy that substitution of 2,2'-bipyridine ligands with four cyanides increases the MLCT excited lifetime by more than two-orders of magnitude.
- (2) Ligand substitution and solvent variation have been shown to vary the MLCT excited state lifetime of Cu(I) coordination complexes by many orders of magnitude. The excited states of these complexes undergo pseudo-Jahn-Teller distortions from roughly tetrahedral to square planar geometries, providing open coordination sites in the excited state. Variation in the ligand torsion about the ligand-metal bond and exciplex formation with strongly coordinating solvents have been proposed to account for the ligand and solvent dependent lifetimes, but robust structural observation of these effects have not been achieved with time resolved methods – be these quantum chemical dynamics simulations or experiment. We believe this can be better achieved with vibrational spectroscopy and diffuse x-ray scattering and have initial results on both experimental fronts.
- (3) We have a long standing (Hartsock 2011) and slowly progressing project where we have studied the excited state dynamics of a bimetallic Ir complex, $[\text{Ir}_2(\text{dimen})_4]^{2+}$, where dimen = 1,8-diisocyno-*p*-menthane, with femtosecond resolution diffuse x-ray scattering. The slow progress reflected the analysis challenges for the area detector at the LCLS, but a recent breakthrough in data analysis has demonstrated the success of the measurement. The initial analysis demonstrates the power of the anisotropic scattering of the photo-excited system and indicates that the vibrational assignments in our prior publication based on UV-visible pump-probe measurements. If true, we believe this will be an excellent example of the power of more direct structural probes of nuclear dynamics in excited state chemical systems.

Mapping the electronic density evolution of charge transfer excited states: The spatial extent of interacting electronic states significantly influences the non-adiabatic coupling and transfer rate between these states. Fast and efficient energy migration and charge separation represent essential steps in molecularly based light-harvesting materials. High symmetry and strong intermolecular coupling facilitate fast energy migration, while solvent disorder leads to the symmetry breaking that facilitates charge separation. The interplay of electronic coupling and disorder, both dynamic and static, has a critical impact on the electron mobility in molecular materials. We propose to use soft x-ray core hole spectroscopy (Kunnus 2012; Kunnus 2013; McFarland 2014) and vibrational spectroscopy (Zhang 2012; Zhang 2012) to track these electron density dynamics.

In previous work, we have used time resolved vibrational anisotropy to study the dynamics of electron localization in the ligand-to-metal charge transfer (LMCT) excited state of $[\text{Fe}(\text{CN})_6]^{3-}$ (Zhang 2012) and the dynamics of twisted intra-molecular charge transfer in julolidine malanonitrile (Zhang 2012). In previous work, we have used time resolved vibrational spectroscopy to determine the rate of excited state localization in $[\text{Fe}(\text{CN})_6]^{3-}$. The single excited state vibrational absorption peak and the absence of excited state anisotropy for the initially generated LMCT excited state of $[\text{Fe}(\text{CN})_6]^{3-}$ strongly indicate the ligand electron hole hops between the equivalent ligands with a rate too high to be resolved with the 200 fs time resolution of the measurement. On the picosecond time scale, we observe the excited state spectrum transition from one to two excited state absorptions with a solvent dependent rate. We attribute

this to a reduction in molecular symmetry induced by hole localization. While vibrational spectroscopy has proven valuable for studying excited state charge dynamics, the interpretation has relied heavily on symmetry considerations and TDDFT calculations.

Our future work will complement this vibrational spectroscopy studies with time resolved soft x-ray resonance Raman measurements – more commonly referred to as resonance inelastic x-ray scattering (RIXS). By resonantly exciting transitions associated with specific atoms in a molecule, such as the N K-edge of the ligand and the Fe L-edge of the metal center in $[\text{Fe}(\text{CN})_6]^{3-}$, we will utilize the spatial localization of the $1s$ orbital of N and the $2p$ orbitals of Fe to provide an atom specific view of the molecular electronic structure. An initial experimental study of the photodissociation dynamics of $\text{Fe}(\text{CO})_5$ with Fe L-edge RIXS has demonstrated the feasibility of the measurements at LCLS (Kunnus 2012; Kunnus 2013). These initial studies of CO photodissociation from $\text{Fe}(\text{CO})_5$ demonstrate that during the initial bond dissociation, the parent molecules fragment into both singlet and triplet spin configurations of the $\text{Fe}(\text{CO})_4$ photoproduct. While the triplet state interacts weakly with the ethanol solvent, the singlet configurations exhibit strong ethanol- $\text{Fe}(\text{CO})_4$ interactions on the 100 fs time scale. Whether the solute-solvent structure in the electronic ground state or the details of the non-adiabatic dynamics along dissociative potential energy surfaces governs the branching ratio for singlet and triplet photoproducts has yet to be determined.

Dynamics of hydrogen bonding and ion assembly in solution: We have phased out this effort from our sub-task (Gaffney 2011; Ji 2011; Ji 2011; Ji 2012; Sun 2013; Sun 2013).

Publications Supported by AMOS Program

- Meyer, D. A., X. N. Zhang, U. Bergmann and K. J. Gaffney (2010). Characterization of charge transfer excitations in hexacyanomanganate(III) with Mn K-edge resonant inelastic x-ray scattering. *J. Chem. Phys.* **132**.
- Gaffney, K. J., M. B. Ji, M. Odelius, S. Park, et al. (2011). H-bond switching and ligand exchange dynamics in aqueous ionic solution. *Chem. Phys. Lett.* **504**: 1.
- Hartsock, R. W., W. K. Zhang, M. G. Hill, B. Sabat, et al. (2011). Characterizing the Deformational Isomers of Bimetallic $[\text{Ir}_2(\text{dimen})_4]^{2+}$ (dimen=1,8-diisocyno-p-menthane) with Vibrational Wavepacket Dynamics. *J. Phys. Chem. A* **115**: 2920.
- Jha, S. K., M. B. Ji, K. J. Gaffney and S. G. Boxer (2011). Direct measurement of the protein response to an electrostatic perturbation that mimics the catalytic cycle in ketosteroid isomerase. *Proc. Natl. Acad. Sci. U. S. A.* **108**: 16612.
- Ji, M. B. and K. J. Gaffney (2011). Orientational relaxation dynamics in aqueous ionic solution: Polarization-selective two-dimensional infrared study of angular jump-exchange dynamics in aqueous 6M NaClO_4 . *J. Chem. Phys.* **134**: 044516.
- Ji, M. B., R. W. Hartsock, Z. Sun and K. J. Gaffney (2011). Interdependence of Conformational and Chemical Reaction Dynamics during Ion Assembly in Polar Solvents *J. Phys. Chem. B* **115**: 11399.
- Jha, S. K., M. B. Ji, K. J. Gaffney and S. G. Boxer (2012). Site-Specific Measurement of Water Dynamics in the Substrate Pocket of Ketosteroid Isomerase Using Time-Resolved Vibrational Spectroscopy. *J. Phys. Chem. B* **116**: 11414.
- Ji, M. B., R. W. Hartsock, Z. Sung and K. J. Gaffney (2012). Influence of solute-solvent coordination on the orientational relaxation of ion assemblies in polar solvents. *J. Chem. Phys.* **136**: 014501.
- Kunnus, K., I. Rajkovic, S. Schreck, W. Quevedo, et al. (2012). A setup for resonant inelastic soft x-ray scattering on liquids at free electron laser light sources. *Rev. Sci. Instr.* **83**.
- Zhang, W. K., M. B. Ji, Z. Sun and K. J. Gaffney (2012). Dynamics of Solvent-Mediated Electron Localization in Electronically Excited Hexacyanoferrate(III). *J. Am. Chem. Soc.* **134**: 2581.

Zhang, W. K., Z. G. Lan, Z. Sun and K. J. Gaffney (2012). Resolving Photo-Induced Twisted Intramolecular Charge Transfer with Vibrational Anisotropy and TDDFT. *J. Phys. Chem. B* **116**: 11527.

Kunnus, K., P. Wernet, M. Odellius, I. Josefsson, et al. (2013). Observation of ultrafast ligand addition and spin crossover following Fe(CO)₅ photodissociation in ethanol. submitted.

Lemke, H. T., C. Bressler, L. X. Chen, D. M. Fritz, et al. (2013). Femtosecond X-ray Absorption Spectroscopy at a Hard X-ray Free Electron Laser: Application to Spin Crossover Dynamics. *J. Phys. Chem. A* **117**: 735.

Sun, Z., W. K. Zhang, M. B. Ji, R. W. Hartsock, et al. (2013). Contact Ion Pair Formation between Hard Acids and Soft Bases in Aqueous Solutions Observed with 2DIR Spectroscopy. *J. Phys. Chem. B*: accepted.

Sun, Z., W. K. Zhang, M. B. Ji, R. W. Hartsock, et al. (2013). Aqueous Mg²⁺ and Ca²⁺ Ligand Exchange Mechanisms Identified with 2DIR Spectroscopy. *J. Phys. Chem. B*: accepted.

McFarland, B. K., J. P. Farrell, S. Miyabe, F. Tarantelli, et al. (2014). Ultrafast X-ray Auger probing of photoexcited molecular dynamics. *Nature Communications* **5**.

Zhang, W. K., R. Alonso-Mori, U. Bergmann, C. Bressler, et al. (2014). Tracking Excited State Charge and Spin Dynamics in Iron Coordination Complexes *Nature* **509**: 345.

Ultrafast Theory and Simulation, Todd J. Martínez PI

Program Scope: This program is focused on developing and applying new methods for describing the interaction of molecular systems with radiation fields. We continue to develop the *ab initio* multiple spawning (AIMS) method which solves the electronic and nuclear Schrodinger equations simultaneously from first principles to describe excited state molecular dynamics including the breakdown of the Born-Oppenheimer approximation. We seek to extend this methodology to incorporate the effects of novel pump and probe pulses using high energy photons, including those obtained from modern x-ray sources such as LCLS. We also focus on understanding the behavior of molecular excited states in paradigmatic phenomena such as light-induced isomerization, ring-opening, excited state proton transfer, and excitation energy transfer.

Recent Progress and Future Plans

Improved methods for electronic structure. Obtaining potential energy surfaces and nonadiabatic derivative couplings accurately and efficiently remains a key issue in the modeling of excited state dynamics. We have been pursuing this project along several lines.

Explicitly correlated methods: We have developed a new method based on the explicit introduction of interelectronic distances in the electronic wavefunction – germinal-augmented multiconfiguration self-consistent field (GA-MCSCF). We showed that this method can be easily interfaced with multireference descriptions such as complete active space self-consistent field (CASSCF). This allows us to describe both static and dynamic electron correlation effects on potential energy surfaces within a variational framework (simplifying the construction of analytic gradients and conferring stability to the numerical procedures).¹ We have been working to extend this theory to arbitrary molecules, which involves the implementation of new integral codes for electron repulsion integrals involving up to four electrons.

Interpolated potential energy surfaces: We have also developed new methods to interpolate potential energy surfaces in the context of multiple electronic states.² The key issue here is to interpolate potential energy surfaces in the adiabatic representation, which is inherently non-smooth because of conical intersections. We showed how this could be done by interpolating *not* the potential energy surfaces but rather effective Hamiltonian matrices. Future work will investigate the use of this method to improve the descriptions of potential energy surfaces. For example, since the effective Hamiltonians are representative of a flexible diabaticization, one can correct these Hamiltonian matrices with low order information. Then only the correction would be interpolated and a zeroth order Hamiltonian would be computed on the fly, e.g. from CASSCF.

Dynamics with Multireference Perturbation Theory: We have implemented multi-state multireference perturbation theory (MS-CASPT2) in the context of AIMS dynamics and applied this to several molecules.³⁻⁷ By incorporating *both* static and dynamic correlation effects, we were able to carry out the first *ab initio* molecular dynamics calculations of excited state dynamics including Rydberg states.³ We found that the Rydberg state manifold was largely uninvolved in the excited state dynamics for ethylene, but that it *did* exert a considerable influence on the time-resolved photoelectron spectrum. Future work will focus on making the MS-CASPT2 method more efficient so that larger molecules can be addressed. The current state of the code limits us to molecules with at most ten atoms due to computational expense.

Exploiting graphical processing units (GPUs): We have explored the use of GPUs for electronic structure theory and *ab initio* molecular dynamics. Density functional methods were implemented⁸ and we have been assessing the possibility of using time-dependent density functional (TDDFT) methods for excited state dynamics. The many difficulties of TDDFT as concerns spurious charge transfer states in large molecules have caused difficulty in this regard. Thus, we have pursued two distinct strategies. For weakly-coupled multichromophoric complexes, it is possible to formulate an effective Hamiltonian of exciton type and then to parameterize this on-the-fly with *ab initio* calculations. Since the chromophores themselves are relatively small (e.g. less than 100 atoms), the problems with TDDFT are not manifest. We showed that this procedure is highly parallelizable and efficient. We were able to carry out *ab initio* molecular dynamics for a system with almost 1000 atoms using this approach.⁹ Future work will extend this to larger systems and investigate the extent to which the *ab initio* exciton model can be *more accurate* than the alternative of calculating excited states with TDDFT for the full system. Secondly, we have recently implemented CASSCF methods on the GPU. These new GPU-accelerated CASSCF methods are as much as 100x more efficient than CPU-based analogs. Future work will incorporate dynamic electron correlation corrections in these methods.

Understanding intersection topography: We have developed a new method to explore the landscape of conical intersections and thereby understand and predict the outcome of excited state molecular dynamics. The seam-space nudged elastic band method allows one to characterize minimal energy paths in the seam space, i.e. within the set of conical intersections.¹⁰ We believe this will become a widely used method to characterize intersections, going beyond the usual approach of focusing on a minimal energy conical intersection. Such a focus can be misleading in many cases. Future work will apply this SS-NEB method to a number of standard molecules such as thymine in order to characterize the dynamics and its relationship to the intersection seam.

Ab Initio Molecular Dynamics for Excited States. We continue to extend the AIMS formalism¹¹ to incorporate more complex pump and probe pulses. We are especially interested in pump/probe pulses corresponding to high photon energies, such as those that are available at modern x-ray sources.

Time-resolved photoelectron spectroscopy (TRPES). Ionization is a universal probe and thus not subject to selection rules that can stymie transient absorption techniques. Unfortunately, one does need to take into account the variation of the ionization potential with molecular geometry. When the probe photon energy is high, one also needs to account for multiple ionization continua which can be accessed by the probe pulse. We have developed a scheme for modeling TRPES that is based on AIMS simulation of the excited state dynamics, followed by computation of ionization potentials along the excited state trajectories and also photoionization cross-sections into each of the possible ionization continua. We have applied this method to several molecular systems,^{4-7,12} aiding in the interpretation of spectra and also predicting new spectra that are yet to be measured.^{3,5}

Strong-field ionization and shaped light fields: Typical applications of AIMS have used a weak-field description of the matter-radiation interaction. We have extended AIMS to allow for direct incorporation of the light field using a dressed state picture.¹³ This scheme allows for probe pulses which are too intense to be described in the weak field limit. Using this method, we were able to shed light on an experimental finding that multiple ionization was enhanced near a conical intersection.¹⁴ Future work will investigate this in more detail and determine if this can

be expected as a signature of dynamics near an intersection, i.e. to what extent this new phenomenon is general and dependent only on the exact or near-degeneracy of two electronic states. We have also used a similar method to understand recent LCLS experiments that probed excited state dynamics with an X-ray pulse that induced fragmentation.¹⁵

Time-resolved absorption spectra: We have explored new approaches to diminish the phase problem that is otherwise encountered in calculations of absorption spectra. The traditional correlation function based approach can be sensitive to the accuracy of the time-evolved wavefunction. In collaboration with Vanicek from EPFL,¹⁶ we showed that a much more stable approach can be devised by a form of phase-averaging (originally suggested by Mukamel). Future work will extend this to arbitrary time-dependent spectra.

Auger probe schemes: We have extended the AIMS method to incorporate Auger spectroscopy as a probe. Preliminary work calculated the Auger spectrum at a variety of geometries (for both ground and excited electronic states) and this was used to interpret recent ultrafast spectroscopy experiments at LCLS.¹⁷ Future work will incorporate this Auger probe calculation in the context of the full excited state dynamics. This is critical in order to fully interpret the experiment and to finally resolve the controversy surrounding the excited state dynamics of thymine, namely whether there exists an excited state (S_2) minimum or “shelf,” or if the Franck-Condon point is instead directly connected to a conical intersection. This is a significant point of disagreement between various theoretical electronic structure methods and provides a rare opportunity to benchmark the various methods.

High harmonic generation (HHG) probes: We have been developing new methods to describe HHG spectra from molecules. These methods are based on Gaussian basis sets including *both* time-dependent and time-independent functions. We have succeeded in benchmarking the basic approach for one and two-electron systems and future work will extend this to arbitrary numbers of electrons and moving nuclei. We were also able to use these techniques to aid in the interpretation of experiments that used HHG as a probe to illuminate molecular dynamics.¹⁸

Applications

Isomerization reactions: We have focused on the understanding of photoinduced isomerization in many different environments.^{3-7,10,13,19-22} We were able to show the role of surrounding electrostatic fields, e.g. nearby point charges, and to contrast this with steric effects. We found that steric effects were much less effective in altering the course of excited state dynamics for a prototypical C=C bond isomerization.²¹ We also investigated isomerization in a protein environment, using AIMS with a reparameterized multireference semiempirical method that we developed. We were able to reproduce experimental findings concerning the different excited state lifetimes in two highly homologous proteins and further to show that this difference was due to electrostatic effects in the region near the chromophore.²² Future work will continue to unravel the complex nature of the isomerization process in unsaturated carbon compounds and determine how the surrounding environment can influence the particular bond that isomerizes, the excited state lifetime, and competing fluorescence pathways. These are critical to a better understanding of light harvesting and energy transport in artificial photosynthetic systems (where isomerization is often an undesired pathway that needs to be suppressed).

Publications Supported by AMOS Program

¹ S. A. Varganov, and T. J. Martinez, Variational geminal-augmented multireference self-consistent field theory: Two-electron systems, *J. Chem. Phys.* **2010**, *132*, 054103.

- ² C. Evenhuis, and T. J. Martinez, A scheme to interpolate potential energy surfaces and derivative coupling vectors without performing a global diabaticization, *J. Chem. Phys.* **2011**, *135*, 224110.
- ³ T. Mori, W. J. Glover, M. S. Schuurman, and T. J. Martinez, Role of Rydberg states in the photochemical dynamics of ethylene, *J. Phys. Chem. A* **2012**, *116*, 2808-2818.
- ⁴ T. S. Kuhlman, W. J. Glover, T. Mori, K. B. Moller, and T. J. Martinez, Between ethylene and polyenes - the non-adiabatic dynamics of cis-dienes, *Faraday Disc.* **2012**, *157*, 193-212.
- ⁵ H. Tao, T. K. Allison, T. W. Wright, A. M. Stooke, C. Khurmi, J. van Tilborg, Y. Liu, R. W. Falcone, A. Belkacem, and T. J. Martinez, Ultrafast internal conversion in ethylene. I. The excited state lifetime, *J. Chem. Phys.* **2011**, *134*, 244306.
- ⁶ T. K. Allison, H. Tao, W. J. Glover, T. W. Wright, A. M. Stooke, C. Khurmi, J. van Tilborg, Y. Liu, R. W. Falcone, T. J. Martinez, and A. Belkacem, Ultrafast internal conversion in ethylene. II. Mechanisms and pathways for quenching and hydrogen elimination, *J. Chem. Phys.* **2012**, *136*, 124317.
- ⁷ T. J. A. Wolf, T. S. Kuhlman, O. Schalk, T. J. Martinez, K. B. Moller, A. Stolow, and A.-N. Unterreiner, Hexamethylcyclopentadiene: time-resolved photoelectron spectroscopy and ab initio multiple spawning simulations, *Phys. Chem. Chem. Phys.* **2014**, *16*, 11770-11779.
- ⁸ N. Luehr, I. S. Ufimtsev, and T. J. Martinez, Dynamical quadrature grids: Applications in density functional calculations In *GPU Computing Gems*; Hwu, W.-M., Ed.; Morgan-Kaufman: San Francisco, 2011, p 35-42.
- ⁹ A. Sisto, D. R. Glowacki, and T. J. Martinez, Ab initio nonadiabatic dynamics of multichromophore complexes: A scalable graphical-processing-unit-accelerated exciton framework, *Acc. Chem. Res.* **2014**, *in press*.
- ¹⁰ T. Mori, and T. J. Martinez, Exploring the conical intersection seam: The seam-space nudged elastic band method, *J. Chem. Theo. Comp.* **2013**, *9*, 1155-1163.
- ¹¹ S. Yang, and T. J. Martinez, Ab initio multiple spawning: First principles dynamics around conical intersections In *Conical Intersections: Theory, Computation and Experiment*; Domcke, W., Koppel, H., Eds.; World Scientific: Singapore, 2011, p 347-374.
- ¹² A. L. Thompson, and T. J. Martinez, Time-resolved photoelectron spectroscopy from first principles: Excited state dynamics of benzene, *Faraday Disc.* **2011**, *150*, 293-311.
- ¹³ J. Kim, H. Tao, J. L. White, V. S. Petrovic, T. J. Martinez, and P. H. Bucksbaum, Control of 1,3-Cyclohexadiene photoisomerization using light-induced conical intersections, *J. Phys. Chem. A* **2012**, *116*, 2758-2763.
- ¹⁴ V. S. Petrovic, S. Schorb, J. Kim, J. L. White, J. P. Cryan, J. M. Glownia, L. Zipp, D. Broege, S. Miyabe, H. Tao, T. J. Martinez, and P. H. Bucksbaum, Enhancement of strong-field multiple ionization in the vicinity of the conical intersection in 1,3-cyclohexadiene ring opening, *J. Chem. Phys.* **2013**, *139*, 184309.
- ¹⁵ V. S. Petrovic, M. Siano, J. L. White, N. Berrah, C. Bostedt, J. D. Bozek, D. Broege, M. Chalfin, R. N. Coffee, J. Cryan, L. Fang, J. P. Farrell, L. J. Frasinski, J. M. Glownia, M. Guehr, M. Hoener, D. M. P. Holland, J. Kim, J. P. Marangos, T. J. Martinez, B. K. McFarland, R. S. Minns, S. Miyabe, S. Schorb, R. J. Sension, L. S. Spector, R. Squibb, H. Tao, J. G. Underwood, and P. H. Bucksbaum, Transient X-ray fragmentation: Probing a prototypical photinduced ring-opening, *Phys. Rev. Lett.* **2012**, *108*, 253006.
- ¹⁶ M. Sulc, H. Hernandez, T. J. Martinez, and J. Vanicek, Relation of exact Gaussian basis methods to the dephasing representation: Theory and application to time-resolved electronic spectra, *J. Chem. Phys.* **2013**, *139*, 034112.
- ¹⁷ B. K. McFarland, J. P. Farrell, S. Miyabe, F. Tarantelli, A. Aguilar, N. Berrah, C. Bostedt, J. D. Bozek, P. H. Bucksbaum, J. C. Castagna, R. N. Coffee, J. P. Cryan, L. Fang, R. Feifel, K. J. Gaffney, J. M. Glownia, T. J. Martinez, M. Mucke, B. Murphy, A. Natan, T. Osipov, V. S. Petrovic, S. Schorb, T. Schultz, L. S. Spector, M. Swiggers, I. Tenney, S. Wang, J. L. White, W. White, and M. Guehr, Ultrafast X-ray Auger probing of photoexcited molecular dynamics, *Nature Comm.* **2014**, *5*, 4235.
- ¹⁸ L. S. Spector, M. Artamonov, S. Miyabe, T. J. Martinez, T. Seideman, M. Guehr, and P. H. Bucksbaum, Axis-dependence of molecular high harmonic emission in three dimensions, *Nature Comm.* **2014**, *5*, 3190.
- ¹⁹ H. Tao, L. Shen, M. H. Kim, A. G. Suits, and T. J. Martinez, Conformationally selective photodissociation dynamics of propanal cation, *J. Chem. Phys.* **2011**, *134*, 054313.
- ²⁰ B. Joalland, T. Mori, T. J. Martinez, and A. G. Suits, Photochemical dynamics of ethylene cation C₂H₄⁺, *J. Phys. Chem. Lett.* **2014**, *5*, 1467-1471.
- ²¹ A. M. Virshup, B. G. Levine, and T. J. Martinez, Steric and electrostatic effects on photoisomerization dynamics using QM/MM ab initio multiple spawning, *Theo. Chem. Acc.* **2014**, *133*, 1506.
- ²² C. Punwong, T. J. Martinez, and S. Hannongbua, Direct QM/MM simulation of photoexcitation dynamics in bacteriorhodopsin and halorhodopsin, *Chem. Phys. Lett.* **2014**, *610-611*, 213-218.

Understanding Photochemistry using Extreme Ultraviolet and Soft X-ray Time Resolved Spectroscopy

*Markus Gühr, SLAC National Accelerator Laboratory, 2575 Sand Hill Road, Menlo Park, CA 94025
mguehr@slac.stanford.edu*

Scope of the program

The scientific scope of this early career program is the site specific probing of chemical processes. For this purpose, we use light in the extreme ultraviolet (EUV) and soft x-ray (SXR) spectral range providing the site specificity due to the distinct absorption and emission features of core electrons. We are especially interested in non-Born-Oppenheimer approximation (non-BOA) dynamics, because of its importance for light harvesting, atmospheric chemistry and DNA nucleobases photoprotection. We use three different technical approaches for our studies: Laboratory based high harmonic generation (HHG) sources in the range of 20-100 eV delivering pulses with a few femtoseconds duration, synchrotrons with a wide spectral range from the EUV to the high SXR and the Linac Coherent Light Source (LCLS) providing high pulse energy femtoseconds pulses in the soft and hard x-ray range.

Progress in 2013/2014

EUV photoelectron/photoion spectroscopy (*T. Wolf, M. Koch (now at TU Graz)*)

During this past year we fully commissioned and performed first experiments with our extreme ultraviolet photoelectron/photoion spectrometer in the SLAC Bldg. 40/101 lab. The setup was described in last years abstract, and its performance as well as first measurements are published or under review¹⁻³. To summarize, we isolate the 9th harmonic (14eV photon energy, 86nm wavelength) of our Ti:Sapph 780 nm pulses using an indium filter/aluminum mirror combination. The pulses generated in this way are used to probe the dynamics on photoexcited molecular states via photoelectron and photoion spectroscopy.

With the high photon energies, we address a challenge which is commonly encountered in photoelectron spectroscopy. For low energy probes, vibrational and electronic relaxation often lead to similar features due to loss of Franck-Condon overlap with the ionic states. As the molecular dynamics distributes energy into several nuclear degrees of freedom and at the same time also other electronic states, an optical photon is not energetic enough for many molecules to provide ionization. The general decay on the photoelectron signal is then not sufficient any more to distinguish vibrational and electronic relaxation.

Figure 1 shows time resolved photoelectron and photoion data of isolated perylene (C₂₀H₁₂) molecules using this new apparatus. In part a, we show the photoelectron spectrum of the ground state (thick black line) emitted by 14 eV ultrafast EUV pulses. The highest kinetic energy features are located at 7 eV since the lowest ionization potential is 7eV. Perylene can be excited by 400 nm UV light (3 eV photon energy) to S₁ state, which then undergoes fluorescence decay in a few nanoseconds. The difference-photoelectron spectrum between perylene in the S₁ state and the ground state (thin line in a) shows features shifted to 10 eV due to the UV excitation and does not exhibit any change in peak position in the 6 ps interval after the UV excitation. Fits to the amplitudes and position of the peaks in the difference spectrum shown in Fig. 1b confirm this.

The apparatus allowed for measuring the perylene transient with an infrared multi-photon absorption, now showing ion signal as a function of delay between 400nm excitation and infrared (IR) probe pulse. The result shown in Fig. 1c clearly *exhibits a decay with a time constant of ~1 ps*. This discrepancy between the 14 eV EUV probe and the multi-photon IR is exciting. The two transitions are sensitive to different states of the molecule. The EUV probe directly leads from the S₁ to the cationic states; the multi-photon probe process involves several neutral resonant states in between the S₁ and cationic states, as we know from signal vs. IR intensity measurements. The energy-difference of S₁ and cationic states is constant along the nuclear geometry change induced by the 400 nm excitation, which leads to no or little modulation in the one photon probed photoelectron signal. The intermediate states in the multi-photon probe are getting shifted out of resonance on this path, explaining the signal decay.

We believe that these findings are important for the whole ultrafast community. Multi-photon infrared probing is a very popular tool due to its simplicity, but the role of intermediate states has never been investigated directly. Perylene does not undergo any intersystem crossing (ISC) or internal conversion (IC). It is ideal to show how signal decay, which might be interpreted as a signature IC or ISC in more complex systems, is purely due to shifting intermediate resonances.

We have finished our initial work on perylene and are currently working on the first EUV probe spectra of photoexcited thymine, which we have investigated at the LCLS. We expect that we obtain data complementary to the soft x-ray probes which will lead to new insight in the nucleobase excited state relaxation.

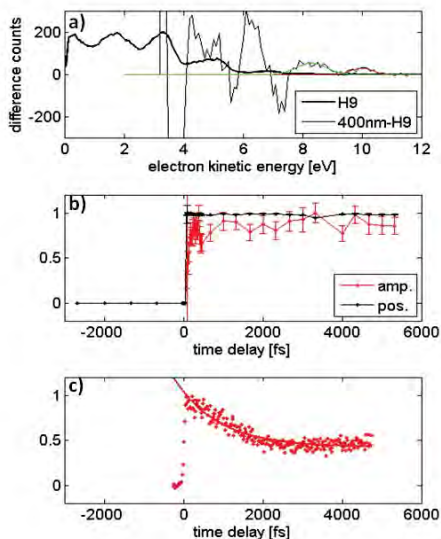


Fig. 1: *a)* Photoelectron spectrum of the perylene electronic ground state (thick black line) obtained with a photon energy of 14eV. Exciting perylene with 400 nm pulses to the S_1 state and subtracting the ground state spectrum leads to the difference spectrum (thin black line). The highest energy features of the ground state shift by 3 eV (corresponding to 400 nm wavelength) in the excited state, resulting in the difference features above 8eV, which are fitted by Gaussians (green). *b)* Amplitude and position of the excited state photoelectron features are stable for many picoseconds. *c)* In contrast, probing the excited state of perylene by an infrared multi-photon transition results in a decay during the first picosecond. This is due to intermediate resonances involved in the multi-photon probing.

EUUV Transient grating spectroscopy (*E. Sistrunk (now at LLNL), J. Grlj (now at EPFL Lausanne)*)

In the last abstract, we gave account on building a transient grating setup that works with EUV probe pulses. This setup is now fully operational and we have first demonstration experiments using VO_2 . The VO_2 possesses an interesting insulator to metal transition switchable by mild temperature changes or by ultrafast optical pulses. Since the vanadium has its M edge (3p – 3d transition) at 40 eV, we can directly address this edge with our EUV continua out of the HHG source. We pump the sample by two infrared pulses that interfere on the substrate under a small angle and thus create an intensity grating. We thereby create a transient grating made of metallic (high laser intensity) and isolating (low laser intensity) stripes. The diffracted EUV harmonic continuum is shown in Fig. 2 and we can identify individual harmonics. We now combined the advantage of transient grating spectroscopy (no background as in transient absorption) with the element selectivity in the M edge range.

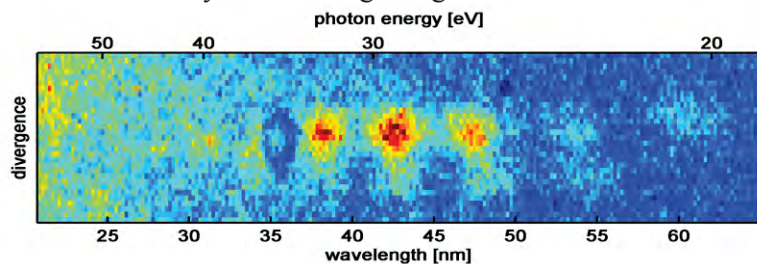


Fig. 2: Transient grating signal as detected by a CCD camera in the far field. The grating is formed by two IR pulses. Its dispersion is strong enough to distinguish individual harmonics.

The transient grating is made up of slow acoustic waves excited by the pump light as well as a fast change of the refractive index due to the metal- to insulator transition. We can identify those in the time delay scans between the grating pump pulses and the EUV probe. We were able to find the signature of the insulator to

metal transition on the vanadium M edge, which shifts to lower photon energies. We are currently summarizing our results in a paper as we continue to improve the time resolution of the apparatus⁴. The results from this work will have direct impact on transient grating and generally four wave mixing techniques at the LCLS. We submitted a proposal to LCLS on the topic of transient grating spectroscopy probed by soft x-ray LCLS pulses.

Soft x-ray probing of nucleobase photoprotection (*together with the nucleobase photoprotection collaboration see author list of Ref.⁵*)

We have finished the final analysis steps and published our work on probing nucleobase photoprotection using probe soft x-ray pulses from the LCLS⁵⁻⁷. We discovered that the Auger spectrum as a function of photoexcitation – X-ray -probe delay contains valuable information about the nuclear and electronic degrees of freedom from an element specific point of view. For the nucleobase thymine, the oxygen Auger spectrum shifts towards high kinetic energies, resulting from a particular C-O bond stretch in the $\pi\pi^*$ photoexcited state. A subsequent shift of the Auger spectrum towards lower kinetic energies displays the electronic relaxation of the initial photoexcited state within 200 fs. Ab-initio simulations reinforce our interpretation and indicate an electronic decay to the $n\pi^*$ state.

It is worth pointing out that we are able to detect a 0.1 Å. Resolving these small changes with hard x-rays requires crystallographic methods, however molecular photophysics in crystals is sufficiently different from the isolated or even the solvated case. Our spectroscopic mechanism can be explained by the fact that the core hole leads to the ejection of two valence electrons in the bond closest to the core hole. The Coulomb repulsion along the bond due to the missing electrons leads to a bondlength dependent shift of the Auger electron kinetic energy. For small bond elongations, the large Coulomb energy between the close lying nuclei leads to lowered Auger kinetic energies. For large bond distances, the Coulomb energy is smaller and more energy is available for the Auger electrons.

More activities at LCLS and other facilities

The data on resonant photoemission on ironpentacarbonyl done at beamline 10 (see last years abstract) at the ALS are analyzed and published⁸. We have developed a method using the resonant photoemission to identify the metal character associated with individual lines in the photoelectron spectra. This will enrich the content of our future time resolved measurements with the EUV source.

We participated in several LCLS beamtimes since the last progress report. The results from a beamtime on C60 fragmentation in strong x-ray fields (lead by N. Berrah with our participation) were analyzed and published in 2014⁹. In FY 2013 we were part of a team investigating uracil excited states by photoelectron spectroscopy at the LCLS. The team was lead by L. Avaldi from Rome. Our knowledge on the nucleobases was of crucial importance for the success of that beamtime and our sample evaporation system was used. The same sample system was used on a beamtime lead by Feiffel (Uppsala), who is also one of our thymine collaborators. We have also participated in investigations on nucleobase excited state investigations at FERMI, the Italian FEL. There, adenine was isolated in helium nanodroplets, which change the excited state dynamics, possibly by freezing out population behind reaction barriers. Furthermore, we helped in a beamtime lead by Nora Berrah and hosted two of her postdocs with their apparatus for preliminary ultrafast measurements preparing for an LCLS beamtime in our laser lab.

Undergraduate project (*M. Gopalakrishnan (CU Boulder)*)

In the framework of a SULI undergraduate project, we designed a motor controlled optical mirror system, which relies on open source hardware¹⁰. Due to its flexibility and low cost and flexibility, the mirror system allows for automatization of whole optical setups in no-access environments.

Plans

- 1) Photoelectron/Photoion EUV spectroscopy: We are currently investigating the excited state dynamics of thymine with probe energies of 14 eV and plan to observe also the dynamics of other nucleobases

- 2) LCLS soft x-ray Auger spectroscopy: We have submitted a proposal to investigate the excited state nuclear dynamics associated with proton transfer. The method allows for observing small sub Angstrom nuclear motion.
- 3) LCLS absorption spectroscopy: to get an indication on the ground state relaxation process of thymine, we have submitted an LCLS proposal using soft x-ray absorption spectroscopy at the O K-edge.
- 4) TG spectroscopy: we are working on covering the full M-edge of 3d transition metals and on a better time-resolution using tilted excitation wavefronts. We also submitted an LCLS proposal transitioning the lab based four wave mixing experience into the soft x-ray range.
- 5) SLACs ultrafast electron diffraction initiative: this task is supporting this initiative in collaboration with M. Centurions group from the University of Nebraska. We will perform ultrafast electron diffraction on photoexcited isolated molecules in the gas phase.

References of this task (or with participation of this task) during the last three years:

1. Koch, M., Wolf, T., Grilj, J., Sistrunk, E. & Gühr, M. Femtosecond photoelectron and photoion spectrometer with vacuum ultraviolet probe pulses. *J. Electron Spectrosc. Relat. Phenom.* **accepted**, (2014).
2. Grilj, J., Sistrunk, E., Koch, M. & Gühr, M. A beamline for time-resolved extreme ultraviolet and soft x-ray spectroscopy. *J. Anal. Bioanal. Tech* **S12**, 005 (2014).
3. Koch, M., Wolf, T. & Gühr, M. Understanding the modulation mechanism in resonance enhanced multi-photon probing of molecular dynamics. **submitted**, (2014).
4. Sistrunk, E. *et al.* Extreme Ultraviolet Transient Grating Spectroscopy of Vanadium Dioxide. *arXiv:1405.5964* (2014).
5. McFarland, B. K. *et al.* Ultrafast X-ray Auger probing of photoexcited molecular dynamics. *Nat. Commun.* **5**, 4235 (2014).
6. McFarland, B. K. *et al.* Experimental strategies for optical pump – soft x-ray probe experiments at the LCLS. *J. Phys. Conf. Ser.* **488**, 012015 (2014).
7. McFarland, B. K. *et al.* Probing nucleobase photoprotection with soft x-rays. *EPJ Web Conf.* **41**, 07004 (2013).
8. Sistrunk, E. *et al.* Resonant photoemission at the iron M-edge of Fe(CO)₅. *J. Chem. Phys.* **139**, 164318 (2013).
9. Murphy, B. F. *et al.* Femtosecond X-ray-induced explosion of C₆₀ at extreme intensity. *Nat. Commun.* **5**, (2014).(this task not lead)
10. Gopalakrishnan, M. & Gühr, M. A low-cost mirror mount control system for optics setups. *Am. J. Phys.* **accepted**, (2014).
11. Spector, L. S. *et al.* Axis-dependence of molecular high harmonic emission in three dimensions. *Nat. Commun.* **5**, (2014). (this task not lead, PULSE ATO task)
12. Gühr, M. Getting Molecular Electrons into Motion. *Science* **335**, 1314–1315 (2012).
13. Cryan, J. P. *et al.* Molecular frame Auger electron energy spectrum from N₂. *J. Phys. B At. Mol. Opt. Phys.* **45**, 055601 (2012). (this task not lead, PULSE SFA task)
14. Petrovic, V. S. *et al.* Transient X-Ray Fragmentation: Probing a Prototypical Photoinduced Ring Opening. *Phys. Rev. Lett.* **108**, (2012). (this task not lead)

Early Career: Strongly-driven attosecond electron-dynamics in periodic media

Shambhu Ghimire, SLAC National Accelerator Laboratory
2575 Sand Hill Rd, Menlo Park, CA, 94025
shambhu@slac.stanford.edu

Scope of the program

Strong-field response in high-density periodic media involves sub-cycle electron dynamics fundamentally different from gas. Recently, the generation of non-perturbative high-order harmonics in bulk crystals has been attributed to these dynamics, which occur in attosecond time-scale. While the basic characteristics of solid-state harmonics are found to be different from the atomic case the mechanism for solid-state HHG is of current debate. The objective of this program is to conduct experiments to investigate the fundamentals of HHG in crystals and thus determine its potential and limitations. This research will advance our fundamental understanding of high-intensity laser matter interactions with a focus on how the strong-field response in bulk crystals differs from that in isolated atoms.

This is a new program beginning August 2014.

Planned Research

1. Measurement of the phase of high order harmonics in bulk crystals:

Measurement of the phase of high-order harmonics is essential for attosecond pulse metrology. That understanding could also help in elucidating the generation mechanism. In atomic HHG this is known as the atto-chirp, whose origin has been understood in the three-step re-collision model [Corkum1993, Schafer1993, Krause1992]. In solid-state HHG this is a subject for investigation.

What do we expect from our model? Basic characteristics of solid-state HHG including high-energy cutoff scaling were consistent to the radiation from driven attosecond Bloch oscillations (ABO) in a single band of the solid [Ghimire2011a, Ghimire2011b, Ghimire2012]. Consider a 1-dimensional simple cosine band: $\varepsilon(q) = \frac{\hbar^2}{m_0^* d^2} [1 - \cos(qd)]$, where m_0^* , q are effective mass and momentum of electron and d is the lattice spacing. For a monochromatic laser field $E(t) = E_0 \cos(\omega t)$, we write the time

dependent group velocity of classical electron as: $v_g(t) = \frac{1}{\hbar} \frac{\partial \varepsilon(q)}{\partial q} = \frac{\hbar}{m_0^* d} \sin \left[\frac{\omega_B}{\omega} \sin(\omega t) + q(0) \right]$, where $\omega_B (= eE_0 d / \hbar)$ is Bloch frequency and $q(0)$ is the initial electron momentum.

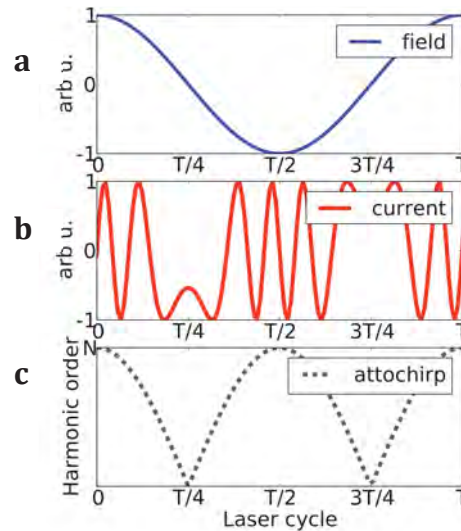


Figure 1: Prediction of harmonic phase from attosecond Bloch oscillation model. a) Laser cycle b) group velocity of classical electron in a 1 dimensional simple cosine band under the influence of the strong laser field, c) Harmonic phase in reference to the laser cycle.

Figure 1 a) is the laser field and figure 1 b) is the plot of group velocity. Figure 1 c) shows harmonic emission time of various harmonics with respect to the laser cycle (T).

As seen in the figure the near cutoff high-order harmonics are likely emitted only at and near the crest or the trough of the electric field of the laser because of the requirement of highest peak fields. In contrast, the lower order harmonic emission could span further away from trough and the crest. Thus depending upon the left (0 to $T/4$) and right ($T/4$ to $T/2$) quarter of the laser cycle the corresponding atto-chirp is negative and positive respectively. This is clearly different from the atto-chirp in atomic HHG, where the near cutoff harmonics are from the electrons released at about 17 degrees from the peak of the field [Dudovich2006].

Experimental Method: We will perform two-color HHG to measure the harmonic phase. In this method, a second harmonic field will be mixed with the driving laser field at a certain phase delay such that a small asymmetry can be introduced in the laser field, which manifests in the form of generation of even order harmonics in addition to the typical odd order harmonics. The strength of second harmonic will be weak so it does not affect HHG substantially but this mixing serves to create “timing gate” for even orders. Then, by scanning the phase delay between two colors we can spectroscopically map-out emission time and thus the pulse duration of individual harmonics with reference to the laser cycle. This method has been successfully used to measure atto-chirp in the gas phase at 800 nm [Dudovich2006].

Theory Support: We obtain theoretical support from Professor Mette Gaarde and her group in the Department of Physics and Astronomy at Louisiana State University. Her research includes modeling the macroscopic aspects of harmonic generation in solids and testing the suitability for attosecond pulse generation. She will develop an ab-initio solution of the time dependent Schrödinger equation that includes both the inter-band and intra-band interactions for HHG in periodic media.

2. Imaging attosecond Bloch Oscillations:

The main goal in this project is to image the driven intra-band oscillations and determine their contribution to the HHG. Our previous HHG results [Ghimire2011b] hinted the presence of full ABOs in ZnO single crystals when the fields strength approached ~ 0.3 V/Å [Ghimire2011b]. For the lattice spacing of 2.8 Å in ZnO this would correspond to the Bloch energy of ~ 0.8 eV, which is just about twice the laser photon energy (0.38 eV). It means that, if the incoherent scattering can be outrun the electrons would have acquired sufficient momentum from the laser field such that they traverse entire Brillouin zone every half cycle.

Attosecond dynamics of electron in atoms, molecules, and surfaces are typically studied experimentally by using isolated attosecond pulses, which makes experiments technically challenging. These difficulties were explored by A. L. Cavalieri *et al.* in the first attosecond time-resolved photoemission (ATPS) experiment in solid crystals, where the photoemission time-delay between 4f and conduction band electrons was measured [Cavalieri2007]. They used a combination of waveform-controlled few cycle 800 nm pulses and 300 *as* XUV pulses in their experiment for streaking photoelectrons as they escape the sample surface. Here, we take a different approach and design the first ATPS experiment without a need of using isolated attosecond pulses.

We take an advantage of the fact that electrons need transverse momentum in order to escape the sample surface. In the case of linearly polarized laser field that is aligned along the sample surface, the electrons in principle would not escape the surface because of the insufficient

transverse momentum. We will use an elliptically polarized MIR laser field $E(t) = E_{0\parallel} \hat{x} \cos(\omega t) + E_{0\perp} \hat{y} \cos(\omega t + \varphi)$ and a sample geometry such that the major and minor axes of ellipse are aligned along and perpendicular to the sample surface respectively. $E_{0\parallel}$ is parallel to the sample surface, which drives ABOs in a high symmetry direction in the crystal. We keep this field component sufficiently large and constant. On the other hand $E_{0\perp}$ is weak and is perpendicular to the sample surface which serves as the photoemission field, and that we vary in the experiment. This variation allows to selectively “streak” the electrons with certain instantaneous parallel momentum off of the sample surface.

Measurement approach: We will orient the <0001> cut single crystal ZnO sample such that the ABO driving field is aligned from Γ to M. This is the crystallographic direction where the width of conduction band is relatively large ($\sim 4 - 5$ eV) and the next higher band is relatively far in the energy. Because ABOs are expected to cover the entire bandwidths for the highest fields, the required energy resolution is coarse (on the order of 0.5 eV). In order to mitigate the photo voltage effects expected in typical wide band gap semiconductors, we have chosen doped samples where the electrical resistivity is low (Ga:ZnO, 0.1-0.01 ohm-cm).

Mitigating background: The use of intense laser pulses in the photoemission experiments often gives substantial background mainly from the unavoidable multiphoton absorption processes [Mathias2007, Dakovski2010]. From our past experience this could extend to about 10 eV. In order to mitigate this difficulty we use high-energy XUV pulse (~ 25 eV) as the pump beam to “aid” photoemission. This is because the XUV pump-pulse provides an additional kinetic energy to the photoelectrons so we can perform measurements where background is expected to be negligible.

Expected signal levels: We expect that about 1% of XUV photons get absorbed within the escape length of the electrons (~ 10 Å for ~ 20 eV electrons) in the ZnO sample. A $\sim 0.05\%$ level of initial conduction band electron density (from doping) corresponds to ~ 500 photoelectrons per pulse. Considering the detector acceptance angle of ± 4 degrees we expect to collect a maximum signal level of ~ 100 electrons per shot. This is in the photon energy from ~ 21 eV to ~ 25 eV thus it can be well separated from the energy range where background from multiphoton absorption is expected (< 10 eV). The photoelectrons from the valance band are well separated from the signal because of the relatively large forbidden gap (~ 3.2 eV).

References

- [Cavaliere2007] “Attosecond spectroscopy in condensed matter”, A. L. Cavaliere *et al.*, Nature, 449, 1029-1032 (2007).
- [Corkum1993] “Plasma perspective on strong field multiphoton ionization”, P. Corkum, Phys. Rev. Lett. 71, 1994–1997 (1993).
- [Dakovski2010] “Tunable ultrafast extreme ultraviolet source for time- and angle-resolved photoemission spectroscopy” Review of scientific instruments 81, 073108 (2010).
- [Dudovich2006] “Measuring and controlling the birth of attosecond XUV pulses”, N. Dudovich *et al.* Nature Physics, 2, 781-786 (2006).
- [Krause1992] “High-order harmonic generation from atoms and ions in the high intensity regime”, J. L. Krause, K. J. Schafer, and K. C. Kulander, Phys. Rev. Lett. 68, 3535 (1992).
- [Safer1993] “Above threshold ionization beyond the high harmonic cutoff” K. J. Schafer, B. Yang, L. F. DiMauro & K. C. Kulander, Phys. Rev. Lett. 70, 1599–1603 (1993).
- [Ghimire2011a] “Observation of high-order harmonic generation in a bulk crystal” S. Ghimire, A. D. DiChiara, E. Sistrunk, P. Agostini, L. F. DiMauro, and D. A. Reis, Nature Physics, 85, 4, 043836 (2011).

- [Ghimire2011b] “Redshift in the Optical Absorption of ZnO Single Crystals in the Presence of an Intense Midinfrared Laser Field” S. Ghimire, A. D. DiChiara, E. Sistrunk, U. Szafruga, P. Agostini, L. F. DiMauro, and D. A. Reis, *Phys. Rev. Lett.* 107, 167407 (2011).
- [Ghimire2012] “Generation and propagation of high-order harmonics in crystals”, S. Ghimire, A. D. DiChiara, E. Sistrunk, G. Ndabashimiye, U. Szafruga, P. Agostini, L. F. DiMauro, and D. A. Reis, *Phys. Rev. A.* 85, 043836 (2012).
- [Mathias2007] “Angle-resolved photoemission spectroscopy with a femtosecond high harmonic light source using a two-dimensional imaging electron analyzer”, *Review of Scientific Instruments* 78, 083105 (2007).
- [Sobota2013] “Direct Optical Coupling to an Unoccupied Dirac Surface State in the Topological Insulator Bi_2Se_3 ” J. A. Sobota, S.-L. Yang, A. F. Kemper, J. J. Lee, F. T. Schmitt, W. Li, R. G. Moore, J. G. Analytis, I. R. Fisher, P. S. Kirchmann, T. P. Devereaux, and Z.-X. Shen, *Phys. Rev. Lett.* 111, 136802 (2013).

University Research Summaries
(by PI)

Page is intentionally blank.

Tracing and Controlling Ultrafast Dynamics in Molecules

Principal Investigator: Andreas Becker

JILA and Department of Physics, University of Colorado at Boulder,
440 UCB, Boulder, CO 80309-0440

andreas.becker@colorado.edu

Program Scope

The emergence of attosecond technology has shifted our perspective in ultrafast science from the time scales intrinsic to nuclear dynamics to that of electron dynamics. With our projects we seek to provide theoretical support to establish new ultrafast concepts and optical techniques to obtain an advanced understanding and interpretation of electron dynamics in atoms and molecules.

Recent Progress and Future Goals

Our activities in the project over the last year can be summarized in the following sub-projects.

A. Finite-range time delays in numerical streaking experiments

The attosecond streak camera technique [1] enables the retrieval of temporal information of ultrafast processes on the attosecond time scale. The basic idea of this technique is that the momentum of a photoelectron, which is ionized by an ultrashort XUV pulse from a target, is streaked by an additional laser pulse, usually a near-infrared pulse. The final momentum of the electron then depends on the vector potential of the streaking field at the time instant of the transition of the electron into the continuum. By scanning the relative delay between the two pulses, time information is mapped onto the streaking trace, i.e., the final electron momentum as a function of the relative delay between the two pulses. In a recent application of the attosecond streaking technique a temporal offset of 21 as between streaking traces of electrons emitted from $2s$ and $2p$ orbitals in a neon atom was reported by Schultze *et al.* [2]. This temporal offset was interpreted as the time delay between the emission of the $2s$ and $2p$ electrons.

For single photoionization the temporal offset observed in numerical attosecond streaking simulations is often considered to involve contributions from the WS time delay [3,4] and the coupling between the streaking field and the Coulomb field. Based on our own quantum streaking simulations as well as a classical trajectory analysis, we have shown that alternatively the observed time delay can be written as a sum or integral of piecewise field-free time delays weighted by the instantaneous streaking field strength, relative to the streaking field strength at the instant of transition of the electron into the continuum [DOE6,DOE8]. This led us to the intuitive interpretation that - for single photoionization - the observed time delay depends on the *finite time* between the transition of the photoelectron from the initial bound state into the continuum and the end of the streaking pulse (or, alternatively the *finite region in space* along the polarization direction over which the electron propagates during this time interval).

Furthermore, our results show that over a long streaking pulse the observed continuum time delay can vary and that in an asymmetric potential it strongly depends on the directions of polarization and photoelectron emission. Finally, we have found that - in case of an atomic-like potential - the shape of the streaking pulse, e.g. pedestal in the trailing part of the pulse, as well

as additional static electric fields have a small influence on the observed continuum time delays only.

Based on our advanced understanding of the continuum time delay (in single photoionization) we have recently shown that the attosecond streaking technique actually provides the perspective to retrieve time-resolved information *during* the transition of the electron from the initial ground state to the continuum in a photoionization process. To this end, we considered two-photon ionization of the helium atom and performed ab-initio simulations to obtain attosecond streaking time delays for different scenarios. Our results show that in a resonant two-photon transition a significant additional time delay that depends on the XUV pulse parameters is acquired by the electron. We assume that this additional time delay is accumulated during the transition to the continuum via the resonant excited state and postulate that the retrieved streaking time delay consists of the sum of an absorption time delay and a continuum time delay [5].

We plan to develop efficient algorithms for the calculation of continuum time delays in streaking experiments and, in the long term, to apply our current understanding to the absorption time delay in molecules.

B. Generation of isolated ultrashort pulses using long driving wavelengths

To date the shortest attosecond pulses have been produced in the extreme UV region of the spectrum below 100 eV, which limits the range of materials and molecular systems that can be explored. These schemes for generating isolated attosecond pulses rely either on very short-duration few-cycle 800 nm driving laser pulses or polarization modulation schemes. In collaboration with the experimental groups of Margaret Murnane and Henry Kapteyn we have examined an alternative path of generating isolated ultrashort pulses by multi-cycle driving laser pulses at midinfrared wavelengths. Our calculations are based on an advanced numerical model, in which the process of harmonic generation is computed via an extension of the strong-field approximation on the microscopic level. Macroscopically, the gas medium is then discretized into elementary radiators and the radiation (harmonic emission) of each of these sources is propagated to the detector and calculated as coherent sum.

Our results indicate, in support of corresponding experimental observations, that a temporal gating of the harmonic emission down to one optical cycle can be achieved via macroscopic phase matching [DOE10]. By increasing the pressure of the gas medium, it is found that the increasing contribution of the neutral atom dispersion induces a phase shift on the front of the pulse, whereas the presence of the free-electron plasma induces a chirp on the trailing edge of the pulse. The combined effect confines the phase-matching window to the center of the pulse, where an isolated linearly chirped attosecond pulse is produced. Surprisingly, our results further indicate that multicycle driving laser pulses can be used and may lead to a more efficient generation of the isolated soft X-ray bursts than in few-cycle pulses, since in the multicycle pulses group velocity walk-off effects between the laser and the X-ray fields are mitigated that otherwise limit the conversion efficiency.

We are currently performing a systematic study regarding the application of this new method to generate isolated attosecond pulses at midinfrared driving wavelengths with respect to the wavelength and other parameters of the laser pulse as well as the gas parameters.

C. Multiple rescattering dynamics at the single atom level

Recent experiments have investigated driving high harmonic generation with midinfrared light, and thus extending the harmonic plateau to keV energies [6]. At these longer wavelengths, it has been proposed that electrons which rescatter multiple times from a parent nucleus play an important role [7], and furthermore may open a way of producing waveforms on zeptosecond time scales [8]. However, detection and resolution of the zeptosecond waveforms, and therefore confirmation of the presence of the multiple rescattering events poses a challenge to current experimental technologies.

We have therefore studied a control scheme based on the interrogation of the process of HHG production by application of a second color of light on the microscopic level either via an attosecond pulse train or an isolated attosecond pulse. This strategy has been explored before in the context of controlling the excursion distance of an electron wave packet and enhancing the HHG signal [9]. We have proposed to extend this strategy and use the control afforded by using an isolated pulse of VUV light to verify the existence of multiple rescatterings. By using VUV light to control the moment of electron ionization, we have demonstrated selective generation of electrons into trajectories which revisit the parent nucleus several times and have examined the signatures of multiple rescatterings in both the temporal and frequency domains of the generated radiation. We additionally suggested a way of employing this technique to advance the frontier of ultrashort light pulse production through the use of two VUV pulses. Instances of coincident rescatterings of two wave packets are shown to occur and modulate the generated XUV light pulses by a rapidly beating substructure through interference. The beating period can be controlled via the energy difference between the simultaneously rescattering wave packets and may offer a perspective to generate ultrashort waveforms.

We plan to extend our studies – on the long term – by including phase-matching and propagation effects in order to show that the effects identified on the single atom level are observable on the macroscopic level as well.

References

- [1] J. Itatani et al., Phys. Rev. Lett. **88**, 173903 (2002).
- [2] M. Schultze et al., Science **328**, 1658 (2010).
- [3] E. P. Wigner, Phys. Rev. **98**, 145 (1955).
- [4] F. T. Smith, Phys. Rev. **118**, 349 (1960).
- [5] J. Su, H. Ni, A. Jaron-Becker, and A. Becker, submitted for publication.
- [6] T. Popmintchev et al., Science **91**, 1287 (2012)
- [7] J. Tate et al., Phys. Rev. Lett. **98**, 013901 (2007)
- [8] C. Hernandez-Garcia et al., Phys. Rev. Lett. **111**, 033002 (2013)
- [9] K. Schafer et al., Phys. Rev. Lett. **92**, 023003 (2004)

Publications of DOE sponsored research

[DOE1] J. Su, S. Chen, A. Jaroń-Becker and A. Becker, *Temporal analysis of non-resonant two-photon coherent control involving bound and dissociative molecular states*, *Physical Review A* **84**, 065402 (2011)

[DOE2] M. Odenweller, N. Takemoto, A. Vredenburg, K. Cole, K. Pahl, J. Titze, L. Ph. H. Schmidt, T. Jahnke, R. Dörner and A. Becker, *Strong field electron emission from fixed in space H_2^+ ions*, *Physical Review Letters* **107**, 143004 (2011)

[DOE3] A. Picon, A. Jaron-Becker and A. Becker, *Enhancement of vibrational excitation and dissociation of H_2^+ in infrared laser pulses*, *Physical Review Letters* **109**, 163002-1-4 (2012)

[DOE4] J. Su, H. Ni, A. Becker and A. Jaron-Becker, *Numerical simulation of time delays in light induced ionization*, *Physical Review A* **87**, 0334201-9 (2013)

[DOE5] A. Becker, F. He, A. Picon, C. Ruiz, N. Takemoto and A. Jaron-Becker, *Observation and control of electron dynamics in molecules*, in *Attosecond Physics: Attosecond Measurements and Control of Physical Systems*, Eds. L. Plaja, R. Torres and A. Zair, Springer Series in Optical Sciences, Vol. 177 (Springer, Berlin - Heidelberg, 2013) p. 207-229

[DOE6] J. Su, H. Ni, A. Becker and A. Jaron-Becker, *Finite-range time delay in numerical streaking experiments*, *Physical Review A* **88**, 023413-1-6 (2013)

[DOE7] J. Su, H. Ni, A. Becker and A. Jaron-Becker, *Theoretical analysis of time delays and streaking effects in XUV photoionization*, *Journal of Modern Optics* **60**, 1484-1491 (2013)

[DOE8] J. Su, H. Ni, A. Becker and A. Jaron-Becker, *Attosecond streaking time delays: Finite-range property and comparison of classical and quantum approaches*, *Physical Review A* **89**, 013404 (2014)

[DOE9] J. Su, H. Ni, A. Becker and A. Jaron-Becker, *Numerical simulations of attosecond streaking time delays in photoionization (invited paper)*, *Chinese Journal of Physics* **52**, 404 (2014)

[DOE10] M.-C. Chen, C. Mancuso, C. Hernández-García, F. Dollar, B. Galloway, D. Popmintchev, P.-C. Huang, B. Walker, L. Plaja, A. A. Jaroń-Becker, A. Becker, M. M. Murnane, H. C. Kapteyn, and T. Popmintchev, *Generation of bright isolated attosecond soft X-ray pulses driven by multicycle midinfrared lasers*, *Proceedings of the National Academy of Sciences of the United States of America* **111**, E2361 (2014)

Probing Complexity using the LCLS and the ALS

Nora Berrah

Physics Department, University of Connecticut, Storrs, CT 06268

e-mail:nora.berrah@uconn.edu

Program Scope

The goal of our research program is to investigate *fundamental interactions between photons and molecular systems* to advance our quantitative understanding of electron correlations, charge transfer and many body phenomena. Our research investigations focus on probing on femtosecond time-scale multi-electron interactions and tracing nuclear motion in order to understand and ultimately control energy and charge transfer processes from electromagnetic radiation to matter. Most of our work is carried out in a strong partnership with theorists.

Our current interests include: **1)** The study of non linear and strong field phenomena in the x-ray regime using free electron lasers (FELs), and in particular, the ultrafast linac coherent light source (LCLS) x-ray FEL facility at the SLAC National Laboratory. **2)** Time-resolved investigations of molecular dynamics using pump-probe techniques. Our experiments probe physical and chemical processes that happen on femtosecond time scales. This is achieved by measuring and examining both electronic and nuclear dynamics subsequent to the interaction of molecules and clusters with LCLS pulses of various fluence and fs (4-500) pulse duration. **3)** The study of dynamics and correlated processes in select molecules as well as anions with vuv-soft x-rays from the Advanced Light Source (ALS) at Lawrence Berkeley Laboratory. We present here results completed and in progress this past year and plans for the immediate future.

Recent Progress

1) Buckyball Explosion by Intense Femtosecond X-Ray Pulses: A Model System for Complex Molecules

We have carried out an experimental and theoretical study of C_{60} molecules interacting with intense x-ray pulses from the LCLS, revealing the influence of processes not previously reported. Specifically, we demonstrated the effects of high per-atom x-ray absorption on the fragmentation dynamics of C_{60} molecules in the gas phase. This work presents an essential step for the rigorous, quantitative understanding of femtosecond molecular dynamics. Measurements guided the development of molecular dynamics simulations suitable for large molecules exposed to intense XFEL pulses. Experimental and simulation data on C_{60} ion dynamics reveal that a complex variety of physical and chemical processes are present in these interactions. Our model demonstrates that full atomic fragmentation of C_{60} occurs at the highest fluences while molecular fragments are generated at medium fluence. We show that ionization suppression occurs for very short pulses (4 fs). While an analogous effect is known for atoms and small molecules, the mechanism for such a large molecule is more complex, as revealed by simulations. Furthermore, our experiment provided evidence that the charged particles produced by exposing an extended quantum system, C_{60} , to high-fluence x rays behave as if they were classical particles. At high fluence, the parent molecule explodes within few tens of fs, giving rise to fragment ions and highly charged state of C atom. In fact, we fully strip C of all of its 6 electrons.

We have compared our experimental data with various modeling scenarios of the atomic ion yields following molecular fragmentation with short (4 fs), medium (60 fs) and long pulse durations (90 fs). Our final Molecular Dynamics (MD) model includes several independent phenomena: bonds between C atoms, bond breaking, molecular Auger decay and secondary

ionization. The final model is compared with models ignoring one of these key ingredients. The discrepancies reveal the relative importance of each physical process implemented in the development of the model, leading to a final model that agrees very well with the data for both pulse durations. The first and second models represent two extreme cases: no chemical bonding and always-present bonding forces, respectively. Turning off the bonding force field and allowing the ions to interact with each other and with electrons only through simple Coulomb forces results in excessive pre-expansion, and an excess of C^{1+} while suppressing higher charge states and eliminating all molecular ion fragments. Second, turning off the bond-breaking mechanism so that ions experience the bonding field regardless of electronic configuration (but fragmentation can still happen due to the dominance of strong Coulomb repulsion over bonding forces). This scenario depletes the C^{1+} channel and results in excess of high charges, since more energetic dissociation prevents recombination following the pulse. The model with no molecular Auger process produces similar results to the scenario without bond-breaking: insufficient C^{1+} and excess high charge states. Finally, the consequence of neglecting secondary ionizations further biases the ion yield toward higher charges, because recombination processes, which occur mainly with slow secondary electrons, are suppressed [1,2].

2) Advanced Instrumentation for LCLS-Based Research

We have built and commissioned a multi-user facility that consists presently of two instruments based at the LCLS and available to any user. They are: 1) the X-Ray Split and Delay (XRSD) to carry out time-resolved experiments utilizing x-ray pump x-ray probe technique and 2) the LAMP instrument which presently houses two imaging detectors and two VMI spectrometers. The later have already been used to measure ion-ion coincidences in molecular experiments.

Future Plans.

The principal areas of investigation planned for the coming year are:

1) Finish analyzing the recent XRSD commissioning data collected during our LCLS May 2013 beamtime. 2) Analyze the data generated during the November 2013 LAMP commissioning beamtime. 3) Analyze the data that resulted from the photodetachment experiment of H^- using single photon ionization from the ALS. 4) Analyze the data that we generated from the photodetachment experiments of the carbon anions chain ($C_2^- - C_{12}^-$) at the ALS.

Publications from DOE Sponsored Research

1. B. F. Murphy, T. Osipov, Z. Jurek, L. Fang, S.-K. Son, L. Avaldi, P. Bolognesi, C. Bostedt, J. Bozek, R. Coffee, J. Eland, M. Guehr, J. Farrell, R. Feifel, L. Frasinski, J. Glowina, D.T. Ha, K. Hoffmann, E. Kukk, B. McFarland, C. Miron, M. Mucke, R. Squibb, K. Ueda, R. Santra, and N. Berrah “Bucky ball explosion by intense femtosecond x-ray pulses: a model system for complex molecules”, *Nature Communication*, **5**, 4281, doi:10.1038/ncomms5281 (2014)
2. N. Berrah, L. Fang, T. Osipov, Z. Jurek, B. F. Murphy, and R. Santra, *Faraday Discussion*, “Emerging photon technologies for probing ultrafast molecular dynamics” Royal Society of Chemistry Publishing, (in press, 2014)
3. N. Berrah and P. H. Bucksbaum, “The Ultimate X-ray Machine” *Scientific American*, **310**, 64, January 2014.
4. B. K. McFarland, J. P. Farrell, S. Miyabe, F. Tarantelli, A. Aguilar, N. Berrah, C. Bostedt, J. Bozek, P.H. Bucksbaum, J. C. Castagna, R. Coffee, J. Cryan, L. Fang, R. Feifel, K. Gaffney, J. Glowina, T. Martinez, M. Mucke, B. Murphy, A. Natan, T. Osipov, V. Petrovic, S. Schorb, Th. Schultz, L. Spector, M. Swiggers, I. Tenney, S. Wang, W. White, J. White and M. Gühr “Delayed Ultrafast X-ray Auger Probing (DUXAP) of Nucleobase Ultraviolet Photoprotection”, *Nature Communication*, **5**, 4235, doi:10.1038/ncomms5235 (2014)

5. L. Fang, D. Rolles, A. Rudenko, V. Petrovich, C. Bostedt, J. D. Bozek, P. Bucksbaum and N. Berrah “Probing ultrafast electronic and molecular dynamics with free electron lasers” *J. Phys. B: At. Mol. Opt. Phys.* **47** 124006 (2014) doi:10.1088/0953-4075/47/12/124006
6. M. Mucke, V. Zhaunerchyk, R.J. Squibb, M. Kamiska, J.H.D. Eland, P. v.d.Meulen, P. Salén, P. Linusson, R.D. Thomas, M. Larsson, L.J. Frasinski, M. Siano, T. Osipov, L. Fang, B. Murphy, N. Berrah, L. Foucar, J. Ullrich, K. Motomura, S. Mondal, K. Ueda, R. Richter, K.C. Prince, M.N. Piancastelli, M. Glownia, J. Cryan, R. Coffee, C. Bostedt, J. Bozek, S. Schorb, M. Messerschmidt, O. Takahashi, S. Wada, and R. Feifel, “Mapping the decay of double core hole states of atoms and molecules”, *Journal of Physics: Conference Series* **488**, 032021 (2014).
7. N. Berrah, L. Fang, T. Osipov, B. Murphy, C. Bostedt and J.D. Bozek, “Multiphoton Ionization and Fragmentation of Molecules with the LCLS X-Ray FEL (J. Elec. Spect and Rela. Phen, in press.)
8. B.K. McFarland, N. Berrah, C. Bostedt, J. Bozek, P. H. Bucksbaum, J. C. Castagna, R. N. Coffee, J. P. Cryan, L. Fang, J. P. Farrell, R. Feifel, K. J. Gaffney, J. M. Glownia, T. J. Martinez, S. Miyabe, M. Mucke, B. Murphy, A. Natan, T. Osipov, V. S. Petrović, S. Schorb, Th. Schultz, L. S. Spector, M. Swiggers, F. Tarantelli, I. Tenney, S. Wang, J. L. White, W. White, and M. Gühr, “Experimental strategies for optical pump – soft x-ray probe experiments at the LCLS” *J. Phys.: Conf. Ser.* **488** 012015 doi:10.1088/1742-6596/488/1/012015(2014).
9. R. C. Bilodeau, N. D. Gibson, C. W. Walter, D. A. Esteves-Macaluso, S. Schippers, A. Muller, R. A. Phaneuf, A. Aguilar, M. Hoener, J. M. Rost, and N. Berrah, “Single-Photon Multiple-Detachment in Fullerene Negative Ions: Absolute Ionization Cross Sections and the Role of the Extra Electron, *Phys. Rev. Lett.* **111**, 043003 (2013).
10. L.J. Frasinski, V. Zhaunerchyk, M. Mucke, R.J. Squipp, M. Siano, J.H.D. Eland, P. Linusson, P.v.d. Meulen, P. Salén, R.D. Thomas, M. Larsson, L. Foucar, J. Ullrich, K. Motomura, S. Mondal, K. Ueda, T. Osipov, L. Fang, B.F. Murphy, N. Berrah, C. Bostedt, J.D. Bozek, S. Schorb, M. Messerschmidt, M. Glownia, J.P. Cryan, R.N. Coffee, O. Takahashi, S. Wada, M.N. Piancastelli, R. Richter, K.C. Prince, and R. Feifel *Phys. Rev. Lett.* **111**, 073002 (2013).
11. V. Zhaunerchyk, M. Mucke, P. Salén, P.v.d. Meulen, M. Kaminska, R.J. Squipp, L.J. Frasinski, M. Siano, J.H.D. Eland, P. Linusson, R.D. Thomas, M. Larsson, L. Foucar, J. Ullrich, K. Motomura, S. Mondal, K. Ueda, T. Osipov, L. Fang, B.F. Murphy, N. Berrah, C. Bostedt, J.D. Bozek, S. Schorb, M. Messerschmidt, J.M. Glownia, J.P. Cryan, R.N. Coffee, O. Takahashi, S. Wada, M.N. Piancastelli, R. Richter, K.C. Prince, and R. Feifel *J. Phys. B: At. Mol. Opt. Phys.* **46**, 164034 (2013).
12. C. Bostedt, J. D. Bozek, P. H. Bucksbaum, R. N. Coffee, J. B. Hastings, Z. Huang, R. W. Lee, S. Schorb, J. N. Corlett, P. Denes, P. Emma, R. W. Falcone, R. W. Schoenlein, G. Doumy, E. P. Kanter, B. Kraessig, S. Southworth, L. Young, L. Fang, M. Hoener, N. Berrah, C. Roedig, and L. F. DiMauro, *J. Phys. B: At. Mol. Opt. Phys.* **46**, 164003 (2013).
13. T Osipov, L Fang, B Murphy, F Tarantelli, E R Hosler, E Kukkk, J D Bozek, C Bostedt, E P Kanter and N Berrah, ” Multiphoton ionization and fragmentation of SF₆ induced by intense free electron laser pulses”, *J. Phys. B: At. Mol. Opt. Phys.* **46** , 164032 (2013).
14. M Larsson, P Salén, P van der Meulen, H T Schmidt, R D Thomas, R Feifel, M N Piancastelli, L Fang, B Murphy, T Osipov, N Berrah, E Kukkk, K Ueda, J D Bozek, C Bostedt, S Wada, R Richter, V Feyer and K C Prince “Double core-hole formation in small molecules at the LCLS free electron laser” *J. Phys. B: At. Mol. Opt. Phys.* **46**, 164030 (2013).
15. J.C. Castagna, B. Murphy, J. Bozek, and N. Berrah, “X-ray split and delay for soft x-rays at LCLS”, *Journal of Physics:Conference Series* **425** 152021, (2013).
16. L. Fang, T. Osipov, B. Murphy, F. Tarantelli, E. Kukkk, J.P. Cryan, M. Glownia, P.H. Bucksbaum, R.N. Coffee, M. Chen, C. Buth, and N. Berrah, “Multiphoton Ionization as a Clock to Reveal Molecular Dynamics with Intense Short X-ray Free Electron Laser Pulses”, *Phys. Rev. Lett.*, **109**, 263001 (2012).

17. B. F. Murphy, L. Fang, M.-H. Chen, J. D. Bozek, E. Kukk, E. P. Kanter, M. Messerschmidt, T. Osipov, and N. Berrah, “Multiphoton L-Shell Ionization of H₂S using Intense X-ray Pulses from the LCLS Free Electron Laser” *Phys. Rev. A* **86**, 053423 (2012).
18. B. Rudek, S. Kil Son, L. Foucar, S. W. Epp, B. Erk, R. Hartmann, M. Adolph, R. Andritschke, A. Aquila, N. Berrah, et al. “Ultra-Efficient Ionization of Heavy Atoms by Intense X-Ray Free-Electron Laser Pulses, *Nature Photonics* **6**, 865 (2012)
19. R.C. Bilodeau, N.D. Gibson, C.W. Walter, A. Aguilar, N. Berrah, “Inner-shell photodetachment: Shape and Feshbach resonances of anions”, *Journal of Electron Spectroscopy and Related Phenomena* **185** 219– 225 (2012).
20. V. S. Petrović, M. Siano, J.L. White, N. Berrah, C. Bostedt, J. D. Bozek, D. Broege, M. Chalfin, R. N. Coffee, J. Cryan, L. Fang, J. P. Farrell, L. J. Frasinski, J. M. Glowina, M. Gühr, M. Hoener, D.M. P. Holland, J. Kim, J. P. Marangos³, T. Martinez, B. K. McFarland, R. S. Minns, S. Miyabe, S. Schorb, R. J. Sension, L. S. Spector, R. Squibb, H. Tao, J. G. Underwood, and P. H. Bucksbaum “Transient X-ray fragmentation: Probing a prototypical photoinduced ring opening”, *Phys. Rev. Lett.* **108**, 253006, (2012).
21. Christian Buth, Ji-Cai Liu, Mau Hsiung Chen, L. Fang, M. Hoener, N. Berrah, “Ultrafast absorption of intense x rays by nitrogen molecules”, *J. Chem. Phys.* **136**, 214310 (2012)
22. P. Salen, P. van der Meulen, H.T. Schmidt, R.D. Thomas, M. Larsson, R. Feifel, M.N. Piancastelli, L. Fang, B. Murphy, T. Osipov, N. Berrah, E. Kukk, K. Ueda, J.D. Bozek, C. Bostedt, S. Wada, R. Richter, V. Feyer and K.C. Prince, “X-ray FEL-induced Two-Site Double Core-Hole Formation for Chemical Analysis”, *Phys. Rev. Lett. PRL* **108**, 153003 (2012)
23. H. Thomas, A. Helal, K. Hoffmann, N. Kandadai, J. Keto, J. Andreasson, B. Iwan, M. Seibert, N. Timneanu, J. Hajdu, M. Adolph, T. Gorkhover, D. Rupp, S. Schorb, T. Möller, G. Doumy, L.F. DiMauro, M. Hoener, B. Murphy, N. Berrah, M. Messerschmidt, J. Bozek, C. Bostedt and T. Ditmire, “Explosions of Xe-clusters in ultra-intense femtosecond x-ray pulses from the LCLS Free Electron Laser”, *Phys. Rev. Lett.* **108**, 133401 (2012).
24. James P. Cryan, J. M. Glowina, Andreasson, A. Belkacem, N. Berrah, C. I. Blaga, C. Bostedt, J. Bozek, N. A. Cherepkov, L. F. DiMauro, L. Fang, O. Gessner, M. Guehr, J. Hajdu, M. P. Hertlein, M. Hoener, O. Kornilov, J. P. Marangos, A. M. March, B. K. McFarland, H. Merdji, M. Messerschmidt, V. Petrovic, C. Raman, D. Ray, D. Reis, S. K. Semenov, M. Trigo, J. L. White, W. White, L. Young, P. H. Bucksbaum, and R. N. Coffee, “Molecular frame Auger electron energy spectrum from N₂” *J. Phys. B: At. Mol. Opt. Phys.* **45**, 055601 (2012).
25. T.Y. Osipov, L. Fang, B.F. Murphy, M. Hoener, and N. Berrah, “X-Ray FEL Induced Double Core-Hole and High Charge State Production”, *Journal of Physics: Conference Series* **388**, 012030, (2012).
26. L. Fang, T. Osipov, B. Murphy, et al. and N. Berrah, Multiple ionization and double core-hole production in molecules using the LCLS x-ray FEL””, *Journal of Physics: Conference Series* **388**, 032028, (2012).
27. T. Osipov, D. Rolles, C. Bostedt, J-C. Castagna, R. Hartman, J. D. Bozek, I. Schlichting, L. Struder, J. Ullrich and N. Berrah, “Next generation endstation for concurrent measurements of charged products and photons in LCLS FEL experiments” *Journal of Physics: Conference Series* **388**, 142025 (2012).
28. P. Salen, P. van der Meulen, R. D. Thomas, H. T. Smith, M. Larsson, R. Feifel, L. Fang, T. Osipov, B. Murphy, N. Berrah, et al. “X-ray FEL-induced double core hole formation in polyatomic molecules, *J. Phys.: Conf. Ser.* **388**, 022083 (2012)
29. B.F. Murphy, L. Fang, T.Y. Osipov, M. Hoener, and N. Berrah, “Intense X-ray FEL-Molecule Physics: Highly Charged Ions” the American Institute of Physics (AIP) Conference Proceedings of ICAPiP, **1438**, 249 (2012).
30. B.F. Murphy, J. Bozek, J.C. Castagna, and N. Berrah, “Split and Delay System for Soft X-ray Pump/Soft X-ray Probe Experiments at the LCLS Free Electron Laser”, *Journal of Physics: Conference Series* **388** 142003 (2012).

Ultrafast Electron Diffraction from Aligned Molecules

Martin Centurion

Department of Physics and Astronomy, University of Nebraska, Lincoln, NE 68588-0299
mcenturion2@unl.edu

Program Scope

The aim of this project is to record time-resolved electron diffraction patterns of aligned molecules and to reconstruct the 3D molecular structure. The molecules are aligned non-adiabatically using a femtosecond laser pulse. A femtosecond electron pulse is then used to record a diffraction pattern while the molecules are aligned. The experiment consists of a laser system, a pulsed electron gun, a gas jet that contains the target molecules and a detector to capture the diffraction patterns. The diffraction patterns are processed to obtain the molecular structure.

Introduction

The majority of known molecular structures have been determined using either x-ray diffraction for crystallized molecules or Nuclear Magnetic Resonance (NMR) spectroscopy for molecules in solution. However, for isolated molecules there has been no method demonstrated to measure the three dimensional structure. Electron diffraction has been the main tool to determine the structure of molecules in the gas phase [1] and also to investigate ultrafast changes in structure[2-4]. In this method the diffraction pattern is compared with a calculated structure iteratively until an appropriate match between experiment and theory is found. Diffraction patterns from randomly oriented molecules contain only one-dimensional information, and thus input from theoretical models is needed to recover the structure. We propose to use pulsed electron diffraction from aligned molecules to recover the three dimensional structure, and to investigate molecular dynamics.

In previous experiments, electron diffraction patterns of aligned molecules have been recorded using adiabatic alignment with long laser pulses (in this case the laser is longer than the rotational period and is present during the alignment)[5], and by selective alignment in a photodissociation reaction[6]. However, in both cases the degree of alignment was found to be too weak to extract structural information. Additionally, in adiabatic alignment the presence of a strong laser field can distort the molecular structure, while selective alignment relies on a change in the structure. In our experiments, the molecules are impulsively aligned with a femtosecond laser pulse and probed with femtosecond electron pulses in a field-free environment at the peak alignment. This ensures that the molecules are not distorted by the laser field when the structure is probed by the electron pulse.

Recent Progress

We have demonstrated experimentally, for the first time, three dimensional imaging of isolated molecules in which the structure was recovered from the diffraction patterns without assuming any previous knowledge of the structure [7]. In order to reach this goal, we had to overcome two major obstacles. First, sub-picosecond resolution was needed to be able to capture the diffraction pattern while the molecules were aligned. Previously, the highest temporal resolution for gas phase diffraction experiments was about 3 ps [6]. We were able to reach a resolution of 850 fs by simultaneously improving on several parts of the experiments. The second challenge was to retrieve structure from diffraction of partially aligned molecules. So far, all existing phase retrieval methods, to our knowledge, only deal with perfectly aligned molecules. Experimentally it is very difficult to achieve very high degrees of alignment, particularly because the densities needed for diffraction are not compatible with the sub-Kelvin temperatures needed for high alignment. We developed a new algorithm that combines several diffraction patterns corresponding to different projections of partially aligned molecules. This allowed us to reconstruct the structure of the CF_3I molecule by combining multiple diffraction patterns with partial alignment [7].

We have now shown numerically that the method can be extended to more complex asymmetric molecules [8] (Figure 1). We use a two-step method for retrieving the 3-D structure of trifluorotoluene ($\text{C}_6\text{H}_5\text{CF}_3$), an asymmetric-top molecule. Two diffraction patterns were used:

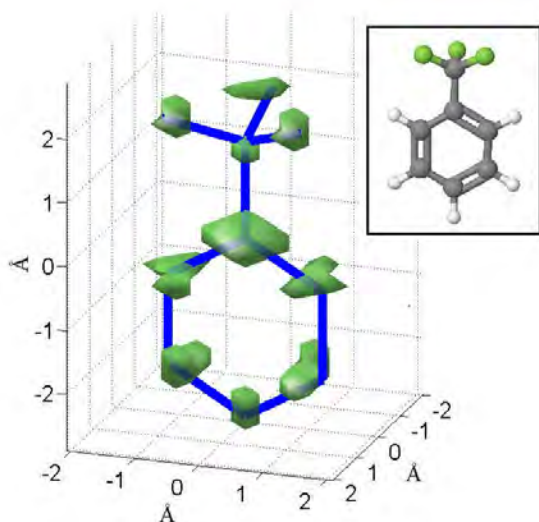


Figure 1. Isosurface rendering of the reconstructed 3-D molecular structure of $\text{C}_6\text{H}_5\text{CF}_3$. The overlapped blue sticks show the frame of the molecule with non-hydrogen atoms in both ends of each stick. The ball-and-stick model of the molecule is shown in the inset. (Reproduced from reference 8).

one corresponding to partial 1-D alignment and the other to randomly oriented molecules. Perfect alignment corresponds to a delta-function-like angular distribution, while partially aligned molecules have a continuous angular distribution. The diffraction pattern of partially aligned molecules can be treated as a convolution of the diffraction pattern of perfectly aligned molecules with the angular distribution. The first step in our method is a deconvolution to retrieve the diffraction pattern corresponding to perfectly aligned molecules from the two input diffraction patterns, using a genetic algorithm. The second step is to reconstruct the molecular structure from the deconvolved diffraction pattern. An iterative phase retrieval algorithm in 3-D cylindrical space is used to reconstruct the full 3-D molecular structure. For this purpose we have modified an existing algorithm [9,10] to apply to the case of

imaging with atomic resolution. The genetic algorithm used in the first step is applicable for the case where a single axis of the molecule is aligned. For asymmetric-top molecules, 1-D alignment affects the angular distribution about two molecular axes. We were able to apply the genetic algorithm by selecting a time at which the angular distribution is narrow along the most polarizable axis and approximately random along the second-most polarizable axis. Figure 1 shows the retrieved molecular structure for $C_6H_5CF_3$. The Hydrogen atoms are not detected due to the small scattering cross section. The green region shows the position of the atoms in the reconstructed structure, while the blue bars show the frame of the molecule from the theoretical structure. The retrieved structure agrees very well with the theoretical model of the molecule.

We have also used ultrafast electron diffraction (UED) to investigate the dynamics following the interaction of carbon disulfide (CS_2) with an intense laser pulse. We use CS_2 as a model molecule because it is a simple polyatomic molecule that can be aligned and that displays many important properties such as the presence of conical intersections and photoexcitation into dissociative

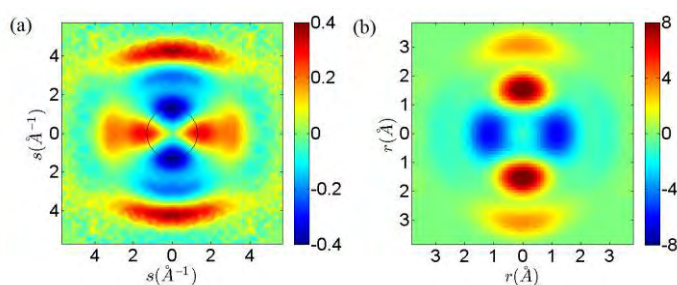


Figure 2. a) Diffraction pattern of aligned CS_2 molecules. b) Fourier Transform (FT) of the diffraction pattern. The structure and angular distribution can be extracted from the FT. The bright spots in the vertical direction correspond to the C-S and S-S distance (1.55\AA and 3.1\AA , respectively).

states. We have investigated a range of laser intensities (10^{12} - 10^{13} W/cm^2) relevant for many experimental methods that involve alignment and/or ionization of molecules. By analyzing diffraction patterns, we were able to characterize the dependence of the alignment on both the intensity and fluence of the laser pulses. We have compared the experimental results with simulations of the alignment, and seen that experimentally the alignment saturates at intensities well below 10^{13} W/cm^2 , while in the simulation the alignment continues to increase. We have also observed a distortion of the molecular structure for intensities on the order of 10^{13} W/cm^2 . While the data analysis is preliminary, it is clear that diffraction provides a lot of information about the angular distribution and structure of the molecules. Figure 2 shows a difference diffraction pattern, it is the difference between the diffraction pattern at the time of maximum alignment and the diffraction pattern of randomly oriented molecules. The Fourier Transform (FT) of the diffraction pattern give the autocorrelation of the object (the molecular structure) convolved with the angular distribution. Figure 2b shows the FT of the diffraction pattern in Fig. 2a. The bright spots in the vertical direction correspond to the C-S and S-S distances (1.55\AA and 3.1\AA , respectively). The angular spread of the spots is determined by the angular distribution. From the FT we can extract both the structure and angular distribution of the molecules. We are currently working on the interpretation of multiple diffraction patterns.

Future Plans

We will further investigate the limits of impulsive laser alignment, based on some discrepancies we have seen between standard alignment theories and experimental measurements. We will also move to use our 3D imaging method to study dynamics where the structure is changing on femtosecond and picosecond time scales. We will focus on photoisomerization reactions, where a change in the molecular structure is initiated by the absorption of a UV photon. We are currently building the experimental setup for this purpose.

References

- [1] P. W. Allen and L. E. Sutton, *Acta Crystallogr.* **3**, 46 (1950).
- [2] H. Ihee, V. A. Lobastov, U. M. Gomez, B. M. Goodson, R. Srinivasan, C. Y. Ruan, and A. H. Zewail, *Science* **291**, 458 (2001).
- [3] C. I. Baga, J. Xu, A. D. DiChiara, E. Sistrunk, K. Zhang, P. Agostini, T. A. Miller, L. F. DiMauro, and C. D. Lin, *Nature* **483**, 194 (2012).
- [4] R. Srinivasan, J. Feenstra, S. Park, S. Xu, and A. Zewail, *Science* **307**, 558 (2005).
- [5] K. Hoshina, K. Yamanouchi, T. Ohshima, Y. Ose, and H. Todokoro, *J. Chem. Phys.* **118**, 6211 (2003).
- [6] P. Reckenthaeler, M. Centurion, W. Fuss, S. A. Trushin, F. Krausz, and E. E. Fill, *Phys. Rev. Lett.* **102**, 213001 (2009).
- [7] C. J. Hensley, J. Yang, M. Centurion, *Phys. Rev. Lett.* **109**, 133202 (2012).
- [8] J. Yang, V. Makhija, V. Kumarappan, M. Centurion, *Struct. Dyn.* **1**, 044101 (2014).
- [9] D. K. Saldin, V. L. Shneerson, D. Starodub, and J. C. H. Spence, *Acta Cryst. A* **66**, 32–37 (2010).
- [10] D. Starodub, J. C. H. Spence, and D. K. Saldin, *Proc. SPIE* **7800**, 78000O (2010).

Publications of DOE sponsored research in the past 3 years

1. Peter Hansen, Cory Baumgarten, Herman Batelaan, Martin Centurion, "Dispersion Compensation for Attosecond Electron Pulses," *Appl. Phys. Lett.* **101**, 083501 (2012).
2. Christopher J. Hensley, Jie Yang, and Martin Centurion., "Imaging of Isolated Molecules with Ultrafast Electron Pulses" *Phys. Rev. Lett.* **109**, 133202 (2012). *Featured in APS Physical Review website on 9/28/2012 as a Focus Story.*
3. Jie Yang, Varun Makhija, Vinod Kumarappan and Martin Centurion, "Reconstruction of three-dimensional molecular structure from diffraction of laser-aligned molecules," *Struct. Dyn.* **1**, 044101 (2014).

Atomic and Molecular Physics in Strong Fields

Shih-I Chu
 Department of Chemistry, University of Kansas
 Lawrence, Kansas 66045
 E-mail: sichu@ku.edu

Program Scope

In this research program, we address the fundamental physics of the interaction of atoms and molecules with intense ultrashort laser fields. The main objectives are to develop new theoretical formalisms and accurate computational methods for *ab initio* nonperturbative investigations of multiphoton quantum dynamics and very high-order nonlinear optical processes of one-, two-, and many-electron quantum systems in intense laser fields, taking into account detailed electronic structure information and many-body electron-correlated effects. Particular attention will be paid to the exploration of the effects of electron correlation on high-harmonic generation (HHG) and multiphoton ionization (MPI) processes, multi-electron response and underlying mechanisms responsible for the strong-field ionization of atoms, and diatomic, and small polyatomic molecules, time-frequency spectrum, coherent control of HHG processes for the development of shorter and stronger attosecond laser pulses, etc.

Recent Progress

1. Sub-optical-cycle Transient HHG Dynamics and Ultrafast Spectroscopy in the Attosecond Time Domain

The recent development of attosecond metrology has enabled the real-time experimental observation of ultrafast electron dynamics and transient sub-cycle spectroscopy in atomic and molecular systems. While they are some recent experimental and theoretical studies of subcycle transient absorption, there has been no study of the subcycle transient behavior of the harmonic emission. We have recently initiated such a direction by extending the *self-interaction-free* TDDFT [1,2] with proper exchange-correlation (xc) energy functional, allowing the correct long-range asymptotic behavior, and the time-dependent generalized pseudospectral (TDGPS) method [1,3] for the first *ab initio* study of the subcycle HHG dynamics of He atoms [1]. We have explored the dynamical behavior of the subcycle HHG for transitions from the excited states to the ground state and found oscillation structures with respect to the time delay between the single extreme ultraviolet (XUV) attosecond pulse (SAP) and near-infrared (NIR) fields. The oscillatory pattern in the photon emission spectra has a period of ~ 1.3 fs which is half of the NIR laser optical cycle, similar to that recently measured in the experiments on transient absorption of He [4]. We present the photon emission spectra from 1s2p, 1s3p, 1s4p, 1s5p, and 1s6p excited states as functions of the time delay. We explore the subcycle a. c. Stark shift phenomenon in NIR fields and its influence on the photon emission process. Our analysis reveals several novel features of the subcycle HHG dynamics and we identify the mechanisms responsible for the observed peak splitting in the photon emission spectra.

2. Coherent Phase-matched VUV Generation by Field-controlled Bound States.

High-order harmonic generation has been the enabling technology for ultrafast science in the VUV and soft-X-ray spectral regions. Recently, ultrafast sources of below-threshold harmonics, with photon energies below the target ionization potential, have been demonstrated. Such harmonics are critical to the extension of time-resolved photoemission spectroscopy to megahertz repetition rates and to the development of high-average-power VUV sources, because they can be generated with relatively low driving laser intensities ($\sim 1 \times 10^{13}$ W/cm²). Ultrafast VUV sources of low-order harmonics are also critical tools for studying wave packet dynamics in bound states of atoms and molecules. However, compared to the high-order above-threshold harmonics, which

have been extensively studied, little attention has been devoted to the development and characterization of below-threshold harmonic sources. Recently in collaboration with the experimental group led by Dr. Z. Chang in UCF, we extend our *self-interaction-free* time-dependent density functional theory (TDDFT) [1,2] and generalized Floquet formalism [5] and demonstrate a new regime of phase-matched below-threshold harmonics generation, for which the generation and phase matching is enabled only near Stark-shifted resonance structures of the atomic target [6]. The coherent VUV line emission exhibits sub-100 meV linewidth, low divergence and quadratic growth with increasing target density, and can be controlled by the sub-cycle field of a few-cycle driving laser with intensity of only 10^{13} W/cm², which is achievable directly from few-cycle femtosecond oscillators with nano Joule energy. This work opens the door to the future development of compact, high flux and ultrafast VUV light sources without the need for cavity or nanoplasmonic enhancement. This work has been recently published in Nature Photonics [6].

3. Multiphoton above-threshold ionization in superintense free-electron x-ray laser fields: Beyond the dipole approximation

We present an accurate and efficient computational approach in *momentum space* for the nonperturbative study of multiphoton above-threshold ionization (ATI) of atoms in superintense and ultrashort-wavelength laser fields beyond the dipole approximation [7, 8]. In this approach, the electron wave function is calculated by solving the *P*-space time-dependent Schrödinger equation (TDSE) in a finite *P*-space volume under a simple zero asymptotic boundary condition. The *P*-space TDSE is propagated accurately and efficiently by means of the TDGPS method with optimal momentum grid discretization and a split-operator time propagator in the *energy* representation. The differential ionization probabilities are calculated directly from the continuum-state wave function obtained by projecting the total electron wave function onto the continuum-state subspace using the projection operator constructed by the continuum eigenfunctions of the unperturbed Hamiltonian. We apply this approach for the investigation of the multiphoton processes of a hydrogen atom exposed to superintense free-electron x-ray laser fields. High-resolution photoelectron energy-angular distribution and ATI spectra have been obtained. We find that, compared to results of the dipole approximation, the nondipole ATI spectra are enhanced substantially in the high-energy regime, and the photoelectron angular distributions are distorted significantly in higher-intensity and/or longer-pulse laser fields; in particular two lobes are induced, one along and one against the laser propagation direction. The origin of these phenomena has been explored in detail.

4. Development of Fast Algorithms for Searching Optimal Control Fields for Controlling Molecular Excitation, Alignment and Orientation

(a) We develop a fast-kick-off two-point boundary-value quantum control paradigm (TBQCP) search algorithm for quickly finding optimal control fields in the state-to-state transition probability control problems, especially those with poorly chosen initial control fields [9]. Specifically, the local temporal refinement of the control field at each iteration is weighted by a fractional inverse power of the instantaneous overlap of the backward-propagating wave function, associated with the target state and the control field from the previous iteration, and the forward-propagating wave function, associated with the initial state and the concurrently refining control field.

(b) Recently, a single-cycle THz pulses have been demonstrated in the laboratory to induce field-free orientation in gas-phase polar molecules at room temperature [10]. In a recent article [11], we explore the maximum attainable field-free molecular orientation with optimally shaped linearly polarized near-single-cycle THz laser pulses of a thermal ensemble. Large-scale benchmark optimal control simulations are performed, including rotational energy levels with the rotational quantum numbers up to $J = 100$ for OCS linear molecules. The simulations are made possible by an extension of the recently formulated fast search algorithm, the two-point boundary-value quantum control paradigm [11], to the mixed-states optimal control problems in the present work. It is shown that a very high degree of field-free orientation can be achieved by strong, optimally shaped near-single-cycle THz pulses.

5. Coherent Control of the Electron Quantum Paths for the Optimal Generation of Single Ultrashort Attosecond Laser Pulse

We report a new mechanism and experimentally realizable approach for the coherent control of the generation of an isolated and ultrashort attosecond (*as*) laser pulse from atoms by means of the optimization of the two-color [12] and three-color [13] laser fields with proper time delays. Optimizing the laser pulse shape allows the control of the electron quantum paths and enables high-harmonic generation from the long- and short-trajectory electrons to be enhanced and split near the cutoff region. In addition, it delays the long-trajectory electron emission time and allows the production of extremely short attosecond pulses in a relatively narrow time duration. As a case study, we show that an isolated 30 *as* pulse with a bandwidth of 127 eV (for the two-color case) and an isolated 23 *as* pulse with a bandwidth of 163 eV (three-color case) can be generated directly from the contribution of long-trajectory electrons alone by superposing the supercontinuum harmonics near the cutoff region. We show that such a metrology can be realized experimentally.

Then we have further investigated the effect of macroscopic propagation on the supercontinuum harmonic spectra and the subsequent attosecond-pulse generation [14]. The effects of macroscopic propagation are investigated in near and far field by solving Maxwell's equation. The results show that the contribution of short-trajectory electron emission is increased when the macroscopic propagation is considered. However, the characteristics of the dominant long-trajectory electron emission (in the single-atom response case) are not changed, and an isolated and shorter *as* pulse can be generated in the near field. Moreover, in the far field, the contribution of long-trajectory electron emission is still dominant for both on-axis and off-axis cases. As a result, an isolated and shorter *as* pulse can be generated directly.

More recently, we propose an efficient method for the generation of ultrabroadband supercontinuum spectra and isolated ultrashort attosecond laser pulses from He atoms with two-color mid-infrared laser fields [15]. High-order harmonic generation (HHG) is obtained by solving the time-dependent Schrodinger equation accurately by means of the time-dependent generalized pseudospectral method. We found that the optimizing two-color midinfrared laser pulse allows the HHG cutoff to be significantly extended, leading to the production of an ultrabroadband supercontinuum. As a result, an isolated 18-attosecond pulse can be generated directly by the superposition of the supercontinuum harmonics. To facilitate the exploration of the ultrashort attosecond generation mechanisms, we perform both a semiclassical simulation and a wavelet time-frequency transform.

6. *Ab Initio* Precision Study of High-Lying Doubly Excited States of Helium in Static Electric Fields: Complex-Scaling Generalized Pseudospectral Method in Hyperspherical Coordinates

We develop a complex-scaling (CS) generalized pseudospectral (GPS) method in hyperspherical coordinates (HSC) for *ab initio* and accurate treatment of the resonance energies and autoionization widths of two-electron atomic systems in the presence of a strong dc electric field [16]. The GPS method allows nonuniform and optimal spatial discretization of the two-electron Hamiltonian in HSC with the use of only a modest number of grid points. The procedure is applied for the first precision calculation of the energies and autoionization widths for the high-lying $^1S^e$, $^1P^o$, $^1D^e$, and $^1F^o$ ($n = 10-20$) doubly excited resonance states of He atoms. In addition, we present a theoretical prediction of the energies and widths of high-lying doubly excited resonance states of $^1P^o$ ($n = 8-15$) in external dc electric field strengths of 3.915–10.44 kV/cm. The calculated dc-field perturbed high-lying resonance energies are in good agreement with the latest experimental data.

7. Sub-cycle Oscillations in Virtual States Brought to Light

Understanding and controlling the dynamic evolution of electrons in matter is among the most fundamental goals of attosecond science. While the most exotic behaviors can be found in complex systems, fast electron dynamics can be studied at the fundamental level in atomic systems, using moderately intense ($\leq 10^{13}$ W/cm²) lasers to control the electronic structure in proof-of-principle experiments. In cooperation with the UCF experimental group, we probe the transient changes in the absorption of an isolated attosecond extreme ultraviolet (XUV) pulse by helium atoms in the presence of a delayed, few-cycle near infrared (NIR) laser pulse, which uncovers absorption structures corresponding to laser-induced “virtual” intermediate states in the two-color two-photon (XUV + NIR) and three-photon (XUV + NIR + NIR) absorption process [4]. These previously

unobserved absorption structures are modulated on half-cycle (~ 1.3 fs) and quarter-cycle (~ 0.6 fs) time scales, resulting from quantum optical interference in the laser-driven atom.

8. We have completed several invited review articles on the recent development of *self-interaction-free* time dependent density functional theory (TDDFT) for the nonperturbative treatment of atomic and molecular multiphoton processes in intense ultrashort laser fields in the past 3 years [17-20].

Future Research Plans

In addition to continuing the ongoing researches discussed above, we plan to initiate the following several new project directions: (a) Extension of the exploration of the coherent control and giant enhancement of MPI and HHG driven by intense frequency-comb laser fields [21, 22] to rare gas atoms. (b) Extension of the TDGPS method in momentum space to the study of HHG/ATI processes in intense ultrashort laser fields. (c) Development of *self-interaction-free* TDDFT with proper *derivative discontinuity* for the treatment of double ionization of complex atoms in intense laser fields [23]. (d) Development of nonperturbative methods for the accurate treatment of transient absorption and subcycle HHG dynamics in NIR+ XUV attosecond pulses.

References Cited (* Publications supported by the DOE program in the period of 2011-2014).

- *[1] J. Heslar, D. A. Telnov, and S. I. Chu, Phys. Rev. A **89**, 052517 (2014).
- [2] S. I. Chu, J. Chem. Phys. **123**, 062207 (2005).
- [3] X. M. Tong and S. I. Chu, Chem. Phys. **217**, 119–130 (1997).
- *[4] M. Chini, X. Wang, Y. Cheng, Y. Wu, D. Zhao, D. A. Telnov, S. I. Chu, and Z. Chang, (Nature) Sci. Rep. **3**, 1105 (2013).
- [5] S. I. Chu and D. A. Telnov, Phys. Rep. **390**, 1-131 (2004).
- *[6] M. Chini, X. Wang, Y. Cheng, H. Wang, Y. Wu, E. Cunningham, P.-C. Li, J. Heslar, D.A. Telnov, S.I. Chu, and Z. Chang, Nature Photonics **8**, 437 (2014).
- *[7] Z. Y. Zhou and S. I. Chu, Phys. Rev. A **83**, 013405 (2011).
- *[8] Z. Y. Zhou and S. I. Chu, Phys. Rev. A **87**, 023407 (2013).
- *[9] S. L. Liao, T. S. Ho, S. I. Chu, and H. Rabitz, Phys. Rev. A **84**, 031401 (2011).
- *[10] S. Fleischer, Y. Zhou, R. W. Field, and K. A. Nelson, Phys. Rev. Lett. **107**, 163603 (2011).
- *[11] S. L. Liao, T. S. Ho, H. Rabitz, and S. I. Chu, and, Phys. Rev. A **87**, 013429 (2013).
- *[12] I. L. Liu, P.-C. Li, and S.I. Chu, Phys. Rev. A **84**, 033414 (2011).
- *[13] P. C. Li, I. L. Liu, and S.I. Chu, Opt. Express **19**, 23857 (2011).
- *[14] P. C. Li and S.I. Chu, Phys. Rev. A **86**, 013411 (2012).
- *[15] P. C. Li, C. Laughlin, and S. I. Chu, Phys. Rev. A **89**, 023431 (2014).
- *[16] J. Heslar and S. I. Chu, Phys. Rev. A **86**, 032506 (2012).
- *[17] S. I. Chu and D. A. Telnov, in *Computational Studies of New Materials II: From Ultrafast Processes and Nanostructures to Optoelectronics, Energy Storage and Nanomedicine*, edited by T.F. George, D. Jelski, R.R. Letfullin, and G. Zhang (World Scientific, 2011), pp. 75–101.
- *[18] D. A. Telnov, J. Heslar, and S.I. Chu, in *Theoretical and Computational Developments in Modern Density Functional Theory*, edited by Amlan K. Roy (Nova Science Publishers, Inc., Hauppauge, NY (USA), 2012), pp. 357- 390.
- *[19] J. Heslar, D. A. Telnov, and S. I. Chu, in *Concepts and Methods in Modern Theoretical Chemistry: Statistical Mechanics*, Volume 2, edited by S.K. Ghosh and P.K. Chattaraj (Taylor & Francis Inc., Bosa Roca, USA, 2013), pp. 37-55.
- *[20] J. Heslar, D.A. Telnov, and S.I. Chu, *Chinese J. Phys.* **52**, 578 (2014).
- *[21] D. Zhao, F. I. Li, and S.I. Chu, Phys. Rev. A **87**, 043407 (2013).
- *[22] D. Zhao, F. I. Li, and S. I. Chu, J. Phys. B: At. Mol. Opt. Phys. **46**, 145403 (2013).
- *[23] J. Heslar and S. I. Chu, Phys. Rev. A **87**, 052513 (2013).

Formation of Ultracold Molecules

Robin Côté

Department of Physics, U-3046
University of Connecticut
2152 Hillside Road
Storrs, Connecticut 06269

Phone: (860) 486-4912
Fax: (860) 486-3346
e-mail: rcote@phys.uconn.edu
URL: <http://www.physics.uconn.edu/~rcote>

Program Scope

Current experimental efforts to obtain ultracold molecules (*e.g.*, photoassociation (PA), buffer gas cooling, or Stark deceleration) raise a number of important issues that require theoretical investigations and explicit calculations.

The main aims of this Research Program are to identify efficient approaches to obtain ultracold molecules, and to understand their properties. To that end, we often need to calculate the electronic properties (energy surfaces, dipole and transition moments, ro-vibrational states, etc.), as well as the interaction of the molecules with their environment (surrounding atoms, molecules, or external fields).

Recent Progress

During FY 2014, we have made progress on 4 main axes of research: 1) Rydberg interactions, 2) Energy surfaces and reactions, 3) Long-range interaction between diatomic molecules, and 4) Formation of dimers and tetramers. Below, we refer to DOE supported articles during the last four years only; new articles published since the last annual report filing (August 2013) are listed as [N...], while those of the prior years since 2010 by [P...].

1) Rydberg interactions

We extended our previous work on Rydberg-Rydberg interactions explaining spectral features observed in ^{85}Rb experiments, namely resonances correlated to the $69p_{3/2} + 71p_{3/2}$ asymptote [J. Stanojevic *et al.*, *Eur. Phys. J. D* **40**, 3 (2006)], and to $69d + 70s$ asymptote [J. Stanojevic *et al.*, *Phys. Rev. A* **78**, 052709 (2008)], to investigate the existence of potential wells of doubly-excited atoms due to ℓ -mixing, first for the 0_g^+ symmetry [P1], and then for other molecular symmetries (0_u^- and 1_u) of Rb_2 Rydberg macrodimers [P2]. We have also explored the possibility of forming metastable long-range *macrotrimers* made of three Rydberg [P3]. Our calculations showed the existence of shallow (roughly 20 MHz deep) long-range wells for three Rydberg atoms forming a linear molecule.

We have recently started to investigate how interactions can be affected by dressing atoms with a Rydberg state. In [N1], we have shown that Rydberg-dressed interactions could be used to tune ultracold chemical reactions. We illustrated the concept with benchmark system, namely $\text{H}_2 + \text{D} \rightarrow \text{HD} + \text{H}$. We also investigate a possible new chemical bound between ground state atoms using Rydberg dressing of the atoms [N2]. The molecular bound states would be extremely long-range, roughly 500 bohr radii, and very weakly bound.

2) Energy surfaces and reactions

A recent effort in my group towards reactive scattering involving cold molecules and molecular ions has started with the calculation of potential energy surfaces (PES). In our previous work, we studied PES for trimers, such as the lowest doublet electronic state of Li_3 ($1^2A'$) [J.N. Byrd *et al.*, *Int. J. of Qu. Chem.*, **109**, 3112 (2009)], or the lowest $^2A''$ surface arising from the $\text{Li}_2[\text{X}^1\Sigma_g^+] + \text{Li}^*[^2P]$ interaction [J.N. Byrd *et al.*, *Int. J. of Qu. Chem* **109**, 3626 (2009)]. In [P4],

we extended this work to obtain accurate long-range *ab initio* PES for the ground state X^2A' of Li_3 , the van der Waals dispersion coefficients and three-body dispersion damping terms for the atom-diatomic dissociation limit. We recently computed the surfaces for RbOH^- and RbOH [N3] to model the associative detachment reaction, paying special attention to the angular dependence of the PES.

Together with my collaborators, we have studied the collisions of trapped molecules with slow beams, particularly of $\text{OH}(J = \frac{3}{2}, M_J = \frac{3}{2})$ molecules with ^4He atoms [P5], and demonstrated the importance of including the effects of non-uniform trapping fields. More recently, we computed rate coefficients for reaction and vibrational quenching of the ultracold collision $\text{D} + \text{H}_2(v, j = 0)$ for a wide range of initial vibrationally excited states v [P6]. The v -dependence of the zero-temperature limit shows two distinct regimes: a barrier dominated regime for $0 \leq v \leq 4$, and a barrierless regime for $v \geq 5$. We extended our study of atom-diatom reactive scattering to $\text{H}_2 + \text{Cl}$ to investigate the effect of resonances near the scattering threshold [N4]. We find a new universal behavior of the inelastic cross section in the s -wave regime scaling as k^{-3} , which can be explained by the proximity of a pole in the complex k -plane.

We extended our previous work on the structure of K_2Rb_2 tetramers and thermochemistry relevant to $\text{KRb} + \text{KRb}$ collisions and reactions [P7] to all possible alkali tetramers formed from $\text{X}_2 + \text{X}_2 \rightarrow \text{X}_4$, $\text{X}_2 + \text{Y}_2 \rightarrow \text{X}_2\text{Y}_2$, and $\text{XY} + \text{XY} \rightarrow \text{X}_2\text{Y}_2$ association reactions [P8], and found two stable structures for the tetramers, rhombic (D_{2h}) and planar (C_s), and that there are barrier-less pathways for the formation of tetramers from dimer association reactions. We are still exploring these systems.

Finally, we have continued our new effort on molecular ions, carefully calculating their energy surface and transition dipole moments. We started with alkaline-earth elements, since they can be cool to very low temperatures. In [P9], we reported *ab initio* calculations of the $X^2\Sigma_u^+$ and $B^2\Sigma_g^+$ states of Be_2^+ , and found two local minima, separated by a large barrier, for the $B^2\Sigma_g^+$, and extended this work to Ca_2^+ in [P10]. We are in the process to complete two other systems: Mg_2^+ [N5] and Sr_2^+ [N6]. More recently, we helped analyzing experimental results on NaCa^+ [N7].

3) Long-range interaction between diatomic molecules

In our previous work on K_2Rb_2 [P7], we calculated the minimum energy path for the reaction $\text{KRb} + \text{KRb} \rightarrow \text{K}_2 + \text{Rb}_2$ and found it to be barrierless. However, we recently showed that long-range barriers originating from the anisotropic interaction due to higher electrostatic, induction, and dispersion contributions could exist and stabilize a molecular sample [P11]. In addition, we showed that by changing the orientation of the molecules using an external DC electric field, and by varying its strength, one could control the effective inter-molecular interaction, switching it from attractive to repulsive (and vice-versa). Recently, we generalized our treatment to the long-range interaction between homonuclear alkali dimers [P12], where there are still anisotropic interactions (e.g. due to quadrupolar terms). and extended this work to the case of heteronuclear diatomic alkali molecules [P13]; in addition to the multipole expansion and van der Waals terms, we also give an analytic expression for molecules in an external (weak) DC electric field. Finally, we summarized some of this work in a book chapter on ultracold molecules for quantum information processing [N8].

4) Formation of dimers and tetramers

In previous papers sponsored by DOE [E. Juarros *et al.*, PRA **73**, 041403(R) (2006); E. Juarros *et al.*, JPB **39**, S965 (2006); N. Martinez de Escobar *et al.*, PRA **78**, 062708 (2008)], we explored the formation of homo- and hetero-nuclear diatomic molecules in their ground electronic state from one- and two-photon photoassociative processes [P14]. We also worked on using many coherent laser pulses [E. Kuznetsova *et al.*, PRA **78**, 021402(R) (2008)], and Feshbach resonances [P. Pellegrini

et al., PRL **101**, 053201 (2008)] to increase the formation rate of ultracold diatomic molecules [P. Pellegrini, and R. Côté, New J. Phys. **11**, 055047 (2009); E. Kuznetsova *et al.*, New J. Phys. **11**, 055028 (2009); J. Deiglmayr, *et al.*, New J. Phys. **11**, 055034 (2009)]. We recently started to explore how Feshbach resonances could enhance the pump-dump scheme to produce ground state molecules [N9], and we are using the same approach to investigate the possible formation of tetramers [N10]. In fact, by controlling the long-range interaction between polar diatomic molecules using external DC electric field [P11], we could increase the shorter-range overlap of the continuum and excited states (as in FOFA – Feshbach Optimized Photo-Association), and thus the formation rate of tetramers.

Future Plans

In the coming year, we expect to carry more calculations on Rydberg interactions, especially the possibility of forming metastable long-range *macrotrimers* made of three Rydberg, and the use of Rydberg-dressed interactions. We will continue and extend our work on computing electronic properties of molecules (PES and moments), especially for the molecular ions, where not much is available. We plan to extend our work on the long-range interaction between molecules to more complex systems (e.g. diatomic + triatomic molecules, etc.). Finally, we will investigate in detail paths to form larger ultracold molecules by controlling the inter-molecular interactions in order to enhance formation rate.

New DOE sponsored publications since August 2013

- N1. Jia Wang, Jason N. Byrd, Ion Simbotin, and Robin Côté, *Tuning ultracold chemical reactions via Rydberg-dressed interactions*. Phys. Rev. Lett. **113**, 025302 (2014).
- N2. Jia Wang and Robin Côté, *A new long-range chemical bound using Rydberg-dressing*. In preparation: to be submitted to Phys. Rev. Lett.
- N3. Jason N. Byrd, H. Harvey Michels, John A. Montgomery, Jr., and Robin Côté, *Associative detachment of rubidium hydroxide*. Phys. Rev. A **88**, 032710 (2013).
- N4. Ion Simbotin, Subhas Ghosal, and Robin Côté, *Threshold resonance effects in reactive processes*, Phys. Rev. A **89**, 040701(R) (2014).
- N5. Sandipan Banerjee, John A. Montgomery, Jr., H. Harvey Michels, and Robin Côté, *Comparison of the Alkaline Earth diatomic homonuclear molecular ions*. In preparation: to be submitted to J. Chem. Phys.
- N6. Sandipan Banerjee, John A. Montgomery, Jr., H. Harvey Michels, and Robin Côté, *Ab initio potential curves for the $X^2\Sigma_u^+$, $A^2\Pi_u$, and $B^2\Sigma_g^+$ states of Sr_2^+* . In preparation: to be submitted to Chem. Phys. Lett.
- N7. W. W. Smith, D.S. Goodman, I. Sivarajah, J.E. Wells, S. Banerjee, R. Côté, H.H. Michels, J.A. Montgomery Jr., and F.A. Narducci, *Experiments with an ion-neutral hybrid trap: cold charge-exchange collisions*, Appl. Phys. B **114**, 75 (2014).
- N8. Robin Côté, *Ultracold molecules: their formation and application to quantum computing*. Advances in Chemical Physics **154**, Chap. 7, pp. 403-448, John Wiley and Sons (New York) (2014).
- N9. M. Gacesa, S. Ghosal, J.N. Byrd, and R. Côté, *Feshbach-optimized photoassociation of ultracold $^6Li^87Rb$ molecules with short pulses*, Phys. Rev. A **88**, 063418 (2013).
- N10. J.N. Byrd, S. Ghosal, and R. Côté, *The formation of tetramers of alkali metals by controlling inter-molecular interactions*. In preparation (to be submitted to Phys. Rev. Lett.).

Prior DOE sponsored publications since 2010

- P1. N. Samboy, J. Stanojevic, and R. Côté, *Formation and properties of Rydberg macrodimers*, Phys. Rev. A **83**, 050501(R) (2011).
- P2. Nolan Samboy and Robin Côté, *Rubidium Rydberg macrodimers*, J. Phys. B **44**, 184006 (2011).
- P3. Nolan Samboy and Robin Côté, *Rubidium Rydberg linear macrotrimers*. Phys. Rev. A **87**, 032512 (2013).
- P4. Jason N. Byrd, H. Harvey Michels, John A. Montgomery, Jr., and Robin Côté, *Long-range three-body atom-diatom potential for doublet Li_3* , Chem. Phys. Lett. **529**, 23 (2012).
- P5. T. V. Tscherbul, Z. Pavlovic, H. R. Sadeghpour, R. Côté, and A. Dalgarno, *Collisions of trapped molecules with slow beams*, Phys. Rev. A **82**, 022704 (2010).
- P6. Ion Simbotin, Subhas Ghosal, and Robin Côté, *A case study in ultracold reactive scattering: $D + H_2$* , Phys. Chem. Chem. Phys. **13**, pp. 19148-19155 (2011).
- P7. J.N. Byrd, J.A. Montgomery (Jr.), and R. Côté, *Structure and thermochemistry of K_2Rb , KRb_2 and K_2Rb_2* , Phys. Rev. A **82**, 010502 (2010).
- P8. Jason N. Byrd, H. Harvey Michels, John A. Montgomery, Robin Côté, and William C. Stwalley, *Structure, energetics, and reactions of alkali tetramers*, J. Chem. Phys. **136**, 014306 (2012).
- P9. S. Banerjee, J. N. Byrd, R. Côté, H. H. Michels, J. A. Montgomery, Jr. *Ab initio potential curves for the $X^2\Sigma_u^+$ and $B^2\Sigma_g^+$ states of the Be_2^+ : Existence of a double minimum*, Chem. Phys. Lett. **496**, 208 (2010).
- P10. Sandipan Banerjee, John A. Montgomery, Jr., Jason N. Byrd, H. Harvey Michels, and Robin Côté, *Ab initio potential curves for the $X^2\Sigma_u^+$, $A^2\Pi_u$, and $B^2\Sigma_g^+$ states of Ca_2^+* , Chem. Phys. Lett. **542**, 138-142 (2012).
- P11. Jason N. Byrd, John A. Montgomery, and Robin Côté, *Controllable Binding of Polar Molecules and Metastability of One-Dimensional Gases with Attractive Dipole Forces*, Phys. Rev. Lett. **109**, 083003 (2012).
- P12. Jason N. Byrd, Robin Côté, and John A. Montgomery, *Long-range interactions between like homonuclear alkali metal diatoms*, J. Chem. Phys. **135**, 244307 (2011).
- P13. Jason N. Byrd, John A. Montgomery, and Robin Côté, *Long-range forces between polar alkali-metal diatoms aligned by external electric fields*, Phys. Rev. A **86**, 032711 (2012).
- P14. E. Juarros, K. Kirby, and R. Côté, *Formation of ultracold molecules in a single pure state: LiH in $a^3\Sigma^+$* . Phys. Rev. A **81**, 060704 (2010).

Optical Two-Dimensional Spectroscopy of Disordered Semiconductor Quantum Wells and Quantum Dots

Steven T. Cundiff
 JILA, University of Colorado & NIST, Boulder, CO 80309-0440
 cundiff@jila.colorado.edu

September 11, 2014

Program Scope: The goal of this program has been to implement optical 2-dimensional coherent spectroscopy and apply it to electronic excitations, including excitons, in semiconductors. Specifically of interest are epitaxially grown quantum wells that exhibit disorder due to well width fluctuations and quantum dots. In both cases, 2-D spectroscopy provides information regarding coupling among excitonic localization sites. During the last year we have begun applying this method to colloidal quantum dots in addition to epitaxially grown materials.

Progress: Quantum dots are often described as “artificial atoms” because they have discrete energy levels. However, quantum dots have an important distinction from atoms, namely they have degrees of freedom associated with motion of the constituent atoms relative to their equilibrium position i.e., vibrational degrees of freedom, which in the case of epitaxial dots corresponds to phonons. In this way, they are more like molecules than atoms. As a consequence, many applications of InAs quantum dots require low temperatures to eliminate decoherence due to the phonons.

The interaction of an exciton confined in an InAs epitaxially grown dot with acoustic phonons can be described in a picture similar to that used for molecular vibrations. The equilibrium position of the excited state within the quantum dot is slightly displaced with respect to the ground state. For a phonon of a given energy, there is a series of vibrational bands in each state, corresponding to the number of phonons. The zero-phonon line is an optical transition between ground and excited states with the same number of phonons. Transitions between states with differing number of phonons results in emission or absorption with an energy difference corresponding to the phonon energy. If the phonon energy were discrete, as for optical phonons, or molecular vibrations, well resolved satellites would result. However, acoustic phonons have a continuous distribution of phonon energies and thus smooth phonon sidebands occur. At low temperature, i.e., around 5 K, the zero phonon line dominates. As the temperature is increased, the phonon sidebands become prominent.

The dephasing of the ground state transition of InAs quantum dots was studied using photon echo spectroscopy. These measurements showed a remarkably long dephasing time, on the order of a nanosecond, which triggered interest in using InAs quantum dots as qubits. At elevated temperature, the phonon sidebands were observed. Since these measurements were based on photon echoes, they provide an ensemble averaged value and no information about how/if the phonon-exciton interactions vary with dot size. In addition, these studies did not provide any information on the dephasing of the excited state transitions.

We have taken 2D spectra at several temperatures, see Fig. 1. At 10K, only the zero-phonon exciton line is seen. These data are fit to a single Lorentzian. At 80K, the exciton line is a combination of the zero-phonon line and the phonon sidebands, thus it is fit to two Lorentzians. The phonon-sideband contribution is actually shifted with respect to the zero-phonon line, this shift depends on temperature. In addition to the exciton line, there is also a peak at lower energy that we attribute to biexcitons. We include a third

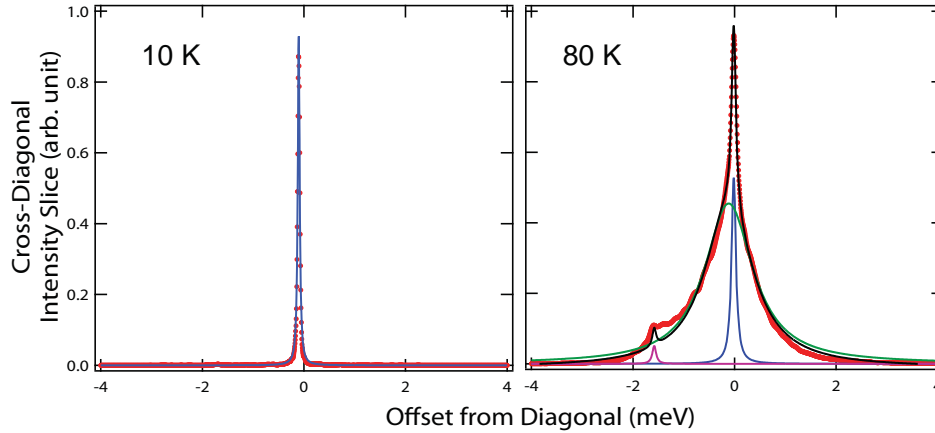


Figure 1: Cross-diagonal slices of the 2D coherent spectrum of InAs self-organized quantum dots at temperatures of 10 K (left) and 80 K (right). The dots are the measurements and the lines are fits.

Lorentzian to fit the biexciton line. It is surprising that the biexciton becomes more apparent at elevated temperature, especially since the temperature is comparable to the biexciton binding energy. These slices were taken at the center of the inhomogeneous distribution. After taking them, we realized that the low-temperature linewidth was actually limited by the spectral resolution of the spectrometer used to perform spectral interferometry. This can be rectified by inserting a field lens between the spectrograph and the CCD camera. This will be done before further data is taken.

The use of self-organized InAs quantum dots as a qubit requires that the exciton can undergo a Rabi oscillation. Because the Rabi frequency depends on detuning, and the excitonic resonance frequency depends on dot size, these measurements have been almost exclusively done on single dots. Ensemble measurements of Rabi flopping showed excess damping attributed to ensemble effects. The ability of 2D spectroscopy to make size-dependent measurements suggests that it could observe Rabi oscillations in an ensemble.

We have performed preliminary measurements to test this idea. These measurements used a prepulse to drive the quantum dot excitons into the excited state. The prepulse was followed by a pulse sequence that produced a 2D spectrum. The results are shown in Fig. 2. Without the prepulse, peaks are observed both on the diagonal and below the diagonal. The diagonal peak is due to a combination of exciton and trion transitions (the trion binding energy is much less than the inhomogeneous distribution). The peak below the diagonal is due absorption on the ground-state to exciton transition and emission on the exciton to biexciton transition. With the prepulse, a new peak appears above the diagonal. This peak occurs because there is already a population of excitons before the 2D pulses arrive. It corresponds to absorption on the exciton to biexciton transition and emission on the exciton to ground-state transition. As the prepulse intensity is increased, the strength of the lower sideband decreases, because the ground-state is depleted and the upper side band increases in strength as the initial population of excitons increases.

These results are consistent with coherently controlling the population of excitons, however to prove it is coherent we need sufficient prepulse intensity to produce at least a π pulse, i.e., see at least half of a Rabi oscillation. When we took these data, we did not have sufficient intensity. One difficulty is that the prepulse spot size on the sample needs to be significantly large than the 2D beams to make sure that the 2D spectrum corresponds to an area of reasonably uniform prepulse intensity. This restricts our ability to simply focus the prepulse tighter to increase the intensity.

During the last year, we began working on obtaining 2D coherent spectra of colloidal quantum dots. As colloidal quantum dots are a substantially different system than the epitaxially grown quantum wells and quantum dots we have studied in the past, there is a substantial period of learning involved.

The first issue to be faced was the substantial difference in wavelength as well as the much slower

relaxation times due to dark states present in colloidal quantum dots. To address both of these issues, we built a second 2D spectrometer that uses an optical parametric amplifier (OPA) pumped by a regenerative ti:sapphire amplifier running at 250 kHz repetition rate as the light source. This system gives much greater wavelength diversity than the ti:sapphire oscillator we had used for studying the epitaxially grown samples, however the lower repetition rate and greater noise, due to the cascaded nonlinearities used in an OPA, presents a challenge to obtaining quality results with this system.

The second issue was dealing with the different type of sample, namely solution phase rather than a wafer. To make things more challenging, we wanted to have the ability to go to low temperature to study phonon-carrier scattering. We tried making thin films using spin casting and drop casting, however we found that these resulted in excess scattering of the incident laser beams, which caused the 2D spectrum to be unacceptably noisy. So to overcome this, we switched to using a glass-forming liquid, namely heptamethylnonane. After some trial and error with sample cell design and the sequence for cooling down, we were able to get acceptable sample quality at low temperature. A typical 2D coherent spectrum is shown in Fig. 3(a). This spectrum clearly shows elongation along the diagonal due to inhomogeneous broadening from the size dispersion of the dots. The cross-diagonal width gives the homogeneous width.

Using this sample, we have performed an initial study of the temperature dependence of the homogeneous linewidth, as shown in Fig. 3(b). The homogeneous linewidth is determined from a cross-diagonal slice at the center of the inhomogeneous distribution.

Future Plans: The preliminary data on the temperature dependence of the cross-diagonal width in InAs dots set the stage for a detailed study of how the exciton-phonon interaction depends on dot size. Our study of how the biexciton binding energy depends on dot size showed that it was independent of size, which contradicted single dot studies. It will be very interesting to see if the results for the phonon-exciton interaction are consistent with single dot studies, or again they show a different behavior. In addition, we will measure the dephasing of the excited state transition. To the best of our knowledge, there have not been any studies of the excited state dephasing.

For the effort towards coherent control of InAs quantum dots, we are currently moving the apparatus to a new optical table and in doing so will reconfigure the focusing optics so that we can use smaller spots, for both prepulse and 2D beams. In addition, we will swap the pump laser for one with slightly higher power, which will give a corresponding increase in the available power. With both of these modifications, we will be able to achieve a pulse area well in excess of π .

For the colloidal dots, our main goals will be to resolve the ambiguities resulting from the photon echo studies of low temperature dephasing in the CdSe/ZnS dots and to determine the biexciton binding energy and the fine structure of the PbSe/CdSe and Ge dots, novel materials for which there is very little known. Of course, both the biexciton binding energy and fine structure will depend on dot size. We will also measure

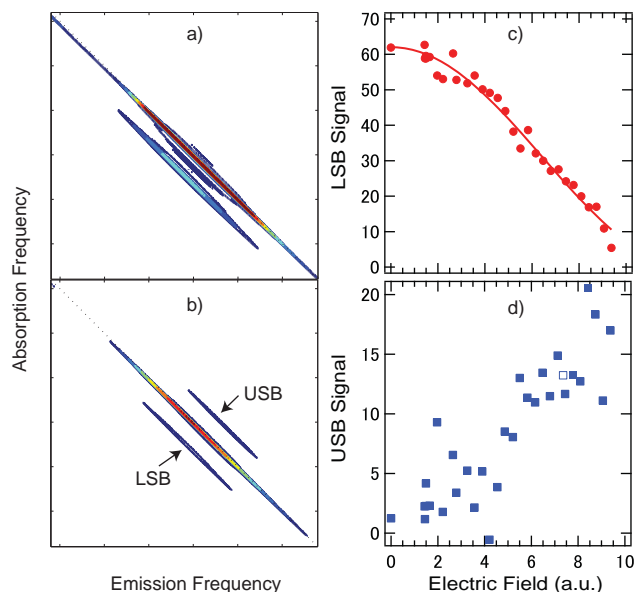


Figure 2: Preliminary results showing coherent control of excitons in InAs quantum dots. (a) 2D spectrum without a prepulse. Lower side band is due to absorption by the ground-state to exciton transition and emission on the exciton-biexciton transition. (b) 2D spectrum with a prepulse, the upper side band (USB) is due to absorption on the exciton to biexciton transition followed by emission on the exciton to ground state transition. (c & d) strength of the side bands as a function of prepulse electric field.

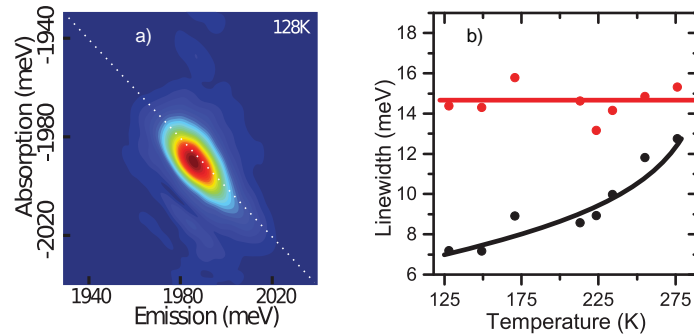


Figure 3: (a) 2D spectrum of CdSe/ZnS core-shell colloidal quantum dots. (b) Temperature dependence of the homogeneous (black) and inhomogeneous widths of determined from the 2D coherent spectra of CdSe/ZnS quantum dots. The lines are guides to the eye.

the dephasing rates in these materials.

Publication during the current grant year:

1. G. Nardin, G. Moody, R. Singh, T.M. Autry, H. Li, F. Morier-Genoud and S.T. Cundiff, "Coherent Excitonic Coupling in an Asymmetric Double InGaAs Quantum Well", *Phys. Rev. Lett.* **112**, 046402 (2014).
2. G. Moody, I.A. Akimov, H. Li, R. Singh, D.R. Yakovlev G. Karczewski, M. Wiater, T. Wojtowicz, M. Bayer and S.T. Cundiff, "Coherent Coupling of Excitons and Trions in a Photoexcited CdTe/CdMgTe Quantum Well", *Phys. Rev. Lett.* **112**, 097401 (2014).

Publication during the prior 2 years from this project:

1. S.T. Cundiff, "Optical two-dimensional Fourier transform spectroscopy of semiconductor nanostructures," *J. Opt. Soc. Am. B* **29**, A69-A81 (2012).
2. S.T. Cundiff, A.D. Bristow, M. Siemens, H. Li, G. Moody, D. Karaiskaj, X. Dai and T. Zhang, "Optical Two-Dimensional Fourier Transform Spectroscopy of Excitons in Semiconductor Nanostructures (Invited)," *IEEE J. Spec. Topics Quantum Electr.* **18**, 318-328 (2012).
3. D. B. Turner, P. Wen, D. H. Arias, K. A. Nelson, H. Li, G. Moody, M. E. Siemens, and S. T. Cundiff, "Measuring many-body interaction dynamics in GaAs quantum wells using two-dimensional electronic correlation spectroscopy," *Phys. Rev. B* **85**, 201303(R) (2012).
4. S.T. Cundiff and S. Mukamel, "Optical multidimensional coherent spectroscopy," *Physics Today* **66**, number 6, p. 44-49 (2013).
5. G. Moody, R. Singh, H. Li, I.A. Akimov, M. Bayer, D. Reuter, A.D. Wieck, A.S. Bracker, D. Gammon and S.T. Cundiff, "Biexcitons in semiconductor quantum dot ensembles," *Physica Status Solidi B* **250**, 1753-1759 (2013).
6. G. Moody, R. Singh, H. Li, I.A. Akimov, M. Bayer, D. Reuter, A.D. Wieck and S.T. Cundiff, "Correlation and dephasing effects on the non-radiative coherence between bright excitons in an InAs QD ensemble measured with 2D spectroscopy," *Solid State Commun.* **163**, 65-69 (2013).
7. G. Moody, R. Singh, H. Li, I.A. Akimov, M. Bayer, D. Reuter, A.D. Wieck and S.T. Cundiff, "Fifth-order nonlinear optical response of excitonic states in an InAs quantum dot ensemble measured with 2D spectroscopy," *Phys. Rev. B* **87**, 045313 (2013).
8. H. Li, G. Moody, S.T. Cundiff, "Reflection optical two-dimensional Fourier-transform spectroscopy," *Opt. Express* **21**, 1687-1992 (2013).
9. G. Moody, R. Singh, H. Li, I.A. Akimov, M. Bayer, D. Reuter, A.D. Wieck, A.S. Bracker, D. Gammon and S.T. Cundiff, "Influence of confinement on biexciton binding in semiconductor quantum dot ensembles measured with 2D spectroscopy," *Phys. Rev. B* **87**, 041304(R) (2013).

SISGR: Understanding and Controlling Strong-Field Laser Interactions with Polyatomic Molecules

DOE Grant No. DE-SC0002325

Marcos Dantus, dantus@msu.edu

Department of Chemistry and Department of Physics and Astronomy, Michigan State University, East Lansing MI 48824

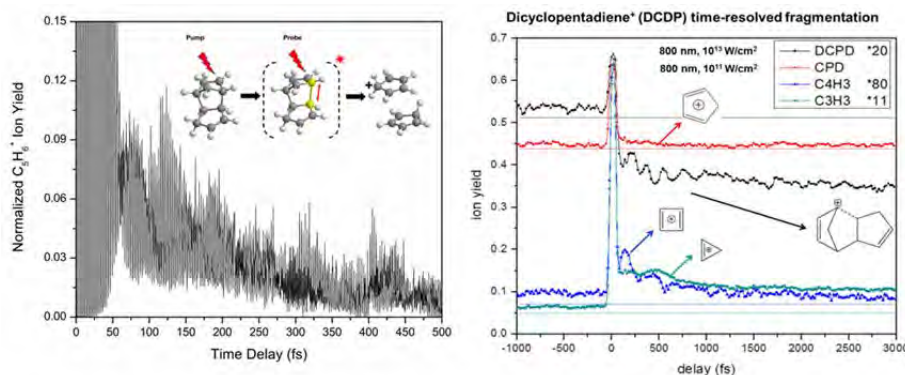
1. Program Scope

When intense laser fields interact with polyatomic molecules, the energy deposited leads to fragmentation, ionization and electromagnetic emission. The objective of this project is to determine to what extent these processes can be controlled by modifying the phase and amplitude characteristics of the laser field according to the timescales for electronic, vibrational, and rotational energy transfer. Controlling these processes will lead to order-of-magnitude changes in the outcome from laser-matter interactions, which may be both of fundamental and technical interest. The proposed work is unique because it seeks to combine knowledge from the field of atomic-molecular-optical physics with knowledge from the fields of analytical and organic ion chemistry. This multidisciplinary approach is required to understand to what extent the shape of the field affects the outcome of the laser-molecule interaction and to which extent the products depend on ion stability. The information resulting from the systematic studies will be used to construct a theoretical model that tracks the energy flow in polyatomic molecules following interaction with an ultrafast pulse.

2. Recent Progress

During the two years of this grant period we have carried out a series of studies to determine the role of electronic and vibrational coherence in large molecules. Our interest in electronic and vibrational coherence and the development of laser pulse shaping approaches led us to some ‘model’ experiments in condensed phase. Results on the coherent response of polyatomic molecules in condensed phase have resulted in four publications and one manuscript in revision. Our work on isolated polyatomic molecules in strong-fields is now summarized in a J. Phys. Chem. A. Feature Article under final revision. We have a second manuscript under revision related to electronic coherence in isolated molecules studied under strong field. In terms of instrument development, we rebuilt our molecular beam and completed a PEPICO instrument.

1. A. Konar, Y. Shu, B. G. Levine, V. V. Lozovoy, and M. Dantus, “Electronic Coherence Mediated Quantum Control of Chemical Reactions in Polyatomic Molecules”, a manuscript being considered by Science.



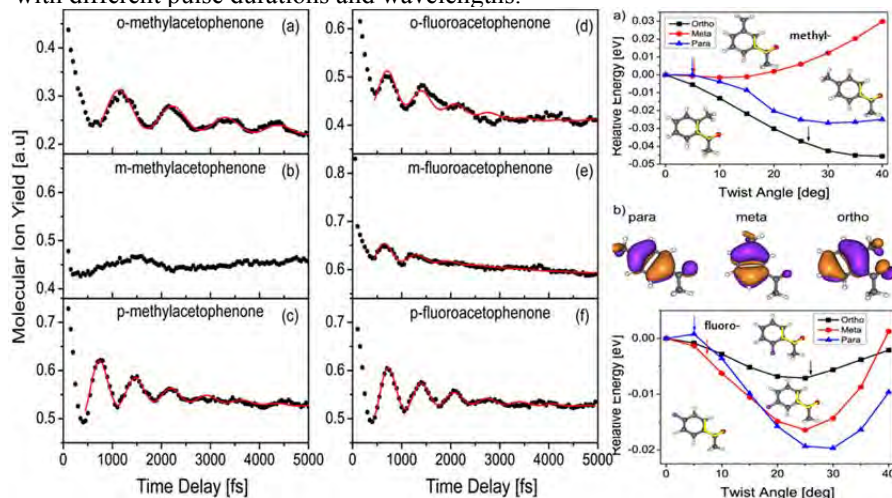
Using lasers to induce coherence onto a molecule and then using constructive or destructive interference with the mixed state to achieve quantum coherent control of its subsequent chemical transformation has been a long-standing dream. Here we report order-of-magnitude quantum coherent control of the yield of photofragment ions

following the creation of electronic coherence in dicyclopentadiene (C₁₀H₁₂) molecules using a pair of phase-locked femtosecond near-infrared laser pulses. The electronic coherence involving Rydberg states, which can preserve phase information for hundreds of femtoseconds, provides a robust platform for quantum coherent control. Control is achieved simply by changing the delay between pump and probe pulses by 400 attoseconds, even at delay times greater than 0.5 picoseconds. Our results serve as a guide on how femtosecond pulses can be used to prepare an electronic superposition intermediate state from which coherent control is possible.

2. A. Konar, Y. Shu, V. V. Lozovoy, J. E. Jackson, B. G. Levine and M. Dantus, “Polyatomic molecules under intense femtosecond laser irradiation,” J. Phys. Chem. A, Feature Article (In press 2014).

In this article we present an experimental quest to better understand the behavior of a large class of aromatic ketones when irradiated with intense femtosecond pulses and consider to what extent molecules retain their molecular identity and properties. Using time-of-flight mass spectrometry in conjunction with pump-probe techniques, we study the dynamical behavior of these molecules while monitoring the ion yield modulation caused by intramolecular motion post ionization. The large group of molecules studied is further divided into smaller

subgroups depending on particular chemical changes to the backbone structure such as positional isomerism of different functional groups. We find that these changes, which energetically amount to a few meV influence the dynamical behavior of the molecules as evident from the time-delay scans even in the presence of such high fields ($V/\text{\AA}$). High level ab initio quantum chemical calculations were performed in order to predict molecular dynamics and single and multiphoton resonances in the neutral and ionic states. We propose the following model of strong-field ionization and subsequent fragmentation for polyatomic molecules. Following single electron tunneling ionization, the cation is left with very little internal energy in the remaining laser field. Further fragmentation takes place as a result of both, further photon absorption modulated by one and two photon resonances and radical cation stability. The proposed ‘sacrificial electron’ hypothesis implies the loss of an electron at a rate that is faster than intramolecular vibrational relaxation and is consistent with the observation of non-statistical photofragmentation of polyatomic molecules as well as experimental results from many other research groups on different molecules and with different pulse durations and wavelengths.

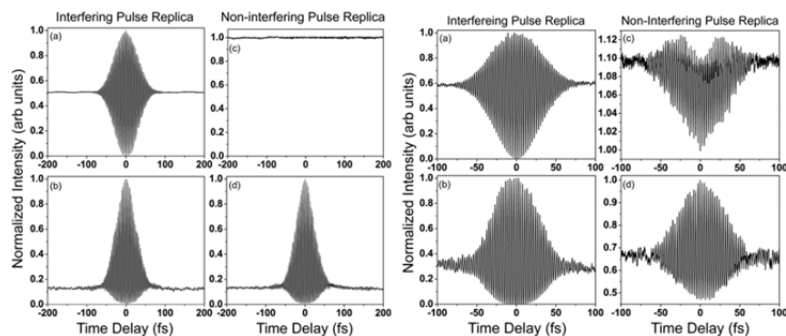


Strong-field pump weak field probe time-resolved transients obtained for ortho-, meta- and para-methylacetophenone and fluoroacetophenone. The coherent oscillations correspond to motion along the twist angle of the carbonyl group with respect to the aromatic ring plane. Note that m-methylacetophenone shows no oscillations, and this is consistent with ab initio calculations (top right panel). All three isomers for fluoroacetophenone show

coherent oscillations as corroborated by calculations. These results are consistent with the explanation that strong-field ionization creates a molecular ion with low internal energy.

3. A. Konar, J. Shah, V. V. Lozovoy and M. Dantus, “Optical Response of Fluorescent Molecules Studied by Synthetic Femtosecond Laser Pulses”, *J. Phys. Chem. Lett.* 3, 1329–1335 (2012).

The optical response of the fluorescent molecule IR144 in solution is probed by pairs of collinear pulses with intensity just above the linear dependence using two different pulse shaping methods. The first pulse-generation approach mimics a Michelson interferometer while the second approach, known as multiple independent-comb shaping (MICS), eliminates spectral interference between the pulses. The comparison of interfering and non-interfering pulses reveals that experimental information can be lost at early delay times because of linear interference between the pulses. In both cases, the delay between the pulses is controlled with attosecond resolution and the sample fluorescence and stimulated emission are monitored simultaneously. An out-of-phase behavior is observed for fluorescence and stimulated emission, with the fluorescence signal having a minimum at zero time delay. Experimental findings are modeled using a two-level system with relaxation that closely matches the phase difference between fluorescence and stimulated emission and the relative intensities of the measured effects. The goal of developing non-interfering pulse pairs was achieved and will be applied to strong field experiments.



(Left) Experimental Data: Interferometric (PA) time delay scans for the (a) laser intensity and (b) second harmonic generation intensity. Non-interfering (MICS) time delay scans for the (c) laser intensity and (d) second harmonic generation intensity. (Right) Experimental results (a) integrated fluorescence and (b) stimulated emission as a function of time delay using phase and amplitude modulation. (c) Integrated fluorescence and (d) stimulated emission

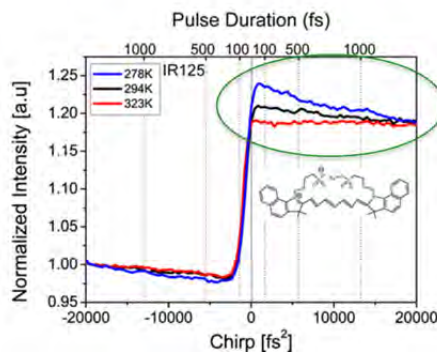
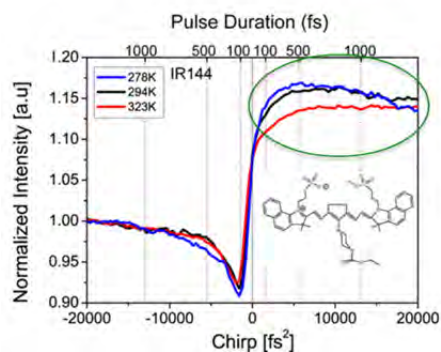
as a function of time delay using MICS phase modulation.

4. A. Konar, J. Shah, V. V. Lozovoy and M. Dantus, "Solvation Stokes-Shift Dynamics Studied by Chirped Femtosecond Laser Pulses", *J. Phys. Chem. Lett.* 3, 2458-2464 (2012).

Chirped pulses can be used to probe fast intramolecular dynamics, and are sensitive to the molecular environment. This study showed that the phase response of large polyatomic molecules is nonlinear in nature, a finding that was very important for the field of coherent control in weak fields.

5. A. Konar, V.V. Lozovoy, and M. Dantus, "Solvent Environment Revealed by Positively Chirped Pulses," *J. Phys. Chem. Lett.* 5, 924–928 (2014).

In terms of pulse shaping experiments, chirp has been used since the nineties with experiments from the Shank and Wilson's groups in the 1990's. Despite the fact that chirp experiments have been performed for decades there have been few systematic studies aimed at figuring out what kind of dynamics are probed by positive and negative chirp experiments. Here we found that positive chirp pulses are more sensitive to intramolecular dynamics while negative chirp experiments are to intermolecular dynamics.

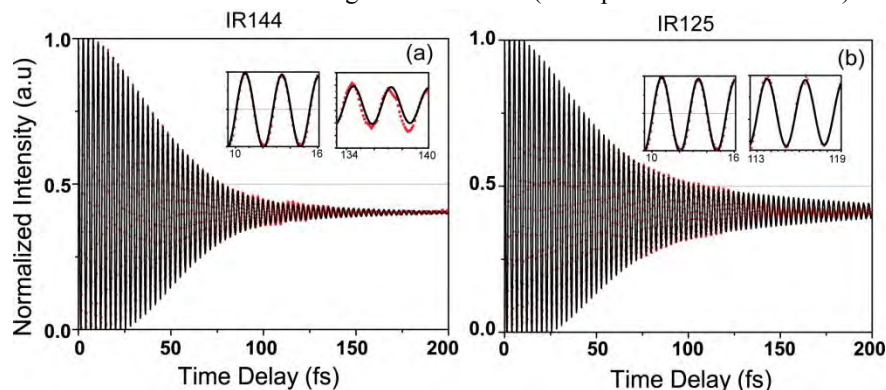


Fluorescence response to chirped pulses for IR144 (left) and for IR125 (right) in ethylene glycol at three temperatures 323K (red), 294K (black), and 278K (blue). The plots have been normalized on the asymptotic value of the chirp effect. These plots show for the first time that negative chirp follows

intramolecular dynamics while positive chirp is more sensitive to intermolecular (solvation) dynamics. These two molecules have a different solvent response; IR144 has a polar while IR125 a non-polar response. Similar results were observed when following stimulated emission, which occurs before vibrational relaxation.

6. A. Konar, V.V. Lozovoy, and M. Dantus, "Electronic dephasing of molecules in solution measured by nonlinear spectral interferometry," *J. Spectrosc. Dyn.* 4, 26 (2014).

The dephasing time for the initial electronic coherence between the ground and excited states is significant because during this time quantum-mechanical phase can be expected to play a role in molecular processes. Dephasing measurements are particularly important for molecules in condensed phase where inhomogeneous broadening, changes in dipole, and solvent reorientation complicate the observables. Here, phase-locked femtosecond pulse pairs are used to measure the coherent third order response from IR144 and IR125 and the measurements are compared with simultaneous fluorescence measurements. Related electronic dephasing experiments were carried out in isolated molecules under strong field excitation (to be published in the future).



Experimental data (red dots) and the best fit curve (black line) for stimulated emission generated by the pair of the delayed pulses for (a) IR144 and (b) IR125. The inset shows the fit quality for both the datasets at early and later times. For long time delays, out-of-phase oscillations for stimulated emission, that persist for approximately 130 fs or 180fs for IR144 or IR125, respectively, are observed.

7. A. Konar, V. V. Lozovoy and M. Dantus, “Coherent quantum control of stimulated emission,” *Phys. Rev. Letters* (in review 2014).

Interaction of light with matter leads to scattering, absorption and stimulated emission. These fundamental processes are well understood and therefore prime for control experiments. We show that applying a sharp spectral phase step in the excitation pulse causes enhanced absorption of the high frequency components and a sharp narrow-band emission of low frequency. We provide a theoretical model that explains how the induced nonlinear optical polarization gives rise to the experimentally observed results. The Mukamel group has developed a theoretical formalism that explains the off-diagonal features. Making this single-shaped laser experiment as powerful as a 2D spectroscopy experiment.⁸⁹

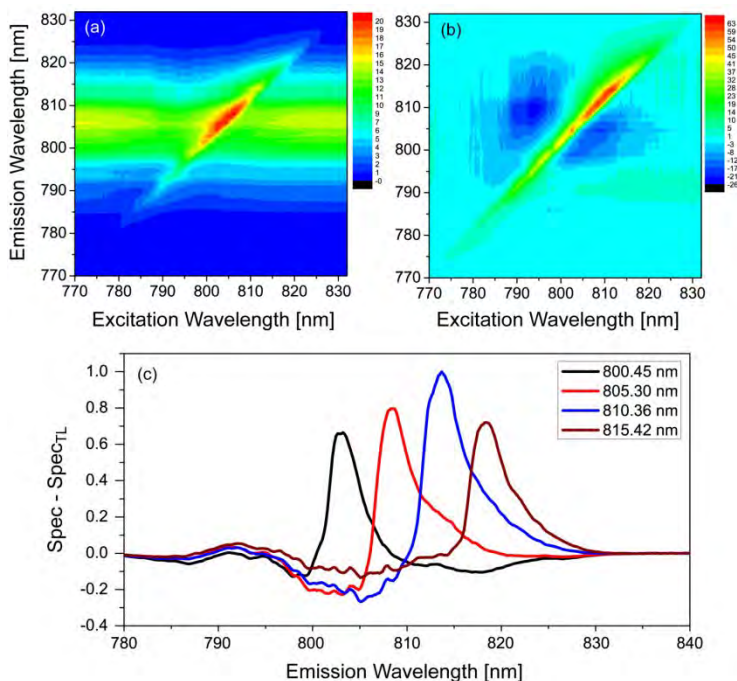


Fig. 8 Experimental data obtained for IR125 solution in methanol. (a) 2D plot of the raw signal spectrum as a function of $\pi/2$ step on the excitation spectrum. (b) Difference 2D spectrum obtained by subtracting the signal due to TL pulses from the raw signal. (c) Sections at 800.45 nm (black), 805.30 nm (red), 810.36 nm (blue) and 815.42 nm (olive) showing the difference spectrum.

3. Future Plans

- We are working on the final revision of a Feature Article in *J. Phys. Chem* on the behavior of polyatomic molecules under strong fields.
- We plan to complete our publication on the electronic coherence involved in laser control of chemical reactions, in particular intense non-resonant fields.
- We plan to complete the studies of IR144, and IR125 in solution, based on a single shaped pulse. We are working with the Mukamel group on simulation of the 2D data.

One of the important goals of our proposed work was to upgrade our molecular beam in order to be able to carry out experiments taking advantage of PEPICO detection, to determine how much energy was deposited in the molecule by the laser field to produce each of the different fragment ions. We will also be able to correlate the origin of the ejected electron with a specific fragment. The system is now operational.

4. Publications

- X. Zhu, V. V. Lozovoy, J. D. Shah and M. Dantus, “Photodissociation dynamics of acetophenone and its derivatives with intense nonresonant femtosecond pulses,” *J. Phys. Chem. A* **115**, 1305–1312 (2011)
- A. Konar, V. V. Lozovoy and M. Dantus, “Solvation Stokes-Shift Dynamics Studied by Chirped Femtosecond Laser Pulses”, *J. Phys. Chem. Lett.* **3**, 2458-2464 (2012)
- A. Konar, J. D. Shah, V. V. Lozovoy and M. Dantus, “Optical Response of Fluorescent Molecules Studied by Synthetic Femtosecond Laser Pulses”, *J. Phys. Chem. Lett.* **3**, 1329–1335 (2012)
- A. Konar, V.V. Lozovoy, and M. Dantus, “Electronic dephasing of molecules in solution measured by nonlinear spectral interferometry,” *J. Spectrosc. Dyn.* **4**, 26 (2014).
- A. Konar, V.V. Lozovoy, and M. Dantus, “Solvent Environment Revealed by Positively Chirped Pulses,” *J. Phys. Chem. Lett.* **5**, 924–928 (2014).
- A. Konar, Y. Shu, V. V. Lozovoy, J. E. Jackson, B. G. Levine and M. Dantus, “Polyatomic molecules under intense femtosecond laser irradiation,” *J. Phys. Chem. A*, Feature Article (In press 2014).
- A. Konar, Y. Shu, B. G. Levine, V. V. Lozovoy, and M. Dantus, “Electronic Coherence Mediated Quantum Control of Chemical Reactions in Polyatomic Molecules”, a manuscript being considered by *Science*

Production and trapping of ultracold polar molecules

D. DeMille

Physics Department, Yale University, P.O. Box 208120, New Haven, CT 06520

e-mail: david.demille@yale.edu

Program scope: The goal of our project is to produce and trap polar molecules in the ultracold regime. Once achieved, a variety of novel physical effects associated with the low temperatures and/or the polar nature of the molecules should be observable. We recently discovered and characterized a simple and efficient method to produce and accumulate ultracold RbCs in its absolute rovibronic ground state and used our findings to predict the properties of trapped samples produced using this technique. Molecules in such a sample will be stable against inelastic collisions and hence suitable for further study and manipulation. Once in place, we will study chemical reactions at ultracold temperatures, dipolar effects in collisions, etc.

Our group earlier pioneered techniques to produce and state-selectively detect ultracold heteronuclear molecules. These methods yielded RbCs molecules at translational temperatures $T < 100 \mu\text{K}$, in any of several desired rovibronic states—including the absolute ground state, where RbCs has a substantial electric dipole moment. Our previous method for producing ultracold, ground state RbCs consisted of several steps. First, laser-cooled and trapped Rb and Cs atoms were bound into an electronically excited state via photoassociation (PA).¹ These states decayed rapidly into weakly bound vibrational levels in the ground electronic state manifold.² Population from one such level could be transferred into the lowest vibronic state $X^1\Sigma^+(v=0)$ of RbCs using a laser “pump-dump” scheme.^{3,4} We detect molecules with vibrational-state selectivity with a resonantly-enhanced multiphoton ionization process (1+1 REMPI) followed by time-of-flight mass spectroscopy. Subsequently, we incorporated a 1D optical lattice trap into our experiments. This made it possible to trap vibrationally-excited RbCs molecules as they were formed. The precursor Rb and Cs atoms could also be trapped. We used this capability to measure inelastic (trap loss) cross-sections for individual RbCs vibrational levels on both Rb and Cs atoms in the ultracold regime, and also developed a simple theoretical model for these collisions.⁵

Recently we have focused on a new method to directly create rovibronic ground-state $X^1\Sigma^+(v=0, J=0)$ RbCs molecules (Fig. 1). Here we drive PA transitions into tightly-bound states of excited electronic potentials. Such states can in decay with substantial probability to the $X^1\Sigma^+(v=0, J=0)$ absolute ground state, which also has small internuclear separation. PA to short-range states was previously believed to be impractical: in the WKB approximation, the scattering-state wavefunction of two colliding atoms has negligible amplitude at distances comparable to the separation of atoms in the molecular ground state,⁶ so Franck-Condon factors (FCFs) for the free-to-bound PA transition were expected to be too small to drive efficiently.

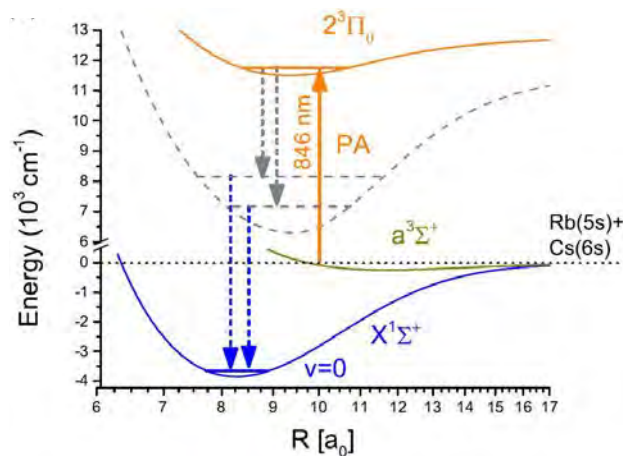


Fig. 1: Scheme for ground state molecule formation via direct short-range photoassociation.

Nevertheless, recent observations from groups working on similar heteronuclear bi-alkali systems has shown that it is sometimes possible to drive PA transitions into tightly-bound states.^{7,8,9,10} In all these cases the PA rate was larger than the naïve expectation, although the underlying mechanisms were sometimes unclear. Most importantly, efficient production of the rovibronic $X^1\Sigma^+(v=0, J=0)$ ground state via decay of a PA level could not be demonstrated in any of these systems.

In our recent work, we have demonstrated that formation of rovibronic ground-state RbCs via short-range PA is indeed viable.¹¹ We first used our REMPI detection method to show that the short-range PA level of Ref. [9] indeed results in population of the $X^1\Sigma^+(v=0)$ state. Using existing spectroscopic data on RbCs,¹² we were able to assign the PA level definitively to the $(2)^3\Pi(0^-)$ state. Subsequently, using existing spectroscopic data for state identification, we demonstrated PA into several vibrational levels of neighboring $(2)^3\Pi(0^+)$ state. Some of these yielded larger rates of $X^1\Sigma^+(v=0)$ formation than using the previously known resonance (Fig. 2).

We subsequently compared the rates of formation of $X^1\Sigma^+(v=0)$, via PA through different $(2)^3\Pi(0^+)[v']$ sublevels, to expectations based on FCFs for the free-bound and bound-bound transitions. We found good qualitative agreement. This model relies on no unusual circumstances such as resonant coupling between bound states or scattering resonances. Rather, it simply takes advantage of the fact that the triplet-state scattering wavefunction is considerably larger than would be expected based on the WKB approximation; and that (non-resonant) spin orbit coupling is strong in bi-alkali molecules containing Cs. We also demonstrated that the PA transition could be saturated under typical experimental conditions, in rough agreement with calculated PA rates based on the FCFs. This means that formation of rovibronic ground state molecules can proceed at a rate given by the unitarity-limited scattering rate (i.e., the theoretical maximum PA rate), times the branching ratio $b \sim 0.2\%$ for decay of the $J = 1$ PA resonance into the $X^1\Sigma^+(v=0, J=0)$ state. In the course of this work, we also developed a straightforward and general method for predicting and analyzing rotational line strengths in PA spectra. This method makes it possible to assign the electronic symmetry of the excited state in a PA spectrum simply, and also to determine the temperature of the trapped atomic sample, as well as the presence of any scattering resonances between atoms. A publication describing this method and its application to previous PA spectra is near completion.

We next made high-resolution “depletion spectroscopy” measurements to explicitly verify that the $X^1\Sigma^+(v=0, J=0)$ state is populated by the decay of the PA resonance. This data showed

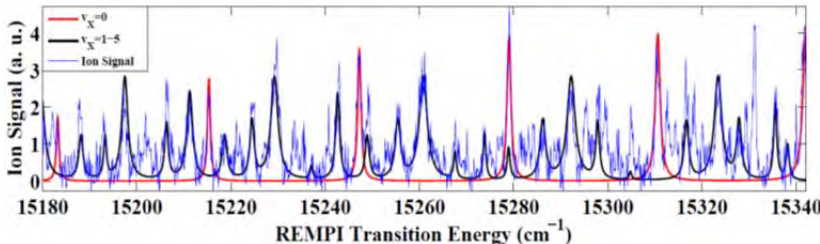


Fig. 2: Population of $X^1\Sigma^+(v=0)$ via short-range PA. Plotted is signal (blue) vs. detection laser frequency, with the PA laser tuned to the short-range $(2)^3\Pi_{0+}[v'=10]$ state. Red and black curves are simulated spectra, based on known energies and FCFs of the $X^1\Sigma^+(v'') \rightarrow (2)^1\Pi[v']$ states transitions. The black [red] curve is for transitions from $X(v''=0)$ [sum of signals from all excited levels $X(v''=1-5)$]. The only free parameters in the fit are an overall scale, and the relative populations of the $X^1\Sigma^+(v'')$ levels. Here the relative population of $X(v''=0)$ is $\sim 20\%$.

that indeed, as expected, up to 1/3 of the $X^1\Sigma^+(v=0)$ population can be produced in the $J=0$ absolute rovibronic ground state.¹³ However, our data showed that, surprisingly, the primary decay path to the ground state is via a two-photon cascade decay. While we observed a higher rate of production of rovibronic ground state molecules than in any experiment, the fact that the production occurs through an

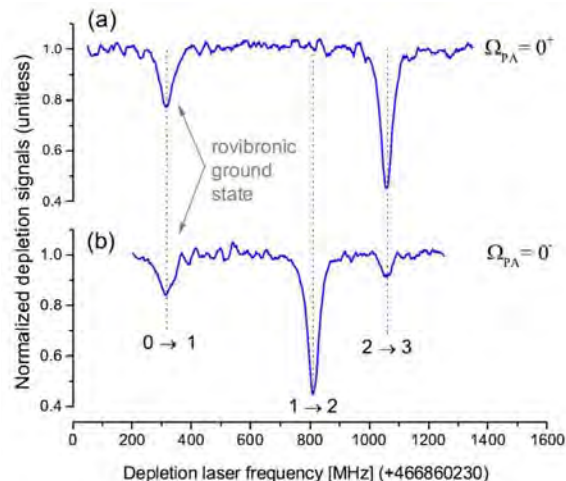


Fig. 3: High-resolution “depletion” spectra showing up to $\sim 1/3$ population in the $J=0$ rotational state for molecules in the $X^1\Sigma^+(v=0)$ vibronic ground state.

molecule production in the presence of dense Rb and Cs vapors can allow the accumulation of large molecular samples. Once the molecule density reaches equilibrium (due to destructive collisions with Rb atoms and residual rovibrationally-excited RbCs* molecules), removal of Rb and continued co-trapping with Cs atoms can “scrub” the sample of RbCs* via inelastic collisions. We have simulated the properties of a trapped sample of $X^1\Sigma^+(v=0, J=0)$ RbCs molecules produced using this approach, based on simple rate equation arguments, and have concluded that it opens a pathway to trapping molecules at sufficient density and number to study collisions and reactions.¹¹ We recently revived our optical trapping apparatus and have co-trapped Rb and Cs again as we last did a few years ago. We next plan to experimentally explore the dynamics of the accumulation and scrubbing processes in this optical trap.

inefficient two-photon process makes it likely that much higher rates can be obtained by finding a more optimal PA pathway.

More generally, our results should make it possible to continuously produce and accumulate $X^1\Sigma^+(v=0, J=0)$ RbCs molecules into an optical trap. This is fundamentally different from existing approaches to form similar molecular samples, which use Feshbach-resonance association followed by stimulated optical transitions to the ground state.¹⁴ In our approach, the dissipation associated with decay of the PA resonance allows irreversible accumulation. Key to this approach is that, unlike many heteronuclear alkali species, RbCs is immune to inelastic, chemically-reactive collisions with itself, and with Cs atoms. Hence,

References

- ¹A.J. Kerman *et al.*, Phys. Rev. Lett. **92**, 033004 (2004).
- ²A.J. Kerman *et al.*, Phys. Rev. Lett **92**, 153001 (2004).
- ³J.M. Sage, S. Sainis, T. Bergeman, and D. DeMille, Phys. Rev. Lett. **94**, 203001 (2005).
- ⁴T. Bergeman *et al.*, Eur. Phys. J. D **31**, 179 (2004).
- ⁵E. R. Hudson, N.B. Gilfoy, S. Kotochigova, J.M. Sage, and D. DeMille, Phys. Rev. Lett. **100**, 203201 (2008). [DOE SUPPORTED]
- ⁶W.C. Stwalley and H.J. Wang, J. Mol. Spectrosc. **195**, 194 (1999)
- ⁷J. Deiglmayr *et al.*, Phys. Rev. Lett. **101**, 133004 (2008)
- ⁸P. Zabawa, A. Wakim, M. Haruza, and N. P. Bigelow, Phys. Rev. A **84**, 061401(R) (2011).
- ⁹C. Gabbanini and O. Dulieu, Phys. Chem. Chem. Phys. **13**, 18905 (2011).
- ¹⁰Z. Ji *et al.*, Phys. Rev. A **85**, 013401 (2012).
- ¹¹C.D. Bruzewicz, M. Gustavsson, T. Shimasaki, and D. DeMille, New J. Phys. **16**, 023018 (2014). [DOE SUPPORTED]
- ¹²Y. Lee, Y. Yoon, S. Lee, J.-T. Kim, and B. Kim, J. Phys. Chem. A **112**, 7214 (2008).
- ¹³T. Shimasaki, M. Bellos, C. D. Bruzewicz, Z. Lasner and D. DeMille, arXiv:1407.7512; to appear in Phys. Rev. A (Rapid Communications) (2014). [DOE SUPPORTED]
- ¹⁴S. Ospelkaus *et al.*, Science **327**, 853 (2010).

Page is intentionally blank.

SPATIAL-TEMPORAL IMAGING DURING CHEMICAL REACTIONS

Louis F. DiMauro
 Co-PI: Pierre Agostini
 Co-PI: Terry A. Miller
 Department of Physics
 The Ohio State University
 Columbus, OH 43210
dimauro@mps.ohio-state.edu
agostini@mps.ohio-state.edu

1.1 PROJECT DESCRIPTION

This document describes the BES funded project (grant #: DE-FG02-06ER15833) entitled “Spatial-temporal imaging during chemical reactions” at The Ohio State University. Imaging, or the determination of the atomic positions in molecules is of central importance in physical, chemical and biological sciences. X-ray and electron diffraction are well-established method to obtain static images with sub-Angstrom spatial resolution. However their temporal resolution is limited to picoseconds. This proposal builds on the “molecule self-imaging” approach, based on bursts of strong-field driven coherent electron wave packets emitted by the molecule under interrogation. We are investigating two complementary self-imaging methods: Laser-Induced Diffraction [1] and high harmonic tomography [2, 3]. Both thrust exploit the wavelength scaling of strong-field interactions to improve the imaging capabilities.

Over the past year, our efforts have focused on several thrusts: (1) development of fixed-angle broadband laser-induced electron scattering (FABLES), (2) application of laser-induced electron diffraction (LIED) to complex molecular systems and (3) high-harmonic tomography of N₂ and CO₂ at mid-infrared wavelengths.

1.2 PROGRESS IN FY13: IMAGING

Direct visualization of isolated molecules undergoing structural transformations can provide insight into the fundamental understanding of chemical processes. Conventional methods based on diffraction and absorption, using electrons or synchrotron-generated X-rays pulses, routinely achieve sub-angstrom resolutions, but their picosecond duration precludes characteristic, femtosecond-scale dynamical molecular imaging. The recent development of femtosecond sources of X-rays, *e.g.* free-electron lasers, and electron beams has enhanced the temporal resolving power of these standard probes for ultrafast molecular dynamics. Femtosecond electron and X-ray diffraction have been successfully demonstrated recently [4-7]. These schemes offer the potential for performing ultrafast dynamic imaging in condensed-phase systems, but their current fluxes are insufficient to achieve good enough signal-to-noise ratios for more rarified systems, *e.g.* gas-phase. Alternatively, since electrons have larger diffraction cross-sections than X-rays, it is advantageous to convert X-ray photons to electrons via core ionization. Femtosecond photoelectron

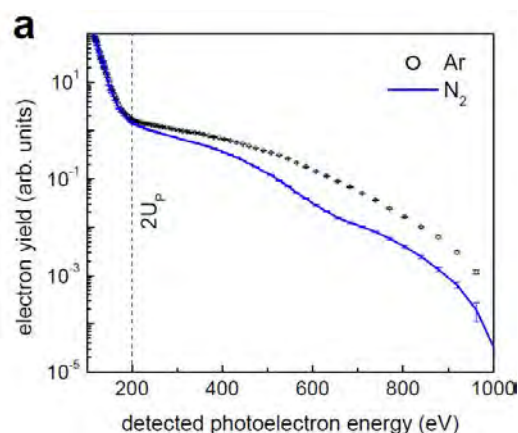


Figure 1: High-resolution photoelectron energy spectra along the laser polarization for N₂ and argon recorded at a wavelength of 2.0 μm and an intensity of 270 TW/cm^2 . The error bars indicate the $N^{-1/2}$ Poisson statistical fluctuations for each time bin, N being the number of detected electrons. The vertical dashed line marks the $2U_p$ energy, electrons below this are direct. Above it, the long plateau corresponds to photoelectrons that are backscattered following ionization. The plateaus are a direct illustration of the broadband nature of the returning electron wave packet.

diffraction/holography has been proposed as a time-resolved imaging method of transient molecules in the gas phase [8,9].

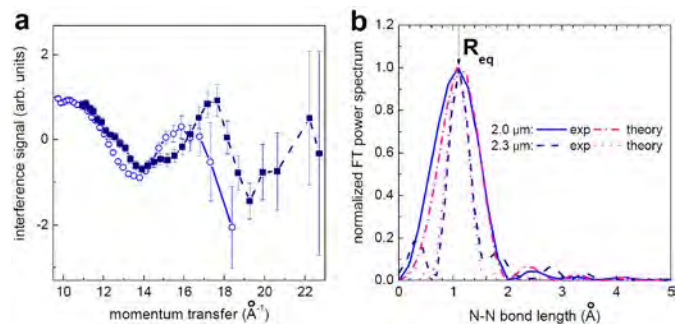


Figure 2: *FABLES* bond length retrieval and Fourier transform. (a) The intramolecular interference fringes extracted from the nitrogen plateau data at 2.0 μm (light blue open circles) and 2.3 μm (dark blue solid squares). The error bars represent the standard deviations of the two data sets which are calculated from measurement errors of their corresponding photoelectron energy distribution by assuming that the theoretical atomic DCS is exact. (b) The mean internuclear distance function obtained by Fourier Transform of the data in (a). The dash-dotted and dotted lines are the FT of the theoretical DCS spanning the same momentum transfer range as the experiments at 2.0 and 2.3 μm , respectively. The vertical arrow in (b) denotes the known N_2 equilibrium distance, R_{eq} . Our retrieved bond lengths deviate from R_{eq} by 0.01 \AA .

recollision electron energy is identical with LIED. For small molecules, it has been demonstrated that mid-infrared wavelengths ($\lambda \geq 1.7 \mu\text{m}$) generate recollision electron wave packet energies sufficient ($\geq 100 \text{ eV}$) to directly probe the “independent” atomic cores in the molecule [10-12].

Fixed-angle broadband laser-driven electron scattering (FABLES). In Nature Communication [13] we introduced fixed-angle broadband laser-driven electron scattering (FABLES) as an alternative to fixed-energy, angle-swept LIED [11]. FABLES is analogous to white light interferometry in optics, and this is the first experimental confirmation that broadband electron wave packet (EWP) can be used for imaging. In FABLES, the energy-dependent DCS, $\sigma(E)$, is retrieved as compared to the angle-dependent DCS, $\sigma(\theta)$, of the LIED method. The main benefit of FABLES is a trivial retrieval of molecular structure via a simple Fourier transform (FT) with no theoretical fitting or modeling, *e.g.* no *a priori* knowledge of laser ionization. Furthermore, the method “visualizes” only bonds *parallel* to the laser polarization and has the potential for routine, real-time imaging in a pump-probe configuration. This unique aspect combined with molecular alignment was shown theoretically to offer a full molecular tomographic reconstruction.

Figure 1 shows the main result of this study. Both N_2 and Ar photoelectron spectrum were recorded under identical laser conditions. The detector collects electrons in a small angle (2°) along the laser polarization direction. The physically relevant difference between N_2 and Ar is the oscillation on the N_2 plateau resulting from the interference of the broadband EWP on the molecular structure.

To retrieve the structural information, we adopt the mature rectification-based analysis method of CED. Figure 2(a) shows the intra-molecular interference fringes extracted from the nitrogen distributions at 2.0 μm and 2.3 μm as a function of the momentum transfer $|\mathbf{q}|$. Following CED’s inversion procedure, a Fourier transform extracts from the momentum-space interferogram the real-space structural information, as illustrated in the power spectra plotted in Fig. 2(b). The retrieved experimental internuclear distance functions peak at nearly the same position, 1.09 and 1.11 \AA for 2.0 and 2.3 μm experiments, respectively. In comparison, the known nitrogen equilibrium distance, R_{eq} , is 1.10 \AA .

Independent of the method, the critical parameter that ultimately controls the spatial resolution is the momentum transfer, $|\mathbf{q}|$, defined as $|\mathbf{q}|=2|\mathbf{k}_r|\sin(\theta_r/2)$, where \mathbf{k}_r and θ_r are the electron’s scattering momentum and angle, respectively. In a typical conventional electron diffraction (CED) experiment $|\mathbf{k}_r|$ is held constant and $|\mathbf{q}|$ is varied by sweeping the angle, usually over a small range in the forward direction. However, similar $|\mathbf{q}|$ ranges can be obtained at a fixed angle (with the most advantageous collision geometry for $\theta_r = 180^\circ$) by varying the electron momentum. In strong field ionization, the backscattering requirement is met along the laser polarization, in which case the photoelectron energy distribution exhibits a long backscattering plateau. The maximum detected electron energy extends to $\sim 10U_p$, where U_p represents a free electron’s cycle-averaged quiver energy (ponderomotive energy). This cutoff corresponds to a $\sim 3U_p$ electron-ion recollision energy, which decreases monotonically for electrons detected at lower energies. The correspondence between detected and

LIED studies of large molecules. We have begun to investigate the applicability of LIED and FABLES to complex molecular systems. The LIED approach is one of the variants of molecular self-probing techniques, which has a simple analog to conventional electron diffraction (CED). In CED, an external multi-kilovolt electron beam elastically scatters from a molecular gas sample and the resulting small-angle, forward-scattering, diffraction pattern conveys information on the molecular structure. The bond-length information can be retrieved from the pattern, assuming some approximations. One key ansatz is that the high-energy electrons penetrate the core and thus, the short range atomic-like potential dominates the electron-molecule scattering, while the bonding valence electrons look transparent. This allows use of the independent atom model (IAM) approximation, which describes the scattering as the contribution from individual atoms and an interference term between atoms (molecular term).

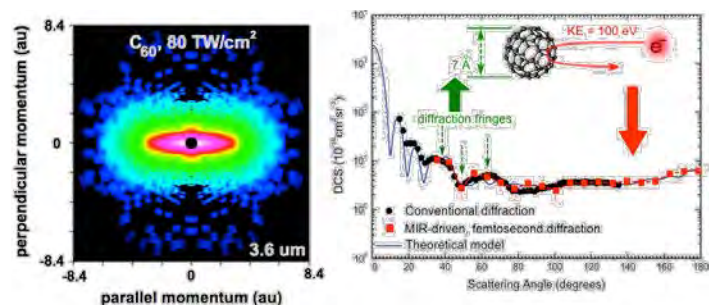


Figure 3: Preliminary electron momentum distribution of C_{60} ionized by femtosecond $4 \mu\text{m}$ pulses. On the right the extracted LIED DCS (red squares) is plotted against CED result and a theoretical scattering calculation. The fringe pattern allows the LIED experiment to measure the overall size (7 \AA) of the fullerene.

the electron is promoted into the continuum and the instant when it rescatters with the molecule. This time difference (propagation time) is easily derived from the classical equation of motion of a field-driven electron.

In an earlier report, we showed the viability of LIED for capturing a time-resolved molecular image of N_2 and O_2 [11]. We are currently exploring the possible extension of LIED to more complex systems. Various saturated hydrocarbon chains are being investigated. The low-binding energy of most molecule's valence electrons ($\sim 10 \text{ eV}$), as compared to low- Z diatomics, requires even longer wavelength mid-infrared fields ($\gg 2 \mu\text{m}$) to produce sufficient return energies via the λ^2 -scaling of the ponderomotive energy. Figure 3 is an example of a preliminary result obtained from a C_{60} fullerene experiment. Our analysis shows that we can extract the field-free DCS and obtain the size of the fullerene. Our theoretical modeling suggests that we should be able to extract the C-C distance and experiments are underway to verify this prediction. This work is being performed in collaboration with Dr. Matthias Kling (MPQ-Garching).

1.3 FUTURE PLANS

LIED and FABLES: Our current efforts are focused on both fundamental and applied tests of the LIED method: 1) the limits of spatial precision, the influence of multiple trajectories (long versus short and higher-order returns) on temporal precision, the dependence of the ionization rate on molecular alignment and the applicability of theoretical tools developed for CED analysis to LIED. 2) Applications of LIED to determine or observe structural changes in more complex systems; studies on isomeric systems and pump-probe interrogations. Larger molecules pose new challenges on experimental precision and theoretical methods in LIED. The inverse Fourier transform of the FABLES image will be further explored as an alternate structural retrieval method.

Tomography: Long wavelength tomography measurements of N_2 and CO_2 are being analyzed and should provide a benchmark for future efforts.

A strategy for imaging chemical dynamics using LIED and FABLES is being evaluated: the aim is to follow unimolecular dissociation using pump-probe schemes. A potential candidate is the breaking of the I-C bond in aligned ICN ($I_p = 10.8$ eV) by exciting from its ground state to its lowest excited, repulsive A state.

1.4 REFERENCES CITED

- [1] M. Meckel *et al.*, Laser-induced electron tunneling and diffraction, *Science* **320**, 1478-1482 (2008).
- [2] J. Itatani *et al.*, Tomographic imaging of molecular orbitals, *Nature* **432**, 867-871 (2004).
- [3] S. Haessler *et al.*, Attosecond imaging of molecular electronic wavepackets, *Nat. Phys.* **6**, 200 (2010).
- [4] B. J. Siwick, J. R. Dwyer, R. E. Jordan & R. J. D. Miller, An atomic-level view of melting using femtosecond electron diffraction, *Science* **302**, 1382 (2003).
- [5] Gao, M. *et al.*, Mapping molecular motions leading to charge delocalization with ultrabright electrons. *Nature* **496**, 343 (2013).
- [6] H. N. Chapman *et al.*, Femtosecond diffractive imaging with a soft-X-ray free-electron laser. *Nature Phys.* **2**, 839 (2006).
- [7] A. Barty *et al.*, Ultrafast single-shot diffraction imaging of nanoscale dynamics. *Nature Photon.* **2**, 415 (2008).
- [8] F. Krasniqi *et al.*, Imaging molecules from within: ultrafast angstrom-scale structure determination of molecules via photoelectron holography using free-electron lasers. *Phys. Rev. A* **81**, 033411 (2010).
- [9] R. Boll *et al.*, Femtosecond photoelectron diffraction on laser-aligned molecules: towards time-resolved imaging of molecular structure. *Phys. Rev. A* **88**, 061402(R) (2013).
- [10] Junliang Xu *et al.*, Laser-induced electron diffraction for probing rare gas atoms, *Phys. Rev. Lett.* **109**, 233002 (2012).
- [11] C. I. Bлага *et al.*, Imaging ultrafast molecular dynamics with laser-induced electron diffraction, *Nature* **483**, 194 (2012).
- [12] J. Xu *et al.*, Self-imaging of molecules from diffraction spectra by laser-induced rescattering electrons. *Phys. Rev. A* **82**, 033403 (2010).
- [13] J. Xu *et al.*, Diffraction using laser-driven broadband electron wave packets, *Nat. Comm.* **5**, 4635 (2014).

1.5 PUBLICATION RESULTING FROM THIS GRANT SINCE 2012

1. "Diffraction using laser-driven broadband electron wave packets", Junliang Xu *et al.* *Nat. Comm.* **5**, 4635 (2014).
2. "Laser-induced electron diffraction for probing rare gas atoms", Junliang Xu *et al.*, *Phys. Rev. Lett.* **109**, 233002 (2012).
3. "Imaging ultrafast molecular dynamics with laser-induced electron diffraction", C. I. Bлага *et al.*, *Nature* **483**, 194 (2012).
4. "Generation and propagation of high-order harmonics in crystals", S. Ghimire *et al.*, *Phys. Rev. A* **85**, 043836 (2012).

1.6 REVIEW ARTICLES ACKNOWLEDGING THIS DOE AWARD

1. "Scaling of high-order harmonic generation in the long wavelength limit of a strong laser field", A. D. DiChiara *et al.*, *IEEE J. Select. Topics Quan. Electro.* **18**, 419-433 (2012).
2. "Atomic and molecular ionization dynamics in strong laser-fields: from optical to X-rays", P. Agostini and L. F. DiMauro, in *Atomic, Molecular, and Optical Physics*, v.61, eds. P. Berman, E. Arimondo and Chun Lin (Elsevier, Maryland Heights, 2012) pp. 117-158.
3. "Strong-field interactions at long wavelengths", M. Kremer *et al.*, in *Attosecond and XUV Physics: Ultrafast Dynamics and Spectroscopy* eds. T. Schultz and M. Vrakking (Wiley-VCH Verlag, Weinheim), Chapter 11.

PROGRAM TITLE: ATTOSECOND AND ULTRA-FAST X-RAY SCIENCE

Louis F. DiMauro
 Co-PI: Pierre Agostini
 Department of Physics
 The Ohio State University
 Columbus, OH 43210
dimauro@mps.ohio-state.edu
agostini@mps.ohio-state.edu

1.1 PROJECT DESCRIPTION

This document describes the BES funded project (grant #: DE-FG02-04ER15614) entitled “Attosecond & Ultra-Fast X-ray Science” at The Ohio State University (OSU). Attosecond light pulses from gases offer a transition to a new time-scale and open new avenues of science while complementing and directly contributing to the efforts at the LCLS XFEL. An objective of this grant is the development of competency in generation and metrology of attosecond pulses using mid-infrared drivers and a strategy of employing these pulses for studying multi-electron dynamics in atomic systems. It focuses on applications in which attosecond pulses are produced and transported to a different region of space and applied to a different target, thus providing the greatest degree of spectroscopic flexibility. The proposal has also a strong thrust at the LCLS XFEL for studying the scaling of strong-field interactions into a new regime of x-ray science and the metrology of ultra-fast x-ray pulses.

Progress over the past year includes (1) measurement of the atomic phase near the Cooper minimum in argon atoms, (2) study of the Wigner delay in photoionization of inert gas atoms and (3) began an experimental study to examine near threshold effects in RABBITT measurements in collaboration with Prof. Robert Jones (Virginia).

1.2 PROGRESS IN FY14: THE ATTOSECOND PROGRAM

The technical approach of the Ohio State University (OSU) group is the use of long wavelength ($\lambda > 0.8 \mu\text{m}$) driving lasers for harmonic and attosecond generation. Through support of this program, the long wavelength approach has been successful and adopted by many groups world-wide. Our program over the last two years has turned towards using these long wavelength generated harmonics for measurements, ultimately of dynamics. We are interested in addressing two basic questions related to attosecond physics. First, can high harmonic spectroscopy extract atomic/molecular structure and second, what is really measured.

Attosecond pulse shaping around a Cooper minimum. One signature of atomic structure, first discussed by Cooper [1], is a local minimum in the photoionization (PI) probability at a specific photon energy. This Cooper minimum (CM) is caused by a sign change, equivalent to a π -phase jump, in the bound-free transition dipole of one angular momentum channel. The CM has been extensively studied using traditional photoionization spectroscopy but the phase of the total transition dipole is not directly accessible, although it strongly influences the measured electron angular distribution and spin polarization. Consequently the Cooper minimum in argon became an excellent candidate for examining the viability of high harmonic spectroscopy.

In high harmonic generation (HHG) the inverse process of broadband PI takes place: an electron wave packet (EWP), promoted and accelerated in the continuum by an intense, optical pulse, returns to the core and gives rise to emission of XUV radiation through photo-recombination. The propagation of the EWP is determined by the laser wavelength and intensity while the recombination process has been shown to be independent of the laser. The EWP thereby acts as a self-probe of the laser-free complex recombination dipole matrix element (RDM). A measurement of the emitted XUV radiation can provide

access to both the amplitude and phase of the RDM and thus can be used to study structural features of the generating atom or molecule, and in particular the CM.

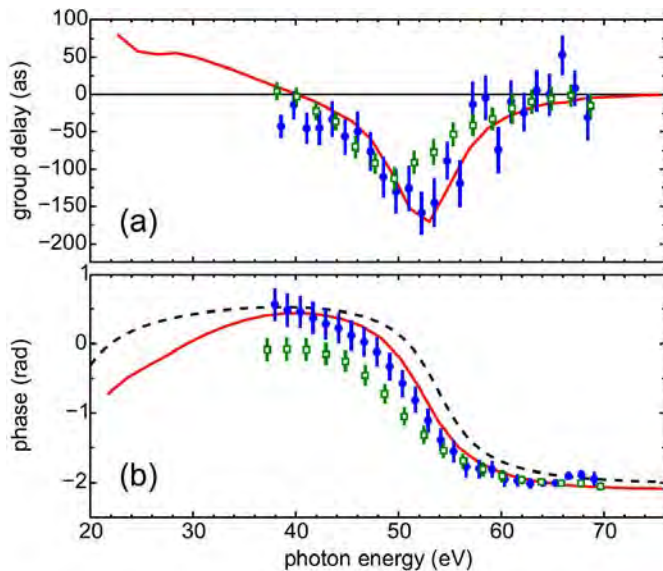


Figure 1: The group delay and phase near the Cooper minimum in argon. High harmonic radiation generated from argon atoms excited by 1.3 and 2 μm pulses are used in the measurements. The total RDM phase evolves by 1.8–2.6 radians over a 20 eV spectral range, even though the d-channel RDM undergoes a sharp π phase shift. The solid line results from calculations performed using the TDSE-MWE method (Gaarde and Schafer). The dashed line is calculated using a simple analytical model (see Ref. [2] for details).

We have investigated the phase modification in the high harmonic emission induced by the 3p Cooper minimum of argon, over a wide spectral range. In the experiment, the derivative of the spectral phase, the group delay (GD), is measured using the resolution of attosecond beating by interference of two-photon transitions (RABBITT) method. The measured RDM phase and amplitude agrees well with predictions based on the scattering phases and amplitudes of the interfering s- and d-channel contributions to the complementary photoionization process (see Fig. 1). The reconstructed attosecond bursts that underlie the HHG process show that the derivative of the RDM spectral phase, the group delay, does not have a straight-forward interpretation as an emission time, in contrast to the usual attochirp group delay. Instead, the rapid RDM phase variation caused by the CM reshapes the attosecond bursts. Most importantly, our results unequivocally establish that direct measurement of the RDM phase near a CM can be extracted from RABBITT. This lays

the foundation for future studies using high harmonic spectroscopy as a probe of atomic and molecular dynamics. This work was performed in collaboration with Profs. Ken Schafer and Mette Gaarde (LSU) and is published in PRL.

RABBITT measurement and the interpretation of the Wigner delay in photoionization.

Photoionization is the process by which an atom in a bound state absorbs a photon and makes a transition to a continuum state in which there is a finite probability to detect the electron at macroscopic distances from the nucleus. Photoionization can be regarded as a quantum jump, which occurs instantaneously at any moment in the field. While there is no such thing as a time operator in quantum mechanics, the delay in photoionization can be a quantum dynamical observable when it is understood as the temporal shift in the departure of the outgoing electron wave packet relative to the arrival of the XUV pulse or when it is treated as the energy-derivative of the time-dependent quantum phase. This is the so-called Wigner delay [3].

Photoionization by an XUV attosecond pulse train in the presence of an infrared pulse (RABBITT method) conveys information about the atomic photoionization delay. By taking the difference of the spectral delays between pairs of rare gases (Ar,He), (Kr,He) and (Ne,He) it is possible to eliminate in each case the larger group delay (“attochirp”) associated with the attosecond pulse train itself and obtain the Ar, Kr and Ne “effective” Wigner delays referenced to calculated He delay. As shown in Fig. 2, our extracted delays have been compared with several theoretical predictions and the results are consistent within 30 as over the energy range from 10-50 eV. Of particular interest are slight deviations which may be potential signatures of resonances. This work is accepted for publication in J. Phys. B.

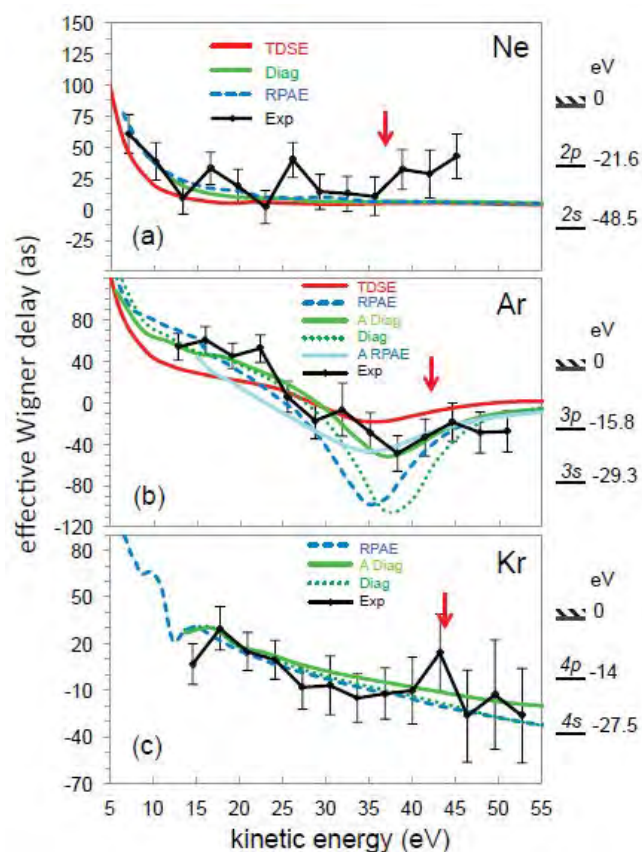


Figure 2: Comparison of the effective Wigner delay from experiment and theory for (a) neon, (b) argon and (c) krypton versus photoelectron kinetic energy, E_e . The photon energy is simply given as $E_p = E_e + I_p$, where I_p is the ionization potential and is 21.6 (Ne), 15.8 eV (Ar) and 14 eV (Kr). The TDSE-SAE calculation is from [4], Diag \equiv diagrammatic calculations from [5], “RPAE” from [6] and Exp \equiv experiment. The calculations shown with a “A” in the legend are angle-integrated. The red arrow in each marks the start of the region of helium doubly excited states. The valence subshell energy levels are shown for Ne, Ar and Kr.

the driver of the electron wave packet (EWP). Subsequent interaction of the EWP with the helium core will promote, among others, the $(e,2e)$ process. The requirement is that $3U_p \geq 54$ eV (He^+ ionization potential) and that the dressing field does not ionize helium. Simple estimates show that this is only possible with mid-infrared dressing fields. If successful, the tunnel simulator will allow exquisite control over the $(e,2e)$ process. We are currently evaluating the technical issues associated with this experiment.

Finally, we have been awarded LCLS time in March 2015. We will explore chemical sensitivity of Auger decay by observing Carbon 1s Auger electrons originating from CO, a simple diatomic molecule as well as from CF_4 , a more complicated yet symmetric system. The experiment will be time-resolved using a Streaking method proposed by our collaboration.

1.3 FUTURE PLANS

The following year we will continue to investigate the applications of high harmonic and attosecond spectroscopy. First, we have begun collaborating with Prof. Robert Jones on a project that aims at measuring the high harmonic group delay (GD) near and below threshold. In these experiments, attosecond pulses are generated in a suitable gas and the atom of interest is interrogated in our RABBITT apparatus. The quasi-classical model predicts the GD obtains a universal value of zero at threshold. However, the influence of the atomic potential cannot be neglected. This should be apparent in the experiment by comparing differences between atoms at fixed frequency. RABBITT measurements at low-energy are technically demanding and over the past year (Prof. Jones has visited the laboratory for 5 weeks) we have made significant progress in characterizing our photoelectron energy spectrometer’s transfer function at low-energy. Preliminary results have been obtained and are being analyzed.

Double ionization is a paradigm for understanding many-body effects. As part of our plans, we will use a tunneling simulator to time-resolved double ionization of helium atoms. In the experiment, attosecond pulses will photoionize helium above the 1e threshold (>24 eV) in the presence of an intense dressing field. The linearly polarized dressing field will quiver the electron in a manner similar to the step-2 in the rescattering model. In this scenario the attosecond photoionization replaces tunnel ionization in a strong low-frequency field while the dressing field acts as

1.4 REFERENCES CITED

- [1] J. W. Cooper, Phys. Rev. **128**, 681 (1962).
- [2] S.B. Schoun, R. Chirila, J. Wheeler, C. Roedig, P. Agostini, L.F. DiMauro, K.J. Schafer, and M.B. Gaarde, Phys. Rev. Lett. **112**, 153001 (2014).
- [3] E. P. Wigner, Phys. Rev. **98**, 145 (1955).
- [4] J. Mauritsson, M. B. Gaarde and K. J. Schafer, Phys. Rev. A **72**, 013401 (2005).
- [5] J. M. Dahlstrom, T. Carette and E. Lindroth, Phys. Rev. A **86**, 061402 (2012).
- [6] A. S. Keifets, Phys. Rev. A **87**, 063404 (2013).

1.5 PUBLICATION RESULTING FROM THIS GRANT FROM 2012-2014

“Measuring the temporal structure of few-femtosecond FEL X-ray pulses directly in the time domain”, W. Helml *et al.*, Nat. Photonics (2014), accepted.

“Atomic delay in helium, neon, argon and krypton”, C. Palatchi, J. Dahlstrom, A. S. Kheifets, I. A. Ivanov, D. M. Canaday, P. Agostini and L. F. DiMauro, J. Phys. B (2014), accepted.

“Attosecond Pulse Shaping around a Cooper Minimum”, S.B. Schoun, R. Chirila, J. Wheeler, C. Roedig, P. Agostini, L.F. DiMauro, K.J. Schafer, and M.B. Gaarde, Phys. Rev. Lett. **112**, 153001 (2014).

“Strong-field interactions at long wavelengths”, M. Kremer, C. I. Blaga, A. D. DiChiara, S. B. Schoun, P. Agostini, and L. F. DiMauro, in Attosecond and XUV Physics: Ultrafast Dynamics and Spectroscopy eds. T. Schultz and M. Vrakking (Wiley-VCH Verlag, Weinheim, 2014), Chapter 11.

“Ultra-fast and ultra-intense X-ray sciences: first results from the Linac Coherent Light Source free-electron laser”, C. Bostedt *et al.*, J. Phys. B **46**, 164003 (2013).

“Driving-frequency scaling of high harmonic quantum paths”, T. Auguste, F. Catoire, P. Agostini, L. F. DiMauro, C. C. Chirila, V. S. Yakovlev and P. Salieres, New J. Phys. **14**, 103014 (2012).

“Angle-resolved electron spectroscopy of laser-assisted Auger decay induced by a few-femtosecond x-ray pulse”, M. Meyer *et al.*, Phys. Rev. Lett. **108**, 063007 (2012).

“Scaling of high-order harmonic generation in the long wavelength limit of a strong laser field”, A. D. DiChiara *et al.*, IEEE J. Select. Topics Quan. Electro. **18**, 419 (2012).

“Atomic and molecular ionization in strong laser fields: from optical to x-rays”, P. Agostini and L. F. DiMauro, in Adv. In Atomic, Molecular and Optical Physics, vol. **61**, eds. E. Arimonda, P. R. Berman and C. C. Lin (Elsevier, Amsterdam, 2012), 118-158.

High Intensity Femtosecond XUV Pulse Interactions with Atomic Clusters

Project DE-FG02-03ER15406

Principal Investigator:
Todd Ditmire

Co-Investigator
John Keto

The Texas Center for High Intensity Laser Science
Department of Physics
University of Texas at Austin, MS C1600, Austin, TX 78712
Phone: 512-471-3296
e-mail: tditmire@physics.utexas.edu

Program Scope:

The nature of the interactions between high intensity infrared laser pulses and atomic clusters of a few hundred to a few thousand atoms have been well studied. Such studies have found that these interactions are more energetic than interactions with either single atoms or solid density plasmas and that the clusters explode with substantial energy. Under the previous phase of BES funding we extended investigation in this interesting area by undertaking a study of the interactions of intense extreme ultraviolet (XUV) pulses with atomic clusters, and more recently, interactions with intense x-ray pulses from the Linac Coherent Light Source (LCLS). Our current work builds on our previous work with a high harmonic (HHG) fs XUV source and seeks to study interactions at two orders of magnitude higher XUV intensity than we obtained in the last phase. This is being accomplished by upgrading our HHG beam line to much higher drive energies on the upgraded THOR laser. We also plan new target clusters, pulse-probe experiments and XUV fluorescence.

Our studies with XUV light are designed to illuminate the mechanisms for intense pulse interactions in the regime of high intensity but low ponderomotive energy by measurement of electron and ion spectra. This regime of interaction is very different from interactions of intense IR pulses with clusters where the laser ponderomotive potential is significantly greater than the binding potential of electrons in the cluster. We are now able to generate short wavelength pulses with up to 1 J of laser drive energy in a #100 focus which is 2.5 times that previously employed.

We have designed experiments using new targets to confirm our hypothesis about the origin of the high charge states [5] in these exploding clusters, an effect which we ascribed to plasma continuum lowering (ionization potential depression) in a cluster nanoplasma. This effect, which is well known in plasma physics, leads to a depression of the ionization potential enabling direct photo-ionization of ion charge states which would otherwise have ionization energies which are above the photon energy employed in the experiment. To do this we will perform experiments in which XUV pulses of carefully chosen wavelength irradiate clusters composed of only low-Z atoms and clusters with a mixture of this low-Z atom with higher Z atoms (eg. SiO₂ and SnO₂). Experiments on clusters from solids will be enabled by development during the past grant period in which we constructed and tested a cluster generator based on the Laser Ablation of Microparticles (LAM) method. Using a LAM device we will explore oxide clusters as well as metal clusters chosen such that the intense XUV pulse rests at a wavelength that coincides with the giant plasma resonance of the metallic cluster. The latter clusters will exhibit higher electron densities and will serve to lower the ionization potential further than in the clusters composed only of low Z atoms. This should have a significant effect on the charge states produced in the exploding cluster.

We will also explore the transition of explosions in these XUV irradiated clusters from hydrodynamic expansion to Coulomb explosion. We observed hints of this transition in our recent work on THOR in which we compared explosions of Xe and Ar clusters irradiated at 38 nm. The work to be performed with the upgraded beamline will explore clusters of a wide range of constituents, including not only clusters from gases (Xe, Ar, N₂, CH₄, and Xe doped CH₄) but also clusters from solids. In particular we are currently studying CH₄ and mixed Xe/CH₄ clusters to compare with previous studies at LCLS.[8]

Progress During the Past Year

Work during this past year has concentrated on optimizing the OPCPA in the upgraded THOR laser, optimization of HHG production in the new beam line, and testing of the new target chamber, and time-of-flight (TOF) detector.

In our past experiments on XUV irradiation of noble gas clusters we produced harmonic radiation by loosely focusing 40 fs pulses with a MgF $f\#60$ lens from our THOR Ti:sapphire laser into an Ar gas jet. These data showed that we were able to produce an $8\mu\text{m}$ spot dia. with the 38 nm pulse, yielding a focal intensity of $\sim 10^{11}$ W/cm² assuming an XUV pulse duration of 10 fs. These harmonics were then focused into the plume of a second, low density cluster jet. The main limitation of this apparatus was that the drive laser pulse energy was limited to ~ 60 mJ by the use of lens and focal geometry constrained by the lab space. This limited the XUV energy per pulse to ~ 0.5 nJ/pulse in the 21st harmonic.

We have now improved this beam line in new expanded lab space. This new beam line is illustrated in Figure 1. It is an all reflective design where the THOR laser sends its full energy (~ 1 J) loosely-focused ($f\#100$) into a gas jet to produce HHG of significant intensity. The XUV is sent to the interaction chamber where one of the harmonics is selected and focused using a Sc/Si mirror into gas



Figure 1: THOR XUV beamline spanning across two laboratory spaces.

clusters or nanoparticles for HED studies. Figure 2 shows a top view of the XUV beamline and the compressor chamber. The beamline is divided in three stages: 1- Focusing, 2- HHG, 3-XUV interaction. In the first stage the compressed 7.5 cm diameter beam is steered 90° in the focusing chamber, sent to a 0° mirror in the retro chamber. There, the beam reflects back onto a $f_l = 5.50$ m, concave spherical mirror that focuses the beam under a rectangular shaped (~ 0.5 mm x 5 mm) conical, gas jet in the HHG stage at fundamental intensities up to 3×10^{15} W/cm². The jet is moved upstream of the focus to keep the intensity near this transition for relativistic motion of quiver electrons. The angle of incidence in the focusing mirror is about 1° which makes spherical aberrations at focus negligible ($1/e^2$ spot diameter of $76\mu\text{m}$, 5.5 mm Rayleigh length). Two stages of differential pumping are used upstream of the harmonic nozzle to limit the pressure to below 10^{-5} Torr in the compressor. Three stages of differential pumping are used downstream to limit the pressures to less than 10^{-7} Torr. At a distance one focal length from the gas jet the fundamental and low harmonics are blocked and high harmonics sent to the XUV interaction chamber. A selected Sc/Si mirror picks a particular harmonic in the 10-60 nm range and focuses it on a gas jet.

Separation of the XUV pulses from the fundamental and low harmonics is done in a two-step process. Initially, the pulse before leaving the compressor goes through a 1 cm diameter mirror (reflective mask) in the center of the beam that creates a donut shape spatial beam profile. This disk is at approximately two focal lengths upstream from the focusing mirror and its image is located at two focal lengths. At this location, right before entering the interaction chamber, an aperture with the size of the circular disk blocks most of the infrared donut shape profile. The XUV, having a much shorter wavelength and divergence propagate through the center of the aperture with a small fraction of the fundamental light that was scattered by the gas jet. Following the aperture, a 200 nm aluminum foil (Luxel Corp.), with approximately 20-50% transmission in the XUV range blocks the remaining fundamental light and low harmonics. Optimization of the HHG yield is achieved by observing the harmonic spectrum using a grazing incident spectrograph with a multichannel plate detector, phosphor plate, and CCD camera. We first varied the location of the gas jet with respect to the laser focus at the maximum fundamental energy. A series of vacuum tubes with different length are swapped before or after the HHG chamber to produce the coarse

positioning (2nd steps) along the laser beam while a xyz-manipulator for the gas jet and translator for the focusing mirror provides fine adjustment. We optimized the HHG production as a function of jet pressure, x-y position of the jet relative to the focus, pulse width of the laser (optimum at minimum pulse width), and laser energy (optimum at maximum fundamental energy). Initially, we observed a 40 fs pulse width from the upgraded THOR laser. Because we found harmonic production peaked at shorter pulse widths, we spent several months optimizing the alignment of the OPCPA to produce 120 nm of bandwidth from the final TiSapphire amplifier. To increase the compressor throughput, we rotated the grating (now nearly 10 years old) by 180 degrees to improve reflectivity and with realignment achieved the current 25 fs pulse width. Using an XUV calibrated photodiode (AXUV100, Opto Diode Corp.) we measured the total energy on target in the 21st harmonic (38 nm) to be 10 nJ. This is a factor of 20 times greater than measured for the previous beam line (Ref. 5 below). Given adjacent, coherent 19th and 23rd harmonics we expect the overall XUV envelope in time ($\Delta t \sim 5$ fs) to be modulated, leading to peak intensities on the order of 10^{14} Wcm⁻². [5]

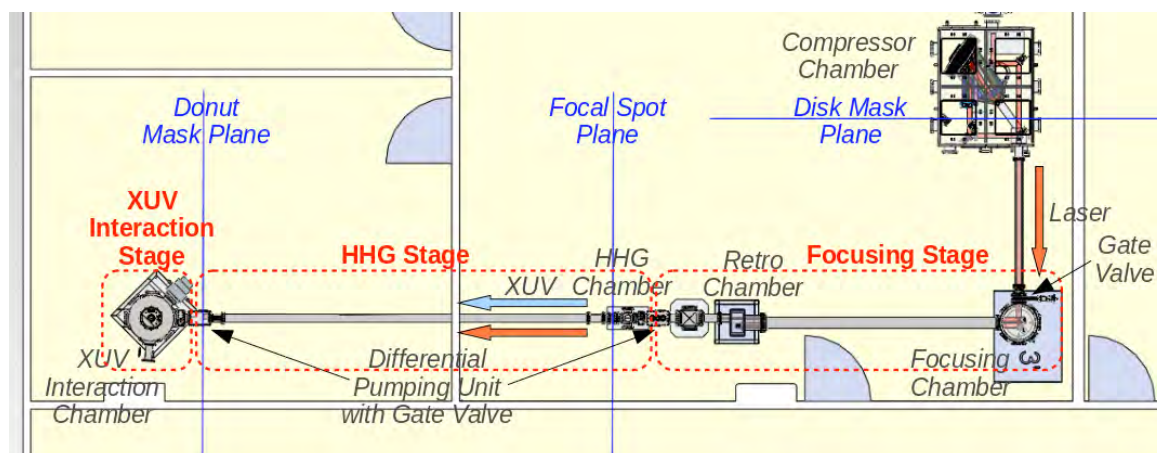


Fig. 2. Top view schematic of the new XUV beamline.

Explosion of CH₄ clusters and Xenon doped CH₄ clusters

We recently studied explosions of CH₄ mixed CH₄/Xe clusters (mean sizes up to 10⁵ molecules) using the x-ray, free-electron laser at LCLS at intensities approaching 10¹⁷ Wcm⁻². [7, 8, 9] For all of the clusters we studied, the interaction with the intense keV photons was dominated initially by single photon photo-ionization and by Auger emission following each inner-shell, photoionization event. The exit of electrons from the cluster successively built a positive charge on the surface until the space charge potential confined the photo- and Auger electrons. This charged surface of the cluster surrounds a quasi neutral plasma core whose temperature was determined by the photo- and Auger electron energies distributed over all the plasma electrons.[4] In methane clusters photoionization of the inner (1s²) shell of carbon is dominant since the photoionization cross section of H is three orders of magnitude smaller than C for 850 keV photons. Subsequent filling of the hole and Auger emission of valence-bond electrons results in the dissociation of hydrogen as protons, rather than an increased charge state of the carbon.

When the cluster size is increased, ion states formed within the cluster produced broadened peaks because ions emitted in the forward and backward directions relative to the TOF have different arrival times dependent upon the distribution in ion energy. Though ions with charge states up to C⁶⁺ are observed in molecular targets in our experiment, these peaks are not broadened in the TOF with increased cluster size, hence they are not produced significantly in clusters. To produce high charge states of carbon all of the protons must be removed from the molecule first, delaying their formation. We find strong peaks from CH₅⁺, C₂H₄⁺, and C₂H₉⁺ due to association of recoil protons and hydrocarbon ions with neutral molecules at the solid densities of the clusters. Again a neutrally charged plasma core is formed, and we find dissociative recombination plays an important role in the population of CH₅⁺ and larger molecules. The Coulomb explosion of the outer shell is dominated by protons because their expansion is more rapid than hydrocarbon ions because of their smaller mass. [8] The plasma core expands much more slowly, increasing the importance of electron-ion recombination.

For 3 fs laser pulses of 2 keV photons, we observed the smallest Coulomb explosion energies. For these pulses we expect fewer than 4% of the molecules to be ionized. While the production of CH_5^+ and larger molecules might be thought to disturb the possibility for x-ray diffraction imaging of the cluster, or comparably a biological molecule, molecular fragmentation occurs only after Auger emission (hole lifetime ~ 7.5 fs) and well after the end of the laser pulse. In effect the hollow molecule formed by the laser delays atomic motion that would distort imaging.

We also observed x-ray interactions with Xe doped Methane clusters, where the Xe doping concentration varied from 1% to 4%. One motivation for this experiment was the study of the interaction of LCLS x-rays with hydrocarbon molecules containing high Z atoms. Earlier simulations on this work showed that the addition of high Z atoms in the sample could accelerate the explosion of one set of species in the sample, while dampening the explosion of the rest of the ions [i]. We observe in Figure 3 that the addition of Xenon in Methane clusters, up to a concentration of 4%, generates higher energy protons as predicted. The Xe atoms are easily ionized to large charge states. Subsequent charge transfer from adjacent hydrogen atoms produces energetic protons. We are now completing similar experiments on the new HHG XUV line with the much lower photon energy

Future Research Plans

Our future plans involve studying continuum lowering in mixed species clusters. We have finished the construction of a micro-particle laser ablation beam to be installed on the beam line in Figure 2. This will allow us to study continuum lowering in mixed low and high Z clusters.

Refereed papers published or submitted on work supported by this grant during the past three years

- 1) W. Bang, M. Barbui, A. Bonasera, G. Dyer, H. J. Quevedo, K. Hagel, K. Schmidt, F. Consoli, R. De Angelis, P. Andreoli, E. Gaul, A. C. Bernstein, M. Donovan, M. Barbarino, S. Kimura, M. Mazzocco, J. Sura, J. B. Natowitz, and T. Ditmire, "Temperature Measurements of Fusion Plasmas Produced by Petawatt-Laser-Irradiated $\text{D}_2\text{-He}^3$ or $\text{CD}_4\text{-He}^3$ Clustering Gases" *Phys. Rev. Lett.* **111**, 055002 (2013).
- 2) W. Bang, G. Dyer, H. J. Quevedo, A. C. Bernstein, E. Gaul, M. Donovan, and T. Ditmire, "Optimization of the neutron yield in fusion plasmas produced by Coulomb explosions of deuterium clusters irradiated by a petawatt laser" *Phys. Rev. E* **87**, 023186 (2013).
- 3) W. Bang, H. J. Quevedo, G. Dyer, J. Rougk, I. Kim, M. McCormick, A. C. Bernstein, A. and T. Ditmire, "Calibration of the neutron detectors for the cluster fusion experiment on the Texas Petawatt Laser" *Rev. Sci. Instruments* **83**, 063504 (2012).
- 4) H. Thomas, N. Kandadai, K. Hoffmann, A. Helal, J. Keto, B. Iwan, N. Timneanu, J. Andreasson, M. Seibert, D. van der Spoel, J. Hajdu, S. Schorb, T. Gorkhover, D. Rupp, M. Adolph, T. Möller, G. Doumy, L.F. DiMauro, C. Bostedt, J. Bozek, M. Hoener, B. Murphy, N. Berrah and T. Ditmire "Explosions of Xe-clusters in ultra-intense femtosecond x-ray pulses from the LCLS X-ray Free Electron Laser" *Phys. Rev. Lett.* **108**, 133401 (2012).
- 5) K. Hoffmann, B. F. Murphy, N. Kandadai, B. Erk, A. Helal, J. Keto, and T. Ditmire, "Rare-gas-cluster explosions under irradiation by intense short XUV pulses" *Phys. Rev. A*, **83**, 043203 (2011).
- 6) B. Erk, K. Hoffmann, N. Kandadai, A. Helal, J. Keto, and T. Ditmire "Observation of shells in Coulomb explosions of rare-gas clusters" *Phys. Rev. A* **83**, 043201 (2011).
- 7) N. Timneanu, B. Iwan, J. Andreasson, M. Bergh, M. Seibert, C. Bostedt, S. Schorb, H. Thomas, D. Rupp, T. Gorkhover, M. Adolph, T. Möller, A. Helal, K. Hoffmann, N. Kandadai, J. Keto, T. Ditmire, "Fragmentation of clusters and recombination induced by intense ultrashort X-ray laser pulses," *Proc. SPIE Vol. 8777*, p. 87770J1-J7, (2013).
- 8) N. Kandadai, H. Thomas, K. Hoffmann, A. Helal, J. Keto, T. Ditmire, B. Iwan, N. Timneanu, J. Andreasson, M. Seibert, D. van der Spoel, J. Hajdu, S. Schorb, T. Gorkhover, D. Rupp, M. Adolph, T. Möller, G. Doumy, L.F. DiMauro, C. Bostedt, J. Bozek, M. Hoener, B. Murphy, N. Berrah, "Explosion of Methane clusters in ultra-intense femtosecond x-ray pulses from the free-electron-laser LCLS", to be published *Phys. Rev. Lett.*
- 9) N. Kandadai, et. al., "Explosion of Xe doped CH_4 clusters in intense femtosecond x-ray pulses", submitted *Phys. Rev. Lett.*

ⁱ Last, I. Schek and J. Jortner, *Energetics and Dynamics of Coulomb Explosion of Highly Charged Clusters*, *J.Chem.Phys.* 107, 6685 (1997).

Electron Correlation in Strong Radiation Fields

J. H. Eberly
University of Rochester, Rochester, NY 14627
eberly@pas.rochester.edu

Introduction

We are interested to understand how very intense laser pulses excite electrons in atoms and molecules, with intensities in the range $I \geq 0.1 \text{ PW/cm}^2$. The combination of phase-coherent character and short-time nature of laser pulses in experimental use creates substantial challenges to theoretical study in this domain. The intensities are high enough to mandate development of non-perturbative approaches. This has been done in several partially conflicting and partially overlapping theoretical methods. We have discussed the successes and listed the still-existing challenges in a recent review [1]. Challenging complications of great interest arise when more than one electron is dynamically active in response to the laser excitation, and here we briefly sketch a new approach to the so far barely examined question of the degree of purely quantum content in electron dynamical behavior.

Conditional Correlation, Quantum and Classical

Origin of correlation is both an intriguing and a fundamental question. Of course atomic ground states are highly correlated, but correlation developing during ionization is a different matter. Does it increase or decrease? Does it remain mostly quantum in character? The familiar strong-field recollision picture implies final-state correlation in non-sequential double ionization (NSDI), but to what degree is that correlation quantum in origin? Our calculations with elliptical polarization [2, 3, 4] led to collaboration [5] with an experimental demonstration and a conclusion that recollision is not the only mechanism that can lead to correlated electron emission in strong field double ionization.

One wants to have better quantitative insight into the quantum content of correlation during high-field ionization. Classical calculations via solution of the time-dependent Newton equations (TDNE) for very large ensembles of one-electron and two-electron atoms are known to give valuable insights in the form of electron and ion trajectories and collisions [6], but quantum correlation is embedded in wave function entanglement and is not available to classical particles or revealed in their trajectories.

We have begun to apply the powerful functional decomposition theorem of Erhard Schmidt [7] to two-particle wave functions. This will allow the systematic extraction of the non-classical aspects in the form of a degree of quantum content, effectively the degree of two-party quantum entanglement. Only this year the first report appeared of success in finding indirect evidence for “true” quantum effects in double ionization [8], but the degree of quantum content was not accessible. In effect, we will be addressing an open question that has been hiding in plain sight. Tools for using

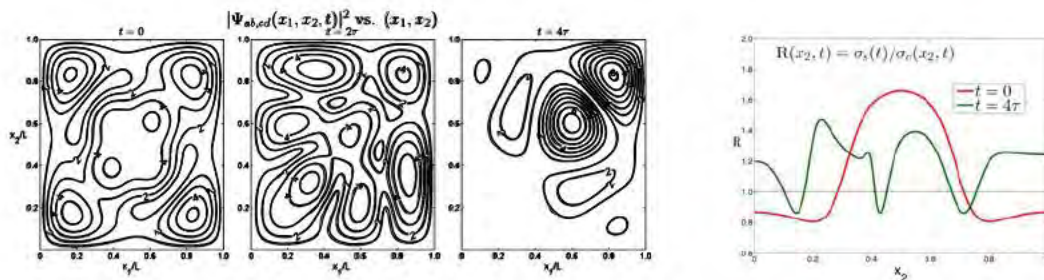


Figure 1: . Left group - Two-particle joint probability densities. Three snapshots of free-particle “flow” toward a nominal “joint ionization” in the form of concentrated two-particle density well removed from the center and near to one box wall. Right figure - Two curves showing the R parameter for the first and last snapshots.

the Schmidt theorem to reach the most useful answers need to be developed. For the answers to be properly interpreted and exploited it will help to have a dictionary of the most important theoretical terms with their connections to each other. Equally important, they must be connected to experimentally accessible counterparts, which we are beginning to develop.

Connection of Theory with Experiment

We know how the degree of entanglement residing in a two-party wave function can be quantified by the wave function’s Schmidt weight, usually written K . Entanglement is a conditional probability amplitude measure, and for two particles in a breakup process such as ionization or dissociation we have identified a conditional parameter that is experimentally measurable. A preliminary study of its connection to entanglement has been made [9]. This parameter, usually denoted R , is the ratio of two measurable standard deviations (in this case momentum):

$$K \approx R \equiv (\Delta p_1)/(\Delta p_1|_{p_2}), \quad (1)$$

where the denominator is the p_1 standard deviation conditioned on a given value for p_2 , the momentum of the other particle. Under conditions of two-party breakup (e.g., laser-driven ionization), R must be tested relative to the Schmidt weight K .

Our first step has been to examine highly simple, but entangled, two-party wave functions (particle-in-box type) to compare R values against known K values in cases where a “flow” within the box could model electron ejection into a specific direction. An example is shown in Fig. 1. The comparison of R with the known $K = 2$ is not good. A second test suggests that this is due to the artificiality of the closed-box context.

Double Ionization Test

Our second series of tests will engage actual ionization - emission of electrons into open-ended continua. We have begun with an experimentally familiar situation in which correlation connected to ionization is widely assumed to be present, non-sequential double ionization. Here TDNE analysis is already available for the standard soft-Coulomb model of helium [6], and we have extended this to calculation of R values using (1). The intensity range where the famous “knee” occurs in ion count data is of particular interest and the first results of R calculations are shown in Fig. 2. One sees that the peaks in the R value clearly occur in the same intensity range where the ion-count knee is seen. This confirms the role of R as a conditionality measure and provides nice support for

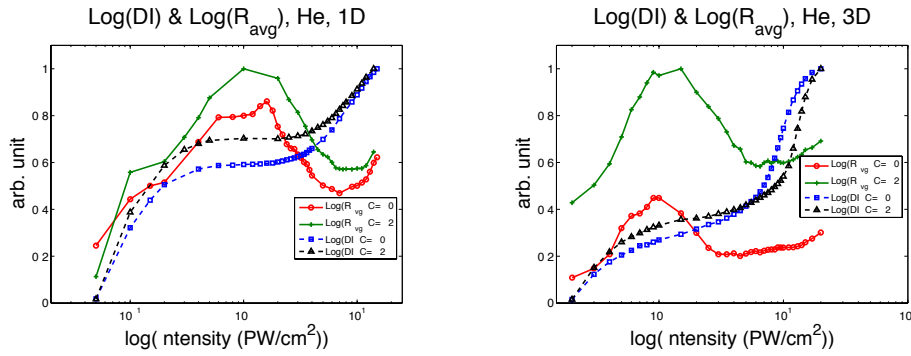


Figure 2: Log plots covering the intensity range for the NSDI knee, showing ion count data (triangles and squares) and the accompanying plots of R values over the same range. R is averaged over the values obtained for the momenta of actually-ionized electrons. It is clear that the R parameter peaks in the same range where the knee appears.

the universal conjecture that the knee arises from two-particle interaction. One also notes that there is semi-quantitative agreement about this conclusion between the one-dimensional (left panel) and full-dimensional (right panel) calculations. They are delivering the same message. The parameter C is a factor that multiplies the e-e interaction potential in the TDNE Hamiltonian. Its effect was also examined in the fully quantum entanglement calculation made more than a decade ago [10]. The R values here and the K values there are in acceptable agreement.

The citations of publications that were supported by DOE Grant DE-FG02-05ER15713 are marked with * in the listing below.**

References

- [1] ***W. Becker, X.J. Liu, P.J. Ho and J.H. Eberly, *Rev. Mod. Phys.* **84**, 1011 (2012).
- [2] ***Xu Wang and J.H. Eberly, *Phys. Rev. Lett.* **103**, 103007 (2009).
- [3] ***Xu Wang and J.H. Eberly, *Phys. Rev. Lett.* **105**, 083001 (2010). See also, ***Xu Wang and J.H. Eberly, *New J. Phys.* **12**, 093047 (2010).
- [4] ***X. Wang and J.H. Eberly, *J. Chem. Phys.* **137**, 22A542 (2012).
- [5] ***A.N. Pfeiffer, C. Cirelli, M. Smolarski, X. Wang, J.H. Eberly, R. Dörner, and U. Keller, *New J. Phys.* **13**, 093008 (2011).
- [6] Phay J. Ho, R. Panfili, S. L. Haan and J. H. Eberly, *Phys. Rev. Lett.* **94**, 093002 (2005). See also Phay J. Ho, *Phys. Rev. A* **74**, 045401 (2005), ***Phay J. Ho and J.H. Eberly, *Phys. Rev. Lett.* **95**, 193002 (2005), ***Phay J. Ho and J.H. Eberly, *Phys. Rev. Lett.* **97**, 083001 (2006), and ***S.L. Haan, L. Breen, A. Karim, and J. H. Eberly, *Phys. Rev. Lett.* **97**, 103008 (2006).
- [7] The original paper is: E. Schmidt, *Math. Ann.* **63**, 433 (1907). For background, see M.V. Fedorov and N.I. Miklin, *Contem. Phys.* **55**, 94 (2014).
- [8] X.L. Hao, J. Chen, W.D. Li, et al. *Phys. Rev. Lett.* **112**, 073002 (2014).
- [9] M.V. Fedorov, et al., *Phys. Rev. A* **69**, 052117 (2004).
- [10] W.-C. Liu, J.H. Eberly, S.L. Haan and R. Grobe, *Phys. Rev. Lett.* **83**, 520 (1999).

Page is intentionally blank.

Image Reconstruction Algorithms

Office of Basic Energy Sciences
Division of Chemical Sciences, Geosciences, and Biosciences
Program in Atomic, Molecular, and Optical Sciences

Veit Elser, Department of Physics
PSB 426, Cornell University
Ithaca, NY 14853
(607) 255-2340
ve10@cornell.edu
uuuuuu.lassp.cornell.edu

Program Scope

The many-orders-of-magnitude gains in X-ray brightness achieved by free-electron laser sources such as the LCLS are driving a fundamental review of the data analysis methods in X-ray science. It is not just a question of doing the old things faster and with greater precision, but doing things that previously would have been considered impossible. Our group at Cornell is working closely with experimental groups at LCLS and elsewhere to develop data analysis tools that exploit the full range of opportunities made possible by the new light sources. More recently we have begun collaborations with David Mueller's electron microscopy group and Sol Gruner's detector group, both at Cornell.

Ultra-low signal experiments

At the RACIRI 2014 Summer School [1] the PI presented a new "roadmap" to single-particle imaging that emphasizes the ultra-low-signal nature of the proposed experiments. The second item on this roadmap, tomographic imaging, had recently been achieved [2]. Our latest results (see Figure 1) address the third milestone of imaging a 3D crystal-diffraction pattern, and were also presented at RACIRI. We have already taken data for the next step in this program, where we propose to determine a protein structure from very sparse data frames. Processing of this data has been delayed as a result of unforeseen circumstances.

At every stage of the new roadmap we are challenging ourselves with the ultra-low signal levels in LCLS single-particle imaging experiment. While the latter is still what drives this research, we may have more impact in the short term on structural biology carried out at lower brightness synchrotron sources. Many of the most interesting targets (*e.g.* membrane proteins) form only micron sized crystals, from which high signal, "indexable" diffraction data can now be obtained at LCLS. But because our methods continue to work in the low-signal regime, the same quality of structure should be achievable at the far greater number of beam lines available at synchrotron sources.

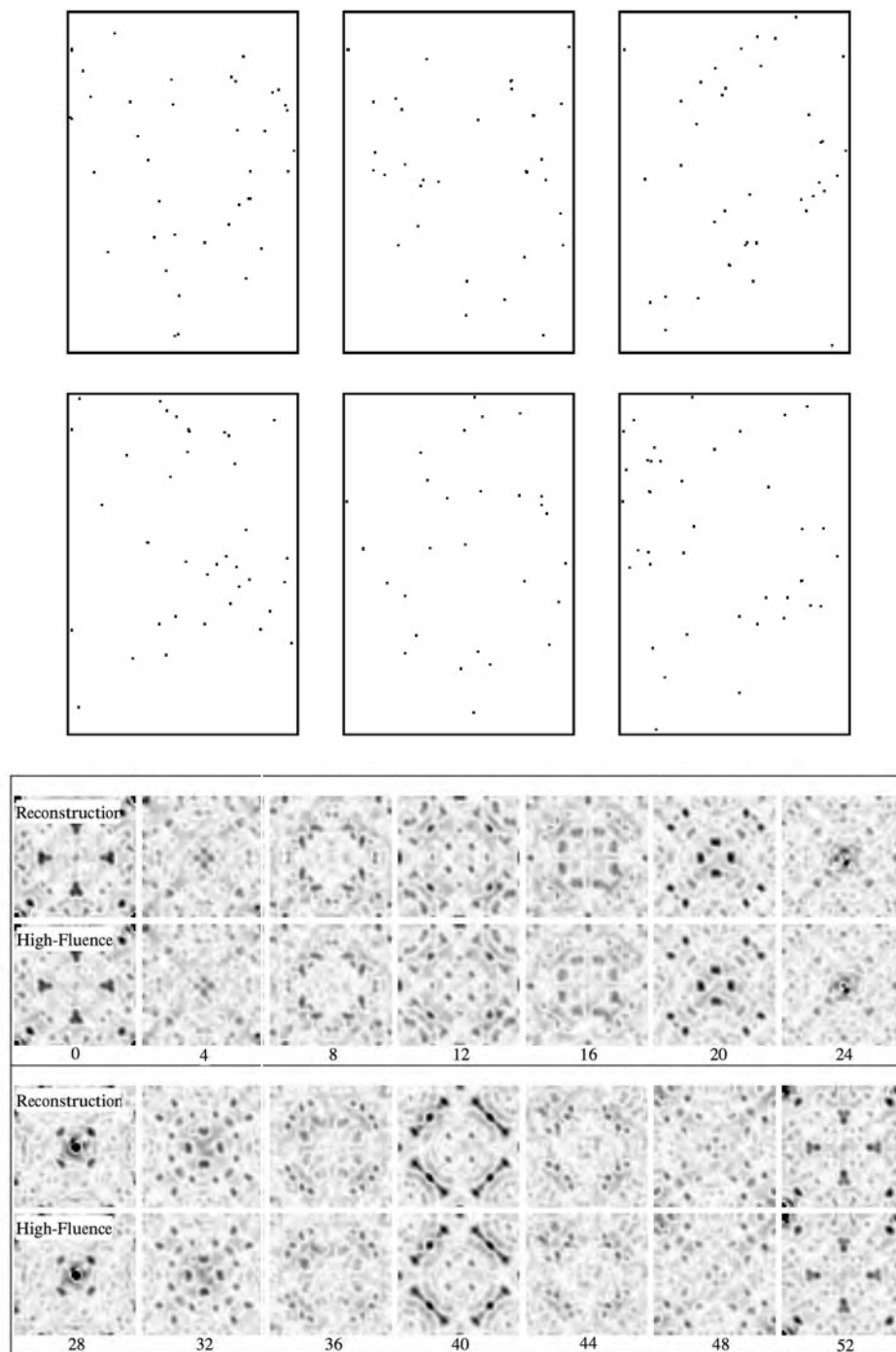


Figure 1: *Top*: Six diffraction data frames of a crystal in one orientation. At these ultra-low-signal levels there are no discernible Bragg peaks to help orient the frames. *Bottom*: Comparison of Patterson maps derived from the true 3D intensity and the intensity reconstructed from 290,000 low-signal data frames.

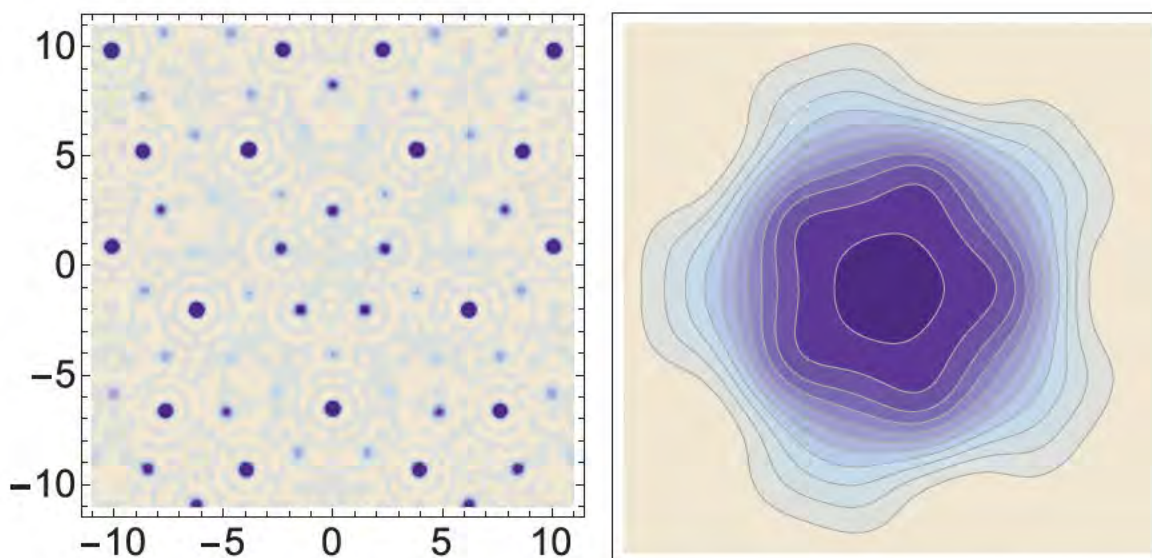


Figure 2: Phase reconstruction of AlCuRh quasicrystal diffraction data. *Left:* Electron density in a 5-fold plane of the decagonal quasicrystal. The very darkest and weakest spots correspond to Rh and Al atoms respectively. Intermediate density spots are Cu and Cu/Al mixed occupancy positions. *Right:* Phase reconstruction of the “superspace atomic surface”, a structure that encodes site occupancy in the quasicrystal more compactly than non-periodic density maps.

Phase reconstruction of quasicrystals

As part of the terms in accepting an invitation to speak on advances in phase reconstruction algorithms at the 2014 IUCr Congress and General Assembly, the PI requested a state-of-the-art quasicrystal diffraction data set from one of the organizers, Walter Steurer [4], to use as a demonstration of the PI’s phasing algorithm. The phase reconstruction proved to be quite easy and was accomplished on the PI’s laptop with Mathematica software written specifically for the lecture demonstration (see Figure 2). Because of the unexpected level of interest in the application of the phasing algorithm to these exotic materials, the PI was persuaded to write an article on the topic [5].

Other projects

Results on other projects reported last year have now been published: soot particle studies at LCLS [6], nanocrystal phasing [7].

References

- [1] V. Elser, *Imaging with few photons* (lecture), RACIRI 2014 Summer School: Imaging with X-Rays and Neutrons in Life and Materials Sciences, Stockholm,
- [2] K. Ayyer, H. T. Philipp, M. W. Tate, V. Elser & S. M. Gruner, *Real-space x-ray tomographic reconstruction of randomly oriented objects with sparse data frames*, Opt. Express **22** 2403 (2014).
- [3] K. Ayyer, H. T. Philipp, M. W. Tate, J. L. Wierman, V. Elser & S. M. Gruner, *Determination of crystallographic intensities from sparse data*, to be published in IUCrJ (2014).
- [4] P. Kuczera, J. Wolny & W. Steurer, *Comparative structural study of decagonal quasicrystals in the systems Al-Cu-Me (Me = Co, Rh, Ir)*, Acta Cryst. B **68** 578 (2012).
- [5] V. Elser, *Phase reconstruction of quasicrystal diffraction data*, to be published (2015).
- [6] H. J. Park *et al.*, *Toward unsupervised single-shot diffractive imaging of heterogeneous particles using X-ray free-electron lasers*, Opt. Express **21** 28729 (2013).
- [7] V. Elser, *Direct phasing of nanocrystal diffraction*, Acta Cryst. A **69** 559 (2013).

Collective Coulomb Excitations and Reaction Imaging

Department of Energy 2013-2014

James M Feagin

Department of Physics

California State University–Fullerton

Fullerton CA 92834

jfeagin@fullerton.edu

Quantum Imaging

In recent years we have seen enormous advances in atomic and molecular physics in the efficiency of many-particle coincidence detection of fragments produced in collisions or by laser light absorption. This progress has placed great demands on theory to develop methods to describe many-particle continua and to explain the plethora of data on multi-particle differential cross sections. The formal expression for the probability amplitude $T_f(t)$ at time t for occupation of a particular final state $\phi_f(t)$ arising from a collision complex described by an exact scattering state $\Psi(t)$ is simply the projection

$$T_f(t) = \langle \phi_f(t) | \Psi(t) \rangle. \quad (1)$$

It is readily shown that this amplitude is also given by

$$T_f(t) = -\frac{i}{\hbar} \int_{-\infty}^t \langle \phi_f(t') | V_f(t') | \Psi(t') \rangle dt', \quad (2)$$

which expresses the exact T-matrix element, where $V_f(t)$ is that part of the total Hamiltonian not diagonalized in the final state $\phi_f(t)$. Historically, almost all calculations of scattering processes have used this form of the T-matrix element (or its time-independent equivalent) as a starting point, since the exact form of $\Psi(t)$ is usually unknown and resort is made to approximations, e.g. Born series expansions of the integral form Eq. (2). More recently, increased computing power has enabled direct numerical evaluation of $\Psi(t)$ for many-particle fragmentation cross sections as pioneered by our colleagues in BES, including C. W. McCurdy and T. N. Rescigno,¹ and F. Robicheaux.² Then a projection of the measured final state at large times becomes a practical way of calculating fragmentation amplitudes according to Eq. (1). This approach has been recently reviewed by J. Macek.³

In calculations, usually the idealization that momentum can be measured to infinite accuracy is assumed. Then, for the simplest case of detection of a single particle in a momentum (planewave) eigenstate with a well defined wave vector \mathbf{k} , $\phi_f = |\mathbf{k}\rangle$, the exact scattering amplitude is given from Eq. (1) to within a phase factor by $T_{\mathbf{k}}(t) \propto \langle \mathbf{k} | \Psi(t) \rangle = \tilde{\Psi}(\mathbf{k}, t)$, where $\tilde{\Psi}(\mathbf{k}, t)$ is the momentum-space wavefunction (Fourier-transform) of the exact spatial scattering state. For the case of many-particle fragmentation, the difficulty with this asymptotic numerical projection onto momentum eigenstates is that a many-dimensional integral, often with strongly oscillatory phase factors, must be performed.

¹ W. Vanroose, F. Martin, T. N. Rescigno, and C. W. McCurdy, Phys. Rev. A **70**, 050703 (R) (2004); Science **310**, 1787 (2005).

² J. Colgan, M. S. Pindzola and F. Robicheaux, J. Phys. B: At. Mol. Opt. Phys. **37**, L377 (2004); Phys. Rev. Lett. **98**, 153001 (2007).

³ J. H. Macek in *Dynamical Processes in Atomic and Molecular Physics*, (Bentham Science Publishers, ebook.com, 2012), G. Ogurtsov and D. Doweck, eds.

A simple and effective solution that mostly circumvents this problem has emerged in recent years. The so-called³ *imaging theorem* (IT) establishes an asymptotic relation for macroscopic times $t \rightarrow \infty$ between the coordinate and momentum wavefunctions, $\Psi(\mathbf{r}_1, \mathbf{r}_2, \dots, t)$ and $\tilde{\Psi}(\mathbf{k}_1, \mathbf{k}_2, \dots, t)$, describing the many-particle state of an arbitrary fragmentation reaction. The relation rests upon the fact that detection is made at macroscopically large distances from the scattering center and leads via stationary phase to the classical connection among the coordinates and the momenta $\mathbf{r}_i = \hbar\mathbf{k}_i t / \mu_i \equiv \mathbf{v}_i t$ of each scattered fragment of mass μ_i . This important asymptotic relation was derived long ago by Kemble in his classic quantum text but perhaps has not been accorded the prominence it deserves in standard scattering theory. However it has been re-discovered in various guises over the intervening years and lately been employed independently by J. Macek, U. Thumm,⁴ and J. Eberly⁵ to efficiently extract scattering amplitudes from numerically-propagated wavefunctions.

Thus, the IT could provide an enormously practical method for extracting scattering amplitudes directly from the asymptotic form of numerically computed multidimensional coordinate wavefunction. Furthermore, the IT opens up the intriguing possibility of direct *experimental* imaging of collision wavefunctions via the measurement of the momentum distribution of the outgoing fragments. This is an aspect we have emphasized in a recent paper.⁶ In another recent paper,⁷ we have extended the IT to electric- and magnetic-field extraction and position-sensitive detection as widely used in cold-target recoil-ion momentum spectrometry (COLTRIMS) and related *reaction microscopes*.

Quantum Scattering, Classical Detection and Time

In another recent paper,⁸ our aim has been to reconcile the wholly quantum time-independent scattering theory with the introduction of position-sensitive detection and a classical time. Modern detector techniques rely more on position detection than energy or momentum detection and, despite the quantum nature of the theory, classical mechanics is used successfully to describe the extraction of charged particles and their passage from the microscopic reaction zone to the macroscopic detector.

At the core of our analysis are three features which are not usually found in text books on scattering theory. The first is the derivation of a wholly time-independent scattering theory for many-particle many-channel fragmentation processes as a direct generalization of the standard two-body single-channel potential scattering. Our derivation is based upon an old but largely neglected work of Gerjuoy.⁹ However, in contrast to Gerjuoy and to standard approaches, we derive the cross section directly in terms of a position measurement. Crucial to our argument is the demonstration that *classical* motion in the asymptotic region emerges naturally and allows a time variable to be defined from a time-independent theory.

The second new feature is to show that this time variable can be identified with the classical clock time of the detection apparatus, which leads to time-dependent expressions for quantum transition amplitudes. Time-dependent scattering theory, involving both time-independent and explicitly time-dependent interaction potentials, is shown to emerge from a time-independent theory in which the detector itself is treated first by quantum mechanics and then allowed to become macroscopically large and describable by time-dependent classical mechanics.

The third feature is to derive the multi-fragment generalization of the IT and emphasize an alternative point of view relevant to quantum imaging. Once the detector time is defined from *time-independent* scattering theory and macroscopic position detection, the IT follows

⁴ B. Feuerstein and U. Thumm, J. Phys. B: At. Mol. Opt. Phys. **36**, 707 (2003).

⁵ X. Wang, J. Tian, and J. H. Eberly, Phys. Rev. Lett. **110**, 243001 (2013).

⁶ J. S. Briggs and J. M. Feagin, J. Phys. B: At. Mol. Opt. Phys. **46**, 025202 (2013).

⁷ J. M. Feagin and J. S. Briggs, J. Phys. B: At. Mol. Opt. Phys. **47**, 115202 (2014).

⁸ J. S. Briggs and J. M. Feagin, Phys. Rev. A, submitted (2014).

⁹ E. Gerjuoy, Annals of Physics **5**, 58 (1958).

and shows that detection of fragments at different times and positions conforms to the classical Newton's equations *even when the particles still obey quantum mechanics*.

Collective Excitations in the Electron-Pair Continuum

Photo double ionization of molecular hydrogen shows a close similarity with the corresponding electron-pair angular distributions well established in helium, especially for relatively low-energy electron pairs.¹⁰ However, Gisselbrecht et al. identified equal-energy-sharing electron-pair configurations in the molecular fragmentation for which the helium-like description categorically fails.¹¹ Their observations were a follow-on to somewhat earlier experiments at the ALS by Th. Weber, A. Belkacem, and coworkers.¹²

In the molecular ground state, the electron-pair total angular momentum $\mathbf{L} = \mathbf{l}_1 + \mathbf{l}_2$ is not a good quantum number, so the helium-like dipole selection rule $^1S^e \rightarrow ^1P^o$ generalizes to $^1S^e, ^1P^e, ^1D^e, \dots \rightarrow ^1P^o, ^1D^o, ^1F^o, \dots$. One readily quantizes the rotations of an outgoing electron-pair momentum plane and constructs electron-pair *momentum* states $\tilde{\psi}_M^{(2S+1)L_\lambda}$ of definite $LS\pi^e$ symmetry for $L \geq 1$ in terms of symmetric-top wavefunctions $\tilde{D}_{Mm}^L(\hat{\mathbf{k}}_-)$ to describe rotations from a Lab frame with z axis along $\hat{\mathbf{z}}_L$ to an electron-pair body frame with z axis along $\hat{\mathbf{k}}_-$ defined by projections $\hbar\lambda \equiv \hbar|m| = \mathbf{L} \cdot \hat{\mathbf{k}}_-$ and $\hbar M = \mathbf{L} \cdot \hat{\mathbf{z}}_L$.

Thus we derived¹³ dipole-allowed states of the molecular electron-pair continuum. For the first two states for *equal-energy* sharing with $\mathbf{k}_+ \cdot \mathbf{k}_- = E_1 - E_2 = 0$, we find

$$\begin{aligned} \tilde{\psi}(^1P_1) &\sim a_{1\Pi 1} \sin\theta_N \hat{\mathbf{e}}_\Pi \cdot \mathbf{k}_+ + a_{1\Sigma 1} \cos\theta_N \hat{\mathbf{K}}_- \cdot \mathbf{k}_+, \\ \tilde{\psi}(^1D_1) &\sim a_{2\Pi 1} \sin\theta_N \left(\hat{\mathbf{e}}_\Pi \cdot \mathbf{k}_+ - 2\hat{\mathbf{K}}_- \cdot \hat{\mathbf{k}}_- \hat{\mathbf{y}}_M \cdot \hat{\mathbf{k}}_- \times \mathbf{k}_+ \right), \end{aligned} \quad (3)$$

where the $a_{L\Lambda\lambda}$ are undetermined dipole amplitudes describing the internal molecular dynamics with $\hbar\Lambda \equiv \hbar|M| = \mathbf{L} \cdot \hat{\mathbf{e}}$. Note, the polarization defines the Lab z axis, $\hat{\mathbf{z}}_L \equiv \hat{\mathbf{e}}$, and has been resolved along the molecular axes with $\hat{\mathbf{e}} \rightarrow \epsilon_\Pi + \epsilon_\Sigma \equiv \sin\theta_N \hat{\mathbf{e}}_\Pi + \cos\theta_N \hat{\mathbf{K}}_-$. We take the molecular frame z_M axis along $\hat{\mathbf{K}}_-$ with $\hat{\mathbf{z}}_M = \hat{\mathbf{K}}_- = \hat{\mathbf{e}}_\Sigma$ and $\hat{\mathbf{x}}_M = \hat{\mathbf{e}}_\Pi$, so that $\hat{\mathbf{y}}_M = \hat{\mathbf{K}}_- \times \hat{\mathbf{e}}_\Pi$.

One sees from Eq. (3) that the molecular continuum introduces a special axial-vector geometry $\mathbf{k}_- \times \mathbf{k}_+ = \mathbf{k}_1 \times \mathbf{k}_2$ into the momentum distribution of the outgoing electron pair not possible in atoms. In the molecule, the pseudo scalar $\hat{\mathbf{y}}_M \cdot \hat{\mathbf{k}}_- \times \mathbf{k}_+$ arises with respect to reflections in the $\hat{\mathbf{e}}_\Sigma, \hat{\mathbf{K}}_-$ plane. We find that these special distributions can be isolated by fixing $\hat{\mathbf{K}}_- \perp \hat{\mathbf{e}}$ while selecting electron pairs with $\mathbf{k}_+ \perp \hat{\mathbf{e}}$, thereby reducing the electron-pair momentum distribution to $\tilde{\psi}(^1P_1 + ^1D_1 + ^1F_1) \sim \hat{\mathbf{K}}_- \cdot \hat{\mathbf{k}}_- \hat{\mathbf{y}}_M \cdot \hat{\mathbf{k}}_- \times \mathbf{k}_+$ where now $\hat{\mathbf{y}}_M \equiv \hat{\mathbf{K}}_- \times \hat{\mathbf{e}}$. The photo double ionization cross section is proportional to the square of this result. Thus we confirmed¹³ this unique ‘axial-vector’ distribution in the close-coupling calculations of J. Colgan, although it proved elusive in the measured data.

However, this past summer A. Huetz (private communication, Orsay) has reexamined his data as a function θ_2 for $\theta_1 \sim \pi - \theta_2$ and integrated them over electronic azimuthal angles and *all* molecular-axis orientations to enhance statistics. Remarkably, he finds an intensified four-lobe structure in this new integrated cross section. To begin to understand his findings, we have combined the 1P_1 and 1D_1 contributions from Eq. (3) and integrated the resulting wavefunction squared. Setting $\theta_1 = \pi - \theta_2$, we obtain

$$\int |\tilde{\psi}(^1P_1 + ^1D_1)|^2 \sin\theta_N d\theta_N d\phi_1 d\phi_2 \sim \cos^2\theta_2 \sin^4\theta_2 + |r_\Sigma - r_\Pi + \cos 2\theta_2|^2 \sin^2\theta_2, \quad (4)$$

¹⁰ T. J. Reddish and J. M. Feagin, J. Phys. B: At. Mol. Opt. Phys. **32**, 2473 (1999); J. M. Feagin, J. Phys. B: At. Mol. Opt. Phys. **31**, L729 (1998).

¹¹ M. Gisselbrecht et al., Phys. Rev. Lett. **96**, 153001 (2006).

¹² Th. Weber et al., Nature (London) **431**, 437 (2004).

¹³ J. M. Feagin, J. Colgan, A. Huetz, and T. J. Reddish, Phys. Rev. Lett. **103**, 033002 (2009).

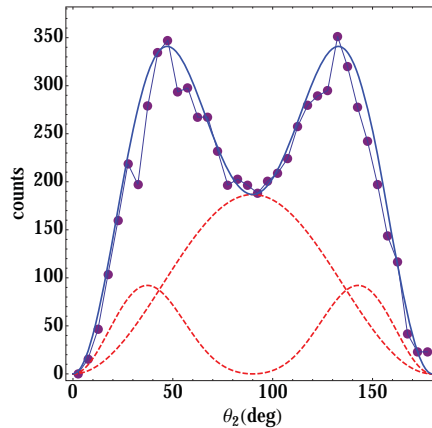


FIG. 1: Photo double ionization data for molecular hydrogen as a function of θ_2 of one outgoing electron and $\theta_1 = \pi - \theta_2$ of the other integrated over electronic azimuthal angles and molecular-axis orientations to enhance statistics. The blue curve is a fit from Eq. (4) arbitrarily scaled with $r_\Sigma - r_\Pi = 2.15$. The red dashed curve with a node at $\theta_2 = \pi/2$ is the pseudo-scalar contribution to Eq. (3), while the red dashed curve with an antinode at $\theta_2 = \pi/2$ is the helium-like contribution to Eq. (3).

where $r_\Sigma \equiv a_{1\Sigma 1}/a_{2\Pi 1}$ and $r_\Pi \equiv a_{1\Pi 1}/a_{2\Pi 1}$. Here the first term arises solely from the pseudo-scalar molecular contribution and has a node at $\theta_2 = \pi/2$, while the second term arises from the remaining $\hat{\mathbf{e}}_\Pi \cdot \mathbf{k}_+$ and $\hat{\mathbf{K}}_- \cdot \mathbf{k}_+$ contributions to Eq. (3), which fill in the node at $\theta_2 = \pi/2$. This second term represents non-molecular atom-like contributions. If helium were used as target the corresponding cross section would be proportional to $\int |\tilde{\psi}({}^1P) + {}^1D_1|^2 d\phi_1 d\phi_2 \sim \sin^2 \theta_2$.

Fig. 1 shows a preliminary comparison of $|\tilde{\psi}({}^1P_1 + {}^1D_1)|^2$ from Eq. (3) integrated over electron azimuthal angles and molecular-axis orientations from Eq. (4). (Of course, the four-lobes manifest themselves in the polar plot for $0 \leq \theta_2 \leq 2\pi$. The cross section is symmetric about $\theta_2 = \pi$.) We find the result an encouraging step towards the first verification of a pseudo scalar contribution to the electron-pair molecular ionization continuum.

Recent Relevant Publications

Scattering Theory, Multi-Particle Detection and Time, J. S. Briggs and J. M. Feagin, Phys. Rev. A, submitted (2014).

Reaction Imaging in Uniform Electric and Magnetic Fields, J. M. Feagin and J. S. Briggs, J. Phys. B: At. Mol. Opt. Phys. **47**, 115202 (2014).

Momentum and Spatial Imaging of Multi-Fragment Dissociation Reactions, J. S. Briggs and J. M. Feagin, J. Phys. B: At. Mol. Opt. Phys. **46**, 025202 (2013).

Loss of Wavepacket Coherence in Stationary Scattering Experiments, J. M. Feagin and L. Hargreaves, Phys. Rev. A **88**, 032705 (2013).

Vortex Kinematics of a Continuum Electron Pair, J. M. Feagin, J. Phys. B: At. Mol. Opt. Phys. **44**, 011001 (2011).

Electron-Pair Excitations and the Molecular Coulomb Continuum, J. M. Feagin, J. Colgan, A. Huetz, and T. J. Reddish, Phys. Rev. Lett. **103**, 033002 (2009).

Transient Absorption and Reshaping of Ultrafast Radiation

DE-FG02-13ER16403

Kenneth J. Schafer (schafer@phys.lsu.edu)

Mette B. Gaarde (gaarde@physics.lsu.edu)

Department of Physics and Astronomy, Louisiana State University

Baton Rouge, LA 70803

September 15, 2014

Program Scope

Our program is centered around the theoretical study of transient absorption of ultrafast extreme ultraviolet (EUV) radiation by atoms and materials interacting with a precisely synchronized near-to-mid infrared (IR) laser pulse. Transient absorption spectroscopy can in principle provide high spectral resolution and high (attosecond) time resolution simultaneously, by spectrally resolving the light transmitted through a sample as a function of delay between the dressing laser pulse and the broadband attosecond EUV probe. As in all transient absorption calculations/measurements, one of the main challenges we confront is the extraction of time-dependent dynamics from delay-dependent information. In addition, we must also account for the reshaping of the broadband XUV light in the macroscopic medium. We study attosecond transient absorption (ATA) using a versatile theoretical treatment that takes account of both the strong laser-atom interaction at the atomic level via the time-dependent Schrodinger equation (TDSE), as well as propagation of the emitted radiation in the non-linear medium via the Maxwell wave equation (MWE), in the single-active electron (SAE) approximation up to now [1]. We are extending our SAE treatment in atoms to fully-active two electron calculations in helium, in both full and reduced dimensions.

Research Projects

We briefly summarize the results of four collaborations with experimental groups carrying out attosecond transient absorption measurements.

Interference between multiple electronic states in attosecond transient absorption in neon

In collaboration with the experimental group of Prof.s S. Leone and D. Neumark at UC Berkeley, the transient absorption of an isolated attosecond pulse (IAP) in an IR-dressed neon gas is studied. The transient absorption spectra show broadband excitation of a range of states below and above the first Ne ionization threshold. Additionally, several of the lines show oscillations with characteristic periods as a function of delay between the IAP and the IR laser when the IAP comes first. In particular, the spin-orbit split $3d$ lines ($J = 1/2$ and $3/2$) exhibit a 40 fs oscillation period, corresponding to their energy separation of approximately 0.1 eV. For this project, in order to include effects of the spin-orbit splitting of the ion core, we solved the TDSE using a basis of states and dipole coupling matrix elements that we had predetermined using the GRASP package which solves the multi-configuration Dirac-Fock equation. We also modeled the transient absorption spectra using few-level essential states models, which uncovered two different scenarios for the origin of the oscillations – one involving coherent interaction of the two $3d$ states, and one involving only incoherent processes. A manuscript detailing our results is under review.

Macroscopic effects in APT transient absorption

In collaboration with the group of Prof. A. Sandhu at the University of Arizona, Tuscon, we are exploring macroscopic propagation effects in the absorption of attosecond pulse trains (APTs) by IR-laser-dressed He

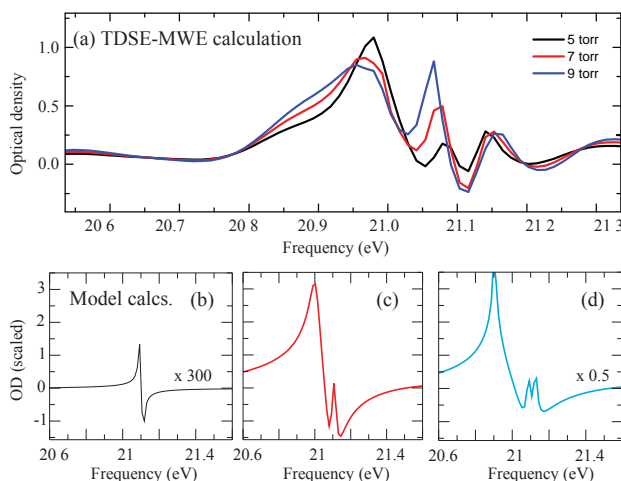


Figure 1: (a) TDSE-MWE calculations of attosecond transient absorption in helium near the $1s2p$ resonance for different gas pressures. (b-d) Model calculations of the transient absorption in this system demonstrating how new spectral features appear. (b) and (c) are calculated at the beginning and the end of the medium, (d) is calculated at the end of the medium for a higher pressure, when a second new feature has appeared.

atoms. Since transient absorption experiments must measure a non-zero (usually substantial) amount of absorption, it is important to understand the absorption lineshape beyond the single atom response, and in particular the interplay of microscopic and macroscopic effects.

Our experimental and theoretical results show that increasing the He pressure generally leads to a broadening of the IR-modified absorption line shape as well as induces new, narrow peaks in the center of the line. This can be seen in Fig. 1(a) which shows the optical density in the vicinity of the helium $1s2p$ absorption line, calculated within our full TDSE-MWE framework, at the end of a 1 mm long gas cell with a varying gas density. The overall dispersive line shape is caused by the perturbation due to the IR field, which adds an extra phase onto the time-dependent polarization field [2, 3], and the line shape is seen to broaden as the pressure increases. However, the detailed line shape is complicated, with additional, narrow features that first appear on line center when the pressure reaches approximately 4 Torr and then move outward with increasing pressure. Figs 1(b-d) show results of a simpler TDSE-MWE calculation, in which the TDSE is solved as a two-level system which is resonant with an attosecond pulse, and where the IR perturbation is modeled as a simple, time-dependent phase. Fig. 1(b) and (c) shows the optical density (OD) at the beginning and end of a medium in which the pressure is just high enough to induce one extra spectral feature. Fig. 1(d) shows the OD at the end of a medium with a higher pressure, in which a second new feature has appeared. We find that the appearance of these new features is caused by the propagation-induced temporal reshaping of the short XUV pulse in the He gas which has narrow-band resonances. The long-lived time-dependent polarization induced in such a medium causes the attosecond XUV pulse to develop a tail in the time-domain, consisting of one or several sub-pulses. These sub-pulses cause both the broadening of the absorption line shape and the appearance of new features. A paper detailing these results will be submitted shortly.

Using multiphoton absorption as a calibration of delay-zero in attosecond spectroscopy

In collaboration with the group of Prof. U. Keller and Dr. L. Gallmann at the ETH in Zurich, Switzerland, we address the question of finding “zero delay” between IR and XUV pulses in an ATA experiment, a quantity that has not been directly measured before. The determination of zero delay relates directly to the phases of wave packet components excited by an XUV pulse. We find that when using an attosecond pulse train in combination with an IR probe pulse, the quarter-cycle (4ω) oscillations in the absorption spectrum are a reliable way to find the overlap between the XUV pulse and the peak of the IR envelope. We have used TDSE calculations in parallel with macroscopic propagation calculations to delineate the conditions under

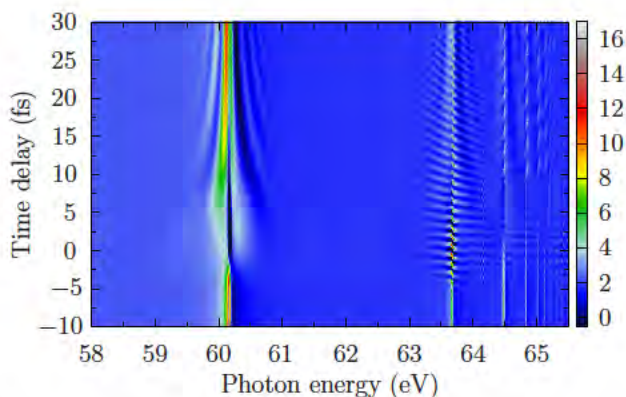


Figure 2: Fully-active two electron calculation of helium single atom transient absorption spectrum near the $sp_{2,n}^+$ resonance series. The 500 as XUV pulse has a central frequency 60 eV (near the $sp_{2,2}^+$ resonance) and a bandwidth of ≈ 4 eV. The IR pulse has a central frequency of 1.7 eV (730 nm) and a FWHM duration of 7.3 fs and a peak intensity of 3.5 TW/cm^2 .

which this *in situ* measurement can be expected to be reliable. This is an example of using a high-order non-linearity to achieve increased temporal precision. A manuscript detailing our results is under review.

Polarization-control of absorption of virtual dressed-states in helium

This project is in collaboration with the experimental group of Prof. G. Sansone at Politecnico Milan, Italy. We have explored the dependence of XUV absorption on the relative polarizations of an isolated attosecond pulse (IAP) and an IR pulse. We find that when the polarization between the two pulses is rotated, the light-induced features in the transient absorption spectrum are strongly modified or even eliminated altogether in some cases. This work demonstrates that the pump-probe polarization (parallel, perpendicular, or something in between) can be used to selectively turn on and off the transient processes that lead to two photon (phase sensitive Raman-like) population transfer in laser-dressed systems. In this work we have used a restricted excitation model which allows for an efficient solution of this three dimensional problem using a two dimensional grid. A manuscript detailing these results is under review.

Future directions

Transient absorption in multi-electron systems

Recently, Dr. Xiaoxu Guan (formerly of Drake University) has joined our group and initiated a program in the study of transient absorption in multi-electron systems. Dr. Guan has developed an ab-initio two-electron TDSE solver for He atoms interacting with electromagnetic fields that he has adapted to calculate absorption. We are currently exploring transient absorption around the low-lying autoionizing resonances in helium. The modification of these (Fano-like) resonance features by an IR dressing field was the subject of a *Science* paper by T. Pfeifer’s group last year [2]. Fig. 2 shows a full two electron active (five dimensional) calculation of the single atom transient absorption in helium for conditions matching those in the experiment. The Autler-Townes-like splitting of the $sp_{2,2}^+$ line near 60 eV results from an almost-resonant two photon coupling to the $sp_{2,3}^+$ state, aided by a “dark state” (the $2p^2(1S)$) that is intermediate between the two. We hope to connect these calculations to work that we have done using transient absorption to study Autler-Townes splitting from a time-domain perspective in a single electron context [4]. Of course true two-electron calculations (in at least five spatial dimensions) are very expensive and so we have also initiated a program, led by a new post-doc, Dr. R. Pazourek, to study lower-dimensional models of two electron systems. We hope to couple these reduced-dimension helium model calculations to the MWE solver to study propagation effects around auto ionizing resonances.

Cited publications

1. M. B. Gaarde *et al.*, Phys. Rev. A **82**, 023401 (2011).
2. C. Ott, *et al.* Science **340** 716 (2013).
3. S. Chen *et al.*, Phys. Rev. A **87**, 013828 (2013).
4. M. Wu *et al.*, Phys. Rev. A **88** 043416 (2013).

Publications supported by this grant, under review:

- A. R. Beck, B. Bernhardt, E. R. Warrick, M. Wu, S. Chen, M. B. Gaarde, K. J. Schafer, D. M. Neumark, and S. R. Leone, *Attosecond transient absorption probing of electronic superpositions of bound states in neon: detecting quantum beats by laser coupling of individual states*, submitted (2014).
- J. Herrmann, M. Lucchini, A. Ludwig, L. Kasmi, L. Gallmann, S. Chen, M. Wu, K. J. Schafer, M. B. Gaarde, and U. Keller, *Multiphoton transitions for delay-zero calibration in attosecond spectroscopy*, submitted (2014).
- M. Reduzzi, J. Hummert, A. Dubrouil, F. Calegari, M. Nisoli, F. Frassetto, L. Poletto, S. Chen, M. Wu, M. B. Gaarde, K. J. Schafer, G. Sansone, *Polarization-control of absorption of virtual dressed-states in helium*, submitted (2014).
- C.-T. Liao, A. Sandhu, S. Camp, K. J. Schafer, and M. B. Gaarde, *Macroscopic propagation effects in absorption lineshapes: Probing dense, laser-dressed Helium with XUV attosecond pulse trains*, to be submitted (2014).

Studies of Autoionizing States Relevant to Dielectronic Recombination

T.F. Gallagher
 Department of Physics
 University of Virginia
 P.O. Box 400714
 Charlottesville, VA 22904-4714
 tfg@virginia.edu

In this research program we have studied doubly excited autoionizing atomic states, the effects of intense low frequency radiation on atomic photoionization, and the high angular momentum bound states of alkaline earth atoms. The systematic study of autoionization has provided us with valuable insight into the reverse process, dielectronic recombination (DR), the recombination of ions and electrons via intermediate autoionizing states. DR's importance is that it provides an efficient recombination mechanism for ions and electrons in astrophysical and laboratory plasmas.¹⁻⁴ In fusion plasmas impurity ions from the wall of the containment vessel capture electrons and radiate power from the plasma, negating efforts to heat the plasma. The most important pathway for DR is through the autoionizing Rydberg states converging to the lowest lying excited states of the parent ion, because of their rapid radiative decay to bound states. Because Rydberg states are involved, DR rates are profoundly influenced by other charged particle collision processes and any small electric and magnetic fields in the plasma.^{5,6} Consequently, a major thrust of this program has been understanding how autoionization rates, and thus DR rates, are affected by external fields. This understanding is broadly useful since DR exhibits similar physics to that found in other contexts, notably zero kinetic energy electron (ZEKE) spectroscopy,⁷ dissociative recombination,⁸ and fluorescence yield spectroscopy.⁹ The isolated core excitation (ICE) method we have used to study autoionizing states also provides a new tool for the spectroscopy of the bound high angular momentum states of alkaline earth atoms. To be specific, it allows us to detect transitions between them. From their energy separations one can determine the polarizabilities and radial matrix elements of the ionic cores.¹⁰⁻¹³ The polarizabilities are important in determining the blackbody frequency shifts of trapped ion based clocks and for parity nonconservation measurements.¹⁴

We originally used a microwave field to mimic the rapidly varying fields which occur in electron collisions with atoms, but the experiments are, in essence, laser photoionization of atoms in the presence of a strong microwave field. An atom in a strong microwave field exposed to visible radiation is very similar to an atom in an intense infrared field exposed to a train of attosecond xuv pulses, a problem under investigation by many research groups.¹⁵⁻¹⁹ More generally, a microwave field strong enough to ionize atoms leaves atoms in highly excited states, a phenomenon also observed in recent laser ionization experiments.²⁰

During the past year we have worked on several projects. First, we have used a novel technique to detect microwave transitions between high angular momentum states of Ba. Specifically, we detected the microwave $\Delta\ell$ transitions using isolated core excitation (ICE), in which the core electron is optically excited while the Rydberg electron remains a spectator.²¹ In Ba the ICE transition from the bound $6sn\ell$ state to the autoionizing $6p_{1/2}n\ell$ state has an optical

cross section which increases by a factor of five for each increase in ℓ of one,²² and we used this difference in the cross sections to detect the 6sng-6sn ℓ microwave transitions for $\ell > 4$. Using this technique, we have measured the Ba 6sng-6snh-6sni-6snk intervals for $15 \leq n \leq 18$. Using our data and the high ℓ data of Snow and Lundeen²³ we extracted new values for the dipole and quadrupole polarizabilities, $\alpha_d = 124.81(25) a_0^3$ and $\alpha_q = 2613(24) a_0^5$, respectively. Our value for α_d is in reasonable agreement with recent experimental determinations and calculations.^{23,24} In contrast, our value for α_q is roughly half the values of both other recent experiments and calculations.^{6,7} A most interesting point is that the discrepancy between the experimental numbers exists not because of a difference in the experimental data but a difference in the method of analysis, in particular, how the non adiabatic effects are taken into account. We are currently in the process of isolating the source of the difference.

The Ca^+ ion is particularly interesting for clock applications, and we have completed analogous microwave resonance measurements of the Ca 4snf-4sng-4snh-4sni-4snk intervals. In this case we have used the fact that the lifetimes of the higher ℓ states are longer than the lifetimes of the 4snf states to detect the 4snf-4sn ℓ microwave transitions. Using the same approach we used for Ba, we have obtained the values $\alpha_d = 80.0(1) a_0^3$ and $\alpha_q = 228(12) a_0^5$. Our value for the dipole polarizability is much closer to the theoretical value than the previous measurement,^{25,26} but α_q is half the theoretical value,²⁶ just as in Ba. The theoretical value for α_q is in agreement with measurements of the Ca^+ 3d lifetimes, so it appears to be correct. These Ba and Ca measurements indicate that the core polarization models need to be re-examined; something appears to be missing. In addition to trying to determine the source of the discrepancy between our values of the quadrupole polarizabilities and the calculated ones, we are recording the spectra of the Ca 4s20k Stark states in very low fields, less than 10 V/cm, in the hope of determining the quantum defects of the high ℓ 4sn ℓ states. If we are able to determine their quantum defects, we can extract the polarizabilities with less uncertainty due to the non adiabatic effects.

We have finished the construction of an experiment to excite Li atoms in the presence of a strong microwave field phase locked to an amplitude modulated laser field. This experiment is motivated by experiments done with a combined xuv attosecond pulse train (APT) and infrared laser field^{15,16} and our experiments in which we excited atoms in a microwave field phase locked to a mode locked laser producing ps pulses^{27,28}. In these experiments the sign and the amount of energy transfer to the electron produced by the xuv or ps laser pulse was dependent on the phase of the low frequency field at which the laser excitation occurred.^{15,16,27,28} According to the theoretical analysis, the coherent effect of the multiple pulses in the APT is important.¹⁵ In our experiments with a single ps pulse we observed a markedly smaller phase dependence, perhaps due to the absence of coherence over multiple microwave cycles, as earlier asserted.¹⁵ In the present experiment we produce the amplitude modulation, at 26 GHz, by combining the beams from two 819 nm diode lasers with frequencies 26 GHz apart. We have phase locked the 26 GHz beat note between the two 819 nm lasers to the second harmonic of a 13 GHz microwave oscillator which provides the microwave field in the Fabry-Perot cavity in which the atoms are excited by the laser. We have amplified the amplitude modulated beam in a tapered amplifier and

a dye amplifier, and we are now in the process of minimizing the stray fields in the apparatus. We are ready to search for a phase dependent signal.

References

1. A. Burgess, *Astrophys. J.* **139**, 776 (1964).
2. A.L. Merts, R.D. Cowan, and N.H. Magee, Jr., Los Alamos Report No. LA-62200-MS (1976).
3. S. B. Kraemer, G. J. Ferland, and J. R. Gabel, *Astrophys. J.* **604** 556 (2004).
4. N. R. Badnell, M. G. O'Mullane, H. P. Summers, Z. Altun, M. A. Bautista, J. Colgan, T. W. Gorczyca, D. M. Mitnik, M. S. Pindzola, and O. Zatsarinny, *Astronomy and Astrophysics*, **406**, 1151 (2003).
5. A. Burgess and H. P. Summers, *Astrophysical Journal* **157**, 1007 (1969).
6. V. L. Jacobs, J. L. Davis, and P. C. Kepple, *Phys. Rev. Lett.* **37**, 1390 (1976).
7. E. W. Schlag, *ZEKE Spectroscopy* (Cambridge University Press, Cambridge, 1998).
8. V. Kokoouline and C. H. Greene, *Phys. Rev. A* **68**, 012703 (2003).
9. C. Sathé, M. Strom, M. Agaker, J. Soderstrom, J. E. Rubenson, R. Richter, M. Alagia, S. Stranges, T. W. Gorczyca, and F. Robicheaux, *Phys. Rev. Lett.* **96**, 043002 (2006).
10. J. E. Mayer and M. G. Mayer, *Phys. Rev.* **431**, 605 (1933).
11. J. H. Van Vleck and N. G. Whitelaw, *Phys. Rev.* **44**, 551 (1933).
12. S. R. Lundeen, in *Advances in Atomic, Molecular, and Optical Physics*, edited by P. Berman and C. Lin (Elsevier Academic Press, San Diego, 2005).
13. E. S. Shuman and T. F. Gallagher, *Phys. Rev. A* **74**, 022502 (2006).
14. M. S. Safronova and U. I. Safronova, *Phys. Rev. A* **83**, 013406 (2011).
15. P. Johnsson, R. Lopez-Martens, S. Kazamias, J. Mauritsson, C. Valentin, T. Remetter, K. Varju, M. B. Gaarde, Y. Mairesse, H. Wabnitz, P. Salieres, Ph. Balcou, K. J. Shafer, and A. L'Huillier, *Phys. Rev. Lett.* **95**, 013001 (2005).
16. P. Ranitovic, X. M. Tong, B. Gramkow, S. De, B. DePaola, K. P. Singh, W. Cao, M. Magrakelidze, D. Ray, I. Bocharova, H. Mashiko, A. Sandhu, E. Gagnon, M. M. Murnane, H. C. Kapteyn, I. Litvinyuk, and C. L. Cocke, *New J. Phys.* **12**, 013008 (2010).
17. P. Johnsson, J. Mauritsson, T. Remetter, A. L'Huillier, and K. J. Schafer, *Phys. Rev. Lett.* **99**, 233001 (2007).
18. X. M. Tong, P. Ranitovic, C. L. Cocke, and N. Toshima, *Phys. Rev. A* **81**, 021404 (2010).
19. P. Riviere, O. Uhden, U. Saalman, and J. M. Rost, *New J. Phys.* **11**, 053011 (2009).
20. T. Nubbemeyer, K. Gorling, A. Saenz, U. Eichmann, and W. Sandner, *Phys. Rev. Lett.* **101**, 233001 (2008).
21. W. E. Cooke, T. F. Gallagher, R. M. Hill, and S. A. Edelstein, *Phys. Rev. Lett.* **40**, 178 (1978).
22. R. R. Jones and T. F. Gallagher, *Phys. Rev. A* **38**, 2846 (1988).
23. E. L. Snow and S. R. Lundeen, *Phys. Rev. A* **76**, 052505 (2007).
24. M. S. Safronova and U. I. Safronova, *Phys. Rev. A* **83**, 013406 (2011).
25. A. G. Vaidyanathan, W. P. Spencer, J. R. Rubbmark, H. Kuiper, C. Fabre, D. Kleppner, and T. W. Ducas, *Phys. Rev. A* **26**, 3346 (1982).
26. U. I. Safronova and M. S. Safronova, *Phys. Rev. A* **79**, 022512 (2009).
27. K. R. Overstreet, R. R. Jones, and T. F. Gallagher, *Phys. Rev. Lett.* **106**, 033002 (2011).

28 K. R. Overstreet, R. R. Jones, and T. F. Gallagher, *Phys. Rev. A* **85**, 055401 (2012).

Publications 2012-2014

1. J. Nunkaew and T. F. Gallagher, "Spectroscopy of barium $6p_{1/2}n_k$ autoionizing states in a weak electric field," *Phys. Rev. A* **86**, 013401 (2012).
2. K. R. Overstreet, R. R. Jones, and T. F. Gallagher, "Phase-dependent energy transfer in a microwave field," *Phys. Rev. A* **85**, 055401 (2012).
3. E. G. Kim, J. Nunkaew, and T. F. Gallagher, "Detection of Ba $6s_{ng} \rightarrow 6s_{nh}$, $6s_{ni}$, and $6s_{nk}$ microwave transitions using selective excitation to autoionizing states," *Phys. Rev. A* **89**, 062503 (2014).

Experiments in Ultracold Molecules

Phillip L. Gould
Department of Physics U-3046
University of Connecticut
2152 Hillside Road
Storrs, CT 06269-3046
<phillip.gould@uconn.edu>

Program Scope:

Recent advances in the production and manipulation of ultracold atoms and molecules have not only benefited atomic, molecular and optical (AMO) physics, but had a broader impact as well. Areas ranging from chemistry and condensed-matter physics to quantum information and fundamental symmetries stand to profit from this progress. Molecules have a much richer level structure than atoms, which introduces challenges in their production and manipulation. Ironically, molecules are of interest mainly because of these multiple internal degrees of freedom: electronic, vibrational, rotational, electron spin, and nuclear spin. The associated energies span a wide range, allowing interactions with a variety of other systems. In addition, heteronuclear molecules can have permanent electric dipole moments, giving rise to dipole-dipole interactions which are long-range, anisotropic and controllable. Molecules have been cooled “directly” using buffer gas cooling, electrostatic slowing, and laser cooling. They have also been produced “indirectly” by assembling cold atoms into molecules via photoassociation and magnetoassociation. The resulting cold molecules have been trapped using optical, magnetic, and electrostatic techniques. Applications of ultracold molecules include: ultracold chemical reactions; ultracold collisions; quantum degenerate gases; novel quantum phases of dipolar gases; tests of fundamental symmetries; time variation of fundamental constants; quantum computation; and simulations of condensed-matter systems. The main goal of our experimental program is to coherently manipulate the dynamics of colliding ultracold atoms using pulses of frequency-chirped light on the nanosecond time scale. We are particularly interested in applying these techniques to the coherent control of photoassociative formation of ultracold molecules.

Our experiments utilize Rb atoms which are laser cooled and confined in a magneto-optical trap (MOT). Rubidium is our species of choice for a number of reasons: 1) its resonance lines at 780 nm and 795 nm are readily accessed with commercially available diode lasers; 2) it has two abundant isotopes, ^{85}Rb and ^{87}Rb ; 3) ^{87}Rb is the most popular atom for BEC studies; and 4) Rb photoassociation, as well as state-selective ionization detection of the resulting Rb_2 , have been thoroughly investigated here at UConn and elsewhere. Our experiments employ a phase-stable MOT which is loaded with cold atoms from a separate “source” MOT. After being loaded, the cold atoms are illuminated with a sequence of pulses of frequency-chirped light. Typically, these pulses are 40 ns FWHM and the chirps cover 1 GHz in 100 ns. The ground-state Rb_2 molecules formed by the chirped photoassociation are detected by ionization with a tunable pulsed dye laser. The resulting molecular ions are distinguished from background atomic ions by their time-of-flight to the detector.

Recent Progress:

We have recently made progress in a number of areas: formation of ultracold ground-state molecules by photoassociation with frequency-chirped light; detection of these molecules by multiphoton ionization; production of faster pulses and chirps using intensity and phase modulators; quantum simulations of chirped photoassociation; quantum simulations of molecule formation optimized by local control of the phase; and calculations of chirped Raman transfer in 3- and 4-level systems.

We recently observed the photoassociative formation of ultracold molecules using pulses of frequency-chirped light. In these experiments, the chirp was centered on a photoassociation resonance located 7.8 GHz below the $5S_{1/2} + 5P_{3/2}$ asymptote. Molecules ending up in the $a^3\Sigma_g^+$ triplet ground state were detected by resonance-enhanced multiphoton ionization (REMPI) with a pulsed dye laser at ~ 600 nm. We found that, with all other parameters fixed, a positive chirp produced more molecules than a negative chirp. We also found that the chirped light could destroy already-existing molecules.

In order to understand the dependence of molecule formation rate on chirp direction, we are collaborating with Shimshon Kallush at ORT Braude and Ronnie Kosloff at Hebrew University (both in Israel) on quantum simulations of this process. This is an extension of our earlier work on inelastic trap-loss collisions, where we now include the bound vibrational levels in both the ground- and excited-state molecular potentials. In our case, the 0_g^- and 1_g excited states are relevant for the photoassociation, and these can in turn populate high vibrational levels of the $a^3\Sigma_g^+$ triplet ground state, either by spontaneous (incoherent) or stimulated (coherent) emission. We find that the simulations generally reproduce the trends of the experiment, most notably the dependence on chirp direction. Examining the time evolution of the various state populations reveals the mechanism. The positive chirp first passes through a photoassociation (free-bound) resonance, producing excited molecules from free atoms, and then through a bound-bound resonance, causing stimulated emission of the excited-state molecules into a ground-state vibrational level. Since this sequence is in the wrong order for the negative chirp, the efficiency of producing ground-state molecules is significantly reduced for this chirp direction.

We have also adapted our quantum simulations to deal with situations other than a linear chirp. For example, we are using the idea of local control of the phase in order to optimize the molecular formation. Local control is a unidirectional and non-iterative time propagation scheme which adjusts the field, in our case the phase, at each instant of time in order to optimize the target at the next time step. We find that the field resulting from such an optimization is a rapid jump in frequency: it is initially resonant with the photoassociation transition, and then jumps to being resonant with the bound-bound transition. This gives a significant enhancement relative to a linear chirp at the same intensity. We also see interesting interference effects when two frequencies and/or two intermediate excited states are present. The parameters emerging from these simulations are compatible with our faster chirped-pulse production technique.

In order to produce fast and arbitrarily-shaped chirped pulses, we are using electro-optic phase and intensity modulators driven by a 4 GHz arbitrary waveform generator (AWG). Although the AWG has only a single channel, we generate

independent waveforms for the two modulators using an rf switch and a delay line. With this scheme, the phase modulator can produce frequency chirps of a few GHz in a few ns with a subnanosecond pulse envelope generated by the intensity modulator. We are also incorporating a tapered amplifier to boost the intensity of the chirped pulses.

Together with Svetlana Malinovskaya (Stevens Institute of Technology), we have performed calculations of Raman transfer using a single chirped pulse on the nanosecond time scale. We examined both 3-level (one excited state) and 4-level (two excited states) systems to see the effects of the additional excited state. We found that the transfer efficiency can be quite high for experimentally achievable parameters, and that under some conditions, the extra excited state does reduce transfer to the target ground state. So far, the calculations have been done for transfer between hyperfine levels of the Rb atom, but they can be adapted to describe the transfer of population between vibrational levels of an ultracold molecule.

Future Plans:

We will build upon our recent chirped molecule formation experiments by going to faster time scales and higher intensities. The more rapid chirps and shorter pulses will allow us to avoid the effects of spontaneous emission, while the higher intensities will enable more adiabatic, and therefore more efficient, molecule formation. Based on the results of our quantum simulations, we will also go beyond linear chirps in order to optimize the production of ground-state molecules in a target vibrational level. For example, the local control simulations indicate that a sudden jump in frequency should be advantageous.

Recent Publications:

“Coherent Control of Ultracold ^{85}Rb Trap-Loss Collisions with Nonlinearly Frequency-Chirped Light”, J.A. Pechkis, J.L. Carini, C.E. Rogers III, P.L. Gould, S. Kallush, and R. Kosloff, *Phys. Rev. A* **83**, 063403 (2011).

“Creation of Arbitrary Time-Sequenced Line Spectra with an Electro-Optic Phase Modulator”, C.E. Rogers III, J.L. Carini, J.A. Pechkis, and P.L. Gould, *Rev. Sci. Instrum.* **82**, 073107 (2011).

“Quantum Dynamical Calculations of Ultracold Collisions Induced by Nonlinearly Chirped Light”, J.L. Carini, J.A. Pechkis, C.E. Rogers III, P.L. Gould, S. Kallush, and R. Kosloff, *Phys. Rev. A* **85**, 013424 (2012).

“Production of Ultracold Molecules with Chirped Nanosecond Pulses: Evidence for Coherent Effects”, J.L. Carini, J.A. Pechkis, C.E. Rogers III, P.L. Gould, S. Kallush, and R. Kosloff, *Phys. Rev. A* **87**, 011401(R) (2013).

“Population Inversion in Hyperfine States of Rb with a Single Nanosecond Chirped Pulse in the Framework of a Four-Level Atom”, G. Liu, V. Zakharov, T. Collins, P. Gould, and S.A. Malinovskaya, *Phys. Rev. A* **89**, 041803(R) (2014).

Page is intentionally blank.

Physics of Correlated Systems

Chris H. Greene

Department of Physics, Purdue University, West Lafayette, IN 47907-2036

chgreene@purdue.edu

Program Scope

Among all physics problems, the challenges of describing tightly coupled interactions among multiple degrees of freedom remains one of the richest but most challenging to describe theoretically. This is because the starting point for most theoretical approaches is a separable or mean-field-type approximation, in which each degree of freedom has its own independent variation, and these variations are approximated as entirely separate except the effects of other degrees of freedom are taken into account in an average way. These uncorrelated methods, commonly known in the description of electronic states of atoms and molecules as the Hartree-Fock method and its generalizations, constitute the usual starting point for investigating a broad range of properties. When low energy electrons, atoms, molecules, and photons undergo collisions, however, it is rather well known by now that the uncorrelated starting point is unable to provide much physical insight and it is also frequently unable to be pushed to the desired level of quantitative accuracy. The work in our group develops theoretical treatments, usually based on nonrelativistic quantum mechanics but occasionally involving semiclassical or classical approximations, which incorporates as much as possible about the correlated interactions in the zeroth-order description. This often involves making an unconventional choice of the coordinate system for the problem, and looking at the development of the theory and its implications from this unconventional point of view. The processes we have been investigating during the past year include three-body recombination at chemically interesting temperatures, treatments of short-pulse laser-atom and laser-molecule interactions in order to describe correlated electron processes such as interatomic Coulombic decay (ICD), and continued improvement of systematic ways to describe the interplay between short-range and long-range quantum mechanics of collisions and resonance properties. The publications listed below [1-11] are the papers that have been supported primarily by this project.

Recent Progress and Immediate Plans

(i) Short laser pulses interacting with an atom, molecule, or cluster.

Opportunities for exploration of attosecond physics have been growing rapidly in recent years, as technical capabilities continue to improve rapidly both with table-top sources and higher energy and intensity photon sources such as free-electron X-ray lasers. A new study published this year [2] discusses these opportunities and suggests promising avenues that are ripe for immediate development. One such opportunity has emerged from our collaboration with the Heidelberg experimental group of Thomas Pfeifer and Christian Ott and the theory group of Jörg Evers and Christoph Keitel which identified a general theoretical connection between the Fano lineshape asymmetry parameter q and the phase ϕ of the dipole oscillations that are created by a short pulse excitation of any Fano resonance [7]. The exploration of further implications of this technique for extending quantum control continues to be a ripe avenue for exploration in the near future. Another area where we have invested considerable effort already is a study of impulsive interatomic Coulombic decay processes. In most ICD processes, a double positively charged system is formed during the decay, leading to a Coulomb explosion, but there is another class we

have been focusing on where the products formed in the decay experience an attractive interaction. The differences and similarities with the more typical type of explosive ICD process will be explored and mapped out in the coming year of this project.

(ii) Electron dynamics in internal and external fields

The theory of the Stark effect was developed in an elegant formulation by Fano and Harmin in the early 1980s, in a powerful combination of quantum defect ideas and local coordinate transformations that is now called local frame transformation theory (LFT). The LFT in its original form accurately described the escape of a photoelectron in the combined spherical atomic field at small distances and the Coulomb plus Stark parabolic coordinate potential applicable beyond about 10 bohr radii. This theory has determined total photoionization cross sections to quantitative accuracy, but a 2012 study by Zhao, Fabrikant, Du, and Bordas has suggested that other observables such as the photoionization microscopy differential cross section are inaccurate in the LFT. Because the LFT has emerged as a major tool for theoretical physics, this year has started a new exploration of this approximation, led by postdoc Panos Giannakeas and in collaboration with Francis Robicheaux. Our preliminary results from investigating this issue imply that the discrepancies suggested by Zhao et al. are not caused by deficiencies of the LFT approximation but rather by technical errors in its implementation. An extensive study of this topic, including a reformulation and generalization of the LFT, will be completed soon.

(iii) Few-body collisions from low energy up to chemically interesting temperatures

A number of advances have been made in understanding three-body recombination at ultracold temperatures during the past 15 years, but comparatively little has been carried out for higher energy collisions of interest in chemical contexts. In this vein, a major effort has been initiated to treat three-body recombination both classically and quantum mechanically, to delineate as clearly as possible the temperature range where these two computational approaches are in agreement. Our first exploration along these lines [1] found that classical and quantum treatments of the lowest total angular momentum for three helium atoms are already in agreement at energies above 1K. This line of research is now continuing with calculations of three-body recombination when one of the bodies is positively charged. Our studies of two-body Fano-Feshbach resonances also continued during the past year, with a collaborative experimental and theoretical study of the S-wave and P-wave magnetic resonances in collisions between a bosonic Cs atom and a fermionic Li atom.[3] Further work along these lines is underway at higher temperatures for the Li-Rb system, both for ground state atomic collisions in a magnetic field and for photoassociation reactions.

Papers published since 2012 that were supported by this grant.

[1] *Comparison of classical and quantal calculations of helium three-body recombination*, J Pérez-Ríos, S Ragole, J Wang, and C H Greene, *J. Chem. Phys.* **140**, 044307-1 to -12 (2014).

- [2] *What will it take to observe processes in 'real time'?*, S R Leone, C W McCurdy, J Burgdörfer, L S Cederbaum, Z Chang, N Dudovich, J Feist, C H Greene, M Ivanov, R Kienberger, U Keller, M F Kling, Z-H Loh, T Pfeifer, A N Pfeiffer, R Santra, K Schafer, A Stolow, U Thumm and M J J Vrakking, *Nature Photonics* **8**, 162-166 (2014).
- [3] Comparison of classical and quantal calculations of helium three-body recombination, R. Pires, M. Repp, J. Ulmanis, E. D. Kuhnle, and M. Weidemueller, T. G. Tiecke, C H Greene, B P Ruzic, J L Bohn, and E Tiemann *Phys. Rev. A* **90**, 012710-1 to -14 (2014).
- [4] *Low-energy electron collisions with O₂: Test of the molecular R-matrix method without diagonalization*, M Tarana and C H Greene, *Phys. Rev. A* **87**, 022710-1 to -13 (2013).
- [5] *Rydberg states of triatomic hydrogen and deuterium*, Jia Wang and C H Greene, *J. Phys. Chem. A* **ASAP**, DOI: 10.1021/jp312462a, pp1-5 (2013).
- [6] *Quantum defect theory for high-partial-wave cold collisions*, B P Ruzic, C H Greene and J L Bohn, *Phys. Rev. A* **87**, 032706-1 to -14 (2013).
- [7] *Lorentz Meets Fano in Spectral Line Shapes: A Universal Phase and Its Laser Control*, C Ott, A Kaldun, P Raith, K Meyer, M Laux, J Evers, C H Keitel, C H Greene, and T Pfeifer, *Science* **340**, 716-720 (2013).
- [8] *Laser-assisted electron-argon scattering at small angles*, N Morrison and C H Greene, *Phys. Rev. A* **86**, 053422-1 to -6 (2012).
- [9] *Estimates of rates for dissociative recombination of NO₂⁺ + e via various mechanisms*, D J Haxton and C H Greene, *Phys. Rev. A* **86**, 062712-1 to -5 (2012).
- [10] *Femtosecond transparency in the extreme-ultraviolet region*, M Tarana and C H Greene, *Phys. Rev. A* **85**, 013411-1 to -11 (2012).
- [11] *Dissociative recombination of highly symmetric polyatomic ions*, N Douguet, A E Orel, C H Greene, and V Kokoouline, *Phys. Rev. Lett.* **108**, 023202-1 to -5 (2012).

Page is intentionally blank.

Using Strong Optical Fields to Manipulate and Probe Coherent Molecular Dynamics

Robert R. Jones, Physics Department, University of Virginia
382 McCormick Road, P.O. Box 400714, Charlottesville, VA 22904-4714
bjones@virginia.edu

I. Program Scope

This project focuses on the exploration and control of dynamics in atoms and small molecules driven by strong laser fields. Our goal is to exploit strong-field processes to implement novel ultrafast techniques for manipulating and probing coherent electronic and nuclear motion within atoms, molecules, and on surfaces. Ultimately, through the application of these methods, we hope to obtain a more complete picture of correlated multi-particle dynamics in molecules and other complex systems.

II. Recent Progress and Results

During the current funding year we have: (i) continued our investigation of transient, field-free orientation of polar molecules induced by combinations of intense optical and THz pulses; (ii) extended our studies of strong-field ionization by intense single-cycle THz pulses, moving from Rydberg atom targets to nano-structured metals; (iii) examined the role of multi-electron dynamics in enhanced multiple-ionization of diatomic molecules; and (iv) begun a collaboration with the DiMauro/Agostini group to characterize the influence of the electronic binding potential on energy transfer between an optical dressing field and near-threshold attosecond photoelectrons. Brief summaries of these on-going projects are provided below.

Several of our projects involve the use of intense, single-cycle THz pulses which are produced using optical rectification of tilted pulse-front, 50-150 fs, 790nm laser pulses in MgO doped stoichiometric Li:NbO₃ [1,2]. Such pulses are interesting in the context of strong-field and ultrafast physics for several reasons. First, the broad frequency spectrum and large field strengths allow for direct rotational excitation of molecules, enabling the creation of controllable, mixed parity rotational wavepackets without electronic excitation, ionization, or strong static fields. Second, the long oscillation period of the field makes it possible to drive free, or quasi-free, electrons to large energies (> 100 eV) without influencing the tightly bound electrons in atoms, molecules, or condensed systems. Accordingly, these pulses might be used as time-resolved probes of photoionization times with a temporal resolution approaching a few or few tens of femtoseconds. Third, the passively CE-phase locked, true single-cycle pulses allow us to explore various strong field phenomena in a regime that has yet to be realized at visible and higher frequencies.

(i) Transient Field-Free Orientation of Polar Molecules using Intense Single-Cycle THz Pulses

Following the first demonstration of field-free orientation of polar molecules by intense THz pulses [3], we recently showed that the degree of achievable orientation could be substantially improved by coherently preparing the molecules in rotational superposition states, via Raman transitions in a short optical pulse, prior to their exposure to the THz radiation. Those results were recently published in PRL [see publication (i)]. Our initial measurements were performed at a low (15 Hz) repetition rate using 20 mJ optical pulses to generate as much THz radiation as

possible. We have improved the design, and are now rebuilding, our molecular beam and detection apparatus in an attempt to produce comparable levels of orientation with weaker THz pulses (produced using only 2 mJ of optical pulse energy) at a 1 kHz repetition rate. This will enable our future studies of high-intensity dissociative ionization control in molecules and high-harmonic generation from oriented molecules.

(ii) Strong-Field Ionization with Single-Cycle THz Pulses

We recently showed, using intense THz pulses, that strong-field atomic ionization and the resulting field-driven electron energy spectrum can be remarkably different when true single-cycle, as opposed to multi-cycle, ionizing pulses are used. Due to the wavelength scaling of the pondermotive potential, electrons that are free to move over large distances can attain energies exceeding 100 eV from our strong THz fields. Therefore, in principle, such pulses might be useful for high-energy streaking of photo-electrons from condensed matter targets, providing a time-resolved probe without causing permanent target damage. In addition, electron field emission from a scanning probe tip, induced by non-damaging ultrashort THz pulses, might enable time-resolved electron microscopy. For the latter application, the 400kV/cm field strengths available in our THz pulses are orders of magnitude too small to induce tunneling ionization from bulk metals as an ultrafast electron source. However, tunneling from nano-structured surfaces should be possible given the substantial field enhancements that can be achieved.

Accordingly, we have begun an investigation of THz induced field-emission from nano-structured metal surfaces. We find that we can produce very high energy electrons (> 4 keV) from single nano-scale tips in tungsten as well as from nano-structured gold black coated wires. We believe that this is the first observation of field emission induced by freely propagating THz radiation. Our preliminary analysis suggests that the ionization mechanism is tunneling, aided by field enhancement near the sharp tips. In some cases, the ionization may be aided by energy transfer to the electrons prior to tunneling and we are continuing to explore the details of the ionization mechanism.

The electron energy spectra from the nano-structured gold black surfaces are nearly flat, extending from zero energy to a sharp, high energy cutoff which scales quadratically with the applied THz field strength. The quadratic field-dependence suggests a pondermotive scaling of the high-energy cutoff of $\sim 250 U_p$, and is not currently understood. In contrast, the electrons emitted from single nano-tips are ejected over a fairly well-defined (THz field-dependent) energy range, and have a maximum energy that scales linearly with the applied THz field. The linear field-scaling is consistent with a static, enhanced-field model, recently invoked to explain the non-pondermotive energy scaling of electrons ejected from nano-tips in infrared laser fields [4]. In this model, the electron energy is essentially determined by the product of the enhanced-field near the nano-tip and the distance over which the field enhancement persists. In optical experiments, typical field enhancements are on the order of 10. Our results suggests a much larger field enhancement, ~ 1000 , for our geometries at THz frequencies. A quasi-static model of the field-enhancement supports this conclusion [5]. Many aspects of the ionization process remain to be explored, from the temporal and angular distributions of the emission, to the size, shape, number, and material composition of the emitters.

(iii) Multi-electron Effects in Enhanced Multiple-Ionization of Nitrogen

As part of a large collaboration involving groups from Germany, China, and the U.S. (see publication (iii) for full list of collaborators), we have performed time-resolved measurements of enhanced ionization of Nitrogen. We have combined results of few-cycle pump-probe measurements performed at MPQ and angular streaking experiments using intense elliptically polarized laser pulses completed in Frankfurt to examine the enhanced ionization dynamics. We have been able to rule out any significant contribution from multi-electron charge transfer processes that apparently play a role in the enhanced multiple ionization of I_2 [6]. Our results suggest that charge transfer may only be significant in longer pulses where the strong field is present while the internuclear separation in the dissociating molecule both approaches, and passes through, a critical value. In the future, we intend to perform pump-probe measurements as a function of the duration of the pump and probe pulses in an attempt to confirm this hypothesis.

(iv) Near Threshold Energy Transfer to Attosecond Photoelectrons

In collaboration with the DiMauro/Agostini group at OSU, we have used attosecond pulse trains to photoionize noble gas atoms near threshold in the presence of a moderately intense, infrared dressing laser. As in the standard RABBITT technique, which has been used to reconstruct the field in attosecond pulse trains, we monitor the amplitude and phase of photoelectron sidebands. These sidebands are produced via energy transfer between the dressing field and the photoelectrons produced directly by the XUV harmonic radiation. By comparing the sideband amplitude and phase for different atoms we hope to extract information about the differences in the potentials seen by the photoelectrons as they move away from their respective parent ions. Our very preliminary analysis suggests that there are differences in the sideband amplitudes and phases that might be attributable to the differences in the binding potentials of the different atoms. More extensive analysis will be required to confirm these results and, potentially, extract atomic information from them. In principal, a variant of these measurements might provide time-resolved information on changes in an atomic/molecular potential due to an external stimulus.

III. Future Plans

In addition to continuing our current projects as discussed briefly in (i)-(iv) above, we are working to improve our experimental capabilities for future measurements. In particular we are attempting to produce sub-6fs ~ 760 nm laser pulses from our hollow-core-fiber compressor to explore the coupled dynamics of electrons and nuclei during asymmetric strong-field multi-electron dissociative ionization. We plan to utilize a CE-phase meter [7], recently installed in our lab, to measure the CE-phase on each laser shot, enabling experiments without actively locking the CE-phase of the intense few-cycle laser.

IV. DOE Sponsored Publications from the Last 3 Years

(i) K. Egodapitiya, Sha Li, and R.R. Jones, "THz Induced Field-Free Orientation of Rotationally Excited Molecules," *Physical Review Letters* **112**, 103002 (2014).

(ii) Sha Li and R.R. Jones, "Ionization of Excited Atoms by Intense Single-Cycle THz Pulses," *Physical Review Letters* **112**, 143006 (2014).

(iii) X. Gong, M. Kunitski, K.J. Betsch, Q. Song, L. Ph. H. Schmidt, T. Jahnke, Nora G. Kling, O. Herrwerth, B. Bergues, A. Senftleben, J. Ullrich, R. Moshhammer, G.G. Paulus, I. Ben-Itzhak,

M. Lezius, M.F. Kling, H. Zeng, R.R. Jones, and J. Wu, "Multielectron Effects in Strong-field Dissociative Ionization of Molecules," *Physical Review A* **89**, 043429 (2014).

(iv) M. Kubel, Nora G. Kling, K. J. Betsch, N. Camus, A. Kaldun, U. Kleineberg, I. Ben-Itzhak, R.R. Jones, G.G. Paulus, T. Pfeifer, J. Ullrich, R. Moshhammer, M.F. Kling, and B. Bergues, "Non-Sequential Double-Ionization of N₂ in a Near Single-Cycle Laser Pulse," *Physical Review A* **88**, 023418 (2013).

(v) K. J. Betsch, Nora G. Johnson, B. Bergues, M. Kubel, O. Herrwerth, A. Senftleben, I. Ben-Itzhak, G. G. Paulus, R. Moshhammer, J. Ullrich, M. F. Kling, and R. R. Jones, "Controlled directional ion emission from the dissociative ionization of CO over multiple charge states in a few-cycle laser field," *Physical Review A* **86**, 063403 (2012).

(vi) K.R. Overstreet, R.R. Jones, and T.F. Gallagher, "Phase dependent energy transfer in a microwave field," *Physical Review A* **85**, 055401 (2012).

(vii) Boris Bergues, Matthias Kübel, Nora G. Johnson, Bettina Fischer, Nicolas Camus, Kelsie J. Betsch, Oliver Herrwerth, Arne Senftleben, A. Max Saylor, Tim Rathje, Itzik Ben-Itzhak, Robert R. Jones, Gerhard G. Paulus, Ferenc Krausz, Robert Moshhammer, Joachim Ullrich, and Matthias F. Kling, "Attosecond Control and Real-Time Observation of Electron Correlations," *Nature Communications* **3**, 813 (2012).

V. References

[1] For a recent review see: Janos Hebling, Ka-Lo Yeh, Matthias C. Hoffman, Balazs Bartal, and Keith A. Nelson, "Generation of High-Power Terahertz Pulses by Tilted-Pulse-Front Excitation and Their Application Possibilities," *J. Opt. Soc. Am. B* **25**, B6 (2008).

[2] H. Hirori, A. Doi, F. Blanchard, and K. Tanaka, "Single-cycle Terahertz Pulses with Amplitudes Exceeding 1MV/cm Generated by Optical Rectification in LiNbO₃," *Appl. Phys. Lett.* **98**, 091106 (2011).

[3] Sharly Fleischer, Yan Zhou, Robert W. Field, and Keith A. Nelson, "Molecular Orientation and Alignment by Intense Single-Cycle THz Pulses," *Phys. Rev. Lett.* **107**, 163603 (2011).

[4] G. Herink, D. R. Solli, M. Gulde, and C. Ropers, "Field-driven photoemission from nanostructures quenches the quiver motion," *Nature* **483**, 190 (2012).

[5] S. Podenok, M. Sveningsson, K. Hansen, and E.E.B. Campbell, "Electric Field Enhancement Factors Around a Metallic, End-Capped Cylinder," *NANO: Brief Reports and Reviews* **1**, 87 (2006).

[6] V. Tagliamonti, H. Chen, and G. N. Gibson, "Multielectron Effects in Charge Asymmetric Molecules Induced by Asymmetric Laser Fields," *Phys. Rev. Lett.* **110**, 073002 (2013).

[7] T. Wittman *et al.*, "Single-shot Carrier-Envelope Phase Measurement of Few-Cycle Laser Pulses," *Nat. Phys.* **5**, 357 (2009).

Molecular Dynamics Probed by Coherent Soft X-Rays

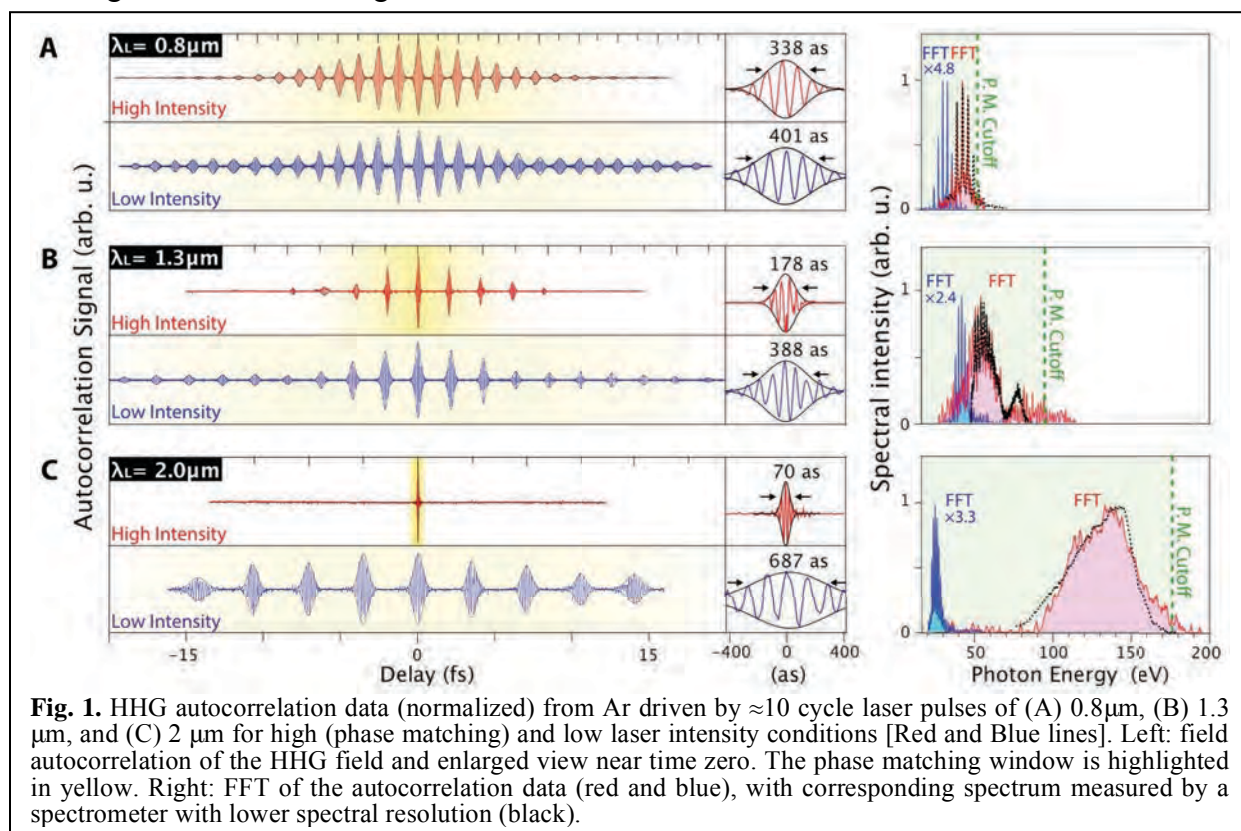
Henry C. Kapteyn and Margaret M. Murnane

JILA and Department of Physics, University of Colorado at Boulder

Phone: (303) 492-8198; FAX: (303) 492-5235; E-mail: kapteyn@jila.colorado.edu

The goal of this work is to develop novel short wavelength probes of molecules and to understand the response of atoms and molecules to strong laser fields. We made exciting advances in several areas.[1-22] We also have very productive collaborations with chemistry colleagues including Profs. Gordana Dukovic and Jose L. Jimenez (CU Boulder), Prof. Keith Nelson (MIT) and Prof. Tamar Seideman (Northwestern), and with physicists Prof. Oren Cohen (Technion) and Prof. Ming-Chang Chen (NTHU). Recent highlights include –

First isolated attosecond soft X-ray pulses [5]: Until recently, attosecond pulses were confined to the EUV region (< 100 eV), limiting the range of molecular/materials systems that could be explored. In work in press in *PNAS*, we experimentally demonstrated a remarkable convergence of physics: when mid-IR lasers are used to drive HHG, the conditions for bright phase-matched soft X-ray generation naturally coincide with the generation of isolated attosecond pulses. Our measurements represent the highest photon energy (≈ 200 eV) isolated attosecond pulses to date. Surprisingly, theory shows that long ~ 10 cycle lasers are required so that collective phase-matching effects isolate a bright attosecond burst.



First photoelectron spectroscopy of isolated quantum dots [3, 8]: In work published in *Nano Letters*, we reported the first studies of isolated quantum dots, i.e. not in solution or in a solid matrix.[8] By coupling a nanoparticle aerosol source to a velocity map imaging photoelectron

spectrometer, we applied robust gas-phase photoelectron spectroscopy techniques to quantum dots, which typically must be studied in a liquid or while bound to a surface. This allowed us to isolate the intrinsic properties of quantum dots independent of coupling to a host or substrate. By measuring the photoelectron yield, we directly probed the evanescent part of the quantum dot excited-state wavefunction for the first time, showing that for smaller dots, the electron wavefunction extends significantly outside the dot itself.

More recently, in order to predict and understand nano-device performance in different environments such as in air and liquid phase, we investigated solvent effects in quantum dot charge transfer processes. Specifically, we compared quantum dot charge transfer processes in the liquid phase and in vacuum using gas-phase photoelectron spectroscopy and solution phase transient absorption spectroscopy. This allowed us to show that hexane, a common solvent for quantum dots, has negligible influence on charge transfer dynamics. Our experimental findings supports the previous hypothesis that the reorganization energy of nonpolar solvents plays a minimal role in the energy landscape of charge transfer in quantum dot devices, implying that measurements in the liquid phase can indeed provide insight into nano-device performance in a wide variety of environments.

Observation of a new regime of collective nanoscale thermal transport [1, 2, 16, 22]:

Understanding thermal transport from nanoscale heat sources is important for a fundamental description of energy flow in materials, as well as for

many technological applications including thermal management in nanoelectronics, thermoelectric devices, nano-enhanced photovoltaics and nanoparticle-mediated thermal therapies. Thermal transport at the nanoscale is fundamentally different from that at the macroscale and is determined by the distribution of carrier mean free paths in a material, the length scales of the heat sources, and the distance over which heat is transported. Past work had shown that Fourier's law for heat conduction dramatically over-predicts the rate of heat dissipation from heat sources with dimensions smaller than the mean free path of the dominant heat-carrying phonons. In new work in collaboration with LBL, we uncovered a new regime of nanoscale thermal transport that dominates when the separation between nanoscale heat sources is small compared with the dominant phonon mean free paths.[1] Surprisingly, the interplay between neighboring heat sources enables better coupling to the full phonon spectrum in the

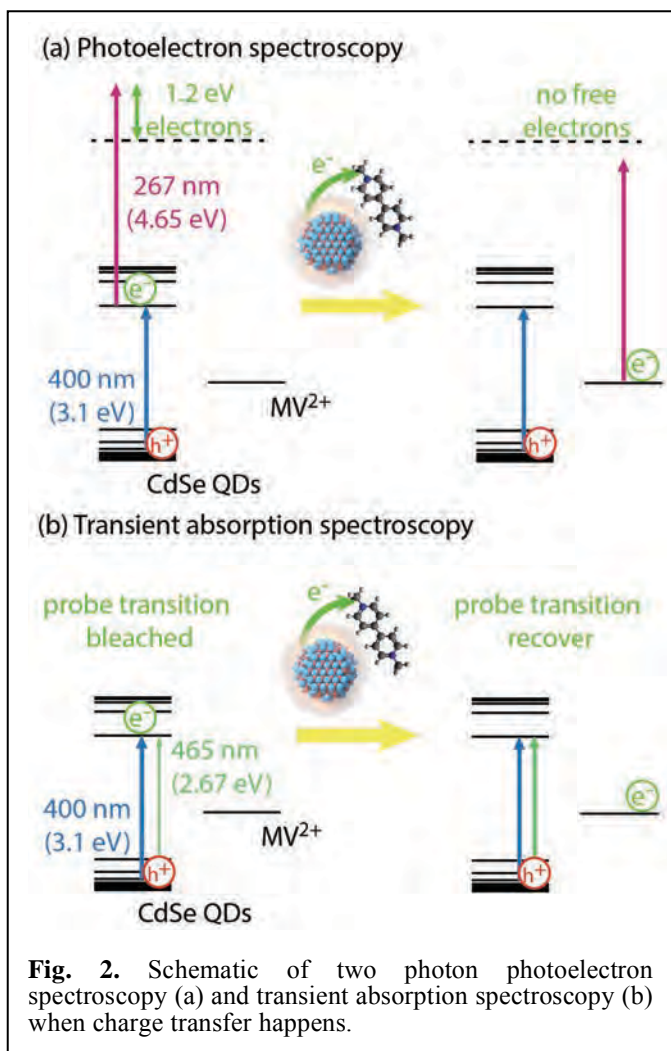
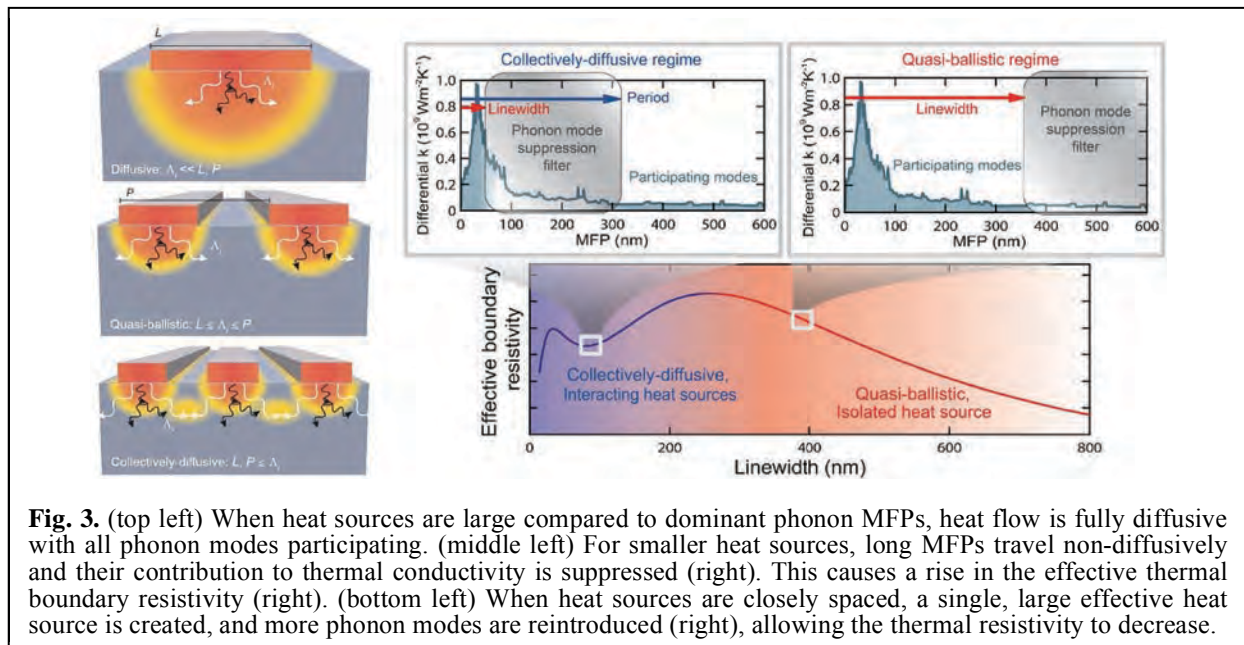


Fig. 2. Schematic of two photon photoelectron spectroscopy (a) and transient absorption spectroscopy (b) when charge transfer happens.

substrate, thus facilitating efficient and diffusive-like heat dissipation, even from the smallest nanoscale heat sources. This finding suggests that thermal management in nanoscale systems including integrated circuits might not be as challenging as projected. Finally, we demonstrated a unique and new capability to extract differential mean free path distributions of phonons in materials, allowing the first experimental validation of differential conductivity predictions from first-principles calculations. This new result is very important both scientifically and technologically.



First bright soft x-ray harmonics at kHz repetition rates [6]: We demonstrated bright soft x-ray harmonics at kHz repetition rates (VUV to $>500\text{eV}$) driven by 1.3 and 2 μm tabletop lasers. This represents a $> \times 1000$ increase in HHG flux beyond all other work to date.

Understanding high harmonic generation from molecules [4, 12, 18]: In collaboration with Tamar Seideman, by studying HHG from molecules undergoing rotational revivals, we showed that electrons gain angular momentum during the HHG process. This led to a surprising new finding - that the maximum HHG emission from molecules is not from linear polarized driving lasers (as is the case for atoms), but rather for non-zero laser ellipticities.

Future work: First, we will use ultra-broad bandwidth, ultrafast HHG soft X-rays to capture coupled charge, spin and structural dynamics in molecular, nanoparticle and materials systems at multiple sites simultaneously. Gas, solid and liquid-phase samples will be excited using mid-IR – UV light, and then probed using soft X-ray HHG supercontinua. Second, we will capture orbital dynamics in molecules and nanosystems using photoelectron spectroscopy. Finally we will characterize circularly and linearly polarized attosecond pulses in the EUV and soft x-ray regions.

Publications and Patents from DOE AMOS support

1. K. Hoogeboom-Pot, J. Hernandez-Charpak, E. Anderson, X. Gu, R. Yang, M. Murnane, H. Kapteyn, D. Nardi, "A new regime of nanoscale thermal transport: collective behavior counteracts dissipation inefficiency", submitted (2014). *Postdeadline paper, International Conference on Ultrafast Phenomena, Japan (2014)*.

2. D. Nardi, K. Hoogeboom-Pot, J. Hernandez-Charpak, M. Tripp, S. King, E. Anderson, M. Murnane, H. Kapteyn, "Probing limits of acoustic nanometrology using coherent EUV beams", submitted (2014).
3. J. Ellis, K. Schnitzenbaumer, D. Hickstein, M. Beernink, B. Palm, J. Jimenez, G. Dukovic, H. Kapteyn, M. Murnane, W. Xiong, "Solvent effects on charge transfer between quantum dots and adsorbates", submitted (2014).
4. P. Sherratt, R. Lock, X. Zhou, H. Kapteyn, M. Murnane, T. Seideman, "Ultrafast elliptical dichroism in high-order harmonics as a dynamic probe of molecular and electronic structure", submitted (2014).
5. M.C. Chen, C. Hernández-García, C. Manusco, B. Galloway, P.C. Huang, F. Dollar, D. Popmintchev, L. Plaja, A. Jaron-Becker, A. Becker, T. Popmintchev, M.M. Murnane, H. C. Kapteyn, "Generation of Bright Isolated Attosecond Soft X-Ray Pulses Driven by Multi-Cycle Mid-IR Lasers," *PNAS* **111** (23) E2361 (2014).
6. C. Ding, W. Xiong, T. Fan, D. D. Hickstein, T. Popmintchev, X. Zhang, M. Walls, M. M. Murnane, and H. C. Kapteyn, "High flux coherent super-continuum soft X-ray source driven by a single-stage, 10mJ, Ti:sapphire amplifier-pumped OPA," *Optics Express* **22**(5), 6194-6202 (2014).
7. X.-M. Tong, P. Ranitovic, D. D. Hickstein, M. M. Murnane, H. C. Kapteyn, and N. Tushima, "Enhanced multiple-scattering and intra-half-cycle interferences in the photoelectron angular distributions of atoms ionized in midinfrared laser fields," *Physical Review A* **88**(1), 013410 (2013).
8. W. Xiong, D. D. Hickstein, K. J. Schnitzenbaumer, J. L. Ellis, B. B. Palm, K. E. Keister, C. Ding, L. Miaja-Avila, G. Dukovic, J. L. Jimenez, M. M. Murnane, and H. C. Kapteyn, "Photoelectron Spectroscopy of CdSe Nanocrystals in the Gas Phase: A Direct Measure of the Evanescent Electron Wave Function of Quantum Dots," *Nano Letters* **13**(6), 2924-2930 (2013).
9. T. Popmintchev, M. Chen, A. Bahabad, M. Murnane, H. Kapteyn, "Method for phase-matched generation of coherent soft and hard x-rays using IR lasers," US Patent # 20110007772, Notice of Allowance March 2013.
10. M. Spanner, J. Mikosch, A. Boguslavskiy, M. Murnane, A. Stolow, S. Patchkovskii, "Strong Field Ionization and High Harmonic Generation during Polyatomic Molecular Dynamics," *Phys. Rev. A* **85**, 033426 (2012).
11. D. Hickstein, P. Ranitovic, S. Witte, X. Tong, Y. Huismans, P. Arpin, X. Zhou, K. Keister, C. Hogle, B. Zhang, C. Ding, P. Johnsson, N. Tushima, M. Vrakking, M. Murnane, H. Kapteyn, "Direct Visualization of Laser-Driven Electron Multiple Scattering and Tunneling Distance in Strong-Field Ionization," *Physical Review Letters* **109**, 073004 (2012).
12. R. Lock, S. Ramakrishna, X. Zhou, H. Kapteyn, M. Murnane, T. Seideman, "Extracting Continuum Electron Dynamics from High Harmonic Emission from Molecules," *Phys. Rev. Lett.* **108**(13), 133901 (2012).
13. X. Zhou, P. Ranitovic, C. W. Hogle, J. H. D. Eland, H. C. Kapteyn, M. M. Murnane, "Probing and controlling non-Born-Oppenheimer dynamics in highly excited molecular ions," *Nature Physics* **8**(3), 232-237 (2012).
14. Qing Li et al., "Generation and Control of Ultrashort-Wavelength 2D Surface Acoustic Waves at Nano-interfaces", *Phys. Rev. B* **85**, 195431 (2012).
15. P. Ranitovic, X. M. Tong, C. W. Hogle, X. Zhou, Y. Liu, N. Tushima, M. M. Murnane, and H. C. Kapteyn, "Laser-Enabled Auger Decay in Rare-Gas Atoms," *Physical Review Letters* **106**(5), 053002 (2011).
16. D. Nardi et al., "Probing Thermomechanics at the Nanoscale: Impulsively Excited Pseudosurface Acoustic Waves in Hypersonic Phononic Crystals", *Nano Letters* **11**, 4126 (2011).
17. T. Popmintchev, M.C. Chen, P. Arpin, M. M. Murnane, and H. C. Kapteyn, "The attosecond nonlinear optics of bright coherent X-ray generation," *Nature Photonics* **4**, 822 (2010). *Featured on cover.*
18. W. Li, A. Becker, C. Hogle, V. Sharma, X. Zhou, A. Becker, H. Kapteyn, M. Murnane, "Visualizing electron rearrangement in space and time during the transition from a molecule to atoms," *PNAS* **107**, 20219 (2010).
19. K. P. Singh et al., "Control of Electron Localization in Deuterium Molecular Ions using an Attosecond Pulse Train and a Many-Cycle Infrared Pulse," *Phys. Rev. Lett.* **104**, 023001 (2010).
20. P. Ranitovic et al, "IR-Assisted Ionization of He by Attosec XUV Radiation," *New J. Phys.* **12**, 013008 (2010).
21. K. S. Raines, S. Salha, R. L. Sandberg, H. D. Jiang, J. A. Rodriguez, B. P. Fahimian, H. C. Kapteyn, J. C. Du, and J. W. Miao, "Three-dimensional structure determination from a single view," *Nature* **463**, 214 (2010).
22. M. Siemens, Q. Li, R. Yang, K. Nelson, E. Anderson, M. Murnane, H. Kapteyn, "Measuring quasi-ballistic heat transport across nanoscale interfaces using ultrafast coherent soft x-rays", *Nature Materials* **9**, 26 (2010).

Imaging Multi-particle Atomic and Molecular Dynamics

Allen Landers

landers@physics.auburn.edu

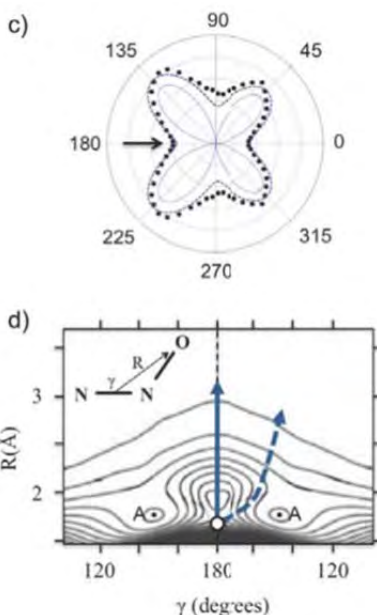
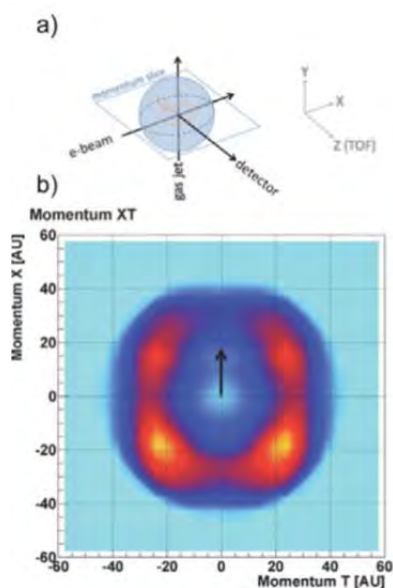
Department of Physics
Auburn University
Auburn, AL 36849

Program Scope: We are investigating phenomena associated with ionization of an atom or molecule by single photons (weak field) or low energy electrons with an emphasis on ionization-driven atomic and molecular dynamics. Of particular interest is untangling the complicated electron-correlation effects and molecular decay dynamics that follow an initial photoionization or electron attachment event. We perform these measurements using variations on the well-established COLTRIMS technique. The experiments take place at the Advanced Light Source at LBNL as part of the ALS-COLTRIMS collaboration with the groups of Reinhard Dörner at Frankfurt and Thorsten Weber at LBNL and at Auburn University in collaboration with Prof. Mike Fogle. Because the measurements are performed in “list mode” over a few days where each individual event is recorded to a computer, the experiments can be repeated virtually with varying gate conditions on computers at Auburn University months following the measurements. We continue to collaborate closely with theoreticians also funded by DOE-AMOS including the groups of F. Robicheaux, C.W. McCurdy, T. Resigno, A. Orel, and D. Haxton.

Recent Progress:

Electron driven Molecular Dynamics:

We have performed a number of dissociative electron attachment measurements on small molecules in collaboration with Prof. Mike Fogle at Auburn, where we have used momentum imaging of the resulting anion in order to explore the dissociation dynamics. Specifically, we have employed a momentum imaging technique to measure the dissociative electron attachment



to a number of small molecules including O_2 , CO_2 , and N_2O . By measuring the momentum distribution of the anion produced we are able to determine the kinetic energy release in the reaction as a function of emission angle over the full 4π solid angle of acceptance. This allows, for example, a comparison with theory that calculates the entrance amplitudes leading to the dissociative resonance being studied. We have found that the high angular resolution of our supersonic crossed-beam experiment has

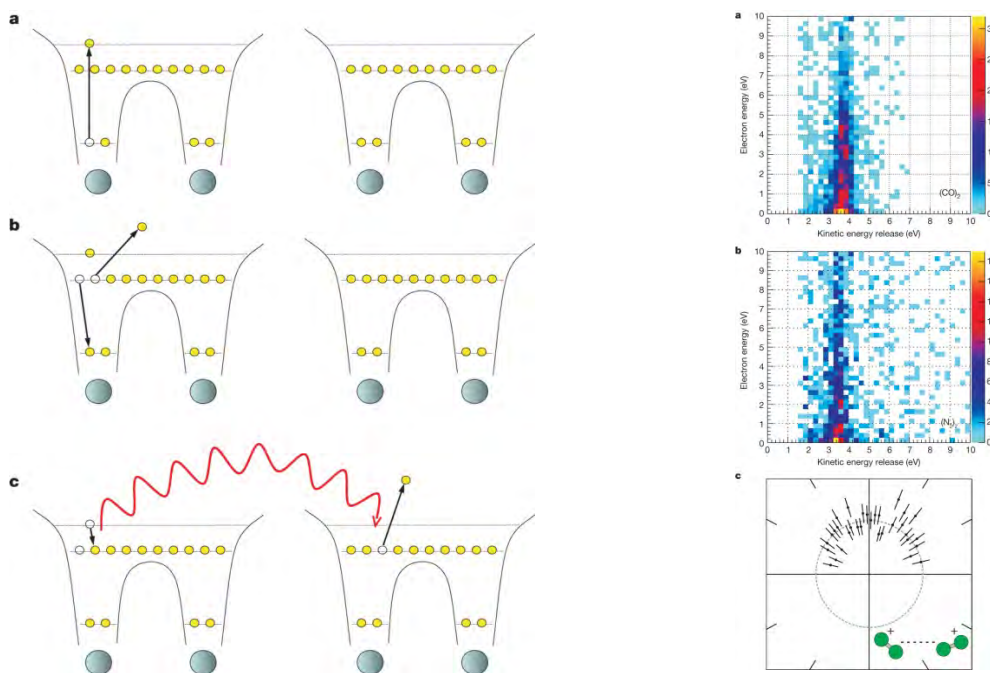
provided new insights into previous measurements of some systems, and has opened the door to

fruitful collaboration with the LBNL theoretical (listed above) and experimental group (Belkacem and Slaughter) also funded within the DOE-AMOS program.

One such example is shown in the figure on the previous page from our recently published results for dissociative electron attachment (DEA) to N_2O at the 2.3eV shape resonance resulting in O^- fragments (Ref. 6). (a) the coordinate system for orienting dissociation events. (b) a weighted momentum space O^- fragment distribution. From this data we can extract the angular distribution of fragments with respect to the incoming electrons, seen (c) and kinetic energy distribution (not shown here). (d) the potential energy landscape of the N_2O^- temporary negative ion state along with possible dissociation dynamics. The solid curve is a direct dissociation across a Renner-Teller reef with no significant bending dynamic, indicative of Π character. The dashed curve represents a significant bending upon dissociation, indicative of a Σ character.

Photoionization experiments at ALS:

Over the past year, Auburn has continued participating in the collaboration with the University of Frankfurt and LBNL groups in COLTRIMS experiments at the Advanced Light Source at LBNL. The most prominent example resulting from this joint effort is a work led by F. Trinter and T. Jahnke (Frankfurt) that was published in *Nature* (Details in Ref. 3). It was recently suggested that inter-coulombic decay (ICD) can be triggered efficiently and site-selectively by resonantly core-exciting a target atom, which then transforms through Auger decay into an ionic species with sufficiently high excitation energy to permit ICD to occur. Here we demonstrated experimentally that resonant Auger decay can indeed trigger ICD in dimers of both molecular nitrogen and carbon monoxide. Our experimental confirmation of this process and its efficiency may trigger renewed efforts to develop resonant X-ray excitation schemes for more localized and targeted cancer radiation therapy.



Previous Page Left: Shown is the series of events involved in resonant-Auger-driven ICD. a, One molecule (left) of the molecular dimer is core-excited. b, The core-excited state decays by a spectator Auger decay to a highly excited state of the molecular ion. c, ICD transfers the excitation energy to the molecular neighbour (right), where a low-energy ICD electron is emitted.

Previous Page Right: **a**, Kinetic energy release of $(\text{CO})_2$ versus energy of one of the two electrons created by ICD after resonant excitation and subsequent Auger decay at a photon energy of 287.4 eV (Π^* excitation of CO). The colour scale shows the intensity in counts. **b**, Same plot for $(\text{N}_2)_2$ recorded at a photon energy of 401.9 eV (Π^* excitation of N_2). **c**, Emission direction of the Auger electron with respect to the molecular axis of the N_2 dimer (with statistical error bars). The dimer is oriented horizontally, as depicted by the green icon. The grey circle is a line to guide the eye, corresponding to isotropic emission.

Future Plans:

We intend to pursue additional experiments as part of our work within the ALS-COLTRIMS collaboration and expand our efforts at Auburn to study electron driven phenomena. Here are some examples:

- Extend electron driven dynamics measurements to include liquid and complex targets (e.g. alcohols, formic acid, clusters)
- Study core-photoionization in similar systems to methane to explore whether or not the imaging effect observed in methane occurs elsewhere (e.g. H_2O , NH_3).
- Measure the Auger electrons in coincidence with fragments to produce molecular frame angular distributions for Auger electrons in order to better identify dissociative pathways following photoionization.
- Study core-hole localization in C_2H_6 using 3D MFPADS.
- Use larger polyatomic molecules (e.g. allene) to probe the limits of extending these measurements to systems of increasing complexity.
- Continue to be guided by and partner with theoreticians to study these fundamental processes.

Refereed Publications: Supported by DOE-AMOS (2011-present)

1. **Hydrogen and fluorine migration in photo-double-ionization** of 1,1-difluoroethylene (1,1- $\text{C}_2\text{H}_2\text{F}_2$) near and above threshold B. Gaire, I. Bocharova, F. P. Sturm, N. Gehrken, J. Rist, H. Sann, M. Kunitski, J. Williams, M. S. Schöffler, T. Jahnke, B. Berry, M. Zohrabi, M. Keiling, A. Moradmand, A. L. Landers, A. Belkacem, R. Dörner, I. Ben-Itzhak, and Th. Weber, *Phys Rev A* **89** 043423 (2014).
2. **Photo-double-ionization of ethylene and acetylene near threshold** B Gaire, SY Lee, DJ Haxton, PM Pelz, I Bocharova, FP Sturm, N Gehrken, M Honig, M Pitzer, D Metz, H-K Kim, M Schöffler, R Dörner, H Gassert, S Zeller, J Voigtsberger, W Cao, M Zohrabi, J Williams, A. Gatton, D Reedy, C Nook, Thomas Müller, AL Landers, CL Cocke, I Ben-Itzhak, T Jahnke, A Belkacem, Th Weber, *Phys Rev A* **89** 013403 (2014).
3. **Resonant Auger decay driving intermolecular Coulombic decay in molecular dimers**, F Trinter, MS Schöffler, H-K Kim, FP Sturm, K Cole, N Neumann, A Vredenburg, J Williams, I Bocharova, R Guillemin, M Simon, A Belkacem, AL Landers, Th Weber, H Schmidt-Böcking, R Dörner, T Jahnke, *Nature* **505** 664-666 (2014).

4. **Dissociative electron attachment to carbon dioxide via the $^2\Pi_u$ shape resonance**, A. Moradmand, D.S. Slaughter, D.J. Haxton, A.L. Landers, C.W. McCurdy, T.N. Rescigno, M. Fogle, A. Belkacem *Phys. Rev. A* **88** 032703 (2013).
5. **Dissociative-electron-attachment dynamics near the 8-eV Feshbach resonance of CO₂**, A. Moradmand, D. Slaughter, A.L. Landers, M. Fogle, *Phys. Rev. A* **88** 022711 (2013).
6. **Momentum imaging of dissociative electron attachment to N₂O**, A. Moradmand, A.L. Landers, M. Fogle, *Phys. Rev. A* **88** 012713 (2013).
7. **Momentum-imaging apparatus for the study of dissociative electron attachment dynamics** A. Moradmand, J. Williams, A. Landers, M. Fogle, *Review of Scientific Instruments* **84**, 033104 (2013).
8. **Ejection of quasi free electron pairs from the helium atom ground state by a single photon**, M. S. Schöffler, C. Stuck, M. Waitz, F. Trinter, T. Jahnke, U. Lenz, M. Jones, A. Belkacem, A.L. Landers, C.L. Cocke, J. Colgan, A. Kheifets, I. Bray, H. Schmidt-Böcking, R. Dörner, and Th. Weber *Phys. Rev. Lett.* **111** 013003 (2013).
9. **Probing the Dynamics of Dissociation of Methane Following Core Ionization Using Three-Dimensional Molecular Frame Photoelectron Angular Distributions**, J. B. Williams, C. S. Trevisan, M. S. Schöffler, T. Jahnke, I. Bocharova, H. Kim, B. Ulrich, R. Wallauer, F. Sturm, T. N. Rescigno, A. Belkacem, R. Dörner, Th. Weber, C. W. McCurdy, and A.L. Landers, *J. Phys. B: At. Mol. Opt. Phys.*, **45** 194003 (2012).
10. **Calculated and measured angular correlation between photoelectrons and Auger electrons from K-shell ionization**, F. Robicheaux, M. P. Jones, M. S. Schöffler, T. Jahnke, K. Kreidi, J. Titze, C. Stuck, R. Dörner, A. Belkacem, Th. Weber, and A.L. Landers *J. Phys. B: At. Mol. Opt. Phys.*, **45** 175001 (2012).
11. **Multi fragment vector correlation imaging - A proposal to search for hidden dynamical symmetries in many-particle molecular fragmentation processes**, F. Trinter, L. Ph. H. Schmidt, T. Jahnke, M. S. Schöffler, O. Jagutzki, A. Czasch, J. Lower, T. A. Isaev, R. Berger, A. L. Landers, Th. Weber, R. Dörner, H. Schmidt-Böcking *Molecular Physics* **110** 1863 (2012).
12. **Imaging polyatomic molecules in three dimensions using molecular frame photoelectron angular distributions**, J. B. Williams, C. S. Trevisan, M. S. Schöffler, T. Jahnke, I. Bocharova, H. Kim, B. Ulrich, R. Wallauer, F. Sturm, T. N. Rescigno, A. Belkacem, R. Dörner, Th. Weber, C. W. McCurdy, and A.L. Landers, *Phys. Rev. Lett.* **108** 233002 (2012).
13. **Dynamic modification of the fragmentation of autoionizing states of O⁺²**, W. Cao, G. Laurent, S. De, M. Schöffler, T. Jahnke, A. S. Alnaser, I. A. Bocharova, C. Stuck, D. Ray, M. F. Kling, I. Ben-Itzhak, Th. Weber, A. L. Landers, A. Belkacem, R. Dörner, A. E. Orel, T. N. Rescigno, and C. L. Cocke, *Phys. Rev. A* **84** 053406, (2011).
14. **Matter wave optics perspective at molecular photoionization: K-shell photoionization and Auger decay of N₂**, M. Schöffler, T. Jahnke, J. Titze, N. Petridis, K. Cole, L. Ph. H. Schmidt, A. Czasch, O. Jagutzki, J.B. Williams, C.L. Cocke, T. Osipov, S. Lee, M.H. Prior, A. Belkacem, A.L. Landers, H. Schmidt-Böcking, R. Dörner, and Th. Weber, *New Journal of Physics* **13** 095013 (2011).
15. **Production of excited atomic hydrogen and deuterium from H₂, HD and D₂ photodissociation** R Machacek , V M Andrianarijaona , J E Furst , A L D Kilcoyne , A L Landers , E T Litaker , K W McLaughlin and T J Gay *J. Phys. B: At. Mol. Opt. Phys.* **44** 045201 (2011).

Exploiting Non-equilibrium Charge Dynamics in Polyatomic Molecules to Steer Chemical Reactions

Wen Li (Lead PI)

Department of Chemistry, Wayne State University, Detroit, MI, 48202

wli@chem.wayne.edu

Raphael D. Levine (PI)

Department of Chemistry and Biochemistry, University of California, Los Angeles, CA, 90095

rafi@chem.ucla.edu

Henry C. Kapteyn (PI)

JILA, University of Colorado at Boulder (PI), Boulder, CO, 80309

Henry.Kapteyn@Colorado.edu

H. Bernhard Schlegel (PI)

Department of Chemistry, Wayne State University, Detroit, MI, 48202

hbs@chem.wayne.edu

Françoise Remacle (Collaborator)

Department of Chemistry, B6c, University of Liège, Liège, Belgium

FRemacle@ulg.ac.be

Margaret M. Murnane (Collaborator)

JILA, University of Colorado at Boulder (PI), Boulder, CO, 80309

Margaret.Murnane@Colorado.edu

Program Scope: The main objectives of this project are to achieve two major research goals of ultrafast science: 1. Creating and probing photo-induced charge migration dynamics of pure electronic origin on the attosecond to few femtoseconds time scales and studying the role of non-equilibrium charge distributions in inducing selectivity of chemical reactions in polyatomic molecules. 2. Achieving mode-selective chemistry in polyatomic molecules using intense ultrashort mid-infrared pulses.

Proposed Studies: For the first objective, coherent electronic wave packets due to the superposition of a few electronic states in molecular cations will be created with strong field photoionization by ultrashort optical pulses and the subsequent charge migration along the molecular backbone will be monitored by various advanced methods including a photoionization probe implemented with intense attosecond pulse trains (APT) coupled with ion-electron coincidence measurements and attosecond transient absorption with high energy attosecond pulses. In the APT ionization experiments, the time-resolved asymmetry parameter of the photoelectron momentum distributions will reveal the charge oscillation dynamics. The central energy and the temporal structure of the APTs will be carefully tuned to yield good sensitivity to the ultrafast electronic dynamics. Because our theoretical models simulate both the pump and the probe steps with minimum approximations, they will provide realistic experimental parameters

and are also well suited to extract electronic dynamics from experimental observations[1-3]. Raphael Levine and Françoise Remacle describe the detailed theoretical background and methods in a separate abstract. In the transient absorption experiments, the time-resolved spectra reflect the instantaneous electron density with element and site specificity and thus charge migration dynamics will be captured in real time. A bright, phase matched attosecond source in the a few hundred eV range has been developed[4-6]. Employing both probing methods, the nuclear dynamics following coherent excitation of electronic states will be monitored on longer time scales to study the influence of transient non-equilibrium charge distributions on the outcome of a chemical reaction. Control schemes will be designed to steer chemical reactions. Systems of interest include the polyatomic molecules 1-azabicyclo[3.3.3]undecane (ABCU, C₁₀H₁₉N) and 2-phenylethyl-N,N-dimethylamine (PENNA), that have already been explored by our team in preliminary work.

For the second goal, we have recently shown in models that mode-selective chemistry can be achieved using intense mid-IR laser excitation through charge polarization on the ground electronic state[7-9]. When the intensity of the excitation laser is much higher than those employed in conventional infrared multiphoton dissociation (IRMPD), nuclear kinetic energy can be efficiently pumped into specific vibrational mode(s) as the result of the very large charge polarization. Molecular axial alignment/orientation is essential to direct the input kinetic energy. Because the large kinetic energy forces reactions to proceed in a prompt fashion, a selected reaction pathway can be complete well within one picosecond, defeating the detrimental effect of intramolecular vibrational redistribution (IVR). The study will be carried out in molecular ions to minimize complications from competing strong field ionization. Mid-IR laser pulses at 3-4 μm will be focused to reach 10^{13} - 10^{14} W/cm² to achieve mode-selectivity in aligned polyatomic molecules. Systems of interest include iodobenzene dication and formyl chloride cation. Additional systems will be designed using computation and simulations.

By exploiting the state-of-the-art in ultrafast laser technologies and attosecond pulse production techniques as well as the theoretical methodologies that we already have available in our laboratories, the proposed research aims to resolve a long-standing challenge in ultrafast molecular science and promises significant advances in understanding, predicting and controlling chemical reactions.

References:

- [1] B. Mignolet, R. D. Levine, and F. Remacle, *Phys. Rev. A* **88**, 021403(R) (2014).
- [2] B. Mignolet, R. D. Levine, and F. Remacle, *J. Phys. B* **47**, 124011 (2014).
- [3] M. Ben-Nun, T. J. Martínez, and R. D. Levine, *J. Phys. Chem. A* **101**, 7522 (1997).
- [4] T. Popmintchev *et al.*, *Nature Photonics* **4**, 822 (2010).
- [5] T. Popmintchev *et al.*, *Science* **336**, 1287 (2012).
- [6] M.-C. Chen *et al.*, *Proc. Natl. Acad. Sci. U. S. A.* **111**, E2361 (2014).
- [7] S. K. Lee *et al.*, *J. Phys. Chem. Lett.*, 2541 (2012).
- [8] S. K. Lee, W. Li, and H. B. Schlegel, *Chem. Phys. Lett.* **536**, 14 (2012).
- [9] S. K. Lee, H. B. Schlegel, and W. Li, *J. Phys. Chem. A* **117**, 11202 (2013).

Raphael D. Levine and Françoise Remacle*
Department of Chemistry and Biochemistry,
University of California Los Angeles, Los Angeles, CA 90095-1569
rafi@chem.ucla.edu

Exploiting Non-equilibrium Charge Dynamics in Polyatomic Molecules to Steer Chemical Reactions

The motion of the electrons determines the forces that act on the atoms of a molecule. Our work seeks to understand how to manipulate the dynamics of the electrons so that we have the ability to alter and to control the onset of chemistry. This control operates on ultrafast time-scales that extend into the few femtosecond domain and requires an electronic motion that is driven out of equilibrium followed by an onset of a motion where the electrons and nuclei are coupled. Our work seeks to model and control this brand new regime of dynamics that can lead to novel, improved and enhanced, chemical reactivity. We here report on our preliminary work that sought to demonstrate the realistic pumping and probing of the non equilibrium electronic dynamics previous to the onset of nuclear motion. In particular we demonstrated that when the initial ultrafast excitation is correctly described it is possible to excite significant electronic disequilibrium. We show this all the way to our recent work on C60 where we needed over 400 stationary states as a basis to represent the non stationary electronic wavepacket. We then report on very preliminary results on the onset of coupling to nuclear dynamics in a diatomic molecule.

Our work is part of an interwoven experimental/theoretical/computational program coordinated by Wen Li of Wayne State University.

Since the seminal work of Born and Oppenheimer (1927) we regard the electrons as instantly adjusting to the given position of the nuclei. Deviations from this limit are possible but these are localized in terms of the molecular geometry and requires a nuclear motion to induce them. In photochemistry we change the forces by arranging for a new equilibrium, stationary state of the electrons. In 2006 we proposed exploring a post Born Oppenheimer regime.¹ The purpose is to induce ultrafast dynamics in molecular systems, on the attosecond timescale, where electrons are pumped to a non-stationary state by a few-cycle light field. On a longer time scale one can study the coupling of electronic and nuclear degrees of freedom, all the way to a measurable chemical outcome. To achieve these aims we seek to demonstrate by concrete realistic computations that it is possible to use non-equilibrium excitation of electrons to drive new chemical and transport processes. Then, through modeling, we take these ideas from the realm of proof-of-principle in simple molecules to systems that are large enough to be of practical interest.

* Permanent address : Department of Chemistry, University of Liège, B4000 Liège, Belgium. fremacle@ulg.ac.be

Our work seeks to explore new schemes and examine new ideas, based on the control of electron dynamics,

- for bond rearrangement and dissociation in photoselective attochemistry,
- for charge-directed reactivity^{2,3} in extended systems (e.g. in biomolecules)
- for charge migration in modular molecules and molecular devices.⁴

The achievement of these objectives requires developing a better understanding of:

the correlation between electronic and nuclear motion. We need to understand how the non-equilibrium electron dynamics is expressed as the forces on atomic nuclei in molecular systems and we need to do it for systems of increasing sizes. The problem for modeling, more technically stated, is that, for a non-equilibrium electronic state, the notion of a single potential energy surface governing atomic motion breaks down. Several electronic states are typically involved in the dynamics during and after an ultrafast excitation. We need to revisit the notion of a force a notion that is only defined within the Born-Oppenheimer approximation.

the correlation between electron and hole dynamics in ionization processes. We need a better understanding of hole-electron dynamics upon ultrafast excitation of the electron density. Ionization will be used both to prepare reactive cations where the electron motion is driven out of equilibrium by ionization and for probing the molecular dynamics after the electron density has been taken out of equilibrium by an ultrashort excitation.

the interplay of multiple time scales (from atto- to picosecond) and how to control the dynamics of molecules subject to rapidly varying fields.

Our first figure, figure 1, is from the original proposal¹ showing few fs charge migration along the backbone of a tetra peptide after instantaneous ionization of a chromophoric amino acid Tyr at one end. Subsequent to this we performed a much more high level computation where both the ionization dynamics and the probing and described correctly for the bifunctional molecule PENNA, figure 2.⁶ Probing is by an as ionization to a dication. The angular distribution of the photoelectron is used to probe the charge migration along the molecular backbone.

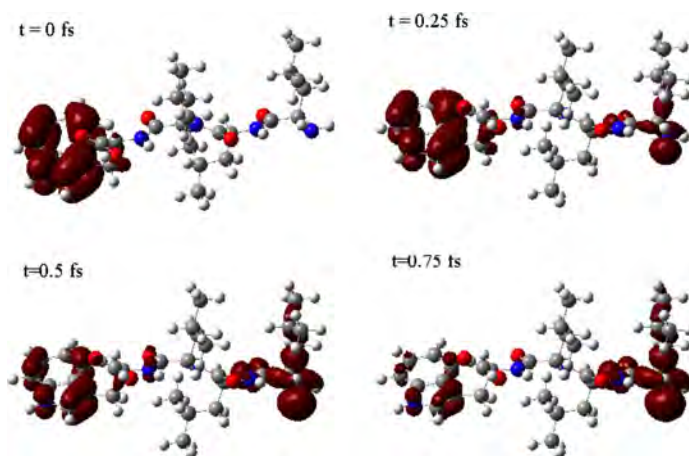


Figure 1. Hole migration in the tetrapeptide cation computed in the sudden ionization limit of the HOMO of the neutral, which is localized on the chromophore Tyrosine end¹.

The half period of the hole migration to the amine end is 0.75 fs. The computation is done for nuclei frozen at the equilibrium geometry of the neutral.

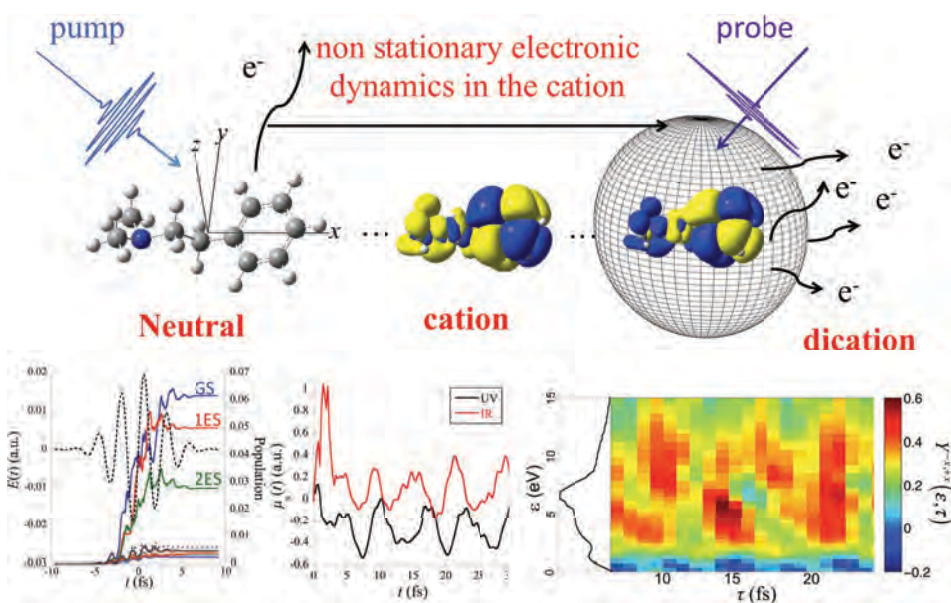


Figure 2. Top : Pump-probe scheme in the modular system PENNA. The pump induces dynamics in the lowest states of the cation by photoionization. The cation non-equilibrium density is probed by photoionization to the dication states using a XUV atto pulse. Bottom left: the population in the three lowest states of PENNA+ created multiphoton ionization by an IR pulse. Middle: the resulting time dependent full polarization, computed for an IR pump (left), but also for a UV pump. Right : The resulting asymmetry parameter for ionization at the phenyl or at the amine moiety, computed as a function of the time-delay between the pump and the probe. The beatings in the anisotropy parameter follow the beating of the charge density of the coherent superposition of states of the cation as shown in the middle panel. From ref. ⁶

Other examples that we recently studies include a high level description of electron dynamics in a tetra peptide.⁷ Here we show results for a functionalized C60 because this is a state of the art computation involving the high density of electronically excited states below the ionization threshold that is below fragmentation threshold, figure 3.

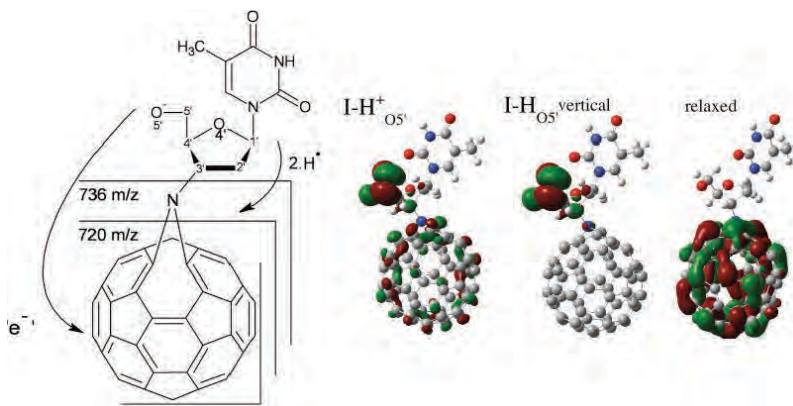


Figure 3. Left: Deoxythymidine-fullerene complex deprotonated on O5 and isocontour amplitudes of the highest occupied MO in the protonated and deprotonated species, computed at the geometry of the protonated one and relaxed. In the deprotonated species, the negative charge moves to the C₆₀ subunit upon geometry relaxation. Adapted from ref. ⁸

Describing the onset of coupling to nuclear motion is demonstrated, Figure 4.

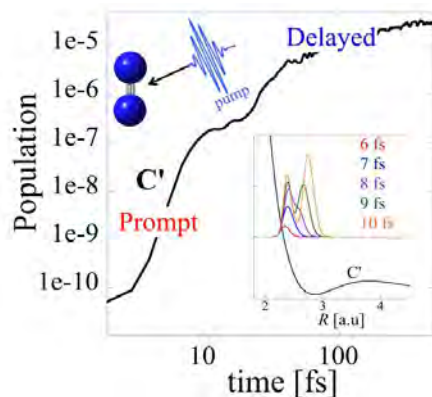


Figure 4. Population in the predissociating triple excited electronic state C' of the N₂ following excitation by an ultrashort XUV pulse⁹. The dissociation exhibits a prompt (on a few fs time scale, see inset) and a delayed branch (on a ps time scale). The prompt dissociation is a probe of the non-equilibrium electron dynamics induced by the pump pulse. The delayed dissociation results from the delocalization of the initial wave packet on the electronic manifold. This behavior is well captured by a Lindeman kinetic model.

References

1. Remacle, F.; Levine, R. D., 2006 *Proc. Natl. Acad. Sci. USA* **103**, 6793-6798.
2. Remacle, F.; Levine, R. D.; Schlag, E. W.; Weinkauff, R., 1999 *J. Phys. Chem. A* **103**, 10149-10158.
3. Remacle, F.; Levine, R. D.; Ratner, M. A., 1998 *Chem. Phys. Lett.* **285**, 25-33.
4. Remacle, F.; Levine, R. D., 2007 *J. Phys. Chem. C* **111**, 2301-2309.
5. Remacle, F.; Levine, R. D., 2011, *Phys Rev A* **83**
6. Mignolet, B.; Levine, R. D.; Remacle, F., 2014 *J. Phys. B: At. Mol. Opt. Phys.* **47**, 124011.
7. Kuś, T.; Mignolet, B.; Levine, R. D.; Remacle, F., 2013 *J. Phys. Chem. A* **117**, 10513-10525.
8. Greisch, J.-F.; Weinkauff, R.; Pauw, E. D.; Kryachko, E. S.; Remacle, F., 2007 *Is. J. Chem.* **47**, 25-35.
9. Muskatel, B. H.; Remacle, F.; Levine, R. D., 2014 *Chem. Phys. Lett.* **601**, 45-48.

Probing electron-molecule scattering with HHG: Theory and Experiment

Robert R. Lucchese, Department of Chemistry, Texas A&M University, College Station, TX, 77843, lucchese@mail.chem.tamu.edu

Erwin Poliakoff, Department of Chemistry, Louisiana State University, Baton Rouge, LA 70803, epoliak@lsu.edu

Program Scope

Understanding electron-molecular scattering dynamics is the overall theme of our program. In recent years, our primary focus was on one-photon molecular ionization and the coupling between vibrational and electronic motion. In particular we studied vibrationally resolved one-photon ionization dynamics in larger molecular systems. This allowed us to disentangle the geometry and energy dependence of the dipole matrix elements that couple the initial bound state to the continuum scattering state. The experimental approach was to obtain vibrationally resolved photoelectron spectra over a broad range of incident photon energies by exploiting the high brightness capabilities at the Advanced Light Source (ALS). On the theory side, we explicitly solved the electron-molecular ion scattering equations to compute the corresponding vibrationally specific matrix elements using the adiabatic approximation. Currently, we have begun to study electron-molecule collisions that occur in high-field processes such as high harmonic generation (HHG) and recollision spectroscopy. Both experimentally and theoretically, this work is being performed in collaboration with the McDonald Laboratory at Kansas State University. All of these research efforts benefit the Department of Energy because the results elucidate structure/spectra correlations that will be indispensable for probing complex and disordered systems of interest to DOE such as clusters, catalysts, reactive intermediates, transient species, and related species.

Recent Progress

High Resolution Photoelectron Spectroscopy

As larger systems are considered, the experimental study of vibrational resolved photoionization cross sections is limited by the increase in the density of states that makes the extraction of vibrationally specific cross sections difficult. This is caused by the number of thermally accessible low-lying tautomers in large molecules, the increase in the density of electronic states of the molecular ion, and to the increase in the density of vibrational states. These limitations are seen in our recent study of the high resolution photoelectron spectrum with partial vibrational resolution of a series of pyrimidine-type nucleobases: thymine, uracil and cytosine. The improved resolution allowed us to identify the electronic origins for the outermost valence electronic states. In the case of cytosine, there has also been much disagreement over which tautomers exist in the gas phase. Better resolution combined with recently published calculated spectra of cytosine tautomers gave insight into which cytosine tautomers exist in the gas phase. Striking similarities in the spectral features of all three pyrimidine-type nucleobases lead us to conclude that the features in the cytosine photoelectron spectrum are not due to contributions from multiple tautomers but instead are from unresolved vibrational progressions. Since these features are practically the same in the spectra for all three molecules, we further

conclude that the dominant vibrational progressions must be due to the pyrimidine back-bone, which all three molecules have in common

Non-Franck-Condon Vibrational Branching Ratios

An example of a recently completed study of vibrationally resolved photoionization is our study of acrolein. In the simplest view of molecular photoionization, one assumes that vibrational and photoelectron motion are decoupled, which leads to the Franck-Condon approximation. Nonresonant and resonant processes can result in coupling molecular vibration and photoelectron motion, with the result that vibrational branching ratios become dependent on photon energy, and that forbidden vibrations can be excited. A convenient way to express the extent of the breakdown of the Franck-Condon approximation for a given mode, represented by the variable q , is via the electronic factor F which is just the logarithmic derivative of the cross section with respect to changes in the coordinate q . This quantity, in the harmonic approximation, can be related to the vibrational branching ratio.

In our experimental and theoretical study of the non-Franck-Condon behavior and electronic factors in the photoionization of acrolein, we found evidence of two localized low energy σ^* resonances, which interact to form two resonant states. Excitation of these states leads to significant non-Franck-Condon effects in the excitation of C-C vinyl stretch and, to a lesser extent, in other modes to which the energies and widths of these resonances are sensitive.

Molecular Aspects of HHG

We have made considerable progress, in collaboration with Profs. Trallero and Lin at the McDonald Laboratory in the study of molecular HHG. We have initiated studies of high harmonic generation in relatively complex molecules, and this work is progressing very well. Preliminary work on the HHG spectrum SF₆ observed noticeable structure in the experimental spectrum. Changing the gas jet position changes the macroscopic propagation and the effective trajectories of the returning electron. The one feature that is consistently present in the experimental data is the minimum in the HHG spectrum at the 17th harmonic. In the theory we have applied the quantitative rescattering (QRS) theory to isolated molecules and considered the ionization of the electrons from the three most weakly bound orbitals, i.e. the highest occupied molecule orbital (HOMO), the HOMO-1, and the HOMO-2. These three orbitals have ionization potentials that are all within 1.5 eV of each other. Predicted single molecule HHG spectra computed using the QRS were not in satisfactory agreement with the experimental data.

The theoretical calculations were performed using relatively simple single-channel static-exchange type calculations for the recombination step in the three step model which is the basis of the QRS. To understand if the source of this disagreement is in the limitations of the recombination calculation, we have explored the validity of the main assumptions in the calculations. First we have considered a calculation including the channel coupling between the different valence ionization channels, which all could conceivably contribute to the HHG spectrum. We found that the single-channel calculations tended to overestimate the strength of the resonances compared to the coupled channel results. We also have studied the effects of the vibrational average resulting from the ground vibrational wave function. The cross section from the $5t_{1u}$ subshell of SF₆ has a narrow resonance at a photon energy of ~ 38 eV for photoelectrons in the e_g photoelectron continuum. Averaging over the symmetric vibration resulted in 15% reduction of the peak resonant cross section, while that over the asymmetric stretching vibration caused 45% reduction. The SF₆ geometry, stretched asymmetrically, supports two shape

resonances which correspond to the degenerate e_g resonance in equilibrium geometry. These two resonances are further moved apart with asymmetric stretching, which in turn causes the reduction of cross section when averaged. We found reasonable agreement between theory and experiment for the one-photon ionization, which suggests that the asymmetric nuclear vibrations reduces the effect of the e_g resonance on the one-electron ionization process and might be important in a QRS treatment of the HHG intensities.

Grid Base Scattering Calculations

Another component of our research program is the development of a next-generation electron-molecule scattering code. This work is being done in collaboration with Bill McCurdy and Tom Rescigno of the Atomic, Molecular, and Optical Theory group at Lawrence Berkeley National Laboratory (LBNL). This code will be based on the complex Kohn approach with a numerical grid-based representation of the scattering wave functions. We have performed preliminary model calculations studying iterative methods for obtaining accurate scattering matrices from the complex Kohn method. Additionally, we have analyzed the methods for implementing an overset grid representation where centered on each nucleus in a molecule there is a local grid which has spherical symmetry around that center. Additionally, these atomic centered grids are combined with an encompassing grid which connects the molecular region and asymptotic regions. These different grids are partially overlapping, thus they are referred to as overset grids.

Future Plans

We will continue to expand our efforts on the studies of molecular HHG. In addition to considering new target molecules, we will also consider variations in parameters that affect the HHG spectrum including laser power, polarization (i.e., ellipticity), and focal position within the target molecular beam. We are also planning to incorporate pump-probe capabilities into our HHG work. Theoretically, we will consider the effects of correlation and vibrational averaging on the recombination step of HHG within the QRS model. The next step in the development of the new scattering code is to implement the overset grid approach for the computation of electron scattering dynamics at the static-exchange level for molecular systems with up to ~ 20 atoms. Subsequently, correlation effects will be incorporated into the new code.

Publications in 2012-2014 Acknowledging Support from DOE

1. Cheng Jin, Julien B. Bertrand, R. R. Lucchese, H. J. Wörner, Paul B. Corkum, D. M. Villeneuve, Anh-Thu Le, and C. D. Lin, Intensity dependence of multiple orbital contributions and shape resonance in high-order harmonic generation of aligned N_2 molecules, *Phys. Rev. A* **85**, 013405:1-7 (2012).
2. Hong Xu, U. Jacovella, B. Ruscic, and S. T. Pratt, and R. R. Lucchese, Near-Threshold Shape Resonance In The Photoionization Of 2-Butyne, *J. Chem. Phys.* **136**, 154303:1-10 (2012).
3. Arnaud Rouzée, Freek Kelkensberg, Wing Kiu Siu, Georg Gademann, R. Lucchese, Marc J. J. Vrakking, Photoelectron kinetic and angular distributions for the ionization of aligned molecules using a HHG source, *J. Phys. B* **45**, 074016:1-11 (2012)
4. C. Wang, M. Okunishi, R. R. Lucchese, T. Morishita, O. I. Tolstikhin, L. B. Madsen, K. Shimada, D. Ding, K. Ueda, Extraction of Electron-Ion Differential Scattering Cross Sections

- for C₂H₄ by Laser-Induced Rescattering Photoelectron Spectroscopy, *J. Phys. B* **45**, 131001:1-5 (2012).
5. J. A. Lopez-Dominguez, D. Hardy, A. Das, E. D. Poliakoff, A. Aguilar, and R. R. Lucchese, Mechanisms of Franck-Condon breakdown over a broad energy range in the valence photoionization of N₂ and CO, *J. Electron Spectrosc. Relat. Phenom.* **185**, 211 (2012).
 6. C. D. Lin, Cheng Jin, Anh-Thu Le, and R. R. Lucchese, Probing molecular frame photoelectron angular distributions via high-order harmonic generation from aligned molecules, *J. Phys. B* **45**, 194010:1-9 (2012).
 7. R. R. Lucchese, H. Fukuzawa, X.-J. Liu, T. Teranishi, N. Saito, and K. Ueda, Asymmetry in the molecular-frame photoelectron angular distribution for oxygen 1s photoemission from CO₂, *J. Phys. B* **45**, 194014:1-11 (2012).
 8. Anh-Thu Le, T. Morishita, R. R. Lucchese, and C. D. Lin, Theory of high harmonic generation for probing time-resolved large-amplitude molecular vibrations with ultrashort intense lasers, *Phys. Rev. Lett.* **109**, 203004:1-5 (2012).
 9. M. C. H. Wong, A.-T. Le, A. F. Alharbi, A. E. Boguslavskiy, R. R. Lucchese, J.-P. Brichta, C.D.Lin, and V.R.Bhardwaj, High Harmonic Spectroscopy of the Cooper Minimum in Molecules, *Phys. Rev. Lett.* **110**, 033006:1-5 (2013).
 10. Anh-Thu Le, R. R. Lucchese, and C. D. Lin, Quantitative rescattering theory of high-order harmonic generation for polyatomic molecules, *Phys. Rev. A* **87**, 063406:1-9 (2013).
 11. Ralph Carey, Robert R. Lucchese, and F. A. Gianturco, Electron scattering from gas phase cis-diamminedichloroplatinum(II): quantum analysis, *J. Chem. Phys.* **138**, 204308:1-10 (2013).
 12. S. Marggi Poullain, K. Veyrinas, P. Billaud, M. Lebech, Y. J. Picard, R. R. Lucchese and D. Dowek, The role of Rydberg states in Photoionization of NO₂ and (NO⁺, O⁻) Ion Pair Formation induced by One VUV Photon, *J. Chem. Phys.* **139**, 044311:1-12 (2013).
 13. Anh-Thu Le, R. R. Lucchese, and C. D. Lin, High-order-harmonic generation from molecular isomers with midinfrared intense laser pulses, *Phys. Rev. A* **88**, 021402:1-5(R) (2013).
 14. J. Jose and R. R. Lucchese, Study of resonances in the photoionization of Ar@C₆₀ and C₆₀, *J. Phys. B* **46**, 215103:1-7 (2013).
 15. K. Veyrinas, C. Elkharrat, S. Marggi Poullain, N. Saquet, D. Dowek, R. R. Lucchese, G. A. Garcia and L. Nahon, Molecular polarimetry: accurate full polarization ellipse determination by electron-ion vector correlations, *Phys. Rev. A* **88**, 063411:1-5 (2013).
 16. J. Jose, R. R. Lucchese, and T. N. Rescigno, Interchannel coupling effects in the valence photoionization of SF₆, *J. Chem. Phys.* **139**, 204305:1-10 (2014).
 17. S. Marggi Poullain, C. Elkharrat, W. B. Li, K. Veyrinas, J.C. Houver, C. Cornaggia, T. N. Rescigno, R. R. Lucchese and D. Dowek, Recoil frame photoemission in multiphoton ionization of small polyatomic molecules: Photodynamics of NO₂ probed by 400 nm femtosecond pulses, *J. Phys. B* **47**, 124024:1-18 (2014).
 18. M.Okunishi, R. R. Lucchese, T. Morishita, and K. Ueda, Rescattering photoelectron spectroscopy of small molecules, *J. Electron Spectrosc. Relat. Phenom.* **195**, 313-319 (2014).
 19. Jesús A. López-Domínguez, Robert R. Lucchese, K. D. Fulfer, David Hardy, E. D. Poliakoff, and A. A. Aguilar, Vibrationally specific photoionization cross sections of acrolein leading to the \tilde{X}^2A' ionic state, *J. Chem. Phys.* **141**, 094301:1-7 (2014).

Program Title:**"Properties of actinide ions from measurements of Rydberg ion fine structure"****Principal Investigator:**

Stephen R. Lundeen
 Dept. of Physics
 Colorado State University
 Ft. Collins, CO 80523-1875
 lundeen@lamar.colostate.edu

Program Scope:

This project determines certain properties of chemically significant Uranium and Thorium ions through measurements of fine structure patterns in high-L Rydberg ions consisting of a single weakly bound electron attached to the actinide ion of interest. The measured properties, such as polarizabilities and permanent moments, control the long-range interactions of the ion with the Rydberg electron or other ligands. The ions selected for initial study in this project, U^{6+} , U^{5+} , Th^{4+} , and Th^{3+} , all play significant roles in actinide chemistry, and are all sufficiently complex that *a-priori* calculations of their properties are suspect until tested. The measurements planned under this project serve the dual purpose of 1) providing data that may be directly useful to actinide chemists and 2) providing benchmark tests of relativistic atomic structure calculations. In addition to the work with U and Th ions, which takes place at the J.R. Macdonald Laboratory at Kansas State University, a parallel program of studies with stable singly-charged ions takes place at Colorado State University. These studies are aimed at clarifying theoretical questions connecting the Rydberg fine structure patterns to the properties of the free ion cores, thus directly supporting the actinide ion studies. In addition, they provide training for students who can later participate directly in the actinide work.

Recent Progress:

Our original project goal was to determine properties of the Rn-like and Fr-like ions of Th and U (Th^{4+} , Th^{3+} , U^{6+} , U^{5+}), as well as properties of the Ni^+ ion, whose Rydberg spectra is similar in complexity to that of the Fr-like ions. We expected the Fr-like ion studies to be much more difficult than the Rn-like ion studies, since the Fr-like ions have $J=5/2$ ground states while the Rn-like ions have $J=0$ ground states, and the number of discrete High-L Rydberg levels for each value of L is $2J+1$. We have now completed successfully the studies of the Th ions and the Ni^+ ion, using both the optical RESIS technique and the more precise microwave/optical RESIS technique. The final results are reported in publications 4, 5, and 6 listed below. In addition, we have reported, in publication 3 below, a quite general derivation of the expected form of the fine structure patterns in high-L Rydberg states bound to ions of any value of J, which clarifies the connection between the spectroscopic measurements and the ion properties.

Unfortunately, we have not yet been able to learn anything about the properties of the two U ions. The case of Rn-like U^{6+} is the most surprising since we expected it to be only slightly more difficult than the successful study of Th^{4+} . In both studies, the only source of information about the core are the frequency differences between the lower L

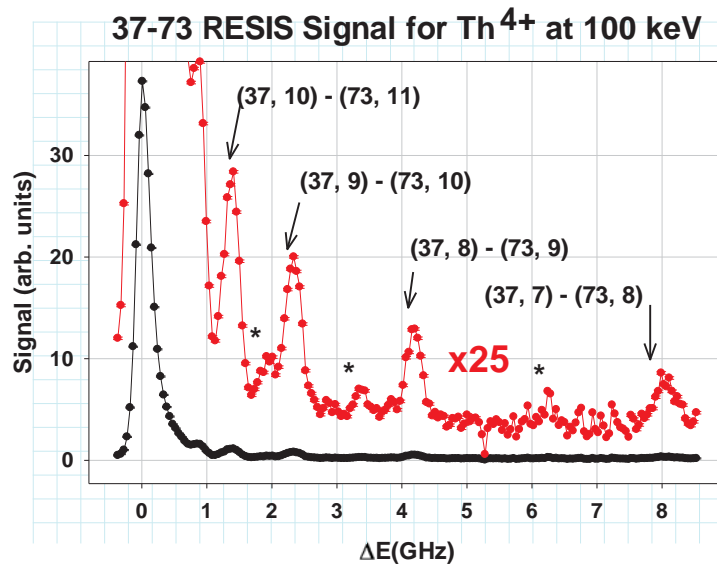


Fig. 1. RESIS excitation signals observed with Rydberg Th^{3+} ions, exciting the 37-73 transitions. The signals in red have been magnified by a factor of 25. Note that the resolved transitions, corresponding to excitation of individual L levels in $n=37$ are 0.5 -3% of the unresolved High-L signal. The x-axis shows the frequency difference between the Doppler-tuned CO_2 laser and the hydrogenic transition frequency between 37 and 73 levels.

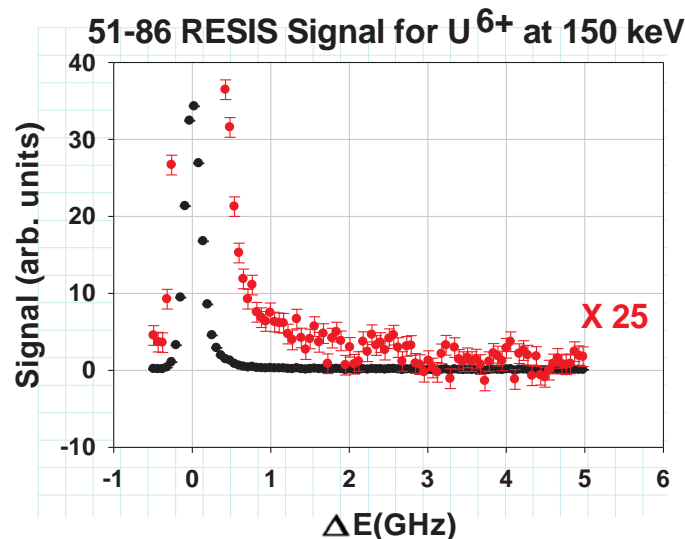


Fig. 2. RESIS excitation signals observed with Rydberg U^{5+} ions, exciting the 51-86 transitions. As in Fig. 1, the signals in red have been magnified by a factor of 25 and the x-axis shows the frequency difference of the Doppler-tuned CO_2 laser from the hydrogenic transition frequency. Note that the resolved signals, if any, are much smaller than in Fig. 1, and do not conform to the simple pattern expected.

RESIS excitations resolved from the much larger RESIS signal corresponding to unresolved excitation of the highest L levels. For the 37-73 RESIS transition of Rydberg electrons bound to Th^{4+} these signals, illustrated in Fig. 1, were several percent of the unresolved high-L signal. For the 51-86 RESIS transition of Rydberg electrons bound to U^{6+} , illustrated in Fig. 2, these signals were much smaller, less than 0.5% of the high-L

signal, and they also failed to present the same type of simple pattern seen in Fig. 1.

Compounding the difficulty posed by the small signals, The U signals were also much more difficult to observe because of a large background that dominated the Signal to Noise of the RESIS signals. Over the past year, we have made considerable progress in understanding the source of that background and reducing it. The dominant cause of the background is the presence of metastable Rn-like ions in the beams extracted from our ECR ion source. These metastable ions capture Rydberg electrons in our Rydberg target, just like the ground state ions in the beam, but unlike the Rydberg states formed with ground state cores, those formed with metastable cores can autoionize after capture. If that autoionization occurs within our detector, it produces a background. The electric fields in the detector that are necessary to Stark ionize the upper levels of the RESIS transition also have the effect of Stark mixing the more stable high-L metastable Rydberg ions that survive to the detector and enhancing their rate of autoionization, producing the background. Such a background is present for both Rn-like ions, Th^{4+} and U^{6+} , but it is much more troublesome in the U^{6+} case because of the smaller resolved signals.

In order to reduce the background, we constructed two additional electric field regions that intercept the metastable Rydberg ions before they reach our detector, Stark mixing them and enhancing their autoionization rate and thereby reducing the background. With these devices, we achieved a reduction by a factor of 3-4 of the background rate, and a comparable reduction in the time necessary to attain a given noise level.

Using these new devices, we were also able to measure the fraction of Rydberg states that contain metastable cores, from which we can infer the metastable fraction of the initial ion beam extracted from the ECR. This appears to be information that is difficult to obtain in any other way. In the case of U^{6+} , for example, more than half of the initial Rydberg beam appears to contain metastable core ions. We were also able to determine, in the case of U^{6+} , that a very large fraction (~95%) of the metastable Rydberg ions autoionize before reaching the detector. This seems to eliminate one of the hypotheses we had proposed to explain the small size and puzzling shape of the U^{6+} resolved RESIS signals, the dilution of the signal by more complex signals from metastable Rydberg ions. On reflection, however, we realized that the "metastable dilution" hypotheses could still be correct IF there are metastable Rydberg levels that are stable against autoionization. In U^{6+} , the metastable levels consist of 1 hole in the 6p shell and one 5f valence electron, forming 12 even parity terms with $1 \leq J \leq 5$, with a total statistical weight 84 times that of the ground state. Most of these levels form Rydberg ions that can readily autoionize to other metastable channels or to the ground state channel by the quadrupole interactions that dominate in high-L levels. However, if the lowest metastable level is the J=1 level, Rydberg electrons bound to that state would be forbidden to autoionize to the ground state channel, and could therefore be stable. The Rydberg ions bound to these J=1 metastable levels could participate in the RESIS signal, perhaps at their statistical weight of 75%, thus reducing the RESIS signals from Rydberg states bound to the ion ground state by a factor of 4 relative to their expected size, and also causing a RESIS signal pattern that reflects the structure of both the J=0 ground state

and of the $J=1$ metastable level. This is currently our best hypothesis to explain the contrast between the signals seen in Figs. 1 and 2. As it turns out, there is some theoretical support for this hypothesis. The calculations of Marianna and Ulyana Safronova (Phys. Rev. A 84, 052515 (2011)) predict that the $J=1$ metastable level is the lowest energy metastable level in U^{6+} , but NOT in Th^{4+} . Thus this hypothesis could answer the question of WHY the two isoelectronic Rn-like ions behave so differently in the RESIS studies.

Immediate Future Plans

We are still working to improve the precision of our RESIS excitation spectra for both the U^{6+} and U^{5+} ions. This has been made much less tedious by the reductions in background levels. We are also planning to extend the metastable fraction measurements to include all four U and Th ions.

Recent Publications:

- 1) "Properties of Fr-like Th^{3+} from spectroscopy of high- L Rydberg levels of Th^{2+} ", Julie A. Keele, M.E. Hanni, Shannon L. Woods, S.R. Lundeen, and C.W. Fehrenbach, Phys. Rev. A 83, 062501 (2011)
- 2) "Polarizabilities of Rn-like Th^{4+} from rf spectroscopy of Th^{3+} Rydberg levels", Julie A. Keele, S.R. Lundeen, and C.W. Fehrenbach, Phys. Rev. A 83, 062509 (2011).
- 3) "Effective Potential Model for high- L Rydberg atoms and ions" Shannon L. Woods and S.R. Lundeen, Phys. Rev. A 85, 042505 (2012)
- 4) "Measurements of dipole and quadrupole polarizabilities of Rn-like Th^{4+} ", Julie A. Keele, Chris S. Smith, S.R. Lundeen, and C.W. Fehrenbach, Phys. Rev. A 85, 064502 (2012)
- 5) "Microwave Spectroscopy of high- L , $n=9$ Rydberg levels of Nickel: Polarizabilities and Moments of the Ni^+ ion", Shannon Woods, Chris Smith, Julie Keele, and S.R. Lundeen, Phys. Rev. A 87, 022511 (2013)
- 6) "Properties of Fr-like Th^{3+} from rf spectroscopy of high- L Th^{2+} Rydberg ions", Julie A. Keele, Chris Smith, S.R. Lundeen, and C.W. Fehrenbach, Phys Rev A 88, 022502 (2013)

Other Reports

"Ion Properties from high- L Rydberg atom spectroscopy: Applications to Nickel", Shannon L. Woods, PhD thesis, Colorado State University, Fall 2012

"Properties of Th^{4+} and Th^{3+} from RF Spectroscopy of high- L Thorium Rydberg Ions", Julie A. Keele, PhD thesis, Colorado State University, Summer 2013

Theory of Atomic Collisions and Dynamics

J. H. Macek

Department of Physics and Astronomy,

University of Tennessee, Knoxville TN 37996-1501 and

Oak Ridge National Laboratory, Oak Ridge TN

(Dated: September 30, 2014)

Abstract

A notable advance made by our group is the verification that vortices occur in the velocity field of wave functions for atomic processes. This advance was made possible by our collaboration with an experimental group in Germany, our use of the advanced adiabatic theory for interactions at small and intermediate distances between targets and projectiles, our use of the Regularized Lattice Time Dependent Schrödinger Equation (RLTDSE) to propagate continuum wave functions to effectively infinite distances where we can employ the Imaging theorem to relate coordinate space wave functions to measured electron distributions. **Grant Number:**DE- FG02-02ER 15283.

Applicant/Institution: The University of Tennessee

Street Address/City/State/Zip: 1534 White Avenue, Knoxville, TN 37996-1529

Principal Investigator: Joseph Macek

Address: 308 South College, 1413 Circle Drive, Knoxville, TN 37996

Telephone Number: (865) 675-5541

Email: jmacek@utk.edu

DOE/Office of Science Program Office: Office of Basic Energy Sciences

DOE/Office of Science Program Technical Program Manager Contact: Jeff Krause, Atomic Molecular and Optical Sciences Program, Fundamental Interactions Team Chemical Sciences, Geosciences and Bioscience Division, Office of Basic Energy Sciences

Statement on unexpended funds: I expect to have no unexpended funds at the end of the grant period.

PACS numbers:

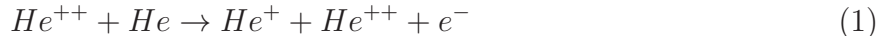
I. INTRODUCTION

Observations of quantum systems are made by examining them after they have moved to macroscopic distances where they can be detected by devices such as photon or particle detectors [1-7]. To our best knowledge, the Regularized Lattice Time-Dependent Schrödinger Equation (RLTDSE) method is the only numerical technique to rigorously compute the time evolution of quantum systems from microscopic to macroscopic scales without fitting onto known or easily computed asymptotic approximations. The RLTDSE provides numerical solutions for species with one active electron in coordinate regions that extend into the macroscopic domain of several thousands of atomic units. Vortices in the velocity field of wave functions for ionized electrons were discovered using the RLTDSE method.

II. RESULTS

Our main new contribution to this field is a joint project with an experimental group in Germany to observe vortex structure and to model the observations theoretically. To do this we found it necessary to treat two electron processes since observations are best made for transfer ionization processes, which are inherently two-electron processes.

The processes



was studied experimentally using COLTIMS. The coordinate system that we use is shown in Fig. 1.

The observed electron distribution is shown in Figs. (1 a) and (1c). Figure (1a) is the distribution seen in the transverse plane for $E=5\text{keF}/\text{amu}$ and $b = 0.5\text{au}$. It shows four zeros (triangular blue regions) arranged around a central maxima and surrounded by a region with four red maxima embedded in a yellow region of intermediate intensity. We modeled this system using the advanced adiabatic theory to compute a two-electron wave function at an internuclear separation of 10 atomic units. The transfer ionization component was projected from this wave function and used as input for and RLTDSE program to propagate the continuum electron to infinite distances. We then use the imaging theorem, namely,

$$\lim_{t \rightarrow \infty} [|\psi(\mathbf{r}, t)|^2 d^3r]_{\mathbf{r}=\mathbf{k}t} = P(\mathbf{k}) d^3k. \quad (2)$$

to extract the electron momentum distribution from the calculated coordinate space wave function.

This equation insures that holes in $P(\mathbf{k})$ relate directly to vortices in $\psi(\mathbf{r}, t)$, provided the vector \mathbf{k} does not point towards a charge center. Because Eq. (1) is fundamental to the way one defines ionization amplitudes, we call this equation the "imaging theorem".

While comparison of computed and measured distributions confirms that zeros related to vortices are observed experimentally, it is also clear that the velocity field itself cannot be observed. To probe the velocity field we have added a strong pulsed laser field in the

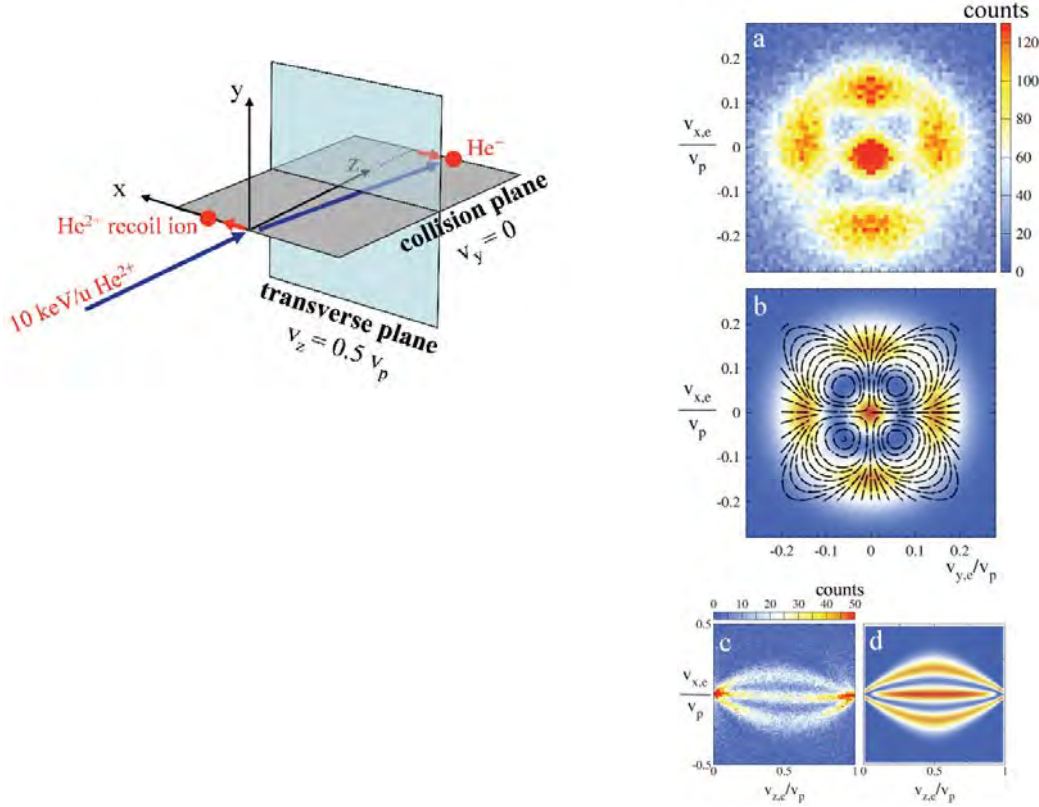


FIG. 1: Left figure: Coordinate system for collisions of He^{++} ions on He atoms. Right figure: Density plot of electrons ejected in the transfer ionization process $He^{++} + He \rightarrow He^+ + He^{++} + e^-$. Here \mathbf{v}_e is the ejected electron velocity and v_p is the magnitude of the projectile velocity. The energy is 5 keV/amu and the impact parameter is $b = 0.5au$. Fig. (1a) is distributions seen in transverse plane while Figs. 1(b) is the corresponding computed distribution where the dark arrows point in direction of the velocity field. Fig. (1c) is the measured distribution in the scattering plane and (1d) is the corresponding calculated distribution.

calculations. We find that a simple pulse does not change the observed distribution thus the use of laser interactions with ejected electron beams do not give any information on the velocity field. This is in accord with general theorems about the interaction of laser pulses with free electrons.

III. PROPOSED RESEARCH

A. Computation of two-electron transfer ionization in $He^{++} + He$ collisions and laser fields.

Our first calculation of how laser pulses modify electron distributions showed no effect of the velocity field. This is in accord with the Lawson-Woodard theorem [7]. Only if the laser pulse is focused and not simply a function of $\mathbf{k} \cdot \mathbf{r} - \omega t$ will there be an effect of the light on the ejected electron distribution. We propose to compute the electron distribution of beams of electrons having vortex structures interacting with focused laser beams. Preliminary results

show that the electron beam passing through a laser beam focused to a gaussian beam of width σ will become asymmetric by an amount Δ that depends upon the strength of the vortex in the velocity field and the degree of focussing σ . This provides a way to observed velocity field circulation directly, at least to the extent that a measurable parameter, Δ relates to the strength of the vortex in the velocity field.

B. Formal anisotropy theory

We will formalize the proposed measurement using standard angular momentum theory and the orientation parameter $\langle J_z \rangle$ for continuum states. This will extend the theory of orientation and alignment to continuum states of atomic species.

IV. SUMMARY

We have made notable strides in showing that vortices discovered in a particular process are observable in electron momentum distributions for charged particle impact. We have also shown that vortices are modified by moderately short electric pulse ionization. In the latter case we have not yet shown that the modifications can be observed. The present projects are directed towards computing atomic wave functions for processes that are amenable to observation.

Our projects are also directed towards understanding mechanisms for angular momentum and energy transfer and their roles in the formation of vortices. The subject is of interest for fundamental reasons, but may also impact quantum information and quantum control.

V. REFERENCES

A. References to DOE sponsored research that appeared in 2010-2013

1. Vortices Associated With The Wavefunction of a Single Electron Emitted in a Slow Ion-Atom Collision, Schmidt, *et. al.*, Phys. Rev. Lett. **112**, 083201 (2014).
2. Vortices in Atomic Processes, J. H. Macek, in *Dynamical Processes in Atomic and Molecular Physics*, ed. by Gennadi Ogurtsov and Danielle Doweck, (Bentham ebooks, 2012) pp 3-28.

B. Other references

3. Sturmian Theory of Electron Energy Distributions in Low Energy Ion-Atom Collisions, S. Yu. Ovchinnikov and J. H. Macek, *Nuc. Inst. Meth. B*, **241**, 78 (2005).
4. Excitation and Polarization of the Emitted light., U. Fano and J. H. Macek, Rev. Mod. Phys. **5**, 553 (1973).
5. Dynamics of Ionization in Atomic Collisions, S. Yu. Ovchinnikov, G. N. Ogurtsov, J. H. Macek and Y. S. Gordeev, *Phys. Rpts.* **389** 119 (2004).
6. D. R. Schultz, C. O. Reinhold, P. S. Krstic, and M. R. Strayer, Phys. Rev. A **65**, 052722 (2002).
7. Acceleration of particles by an asymmetric Hermite-Gaussian laser beam, E. J. Bochove, G. T. Moore, and M. O. Scully, Phys. Rev. A **46**, 6640 (1992).

Photoabsorption by Free and Confined Atoms and Ions

Steven T. Manson, Principal Investigator

Department of Physics and Astronomy, Georgia State University, Atlanta, Georgia 30303
smanson@gsu.edu

Program Scope

The goals of this research program are: to provide theoretical support to, and collaboration with, various experimental programs that employ latest generation light sources, particularly ALS, APS and LCLS; to further our understanding of the photoabsorption process; and to study the properties (especially photoabsorption) of confined atoms and ions. Specifically, calculations are performed using and upgrading state-of-the-art theoretical methodologies to help understand the physics of the experimental results; to suggest future experimental investigations; and seek out new phenomenology, especially in the realm of confined systems. The primary areas of programmatic focus are: nondipole and relativistic effects in photoionization; photoabsorption of inner and outer shells of atoms and atomic ions (positive and negative); dynamical properties of atoms endohedrally confined in buckyballs, primarily C₆₀; studies of time delay on the attosecond scale in photoionization of free and confined atomic systems. Flexibility is maintained to respond to opportunities.

Highlights of Recent Progress

1. Confined Atoms

The study of confined atoms is fairly new. There are a number of theoretical investigations of various atoms endohedrally confined in C₆₀ [1,2], but experimental studies are sparse [3-6]. Thus, we are conducting a program of calculations at various levels of approximation, aimed at delineating the properties of such systems, especially photoionization, to guide experiment. Among our major results, we have found that a huge transfer of oscillator strength from the C₆₀ shell, in the neighborhood of the giant plasmon resonance, to the encapsulated atom for both Ar@C₆₀ [7] and Mg@C₆₀ [8]. In addition, confinement resonances [9], oscillations that occur in the photoionization cross section of an endohedral atom owing to the interferences of the photoelectron wave function for direct emission with those scattered from the surrounding carbon shell have been predicted in a broad range of cases; recently, the existence of confinement resonances has been confirmed experimentally [5,6]. Further, the photoionization of endohedral atoms within nested fullerenes, has shown that, as a result of the multi-walled confining structures, the confinement resonances become considerably more complicated [10]. And we have shown that confinement resonances induce resonances in the time-delay of photoelectron emission [11].

Considering a Xe atom endohedrally confined in C₆₀ the formation of a new type of atom-fullerene hybrid state was discovered [12]. These dimer-type states arise from the near-degeneracy of inner levels of the confined atom and the confining shell, in contrast to the known overlap-induced hybrid states around the Fermi level of smaller compounds, and are found to occur in confined noble gas, alkali-earth atoms [13] and the Zn series [14,15]. The photoionization cross sections of these hybrid states exhibit rich structures and are radically different from the cross sections of free atomic or fullerene

states. This also occurs in buckyonions, nested fullerenes [16] which suggests the possibility of creating buckyonions with plasmons of specified character, i.e., *designer resonances*.

We have also explored the interatomic Coulomb decay (ICD) phenomenon in confined atoms and found, owing to hybridization between atomic and shell orbitals, that ICD occurs both ways, from atom to shell and shell to atom, and the rates (widths) are often much larger than the ordinary Auger rates [17].

2. Atomic/Ionic Photoionization

A relativistic random phase approximation study has explained the significant structure in subshell photoionization cross sections many keV above their thresholds found experimentally in Ag [18]; the structure is nonresonant and about 50 eV wide. It was found to be induced by interchannel coupling with inner-shell ionization channels, in the vicinity of the inner-shell thresholds. Of significance is that this kind of structure should be a general phenomenon in photoionization throughout the Periodic Table.

The photoionization parameters for Xe 5s were explored using the relativistic multiconfiguration Tamm–Dancoff (RMCTD) approximation which we are developing [19]. Encouragingly, we find that RMCTD provides significantly improved agreement with experiment, compared other relativistic many body approximations over the entire photon energy region bracketing the near-threshold 5s Cooper minimum, from the 5s threshold up to about 70 eV. The RMCTD results in the length form are in much better agreement with the experiment than those in the velocity form, suggesting that residual correlations of importance are not yet included; further development is thus required.

Future Plans

Our future plans are to continue on the paths set out above. In the area of confined atoms, expand on our studies of interatomic Coulomb decay (ICD) of resonances. We will also work on ways to enhance the time-dependent local-density approximation to make it more accurate in our calculations of confined atoms. In addition, we shall work towards upgrading our theory to include relativistic interactions to be able to deal with heavy endohedrals with quantitative accuracy. We will also look at the attosecond time delay in photoionization that has been found in various experiments, and we work to further our understanding of how confinement might affect this time delay. Developmental work on enhancing our relativistic multiconfiguration Tamm–Dancoff (MCTD) theory shall continue with an eye towards dealing more accurately with situations like Ba 5s (discussed above). In addition, the search for cases where nondipole effects are likely to be significant, as a guide for experiment, and quadrupole Cooper minima, will continue. And we shall respond to new experimental results that are in need of interpretation as they come up.

Publication over the Past 3 Years Citing DOE Support

- “Cooper Minima: A Window on Nondipole Photoionization at Low Energy,” G. B. Pradhan, J. Jose, P. C. Deshmukh, L. A. LaJohn, R. H. Pratt, and S. T. Manson, *J. Phys. B* **44**, 201001-1-6 (2011).
- “Electron correlation effects near the photoionization threshold: The Ar isoelectronic sequence,” J. Jose, G. B. Pradhan, V. Radojević, S. T. Manson, and P.C. Deshmukh, *J. Phys. B* **44**, 195008-1-8 (2011).

- “Plasmon-plasmon coupling in nested fullerenes: Creation of interlayer plasmonic cross modes,” M. A. McCune, R. De, M. E. Madjet, H. S. Chakraborty, and S.T. Manson, *J. Phys. B* **44**, 241002-1-5 (2011).
- “Magnetic dichroism in K-shell photoemission from laser excited Li atoms,” M. Meyer, A. N. Grum-Grzhimailo, D. Cubaynes, Z. Felfli, E. Heinecke, S. T. Manson, and P. Zimmermann, *Phys. Rev. Letters* **107**, 213001-1-4 (2011).
- “Interference in Molecular Photoionization and Young’s Double-Slit Experiment,” A. S. Baltenkov, U. Becker, S. T. Manson, and A. Z. Msezane, *J. Phys. B* **45**, 035202-1-12 (2012).
- “A Mathematical Model of Negative Molecular Ions,” A. S. Baltenkov, S. T. Manson, and A. Z. Msezane, *Proceedings of Dynamic Systems and Applications 6* (Dynamic Publishers, Atlanta, Georgia, 2012), pp. 53-57.
- “Valence photoionization of small alkaline earth atoms endohedrally confined in C₆₀,” M. H. Javani, M. R. McCreary, A. B. Patel, M. E. Madjet, H. S. Chakraborty and S. T. Manson, *Eur. Phys. J. D* **66**, 189-1-7 (2012).
- “Radiation Damping in the Photoionization of Fe¹⁴⁺,” M. F. Hasoglu, T. W. Gorczyca, M. A. Bautista, Z. Felfli, and S. T. Manson, *Phys. Rev. A* **85**, 040701(R)-1-4 (2012).
- “Photoionization of atomic krypton confined in the fullerene C₆₀,” J. George, H. R. Varma, P. C. Deshmukh and S. T. Manson, *J. Phys. B* **45**, 185001-1-6 (2012).
- “Photoionization of ground and excited states of Ca⁺ and comparison along the isoelectronic sequence,” A. M. Sossah, H.-L. Zhou, S. T. Manson, *Phys. Rev. A* **86**, 023403-1-10 (2012).
- “Photoionization of Endohedral Atoms Using R-matrix Methods: Application to Xe@C₆₀,” T. W. Gorczyca, M. F. Hasoğlu, and S. T. Manson, *Phys. Rev. A* **86**, 033204-1-9 (2012).
- “Atom-fullerene hybrid photoionization mediated by coupled *d*-states in Zn@C₆₀,” Jaykob N. Maser, Mohammad H. Javani, Ruma De, Mohamed E. Madjet, Himadri S. Chakraborty, and Steven T. Manson, *Phys. Rev. A* **86**, 053201-1-5 (2012).
- “Photoionization of Confined Ca in a Spherical Potential Well,” M. F. Hasoğlu, H.-L. Zhou, T. W. Gorczyca, and S. T. Manson, *Phys. Rev. A* **87**, 013409-1-5 (2013).
- “Core Correlation Effects in the Valence Photodetachment of Cu⁻,” J. Jose, H. R. Varma, P. C. Deshmukh, S. T. Manson, and V. Radojević, *Proceedings of the 26th Summer School and International Symposium on the Physics of Ionized Gases (SPIG 2012), 27th-31st August 2012, Zrenjanin, Serbia, Book of Contributed Papers & Abstracts of Invited Lectures and Progress Reports*, editors: M. Kuraica and Z. Mijatović (University of Novi Sad, Novi Sad, Serbia, 2012), pp. 39-42.
- “Photoionization of Endohedrally Confined Ca (Ca@C₆₀),” M. F. Hasoglu, P. Prabha, M. H. Javani, H. L. Zhou, and S. T. Manson, *J. Phys. Conf. Ser.* **388**, 022026 (2012).
- “Dipole and Quadrupole Photoionization of Intermediate Subshells of Atomic Mercury,” T. Banerjee, Hari R. Varma, P. C. Deshmukh, and S. T. Manson, *J. Phys. Conf. Ser.* **388**, 022076 (2012).
- “Dipole and quadrupole photodetachment/photoionization studies of the Ar isoelectronic sequence,” J. Jose, G. B. Pradhan, V. Radojević, S. T. Manson and P. C. Deshmukh, *J. Phys. Conf. Ser.* **388**, 022098 (2012).
- “Effect of Interchannel Coupling and Confinement on the Photoionization of Kr,” J. George, Hari R. Varma, P. C. Deshmukh and S. T. Manson, *J. Phys. Conf. Ser.* **388**, 022009 (2012).
- “Pronounced Effects of Interchannel Coupling In High-Energy Photoionization,” W. Drube, T.M. Grehk, S. Thiess, G. B. Pradhan, H. R. Varma, P. C. Deshmukh and S. T. Manson, *J. Phys. B* **46**, 245006-1-6 (2013).
- “Positron differential studies: Comparison to photoionization,” A. C. F. Santos, R. D. DuBois and S. T. Manson, *AIP Conference Proceedings* **1525**, 441-443 (2013).
- “Innershell Photoionization of Atomic Chlorine,” W. C. Stolte, Z. Felfli, R. Guillemin, G. Ohrwall, S.-W. Yu, J. A. Young, D. W. Lindle, T. W. Gorczyca, N. C. Deb, S. T. Manson, A. Hibbert, and A. Z. Msezane, *Phys. Rev. A* **88**, 053425-1-11 (2013).
- “Photoionization of the 5s subshell of Ba in the region of the second Cooper minimum: cross sections and angular distributions,” A. Ganesan, S. Deshmukh, G. B. Pradhan, V. Radojevic, S. T. Manson and P. C. Deshmukh, *J. Phys. B* **46**, 185002-1-5 (2013).

- “Probing confinement resonances by photoionizing Xe inside a C_{60}^+ molecular cage,” R. A. Phaneuf, A. L. D. Kilcoyne, N. B. Aryal, K. K. Baral, D. A. Esteves-Macaluso, C. M. Thomas, J. Hellhund, R. Lomsadze, T. W. Gorczyca, C. P. Ballance, S. T. Manson, M. F. Hasoglu, S. Schippers, and A. Müller, *Phys. Rev. A* **88**, 053402-1-7 (2013).
- “A Comprehensive X-ray Absorption Model for Atomic Oxygen,” T. W. Gorczyca, M. A. Bautista, M. F. Hasoglu, J. Garcia, E. Gatzuz, J. S. Kaastra, T. R. Kallman, S. T. Manson, C. Mendoza, A. J. J. Raassen, C. P. de Vries and O. Zatsarinny, *Astrophys. J.* **779**, 78-1-11 (2013).
- “Photoionization study of Xe 5s: Ionization Cross Sections and Photoelectron Angular Distributions,” G. Aarthi, J. Jose, S. Deshmukh, V. Radojević, P. C. Deshmukh and S. T. Manson, *J. Phys. B* **47**, 025004-1-5 (2014).
- “Valence Photoionization of Noble Gas Atoms Confined in the Fullerene C_{60} ,” M. H. Javani, H. S. Chakraborty, and S. T. Manson, *Phys. Rev. A* **89**, 053402-1-12 (2014).
- “Resonant Auger-intersite-Coulombic hybridized decay in the photoionization of endohedral fullerenes” by M. H. Javani, J. B. Wise, R. De, M. E. Madjet, H. S. Chakraborty, and S. T. Manson, *Phys. Rev. A* **89**, 063420-1-4 (2014).
- “Attosecond time delay in the photoionization of endohedral atoms $A@C_{60}$: A new probe of confinement resonances,” P. C. Deshmukh, A. Mandal, S. Saha, A. S. Kheifets, V. K. Dolmatov and S. T. Manson, *Phys. Rev. A* **89**, 053424-1-4 (2014).
- “Photoionization of Ca 4s in a spherical attractive well potential: dipole, quadrupole and relativistic effects,” A. Kumar, G. B. Pradhan, H. R. Varma, P. C. Deshmukh and S. T. Manson, *J. Phys. B* **47**, 185003-1-8 (2014).
- “Photoionization of bonding and antibonding-type atom-fullerene hybrid states in $Cd@C_{60}$ vs $Zn@C_{60}$,” M. H. Javani, R. De, M. E. Madjet, S. T. Manson and H. S. Chakraborty, *J. Phys. B* **47**, 175102-1-7 (2014).

References

- [1] V. K. Dolmatov, A. S. Baltenkov, J.-P. Connerade and S. T. Manson, *Radiation Phys. Chem.* **70**, 417 (2004) and references therein.
- [2] V. K. Dolmatov, *Advances in Quantum Chemistry*, **58**, 13 (2009) and references therein.
- [3] A. Müller *et al.*, *Phys. Rev. Lett.* **101**, 133001 (2008).
- [4] R. Phaneuf *et al.*, *Bull. Am. Phys. Soc.* **55**(5), 40 (2010) and private communication.
- [5] A. L. D. Kilcoyne, A. Aguilar, A. Müller, S. Schippers, C. Cisneros, G. Alna'Washi, N. B. Aryal, K. K. Baral, D. A. Esteves, C. M. Thomas, and R. A. Phaneuf, *Phys. Rev. Lett.* **105**, 213001 (2010).
- [6] R. A. Phaneuf, A. L. D. Kilcoyne, N. B. Aryal, K. K. Baral, D. A. Esteves-Macaluso, C. M. Thomas, J. Hellhund, R. Lomsadze, T. W. Gorczyca, C. P. Ballance, S. T. Manson, M. F. Hasoglu, S. Schippers, and A. Müller, *Phys. Rev. A* **88**, 053402-1-7 (2013).
- [7] M. E. Madjet, H. S. Chakraborty and S. T. Manson, *Phys. Rev. Letters* **99**, 243003 (2007).
- [8] M. E. Madjet, H. S. Chakraborty, J. M. Rost and S. T. Manson, *Phys. Rev. A* **78**, 013201 (2008).
- [9] V. K. Dolmatov and S. T. Manson, *J. Phys. B* **41**, 165001 (2008).
- [10] V. K. Dolmatov and S. T. Manson, *J. Phys. Rev. A* **78**, 013415 (2008).
- [11] P. C. Deshmukh, A. Mandal, S. Saha, A. S. Kheifets, V. K. Dolmatov and S. T. Manson, *Phys. Rev. A* **89**, 053424 (2014).
- [12] H. S. Chakraborty, M. E. Madjet, T. Renger, J.-M. Rost and S. T. Manson, *Phys. Rev. A* **79**, 061201(R) (2009).
- [13] M. H. Javani, M. R. McCreary, A. B. Patel, M. E. Madjet, H. S. Chakraborty and S. T. Manson, *Eur. Phys. J. D* **66**, 189 (2012).
- [14] J. N. Maser, M. H. Javani, R. De, M. E. Madjet, H. S. Chakraborty, and S. T. Manson, *Phys. Rev. A* **86**, 053201 (2012).
- [15] M. H. Javani, R. De, M. E. Madjet, S. T. Manson and H. S. Chakraborty, *J. Phys. B* **47**, 175102 (2014).
- [16] M. A. McCune, R. De, M. E. Madjet, H. S. Chakraborty, and S. T. Manson, *J. Phys. B* **44**, 241002 (2011).
- [17] M. H. Javani, J. B. Wise, R. De, M. E. Madjet, H. S. Chakraborty, and S. T. Manson, *Phys. Rev. A* **89**, 063420 (2014).
- [18] W. Drube, T.M. Grehk, S. Thiess, G. B. Pradhan, H. R. Varma, P. C. Deshmukh and S. T. Manson, *J. Phys. B* **46**, 245006 (2013).
- [19] G. Aarthi, J. Jose, S. Deshmukh, V. Radojević, P. C. Deshmukh and S. T. Manson, *J. Phys. B* **47**, 025004 (2014).

ABSTRACT**ELECTRON-DRIVEN PROCESSES IN POLYATOMIC MOLECULES****Investigator: Vincent McKoy**

A. A. Noyes Laboratory of Chemical Physics

California Institute of Technology

Pasadena, California 91125

email: mckoy@caltech.edu**PROJECT DESCRIPTION**

The focus of this project is the development, extension, and application of accurate, scalable computational methods for studying low-energy electron–molecule collisions, with emphasis on larger polyatomic molecules relevant to electron-driven chemistry in biological and materials-processing contexts. Because the required calculations are numerically intensive, efficient use of large-scale parallel computers is essential, and the computer codes developed for the project are designed to run both on tightly-coupled parallel supercomputers and on workstation clusters.

HIGHLIGHTS

The past year saw progress on several significant projects, each involving collaboration with experimentalists to study an electron–molecule collision problem related to biomolecules or biofuels. Highlights include:

- Completed a collaborative study of angle-resolved dissociative electron attachment to uracil
- Extended our investigation of structural effects on resonant scattering patterns by completing a joint experimental/theoretical study of scattering from several alkyl amines and from isobutanol
- Completed a study of elastic electron scattering from acetaldehyde
- Neared completion of a study of electron-impact excitation of the simplest alcohol, methanol

ACCOMPLISHMENTS

During 2014 we developed computational procedures necessary to explore angle-resolved dissociative electron attachment processes while continuing to explore electron scattering processes in biologically relevant molecules. Each of our investigations was carried out collaboratively with experimental colleagues and in some cases with fellow computational scientists. The principal developments over the course of the year are summarized below.

In collaboration with the Belkacem group (Lawrence Berkeley National Laboratory), who performed the relevant experimental measurements, we have completed a study of angle-resolved dissociative attachment to the uracil molecule. As the simplest nucleobase, uracil is a prototype for studying dissociative attachment processes that can mediate electron-induced damage to DNA and RNA. Our results are obtained by computing entrance amplitudes that describe how the probability of attaching an electron during a collision varies depending on the direction from which the electron approaches the molecule. We find, consistent with the Belkacem group’s measurements, that the most likely source of the energetic H^- ions formed via attachment of electrons with ~ 6 eV of kinetic energy is breaking of the N1–H1 bond; this conclusion is also consistent with previous isotopic-substitution studies. These results have been written up in a joint paper that has been submitted for publication.

For some time we have been interested in electron collisions with alcohols, which are actual or potential biofuels. One fundamental issue that has arisen in our studies is the connection between the angular scattering pattern and the molecular structure. Specifically, in the 6 to 10 eV range of collision energies, straight-chain alcohols tend to show an f -wave scattering pattern and branched alcohols a d -wave pattern [1–4]. A similar pattern is known in alkanes. To explore this further, we collaborated with the experimental group of Murtadha Khakoo (California State University, Fullerton) and the computational group of Márcio Bettega (Federal

University of Paraná, Brazil) to investigate additional, related molecules. The Khakoo group measured cross sections for isobutanol, a molecule for which we had previously computed results [3], while we worked with the Bettega group to calculate cross sections for a number of alkyl amines, isoelectronic analogues of the alcohols in which an NH_2 group replaces the OH group. We found that, with a few exceptions, the same pattern persists in the amines. This work recently appeared in *Physical Review A* [5].

Also in collaboration with the Khakoo group, we completed and published [6] a study of elastic scattering by acetaldehyde, a prototype system for biomolecules containing C–O π^* resonances, and we are nearing completion of a study of electron-impact excitation of methanol (CH_3OH) to several of its low-lying electronic states. The latter work both extends our studies of alcohols to inelastic process and builds on our previous study of electron-impact excitation of the related molecule water [7,8]. Like water, methanol presents both experimental and computational challenges that necessitate a careful treatment, but this work is in its final stages and will be submitted for publication in the near future.

PLANS FOR COMING YEAR

We plan to continue collaborating on angle-resolved dissociative attachment with our experimental colleagues at LBL. We are currently discussing a suitable target to follow up our study of uracil—ideally, either another pyrimidine nucleobase, or an analogue such as pyrazine or pyrimidine itself. One constraint is that such a target must exhibit at least one impulsive, two-body dissociation process so that the axial-recoil approximation can be applied.

We also plan to continue our collaboration with the groups of Murtadha Khakoo and Leigh Hargreaves at California State University, Fullerton, on elastic and inelastic electron–molecule collision problems of mutual interest. In the coming year we will wrap up our study of methanol and move on to electron-impact excitation of the next larger alcohol, ethanol. In that work we will apply many of the insights gained during our studies of methanol and, prior to that, water. We also plan to complete work under way on elastic scattering by chloromethane (CH_3Cl) and chloroethane ($\text{C}_2\text{H}_5\text{Cl}$) before moving on to study vibrational excitation of CH_3Cl and, further down the road, dissociative attachment to CH_3Cl .

Finally, we will begin exploring the use of localized-orbital techniques to improve the scaling of accurate electron-scattering calculations in larger molecules, with an initial focus on DNA or RNA base pairs.

REFERENCES

- [1] M. A. Khakoo, J. Blumer, K. Keane, C. Campbell, H. Silva, M. C. A. Lopes, C. Winstead, V. McKoy, R. F. da Costa, L. G. Ferreira, M. A. P. Lima, and M. H. F. Bettega, *Phys. Rev. A* **77**, 042705 (2008).
- [2] M. A. Khakoo, J. Blumer, K. Keane, C. Campbell, H. Silva, M. C. A. Lopes, C. Winstead, V. McKoy, E. M. de Oliveira, R. F. da Costa, M. T. do N. Varella, M. H. F. Bettega, and M. A. P. Lima, *Phys. Rev. A* **78**, 062714 (2008).
- [3] M. H. F. Bettega, C. Winstead, and V. McKoy, *Phys. Rev. A* **82**, 062709 (2010).
- [4] M. H. F. Bettega, C. Winstead, V. McKoy, A. Jo, A. Gauf, J. Tanner, L. R. Hargreaves, and M. A. Khakoo, *Phys. Rev. A* **84**, 042702 (2011).
- [5] K. Fedus, C. Navarro, L. R. Hargreaves, M. A. Khakoo, F. M. Silva, M. H. F. Bettega, C. Winstead, and V. McKoy, *Phys. Rev. A* **90**, 032708 (2014).
- [6] A. Gauf, C. Navarro, G. Balch, L. R. Hargreaves, M. A. Khakoo, C. Winstead, and V. McKoy, *Phys. Rev. A* **89**, 022708 (2014).
- [7] L. R. Hargreaves, K. Ralphs, G. Serna, M. A. Khakoo, C. Winstead, and V. McKoy, *J. Phys. B* **45**, 201001 (2012).
- [8] K. Ralphs, G. Serna, L. R. Hargreaves, M. A. Khakoo, C. Winstead, and V. McKoy, *J. Phys. B* **46**, 125201 (2013).

PROJECT PUBLICATIONS AND PRESENTATIONS, 2012–2014

1. “Low-Energy Electron Scattering by Tetrahydrofuran,” A. Gauf, L. R. Hargreaves, A. Jo, J. Tanner, M. A. Khakoo, T. Walls, C. Winstead, and V. McKoy, *Phys. Rev. A* **85**, 052717 (2012).
2. “Electron-Biomolecule Collision Studies Using the Schwinger Multichannel Method,” C. Winstead and V. McKoy, in *Radiation Damage in Biomolecular Systems*, G. García Gómez-Tejedor and M. C. Fuss, editors (Springer, Dordrecht, 2012), p. 87.
3. “Excitation of the \tilde{a}^3B_1 and \tilde{A}^1B_1 States of H₂O by Low-Energy Electron Impact,” L. R. Hargreaves, K. Ralphs, G. Serna, M. A. Khakoo, C. Winstead, and V. McKoy, *J. Phys. B* **45**, 201001 (2012) (*Fast-Track Communication*).
4. “Low-Energy Electron Collisions with Biomolecules,” C. Winstead and V. McKoy, *J. Phys. Conf. Ser.* **388**, 012017 (2012).
5. “Low-Energy Elastic Electron Scattering by Acetylene,” A. Gauf, C. Navarro, G. Balch, L. R. Hargreaves, M. A. Khakoo, C. Winstead, and V. McKoy, *Phys. Rev. A* **87**, 012710 (2013).
6. “Excitation of the 6 Lowest Electronic Transitions in Water by 9 to 20 eV Electrons,” K. Ralphs, G. Serna, L. R. Hargreaves, M. A. Khakoo, C. Winstead, and V. McKoy, *J. Phys. B* **46**, 125201 (2013).
7. “Low-Energy Elastic Electron Scattering by Acetaldehyde,” A. Gauf, C. Navarro, G. Balch, L. R. Hargreaves, M. A. Khakoo, C. Winstead, and V. McKoy, *Phys. Rev. A* **89**, 022708 (2014).
8. “Low-Energy Elastic Electron Scattering from Isobutanol and Related Alkyl Amines,” K. Fedus, C. Navarro, L. R. Hargreaves, M. A. Khakoo, F. M. Silva, M. H. F. Bettega, C. Winstead, and V. McKoy, *Phys. Rev. A* **90**, 032708 (2014).
9. “Simulating Quantum Collisions,” V. McKoy, School of Computing and Information Sciences, Florida International University, March 23, 2012 (*invited talk, Distinguished Lecture Series*).
10. “Low-Energy Electron Interactions with Biomolecules,” C. Winstead, Forty-Third Annual Meeting of the APS Division of Atomic, Molecular and Optical Physics, Orange County, California, June 4–8, 2012 (*invited talk*).
11. “Low-Energy Electron Scattering from Water Vapor,” K. Ralphs, G. Serna, L. Hargreaves, M. A. Khakoo, C. Winstead, and V. McKoy, Forty-Third Annual Meeting of the APS Division of Atomic, Molecular and Optical Physics, Orange County, California, June 4–8, 2012.
12. “Low-Energy Elastic Scattering and Electronic Excitation of Water and Methanol by Electron Impact,” M. A. Khakoo, L. R. Hargreaves, K. Varela, K. Ralphs, C. Winstead, and V. McKoy, XVIII International Symposium on Electron-Molecule Collisions and Swarms, Kanazawa, Japan, July 19–21, 2013.

Page is intentionally blank.

ELECTRON/PHOTON INTERACTIONS WITH ATOMS/IONS

Alfred Z. Msezane (email: amsezane@cau.edu)

Clark Atlanta University, Department of Physics and CTSPS, Atlanta, Georgia 30314

PROGRAM SCOPE

The project's primary objective is to gain a fundamental understanding of the near-threshold electron attachment mechanism as well as identify and delineate resonances. The complex angular momentum (CAM) methodology [1], wherein is embedded the crucial electron-electron correlations and the core polarization interaction, is used for the investigations. Regge trajectories allow us to probe electron attachment at its most fundamental level near threshold, thereby uncovering new manifestations, including the mechanism of nanocatalysis, and determine the reliable electron affinities (EAs).

The time-dependent-density-functional theory is utilized to investigate the photoabsorption spectra of encapsulated atoms, focusing on the confinement resonances. Methods are developed for calculating the generalized oscillator strength, useful in probing the intricate nature of the valence- and open-shell as well as inner-shell electron transitions. Standard codes are used to generate sophisticated wave functions for investigating CI mixing and relativistic effects in atomic ions. The wave functions are also used to explore correlation effects in dipole and non-dipole studies as well as in R-matrix calculations of the photoionization process.

SUMMARY OF RECENT ACCOMPLISHMENTS

A. Intersection of low-energy electron-atom scattering and photodetachment of negative ions

The extensive exploration of the role of atomic particles and nanoparticles in catalysis has now added the novel atomic negative ions. The interplay between Regge resonances and Ramsauer-Townsend (R-T) minima in the electron elastic total cross sections (TCSs) for Au and Pd atoms along with their large electron affinities (EAs) has been identified as the fundamental atomic mechanism underlying nanoscale catalysis [2]. In electron-atom collision, the atom and electron system can be regarded as a temporary negative ion which is embedded in the continuum of states of the free electron and atom, namely as a resonance in the electron scattering cross section [3].

Regge trajectories allow us to probe electron attachment at its most fundamental level near threshold, thereby uncovering new manifestations such as the origin of resonances (shape resonances, binding energies (BEs) of ground and excited negative ions) formed during the slow electron collisions. They also lead to a fundamental understanding of nanocatalysis through negative ion resonances and the extraction of the reliable EAs. The EA of atoms, important *inter alia* in chemical reaction dynamics, including catalysis, provides a stringent test of theoretical methods when the results are compared with those from reliable measurements since the EA calculations probe the many-body effects.

Here we investigate using the CAM method the near-threshold electron elastic scattering from the Rh, Sn, Sb, Te, W and At atoms, resulting in electron attachment to identify and delineate the resonances. This is also the energy region of the intersection of low-energy electron-atom scattering and photodetachment of negative ions, commonly explored experimentally using the Wigner Threshold Law. The objective is to gain a fundamental understanding of the mechanism of electron attachment leading to the formation of temporary negative ions as Regge resonances. From the calculated elastic TCSs we extract the EAs, shape resonances (SRs), R-T minima and BEs of the negative ions formed during the collisions as resonances; these generally characterize the near-threshold electron elastic TCSs.

Our calculated Data for the Rh, Sn, Sb, Te and W atoms are summarized in the Table 1, where they are compared with other measured and calculated values. Included are also the theoretical EAs for the At atom to assess the importance/unimportance of relativistic effects. As seen from Table 1, for the W atom our SR and the measured EA [8] are very close together, namely 0.86 eV and 0.816 eV,

respectively. Furthermore, for the excited Rh^- ion our calculated BE is 0.35 eV while the measured value is less than 0.385 eV [4]. Our SR for Rh is 1.70 eV while the measured EA is 1.143 eV [4] (this should be compared with our calculated EA of 3.12 eV). Consequently, these discrepancies call for both experimental and theoretical investigations for resolution. Also of interest is that the three theoretical calculations agree on the large EA value for the At atom.

Table 1: Electron affinities (EAs), Shape Resonances (SRs), Ramsauer-Townsend (R-T) minima and Binding energies (BEs) of the excited negative ions, all in eV, for Rh, Sn, Sb, Te, W and At atoms. Extd, Expt. and Present denote excited state, experiment and present calculation, respectively.

Atom	Z	1 st R-T Minimum	SR	2 nd R-T Minimum	EA Present	EA Expt.	BE (Extd) Present	BE (Extd) Expt.
Rh	45	0.880	1.70	3.06	3.120	1.143 [4]	0.350	< 0.385 [4]
Sn	50	0.054	0.312	--	1.100	1.112 [6]	0.285	
Sb	51	0.516	0.774	1.250	1.258	1.047 [5]	0.605	
Te	52	0.557	0.869	1.656	1.745	1.973 [7]	0.530	
W	74	0.580	0.860	1.560	1.590	0.816 [8]	0.610	
At	85	0.810	1.200	2.490	2.510	2.80 [9]* 2.415[10]*	0.292	

* Theoretical values. The MCDHF [10] calculated EA value deviates from the CAM calculated one by about 3.8 %. (This indicates the contribution of relativistic effects to the EA calculation for At).

B. Photoabsorption spectra of Xe atoms encapsulated inside fullerenes

The photoabsorption spectra of Xe atoms encapsulated inside C_{180} and C_{240} have been investigated using the time-dependent density-functional theory (TDDFT). The geometry optimization was effected for the C_{180} and the C_{240} using the generalized-gradient approximation to the density-functional theory, with the PBE exchange-correlation functional, along with the DNP basis sets as implemented in the DMol3 Package. The Kohn-Sham equation was then solved to yield the eigenvalues and eigenvectors for the ground state, when the Xe atom was introduced inside the C_{180} and the C_{240} . The dynamical polarizability of the ground state due to the external electric perturbation was evaluated using the TDDFT. The calculations have been performed in the energy region of the Xe 4d giant resonance. The main features of the confinement resonances for the Xe atoms inside C_{180} and C_{240} may be predicted by the approximate formula $E(\text{eV}) = 67.55 + (12.25n/2r)^2$, where r is the radius in \AA of the fullerene, n is the integer number 2,3,4,5 · · · , and $E(\text{eV})$ is the location of a confinement peak. The calculations indicate that the main peak positions are usually located at the photon energy when the photoelectron takes both the Xe atom and the carbon cage as the wave nodes [11].

The photoabsorption spectra of Xe atoms engaged inside C_{58} , C_{56} and C_{54} have also been studied in the same manner as the C_{180} and C_{240} . The results demonstrate that, except for the Xe atom inside C_{58} , which has similar confinement resonances as those of the Xe atom inside C_{60} , the Xe atoms inside C_{54} and C_{56} have completely different spectra. This is related to the larger deformation parameter for the C_{56} and C_{54} . It is concluded that the quantum confinement resonances will be destroyed if the shape of the fullerene is deformed significantly from a sphere [11].

C. Inner-shell Photoionization of Atomic Chlorine

A few years ago, our group in collaboration with the Queen's University of Belfast, generated the elaborate wave functions that are being used in the current experimental/theoretical investigation of the inner-shell photoionization of open-shell Atomic Chlorine [12], which now involves the collaboration of many national/international institutions.

The theoretical challenges encountered in inner-shell photoionization calculations include radiative decay along with participator and spectator Auger decay; the open-shell character that leads to multiplet structures which in turn translate to multiple inner-shell thresholds and channels; and radiationless Coster-Kronig-like transitions among these multiplet channels. Additional to the basic physics being investigated the data generated are also needed in for example astrophysics and astronomy.

D. Leadership

In the article "Nelson Mandela's Leadership", published by the APS, NEWS, The Back Page, the authors [13] use Mandela to illustrate the qualities of an outstanding leader. His triumph over Apartheid and vision for science led, *inter alia*, to the selection of South Africa and Australia as the two major sites for the international Square Kilometer Array (SKA). It will be the world's largest radio telescope and one of the biggest scientific projects ever to be constructed.

CONTINUING RESEARCH

We continue with the theoretical investigations of low-energy electron scattering from simple and complex atoms to identify possible negative ion catalysts, photoabsorption of endohedral fullerenes, strongly correlated systems and atomic structure energy levels. Sophisticated and elaborate wave functions will be constructed for use in R-matrix calculations as in C. above. New accurate EAs for complex atoms will be obtained and nanocatalysts will be investigated and identified as well. Our recent CAM method [1] will be employed as well as extended to investigate Feshbach resonances.

REFERENCES AND SOME PUBLICATIONS

- [1] D. Sokolovski *et al*, Phys. Rev. A **76**, 012705 (2007)
- [2] A. Z. Msezane, Z. Felfli and D. Sokolovski, J. Phys. B **43**, 201001 (2010) (FAST TRACK)
- [3] P. D. Burrow, J. A. Michejda and J. Comer, J. Phys. B **9**, 3225 (1976)
- [4] M. Scheer, C. A. Brodie, R. C. Bilodeau and H. K. Haugen, Phys. Rev. A **58**, 2015 (1998)
- [5] M. Scheer, H. K. Haugen and D. R. Beck, Phys. Rev. Lett. **79**, 4104 (1997)
- [6] M. Vandevraye, C. Drag and C. Blondel, J. Phys. B. **46**, 125002 (2013)
- [7] T. Andersen, H. K. Haugen and H. Hotop, J. Phys. Chem. Ref. Data **28**, 6 (1999)
- [8] A. O. Lindahl, *et al*, Eur. Phys. J. D **60**, 219 (2010)
- [9] R. J. Zollweg, J. Chem. Phys. **50**, 4251 (1969)
- [10] J. Li, Z. Zhao, M. Andersson, X. Zhang and C. Chen, J. Phys. B **45**, 165004 (2012)
- [11] Zhifan Chen and Alfred Z. Msezane, Euro. Phys. J. D, Submitted (2014)
- [12] W. C. Stolte, Z. Felfli, R. Guillemin, G. Ohrwall, S.-W. Yu, J. A. Young, D. W. Lindle, T. W. Gorczyca, N. C. Deb, S. T. Manson, A. Hibbert, and A. Z. Msezane, Phys. Rev. A **88**, 053425 (2013).
- [13] "Nelson Mandela's Leadership", A. Z. Msezane and S. K. Mtingwa, American Physical Society, APS NEWS, The Back Page <http://www.aps.org/publications/apsnews/201405/backpage.cfm>

SOME RESEARCH PUBLICATIONS 2012-2014 Acknowledging the DOE Grant

- [1] "Slow electron elastic scattering cross sections for In, Tl, Ga and At atoms", Z. Felfli, A.Z. Msezane and D. Sokolovski, J. Phys. B **45**, 045201 (2012)
- [2] "Self-intersecting Regge trajectories in multi-channel scattering", D. Sokolovski, Z. Felfli, A.Z. Msezane, Physics Letters A **376**, 733-736 (2012)
- [3] "Photoabsorption spectrum of the Xe@ C₆₀ endohedral fullerene", Zhifan Chen and Alfred Z. Msezane, Euro. Phys. J. D **66**, 184, (2012)

- [4] “Interference in Molecular Photoionization and Young’s Double-Slit Experiment”, A. S. Baltentkov, U. Becker, S. T. Manson and A. Z. Msezane, *J. Phys. B* **45**, 035202 (2012)
- [5] “Identification of strongly correlated spin liquid in Herbertsmithite”, V. R. Shaginyan, A. Z. Msezane, K. G. Popov, G. S. Japaridze and V. A. Stephanovich, *Euro. Phys. Lett.* **97**, 56001 (2012)
- [6] “Slow electron scattering from Ag, Pd, Pt, Ru and Y atoms: Search for nanocatalysts”, A. Z. Msezane, Z. Felfli, and D. Sokolovski, *Journal of Physics: Conference Series* **388**, 042002 (2012)
- [7] “Fine-Structure energy levels, radiative rates and lifetimes in Si-like Nickel”, G. P. Gupta and A. Z. Msezane, *Phys. Scripta* **86**, 015303 (2012)
- [8] “Atomic Gold and Palladium Negative-ion Catalysis of Light, Intermediate, and Heavy Water to Corresponding Peroxides”, A. Tesfamichael, K. Suggs, Z. Felfli, Xiao-Qian Wang and A. Z. Msezane, *J. Phys. Chem. C* **116**, 18698 (2012)
- [9] “Gold anion catalysis of methane to methanol”, A. Z. Msezane, Zineb Felfli, Aron Tesfamichael, Kelvin Suggs, and Xiao-Qian Wang, *Gold Bulletin*, DOI10.1007/s13404-012-0056-7 (2012)
- [10] “Atomic Gold and Palladium Negative Ion-Catalysis of Water to Peroxide: Fundamental Mechanism”, A. Tesfamichael, K. Suggs, Z. Felfli, Xiao-Qian Wang and A. Z. Msezane, *J. Nanoparticles Research* **15**, 1333 (2013)
- [11] “Photoabsorption spectrum of the $\text{Sc}_3\text{N}@C_{80}$ molecule”, Zhifan Chen and Alfred Z. Msezane, *J. Phys. B* **45**, 235205 (2012)
- [12] “Effect of C60 giant resonance on the photoabsorption of encaged atoms”, Zhifan Chen and Alfred Z. Msezane, *Phys. Rev. A* **86**, 063405 (2012)
- [13] “Scaling in dynamic susceptibility of herbertsmithite and heavy-fermion metals”, V. R. Shaginyan, A. Z. Msezane, K.G. Popov and V.A. Khodel, *Physics Letters A* **376**, 2622 (2012)
- [14] “Magnetic field dependence of the residual resistivity of the heavy-fermion metal CeCoIn_5 ”, V. R. Shaginyan, A. Z. Msezane, K. G. Popov, J. W. Clark, M. V. Zverev, and V. A. Khodel, *Phys. Rev. B* **86**, 085147 (2012)
- [15] “Methane Oxidation to Methanol without CO_2 Emission: Catalysis by Atomic Negative Ions”, Aron Tesfamichael, Kelvin Suggs, Zineb Felfli, and Alfred Z. Msezane, <http://arxiv.org/abs/1403.0597> (2014)
- [16] “Excitation energies, oscillator strengths and lifetimes in Mg-like Vanadium”, G. P. Gupta and A. Z. Msezane, *Phys. Scr.* **88**, 025301 (2013)
- [17] “Fine-structure energy levels, oscillator strengths and lifetimes in Al-like Chromium”, G P Gupta and A Z Msezane, *Indian Journal of Physics*, DOI 10.1007/s12648-013-0372-7 (2013)
- [18] “Energy levels and radiative rates for transitions in Ti VI”, K M Aggarwal, F P Keenan and A Z Msezane, *Phys. Scr.* **88**, 025302 (2013)
- [19] “Common quantum phase transition in quasicrystals and heavy-fermion metals”, V. R. Shaginyan, A. Z. Msezane, K. G. Popov, G. S. Japaridze, V. A. Khodel, *Phys. Rev. B* **87**, 245122 (2013)
- [20] “Flat Bands and Enigma of Metamagnetic Quantum Critical Regime in $\text{Sr}_3\text{Ru}_2\text{O}_7$ ”, V. R. Shaginyan, A. Z. Msezane, K. G. Popov, J. W. Clark, M. V. Zverev, and V. A. Khodel, *Physics Letters A*, Volume **377**, Issue 39, p. 2800-2805 (2013)
- [21] “Photoabsorption spectra of the Ce atom encapsulated inside a C82 fullerene”, Zhifan Chen and Alfred Z. Msezane, *PHYSICAL REVIEW A* **88**, 043423 (2013)
- [22] “Innershell Photoionization of Atomic Chlorine,” W. C. Stolte, Z. Felfli, R. Guillemin, G. Ohrwall, S.-W. Yu, J. A. Young, D. W. Lindle, T. W. Gorczyca, N. C. Deb, S. T. Manson, A. Hibbert, and A. Z. Msezane, *Phys. Rev. A* **88**, 053425 (2013)
- [23] “Off-center effect on the photoabsorption spectra of encapsulated Xe atoms”, Zhifan Chen and Alfred Z. Msezane, *Phys. Rev. A* **89**, 025401 (2014)
- [24] “General properties of phase diagrams of heavy-fermion metals”, V.R. Shaginyan, A.Z. Msezane, K.G. Popov, G.S. Japaridze and V.A. Khodel, *EPL (European Phys. Letters)* **106**, 37001 (2014)
- [25] “Near-threshold electron elastic scattering cross sections for Ta, W, Re, Mo, Tc and Rh atoms: Determination of electron affinities and Ramsauer-Townsend minima”, Zineb Felfli, Alfred Msezane, and Dmitri Sokolovski, *Journal of Physics: Conference Series* **488**, 042019 (2014)

Theory and Simulation of Nonlinear X-ray Spectroscopy of Molecules

Shaul Mukamel

University of California, Irvine, CA 92697

Progress Report 2014, August 22, 2014

DOE DE-FG02-04ER15571

Program Scope

Nonlinear X-ray spectroscopy experiments, which use sequences of coherent broadband X-ray pulses, are made possible by new X-ray free electron laser (XFEL) and high harmonic generation (HHG) sources. These provide a unique window into the motions of electrons and nuclei in molecules and materials. This program is aimed at the design of novel X-ray pulse sequences for probing valence electronic excitations, the development of computational approaches for describing core-excited states, and the application of these techniques to specific molecular systems. Nonlinear spectroscopy techniques widely used in the visible and infrared regimes (e.g. time-resolved photoelectron spectroscopy, time-resolved broadband stimulated Raman, coherent control and frequency combs) are extended to the X-ray regime. Applications are made to energy transfer in metalloporphyrin heterodimers, effects of electronic coherence in nanostructured photovoltaics, charge and energy transfer between different metal centers in mixed-valence complexes, and delocalized carbon core excitations in conjugated hydrocarbons. Signatures of vibrational motions and nonadiabatic dynamics in photo-excited molecules are identified via two-dimensional X-ray correlation spectroscopy of multiple core states, time-, frequency-, and wavevector- resolved X-ray diffraction from single molecules as well as photon coincidence detection of multidimensional attosecond X-ray scattering.

Recent Progress

Multiporphyrin arrays are good candidates for artificial photosynthesis and molecular electronics applications. Understanding the excitation energy transfer (EET) pathways in these systems is of considerable interest. Stimulated X-ray Raman spectroscopy (SXRS) signals of various porphyrin heterodimers with different linkers, bonding structures, and geometries were predicted. The time-domain one- and two-color SXRS signals show coherent excitonic motions, which can be directly mapped into the excited state doorway wavepacket created by the pump pulse, which probes the EET (Fig. 1). SXRS signals are demonstrated to be very sensitive to the chemical bonding and local geometrical environment, and offer a novel window for photophysical and photochemical processes that could help the design of efficient solar energy devices.

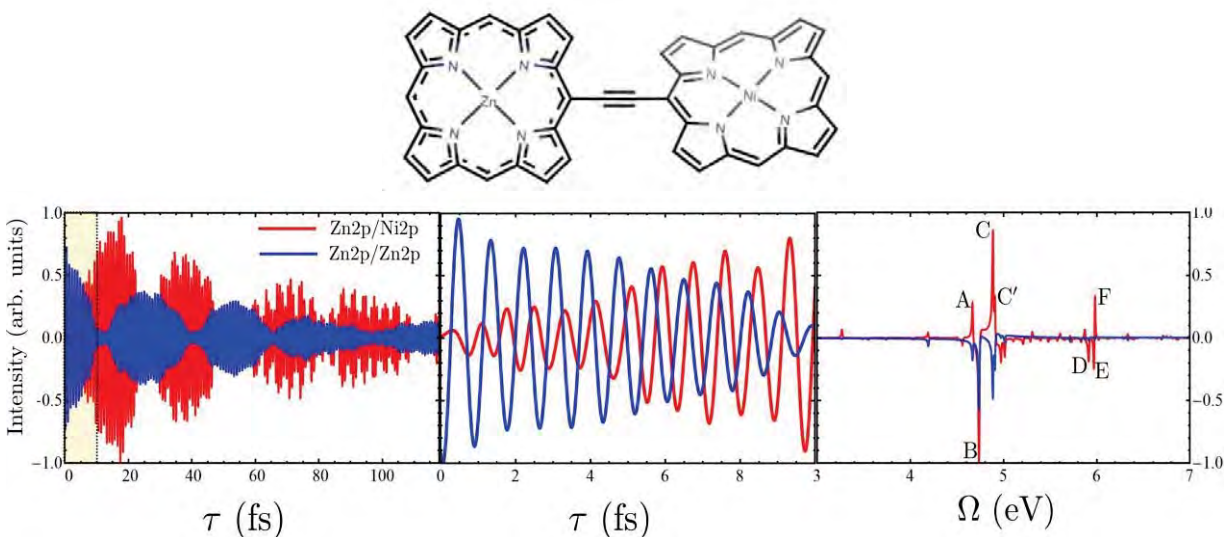


Fig. 1: Left: The time-resolved I2P-SXRS signals for the Zn-Ni porphyrin dimer for 0-120 fs. Single-color Zn2p/Zn2p (in blue) and two-color Zn2p/Ni2p signal, with a zinc pump and nickel probe, (in red). Middle: The first ten femtoseconds of the signals (shaded region in the left panel), on an expanded scale. Right: Fourier transform of the left panel.

The SXRS technique was further extended to multiple core excitation states of the same element. Carbon K-edge signals were simulated for the furan molecule with two types of carbons, C_α and C_β . We studied the interference between pathways contributing to the signals from different sites. There are four channels $\alpha\alpha$, $\beta\beta$, $\alpha\beta$, and $\beta\alpha$ (Fig. 2), where, for example, $\alpha\beta$ denotes C_α 1s excitations by the pump pulse followed by C_β 1s excitations by the probe pulse. We found that direct addition of the pure signals ($\alpha\alpha + \beta\beta$) differs from the total signal ($\alpha\alpha + \beta\beta + \alpha\beta + \beta\alpha$) owing to the significant contribution of the mixed channels ($\alpha\beta + \beta\alpha$). We also investigated the influence of vibronic coupling on SXRS signals by using the linear coupling exciton-phonon model and the cumulant expansion. Fine-structure features were obtained. The nuclei act as a bath for electronic transitions which accelerates the decay of the time-domain signal.

Our previously-developed description of time- and frequency-resolved detection of spontaneous emission was extended to the detection of diffracted X-rays. This extension showed the contribution of inelastic scattering events and provided a way to select them in the diffraction signal. Inelastic terms, which do not contribute to the diffraction from crystals, must be taken into account for scattering from single-molecule samples. This work was further extended to multidimensional X-ray diffraction in which several X-ray pulses are scattered from the sample. These create a non-stationary state which is probed by the scattering of a final X-ray pulse. X-ray photon coincidence detection was also explored.

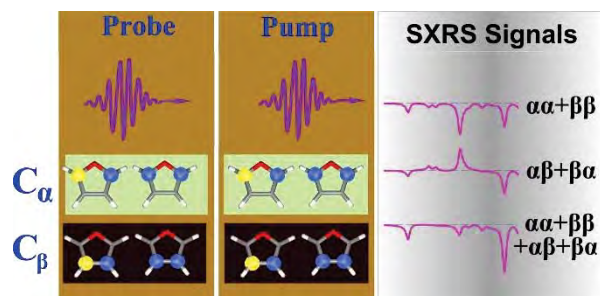


Fig. 2: Interactions of the pump (middle) and probe (left) X-ray pulses with furan. Both pulses are tuned at the C K-edge to resonate with core excitations from the C_α and C_β $1s$ orbitals. Right: Simulated SXRS signals with contributions from different core-excitation pathways. $\alpha\alpha$, $\beta\beta$, $\alpha\beta$, or $\beta\alpha$ distinguish the two core excitations in furan during the interaction with the pump and probe pulses.

Future Plans

In addition to the linear response TDDFT approach, we shall employ the real-time TDDFT method in X-ray nonlinear spectroscopy simulations. At this level of theory, all physical properties of the system are solely determined by the time-dependent charge density obtained from direct propagation of the time-dependent Kohn-Sham equation. TDDFT avoids calculating the more complicated many-body wavefunction and is computationally more affordable than conventional post-Hartree-Fock methods. Real-time TDDFT provides a convenient way for calculating the high-order response properties of the system, without the evaluation of very complicated functional derivatives. High-order responses are important in nonlinear spectroscopy experiments with intense laser fields. TDDFT has been implemented in standard quantum chemistry packages such as Gaussian, NWChem and Octopus. It will be employed to study the electronic relaxation dynamics after a sudden core ionization and photoinduced electron-transfer dynamics between donor-acceptor pairs. *Ab initio* Ehrenfest dynamics simulations will be carried out to include nuclear motions and nonadiabatic reaction dynamics.

Previously, we proposed the X-ray photon-echo signals. Calculations were implemented at a low level by using the equivalent-core-hole method. We plan to use the state-averaged multi-configurational self-consistent-field (MCSCF) method to obtain more accurate signals. We will investigate the aminophenol molecule, which has single N and O centers. Valence excited states, single core excited states ($N1s^{-1}$ and $O1s^{-1}$), and double core excited states ($N1s^{-1}O1s^{-1}$, $N1s^{-1}N1s^{-1}$ and $O1s^{-1}O1s^{-1}$) will be simulated. In addition, we plan to calculate the double-quantum-coherence signals, which reveal the coupling between doubly and singly excited states.

Time-resolved photoelectron and Auger-electron spectroscopy signals will be simulated. These techniques provide sensitive probes of electronic and nuclear dynamics and can track radiationless decay of electronic excited states through non Born-Oppenheimer dynamics. The simulation of these processes involves many different degrees of freedom (core, valence, and continuum electronic levels as well as internal vibrations and environmental degrees of freedom) and our approach will give a unified, practical way of treating them at different levels of theory.

Publications Resulting from the Project

- P1. "Watching Energy Transfer in Metalloporphyrin Heterodimers Using X-ray Raman Spectroscopy", J.D. Biggs, Y. Zhang, D. Healion, and S. Mukamel. *PNAS*, 110, 15597-15601 (2013)
- P2. "Multiple Core and Vibronic Coupling Effects in attosecond Stimulated X-ray Raman Spectroscopy", Weijie Hua, Jason Biggs, Yu Zhang, Daniel Healion, Hao Ren, and Shaul Mukamel. *J. Chem. Theory and Computation*. 9, 5479-5489 (2013)
- P3. "Two-dimensional X-ray Correlation Spectroscopy of Remote Core States", D. Healion, Y. Zhang, J.D. Biggs, W.Hua, and S. Mukamel. *Structural Dynamics*, 1, 014101 (2014).
- P4. "Multidimensional Scattering of Attosecond X-ray Pulses Detected by Photon Coincidence", J. D. Biggs, K. E. Bennett, Y. Zhang, and S. Mukamel. *J. Phys. B: At. Mol. Opt. Phys* (submitted, 2013)
- P5. "Time Resolved Photoelectron Spectroscopy of Thioflavin T Photoisomerization; A simulation study", H. Ren, B. Fingerhut, and S. Mukamel. *J. Phys. Chem*, 117, 6096-6104 (2013)
- P6. "Loss and Gain Signals in Broad-band Stimulated-Raman Spectra; Theoretical Analysis", U. Harbola, S. Umapathy, and S. Mukamel. *Phys Rev A*, 88, 011801 (2013)
- P7. "Nonlinear Transmission Spectroscopy with Dual Frequency Combs", R. Glenn and S. Mukamel. *Phys Rev. A*, 90, 023804 (2014)
- P8. "Time-Resolved Broadband Raman Spectroscopies; A Unified Six-wave mixing Representation", K.E. Dorfman, B.P. Fingerhut, and S. Mukamel. *J. Chem. Phys.* 139, 124113 (2013)
- P9. "Coherent Control of Linear Signals; Frequency-domain Analysis", S. Mukamel. *J. Chem. Phys.* 139, 164113 (2013)
- P10. "Indistinguishability and Correlations of Photons Generated by Quantum Emitters Undergoing Spectral Diffusion", K.E. Dorfman and S. Mukamel. *Scientific Reports*, 4, 3996 (2014)
- P11. "Understanding Excitation Energy Transfer in Metalloporphyrin Heterodimers with Different Linkers, Bonding Structures, and Geometries through Stimulated X-Ray Raman Spectroscopy ", Y. Zhang, J.D. Biggs, and S. Mukamel. *J. Mod. Optics*, DOI: 10.1080/09500340.2014.899734 (2014)
- P12. Comment on "Coherence and Uncertainty in Nanostructured Photovoltaics", S. Mukamel. *J. Phys. Chem A*, DOI: 10.1021/jp4071086 (2013)
- P13. "Nonlinear Spectroscopy of Trapped Ions", F. Schlawin, M. Gessner, S. Mukamel and A. Buchleitner. *Phys Rev A*, 90, 023603 (2014)
- P14. "Time, Frequency, and Wavevector Resolved X-ray Diffraction from Single Molecules", K. Bennett, J. D. Biggs, Y. Zhang, K.E. Dorfman, and S. Mukamel. *J.Chem.Phys.* 140, 204311(2014).

Nonlinear Photoacoustic Spectroscopies Probed by Ultrafast X-Rays

Keith A. Nelson
 Department of Chemistry
 Massachusetts Institute of Technology
 Cambridge, MA 02139
 Email: kanelson@mit.edu

Margaret M. Murnane
 JILA
 University of Colorado and National Institutes of Technology
 Boulder, CO 80309
 E-mail: murnane@jila.colorado.edu

Program Scope

In this project, ultrashort electromagnetic pulses in the visible, extreme ultraviolet (EUV), and x-ray spectral ranges are all used in complementary efforts to gain experimental access to elementary material excitations and fundamental condensed matter processes on ultrafast time scales and mesoscopic length scales. Of primary interest are heat transport, whose nondiffusive character at short length scales plays important roles in thermoelectric materials and nanoscale devices, and structural evolution in disordered media, which shows dynamics on wide-ranging time scales that have long eluded first-principles description. Central to these phenomena are acoustic phonons, which mediate both thermal transport and the compressional and shear components of structural relaxation. In addition to direct time-resolved observation of thermal transport, longitudinal, transverse, and surface acoustic wave generation and detection are key elements of our experiments in all spectral ranges.

We develop and use a variety of methods to excite and monitor acoustic waves and thermal transport on a wide range of length and time scales. For length scales in the roughly 1-100 micron range, we use crossed optical pulses to form an interference or "transient grating" (TG) pattern, directly generating thermoelastic responses with the grating period Λ (i.e. with wavevector magnitude $q = 2\pi/\Lambda$). The responses are monitored by time-resolved diffraction of probe laser light, revealing damped acoustic oscillations (from which acoustic speeds and attenuation rates, and elastic and loss moduli, are determined) and showing the kinetics of thermal transport from the heated interference maxima (the transient grating "peaks") to the unheated minima ("nulls"). The acoustic frequencies at these wavelengths are in the MHz or low GHz range. In order to reach higher acoustic frequencies and to monitor heat transport on length scales far less than 1 μm , we are working to extend transient grating methods to EUV wavelengths, taking advantage of ever-increasing EUV pulse energies produced through high harmonic generation (HHG), and to hard x-ray wavelengths using the LCLS facility at Stanford. Alternatively, spatially periodic structures can be deposited onto substrate surfaces so that optical irradiation produces thermoelastic responses at the specified periods which may be as small as a few tens of nanometers. Time-resolved diffraction of variably delayed EUV pulses reveals the corresponding surface acoustic wave oscillations and thermal transport kinetics with extremely high sensitivity. To excite bulk acoustic waves up to THz frequencies, irradiation of a superlattice structures of alternating layers with different optical absorption spectra generates a thermoelastic response including a compressional acoustic wave with the superlattice period. A thin opaque layer also may be irradiated so that its thermal expansion launches an acoustic wave into a substrate. The bulk acoustic waves generated in these methods may be detected by time-resolved reflectivity, interferometry, or other optical probes.

Recent Progress

Nanoscale thermal transport and acoustics with EUV pulses

Generation and Control of Ultrashort-Wavelength Surface and Longitudinal Acoustic Waves at Nanoscale Interfaces: In a collaboration between JILA, MIT and Berkeley, we generated and probed the

shortest wavelength surface acoustic waves (SAW) to date, at 45 nm (frequency ~ 80 GHz), with corresponding penetration depths of ~ 10 nm. [1,2] This result is significant for nanoscale materials physics because it makes it possible to selectively probe the mechanical properties of very thin films and interfaces, as well as nanostructures deposited on or embedded within a surface. We characterized the acoustic velocity dispersion of 1D and 2D Ni nanostructures with periods 45 nm – 4 μm . As the SAW wavelength and penetration depth decrease, the velocity deviates significantly from that of the stiffer sapphire substrate. A single optical pump pulse excited multiple SAW modes, but pairs of pulses timed to arrive in or out of phase with the first-order SAW mode frequency selectively excited either the first or second-order mode. A detailed finite element analysis of pseudo-SAW eigenmodes in 1D and 2D phononic crystal structures was also performed. [2] The SAW velocity dispersion calculated through this finite element analysis is shown as a blue dashed line in Fig. 1b, in very good agreement with the data. The deviation from the substrate Rayleigh velocity yields information about the mechanical properties of the nanostructure, and offers a new method for surface nanometrology using picosecond SAWs at ultrashort wavelengths.

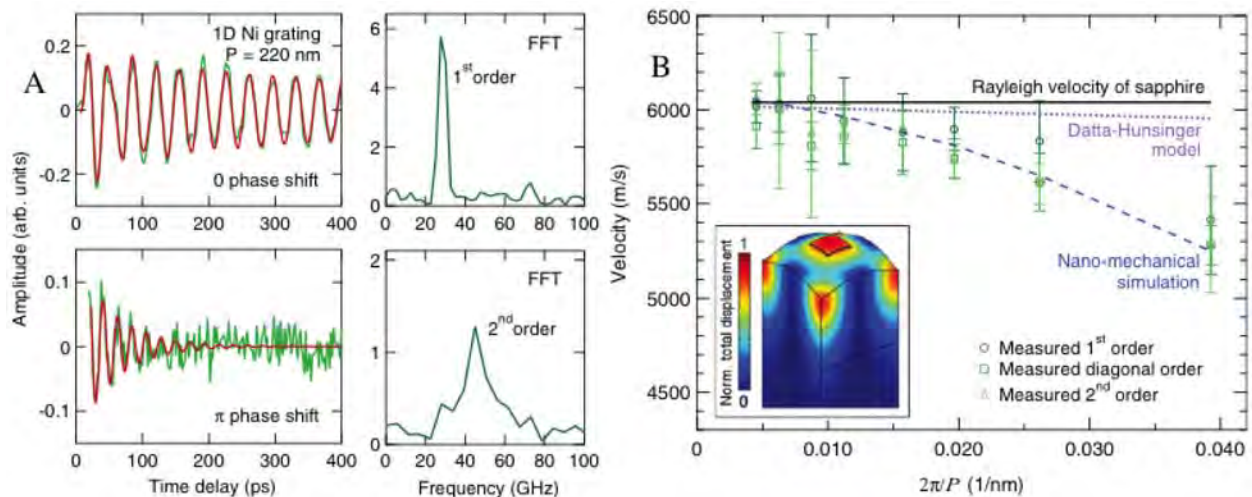


Fig. 1. (A) Selective acoustic wave generation in a 220 nm period Ni nano-grating using optical pulse sequences. Pulse pairs timed to drive the first-order SAW mode in phase (top left) and out of phase (lower left) generated the first and second order mode respectively as shown by the FFT spectra on the right. (B) Velocity dispersion curves for 2D nickel-on-sapphire structures with various periods P . Fundamental, second order, and diagonal SAW mode oscillations were observed. The blue dashed line is from finite element simulations that also show the displacement profiles of the modes, illustrated in the inset for the fundamental mode.

In addition to surface acoustic waves, optical excitation launches longitudinal acoustic waves within surface nanostructures [1,2]. The acoustic "echoes" can be detected after reflection when they return to the free surface, as in conventional picosecond ultrasonics measurements. However, EUV detection has distinct advantages in that the smaller probing wavelength leads to intrinsically higher sensitivity to surface displacements and the EUV reflectivity is insensitive to electronic excitation. In current work on the mechanical properties of ultrathin (0-6 nm, with increments as small as one atomic layer) Ta layers deposited on 10 nm of Ni by XRR-calibrated sputter deposition, a single nanometer of Ta visibly changes the acoustic frequency. Mechanical properties of materials can be studied as a function of layer thickness.

Optical measurements of GHz-THz acoustics: structural relaxation dynamics & thermal transport

Structural relaxation dynamics and scaling behavior of supercooled liquids: As is well known from ordinary experience with viscous liquids as they are taken from warm to cool temperatures, their dynamical behavior spans an extraordinary range of time scales. The challenges posed to experimental measurements of structural relaxation dynamics from picosecond to many-second time scales have left the most fundamental questions unanswered despite decades of study. Do supercooled liquids show "universal" characteristics, at least within some classes of materials? Do they show critical phenomena,

with scaling laws and relations among critical exponents that transcend individual substances? The liquid-glass transition is not a phase transition, but a first-principles *mode-coupling theory* (MCT) has predicted that the dynamics of supercooled liquids can be understood in terms of a transition at a critical temperature T_c from an ergodic, equilibrium liquid to a non-ergodic, nonequilibrium state in which the liquid is kinetically constrained from reaching many of its energetically accessible configurations. The theory predicts the two main dynamical features seen in simple glass formers such as van der Waals organic liquids, namely the primary (alpha), strongly temperature-dependent relaxation dynamics that we associate with viscous fluids, involving the breakup and reformation of intermolecular "cage" geometries, and the faster (beta), nearly temperature-independent relaxation among multiple local configurations within existing geometries. Two key dynamical scaling predictions have never been tested directly because they require experimental measurements of structural relaxation dynamics over an extremely wide range of time (or frequency) scales. We conducted photoacoustic measurements spanning the 1 MHz - 100 GHz frequency range and a collaborating group from Roskilde University (Denmark) conducted dynamic mechanical measurements in the mHz-kHz range to determine the complex elastic modulus (or its inverse, the compliance) over 13 decades of frequency with less than three decades of gaps. The effort was by many decades the most comprehensive study of viscomechanical dynamics ever performed on a single material (the single-component liquid tetramethyl-tetraphenyl-trisiloxane, sold as a commercial oil with the trade name DC704). It also required the first MCT analysis of density dynamics across mHz through GHz frequencies. The analysis has now been completed. [3]

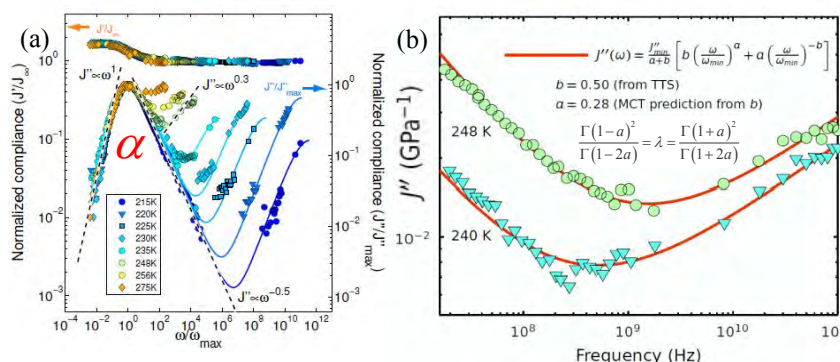


Fig. 2. Supercooled liquids and scaling relations consistent with mode-coupling theory (MCT). (a) Scaling of loss compliance spectra $J''(\omega)$ by peak frequency shows time-temperature superposition of the alpha relaxation dynamics over an unprecedented 13 decades. (b) Power-law exponents a and b from the two seemingly disparate alpha and beta dynamical regimes show the predicted relation between them.

The data show agreement over all 13 decades with "time-temperature scaling" (TTS) of the alpha relaxation spectrum which moves from GHz frequencies at high T to millihertz frequencies at low T . TTS means that the relaxation spectrum, plotted on a $\log(\omega)$ scale, appears identical at all temperatures, with the same frequency-dependent form and width, and simply shifts from high to low frequency without any other change as T is reduced. Figure 2a shows that the alpha spectra, after scaling by their peak frequencies ω_{\max} , do indeed superpose as predicted. Although TTS is often assumed in practical applications such as polymer processing, this is the first direct, comprehensive test of the prediction. Note that the high-frequency wings of the alpha spectra can be fit by a power-law frequency-dependence ω^{-b} with $b = 0.5$. As $T_c = 240$ K is approached, the low-frequency wings of the beta spectra (which all overlap at GHz frequencies before scaling) also show a power-law dependence ω^a with $a = 0.3$. As shown in Fig. 2b, that value is consistent with a MCT prediction of a Gamma-function relation (shown) between the dynamic critical exponents. Direct testing of this crucial MCT prediction, which connects the seemingly disparate alpha and beta relaxation kinetics, has been elusive because it requires measurement of the 10-100 GHz beta relaxation dynamics as well as the much slower alpha relaxation dynamics.

GHz-THz acoustic phonon-mediated thermal transport: We made significant progress on GHz and even THz acoustic wave generation and detection on several fronts. We measured acoustic attenuation mechanisms for acoustic waves in the 0.5-THz frequency range, a step toward mapping the mean free paths of phonons and thereby determining their contributions to thermal transport. [4,5] Going further, using a superlattice (SL) formed by GaN/InGaN multiple quantum wells with a strongly asymmetric unit cell (3 nm and 19 nm respective layer thicknesses), we generated a frequency comb comprising seven

acoustic modes spanning a range from 360 GHz to 2.5 THz, the highest coherent acoustic frequency (corresponding to an acoustic wavelength of ~ 3 nm) generated and measured to date to our knowledge. [6] We also showed that optical reflectivity can be used to detect THz-frequency acoustic waves [7] even though the probe light penetrates deeper than the acoustic wavelength, which would suggest that the measurement would average over acoustic cycles rather than resolving their time-dependent profiles. Instead, the signal generated as the acoustic wave reaches a free surface distinguishes its ultrashort character and allows a time-resolved optical measurement. Our measurements are providing increased access to GHz-THz acoustic waves that mediate nondiffusive thermal transport.

Future Plans

In a collaboration among MIT-JILA-LBL, we will extend our understanding of nanoscale heat flow from isolated 1D and 2D hot spots as well as dense arrays of nanoheaters. We have found that thermal transport from isolated nanosystems is significantly slower than diffusive predictions at length scales <100 nm for most crystalline materials, while densely packed arrays of similarly sized sources retain diffusive transport kinetics on the length scale of the distance between nanoelements. [8,9] Shorter EUV and soft x-ray wavelengths will probe more deeply into the nanoscale. Collaborative effort involving these and optical wavelengths will also characterize phonon mean free path spectra and compare them to measured thermal transport kinetics. We will implement full-field dynamic imaging of nanoscale heat flow and acoustic dynamics using coherent diffractive imaging. Further work on supercooled liquids will extend the frequency range to approach 1 THz and will include shear as well as compressional measurements. Finally, transient grating measurements will be extended to high wavevectors using EUV wavelengths at JILA and x-ray wavelengths at FEL facilities.

References and Selected Additional Publications (all from current DOE AMOS Support)

1. D. Nardi et al., "Probing limits of acoustic nanometrology using coherent EUV beams", submitted (2014).
2. Qing Li et al., "Generation and control of ultrashort-wavelength 2D surface acoustic waves at nano-interfaces," *Phys. Rev. B* **85**, 195431 (2012).
3. T. Hecksher et al., "Direct test of supercooled liquid scaling relations," under revision.
4. A.A. Maznev et al., "Lifetime of sub-THz coherent acoustic phonons in a GaAs-AlAs superlattice", *Appl. Phys. Lett.* **102**, 041901 (2013).
5. F. Hofmann et al., "Intrinsic to extrinsic phonon lifetime transition in a GaAs-AlAs superlattice", *J. Phys.: Condens. Matter* **25**, 295401 (2013).
6. A.A. Maznev et al., "Broadband terahertz ultrasonic transducer based on a laser-driven piezoelectric semiconductor superlattice", *Ultrasonics* **52**, 1-4 (2012).
7. K. J. Manke et al., "Detection of shorter-than-skin-depth acoustic pulses in a metal film via transient reflectivity," *Appl. Phys. Lett.* **103**, 173104 (2013).
8. K. Hoogeboom-Pot et al., "A new regime of nanoscale thermal transport: collective behavior counteracts dissipation inefficiency", submitted (2014). *Postdeadline paper, Int'l. Conf. on Ultrafast Phenomena, Japan (2014)*.
9. D. Nardi et al., "Probing thermomechanics at the nanoscale: Impulsively excited pseudosurface acoustic waves in hypersonic phononic crystals", *Nano Letters* **11**, 4126 (2011).
10. K. M. Hoogeboom-Pot et al., "A new regime of nanoscale thermal transport: collective diffusion counteracts dissipation inefficiency", submitted (2014).
10. C. Klieber, T. Pezeril, S. Andrieu, and K. A. Nelson, "Optical generation and detection of gigahertz-frequency longitudinal and shear acoustic waves in liquids: Theory and experiment," *J. Appl. Phys.* **112**, 013502 (2012).
11. A.A. Maznev, K.J. Manke, C. Klieber, K.A. Nelson, S. H. Baek, and C.-B. Eom, "Coherent Brillouin spectroscopy in a strongly scattering liquid by picosecond ultrasonics", *Opt. Lett.* **36**, 2925-2927 (2011).
12. C. Klieber et al., "Narrow-band acoustic attenuation measurements in vitreous silica at frequencies between 20 and 400 GHz," *Appl. Phys. Lett.* **98**, 211908 (2011).
13. C. Klieber et al., "Mechanical spectra of glass-forming liquids. II. Gigahertz-frequency longitudinal and shear acoustic dynamics in glycerol and DC704 studied by time-domain Brillouin scattering," *J. Chem. Phys.* **138**, 12A544-1-12 (2013).

Electron and Photon Excitation and Dissociation of Molecules

A. E. Orel
 Department of Chemical Engineering and Materials Science
 University of California, Davis
 Davis, CA 95616
 aeorel@ucdavis.edu

Program Scope

This program will study how energy is interchanged in electron and photon collisions with molecules leading to excitation and dissociation. Modern *ab initio* techniques, both for the photoionization and electron scattering, and the subsequent nuclear dynamics studies, are used to accurately treat these problems. This work addresses vibrational excitation and dissociative attachment following electron impact, and the dynamics following inner shell photoionization. These problems are ones for which a full multi-dimensional treatment of the nuclear dynamics is essential and where non-adiabatic effects are expected to be important.

Recent Progress

Molecular-Frame Photoelectron Angular Distributions (MFPADs)

Core-level and, in some cases, inner-valence level photoionization can lead to direct or indirect double ionization through Auger or autoionization processes that frequently populate dissociative dication states. In such instances, coincident measurement of photoelectrons and fragment ion momenta allows one to study photoelectron angular distributions in the molecular-frame. We have used the complex Kohn variational method to compute these fixed-nuclei photoionization amplitudes. We have applied this to problems such as the isomerization of acetylene (Publication #3, #4) and the isomerization of C_2H_4 (Publication #7). We have begun studies on using the complex Kohn variational method to calculate MFPADs for carbon 1s core ionization of neutral acetylene. We then have then substituted hydrogen for fluorine, breaking the *gerade*, *ungerade* symmetry and compare these MFPADs to the acetylene results. We have then computed the MFPADs for FCCF, restoring the the *gerade*, *ungerade* symmetry but studying the effect of a strongly electronegative atom on the angular distribution. In addition, we have studied the results of ionizing the fluorine 1s instead of the carbon.

Ion-momentum imaging of dissociative electron attachment dynamics in acetylene

Previously we had studied dissociative electron attachment (DEA) of the acetylene molecule. These calculations showed that there was a barrier to reaction in linear geometry. Bending the molecule, which broke the $D_{\infty h}$ symmetry and allowed coupling between the ground Σ state of the anion and a component of the Π excited state of the anion lowered the barrier and allowed the reaction to proceed. These calculations produced cross sections and isotope effects that were in good agreement with experiment. Recently, the Auburn group have carried out ion-momentum imaging of the products of dissociative electron attachment in acetylene. The entrance amplitude for this process was calculated to obtain an attachment probability which was integrated over the angle azimuthal to the recoil axis to produce an observable angular distribution. This coincides with the measured angular distribution if the overall rotation of the molecule is slow compared to dissociation and if the fragments recoil at a given angle in the molecular frame, i.e., if the molecular frame recoil axis R is constant over the Franck-Condon region of the neutral. As expected, since theory predicted significant bending during dissociation, this was not found to be the case. However, if the recoil axis was rotated by a fixed amount before averaging the attachment probability over the azimuthal angle the effect of bending can be included (since the H fragment is light, its rotation angle is nearly equal to the C-C-H bending angle). The results with a bending angle around 27 degrees was found to be in good agreement with the observed experimental fragment angular distribution, although the forward/backward asymmetry seen in the experiment is not completely

reproduced by the theory. A paper on this work has been submitted to Physical Review A (Publication #10).

Future Plans

Molecular-Frame Photoelectron Angular Distributions (MFPADs)

We plan to complete our studies of FCCF, FCCH and HCCH, obtaining the MFPADs from the carbon and fluorine 1s photoionization. We will then look at systems such as Lithium Carbide (Li-C-C-Li) and Sodium Carbide (Na-C-C-Na) where now the hydrogen and fluorine are replaced by electropositive atoms.

Publications

1. Dissociative Recombination of Highly Symmetric Polyatomic Ions, Nicolas Douguet, Ann E. Orel, Chris H. Greene, and Viatcheslav Kokoouline, *Phys. Rev. Lett.* **108** 023202 (2012).
2. Breaking a tetrahedral molecular ion with electrons: study of NH_4^+ , N. Douguet, V. Kokoouline and A. E. Orel, *J. Phys. B: At. Mol. Opt. Phys.* **45** 051001 (2012).
3. Time-resolved molecular-frame photoelectron angular distributions: Snapshots of acetylene-vinylidene cationic isomerization, N. Douguet, T. N. Rescigno, and A. E. Orel, *Phys. Rev. A* **86**, 013425 (2012).
4. Imaging Molecular Isomerization Using Molecular-Frame Photoelectron Angular Distributions, T. N. Rescigno, Nicolas Douguet and A. E. Orel, *J. Phys. B: At. Mol. Opt. Phys.* **45** 194001(2012).
5. Resonant enhanced electron impact dissociation of molecules, D S Slaughter, H Adaniya, T N Rescigno, D J Haxton, C W McCurdy, A Belkacem, Å Larson and A E Orel, *J. Phys.: Conf. Ser.* **388** 012016 (2012).
6. Theoretical study of excitation of the low-lying electronic states of water by electron impact, T. N. Rescigno, and A. E. Orel, *Phys. Rev. A* **88** 012703 (2013).
7. Carbon-K-shell molecular-frame photoelectron angular distributions in the photoisomerization of neutral ethylene, N. Douguet, T. N. Rescigno, and A. E. Orel, *Phys. Rev. A* **88** 013412 (2013).
8. Theory of radiative electron attachment to molecules: Benchmark study of CN^- , Nicolas Douguet, Samantha Fonseca dos Santos, Maurice Raoult, Olivier Dulieu, Ann E. Orel, and Viatcheslav Kokoouline, *Phys. Rev. A* **88** 052710 (2013).
9. Scattering matrix approach to the dissociative recombination of HCO^+ and N_2H^+ , S. Fonseca dos Santos, N. Douguet, V. Kokoouline and A. E. Orel *J. Chem. Phys.* **140** 164308 (2014).
10. Ion-momentum imaging of dissociative electron attachment dynamics in acetylene M. Fogle, D. J. Haxton, A. L. Landers, A. E. Orel, and T. N. Rescigno *Phys. Rev. A* submitted.
11. Simplified model to describe the dissociative recombination of linear polyatomic ions of astrophysical interest N. Douguet, S. Fonseca dos Santos, V. Kokoouline and A. E. Orel *European Physics Journal, Web of Conferences*, **XX** XXXX (2014).

2014 Abstract for Program: DOE-FG02-02ER15337
“Low-Energy Electron Interactions with Complex Molecules and Biological Targets”
Thomas M. Orlando

School of Chemistry and Biochemistry and School of Physics,
 Georgia Institute of Technology, Atlanta, GA 30332-0400
 Thomas.Orlando@chemistry.gatech.edu, Phone: (404) 894-4012, FAX: (404) 894-7452

Project Scope: The primary objectives of this program are to investigate the fundamental physics and chemistry involved in low-energy (1-250 eV) electron and soft x-ray interactions with complex targets. There is a particular emphasis on understanding correlated electron interactions and energy exchange in the deep valence and shallow core regions of the collision targets. The energy loss channels associated with these types of excitations involve ionization/hole exchange and negative ion resonances. Thus, the energy decay pathways are extremely sensitive to many body interactions and changes in local potentials. Our proposed investigations should help determine the roles of hole exchange via inter-atomic and intermolecular Coulomb decay (ICD) and energy exchange via localized shape and Feshbach resonances in the non-thermal damage of biological interfaces.

Recent Progress: We have worked on three major tasks during the previous funding cycle. The first task focused on experimental studies of ICD at interfaces and in the condensed phase. The second examined low-energy electron induced damage of DNA adsorbed on graphene. The third probed the role of secondary electrons and substrate interactions in x-ray induced DNA damage.

Project 1. Intermolecular Coulomb decay (ICD) and Coulomb explosions.

We recently demonstrated that ejection of $H^+(H_2O)_{n=1-8}$ from low energy electron irradiated water clusters adsorbed on graphite and overlayers of Ar, Kr or Xe results from ICD at the mixed interface. Inner valence holes in water ($2a_1^{-1}$), Ar ($3s^{-1}$), Kr ($4s^{-1}$) and Xe ($5s^{-1}$) correlate with the cluster appearance thresholds and initiate ICD. Proton transfer occurred during or immediately after ICD and the resultant Coulomb explosions lead to $H^+(H_2O)_{n=1-8}$ desorption with kinetic energies that vary with initiating state, final state and inter-atomic/molecular distances.

The primary threshold energies for direct ejection of $H^+(H_2O)_{n=4}$ are 35 ± 2 eV, 29 ± 2 eV, 29.8 ± 2 eV and 23 ± 2 eV for $H^+(H_2O)_n$ from < 0.5 ML of $(H_2O)_n$ on graphite and Ar, Kr and Xe covered graphite, respectively. The low threshold energies and slow KE distributions (relative to multilayer water) indicate that formation/desorption of $H^+(H_2O)_n$ from < 0.5 ML of $(H_2O)_n$ on graphite and Ar, Kr and Xe covered graphite involves ICD. Though the observed cluster sizes reflected the nascent deposited cluster distribution, the two-component energy distributions reflected the initial hole identities and eventual charge locations produced via ICD. *These previous studies established that energy resolved electron beam induced desorption of cations can directly examine ICD on surfaces and in the condensed phase.*

Project 2. Low-energy electron induced damage of DNA on a novel graphene platform

We have used a sensitive chemical vapor deposited graphene platform for controlled and enhanced sequence dependent DNA damage studies. The use of p-doped graphene

substrates enhances DNA breakage due to phosphate mediated parallel adsorption geometries and direct ballistic electron transfer to phosphate σ^* levels. Graphene adsorbed on Au-thin films also provides enhanced electric fields for Surface Enhanced Raman microscopy. *The combination of these effects allows direct and fast assessment of ≤ 5 eV electron induced DNA damage as a function of base sequence without separations and amplification steps.*

We have recently examined LEE induced damage of nucleotides that have a minor change in the structure of the sugar. Specifically, we have examined the LEE induced damage of deoxyadenosine monophosphate (dAMP) and adenosine monophosphate (rAMP) using the graphene Raman micro-spectroscopy approach described above. The Raman spectra of the LEE irradiated thin-films of dAMP and rAMP are shown in Figure 1. The black line represents the pristine unirradiated sample and shows well defined Raman signatures. There

is no observable changes in the Raman spectra after 1 eV electron irradiation, despite the fact that resonances below 1 eV are expected based on gas-phase studies of the constituent sugars and bases.

However, as

shown in the blue line, significant damage of dAMP (labeled dA in the left frame of Figure 1) occurs after 2 eV electron bombardment. In fact, in addition to the breaking the C-O-P bond, several bonds in the sugar ring and base are also broken. *The situation is not the same for the rAMP (labeled rA in the right frame). There is limited damage even at 2 eV.* Remarkably, the simple addition of an -OH group to the 2'-C site dramatically changes the stability of the nucleotide with respect to glycosidic bond cleavage and base damage. This is likely related to the nature of the sugar shape resonances and decay products and the ability of charge to be transferred to the phosphate σ^* levels.

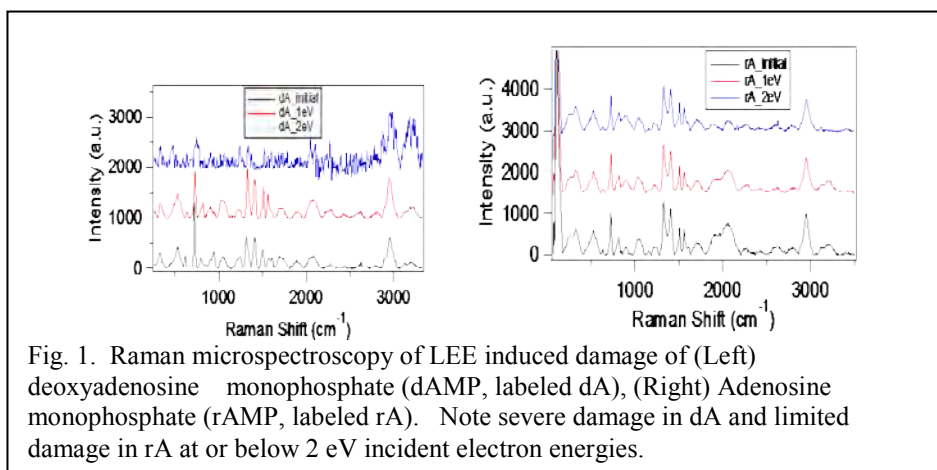


Fig. 1. Raman microspectroscopy of LEE induced damage of (Left) deoxyadenosine monophosphate (dAMP, labeled dA), (Right) Adenosine monophosphate (rAMP, labeled rA). Note severe damage in dA and limited damage in rA at or below 2 eV incident electron energies.

Project 3. X-ray induced damage of DNA and spin-filtering of electrons.

Our collaboration at Argonne National Laboratory has recently focused on examining x-ray damage of DNA adsorbed on Au in two different conformations. The first is a thiolated form which binds via a S bond and the other is direct adsorption via the bases. Differences in the damage cross sections are observed which can be related to the degree of charge exchange with the surface. Specifically, we performed a comparison of the radiation damage occurring in DNA adsorbed on gold in two different conformations, when the DNA is thiolated and bound covalently to the substrate and when it is unthiolated and interacts with the substrate through the bases. Both molecules were found to organize so as to protrude from the surface at ~ 45 degrees. Distinct differences were found in the N 1s X-ray absorption

spectra corresponding to the lowest unoccupied molecular orbitals (LUMOs) of the isolated molecule.

In the case of the adsorbed thiolated DNA, this state is less populated as compared to the adsorbed unthiolated molecules. This is a result of electron transfer from the substrate to the unthiolated adsorbed DNA. Changes in the time-dependent C 1s and O 1s X-ray photoelectron (XP) spectra resulting from irradiation were interpreted to arise from cleavage of the phosphodiester bond and possibly COH desorption. By fitting the time-dependent XP spectra to a simple kinetic model, time constants were extracted, which were converted to cross sections and quantum yields. The damage cross section was found to be significantly higher for the thiolated DNA, probably resulting from the LUMO initially being less populated and hence more effective in capturing of low energy secondary electrons.

We have also contributed to an experimental and theoretical study of the kinetic energy dependence of spin filtering of electrons by organized layers of DNA adsorbed on a gold substrate. Using synchrotron radiation excitation, X-ray Photoelectron Spectroscopy Circular Dichroism measurements were made of electrons with energies in the range 30 to 760 eV. In all cases there was no evidence of any significant dichroism. These results are explained by a model in which the longitudinal polarization is strongly dependent of the k-vector, and hence the energy or the de Broglie wavelength. For a helix with a fixed number of turns, this dependence is due to a coherent process associated with multiple scattering. This model predicts that there is a window of energies where changes in the polarization should be expected. Two competing effects determine this window: the de Broglie wavelength must be small enough to be comparable to the spatial extension of the helix and it must be large enough so that the residence time of the electron in the scattering region allows for at least double scattering to take place.

Publications acknowledging support from this program

1. G. A. Greives, J. L. McLain, and T. M. Orlando, "Low-energy stimulated reactions in nanoscale water films and water:DNA interfaces", Chapter 18, *Charge Particle Interactions with Matter: Recent Advances, Applications and Interfaces*, Taylor, Francis Publishing Co. (2010).
2. G. A. Greives and T. M. Orlando, "Intermolecular Coulomb decay at weakly coupled heterogeneous interfaces", *Phys. Rev. Lett.* 107, 016104 (2011).
3. R. Rosenberg, J. M. Symonds, T. Z. Markus, T. M. Orlando and R. Naaman, "The lack of spin selectivity in low-energy electron induced damage of DNA films", *J. Phys. Chem. C*. doi: 10.1021/jp402387y (2013).
4. A. N. Sidorov and T. M. Orlando, "Monolayer graphene platform for the study of DNA damage by low-energy electron irradiation", *J. Phys. Chem. Lett.*, 4 (14), 2328–2333 (2013).
5. R. A. Rosenberg, J. M. Symonds, V. Kalyanaraman, T.Z. Markus, T. M. Orlando and R. Naaman, "The relationship between interfacial bonding and radiation damage in adsorbed DNA", *Phys. Chem. Chem. Phys.* 2014, Advance Article DOI: 10.1039/C4CP01649A (2014).
6. A. N. Sidorov and T. M. Orlando, "Shape resonance induced damage of dAMP and rAMP", *in prep, Phys. Rev. Lett.*

Presentations acknowledging support from this program

1. T. M. Orlando, "Very low energy electron-induced damage of DNA", Dept. of Physics, Auburn University, March 21, 2014.
2. T. M. Orlando, "Very low energy electron-induced damage of DNA", Dept. of Physics, University of Georgia, March 21, 2014.
3. T. M. Orlando, "Very low energy electron-induced damage of DNA", CUNY, Dec. 6, 2013.
4. T. M. Orlando, "A monolayer graphene:Au surface enhanced Raman micro-spectroscopy platform for DNA damage studies", SERMACS, Atlanta, GA Nov. 13, 2013.

5. T. M. Orlando, "Very low energy electron-induced damage of DNA", Dept. of Physics, Vanderbilt University, Jan. 31, 2013.
6. T. M. Orlando, "Very low-energy electron-induced damage of DNA", University of Rome, LaSapienza, July 10, 2012.
7. T. M. Orlando, "Very low-energy electron-induced damage of DNA", Gaseous Electronics Conference, Univ. of Texas, Austin, Oct. 2012.
8. T. M. Orlando, "The interaction of very low-energy electrons with complex biological targets", Institute of Theoretical Atomic and Molecular Physics Symposium, Harvard University, Dec. 4-6, 2012.

Structure from Fleeting Illumination of Faint Spinning Objects in Flight

A. Ourmazd, A. Dashti, R. Fung, A. Hosseinizadeh, and P. Schwander

Dept. of Physics, University of Wisconsin Milwaukee
1900 E. Kenwood Blvd, Milwaukee, WI 53211
ourmazd@uwm.edu

The hard X-ray Free Electron Laser (XFEL) is a revolutionary new tool for the study of key systems and processes in the energy, physical, and life sciences. The unprecedented ability to record femtosecond X-ray snapshots offers the potential to understand and control the structural and dynamical properties of atoms, molecules, and nanostructures with superb spatial and temporal resolution.

To realize their full potential, revolutionary experimental tools must be accompanied by powerful theoretical frameworks. There is an urgent need for new data-analytical approaches capable of efficiently extracting reliable information from XFEL datasets in the presence of sample heterogeneity and timing uncertainty.

Methods recently developed in our group offer the possibility to extract conformational, ensemble-kinetic, and dynamical information from such datasets [1-7]. These methods combine techniques from Riemannian geometry, graph-theoretical dimensionality reduction (“manifold embedding”), and scattering physics. Fundamentally, however, they are based on two simple observations. First, most experimental datasets are heterogeneous, in the sense that they stem from collections of *non-identical* objects, differing, for example, in their conformational state. Second, *each* snapshot in a heterogeneous dataset provides information about *all* observed states of the system. For example, the view from the back of a person’s head has valuable information about the full-frontal view, because it reveals where the ears are – irrespective of whether the person is smiling or not. By substantially increasing the extracted information, this approach enables one to operate at exceptionally low signal levels. More importantly, it offers the exciting possibility to use the information from *all* observed states of a system to reconstruct *each* state.

Mapping discrete and continuous conformations of nanomachines

We have developed a new generation of algorithms capable of determining the structure and conformations of nanomachines from large noisy ensembles of heterogeneous snapshots, and demonstrated this capability in the context of simulated XFEL diffraction snapshots from discrete conformations, and experimental cryo-electron microscope (cryo-EM) image snapshots for continuous conformational changes.

Fig.1 show the sorting of two million simulated diffraction snapshots from 10 discrete conformations of the biologically important enzyme adenylate kinase (ADK), able to assume any orientation in three-dimensional space. All 10 conformations are correctly sorted. Fig. 2 shows the accurate sorting of simulated cryo-EM snapshots emanating from two discrete conformations of the ribosome responsible for protein synthesis in all cells. The signal-to-noise ratio of the input snapshots was -12dB (0.06 on a linear scale).

The application of these approaches to experimental cryo-EM snapshots of the ribosome has allowed us to determine the energy landscape associated with the protein-synthesis (elongation) cycle, and compile three-dimensional movies of the continuous conformational changes during the work cycle of this important nanomachine (Fig. 3).

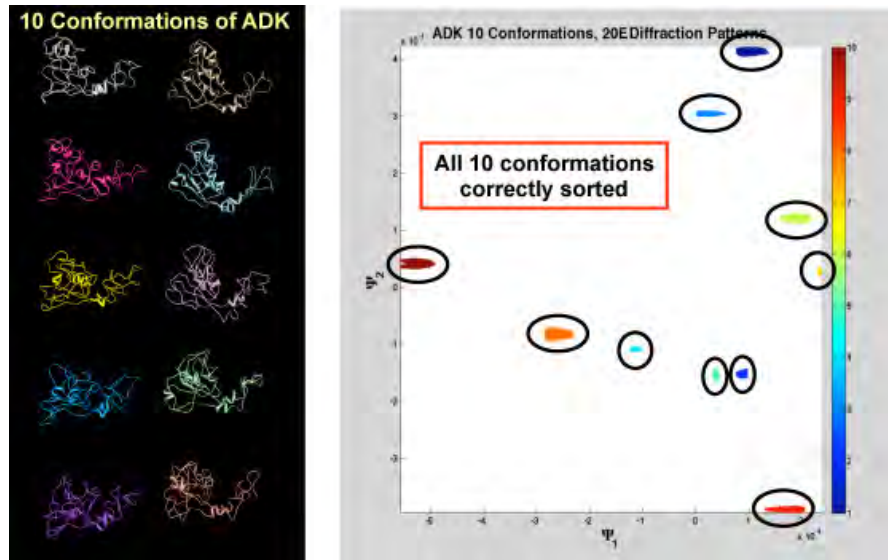


Fig. 1. Sorting of discrete conformations. 10 conformations of the enzyme adenylate kinase sorted by unsupervised manifold embedding. The axes are the first two eigenvectors of the Diffusion Map algorithm.

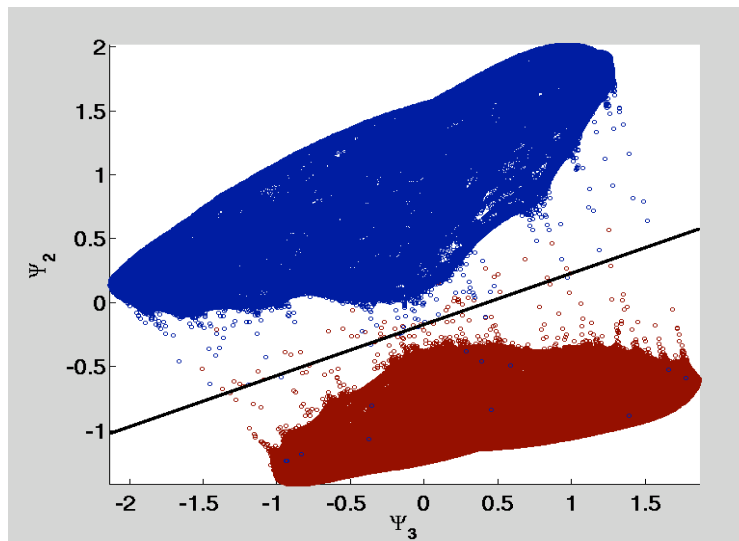


Fig. 2. Sorting of two discrete ribosome conformations (with and without EFG) with 99.96% accuracy. The signal-to-noise ratio of the input snapshots was 0.06.

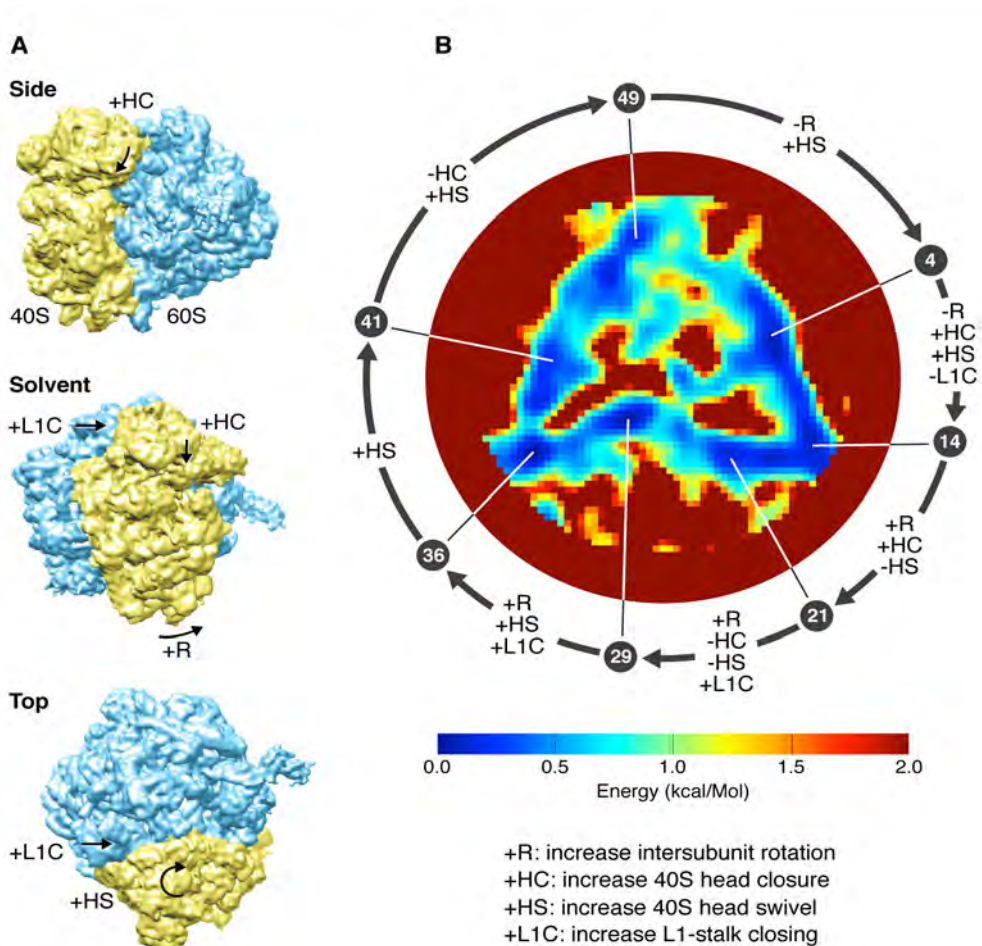


Fig. 3. (A) Three views of a map of the 80S ribosome recovered by our approach. Arrows indicate four key conformational changes associated with the elongation work cycle of the ribosome. **(B) The energy landscape** traversed by the ribosome. The color bar shows the energy scale (uncertainty: ± 0.05 kcal/Mol). The roughly triangular minimum-free-energy trajectory is divided into 50 states. Arrows indicate the structural changes between seven selected states, each identified by its place in the sequence of 50 states. The signal-to-noise ratio of the input experimental snapshots was ~ 0.06 .

Publications from DoE sponsored research

The following papers report on results obtained in the course of this project:

1. D. Giannakis, P. Schwander, and A. Ourmazd, Symmetries of image formation: I. Theoretical framework, *Optics Express* **20**, 12799 (2012).
2. P. Schwander, D. Giannakis, C.H. Yoon, and A. Ourmazd, Symmetries of image formation: II. Applications, *Optics Express* **20**, 12827 (2012).
3. J.M. Glowonia, A. Ourmazd, R. Fung, J. Cryan, A. Natan, R. Coffee, and P.H. Bucksbaum, Sub-cycle strong-field influences in X-ray photoionization, *CLEO Technical Digest*, QW1F.3 (2012).
4. P. Schwander, R. Fung, A. Ourmazd, Conformations of macromolecules and their

complexes from heterogeneous datasets, *Phil Trans Roy Soc B* **369**, 20130567 (2014).

5. A. Hosseinizadeh, P. Schwander, A. Dashti, R. Fung, R.M. D'Souza, A. Ourmazd, High resolution structure of viruses from random snapshots *Phil Trans Roy Soc B* **369**, 20130326 (2014).
6. Tenboer et al., Time-resolved serial femtosecond crystallography captures high-resolution intermediates of Photoactive Yellow Protein, submitted (2014).
7. A. Dashti, P. Schwander, R. Langlois, R. Fung, W. Li, A. Hosseinizadeh, H.Y. Liao, J. Pallesen, G. Sharma, V.A. Stupina, A. E. Simon, J. Dinman, J. Frank, A. Ourmazd, Trajectories of a Brownian machine: the ribosome, submitted (2014).

References

- [1] Fung R, Shneerson V, Saldin DK, Ourmazd A, (2009) Structure from fleeting illumination of faint spinning objects in flight. *Nature Physics*: **5**(1):64-67, <http://www.nature.com/nphys/journal/v5/n1/abs/nphys1129.html>
- [2] Schwander P, Fung R, Phillips GN, Ourmazd A, (2010) Mapping the conformations of biological assemblies. *New Journal of Physics*: **12**:1-15, <http://iopscience.iop.org/1367-2630/12/3/035007>
- [3] Giannakis D, Schwander P, Ourmazd A, (2012) The symmetries of image formation by scattering. I. Theoretical framework. *Optics Express*: **20**(12):12799 - 12826, <http://www.opticsinfobase.org/oe/abstract.cfm?uri=oe-20-12-12799>
- [4] Schwander P, Giannakis D, Yoon CH, Ourmazd A, (2012) The symmetries of image formation by scattering. II. Applications. *Optics Express*: **20**(12):12827-12849, <http://www.opticsinfobase.org/oe/abstract.cfm?uri=oe-20-12-12827>
- [5] Yoon CH, Schwander P, Abergel C, Andersson I, Andreasson J, Aquila A, Bajt S, Barthelmess M, Barty A, Bogan MJ, Bostedt C, Bozek J, Chapman HN, Claverie JM, Coppola N, Deponte DP, Ekeberg T, Epp SW, Erk B, Fleckenstein H, Foucar L, Graafsma H, Gumprecht L, Hajdu J, Hampton CY, Hartmann A, Hartmann E, Hartmann R, Hauser G, Hirsemann H, Holl P, Kassemeyer S, Kimmel N, Kiskinova M, Liang M, Loh NT, Lomb L, Maia FR, Martin AV, Nass K, Pedersoli E, Reich C, Rolles D, Rudek B, Rudenko A, Schlichting I, Schulz J, Seibert M, Seltzer V, Shoeman RL, Sierra RG, Soltau H, Starodub D, Steinbrener J, Stier G, Struder L, Svenda M, Ullrich J, Weidenspointner G, White TA, Wunderer C, Ourmazd A, (2011) Unsupervised classification of single-particle X-ray diffraction snapshots by spectral clustering. *Optics Express*: **19**(17):16542-16549, <http://www.opticsinfobase.org/abstract.cfm?URI=oe-19-17-16542>
- [6] Hosseinizadeh A, Schwander P, Dashti A, Fung R, D'Souza RM, Ourmazd A, (2014) High-resolution structure of viruses from random diffraction snapshots. *Phil. Trans. R. Soc. B*: **369**:20130326, <http://dx.doi.org/10.1098/rstb.2013.0326>
- [7] Schwander P, Fung R, Ourmazd A, (2014) Conformations of macromolecules and their complexes from heterogeneous datasets. *Phil. Trans. R. Soc. B*: **369**:20130567, <http://dx.doi.org/10.1098/rstb.2013.0567>

Control of Molecular Dynamics: Algorithms for Design and Implementation

Herschel Rabitz and Tak-San Ho

Princeton University, Frick Laboratory, Princeton, NJ 08540

hrabitz@princeton.edu, tsho@princeton.edu

A. Program Scope:

This research is for the systematic study of several interrelated topics in the general area of controlled quantum dynamics phenomena. The goal of the research is to develop a deeper understanding of the principles of quantum control as well as to provide new algorithms to extend the laboratory control capabilities.

B. Research Progress:

In the past year, a broad variety of research topics were pursued in the general area of controlling quantum dynamics phenomena. A summary of these activities is provided below.

[1] **Open quantum system control landscapes**¹ This study laid out a formal prescription for assessing open system control landscapes and rigorously proved that for a single spin, the landscape should be trap-free, although not every state is reachable. This analysis was also confirmed in simulations and represents a first step towards a fuller understanding of this important operational regime.

[2] **Exploring quantum control landscape structure**^{2,3} In this work, an initial study was performed theoretically examining landscape structural features with the surprising conclusion that there appears to be a rather universal lack of any gnarled features. A good understanding of these landscape structural features is very important since it can greatly influence the efficiency of finding controls in the laboratory.

[3] **Control principles in the chemical sciences**^{4,5} In this study we examined control principles for different families of molecules, all related through various moieties bonded to a common molecular scaffold, utilizing NMR and IR spectral data as the properties of interest. Chemical rules for the associated spectroscopies were found consistent with known relations, and the analysis went further to reveal broader, overarching rules.

[4] **Control landscapes for laser-driven molecular fragmentation**⁶ In this study we examined the landscape principles for laser-driven molecular fragmentation. These principles guided a series of experimental efforts examining the landscapes for molecular dissociative ionization of halo-methane molecules. The landscape principles provide a natural basis to consider “photonic reagents” as equal partners with chemical reagents. The systematics found in the study of halo-methane molecules takes a step towards identifying photonic reagents as having their own associated “chemistry” for inducing reactive dynamics.

[5] **Quantum control algorithm development**⁷ In this study a new class of algorithm was developed, utilizing sampling-based learning control, as a means for optimally manipulating an ensemble (collection) of quantum systems where each member has a slightly different Hamiltonian due to environmental circumstances. The algorithm was efficient for identifying an optimal field utilizing even a modest sample of ensemble members in the training phase. The

procedure has both simulation and laboratory significance.

[6] **Invariance of quantum optimal control fields to experimental parameters**⁸ This work utilized landscape principles to establish when an optimal field can maintain optimal system performance even when experimental conditions are varying. This analysis rests on the fact that an optimal field serves to create a particular permutation matrix as the dynamical unitary transformation. In particular, this work showed that an optimal field at one temperature will remain optimal at other temperatures, which has broad practical significance in the laboratory.

[7] **Exploring the impact of resource constraints upon control performance**^{9,10} This work laid out the detailed mathematical foundation for systematically exploring how ever increasing constraints encroach on the ability to obtain good, if not optimal, control performance. This formulation functioned by linking the so-called ‘kinematic’ and ‘dynamic’ landscape analysis frameworks to provide a basis for developing practical algorithms to assess the impact of control constraints.

[8] **Control of ozone isomerization dynamics**¹¹ The ozone transformation from the normal open configuration to a potential cyclic form has garnered interest for many years. Even with three atoms, a full dynamics study of ozone under control is a highly complex task. This study took a further step in this direction based on a bending reaction coordinate model utilizing electronic excited states.

[9] **Gene network robustness analysis based on saturated fixed point attractor**¹² This work drew on our general network analysis tools to show that they apply as well for determining the fixed point attractors of gene networks. Analytical treatment was presented based on determination of the saturated fixed point attractors for a sigmoidal function model. The analytical treatment make it possible to properly define and accurately determine robustness to noise and mutation for gene networks.

[10] **Control of atomic collisions**¹³ This work explored the long-standing goal of controlling collisional events with tailored fields. Specifically, we showed that charge transfer between H^+ + D collisions can be significantly manipulated by suitable pulses.

[11] **Control landscapes for nonlinear quantum systems**¹⁴ This work extended the analysis of control landscape topology to nonlinear quantum dynamics with the objective of steering a finite-level quantum system from an initial state to a final target state. Extensive numerical simulations on finite-level models of the Gross-Pitaevskii equation confirm the trap-free nature of the landscape as well as the Hessian rank analysis, using either an applied electric field or a tunable condensate two-body interaction strength as the control. In addition, the control mechanisms arising in the numerical simulations are qualitatively assessed.

[12] **Quantum control landscape practice and theory**^{15,16} In this work an experimental study was carried out to explore the landscape for the control of a single spin in NMR, which implemented a laboratory incarnation of the same algorithms used in our computer simulations. The experimental landscape findings are consistent with the theoretical predictions. Moreover, a landscape theoretical topology analysis was carried out for unitary transformation targets, considering the landscape maxima/minima and saddle features.

[13] **Minimal time population transfer for two-level systems driven by two bounded controls**¹⁷ This work analyzed the minimum time population transfer problem for a two level quantum system driven by two external fields with bounded amplitude. The controls were

modeled as real functions and we do not use the Rotating Wave Approximation. After projection on the Bloch sphere, the time-optimal control problem was treated with techniques of optimal synthesis on 2D manifolds.

[14] **Quantum optimal control fields in the presence of singular critical points**¹⁸ This work explored how gradient searches for globally optimal control fields are affected by deviations from the assumption that the Jacobian of the map from the control field to the evolution operator is full rank. Using optimal control simulations, we showed that search failure is only observed when a singular critical point, at which the Jacobian is rank deficient, is also a second-order trap, which occurs if the control problem meets additional conditions involving the system Hamiltonian and/or the control objective. All known second-order traps occur at constant control fields, and we also show that they only affect searches that originate very close to them. As a result, even when such traps exist on the control landscape, they are unlikely to affect well-designed gradient optimizations under realistic searching conditions.

[15] **Selectively addressing optically nonlinear nanocrystals by polarization-shaped ultrafast laser pulses**¹⁹ This work theoretically studied second-harmonic generation (SHG) and sum-frequency generation (SFG) signals produced by nanocrystals driven with broad-bandwidth laser pulses. Several simulations explored the influence of the field polarization and temporal pulse profile. The latter two factors are decoupled in their influence upon the SHG and SFG signals, and thus polarization and temporal shaping can be independently performed to modulate a nanocrystals' second-order emission. We considered the possibility of enhancing (suppressing) the signal from one nanocrystal among others by choosing the appropriate polarization, thereby opening up the prospect of selectively addressing optically nonlinear nanocrystals.

C. Future Plans:

The research in the coming year will include the following: (1) We plan to analyze the advanced aspects of quantum control landscape and explore its practical implications. In particular, we will closely examine the physical basis for the satisfaction of the Assumptions underlying landscape analysis. (2) We plan to carefully explore and build a framework for identifying essential model features as a basis for analyzing additional emerging laboratory Hessian investigations of optimal control results. The Hessian is the second derivative matrix of the objective being optimized with respect to the control variables. The Hessian, evaluated at the field producing the maximum control yield, was introduced as a means of characterizing control solutions. Importantly, the number and nature of the Hessian eigenvalues at the top of the landscape indicate the complexity of the underlying controlled dynamics, and the associated eigenvectors reveal the cooperative aspects of the optimal field components. (3) We plan to establish conditions for when a control field remains optimal, regardless of the values of the experimental parameters, such that an optimal field determined at one set of parameter values will again produce an optimal outcome at any other values of the parameters. An understanding of the physical conditions consistent with such an invariance property for the optimal control field would be important in the laboratory (as well as for performing control designs) in order to avoid performing unnecessary new control experiments. (4) We plan to build on our current study, in collaboration with Dr. Yuzuru Kurosaki in Japan, to form a more elaborate assessment of the prospects of performing ozone isomerization by executing OCT calculations utilizing multi-state models, beyond the current reaction coordinate picture to include neighboring potential features.

D. References

1. Exploring the transition-probability-control landscape of open quantum systems: Application to a two-level case, F. Yang, S. Cong, R. Long, T. Ho, R. Wu, and H. Rabitz, *Phys. Rev. A*, **88**, 033420, (2013).
2. Exploring quantum control landscape structure, A. Nanduri, A. Donovan, T.-S. Ho, and H. Rabitz, *Phys. Rev. A*, **88**, 033425, (2013).
3. Relation of quantum control mechanism to landscape structure, A. Nanduri, A. Donovan, T.-S. Ho, and H. Rabitz, *Phys. Rev. A*, **90**, 013406, (2014).
4. Systematic Trends in Photonic Reagent Induced Reactions in a Homologous Chemical Family, K. Moore Tibbetts, X. Xing, and H. Rabitz, *J. Phys. Chem A.*, **117**, 8205-8215, (2013).
5. Optimal control of molecular fragmentation with homologous families of photonic reagents and chemical substrates, K. Moore Tibbetts, X. Xing, and H. Rabitz, *Phys. Chem. Chem. Phys.*, **15**, 18012, (2013).
6. Exploring control landscapes for laser-driven molecular fragmentation, K. Moore Tibbetts, X. Xing, and H. Rabitz, *J. Chem. Phys.*, **139**, 144201, (2013).
7. Sampling-based learning control of inhomogeneous quantum ensembles, C. Chen, D. Dong, R. Long, I. Petersen, and H. Rabitz, *Phys. Rev. A*, **89**, 023402, (2014).
8. Invariance of quantum optimal control fields to experimental parameters, E. de Lima, T.-S. Ho, and H. Rabitz, *Phys. Rev. A*, **89**, 043421, (2014).
9. Investigating constrained quantum control through a kinematic-to-dynamic-variable transformation, A. Donovan and H. Rabitz, *Phys. Rev. A*, **90**, 013408, (2014)
10. Local topology at limited resource induced suboptimal traps on the quantum control landscape, A. Donovan, V. Beltrani, and H. Rabitz, *J. Math. Chem.*, **52**, 407-429, (2014).
11. Quantum optimal control pathways of ozone isomerization dynamics subject to competing dissociation: A two-state one-dimensional model, Y. Kurosaki, T.-S. Ho, and H. Rabitz, *J. Chem. Phys.*, **140**, 084305, (2014).
12. Analysis of gene network robustness based on saturated fixed point attractors, G. Li and H. Rabitz, *EURASIP Journal*, **4**, (2014).
13. Optimal control of charge transfer for slow H(+)+D collisions with shaped laser pulses, W. Zhang, C.-C. Shu, T.-S. Ho, H. Rabitz, and S.-L. Cong, *J. Chem. Phys.*, **140**, 094301, (2014).
14. Exploring the control landscape for nonlinear quantum dynamics, J. Yan, D. Hocker, R. Long, T.-S. Ho, and H. Rabitz, *Phys. Rev. A*, **89**, 063408, (2014).
15. Experimental exploration over a quantum control landscape through nuclear magnetic resonance, Q. Sun, I. Pelczer, G. Riviello, R.-B. Wu, and H. Rabitz, *Phys. Rev. A*, **89**, 033413, (2014).
16. Characterization of the Critical Sets of Quantum Unitary Control Landscapes, J. Dominy, T. S. Ho, and H. Rabitz, *IEEE Trans. Autom. Control*, **59**, 2083 (2014).
17. Minimal time trajectories for two-level quantum systems with two bounded controls, U. Boscain, F. Gronberg, R. Long, and H. Rabitz, *J. Math. Phys.*, **55**, 062106, (2014).
18. Searching for quantum optimal control fields in the presence of singular critical points, G. Riviello, C. Brif, R. Long, R.-B. Wu, K. Moore Tibbetts, T.-S. Ho, and H. Rabitz, *Phys. Rev. A*, **90**, 013404, (2014).
19. Selectively addressing optically nonlinear nanocrystals by polarization-shaped ultrafast laser pulses, Y. Paskover, D. Xie, F. Laforge, and H. Rabitz, *J. Opt. Soc. Am. B*, **31**, 1165, (2014).

“Atoms and Ions Interacting with Particles and Fields”

F. Robicheaux

*Purdue University, Department of Physics, 525 Northwestern Ave, West Lafayette
IN 47907 (robichf@purdue.edu)*

Program Scope

This theory project focuses on the time evolution of systems subjected to either coherent or incoherent interactions represented by fields and particles, respectively. This study is divided into three categories: (1) coherent evolution of highly excited quantum states, (2) incoherent evolution of highly excited quantum states, and (3) the interplay between ultra-cold plasmas and Rydberg atoms. Some of the techniques we developed have been used to study collision processes in ions, atoms and molecules. In particular, we have used these techniques to study the correlation between two (or more) continuum electrons and electron impact ionization of small molecules.

Recent Progress 2013-2014

Hole-burning in attosecond ionization: We modified our time dependent Schrodinger equation programs to perform calculations of attosecond laser-atom interactions for laser intensities where interesting two- and three-photon effects become relevant.[15] We focused on the case of “hole burning” in the initial orbital. Hole burning is present when the laser-pulse duration is shorter than the classical radial period because the electron preferentially absorbs the photon near the nucleus. By changing the laser frequency, chirp and duration, we were able to show that the main effects were almost solely due to the duration. The hole burning can be described a Raman process caused by the coherent absorption then re-emission of a photon and is, thus, a two photon process. We also showed that the hole burning can affect the time delay of ejected electrons for strong attosecond fields.

Imaging of quantum state inside atom: We were involved in an experimental/computational project to image a part of the wave function inside an atom.[20] The experiments used photoionization microscopy to image the variation in the wave function perpendicular to the electric field. The calculations involved a direct solution of the time dependent Schrodinger equation in a region $\sim 30,000$ Bohr radii by using a mixture of spherical harmonics (up to 300) and time dependent radial functions on a grid of points. In this study, we investigated the behavior of Stark states near avoided crossings. Near an avoided crossing, the interacting states may have decay amplitudes that cancel each other, decoupling one of the states from the ionization continuum. This well-known interference narrowing was studied in He atoms with photoionization microscopy; with this visualization, the character of the Stark states are revealed. The interference narrowing allows measurements of the nodal patterns of red Stark states, which are otherwise not observable due to their intrinsic short lifetime.

Classical-quantum correspondence in a Rydberg system: We performed classical calculations of one of the iconic effects of Rydberg atoms in electric fields.[14] For low angular momentum states, a rising electric field mixes angular

momenta and gives rise to Stark states. If the initial state has slightly lower (higher) energy than the degenerate manifold, then the state adiabatically connects to a Stark state with the electron on the low (high) potential energy side of the atom. We showed that purely *classical* calculations for non-hydrogenic atoms have an adiabatic connection to extreme dipole moments similar to quantum systems. We developed a simple map to show that the classical dynamics arises from the direction of the precession of the Runge-Lenz vector when the electric field is off. As a demonstration of the importance of this effect, classical calculations of charge exchange showed that the total cross sections for charge transfer and for ionization strongly depend on whether or not a pure Coulomb potential is used.

Quasistable states in a strong microwave field: We were involved in an experimental/theoretical study of how atoms can have resonance states in extremely strong microwave fields.[18] As had been seen earlier, when atoms are exposed to intense laser or microwave pulses, $\sim 10\%$ of the atoms are found in Rydberg states subsequent to the pulse, even if it is far more intense than required for static field ionization. We investigated the spectrum of these quasistable states. Lithium atoms were excited to near threshold by a laser while a strong microwave field was on. The microwave field was then reduced to zero over a time scale longer than the Rydberg period. We were able to measure the fraction of surviving atoms as a function of the detuning of the laser from threshold as a function of the microwave parameters. For a 38 GHz microwave field, the spectra exhibit a periodic train of peaks 38 GHz apart. One peak is just below the limit. This train of peaks can extend from a substantial energy below threshold to above threshold. At 90 V/cm field amplitude, the train extends from 3000 GHz below the zero field limit to 300 GHz above the limit. The spectra and quantum mechanical calculations imply that the atoms survive in quasistable states in which the Rydberg atom is in a weakly bound orbit infrequently returning to the ionic core during the intense pulse.

Many-body ionization: We performed calculations to investigate how many simultaneously excited atoms can exchange energy and ionize.[19] These calculations were inspired by experimental results from T.F. Gallagher's group that found substantially increased ionization at very early times when the atom density was high. They reported ionization in Rydberg gases for densities two orders of magnitude less than expected from ionization between pairs of atoms. They argued the results were due to the simultaneous interaction between many atoms. We performed classical calculations for many interacting Rydberg atoms with the ions fixed in space. We found that the many-atom interaction does allow ionization at lower densities than estimates from two-atom interactions. However, we found that the density fluctuations in a gas play a larger role than the many-atom interactions. Our calculations did give less ionization than was measured which suggests at least one other unidentified mechanism strongly affects ionization.

Relativistic double ionization: We performed calculations of single and double photoionization of Ne^{8+} by direct solution of the time-dependent Dirac equation.[16] We expanded the two-electron wave function in coupled spin-orbit eigenfunctions to obtain time-dependent close-coupled equations for quad-spinor radial wave functions. The repulsive interaction between electrons included both Coulomb and Gaunt interactions. We obtained the fully-correlated ground state

radial wave function by solving a time-independent inhomogeneous set of close coupled equations instead of a relaxation of the time-dependent close-coupled equations in imaginary time. A Bessel function expansion was used to include both dipole and quadrupole effects in the radiation field for both the ‘velocity’ and ‘length’ gauges. Our results for the single and double photoionization cross sections should be easily accessible at advanced free electron laser facilities.

Ion-molecule scattering in a magnetic field: We performed calculations of elastic and inelastic scattering of neutral molecules and cold ions in a magnetic field.[17] The molecule was assumed to have a magnetic and electric dipole moment. The external magnetic field splits the ground rovibrational levels of the molecule. The highest energy state within the ground rovibrational manifold increases in energy as the distance to the ion decreases leading to a repelling potential. At low energy, inelastic collisions are strongly suppressed due to the large distance of closest approach. Thus, a collision between a neutral molecule and a cold ion will lead to a decrease in the molecule’s kinetic energy with no change in internal energy. We also performed molecular dynamics simulations of ions and molecules in a combined Paul trap and time-averaged orbiting potential trap; our results suggest that sympathetic cooling of neutral molecules by ions would be possible.

Finally, this program has several projects that are strongly numerical but only require knowledge of classical mechanics. This combination is ideal for starting undergraduates on publication quality research. Since 2004, twenty four undergraduates have participated in this program. Most of these students have completed projects published in peer reviewed journals. Two undergraduates, Michael Wall in 2006 and Patrick Donnan in 2012, were one of the 5 undergraduates invited to give a talk on their research at the undergraduate session of the DAMOP meeting. Three publications during the past year [14,15,19] had an undergraduate supported by DOE as first author or coauthor.

Future Plans

Single cycle ionization: R.R. Jones recently published results in PRL on single cycle ionization of highly excited atoms. Inspired by these experiments we will perform systematic studies of single cycle ionization of atoms, from highly excited states down to the ground state. There are several parameters that should depend on the binding energy and duration of the pulse. We will investigate the field strength needed to ionize 10% of the atoms, the energy distribution of the ionized electrons, the asymmetry of the ejected electrons, the correlation between ejection angle and electron energy, ...

Rydberg Physics We have performed several calculations of how electrons emerge from atoms in electric fields that were joint experimental/theoretical studies.[12,13,20] We will test some of the basic theories of how to describe the long range behavior of the electron leaving the atom by comparing full quantum calculations with approximations based on the local frame transformation. The local frame transformation has been used in many different situations in atomic and molecular systems. This test will allow us to ascertain whether recent papers describing the limitations of this approximation are accurate.

Two electron physics We have recently developed a method for dealing with the quantum mechanics when two electrons extend over very large regions and/or interact for a long time.[7,8,10] We will use our fully quantum method to test the range of validity of some of the approximations that are standard in PCI. We are also interested in further pursuing the time dependent double Rydberg system[10] but explicitly putting in quantum defects for the electrons and exploring the case where the two electrons have unequal excitation.

DOE Supported Publications (9/2011-8/2014)

- [1] J. Colgan, M.S. Pindzola, F. Robicheaux, and M.F. Ciappina, *J. Phys. B* **44**, 175205 (2011).
- [2] P.H. Donnan, K. Niffenegger, T. Topcu, and F. Robicheaux, *J. Phys. B* **44**, 184003 (2011).
- [3] M.S. Pindzola, Sh. A. Abdel-Naby, J.A. Ludlow, F. Robicheaux, and J. Colgan, *Phys. Rev. A* **85**, 012704 (2012).
- [4] I. Yavuz, E.A. Bleda, Z. Altun, and T. Topcu, *Phys. Rev. A* **85**, 013416 (2012).
- [5] P.H. Donnan and F. Robicheaux, *New. J. Phys.* **14**, 035018 (2012).
- [6] M.S. Pindzola, Sh. A. Abdel-Naby, F. Robicheaux, and J. Colgan, *Phys. Rev. A* **85**, 032701 (2012).
- [7] F. Robicheaux, *J. Phys. B* **45**, 135007 (2012).
- [8] F. Robicheaux, M.P. Jones, M. Schoffler, T. Jahnke, K. Kreidi, J. Titze, C. Stuck, R. Dorner, A. Belkacem, Th. Weber, and A.L. Landers, *J. Phys. B* **45**, 175001 (2012).
- [9] T. Topcu and F. Robicheaux, *Phys. Rev. A* **86**, 053407 (2012).
- [10] X. Zhang, R. R. Jones, and F. Robicheaux, *Phys. Rev. Lett.* **110**, 023002 (2013).
- [11] M. S. Pindzola, C. P. Balance, Sh. A. Abdel-Naby, F. Robicheaux, G. S. J. Armstrong, and J. Colgan, *J. Phys. B* **46**, 035201 (2013).
- [12] S. Cohen, M. M. Harb, A. Ollagnier, F. Robicheaux, M. J. J. Vrakking, T. Barillot, F. Lepine, and C. Bordas, *Phys. Rev. Lett.* **110**, 183001 (2013).
- [13] A. S. Stodolna, A. Rouzee, F. Lepine, S. Cohen, F. Robicheaux, A. Gijsbertsen, J. H. Jungman, C. Bordas, and M. J. J. Vrakking, *Phys. Rev. Lett.* **110**, 213001 (2013).
- [14] G.W. Gordon and F. Robicheaux, *J. Phys. B* **46**, 235003 (2013).
- [15] P.L. Price, L.D. Noordam, H.B. van Linden van den Heuvell, and F. Robicheaux, *Phys. Rev. A* **89**, 033414 (2014).
- [16] M.S. Pindzola, Sh.A. Abdel-Naby, F. Robicheaux, and J. Colgan, *J. Phys. B* **47**, 085002 (2014).
- [17] F. Robicheaux, *Phys. Rev. A* **89**, 062701 (2014).
- [18] A. Arakelyan, T. Topcu, F. Robicheaux, and T.F. Gallagher, *Phys. Rev. A* **90**, 013413 (2014).
- [19] F. Robicheaux, M.M. Goforth, and M.A. Phillips, *Phys. Rev. A* **90**, 022712 (2014).
- [20] A.S. Stodolna, F. Lepine, T. Bergeman, F. Robicheaux, A. Gijsbertsen, J.H. Jungmann, C. Bordas, and M.J.J. Vrakking, *Phys. Rev. Lett.* **113**, 103002 (2014).

Generation of Bright Soft X-ray Laser Beams

Jorge J. Rocca

Department of Electrical and Computer Engineering and Department of Physics
Colorado State University, Fort Collins, CO 80523-1373

jorge.rocca@colostate.edu

Program description

This research addresses the challenge of the efficient generation of bright x-ray laser beams. In table-top experiments conducted during this grant period we extended gain-saturated table-top lasers down to $\lambda = 8.8$ nm, and demonstrated 100 Hz repetition rate soft x-ray laser operation with a record average power of 0.15 mW at $\lambda = 18.9$ nm. We have also collaborated in an experiment at LCLS that demonstrated strong stimulated x-ray Raman scattering by resonantly exciting a dense gas target with high-intensity femtosecond x-ray free-electron laser pulses. Recently we completed the first x-ray pump-x-ray probe measurement of the non-linear response of a soft x-ray laser plasma amplifier perturbed by a strong ultrashort soft x-ray pulse [1]. The measured fast gain recovery time of ~ 1.75 ps supports the possibility to generate ultra-intense fully phase-coherent soft x-ray laser by chirped-pulse-amplification in plasma amplifiers. Although such gain recovery time is one of the most fundamental parameters for soft x-ray lasers, it has never been measured. In a separate experiment the linewidth of a $\lambda = 14.7$ nm Ni-like Pd soft x-ray laser was measured in a single shot with a soft x-ray diffraction grating interferometer that uses the time delay introduced by the gratings across the beam to measure the temporal coherence [2]. The spectral linewidth of the $4d^1S_0-4p^1P_1$ Ni-like Pd lasing line was measured to be $\Delta\lambda/\lambda = 3 \times 10^{-5}$ from the Fourier transform of the fringe visibility. This single shot linewidth measurement technique can contribute to the development femtosecond plasma-based soft x-ray lasers.

Gain dynamics in a soft x-ray laser amplifier perturbed by a strong injected x-ray field

While the population inversion dynamics of plasma-based soft x-ray lasers (SXRL) running in the amplified spontaneous emission mode (ASE) is controlled by thermodynamics and hydrodynamics processes that have been extensively studied, seeding these amplifiers with a high intensity soft x-ray beam uncovered new processes. The non-linear interaction of the strong seed field with the lasing ions modifies the population inversion dynamics, leading for example to the creation and amplification of a picosecond wake field. Maxwell-Bloch equations are suited to model the interaction of soft x-ray electromagnetic field and ionic populations. However, the assumptions and simplifications implied by these set of equations raises the question of its range of validity when predicting the ionic response to the seed with the peculiar complexity related to the high-field regime. No experiment has directly probed the non-linear dynamic of ionic levels in plasma after being perturbed by an external intense soft X-ray seed pulse. In work published in Nature Photonics we have recently reported the first experimental and numerical study of the temporal evolution of the non-linear response of a soft x-ray plasma amplifier following an intense resonant seed pulse [1], of which we had presented preliminary results in a previous report. A sequence of two time-delayed spatially-overlapping high harmonic (HH) pulses was seeded into an 18.9 nm wavelength Ni-like Mo plasma amplifier to measure the rapid regeneration of the population inversion that follows the gain depletion caused by the amplification of a strong seed pulse.

To conduct the experiment a Ti:Sapphire laser beam was separated into two. The first beam has a sequences of pulses that create and ionize the plasma to the nickel-like state, and subsequently rapidly heats it to generate a large transient population inversion by collisional electron impact excitation. The second beam was split to create a sequence of two independently controllable HH seed pulses (~ 60 fs duration), hereafter called the “HH pump” (in the sense that it strongly perturbs the lasing ion excited level populations), and the “HH probe” (in the sense that it is used to analyzed the temporal evolution of the perturbed population). The duration of the amplification was probed by seeding the plasma amplifier with a single HH pulse, whose time of arrival was scanned, taking as a reference the arrival of the plasma heating infrared short pulse. Figure 1(a) shows the measured variation of the energy of the amplified HH seed pulse as a function of time delay respect to the peak of the short plasma heating pulse ($T_0=0$ ps). The

amplification period is observed to last ~ 10 ps with a maximum occurring at ~ 5 ps after T_0 , in good agreement with our simulations (solid line in Fig 1a) using 2D hydrodynamic modeling post-processed by a Maxwell-Bloch code. The modeling shows that the duration of the amplification is mainly governed by the ionization dynamic (over-ionization) linked to the strong plasma heating due to the short infrared pulse. Figure 1b displays the energy of the HH probe after amplification through the plasma, allowing measurement of the depletion of the population inversion and its subsequent recovery due to collisional excitation. Measurements were conducted for two different times of injection of the HH pump pulse respect to the short infrared heating pulse: 3 ps and 6 ps (black and red curves respectively). As a first step, the HH probe was amplified alone (i.e. the HH pump was blocked) giving as a reference the output energy for the unperturbed plasma. The amplified HH probe energy was about 50% lower than of the HH pump alone at the same time delay, because its weaker input energy. Subsequently the HH probe was added at $T_0=3$ ps relative to the short infrared plasma heating pulse, and the pump-probe delay, Δt , was varied from 250 fs to 7 ps (Fig. 1b black line). At $\Delta t = 250$ fs, the output energy of the HH probe was

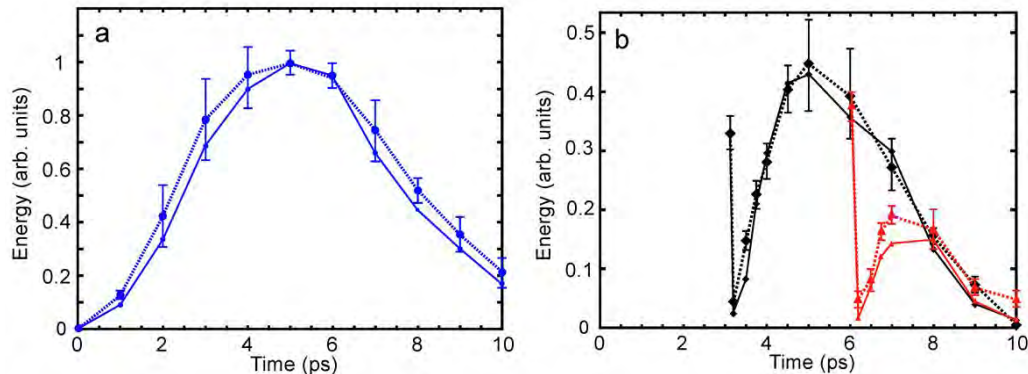


Figure 1. Experimental measurement of the gain dynamics in soft x-ray plasma Ni-like Mo amplifier compared with results from a Maxwell-Bloch simulation. (a) measured (dotted line) and simulated (solid line) variation of the energy of a single amplified HH seed pulse as a function of time delay respect to the peak of the short plasma heating pulse ($T=0$ ps). (b) measured (dotted line) and measured (solid line) variation of the energy of a HH probe pulse as a function of time starting at the time of injection of a preceding pump HH pulse injected at 3 ps (black) and 6 ps after the peak of the short plasma pump heating pulse. The negligible energy of the amplified HH probe 250 fs after arrival of the HH pump shows a nearly complete bleaching of the population inversion by the HH pump, while for delays larger than about 0.5 ps strong probe amplification demonstrates the rapid gain recovery process. The measurement confirms the gain recovery of 1.75 ps predicted by the model.

near or below the detection threshold, which is the signature of negligible amplification and thus practically complete depletion of the population inversion by the HH pump. Indeed, our modeling shows that the HH pump enters in the plasma at an intensity of several 10^8 Wcm^{-2} to exit at $\sim 10^{11}$ Wcm^{-2} i.e. 10 times the intensity necessary to start to saturate the gain. In the case in which the HH pump is seeded at 3 ps, the point acquired with the HH probe delayed by 0.5 ps already shows amplification, but not yet a full recovery of the gain. At $\Delta t=1.5$ ps, the energy of the amplified HH probe equals its value without the HH pump and continues to increase reaching a maximum for a delay of 1.75 ps. When the HH pump is seeded at 6 ps, the HH probe follows the same behavior of fast recovery, but never reaches the energy attained at 6 ps without HH pump, because at this time the gain is already rapidly dropping. Simulations have also been conducted to estimate the maximum energy extractable by a fully coherent source from such plasma produced by a 0.8 J of infrared laser. For two 60 fs seed pulses with equal input energy separated by $\Delta t=1.5$ ps (Fig. 2a) the output energy is practically double the energy extracted using a single HH seed pulse, while a single 6 ps FWHM duration seed pulse extracts 17 times more energy than a single 60 fs HH seed (Fig 2b).

This first X-ray pump- X-ray probe experiment in a soft x-ray plasma amplifier not only uncovers the gain recovery dynamics due to electron collisions but also serves as a diagnostic of the ionization mechanisms in the hot dense plasma with a resolution of hundreds of femtoseconds. The measured rapid recovery of the gain also confirms that it should be possible to continuously extract energy from any long

gain soft x-ray plasma amplifier with a stretched seed pulse. When combined with x-ray CPA this type of injection seeding has the potential to generate ultra-intense fully phase-coherent soft x-ray laser pulses.

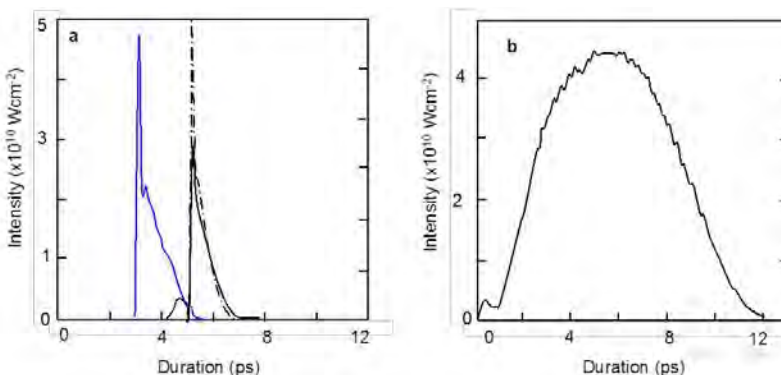


Figure 2. Simulation of energy extracted seeding the plasma soft x-ray amplifier with multiple seed pulses or with an single stretched seed pulse. (a) Amplified sequence of two 60 fs HH seed pulses separated by 1.5 ps. The solid lines correspond to the experimental conditions, the dashed line to injected pulses of equal intensity. (b) Amplified single HH seed pulse of 6 ps duration (FWHM). The extracted energy in this case is 17 times higher than of a single 60 fs HH seed.

Soft x-ray laser linewidth measurement in a single shot

The linewidth of atomic SXRLs is an important parameter that determines the gain, the saturation behavior, and the shortest pulsewidth that can be obtained. In collisional SXRLs the atomic linewidth is dominated by a combination of Doppler and collisional broadening and is affected by gain-narrowing effects during the amplification and by potential re-broadening during gain-saturation. Its measurement is challenging because the linewidths of atomic SXRLs are very narrow, typically $\Delta\lambda/\lambda < 5 \times 10^{-5}$, requiring a resolution that greatly exceeds commonly available spectrometers. A previous SXRL linewidth measurement was performed using a spectrometer with an 8 m long arm. Measurements for transient collisional lasers were also obtained using an amplitude division Michelson interferometer, and with a wavefront division interferometer consisting of a pair of slightly tilted dihedrons. However these measurements required numerous laser shots to obtain the visibility curve, which makes them dependent on the source stability. We conducted the first single-shot linewidth measurement of a transient SXRL using a soft x-ray Mach-Zehnder interferometer that takes advantage of the time delay introduced by diffraction gratings, a concept we had published before but never demonstrated.

The experimental setup of the interferometer is shown in Fig. 3a. Its geometry is a variation of a Mach-Zehnder interferometer we have used for the diagnostics of dense plasmas, in which diffraction gratings are used to split the beam. The key difference is that in the configuration for linewidth measurements the second grating doubles the time delay, which makes the measurement of a linewidth in a single shot possible. The new instrument consists of two flat diffraction gratings (G1 and G2) positioned at grazing incidence to act as beam splitters and a set of four grazing incidence mirrors (M1-M4), two in each of the arms of the interferometer. The zero order and first order beams from the first grating are redirected by reflections from mirrors (M1-M4) to emerge collinearly after diffraction on the second grating (G2). The interference pattern is recorded with a back-thinned CCD array detector.

A time delay between the wavefront of the zero and first order beams is introduced when the pulse is diffracted by the two gratings (G1 and G2), and reflected by the two grazing incidence mirrors, as illustrated in Fig. 3b. Here L is the input beam diameter ($L=AB$), θ_1 is the grazing incidence angle on grating G1 (3° in our experiment), and θ_2 is the output angle. Grating G1 introduces a tilt in the wavefront that produces a time delay across the beam relative to the zero order beam. The second grating doubles the delay when recombining the two interferometer arms into a collinear path. The time delay is given by: $\Delta t = 2(l_1 - l_2)/c = 2L\delta\lambda/(c \sin(\theta_1))$, where $l_1=AC$, $l_2=BD$ (Fig.3 b), c is the speed of light, δ is the grating groove density (900 lines/mm) and λ the laser wavelength. The incidence angle onto the grating G1 is selected to split the energy evenly between the zero and the first diffraction orders. However, an angle of 3 degree was chosen to ensure that the time delay is sufficient to record the complete visibility curve. The alignment of the interferometer was facilitated using a semiconductor laser with a similar coherence length and custom gratings (inset in Fig.3 a) in which the top and the bottom

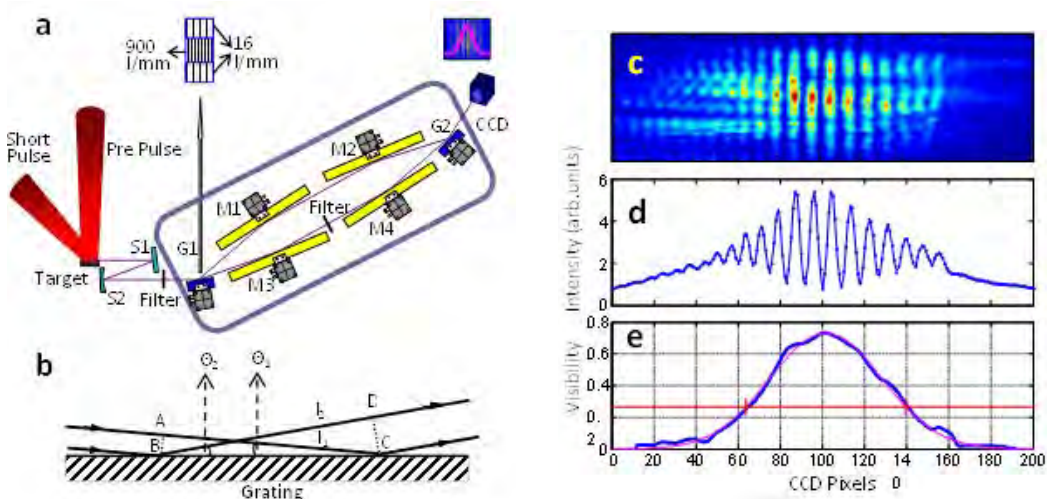


Figure 3 (a) Single-shot SXR linewidth measurement interferometer set up. The SXRL enters the interferometer from the left ; S1, S2: normal-incidence Mo-Si mirrors, S1 is a flat mirror, S2 is spherical mirror, $f=37.5$ cm; G1, G2: flat gold coated diffraction gratings; M1-M4: gold coated grazing incidence mirrors; (b) Wavefront delay introduced by the diffraction grating. The input beam diameter is $L=AB$; θ_1 is the input grazing incidence angle. l_1-l_2 is the path difference, where $l_1=AC$, $l_2=BD$. The coherence length is measured to be $260 \mu\text{m}$. (c) Single shot interferogram for a transient collisional Ni-like Pd laser at $\lambda=14.7$ nm, (d) vertical integration of (c), (e) measured visibility curve (blue) and Gaussian fit (magenta).

regions are ruled with a groove density designed to diffract the infrared laser diode along the same path of the SXRL. A $\lambda=14.7$ nm Pd soft x-ray laser beam was generated by amplification of spontaneous emission in a transient population inversion created between the $4d^1s_0-4p^1p_1$ levels of Ni-like Pd by collisional electron impact excitation in a laser-created plasma produced by irradiating a Pd slab target at grazing incidence with a high-intensity pulse from a Ti:Sa CPA laser. A single-shot SXRL interferogram for the Ni-like Pd laser is shown in Fig. 3c. A Gaussian fit to the fringe visibility yields a coherence length of $260 \mu\text{m}$ ($1/e$ half-width). The average of 30 single-shot interferograms give a coherence length of $(260 \pm 18) \mu\text{m}$ corresponding to a linewidth of $\Delta\lambda/\lambda \sim 3.0 \times 10^{-5}$. This bandwidth can support a pulsewidth of 720 fs assuming a Gaussian line profile. This fast and reliable linewidth measurement can contribute to the development of the next generation soft x-ray lasers.

Journal publications resulting from DOE-BES supported work (2012-2014)

1. Y. Wang, S. Wang, E. Oliva, L. Lu, M. Berrill, L. Ying, J. Nejd, B. Luther, C. Proux, T.T. Le, J. Dunn, D. Ros, P. Zeitoun, J. Rocca, "Gain dynamics in a soft X-ray laser amplifier perturbed by a strong injected X-ray field," *Nature Photonics* **8**, 381 (2014)
2. Y. Wang, L. Yin, S. Wang, M. C. Marconi, J. Dunn, E. Gullikson, J. J. Rocca, "Single-shot soft X-ray laser linewidth measurement using a grating interferometer," *Optics Letters* **38**, 5004 (2013).
3. C. Weninger, M. Purvis, D. Ryan, R. A. London, J. D. Bozek, C. Bostedt, A. Graf, G. Brown, J. J. Rocca, N. Rohringer, "Stimulated electronic X-ray Raman scattering," *Physical Review Letters*, **111**, (2013).
4. B. A. Reagan, W. Li, L. Urbanski, K. Wernsing, C. Salisbury, C. Baumgarten, M. Marconi, C. S. Menoni, and J. J. Rocca, "Hour-long continuous operation of a table-top soft X-ray laser at 50-100 Hz repetition rate," *Opt. Express* **21**, 28320 (2013).
5. Lu Li, Y. Wang, S. Wang, E. Oliva, L. Ying, T.T. Thuy Le, S. Daboussi, D. Ross, G. Maynard, S. Sebban, B. Hu, J.J. Rocca P. Zeitoun, "Wavefront improvement in injection-seeded soft x-ray laser based on solid-target plasma amplifier" , *Optics Letters* *Optics Letters*, **38**, 4011 (2013)
6. N.Rohringer, D. Ryan, R. London, M. Purvis, F. Albert, J. Dunn, J.D.Bozek, C.Bostedt, A. Graf, R. Hill, S.P. Hau-Ridge, J.J. Rocca,, "Inner-shell X-ray laser at 1.46 nm pumped by an X-ray free electron laser", *Nature*, **481**,488, (2012).
7. L. Urbanski, M.C. Marconi, L.M. Meng, M. Berrill, O. Guilbaud, A. Klisnick, J.J. Rocca, "Spectral linewidth of a capillary discharge Ne-like Ar soft X-ray laser: dependence on amplification beyond gain saturation", *Phys. Rev.* **A87**, 033837, (2012).
8. S. Carbajo, I. Howlett, F. Brizuela, K.Buchanan, M. Marconi, W. Chao, E. Anderson, I. Artioukov, A. Vinogradov, J.J. Rocca and C.S. Menoni, "Sequential single-shot imaging of nano-scale dynamic interactions with a table-top soft x-ray laser", *Optics Letters*, **37**, 2994 (2012).
9. H. Bravo , B.T. Szapiro , P. Wachulak,, M.C. Marconi, W. Chao , E.H. Anderson, D.T. Attwood, C.S. Menoni, J.J. Rocca, " Demonstration of nanomachining with focuses EUV laser beams", *IEEE J. of Selec Top. in Quant. Elect*, **18**, 443, (2012).
10. B. Reagan, K. Wernsing, A. Curtis, F. Furch, B. Luther, D. Patel, C.S. Menoni ,J.J. Rocca, " Demonstration of a 100 Hz repetition rate gain-saturated diode-pumped soft x-ray laser". *Optics Letters* ,**37**, 3624 (2012).

Spatial Frequency X-ray Heterodyne Imaging and Ultrafast Nanochemistry

Christoph G. Rose-Petruck

Department of Chemistry, Box H, Brown University, Providence, RI 02912
phone: (401) 863-1533, fax: (401) 863-2594, Christoph_Rose-Petruck@brown.edu

1 Program Scope

Materials are organized in hierarchical structures. Atoms combine to molecules, molecules and atoms combine to nano-scale structures, which, in turn are often embedded in microscopic media. The time scales of processes vary accordingly from femto- and picoseconds for the chemical dynamics of molecules, to hundreds of picoseconds for the transformations of nanoparticles, and finally to microseconds for larger bulk motion. The goal of this research program is the study of the complex interplay between the processes at their varying length and time scales. We address this breadth of time a length scales by studying the structure and dynamics of nanometer-sized materials using Spatial Frequency Heterodyne Imaging (SFHI), an x-ray imaging modality developed during the past DOE funding cycle. Ultrafast dynamics of molecules in their solvation environment are studied with picosecond x-ray absorption fine structure (XAFS) spectroscopy using an endstation that we developed in collaboration with Bernhard Adams at 7ID-C of the Advanced Photon Source, Argonne National Laboratory.

The results of the current funding cycle are summarized in Figure 1. During the previous funding cycle (2011 – 2014) 12 published papers acknowledge this DOE grant.¹⁻¹² Additionally, 2 manuscripts are in preparation.^{13,14} As a direct consequence of this DOE funding one US patent¹⁵ on SFHI in combination with nanoparticles was filed with the USPTO. Three Ph.D. theses were entirely or partially supported by the DOE grant. These outcomes lay the foundation for our continuing research on nano-scale dynamics at the solid-liquid interface.

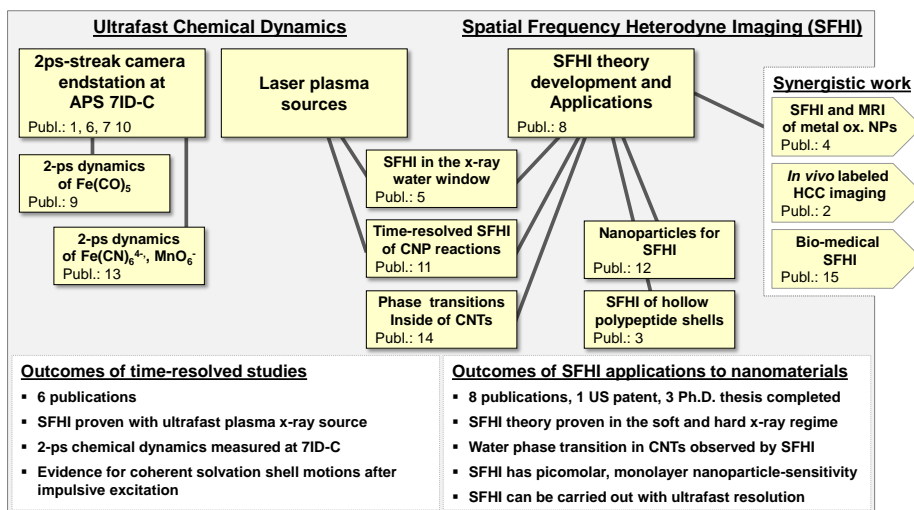


Figure 1: Research outcomes of the last funding cycle.

During the last funding cycle, we have used both, SFHI and XAFS with high temporal resolution. We completed the streak camera endstation^{1,6,7,10} at 7ID-C of the APS and carried out 2-ps XAFS measurements^{1,6,9,13} using this endstation. Using SFHI we observed the liquid-vapor phase transition of water confined in CNTs¹⁴. We have developed SFHI in the hard^{8,11} and soft (water window)⁵ x-ray regimes. We demonstrated that this modality is sensitive enough to image 10-picomolar nanoparticle concentrations, which corresponded for the samples used to a nanoparticle monolayer on a substrate.⁴ Using our laser-driven plasma x-ray source at Brown University we carried out SFHI of large scale bulk motions¹¹ in response to photo thermal nanoparticle chemical reactions in liquid suspensions with micrometer spatial and ultrafast temporal resolution. Not only high-density, for instance, gold or carbon nanoparticles can be imaged by SFHI but hollow particles can be detected as well. We demonstrated this effect using gas-filled polypeptide shells of 12-nm and 62-nm diameter.³ Thus, we will be able to image, for instance, cavitation gas bubbles that often develop within 100 ps around laser-heated nano particles (NPs). SFHI has implication for research areas that transcend the direct interests of the DOE. We used SFHI for the detection of liver cancers labeled with nano-particles.^{2,4,12} We demonstrated that SFHI detects NP-labeled cells with sensitivity nearly equal to that of Magnetic Resonance Imaging (MRI).⁴ Considering that MRI is under development and use for nearly 50 years while we develop SFHI since its first DOE-funding 4 years ago, we believe that SFHI has great promise to develop into a superbly sensitive imaging modality for nanomaterials.

Selected research results are presented in the following paragraphs.

1.1 SFHI of water phase transitions in carbon nanotubes

Water in confined spaces can show unusual properties that are not observed in the bulk. Carbon Nanotubes

(CNTs) are made of hydrophobic graphene sheets. Despite the hydrophobic nature of the graphene sheets, experimental studies have revealed that water can be confined in CNTs. Transmission Electron Microscopy and x-ray diffraction have been used to probe the behavior of water in CNTs. Our objective is to develop SFHI as an X-ray detection method suitable for studying phase transitions in nanomaterials.

SFHI is related to small angle x-ray scattering (SAXS), but simultaneously measures at thousands of points in a sample the integrals of the SAXS profiles in a single x-ray exposure. The data from each sample point form an image that can be numerically decomposed into a pure absorption image and several images that only contain the scattered x-rays. As SAXS is particularly sensitive to the nano and mesoscopic structures of a sample, SFHI images the distribution, size, and orientation nanostructures in a sample. Since all image points are measured simultaneously and only a single x-ray exposure is needed to obtain a complete image of the sample, ultrafast time-resolved imaging of an entire sample is possible. The imaging setup does not require any x-ray optics between the x-ray source and the sample and is equally well-suited for use with point x-ray sources as well as accelerator-based sources. This feature enables future measurements of the dynamics of nanomaterials on an ultrafast time scale with the nanometer-sensitivity typical of conventional SAXS.

Multi-walled carbon nanotubes (MWCNTs) produced by chemical vapor deposition were obtained from Nano Lab. Inc. The MWCNTs were reported to have an inner diameter of 7 ± 2 nm, outer diameter of 15 ± 5 nm and lengths of 1-5 microns. A portion of the as purchased MWCNTs were placed in a Pyrex tube, and heated to 500°C in air for twenty four hours in order to uncap the ends of the CNTs through annealing and partial oxidation, as shown in Figure 2. Two heat-treated and two as-purchased 60-mg samples of MWCNTs were vacuum sealed in NMR tubes. Prior to sealing the samples one of the as-purchased and one of the heat-treated samples each had $250 \mu\text{l}$ of nano-pure water added to them. The four samples were then placed in an aluminum holder fitted with two heating elements and a thermocouple. The CNTs were packed in one end of the sealed NMR tube such that the vacant opposite end extended well beyond the end of the aluminum holder. This allowed for one end of the evacuated NMR tubes to remain near room temperature throughout the experiment, establishing a thermal gradient within the tube at elevated temperatures. The gradient promoted water to condense outside of the field of view during heating. The volume occupied by the CNTs did not exceed the dimensions of the holder. Many SFH images were measured at various sample temperatures. An example for the results for these experiments is shown in Figure 3. The CNTs were quickly heated to 95°C and SFH images were measured at regular intervals. The signal from the wet CNTs were normalized by that of the dry CNTs. The X-ray absorption signals measure the filling of the CNTs with water. These values are plotted on the left scale. The SFHI signals measure the shape change of the CNTs and the formation of nano-vapor bubbles inside of the CNTs. These values are plotted on the right scale. The total experimental time was 3 hours. After the CNTs have partially emptied the x-ray scatter signal increases in a distinctive 2-step pattern. The patterns for both kinds of CNTs are identical but their relative timescales are different. Running the experiments at lower temperatures does not change the signal shapes but elongates the time scale (to 3 days at 45°C) and shifts the heat-treated CNT curves to later times. However, the shape of the observed curves does not change. Currently x-ray scatter simulations of the CNTs with varying amounts of water filling are done but the current results indicate that the reason for the scatter signal is the deformation of the CNTs at reduced water filling. This effect likely is a consequence of the formation of menisci as the water evaporates. At lower temperatures (45°C) functionalization of the heat treated sample causes the events to occur on a longer time scale relative to the original CNTs because functionalization decreases the contact angle and strengthens the CNT-water interaction. As the temperature is increased the thermal energy overcomes the increased CNT water interaction, and events occur on a shorter time scale relative to the original sample due to exaggerated CNT defects as a result of heat treatment. Kinetic effects start to overcome the increased interaction potential and heat treated tubes empty faster than untreated tubes because

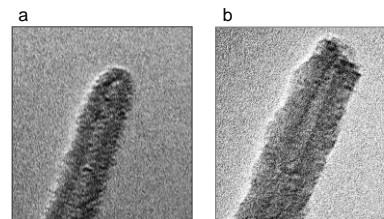


Figure 2: 200-kV TEM images at a magnification of 300,000; **a:** Closed CNTs before heat treatment. **b:** Open CNTs after heat treatment.

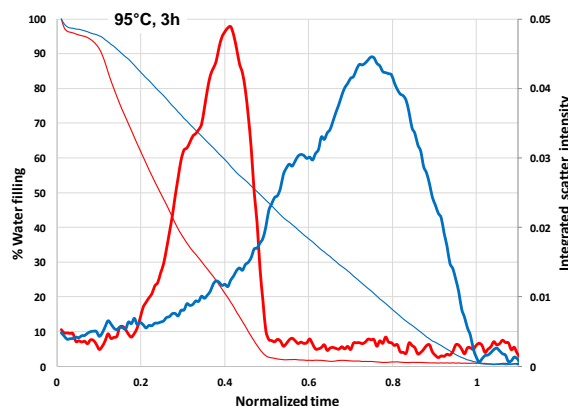


Figure 3: Water content in CNTs (thin lines, left scale) and x-ray scatter signal (heavy lines, right scale) of wet nanotubes normalized by that of dry nanotubes. The signals from the heat-treated CNTs are plotted in red and from the untreated CNTs in blue.

the heat treatment has opened the CNT ends as shown in Figure 2.

1.2 Time resolved XAFS endstation at 7ID-C, Advanced Photon Source

We measured the ligand substitution and charge transfer to solvent (CTTS) of iron hexacyanoferrate in water. This complex serves as a probe molecule for measuring the longitudinal response of the solvation shells after impulsive reduction of the electrostriction after CTTS. Three streaks for the reactions of $\text{Fe}(\text{CN})_6^{4-}$ photo excited with 266-nm, 50-fs laser pulses are shown in Figure 4. The x-ray energies center on the 1st absorption maximum of the XANES spectrum at the iron K-edge. An instrument-limited increase of the transmittance can be seen at time-zero, followed by a slower decay. At about 17 ps, a peak exists followed by a substantial increase of the signal above 30 ps. The three x-ray energies shown correspond to the peak of the Fe-K edge (7130 eV), one energy 2 eV above and one 2 eV below this peak. The black curve is the average of all three curves. Data points every 1.3 ps are shown. For reference, the average flat field curve is shown. This curve is measured without laser pulse excitation but it is acquired and processed identically to the other curves. Its std. deviation is about 0.05% for a data acquisition time of 50 minutes. We interpret the data as follows: the 1st peak close to time-zero is likely due to molecular orbital shifting and electronic excitation during the pump-laser pulse illumination of the sample solution with an intensity of about $5 \times 10^{13} \text{ W/cm}^2$. The rise time of this peak is instrument-limited and serves as a cross-correlation between the laser and x-ray pulses. CTTS product ($\text{Fe}(\text{CN})_6^{(4-x)-}$) formation occurs in less than 500 fs. After about 30 ps a photoaquation product such as $[\text{Fe}(\text{CN})_5\text{H}_2\text{O}]^{3-}$ forms. Most interesting is the peak at 17 ps. We hypothesize that it is caused by coherent solvent shell oscillation in radial direction after the impulse change of the electrostriction after CTTS. A similar effect appears in Figure 5 for KMnO_4 in aqueous solution. The tetrahedral symmetry of the permanganate ion causes a pre-edge peak at 6542.8 eV. We carried out three measurements, one at the line, one below, and one above. As before the rise time at time zero is instrument limited. The relaxation process (thermalization) occurs within about 4-ps. Coherent oscillations follow with an oscillation period only slightly shorter than for iron hexacyanide. Since both solutes are entirely different the similarity supports the interpretation that the XAFs modulations are caused by the solvation shells acting upon the metal-ligand distances, thereby modulating the XAFs signal.

Figure 6 shows the fit with three functions to the

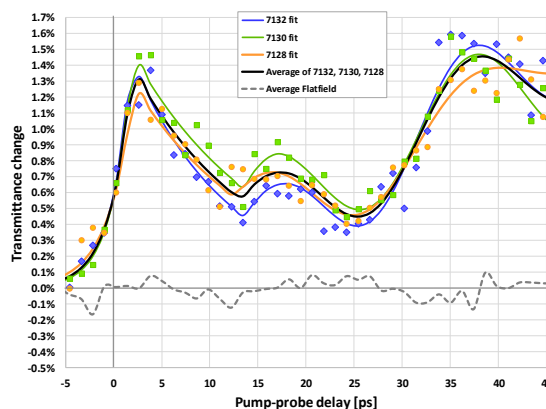


Figure 4: Changes of the x-ray transmittance vs. time after excitation of IHC with 50-fs, 266nm laser pulses at various x-ray energies. The sum of all curves is shown in black. The flatfield curve is dashed.

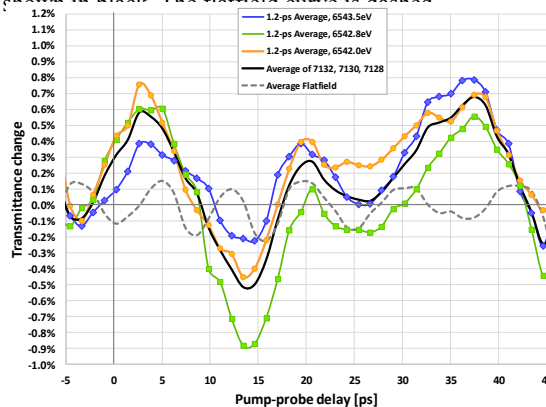


Figure 5: Changes of the x-ray transmittance vs. time after excitation of IHC with 50-fs, 266nm laser pulses at various x-ray energies. The sum of all curves is shown in black. The flatfield curve is dashed.

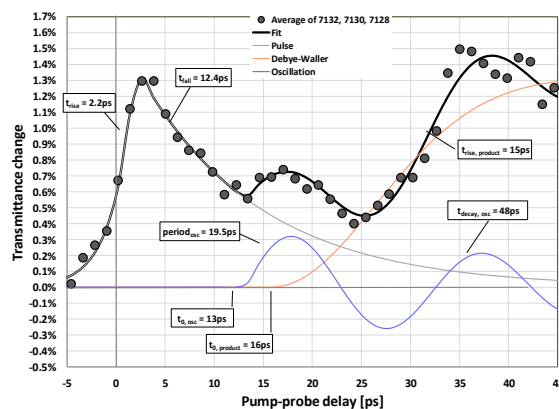


Figure 6: Decomposition of the total x-ray transmittance vs. time after excitation of IHC with 50-fs, 266nm laser pulses. Fit functions are: a double-exponential function, a sigmoidal function, and a dampened sinusoidal function. Relevant function parameters are indicated.

average curve shown in Figure 4. The peak at time-zero is fitted with an exponential rise and an exponential drop. The rise time constant of 2.2 ps is instrument-limited, indicating that the rise of underlying physical effect is instantaneous. The peak decays with a 12.4-ps time constant, which may be the electronic relaxation of the highly excited reaction intermediate. The resulting heating of the complex launches a longitudinal acoustic wave with a period of 19.5 ps. This wave exponentially decays with a 48-ps time constant, i.e., the wave decays within 3 periods. The acoustic wave modulates the Fe-CN bond lengths. A bond length decrease shifts the XANES maximum to lower energies by 0.2 eV/pm, a bond length reduction shift the XANES maximum to higher energies. Since the measured spectra are located in the vicinity of the XANES maximum, they will respond sensitively to bond length changes. It is reasonable to assume an initial bond lengths reduction cause by the increased heating and resulting pressure in the domain. Assuming a sound speed of 1433 m/s, the oscillation period corresponds to a domain diameter of 26 nm. This estimate assumes a sharp boundary between the domain and the surrounding solvent. Since this is an admittedly unrealistic assumption, the number can only serve as an approximate indicator of the average domain diameter. The increase of the transmittance at later times is likely due to the formation of photoaquation products. All conceivable stable photo-products result in a reduction of the XANES amplitude, which causes an increase in x-ray transmittance. More details of the data analysis are discussed in a forthcoming publication.¹³

2 Future plans

We will continue the research on Spatial Frequency Heterodyne Imaging and related techniques and further use the ultrafast XAFS endstation at 7ID-C for the study of nanomaterials in the liquid phase as well as nanoscopic motions of solvation shells surrounding molecular solutes. Specifically, we will

1. continue the development of the theoretical framework of X-ray Spatial Frequency Heterodyne Imaging;
2. continue hard x-ray SFHI experiments at Brown University. Primary application: phase transitions in nanoparticle suspensions and in clathrate hydrate slurries.
3. Extend the studies on CNTs to dynamics measurements of the phase transitions in CNTs after laser excitation;
4. Continue to carry out ultrafast XAFS studies at 7 ID-C;
5. We seek collaborations providing theoretical support for the ultrafast nano-dynamics research.

3 Papers acknowledging this DOE grant

- (1) Adams, B. *et al. Review of Scientific Instruments* **2014**, submitted.
- (2) Rand, D. *et al. Academic Radiology* **2014**, submitted.
- (3) Rand, D. *et al. Optics Express* **2014**, 22, 23290
- (4) Rand, D. *et al. Physics in Medicine and Biology* **2014**, accepted.
- (5) Bruza, P. *et al. Applied Physics Letters* **2014**, 104, 254101.
- (6) Adams, B. *et al. Journal of Synchrotron Radiation* **2014**, in press.
- (7) Chollet, M. *et al. IEEE Journal of Selected Topics in Quantum Electronics* **2012**, 18, 66.
- (8) Wu, B. *et al. Applied Physics Letters* **2012**, 100, 061110.
- (9) Ahr, B. *et al. Phys. Chem. Chem. Phys.* **2011**, 13 (Also PCCP Cover Page, April 2011), 5590.
- (10) Chollet, M. *et al. Nuclear Instruments and Methods in Physics Research A* **2011**, 649, 70
- (11) Liu, Y. *et al. Optics Letters* **2011**, 36, 2209.
- (12) Rand, D. *et al. NanoLetters* **2011**, 11, 2678.
- (13) Jiao, Y. *et al. PCCP* **2014**, to be submitted.
- (14) Schunk, F. *et al. Journal of Physical Chemistry* **2014**, to be submitted.
- (15) Rose-Petruck, C. *et al.*, US Patent Appl. Number: 61/544,419, (2011)

4 Publications and Ph.D. theses related to this DOE grant

1. "Chemical Dynamics in the Condensed Phase: Time-resolved X-ray Imaging and Ultrafast X-ray Absorption Spectroscopy" B. Ahr, Brown University, 2011.
2. "Pulse Plasma Soft X-ray Source in Biomedical Research" P. Bruza, Czech Technical University, 2014.
3. "X-Ray Spatial Frequency Heterodyne Imaging of Hepatocellular Carcinoma Using Nanoparticle Contrast Agents" D. Rand, Brown University, 2014.
4. "A fickle molecule caught in the act," D. Bradley, 2011 Annual Report of the Advanced Photon Source (2012).

Time-Resolved High Harmonic Spectroscopy: A Coherently Enhanced Probe of Charge Migration

ATTO-CM Team: Kenneth Schafer¹, Mette Gaarde¹, Kenneth Lopata¹

Louis DiMauro², Pierre Agostini², Robert Jones³

¹*Department of Physics and Astronomy, Louisiana State University, Baton Rouge, LA*

²*Department of Physics, The Ohio State University, Columbus, OH*

³*Physics Department, University of Virginia, Charlottesville, VA*

September 26, 2014

Program Scope

Understanding the quantum transport of electrons and holes, and the correlations between them, provides an avenue toward improving the efficiency of chemical processes including energy conversion and catalysis. The relevant electron dynamics evolve on exceedingly fast time scales down to the natural time scale of the electron, the attosecond. For this reason attosecond science has increasingly focused on the possibilities for measuring and controlling correlated electron motion in complex many body systems such as polyatomic molecules as one of the key applications of this new science.

There are two broad motivations for extending the measurement of electron/hole dynamics in chemical systems to the attosecond time scale. The first is the study of electron correlation itself. Though electrons interact on an attosecond time scale, currently measurements are made over much longer time scales, meaning that two and many-electron interactions are averaged over. Attosecond studies offer a new perspective on these interactions beyond the mean-field picture and without time-averaging. The second motivation is the study of the earliest phase of charge transfer reactions. These reactions are among the simplest processes in chemistry yet the efficiency with which electrons move around in a molecule is one of the primary regulation mechanisms in biology. As an example of correlated electron dynamics in many-body systems we will study ultrafast charge migration in complex chemical environments. Charge migration refers to the rapid movement (femtosecond or faster) of positively charged holes in a molecule following localized excitation or ionization. The charge can migrate through the system, driven by many-electron correlation and relaxation effects. This can result in charge transfer that is driven by electronic effects, weakly coupled to nuclear motion.

The objective of the ATTO-CM team is to advance ultrafast science in the US both on small-scale and large-scale facilities using a concerted effort of both theorists and experimentalist solving these. Our emphasis is to evaluate high harmonic spectroscopy as a sensitive probe for studying charge migration dynamics in chemical systems by developing a symbiotic relationship between theory and experiment. The initial experimental campaigns will be laboratory based but with the probes maturation they will translate onto a large-scale facility, like LCLS, a natural progression for the science.

Recent Progress

Because the project was awarded in August 2014, there are no publications to report at this time. However, work is underway at the respective sites, assembling the personnel who will extend current theory and computational methods to guide and interpret attosecond charge transfer measurements and develop new (or modify existing) apparatus to enable those measurements. In addition, a “kick-off” workshop designed to explore the current state of theory and experiment in this area and the most promising paths for initial efforts is being planned for Spring 2015.

Page is intentionally blank.

Tamar Seideman
Department of Chemistry, Northwestern University
2145 Sheridan Road, Evanston, IL 60208-3113
t-seideman@northwestern.edu

Strong-Field Control in Complex Systems

1. Program Scope

Our AMOS-supported research can be broadly categorized into two related topics: (1) the design and control of complex material system with strong field concepts developed in our earlier AMOS work, including alignment, 3D alignment, torsional alignment and molecular focusing; and (2) the physics, theory, and potential applications of high harmonics generated from aligned molecules. Whereas the first topic is a generalization of the thrust of our original AMOS-supported research, the second has been motivated by the intense interest of the AMOS Program in attosecond science and rescattering electrons physics, and has been carried out in collaboration with AMOS experimentalists colleagues.

Our work during the past year within the first part is summarized in Secs. 2.4–2.7 and includes two theory development projects and two collaborative research projects with different experimental laboratories. Research in the next year on the problem of strong field coherent control in complex molecular and material systems is discussed in Sec. 3.1. Within the second part of our AMOS-supported research during the past year (2.1–2.3), we combined joint research with several AMOS colleagues with a theory of rotational wavepacket imaging via high harmonic generation (HHG). Our plans for further research in the area of attosecond physics and HHG during the next year is outlined in Sec. 3.2. Citations refer to the list of AMOS-supported publications from the 2012–Aug. 2014 period, Sec. 4.

2. Progress during the past year

2.1 Axis-Dependence of Molecular High Harmonic Emission in Three Dimensions

Our recent research in collaboration with AMOS colleagues Bucksbaum, Martinez and Guehr, illustrates how to extract full body-frame high harmonic generation information for molecules with complicated geometries by utilizing the methods of coherent transient rotational spectroscopy and an analytical theory of the associated angular momentum algebra. To demonstrate our approach, we determined the relative strength of harmonic emission along the three principal axes in the asymmetric top sulfur dioxide. This greatly simplifies the analysis task of high harmonic spectroscopy and extends its usefulness to complex molecules. An article appeared in Nature Communications.¹

2.2 Ultrafast Elliptical Dichroism in High-Order Harmonics as a Probe of Molecular Structure and Electron Dynamics

Molecules illuminated by an elliptically polarized, high intensity laser field emit elliptically polarized high-order harmonics. In a submitted article², we discuss collaborative experimental and theoretical work with AMOS colleagues Murnane and Kapteyn, where surprising experimental observations of ultrafast elliptical dichroism in the harmonic emission as the ellipticity of the driving field and the molecular alignment are scanned are explained and generalized. To that end we develop a simple model in which both the collision angle of the continuum electron with the molecule and the interference between recombination at multiple charge centers play a role. Our analysis ties the

observed elliptical dichroism to the journey of the continuum electron in the field and the underlying bound state of the molecular ion. These results show how to use molecular structure and alignment to manipulate the polarization state of high-order harmonics, and also present a potential new attosecond probe of the underlying molecular system. Specifically, information about the bound state orbital structure and the continuum electron dynamics is contained in the variation of the dichroism with the laser ellipticity, the molecular alignment with respect to the field polarization, and the harmonic order.

2.3 Rotational Wave Packet Imaging

In 3, We propose and illustrate numerically the possibility of imaging rotational wave packets in angular space and time by using different pump-probe spectroscopic techniques. A general theoretical framework to perform such rotational mapping is derived and three specific spectroscopies, namely, birefringence, high harmonic generation, and angle-resolved photoelectron spectroscopy, are numerically explored. All three approaches are shown to provide direct mapping of the rotational coherences of molecules but they are not equivalent; comparison of their results yields interesting insights into their relative merits. Finally, we illustrate the role played by the symmetry of the molecular orbitals in determining the quality of the images generated by high harmonic and photoelectron signals. The potential of rotational imaging as a route to both intramolecular coupling mechanisms and the interaction of molecules with different environments is discussed.

2.4 Dissipation and Rotational Quasi-Revivals in Asymmetric-Top Molecules

Joint theoretical and experimental research with Phil Bucksbaum and his group observed quasi-periodic revivals out to 27 ps in an impulsively-aligned asymmetric-top molecule, sulfur dioxide (SO_2), at high sample temperature and density (295 K, 0.5 bar). We found that the asymmetric top exhibits a strong correlation between population alignment and population lifetime ($r = 0.97$), in accordance with trends observed in linear molecules. Using a linear birefringence measurement fit to a full quantum simulation of the asymmetric rotor, we separately determined both the population (T_1) and the coherence (T_2^*) lifetimes of the rotational wavepacket. Additionally, we inferred a high rate of elastic decoherence ($T_2 = 9.6$ ps), which we attributed to long-range interactions mediated by the permanent dipole of the SO_2 molecule. We proposed the use of birefringence measurements to study intermolecular interactions in a coherent ensemble, as a step toward using field-free alignment to investigate reaction dynamics. A manuscript will be submitted for publication shortly.

2.5 Strong Field Multiple Ionization as a Route to Electron Dynamics in a van der Waals Cluster

In a Phys. Rev. Lett. article co-authored by an overseas experimental group,⁵ we study the order in which a strong laser field removes multiple electrons from an aligned van der Waals (vdW) cluster. The N_2Ar , with an equilibrium T-shaped geometry, contains both a covalent and a vdW bond and serves as a simple yet rich example. Interestingly, the fragmenting double and triple ionizations of N_2Ar with vdW bond breaking are favored when the vdW bond is aligned along the laser field polarization vector. However, the orientation of the covalent bond with respect to the laser field rules the triple ionization when both the covalent and vdW bonds are simultaneously broken. Electron-localization-assisted enhanced ionization and molecular orbital profile-dominated, orientation-dependent ionization are discussed to reveal the order of electrons release from different sites of N_2Ar .

2.6 Molecular Junctions: Can Pulling Influence Optical Controllability?

The field of molecular electronics has seen rapid progress in recent years, motivated both by the ex-

citing challenges in fundamental chemical physics and by the potential for technological applications. Although both optical and mechanical control of transport via junctions were demonstrated, both are limited by damage thresholds. Their combination, however, is promising. In 6 we propose use of a mechanical force to enhance a molecule's susceptibility for optical control. Specifically, we suggest the combination of single molecule pulling and optical control as a way to enhance control over the electron transport characteristics of a molecular junction. We illustrate the concept using a model junction consisting of biphenyl-dithiol coupled to gold contacts. The junction is pulled while the method of torsional alignment, introduced in our earlier AMOS-supported work, is applied to control the dihedral angle between the two rings. Quantum dynamics simulations show that molecular pulling enhances the degree of control over the dihedral angle and hence over the transport properties.

2.7 Dissipative Dynamics of Laser-Induced Torsional Coherences

The concept of torsional alignment, introduced in our earlier AMOS-supported research, opens several interesting phenomena in the dynamics of strong field-triggered torsional wavepackets. The results of a recent publication⁷ point to the origin and consequences of the fundamental differences between rotational and torsional coherences. In addition we provide design guidelines for torsional control experiments by illustrating the role played by the laser intensity, pulse width, temperature, and molecular parameters. Specifically as an example of two classes of molecules expected to make suitable candidates for laboratory experiments, we explore the torsional control of 9-[2-(anthracen-9-yl)ethynyl]anthracene and contrast it with that of biphenyl. Finally we propose several potential applications for coherent torsional control in chemistry, physics, and material science.

More interesting, and more relevant to experiments, is the case of torsional alignment subject to a dissipative environment, discussed in 8, where we explore the controllability of molecular torsions subject to dissipative media and the way in which phase information is exchanged between torsional modes and a dissipative environment. Our theory is based on a density matrix formalism, where dissipation is accounted for within a multilevel Bloch equation model. Our results point to new and interesting phenomena in wavepacket dissipation dynamics that are unique to torsions and also enrich our general understanding of wavepacket phenomena. In addition, we suggest guidelines for designing torsional control experiments for molecules interacting with a dissipative bath.

3. Future Plans

3.1 Strong Field Coherent Control in Complex Material and Molecular Systems

Several ongoing projects will be completed and submitted within the next few months. One is a study of alignment and orientation of semiconductor nanorods. A second explores the control of plasmonic phenomena using laser alignment of a surface-adsorbed molecular layer to modulate with time the dielectric function of the medium of the nanoconstruct. A third develops a Wigner representation of the rotations of rigid bodies, with a view to semiclassical studies of alignment of heavy systems at elevated temperatures.

3.2: The physics, Numerical Methodology and Applications of High Harmonics from Aligned Molecules

A goal of future research, which will hopefully be largely accomplished within the next year, is to develop an approach for accurate modeling of the continuum electronic wavefunction underlying harmonic signals and combine it with our rotational theory of HHG. The method will be first applied to linear systems, but my main interest is in the case of 3D aligned (e.g., by means of an elliptically polarized field) asymmetric top molecules as targets for the recolliding continuum electron. These I expect

to allow both a new view of the electronic structure and dynamics in complex polyatomic molecules and a new and interesting approach to probe the (classically unstable) rotations of asymmetric tops in the fully quantum domain.

4. Publications from DOE sponsored research(2012–August 2014, in citation order)

1. L. S. Spector, M. Artamonov, S. Miyabe, Todd Martinez, T. Seideman, M. Guehr, and P. H. Bucksbaum, *Axis-Dependence of Molecular High Harmonic Emission in Three Dimensions*, *Nature Communications* **5**, 3190 (2013).
2. P. A. J. Sherratt, R. M. Lock, X. Zhou, H. C. Kapteyn, M. M. Murnane, and T. Seideman, *Ultrafast Elliptical Dichroism in High-Order Harmonics as a Probe of Molecular Structure and Electron Dynamics*, submitted for publication in *Phys. Rev. Lett.*
3. S. Ramakrishna and T. Seideman, *Rotational Wave Packet Imaging of Molecules*, *Phys. Rev. A* **87**, 023411 (2013).
4. I. F. Tenney, M. Artamonov, T. Seideman and P. H. Bucksbaum, *Collisional decoherence and rotational quasi-revivals in asymmetric-top molecules*, submitted.
5. J. Wu, X. Gong, M. Kunitski, L. Ph. H. Schmidt, T. Jahnke, A. Czasch, T. Seideman, and R. Dorner, *Sequencing Strong Field Multiple Ionization of a Multicenter Multibond Molecular System*, *Phys. Rev. Lett.* **111**, 083003 (2013)
6. S. M. Parker, M. Smeu, I. Franco, M. A. Ratner, and T. Seideman, *Molecular Junctions: Can Pulling Influence Optical Controllability?*, *NanoLett.* in press.
7. B. Ashwell, S. Ramakrishna and T. Seideman, *Laser-Driven Torsional Coherences*, *J. Chem. Phys.* **138**, 044310 (2013).
8. B. Ashwell, S. Ramakrishna and T. Seideman, *Dissipative Dynamics of Laser-Induced Torsional Coherences*, Special Issue of *J. Phys. Chem. C* **117**, 22391 (2013) (**invited**).
9. M. Artamonov and T. Seideman, *Predicted Ordered Assembly of Ethylene Molecules Induced by Polarized Off-Resonance Laser Pulses*, *Phys. Rev. Lett.* **109**, 165408 (2012).
10. M. Reuter, M. A. Ratner and T. Seideman, *Laser Alignment as a Route to Ultrafast Control of Electron Transport through Junctions* *Phys. Rev. A* **86** 013426 (2012).
11. S. M. Parker, M. A. Ratner and T. Seideman, *Coherent Optimal Control of Axial Chirality*, Special Issue of *Mol. Phys.* **110**, 1941 (2012) (**invited**).
12. J. Floss, T. Grohmann, M. Leibscher, and T. Seideman, *Nuclear Spin Selective Torsional Control*, *J. Chem. Phys.* **136**, 084309 (2012).
13. A. Przystawik, A. Al-Shemmary, S. Dusterer, M. Harmand, A. Kickermann, H.Redlin, L. Schroedter, M. Schulz, N. Stojanovic, S. Toleikis, T. Laarmann, A. M. Ellis, K. von Haefen, F. Tavella, J. Szekeley and T. Seideman, *Generation of the Simplest Rotational Wave Packet in a Diatomic Molecule: Microwave Spectroscopy in the Time Domain without Microwaves*, *Phys. Rev. A* **85**, 052503 (2012).
14. R.M. Lock, S. Ramakrishna, X. Zhou, H.C. Kapteyn, M.M. Murnane, and T. Seideman, *Extracting Continuum Electron Dynamics from High Harmonic Emission from Molecules*, *Phys. Rev. Lett.* **108**, 133901 (2012).
15. S. Ramakrishna and T. Seideman, *On the Information Content of Time- and Angle-Resolved Photoelectron Spectroscopy*, Special Issue of *J. Phys. B* **45**, 194012 (2012) (**invited**).
16. M. Artamonov and T. Seideman, *Three-Dimensional Laser Alignment of Polyatomic Molecular Ensembles*, Special Issue of *Mol. Phys.* **110**, 885 (2012) (**invited**).

Inelastic X-ray Scattering Under Extreme and Transitional Conditions

Gerald T. Seidler, seidler@uw.edu,
 Department of Physics
 University of Washington
 Seattle, WA 98195-1560

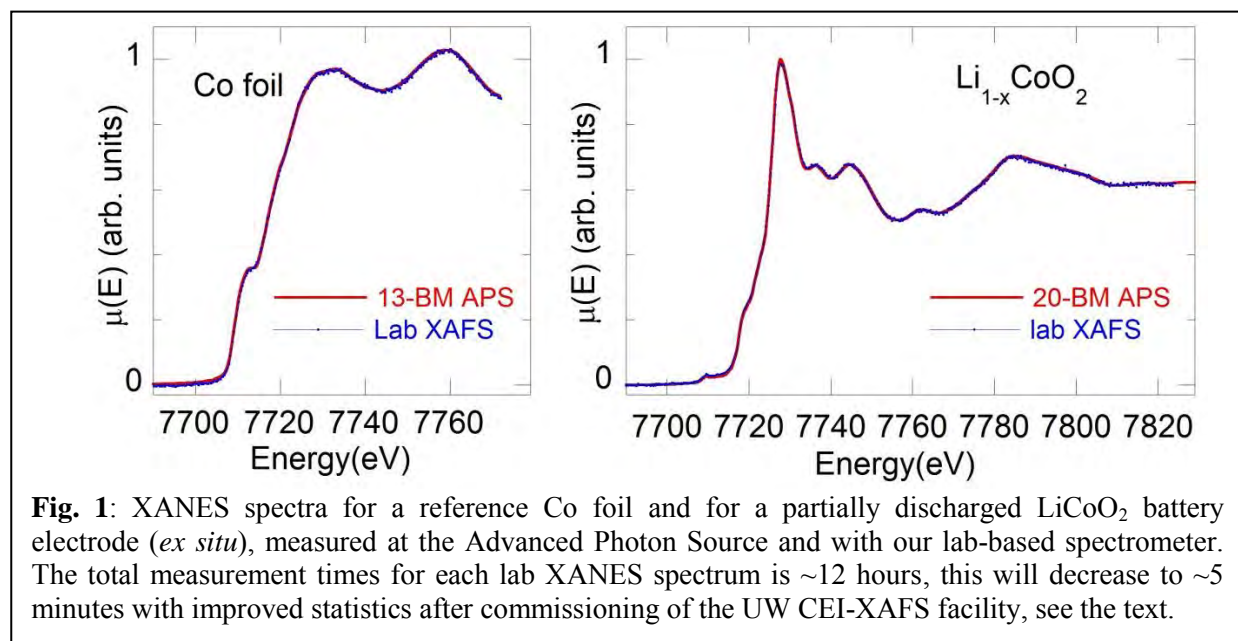
Program Scope

The goal of this program is to expand the scope and scientific potential of time-resolved inelastic x-ray scattering (IXS). First, we are using x-ray spectroscopies, soon to include resonant inelastic x-ray scattering, to gain new insight into the energy transfer mechanisms of lanthanide-based phosphors and related luminescent materials and to study the time dynamics of the electronic and structural changes at metal-insulator transitions. Second, we are performing combined theoretical and experimental work to critically test, and substantially improve, the use of IXS methods in the study of dense plasmas, such as in the transitional, ‘warm dense matter’ regime. Third, we are continuing several collaborations based on IXS instrumentation and methods developed by the PI, including studies of the time-dynamics of energy transfer in photosynthetic proteins and of the f-electron physics of lanthanide elements and compounds at high pressures. Finally, our side-project for laboratory-based XAFS and XES is showing high promise for impact in DOE-relevant research on electrical energy storage, catalysis, and actinide materials.

Selected Recent Progress and Future Directions

I. A Rejuvenation of Laboratory-based High-Resolution X-ray Spectroscopies

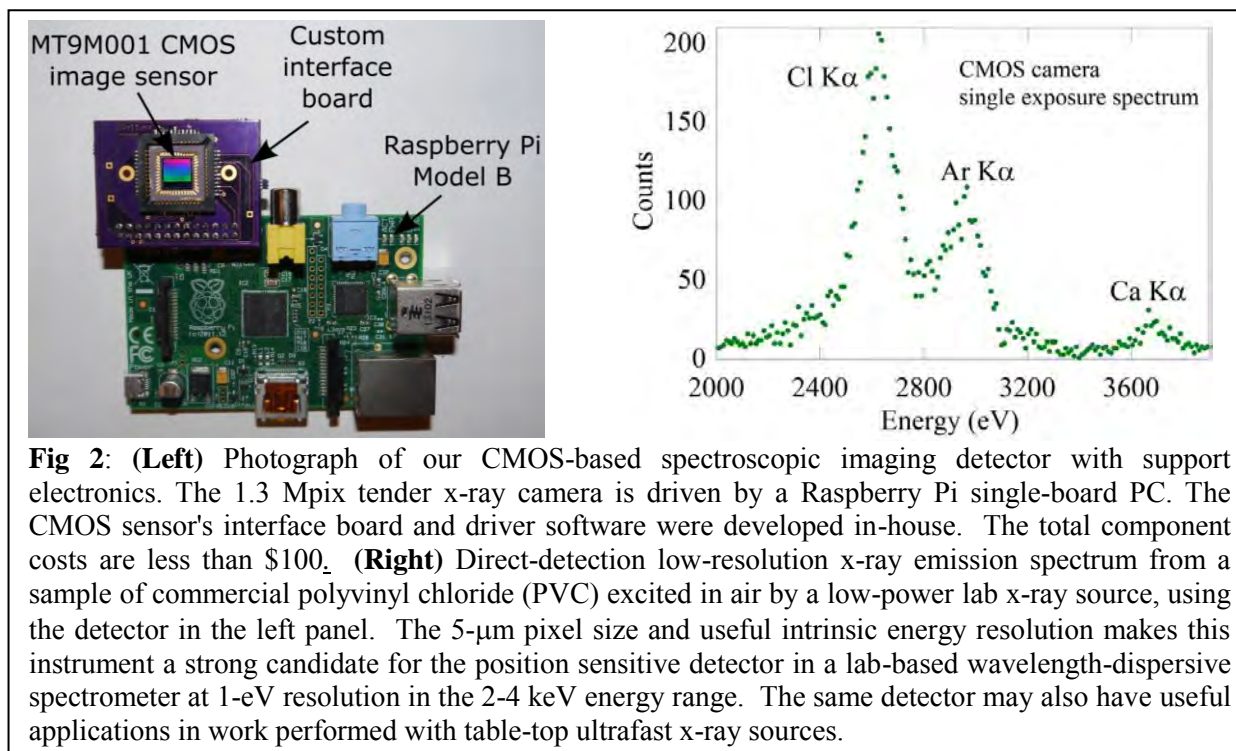
In October 2013 we commissioned a new type of inexpensive lab-based spectrometer for high-resolution x-ray studies, including x-ray absorption fine structure (XAFS) and x-ray emission spectroscopy (XES). In the subsequent year we have fine-tuned our experimental technique and now regularly achieve data that is in essentially perfect agreement with



synchrotron-based results, see Fig. 1. The instrumentation paper for our lab spectrometer has been submitted to the Review of Scientific Instruments.

The startling performance of this modest instrument has garnered significant interest that, we emphasize, has been solely focused on DOE-priority research issues and that does not have the character of competition with synchrotron facilities. In addition to providing a true introductory capability that can help attract and educate entire new user communities, laboratory-based XAFS enables measurements that, for reasons of long duration, sample preparation complexity, chemical hazards, or radioisotope hazards, cannot be performed with regularity or certainty at synchrotron light sources. To this end, under funding from the University of Washington, we are building a mid-scale lab XAFS user facility for the UW Clean Energy Institute (CEI); this new instrument builds directly on the new technology developed under the present award; the CEI-XAFS facility will see extensive use in long-baseline studies of electrical energy storage that cannot, due to the long experimental duration, be completed with regularity at synchrotron beamlines. It will reach a flux of mid- 10^6 /sec on each of two independent beamlines.

We are also assisting collaborators at LANL and ANL with the design and construction of XES spectrometers for the lower-energy range of 2-4 keV, e.g., for S XES in Li-S batteries or in air-sensitive actinide-sulfur compounds that cannot be reliably transported to the light source. In support of the effort to extend lab-based XES to lower energies we have initiated a project to develop an inexpensive x-ray camera for the 2-4 keV ‘tender’ x-ray range. Our first results are promising, see Fig. 2. This 1.3Mpix spectroscopic imaging detector may also prove useful in ultrafast x-ray spectroscopies, such as with table-top laser-pumped x-ray sources.



II. X-ray Heating Studies at LCLS/MEC

The recent LD67 campaign at LCLS/MEC was led by the PI. While this beamrun emphasized laser-shock heating of multicomponent targets (supported by a grant from

DOE/FES), complementary x-ray heating experiments were also performed as part of the WDM research under the present award. The results are still under analysis, but show interesting effects in the electronic structure of metallic and more complex intermediate-Z alloys and compounds. For example, the ability to compare response across multiple intermediate-Z species in alloys will allow a detailed interrogation of the correct theoretical treatment of the electronic structure of isochorically heated matter.

III. Time-resolved Studies of Energy Transfer and Electron Correlations

Lanthanide compounds and coordination complexes are responsible for a wide range of light-gathering and light-emitting applications, including as commercial phosphors in lighting applications, as tools to better match the solar spectrum to the function of photovoltaic devices, and as a critical component in many bioassays. In this lattermost role, an organic ‘antenna’ acts as a strong near-UV photoabsorber before nonradiatively transferring energy to a chelated, trivalent lanthanide ion via a 4f-4f intrashell excitation. This dipole-forbidden excitation subsequently decays through the so-called ‘hypersensitive’ pseudo-quadrupolar decay, giving light at delays of order msec after the initial excitation due to the long lifetime for the 4f excitation. This long time-delay allows simplest time-gate filtering of the emission from the luminescent lanthanide complex from that of the host biological system.

The microscopic physics underlying each step in the energy transfer pathway in the luminescent lanthanides, and indeed in all materials used for the applications described above, remain incompletely understood. Our recent work at the Advanced Photon Source on luminescent lanthanide complexes demonstrate an unexpected, but clear expression of the 4f intrashell excitation in the time-resolved x-ray absorption near-edge spectrum (XANES) of the lanthanide ion.[Pacold, et al., JACS 2014] Our leading explanation requires a surprisingly dynamic coupling between the 4f and 5d orbitals of the lanthanide ion. In any event, this discovery opens up new opportunities to use the LCLS to directly monitor the energy transfer onto the lanthanide species, giving an important complement to studies of the de-excitation of multiple ligand states by transient optical absorption.

We have recently extended this project with time-resolved x-ray excited optical luminescence (TR-XEOL) studies performed at the Advanced Photon Source. The high flux-density of the 20-ID microprobe endstation allowed us to reach a nonlinear XEOL regime where the time scales for different steps in the energy relaxation cascade in Bi-sensitized $Y_2O_3:Eu$ phosphors can be separated.

Manuscripts and Publications in the Last 3 Years of this Award

1. G.T. Seidler, D.R. Mortensen, A.J. Remesnik, J.I. Pacold, N.A. Ball, N. Barry, M. Styczinski, O.R. Hoidn, “A Laboratory-based Hard X-ray Monochromator for High-Resolution X-ray Emission Spectroscopy and X-ray Absorption Near Edge Structure Measurements,” *submitted*, Review of Scientific Instruments (2014).
2. M.J. Lipp, D.R. Mortensen, H. Cynn, W.J. Evans, G.T. Seidler, Y. Xiao, P. Chow, “4f moment and magnetic susceptibility of cerium under pressure: Comparison with lanthanum and CeO_2 ,” *submitted* Journal of Physics: Condensed Matter (2014).
3. Brian A. Mattern, Gerald T. Seidler, Joshua J. Kas, “Condensed Phase Effects on the Electronic Momentum Distribution in the Warm Dense Matter Regime,” *submitted*, Physical Review Letters (2013).
4. Matthew Gliboff, Dana Sulas, Dennis Nordlund, Dane W. deQuilettes, Phu Nguyen, Gerald T. Seidler, Xiaosong Li, David S. Ginger, “Direct Measurement of Acceptor Group Localization on Donor-Accepted Polymers using Resonant Auger Spectroscopy,” Journal of Physical Chemistry C **118**, 5570 (2014).

5. Joseph I. Pacold, David S. Tatum, Gerald T. Seidler, Kenneth N. Raymond, Xiaoyi Zhang, Andrew B. Stickrath, and Devon R. Mortensen, "Direct Observation of 4f Intrashell Excitation in Luminescent Lanthanide Complexes by Time-Resolved X-ray Absorption Near Edge Spectroscopy," *Journal of the American Chemical Society* **136**, 4186 (2014). (doi: 10.1021/ja407924m).
6. D.R. Mortensen, G.T. Seidler, J.A. Bradley, M.J. Lipp, W.J. Evans, P. Chow, Y.-M. Xiao, G. Boman, and M.E. Bowden, "A Versatile Medium-Resolution X-ray Emission Spectrometer for Diamond Anvil Cell Applications," *Review of Scientific Instruments* **84**, 083908 (2013).
7. Steven D. Conradson, *et al.*, "Bose condensate-type behavior from a collective excitation in the chemically and optically doped Mott-Hubbard system, UO_2+x ," *Physical Review B* **88**, 115135 (2013).
8. K.M. Davis, I. Kosheleva, R.W. Henning, G.T. Seidler, Y. Pushkar, "Kinetic Modeling of the X-ray-induced Damage to a Metalloprotein," *Journal of Physical Chemistry B* **117**, 9161 (2013).
9. Matthew Gliboff, Hong Li, Kristina M. Knesting, Anthony J. Giordano, Dennis Nordlund, Gerald T. Seidler, Jean-Luc Bredas, Seth R. Marder, and David S. Ginger, "Competing Effects of Fluorination on the Orientation of Aromatic and Aliphatic Phosphonic Acid Monolayers on ITO," *Journal of Physical Chemistry C* **117**, 15139 (2013).
10. Matthew Gliboff, Lingzi Sang, Kristina M. Knesting, Matthew C. Schalnat, Anoma Mudalige, Erin L. Ratcliff, Hong Li, Ajaya K. Sigdele, Joseph J. Berry, Dennis Nordlund, Anthony Giordano, Gerald T. Seidler, Jean-Luc Brédas, Seth R. Marder, Jeanne E. Pemberton, David S. Ginger, "Orientation and Order of Phenylphosphonic Acid Self-assembled Monolayers on Transparent Conductive Oxides: A Combined NEXAFS, PM-IRRAS and DFT Study," *Langmuir* **29**, 2166 (2013).
11. Stefan G. Minasian, *et al.*, "Covalency in Metal–Oxygen Multiple Bonds Evaluated Using Oxygen K-edge Spectroscopy and Electronic Structure Theory", *Journal of the American Chemical Society* **135**, 1864 (2013).
12. Brian A. Mattern and Gerald T. Seidler, "Theoretical Treatments of the Bound-Free Contribution and Experimental Best Practice in X-ray Thomson Scattering from Warm Dense Matter," *Physics of Plasmas* **20**, 022706 (2013).
13. S.M. Heald, G.T. Seidler, D. Mortensen, B. Mattern, J.A. Bradley, N. Hess, M. Bowden, "Recent Tests of X-ray Spectrometers Using Polycapillary Optics," in *Advances in X-Ray/EUV Optics and Components VII*, edited by Shunji Goto, Christian Morawe, Ali M. Khounsary, Proc. of SPIE Vol. 8502 (2012), article number 85020I.
14. K.M. Davis, B.A. Mattern, J.I. Pacold, T. Zakharova, D. Brewwe, I. Kosheleva, R.W. Henning, T.J. Graber, S.M. Heald, G.T. Seidler, Y. Pushkar, "Fast Detection Allowing Analysis of Metalloprotein Electronic Structure by X-ray Emission Spectroscopy at Room Temperature," *Journal of Physical Chemistry Letters* **3**, 1858 (2012).
15. B.A. Mattern, G.T. Seidler, J.J. Kas, J.I. Pacold, J.J. Rehr, "Real-Space Green's Function Calculation of Compton Profiles," *Phys. Rev. B* **85**, 115135 (2012).
16. J.A. Bradley, K.T. Moore, M. J. Lipp, B.A. Mattern, J.I. Pacold, G. T. Seidler, P. Chow, E. Rod, Y. Xiao, and W. J. Evans, "4f electron delocalization and volume collapse in praseodymium metal," *Phys. Rev. B* **85**, 100102 (2012).
17. J.I. Pacold, J.A. Bradley, B.A. Mattern, M.J. Lipp, G.T. Seidler, P. Chow, Y. Xiao, E. Rod, B. Rusthoven, and J. Quintana, "A miniature X-ray emission spectrometer (miniXES) for high-pressure studies in a diamond anvil cell," *J. Synch. Rad.* **19**, 245 (2012).
18. B.A. Mattern, G.T. Seidler, M. Haave, J.I. Pacold, R.A. Gordon, J. Planillo, J. Quintana, B. Rusthoven, "A Plastic Miniature X-ray Emission Spectrometer (miniXES) based on the Cylindrical von Hamos Geometry," *Rev. Sci. Instrum.* **83**, 023901 (2012).
19. J.A. Bradley, A. Sakko, G.T. Seidler, A. Rubio, M. Hakala, K. Hamalainen, G. Cooper, A.P. Hitchcock, K. Schlimmer, K.P. Nagle, "Revisiting the Lyman-Birge-Hopfield Band of N_2 ," *Physical Review A* **84**, 022510 (2011).

DYNAMICS OF FEW-BODY ATOMIC PROCESSES

Anthony F. Starace, P.I.

*The University of Nebraska, Department of Physics and Astronomy
855 North 16th Street, 208 Jorgensen Hall, Lincoln, NE 68588-0299*

Email: astarace1@unl.edu

PROGRAM SCOPE

The goals of this project are to understand, describe, control, and image processes involving energy transfers from intense electromagnetic radiation to matter as well as the time-dependent dynamics of interacting few-body, quantum systems. Investigations of current interest are in the areas of strong field (intense laser) physics, attosecond physics, high energy density physics, and multiphoton ionization processes. Nearly all proposed projects require large-scale numerical computations, involving, e.g., the direct solution of the full-dimensional time-dependent or time-independent Schrödinger equation for two-electron (or multi-electron) systems interacting with electromagnetic radiation. In some cases our studies are supportive of and/or have been stimulated by experimental work carried out by other investigators funded by the DOE AMOS physics program. Principal benefits and outcomes of this research are improved understanding of how to control atomic processes with electromagnetic radiation and how to transfer energy optimally from electromagnetic radiation to matter.

RECENT PROGRESS

A. Validity of Factorization of the High-Energy Photoelectron Yield in Above-Threshold Ionization of an Atom by a Short Laser Pulse

We have derived quantum mechanically an analytic result for the above-threshold ionization (ATI) probability that is valid in the high-energy part of the ATI plateau for a short laser pulse of any shape and duration. Factorization of this probability in terms of an electron wave packet function (dependent primarily on laser field parameters) and the field-free cross section for elastic electron scattering (EES) (dependent primarily on the target atom) is shown to occur only for the case of an ultrashort pulse. In general, the probability involves interference of different EES amplitudes involving laser-field-dependent electron momenta. These analytic results allow one to describe very accurately the left-right asymmetry as well as the large-scale (intracycle) and fine-scale (intercycle) oscillations in ATI spectra. In fact, agreement with results of accurate numerical solutions of the time-dependent Schrödinger equation is excellent. To use our results, only the field-free EES amplitude for the target atom and the solutions of certain classical equations describing the active electron motion for a given short laser pulse are needed. Our analytic formulas thus provide an efficient tool for the quantitative description of short-pulse ATI spectra, both elucidating the physics of the process and allowing experimentalists to plan and/or control the processes they investigate. (*See reference [5] in the publication list below.*)

B. Enhanced Asymmetry in Few-Cycle Attosecond Pulse Ionization of He in the Vicinity of Autoionizing Resonances

By solving the two-active-electron, time-dependent Schrödinger equation in its full dimensionality, we have investigated the carrier-envelope-phase (CEP) dependence of single ionization of He to the $\text{He}^+(1s)$ state triggered by an intense few-cycle attosecond pulse with carrier frequency ω corresponding to the energy $\hbar\omega = 36$ eV. Effects of electron correlations were probed by comparing projections of the final state of the two-electron wave packet onto (i) field-free highly-correlated Jacobi matrix wave functions with (ii) projections onto uncorrelated Coulomb wave functions. Significant differences are found in the vicinity of autoionizing resonances. Owing to the broad bandwidths of our 115-as and 230-as pulses and their high intensities (1-2 PW/cm²), asymmetries are found in the differential probability for ionization of electrons parallel and antiparallel to the linear polarization axis of the attosecond laser pulse. These asymmetries stem from interference of the one- and two-photon ionization amplitudes for producing electrons with the same momentum along the linear polarization axis. Whereas these asymmetries generally decrease with increasing ionized electron kinetic energy, we find a large enhancement of this asymmetry in the vicinity of two-electron doubly-excited (autoionizing) states on an energy scale comparable to the widths of the autoionizing states. The CEP-dependence of the energy-integrated asymmetry agrees very well with the predictions of time dependent perturbation theory [*Phys. Rev. A* **80**, 063403 (2009)]. (See reference [6] below.)

C. Asymmetries in Production of $\text{He}^+(n=2)$ with an Intense Few-Cycle Attosecond Pulse

By solving the two-electron time-dependent Schrödinger equation, we studied carrier-envelope-phase (CEP) effects on ionization plus excitation of He to $\text{He}^+(n=2)$ states by a few-cycle attosecond pulse with a carrier frequency of 51 eV. For most CEPs the asymmetries in the photoelectron angular distributions with excitation of $\text{He}^+(2s)$ or $\text{He}^+(2p)$ have opposite signs and are two orders of magnitude larger than for ionization without excitation. These results indicate that attosecond pulse CEP effects may be significantly amplified in correlated two-electron ionization processes. (See reference [7] in the publication list below.)

D. Carrier-Envelope-Phase-Induced Asymmetries in Double Photoionization of He by an Intense Few-Cycle XUV Pulse

The carrier-envelope-phase (CEP) dependence of electron angular distributions in double ionization of He by an arbitrarily-polarized, few-cycle, intense XUV pulse is formulated using perturbation theory in the pulse amplitude. Owing to the broad pulse bandwidth, interference of first and second order perturbation amplitudes produces asymmetric angular distributions that are sensitive to the CEP. Our perturbation theory parametrization is shown to be valid by comparing with results of solutions of the full-dimensional, two-electron time-dependent Schrödinger equation for the case of linear polarization. (See reference [8] in the publication list below.)

E. High-Order Harmonic Generation of Be in the Multiphoton Regime

The high-order harmonic generation (HHG) spectrum of Be is investigated in the multiphoton regime by solving the full-dimensional, two-active-electron, time-dependent Schrödinger

equation in an intense (10^{13}W/cm^2), 30-cycle laser field. As the laser frequency ω_L varies from 1.7 to 1.8 eV (which is in the tunable range of a Ti:sapphire laser), the 7th harmonic becomes resonant sequentially with the transition between the ground state and two doubly-excited autoionizing states while the 3rd harmonic becomes resonant with the $2s2p(^1P)$ singly-excited state. At each resonant frequency, the HHG power spectrum increases by an order of magnitude over a range of harmonics that form a plateau, extending from the resonant harmonic up to a cutoff at the 25th harmonic. In contrast to the well-known rescattering plateau cutoff law appropriate in the tunneling regime (which predicts a cutoff at the 5th or 7th harmonic), the multiphoton regime plateau we find for Be originates from atomic resonance effects. Off-resonance, the Be HHG spectrum decreases monotonically with harmonic order. By taking the ratio of the integrated harmonic power of the 7th harmonic to that of the 5th harmonic, one can isolate the resonant effects of the two doubly-excited states in the HHG spectrum from those of singly-excited resonance states. These ratios exhibit resonance profiles for driving laser pulse durations much longer than the lifetimes of these autoionizing states. The energy widths of these resonance features are comparable to the widths of the laser pulse and are much smaller than the autoionizing state widths. These results demonstrate an important role for electron correlations in enhancing harmonic generation rates in the multiphoton regime. (*See reference [9] below.*)

F. Potential Barrier Features in Three-Photon Ionization Processes in Atoms

Resonance-like enhancements of generalized three-photon cross sections for XUV ionization of Ar, Kr, and Xe have been demonstrated and analyzed within a single-active-electron, central-potential model. The resonant-like behavior is shown to originate from the potential barriers experienced by intermediate- and final-state photoelectron wave packets corresponding to absorption of one, two, or three photons. The resonance-like profiles in the generalized three-photon ionization cross sections are shown to be similar to those found in the generalized two-photon ionization cross sections [*Phys. Rev. A* **82**, 053414 (2010)]. The complexity of Cooper minima in multiphoton ionization processes is also discussed. Owing to the similar resonance-like profiles found in both two- and three-photon generalized cross sections, we expect such potential barrier effects to be general features of multiphoton ionization processes in most atoms with occupied *p*- and *d*-subshells. (*See reference [10] in the publication list below.*)

FUTURE PLANS

Our group is currently carrying out research on the following additional projects:

(1) Vacuum Acceleration of Electrons Initially Bound in Highly-Charged Ions. We are carrying out a large set of simulations for the final-state energy and angular dependences of electrons ionized from highly-charged ions by super intense laser pulses. Such ions ensure that the electrons only become ionized near the peak of the laser pulse intensity. We are mapping out the dependences of these distributions on the experimentally-controllable parameters: (a) the *focal width* of the laser pulse, (b) the *polarization* of the laser pulse, and (c) the *intensity* of the laser pulse. The relativistic classical trajectory Monte Carlo (CTMC) method is used. An advantage of the CTMC approach is that it is very well suited to parallel computation. Moreover, the initial locations of the trajectories leading to maximum energy gains can easily be determined. Our calculations indicate that *the location of the target ion relative to the focus is an additional important parameter* affecting the electron energy and angular distributions.

(2) Control of double ionization of He by means of the polarization and carrier-envelope-phase (CEP) of an intense, few-cycle XUV pulse. We are able to solve numerically the six-dimensional two-electron, time-dependent Schrödinger equation for He interacting with an elliptically-polarized XUV pulse. Guided by perturbation theory, we have discovered a new nonlinear dichroic effect that is sensitive to the CEP, ellipticity, peak intensity, and temporal duration of the pulse. This dichroic effect (i.e., the difference of the two-electron angular distributions for opposite helicities of the ionizing XUV pulse) originates from interference of first- and second-order perturbation theory amplitudes, allowing one to probe and control *S*- and *D*-wave channels of the two-electron continuum. We show that the back-to-back in-plane geometry with unequal energy sharing is the best one for observing this dichroic effect that occurs only for an elliptically-polarized, few-cycle attosecond pulse.

PUBLICATIONS STEMMING FROM DOE-SPONSORED RESEARCH (2011 – 2014)

- [1] J.M. Ngoko Djiokap and A.F. Starace, “Evidence of the $2s2p(^1P)$ Doubly Excited State in the Harmonic Generation Spectrum of He,” *Phys. Rev. A* **84**, 013404 (2011).
- [2] E.A. Pronin, A.F. Starace, and L.-Y. Peng, “Perturbation Theory Analysis of Ionization by a Chirped, Few-Cycle Attosecond Pulse,” *Phys. Rev. A* **84**, 013417 (2011).
- [3] M. Xu, L.-Y. Peng, Z. Zhang, Q. Gong, X.-M. Tong, E.A. Pronin, and A. F. Starace, “Attosecond Streaking in the Low-Energy Region as a Probe of Rescattering,” *Phys. Rev. Lett.* **107**, 183001 (2011).
- [4] Z. Zhang, L.-Y. Peng, M.-H. Xu, A. F. Starace, T. Morishita, and Q. Gong, “Two-Photon Double Ionization of Helium: Evolution of the Joint Angular Distribution with Photon Energy and Two-Electron Energy Sharing,” *Phys. Rev. A* **84**, 043409 (2011).
- [5] M.V. Frolov, D.V. Knyazeva, N.L. Manakov, A.M. Popov, O.V. Tikhonova, E.A. Volkova, M.-H. Xu, L.-Y. Peng, and A.F. Starace, “Validity of Factorization of the High-Energy Photoelectron Yield in Above-Threshold Ionization of an Atom by a Short Laser Pulse,” *Phys. Rev. Lett.* **108**, 213002 (2012).
- [6] J.M. Ngoko Djiokap, S.X. Hu, W.-C. Jiang, L.-Y. Peng, and A.F. Starace, “Enhanced Asymmetry in Few-Cycle Attosecond Pulse Ionization of He in the Vicinity of Autoionizing Resonances,” *New J. Phys.* **14**, 095010 (2012). [*Published in the Focus Issue on “Correlation Effects in Radiation Fields.”*]
- [7] J.M. Ngoko Djiokap, S.X. Hu, W.-C. Jiang, L.-Y. Peng, and A.F. Starace, “Asymmetries in Production of $\text{He}^+(n=2)$ with an Intense Few-Cycle Attosecond Pulse,” *Phys. Rev. A* **88**, 011401(R) (2013).
- [8] J.M. Ngoko Djiokap, N.L. Manakov, A.V. Meremianin, and A.F. Starace, “Carrier-Envelope-Phase-Induced Asymmetries in Double Photoionization of He by an Intense Few-Cycle XUV Pulse,” *Phys. Rev. A* **88**, 053411 (2013).
- [9] J.M. Ngoko Djiokap and A.F. Starace, “Resonant Enhancement of the Harmonic Generation Spectrum of Beryllium,” *Phys. Rev. A* **88**, 053412 (2013).
- [10] L.-W. Pi and A.F. Starace, “Potential Barrier Effects in Three-Photon Ionization Processes,” *Phys. Rev. A* **90**, 023403 (2014).

FEMTOSECOND AND ATTOSECOND LASER-PULSE ENERGY TRANSFORMATION AND CONCENTRATION IN NANOSTRUCTURED SYSTEMS

DOE Grant No. DE-FG02-01ER15213

Mark I. Stockman, PI

Department of Physics and Astronomy, Georgia State University, Atlanta, GA 30303

E-mail: mstockman@gsu.edu, URL: <http://www.phy-astr.gsu.edu/stockman>

Current Year Grant Period of 2013-2014 (Publications 2012-2014)

1 Program Scope

The program is aimed at theoretical investigations of a wide range of phenomena induced by ultrafast laser-light excitation of nanostructured or nanosize systems, in particular, metal/semiconductor/dielectric nanocomposites and nanoclusters. Among the primary phenomena are processes of energy transformation, generation, transfer, and localization on the nanoscale and coherent control of such phenomena.

2 Recent Progress and Publications

Publications resulting from the grant during the period of 2012-2014 are: [1-14]. During the current grant period of 2012-2013, the following articles with this DOE support have been published [7, 9, 11-15]. The following articles received, as acknowledged, supplementary support of this grant during 2012-2013: [8, 10, 16-21]. Below we highlight selected articles that we consider most significant.

2.1 Attosecond Control of Dielectrics [9]

Control of the electric and optical properties of semiconductors with microwave fields forms the basis of modern electronics, information processing and optical communications. Extension of such control to optical frequencies calls for wideband materials such as dielectrics, which require strong electric fields to control their physical properties. Few-cycle laser pulses permit damage-free exposure of dielectrics to electric fields of several V/Å and significant modifications in their electronic system. Fields of such strength and temporal confinement can turn a dielectric from an insulating state to a conducting state within the optical period. In this article [9], we study the underlying strong-field-induced electron processes within sub-femtosecond intervals. We have established the feasibility of manipulating the electronic structure and electric polarizability of a dielectric reversibly with the electric field of light. The established ultrafast reversibility of the effects implies that the physical properties of a dielectric can be controlled with the electric field of light, offering the potential for petahertz-bandwidth signal manipulation.

2.2 Metal Nanofilm in Strong Ultrafast Optical Fields [11]

In this article, we predict that a metal nanofilm subjected to an ultrashort (near-single oscillation) optical pulse of a high field amplitude ~ 3 V/Å at normal incidence undergoes an ultrafast (at subcycle times ~ 1 fs) transition to a state resembling semimetal. Its reflectivity is greatly reduced, while its transmissivity and the optical field inside the metal are greatly increased. Despite the metal being a centrosymmetric medium, the strong pulse causes net charge transfer in the direction determined by the carrier envelope phase (CEP) of the pulse, which is opposite to the direction of the maximum field.

2.3 Hot-Electron Nanoscopy Using Adiabatic Compression of Surface Plasmons [12]

Surface plasmon polaritons are a central concept in nanoplasmonics and have been exploited to develop ultrasensitive chemical detection platforms, as well as imaging and spectroscopic techniques at the nanoscale. Surface plasmons decay to form highly energetic (or hot) electrons in a process that is usually thought to be parasitic for applications, because it limits the lifetime and propagation length of surface plasmons and therefore has an adverse influence on the functionality of nanoplasmonic devices. Recently, however, it has been shown that hot electrons produced by surface plasmon decay can be harnessed to produce useful work in photodetection, catalysis and solar energy conversion. Nevertheless, the surface-plasmon-to-hot-electron conversion efficiency has been below 1% in all cases.

In this article [12], we show that adiabatic nanofocusing of surface plasmons on a Schottky diode-terminated tapered tip of nanoscale dimensions allows for a plasmon-to-hot-electron conversion efficiency of ~30%. This effect is predicted and described theoretically [12] to be due to (i) adiabatic slowing down and asymptotic stopping of plasmons at the tip, and (ii) turning of the collision direction of the electrons with the taper surface toward the normal as a result of collisions with this surface. We further demonstrate theoretically and experimentally that, with such high efficiency, hot electrons can be used for a new nanoscopy technique based on an atomic force microscopy set-up. We show that this hot-electron nanoscopy preserves the chemical sensitivity of the scanned surface and has a spatial resolution below 50 nm, with prospects for improvement.

2.4 Electric Spaser in the Extreme Quantum Limit [7]

We consider theoretically the spaser that is excited electrically via a nanowire with ballistic quantum conductance. We show that, in the extreme quantum regime, i.e., for a single conductance-quantum nanowire, the spaser with a core made of common plasmonic metals, such as silver and gold, is fundamentally possible. For ballistic nanowires with multiple-quanta or nonquantized conductance, the performance of the spaser is enhanced in comparison with the extreme quantum limit. The electrically pumped spaser is promising as an optical source, nanoamplifier, and digital logic device for optoelectronic information processing with a speed of ~100 GHz to ~100 THz.

2.5 Optical-Field-Induced Current in Dielectrics [8]

The time it takes to switch on and off electric current determines the rate at which signals can be processed and sampled in modern information technology. Field-effect transistors are able to control currents at frequencies beyond ~100 GHz, but electric interconnects hamper progress towards the terahertz (THz) frontier. In reality, charging of these interconnects limits processor speed to 2-4 GHz only. All-optical injection of currents via interfering photo-excitation pathways or photoconductive switching of THz transients has permitted controlling electric current on a subpicosecond time scale in semiconductors. Insulators have been deemed unsuitable for both concepts, because of the need for either UV light or high fields, which induce either slow damage or ultrafast breakdown, respectively. In this article [8], we report the feasibility of electric signal manipulation in a dielectric. A few-cycle optical waveform increases reversibly – free from breakdown – the (ac) conductivity of amorphous silicon dioxide (fused silica) by more than 18 orders of magnitude within 1 femtosecond, allowing electric currents to be driven, directed, and switched by the *instantaneous field of light*. This work opens a route to extending electronic signal processing and high-speed metrology into the petahertz domain.

2.6 Theory of Dielectric Nanofilms in Strong Ultrafast Optical Fields [2]

We have theoretically predicted that a dielectric nanofilm subjected to a normally incident strong but ultrashort (a few optical oscillations) laser pulse exhibits deeply nonlinear (nonperturbative) optical responses which are essentially reversible and driven by the instantaneous optical field. Among them is a high optical polarization and a significant population of the conduction band, which develop at the peak of the pulse and almost disappear after its end. There is also a correspondingly large increase of the pulse

reflectivity. These phenomena are related to Wannier-Stark localization and anticrossings between the Wannier-Stark ladders originating from the valence and conduction bands leading to optical “softening” of the dielectric. Theory is developed by solving self-consistently the Maxwell equations and the time-dependent Schrödinger equation. The results point out to a fundamental possibility of optical-field effect devices with the bandwidth on the order of optical frequency.

2.7 Interaction of Graphene Monolayer with Ultrashort Laser Pulse [13]

In this work, we study the interaction of graphene with ultrashort a few femtosecond long optical pulse. For such a short pulse, the electron dynamics is coherent and is described within the tight-binding model of graphene. The interaction of optical pulse with graphene is determined by strong wave vector dependence of the interband dipole matrix elements, which are singular at the Dirac points of graphene. The electron dynamics in optical pulse is highly irreversible with large residual population of the conduction band. The residual conduction band population as a function of the wave vector is nonuniform with a few localized spots of high conduction band population. The spots are located near the Dirac points and the number of spots depends on the pulse intensity. The optical pulse propagating through graphene layer generates finite transferred charge, which, as a function of pulse intensity, changes its sign. At small pulse intensity, the charge is transferred in the direction of the pulse maximum, while at large pulse intensity, the direction of the charge transfer is opposite to the direction of pulse maximum. This property opens unique possibility of controlling the direction of the charge transfer by variation of the pulse intensity.

3 Directions of Work for the Next Period

We will develop the present success in the optics of ultrastrong and ultrafast fields on the nanoscale. We will extend the existing theory to other dielectrics, semimetals, and metals, in particular sapphire and graphene. We will invoke more realistic models for the crystal structure of the materials involved, in particular using tight-binding model with experimentally known geometry of the unit cell or pseudopotential model. We will extend theory to describe photoelectron emission caused by the strong ultrashort pulses and probe attosecond XUV pulses in thin films and graphene. We will develop theory of materials subjected to several strong fields of different frequencies, e.g., near-infrared/visible and terahertz/static. We will extend theory to describe generation of high harmonics in solids in strong ultrafast optical fields. In ultrafast active plasmonics, we will study properties of the spaser with optical pumping as ultrabright label for biomedical diagnostics and laser therapy.

References

1. V. Apalkov and M. I. Stockman, *Metal Nanofilm in Strong Ultrafast Optical Fields*, arXiv:1209.2245 [cond-mat.mes-hall], 1-5 (2012).
2. V. Apalkov and M. I. Stockman, *Theory of Dielectric Nanofilms in Strong Ultrafast Optical Fields*, Phys. Rev. B **86**, 165118-1-13 (2012).
3. S. H. Chew, F. Sussmann, C. Spath, A. Wirth, J. Schmidt, S. Zherebtsov, A. Guggenmos, A. Oelsner, N. Weber, J. Kapaldo, A. Gliserin, M. I. Stockman, M. F. Kling, and U. Kleineberg, *Time-of-Flight-Photoelectron Emission Microscopy on Plasmonic Structures Using Attosecond Extreme Ultraviolet Pulses*, Appl. Phys. Lett. **100**, 051904-4 (2012).
4. D. Li and M. I. Stockman, *Electric Spaser in the Extreme Quantum Limit*, arXiv:1211.0366 [cond-mat.mes-hall], 1-5 (2012).
5. A. Schiffrin, T. Paasch-Colberg, N. E. Karpowicz, V. Apalkov, D. Gerster, S. Mühlbrandt, M. Korbman, M. Schultze, S. Holzner, J. Reichert, J. Barth, R. Kienberger, R. Ernstorfer, V. Yakovlev, M. I. Stockman, and F. Krausz, in Laser Science (LS), *Subfemtosecond Photoconductive Switching in Dielectrics* (Optical Society of America, Rochester, NY (USA), 2012), p. LW4H.3.

6. V. Apalkov and M. I. Stockman, *Graphene Spaser*, arXiv:1303.0220 [cond-mat.mes-hall], 1-5 (2013).
7. D. Li and M. I. Stockman, *Electric Spaser in the Extreme Quantum Limit*, Phys. Rev. Lett. **110**, 106803-1-5 (2013).
8. A. Schiffrin, T. Paasch-Colberg, N. Karpowicz, V. Apalkov, D. Gerster, S. Muhlbrandt, M. Korbman, J. Reichert, M. Schultze, S. Holzner, J. V. Barth, R. Kienberger, R. Ernstorfer, V. S. Yakovlev, M. I. Stockman, and F. Krausz, *Optical-Field-Induced Current in Dielectrics*, Nature **493**, 70-74 (2013).
9. M. Schultze, E. M. Bothschafter, A. Sommer, S. Holzner, W. Schweinberger, M. Fiess, M. Hofstetter, R. Kienberger, V. Apalkov, V. S. Yakovlev, M. I. Stockman, and F. Krausz, *Controlling Dielectrics with the Electric Field of Light*, Nature **493**, 75-78 (2013).
10. M. I. Stockman, *Spaser, Plasmonic Amplification, and Loss Compensation*, in *Active Plasmonics and Tuneable Plasmonic Metamaterials*, edited by A. V. Zayats and S. Maier (John Wiley and Sons, Hoboken, NJ, 2013).
11. V. Apalkov and M. I. Stockman, *Metal Nanofilm in Strong Ultrafast Optical Fields*, Phys. Rev. B **88**, 245438-1-7 (2013).
12. A. Giugni, B. Torre, A. Toma, M. Francardi, M. Malerba, A. Alabastri, R. Proietti Zaccaria, M. I. Stockman, and E. Di Fabrizio, *Hot-Electron Nanoscopy Using Adiabatic Compression of Surface Plasmons*, Nat. Nano **8**, 845-852 (2013).
13. H. K. Kelardeh, V. Apalkov, and M. I. Stockman, *Interaction of Graphene Monolayer with Ultrashort Laser Pulse*, arXiv:1401.5786 [cond-mat.mes-hall], 1-11 (2014).
14. M. I. Stockman, *Nanoplasmonics: From Present into Future*, in *Plasmonics: Theory and Applications*, edited by T. V. Shahbazyan and M. I. Stockman (Springer, Dordrecht, Heidelberg, New York, London, 2013), Vol. 15, p. 1-101.
15. V. Apalkov and M. I. Stockman, *Metal Nanofilm in Strong Ultrafast Optical Fields*, Phys. Rev. B **88**, 245438-1-7 (2013).
16. V. Apalkov and M. I. Stockman, *Proposed Graphene Nanospaser*, Light Sci. Appl. **3**, e191-1-6 (2014).
17. V. Apalkov and M. I. Stockman, *Proposed Graphene Nanospaser*, arXiv:1303.0220 [cond-mat.mes-hall], 1-5 (2014).
18. H. K. Kelardeh, V. Apalkov, and M. I. Stockman, *Wannier-Stark States of Graphene Monolayer in Strong Electric Field*, Phys. Rev. B **90** (2014).
19. H. K. Kelardeh, V. Apalkov, and M. I. Stockman, *Wannier-Stark States of Graphene Monolayer in Strong Electric Field*, arXiv:1405.1141, 1-11 (2014).
20. F. Krausz and M. I. Stockman, *Attosecond Metrology: From Electron Capture to Future Signal Processing*, Nat. Phot. **8**, 205-213 (2014).
21. Y.-J. Lu, C.-Y. Wang, J. Kim, H.-Y. Chen, M.-Y. Lu, Y.-C. Chen, W.-H. Chang, L.-J. Chen, M. I. Stockman, C.-K. Shih, and S. Gwo, *All-Color Plasmonic Nanolasers with Ultralow Thresholds: Autotuning Mechanism for Single-Mode Lasing*, Nano Lett. **14**, 4381-4388 (2014).

Laser-Produced Coherent X-Ray Sources

Donald Umstadter

Department of Physics and Astronomy

257 Behlen Laboratory, University of Nebraska, Lincoln, NE 68588-0111

donald.umstadter@unl.edu

Program Scope

X-ray synchrotrons and x-ray free-electron lasers have proven to be transformational technologies for physical and biological sciences. As part of this project, we developed a new type of x-ray source, one which—by virtue of its unique characteristics—may have similar transformational potential. Not only does its x-ray peak brightness and photon energy rival that of 3rd generation x-ray synchrotrons, but its femtosecond x-ray pulse duration is comparable to x-ray free-electron lasers. Moreover, the device is small enough to fit in a university laboratory.

The new light source is based on inverse Compton back-scattering, driven by two intense light pulses, each of which are amplified by a single high-power laser system. One laser pulse rapidly accelerates electrons (~ 3 GeV/cm) by means of the laser-wakefield mechanism; and the other laser pulse Thomson-backscatters from the relativistic electrons. The scattered light Doppler-upshifts relativistically to high photon energy.

Our most recent progress was demonstration of x-ray beams with several additional unique features: quasi-monoenergetic spectral width ($\Delta E/E \sim 50\%$), large energy-tuning range ($50 \text{ keV} \leq h\nu \leq 10 \text{ MeV}$), and small angular divergence (10-mrad) [Powers et al (2014)].

The new source has advantages for x-ray science in general, and for the study of ultrafast phenomena in particular. Its exceptionally large x-ray-energy tuning range facilitates probing of almost any element's inner-shell atomic structure. Its femtosecond x-ray pulse duration, coupled to high photon energy, enables ultrafast time-resolved studies with atomic-scale spatial and temporal resolutions. Its synchronization with ultra-high-intensity laser light pulses ($\leq 10^{22} \text{ W/cm}^2$, $a_0 \sim 100$) can merge ultrafast science with high field science; for example, ultrafast dynamics of either highly stripped atoms or extreme states of matter can be investigated.

Several of our near-term project objectives include: (i) reduction of the x-ray spectral width, (ii) measurement of the x-ray pulse duration (inferred to be < 10 fs), and (iii) demonstration of an x-ray pump-probe capability.

Recent Progress

Bright and well-collimated energetic x-ray beams

The x-ray source is driven by the DIOCLES laser at the University of Nebraska, Lincoln [Liu et al. (2013)]. For the experiments described here, 3-J, 35-fs, 805-nm laser pulses were produced at 10-Hz repetition rate. In the initial implementation of the x-ray source [Chen et al (2013)], the amplified and compressed laser beam was split into two separate beams by means of a beam-splitter (80% reflecting, 20% transmitting), which was located after the pulse compressor. The reflected beam (the drive pulse) had 1.9-J energy and 35-fs duration. Its wavefront was corrected with an adaptive feedback loop between a wavefront sensor and a deformable mirror. It was focused by a 1-m parabolic reflector onto the front edge of a supersonic gas jet.

The focal spot had a Gaussian spatial profile, and is near-diffraction limited, corresponding to full width at half maximum (FWHM) of 20 μm . Thirty-three percent of the laser energy was enclosed in the FWHM width, corresponding to a peak intensity of $\sim 10^{19}$ W cm^{-2} (normalized vector potential $a_0 \sim 2$). Another adaptive feedback loop was also used to optimize the spectral phase of the drive laser pulse, creating a transform-limited pulse at the interaction point. Complete spatial and spectral characterization and optimization of the laser pulse was performed on target and in vacuum [Liu et al (2014a)].

The beam transmitted through the beam-splitter (the scattering pulse) had energy 0.5 J, and counter-propagated (with respect to both the drive beam and electron beam) at a near-back-scattering angle (~ 170 deg). It was focused by a 1-m focal-length lens. On account of dispersion in the beam-splitter, its pulse duration was 120 fs. B-integral effects led to a focal spot with 22 μm diameter (FWHM) and 16% enclosed energy in the central spot. The corresponding intensity at the focus of the scattering pulse was $\sim 3 \times 10^{17}$ W cm^{-2} , corresponding to a normalized vector potential a_0 of 0.4 and linear non-relativistic scattering.

Mixed gas targets (99% He + 1% N₂) were used for the generation of high-energy electron beams. A supersonic nozzle with a 2-mm diameter orifice was used to produce a high density gas flow ($n_e = 10^{19}$ cm^{-3}). The drive pulse was focused onto the front edge of the flow. The medium was fully ionized by the foot of the laser pulse. The peak of the pulse was self-guided in the medium, and drove a laser-wakefield in the underdense plasma.

The energy and charge of the accelerated electron beam were measured with a magnetic spectrometer and fluorescent screen (LANEX), which was imaged by a 12-bit CCD and the response of the detection system was calibrated independently [Banerjee et al (2013)]. Under optimal conditions, beams with cutoff energy < 300 MeV were produced with charge ~ 100 pC for energy > 50 MeV. The accelerator had stable reproducible shot-to-shot characteristics.

The position in space where the scattering took place was located 1-mm downstream of the nozzle. This location is close enough to the exit of the accelerator to ensure that the transverse sizes of the electron beam and focused scattering pulse are nearly matched, while also being far enough to ensure that focusing of the scattering pulse is unaffected by the gas target. The pointing fluctuation of the scattering pulse on target was 5 μrad , and the angular jitter of the electron beam is 5-10 mrad.

The generated x-rays were detected by a CsI detector imaged with a 14-bit EMCCD camera. The CsI array consists of 1-mm diameter, 10-mm long voxels, which are separated by epoxy. The angular divergence of the x-ray beam was measured to be 12 mrad.

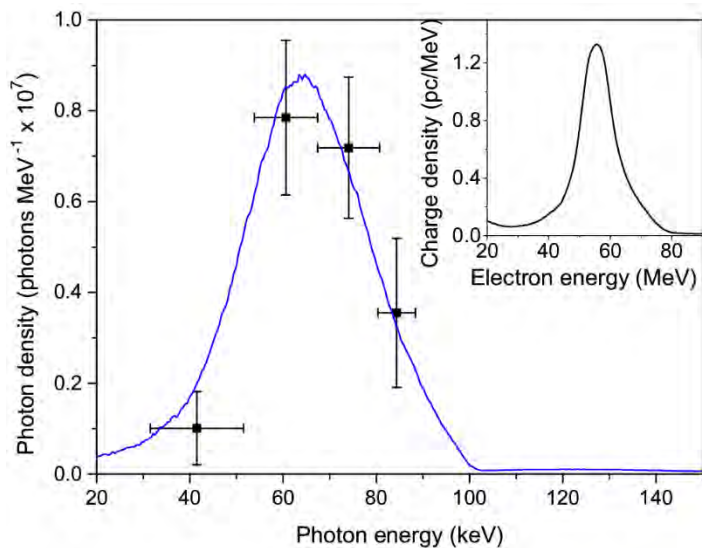
A detailed numerical model that takes into account the spatial profile of the focused scattering pulse was used to compute the spectrum of the scattered x-rays [Ghebregziabher et al. (2013)]. The distribution of electrons in phase space was constructed using the measured angular profile and the energy spectrum of the electron beam.

The x-ray spectrum is determined from measurements of the amount of x-rays transmitted through each of four quadrant attenuation filters. The measurements are found to be in excellent agreement with the values predicted by the above-mentioned numerical model. Based on the absolute detector response, we determined that 10^8 photons s^{-1} were produced. The size of the x-ray source was found to be 5 μm , measured using a cross-correlation technique, in which the scattering pulse was scanned along the vertical direction, and sampled different parts of the electron beam. The peak x-ray spectral brightness was found to be 2×10^{19} photons $\text{s}^{-1} \text{mm}^{-2} \text{mrad}^{-2}$ (0.1% BW), based on the above measurements, and assuming an electron-beam pulse duration that was measured in prior studies under conditions similar to our experiment. This peak

brightness is nearly four orders of magnitude higher than from inverse Compton sources based on the scattering of a high-intensity laser pulse off an electron beam produced by a conventional accelerator.

Tunable and quasi-monoenergetic x-rays

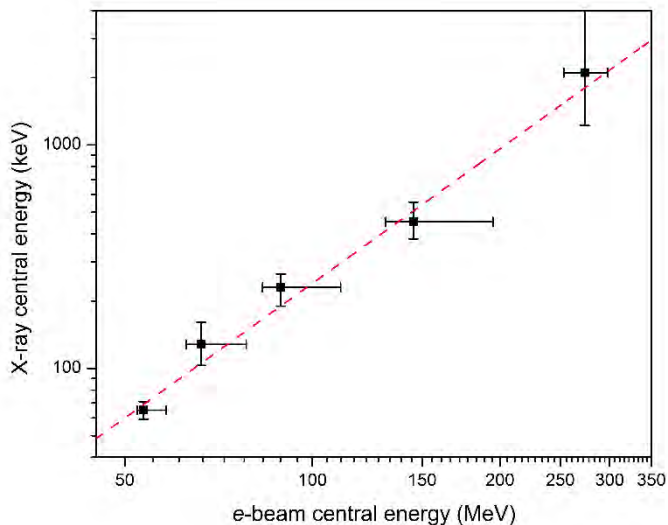
In more recent experiments [Powers et al (2014)], quasi-monoenergetic x-ray beams were generated. The



gas target was redesigned to produce narrowband electron beams that are tunable over a large energy range (50 MeV to 300 MeV), while holding constant the other important electron-beam parameters, such as energy spread and charge. The gas-target comprises two independently controllable gas jets: the first jet flowed a gas mixture (99% He, 1% N₂), functioning as the electron injector; while the second jet flowed pure helium, functioning as the accelerator.

Figure 1: X-ray spectrum (inset: electron spectrum [Powers et al (2014)]).

To measure the energy spread of the x-ray beam more precisely than in the original experiments, a Ross-filter technique was implemented. It relies on measurement of transmission through various different



materials near their K-edges. The detection system was again the voxelated CsI detector. The measured spectrum is shown in Fig. 1.

Figure 2: X-ray energy versus electron energy [Powers et al (2014)].

The photon energy of the x-rays was tuned from 50 keV to 1 MeV by tuning the electron energy from 50 MeV to 250 MeV. The results, as shown in Fig. 2, confirm the theoretically predicted quadratic relationship between x-ray and electron energies. Using the absolute response of the detection system, it is inferred that

$\sim 2 \times 10^7$ photons s^{-1} are produced at the 10-Hz repetition rate of the laser system. The average energy spread is 40-50%, consistent with the 20% spread in the energy of the electron beam; the fluctuation in the photon number was $\sim 50\%$ on a shot-to-shot basis [Powers et al. (2014)].

Two further improvements to the x-ray source were recently implemented. The beam was split before the pulse compression system in order to mitigate the effects of B-integral [Liu et al (2014b)]. Two separate pulse compressors were used to independently compress and optimize the temporal characteristics of the scattering pulse. A frequency-doubling crystal was used in the scattering beam-line to convert the incident

800-nm light to 400 nm. Doubling the photon energy of the scattering pulse reduces the electron energy required in order to produce x-rays of a given photon energy.

We believe that this hard x-ray source—which is tunable, quasi-monoenergetic, short-pulse, and well-collimated—represents a significant advance, since the beams produced by previous alternative approaches are highly divergent and/or spectrally broadband.

Future Plans:

By means of dispersive and single-photon-counting spectroscopies, we are currently studying femtosecond x-ray excitation and absorption of high-Z atoms. We are also preparing pump-probe experiments to study ultrafast photo-induced changes in atomic structure.

Publications supported the in part by DOE (published within last three years)

1. C. Liu et al., “Generation of 9-MeV γ -rays by all-laser-driven Compton scattering with second-harmonic laser light,” *Opt. Lett.* **39**, 14, 4132-4135 (2014).
2. C. Liu et al., "Adaptive-feedback spectral-phase control for interactions with transform-limited ultra-short high-power laser pulses," *Opt. Lett.* **39**, 1, 80-83 (2014).
3. N. D. Powers et al., "Tunable and quasi-monoenergetic x-rays from a laser-driven Compton light source," *Nat. Photonics* **8**, 28-31 (2014).
4. S. Chen et al., "MeV-energy x-rays from inverse Compton scattering with laser-wakefield accelerated electrons," *Phys. Rev. Lett.* **110**, 155003 (2013).
5. S. Banerjee et al., “Stable, tunable, quasimonoenergetic electron beams produced in a laser wakefield near the threshold for self-injection,” *Phys. Rev. ST Accel. Beams* **16**, 031302 (2013).
6. I. Ghebregziabher et al., "Spectral bandwidth reduction of Thomson scattered light by pulse chirping," *Rev. ST Accel. Beams* **16**, 030705 (2013).
7. J. Silano et al., “Selective activation with all-laser-driven Thomson γ -rays,” *Proceedings of the 2013 IEEE International Conference on Technologies for Homeland Security*, 429 - 434 (Waltham, MA, 2013).
8. S. Banerjee et al., "Generation of tunable, 100-800 MeV quasi-monoenergetic electron beams from a laser-wakefield accelerator in the blowout regime," *Phys. Plasmas* **19**, 056703 (2012).
9. B. M. Cowan et al., "Computationally efficient methods for modeling laser wakefield acceleration in the blowout regime," *J. Plasma Phys.* **78**, 469 (2012).
10. S. Y. Kalmykov et al., "Electron self-injection into an evolving plasma bubble: quasi-monoenergetic laser-plasma acceleration in the blowout regime," *Phys. Plasmas* **18**, 056704 (2011).

Combining High Level *Ab Initio* Calculations with Laser Control of Molecular Dynamics

Thomas Weinacht
 Department of Physics and Astronomy
 Stony Brook University
 Stony Brook, NY
 thomas.weinacht@stonybrook.edu

and

Spiridoula Matsika
 Department of Chemistry
 Temple University
 Philadelphia, PA
 smatsika@temple.edu

1 Program Scope

We use intense, shaped, ultrafast laser pulses to follow and control molecular dynamics, and high level *ab initio* calculations to interpret the dynamics and guide the control.

2 Recent Progress

Our accomplishments in the past three years of DOE support are detailed in the 12 papers which we have written.¹⁻¹² Our principal findings/accomplishments are:

- *Development of time resolved strong field dissociative ionization spectroscopy for probing and interpreting excited state molecular dynamics*
- *Studying neutral to ionic state correlations in strong field molecular ionization*
- *Observing strong field molecular ionization from multiple orbitals*
- *Obtaining insight into the dynamics of the radical cations produced via strong field ionization*

Our main experimental results from the past year have focused on developing a new ultrafast VUV source as an ionization probe of excited state dynamics and using velocity map imaging to try and characterize the ultrafast relaxation and dissociation of excited molecular cations. In terms of theory, we have employed two parallel approaches for following the dynamics of excited molecular cations in order to understand how relaxation competes with dissociation.

2.1 Development of the VUV source

Figure 1 highlights our progress in developing a UV pump VUV probe apparatus for pump probe measurements of excited state dynamics and a comparison of weak and strong field ionization of excited states. The central part of the figure shows the apparatus we are constructing. Also shown are the VUV intensity as a function of UV and IR delay in generating the VUV via four wave mixing in Argon (on the left) and a cartoon of the potential energy surfaces involved in a pump probe measurement (on the right). The VUV intensity was measured using ionization of a gold surface. The pump probe apparatus is almost completed and about to be tested.

2.2 Velocity Map Imaging measurements of relaxation in excited molecular cations

We ionize the molecule in question using our strong field IR laser pulses. Ionization can proceed to a range of ionic states, as we have seen in both calculations and experiment. By measuring the photoelectrons in coincidence with the fragment ions produced by ionization, we can determine the ionic state of the molecule immediately after ionization. Then, the velocity map imaging measurement of the fragment ion measured in coincidence with the photoelectron can be used to determine the kinetic energy release in dissociation for the case of ionization to a dissociative cationic state. A signature of relaxation prior to dissociation (as long as the excited state does not lead to the same dissociation limit as the ground state) is the measurement of fragment ions with

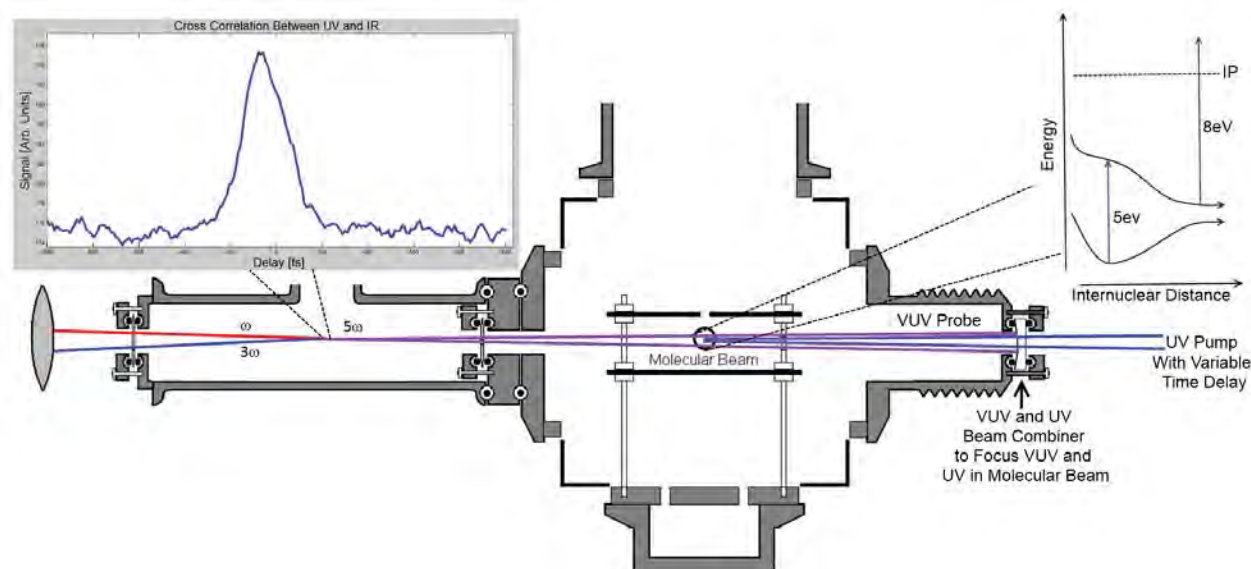


Figure 1: UV pump VUV probe apparatus, preliminary measurements and cartoon illustrating proposed experiments.

kinetic energy release equal to the energy difference between the initial ionic state and ground ionic state at the FC point minus the dissociation energy on the ground state.

Figure 2 illustrates the velocity map imaging of ionic fragments for the case of 1-3 Cyclohexadiene. These initial measurements show at least two dissociation channels, suggesting that there is competition between relaxation and dissociation, with dissociation taking place on multiple electronic states of the molecular cation.

2.3 Ultrafast relaxation in molecular cations

In strong field dissociative ionization techniques several excited ionic states can be created during the ionization step followed by fragmentation, and it is not clear whether the fragments are produced directly in the excited ionic states or if fast relaxation to the ground ionic state occurs first and fragmentation follows, i.e. does fragmentation of an excited molecular cation with energy above the dissociation barrier take place on the excited or ground state of the cation? In order to better understand the processes occurring after ionization and interpret the experimental observables, we have theoretically investigated dynamics of excited radical cations.

Polyatomic radical cations often have closely spaced electronic states with several two and three-state conical intersection seams making the dynamics particularly interesting. We have applied trajectory surface hopping (TSH) molecular dynamics and the Multi-Configurational Time-Dependent Hartree (MCTDH) approach to study the dynamics of the uracil radical cation as well as cyclohexadiene (CHD) and hexatriene (HT) radical cations. The uracil cation has been used before in our work on neutral uracil excited state dynamics, while the other two cations were involved in our probing of the CHD to HT isomerization reaction.

Dynamics on the uracil cation were studied in detail using the Linear Vibronic Coupling (LVC) Hamiltonian where 10 modes were included and the MCTDH approach for solving the time-dependent Schrödinger equation. The EOM-IP-CCSD/6-311+G* *ab initio* method was used to produce 1-dimensional scans along normal modes which were then fitted using the LVC model. The method reproduces the experimental photoelectron spectrum reasonably well, giving us confidence

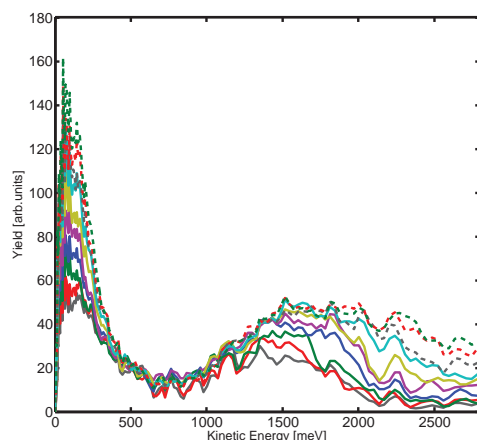


Figure 2: Preliminary velocity map imaging measurements of $C_4H_n^+$ ($n=1-4$) fragments from 1-3 Cyclohexadiene ionized by an intense femtosecond laser pulse. The raw VMI images have been inverse Abel transformed and then processed to generate the kinetic energy release spectrum for several different laser intensities

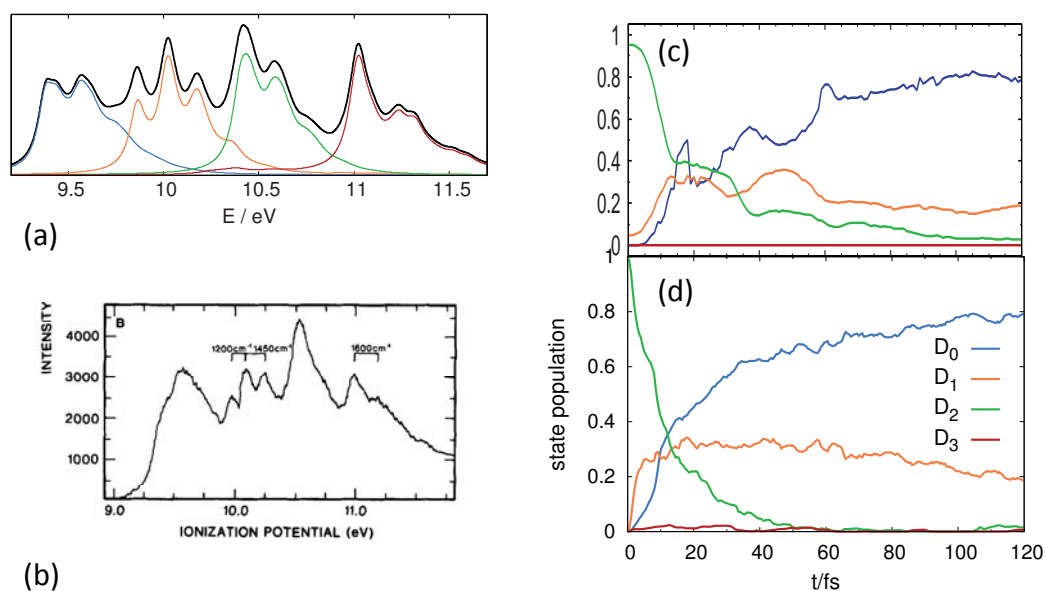


Figure 3: (a) Photoelectron spectrum of uracil calculated using MCTDH and (b) taken from the literature (Biochemical and Biophysical Research Communications **60**, 1262 (1974)).(c,d) Adiabatic state populations generated from dynamics on uracil cation starting on D_2 . (c) shows results from the MCTDH approach while (d) shows results from TSH.

in our approach (see Figure 3a,b). The TSH approach was also used for the dynamics and in this case all the degrees of freedom were included. Both methods give similar results for the decay (see Figure 3c,d). The decay of the excited ionic states is very fast (population of D_2 goes from 1 to 0 in 50-100 fs), indicating that in this system decay will occur faster than dissociation. We have also found that both two- and three-state conical intersections play an important role in the decay.

3 Future Plans

We have two goals for the immediate future:

1. *Comparing strong and weak field ionization from excited states.* We have developed a new ultrafast VUV light source at about 8 eV, which can serve as both an ideal probe of excited state dynamics, and as a basis for direct comparison between weak and strong field ionization. This approach will test our recent ideas about the differences between strong and weak field ionization and whether Dyson norms can be used as predictors of which ionic states are populated.
2. *Ultrafast relaxation in molecular cations.* As already described above we are interested in how ultrafast relaxation of excited state molecular cations competes with direct dissociation. Experimentally, we will use photoelectron and photoion coincidence velocity map imaging in order to determine whether relaxation precedes dissociation. Measurements of the photoelectron energy resulting from ionization can be used to label the initial electronic state of the cation immediately after ionization. Measuring the kinetic energy release of the fragment ions will allow us to determine how much energy went into kinetic energy during the dissociation process. Theoretically, we will continue our studies on dynamics of cations using TSH and MCTDH in order to establish some guidelines about the competition between radiationless decay and dissociation.

References

- [1] M. Kotur, T. C. Weinacht, C. Zhou, K. Kistler, and S. Matsika, *J. Chem. Phys.* **134**, 184309 (2011).
- [2] P. Krause, S. Matsika, M. Kotur, and T. Weinacht, *J. Chem. Phys.* **137**, 22A537 (2012).
- [3] M. Kotur, T. C. Weinacht, C. Zhou, and S. Matsika, *Phys. Rev. X* **1**, 021010 (2011).
- [4] S. Matsika, C. Zhou, M. Kotur, and T. C. Weinacht, *Faraday Discussions* **153**, 247 (2011).
- [5] C. Zhou, S. Matsika, M. Kotur, and T. C. Weinacht, *J. Phys. Chem. A* **116**, 9217 (2012).
- [6] M. Kotur, T. C. Weinacht, C. Zhou, and S. Matsika, *IEEE J. Sel. Topics Quantum Electron.* **18**, 187 (2012).
- [7] C. Tseng, P. Sandor, M. Kotur, T. C. Weinacht, and S. Matsika, *J. Phys. Chem. A* **116**, 2654 (2012).
- [8] M. Spanner, S. Patchkovskii, C. Zhou, S. Matsika, M. Kotur, and T. C. Weinacht, *Phys. Rev. A* **86**, 053406 (2012).
- [9] M. Kotur, C. Zhou, S. Matsika, S. Patchkovskii, M. Spanner, and T. C. Weinacht, *Phys. Rev. Lett.* **109**, 203007 (2012).
- [10] O. Njoya, S. Matsika, and T. Weinacht, *ChemPhysChem* **14**, 1451 (2013).
- [11] S. Matsika, M. Spanner, M. Kotur, and T. C. Weinacht, *J. Chem. Phys.* **117**, 12796 (2013).
- [12] A. Moradmand, D. S. Slaughter, D. J. Haxton, T. N. Rescigno, C. W. McCurdy, T. Weber, S. Matsika, A. L. Landers, A. Belkacem, and M. Fogle, *Phys. Rev. A* **88**, 032703 (2013).

New scientific frontiers with ultracold molecules

Jun Ye

JILA, NIST and University of Colorado

Ye@jila.colorado.edu

PROGRAM SCOPE

Following the demonstration of a two-dimensional magneto-optical trap for molecular YO, we have been working on the implementation of a three-dimensional MOT. Collaborating with John Doyle's group in Harvard, we have prepared a slow YO molecule beam with a center velocity of 70 m/s from a dual stage buffer gas cooled laser ablation source. We have successfully demonstrated the slowing and cooling of this molecular beam to 20 m/s, and are working now to further cool this beam for loading into a 3D MOT. We expect to achieve this result soon.

Evaporation of the hydroxyl radical (OH) remains an exciting prospect for further cooling of chemically interesting molecules and increasing their phase space density. Thus far evaporation efficiency has been limited by collision rate and vacuum lifetime, prompting an investigation of possible improvements. We have designed a new permanent magnetic trap with a factor of 2 steeper gradient and a more favorable loading geometry. Using this trap, we show an order of magnitude increase in the initial density and in collision rate of OH molecules. We are currently working on a detailed investigation of the inelastic and elastic collisions of OH free radicals.

On the front of dipolar molecules in the quantum regime, we have recently realized a lattice spin model. By encoding spin in rotational states, we have observed spin exchanges of ultracold polar KRb molecules that are confined in a deep three-dimensional optical lattice. The interactions manifest as a density dependent decay of the spin coherence of the system. In addition to decaying, the spin contrast oscillates, with frequency components that are consistent with the dipolar interaction energies. We have studied these spin exchanges for two different pairs of rotational states, which differ by a factor of two in interaction strength, and find the decay and oscillations to be roughly twice as fast in the case of stronger interactions. A theory comparison based on a cluster expansion agrees quantitatively with our data. These observations were made in a regime where the lattice filling is quite dilute. Our current experimental efforts are focused on increasing the filling fraction. Higher lattice fillings will enable the study of richer physics, such as transport of excitations in an out of equilibrium long-range interacting system.

While we have used dipolar interactions of polar molecules pinned in a three-dimensional optical lattice to realize the spin exchange model, the absence of an external electric field precludes the study of the full spin-1/2 Hamiltonian that includes the Ising interaction. Moreover, advanced manipulation of dipolar properties of a bulk molecular gas is also strongly desired. In the near future we will commission the second generation of our KRb polar molecule apparatus that allows large electric fields with the

flexibility to apply gradients of the field in arbitrary directions. The same electrodes that supply large DC electric fields also provide AC fields for driving rotational transitions to encode spin. The relative angle between the AC and DC fields can be tuned to control the polarization of the microwave field for high fidelity rotational state transfer. Moreover, the geometry of the system is amenable to high resolution optical detection of the molecules. A high NA microscope objective allows for the first microscopic studies of molecular quantum gases. We plan to implement these tools to perform direct evaporative cooling of our spin-polarized fermionic molecular gas to realize a molecular Fermi gas deep in degeneracy.

Publications over the past 12 months:

N. Y. Yao, A. V. Gorshkov, C. R. Laumann, A. Läuchli, J. Ye, and M. D. Lukin, "Realizing Fractional Chern Insulators with Dipolar Spins," *Phys. Rev. Lett.* 110, 185302 (2013). (Editor's Suggestion; Selected for a Viewpoint in Physics.)

B. K. Stuhl, M. Yeo, M. T. Hummon, and J. Ye, "Electric-field-induced inelastic collisions between magnetically trapped hydroxyl radicals," *Molecular Physics* 111, 1798 – 1804 (2013). (Invited Article)

B. Yan, S. A. Moses, B. Gadway, J. P. Covey, K. R. A. Hazzard, A. M. Rey, D. S. Jin, and J. Ye, "Observation of dipolar spin-exchange interactions with lattice-confined polar molecules," *Nature* 501, 521 – 525 (2013).

B. K. Stuhl, M. T. Hummon, and J. Ye, "Cold State-Selected Molecular Collisions and Reactions," *Annu. Rev. Phys. Chem.* 65, 501 – 518 (2014). (Invited Review)

B. Zhu, B. Gadway, M. Foss-Feig, J. Schachenmayer, M. L. Wall, K. R. A. Hazzard, B. Yan, S. A. Moses, J. P. Covey, D. S. Jin, J. Ye, M. Holland, A. M. Rey, "Suppressing the loss of ultracold molecules via the continuous quantum Zeno effect," *Phys. Rev. Lett.* 112, 070404 (2014). (Editor's Suggestion)

List of Participants

Page is intentionally blank.

Andreas Becker
University of Colorado
440 UCB
Boulder, CO 80309
Phone: 303-492-7825

Ali Belkacem
Lawrence Berkeley National Laboratory
One Cyclotron Road, MS: 70AR03307
Berkeley, CA 94720
Phone: 510-486-6382

Itzik Ben-Itzhak
Kansas State University
116 Cardwell Hall
Manhattan, KS 66506
Phone: 785-532-1636

Nora Berrah
University of Connecticut
2152 Hillside Road
Storrs, CT 6268
Phone: 860-486-4924

Philip Bucksbaum
SLAC National Accelerator Laboratory
2575 Sand Hill Road
Menlo Park, CA 94025
Phone: 650-926-5337

Martin Centurion
University of Nebraska
855 North 16th Street
Lincoln, NE 68510
Phone: 402-472-5810

Shih-I Chu
University of Kansas
Department of Chemistry
Lawrence, KS 66045
Phone: 785-864-4094

Robin Cote
University of Connecticut
2152 Hillside Road, U-3046
Storrs, CT 6269
Phone: 860-486-4912

Steven Cundiff
University of Colorado
440 UCB
Boulder, CO 80302
Phone: 303-492-7858

Marcos Dantus
Michigan State University
578 Shaw Lane, Room 58
East Lansing, MI 48824
Phone: 517-881-4562

David DeMille
Yale University
PO Box 208120
New Haven, CT 0
Phone: 203-432-3833

Louis DiMauro
The Ohio State University
191 West Woodruff Avenue
Columbus, OH 43210
Phone: 614-688-5726

Todd Ditmire
University of Texas at Austin
2515 Speedway Stop C1600
Austin, TX 78712
Phone: 512-471-3296

Gilles Doumy
Argonne National Laboratory
9700 S. Cass Ave.
Argonne, IL 60439
Phone: 630-252-2588

joseph eberly
University of Rochester
600 Wilson Blvd
Rochester, NY 14627
Phone: 585-275-4351

Brett Esry
Kansas State University
116 Cardell Hall
Manhattan, KS 66506
Phone: 785-532-1620

Jim Feagin
California State University
800 N State College
Fullerton, CA 92834
Phone: 657-278-4827

Christopher Fecko
U. S. Department of Energy
19901 Germantown Road
Germantown, MD 20874
Phone: 301-903-1303

Kelly Gaffney
SLAC National Accelerator Laboratory
2575 Sand Hill Road
Menlo Park, CA 94025
Phone: 650-926-2382

Thomas Gallagher
University of Virginia
Dept. of Physics
Charlottesville, VA 22904
Phone: 434-924-6817

Oliver Gessner
Lawrence Berkeley National Laboratory
One Cyclotron Road
Berkeley, CA 94720
Phone: 510-486-6929

Shambhu Ghimire
SLAC National Accelerator Laboratory
2575 Sand Hill Rd
Menlo Park, CA 94025
Phone: 650-926-2071

John Gillaspay
National Science Foundation
4201 Wilson Blvd
Arlington, VA 22230
Phone: 703-292-7173

Phillip Gould
University of Connecticut
U-3046, 2152 Hillside Rd
Storrs, CT 6269
Phone: 860-486-2950

Chris Greene
Purdue University
525 Northwestern Avenue
West Lafayette, IN 47907
Phone: 765-496-1859

Markus Guehr
SLAC National Accelerator Laboratory
2575 Sand Hill Road
Menlo Park, CA 94025
Phone: 650-926-5550

Daniel Haxton
Lawrence Berkeley National Laboratory
One Cyclotron Road
Berkeley, CA 94720
Phone: 510-495-2508

Robert Jones
University of Virginia
382 McCormick Road
Charlottesville, VA 22904
Phone: 434-924-3088

Elliot Kanter
Argonne National Laboratory
9700 S. Cass Avenue
Lemont, IL 60439
Phone: 908-617-1622

Henry Kapteyn
University of Colorado
440 UCB
Boulder, CO 80309
Phone: 303-492-8198

Victor Klimov
Los Alamos National Laboratory
MS-J567
Los Alamos, NM 87545
Phone: 505-665-8284

Bertold Kraessig
Argonne National Laboratory
9700 S. Cass Avenue
Argonne, IL 60439
Phone: 630-252-9230

Jeffrey Krause
U. S. Department of Energy
19901 Germantown Road
Germantown, MD 20874
Phone: 301-903-5827

Prem Kumar
DARPA/DSO
675 N. Randolph St
Arlington, VA 22203
Phone: 703-526-2709

Vinod Kumarappan
Kansas State University
328 Cardwell Hall
Manhattan, KS 66506
Phone: 785-532-3415

Allen Landers
Auburn University
216 Allison Lab, Physics
Auburn, AL 36849
Phone: 334-844-4048

Anh-Thu Le
Kansas State University
116 Cardwell Hall
Manhattan, KS 66506
Phone: 785-532-1635

Stephen Leone
University of California and LBNL
Department of Chemistry
Berkeley, CA 94720
Phone: 510-643-5467

Wen Li
Wayne State University
5101 Cass ave.
Detroit, MI 48202
Phone: 313-577-8658

Chii-Dong Lin
Kansas State University
Department of Physics
Manhattan, KS 66506
Phone: 785-532-1617

Kenneth Lopata
Louisiana State University
742 Choppin Hall
Baton Rouge, LA 70808
Phone: 225-578-2063

Robert Lucchese
Texas A&M University
Department of Chemistry
College Station, TX 0
Phone: 979-845-0187

Stephen Lundeen
Colorado State University
200 W. Lake St
Fort Collins, CO 0
Phone: 970-491-6647

Joseph Macek
University of Tennessee
Department of Physics and Astronomy
Knoxville, TN 37934
Phone: 865-974-0770

Steven Manson
Georgia State University
Department of Physics & Astronomy
Atlanta, GA 30303
Phone: 404-413-6046

Diane Marceau
U. S. Department of Energy
19901 Germantown Road
Germantown, MD 20874
Phone: 301-903-0235

Anne Marie March
Argonne National Laboratory
9700 S. Cass Ave.
Argonne, IL 60439
Phone: 630-252-4099

Todd Martinez
SLAC National Accelerator Laboratory
2575 Sand Hill Rd
Menlo Park, CA 94025
Phone: 650-736-8860

Spiridoula Matsika
Temple University
1901 N.13th Street
Philadelphia, PA 19122
Phone: 215-204-7703

William McCurdy
Lawrence Berkeley National Laboratory
One Cyclotron Road
Berkeley, CA 94720
Phone: 510-486-4283

Vincent McKoy
California Institute of Technology
1200 E. California Blvd
Pasadena, CA 91125
Phone: 626-395-6545

ALFRED MSEZANE
Clark Atlanta University
Department of Physics
Atlanta, GA 30314
Phone: 404-880-8360

Shaul Mukamel
University of California
1102 Natural Sciences II
Irvine, CA 0
Phone: 949-824-7600

Keith Nelson
MIT
MIT Room 6-235
Cambridge, MA 2139
Phone: 617-253-1423

Ann Orel
National Science Foundation
4001 N 9th #1806
Arlington, VA 22203
Phone: 703-292-2163

Thom Orlando
Georgia Institute of Technology
901 Atlantic Drive NW
Atlanta, GA 30332
Phone: 404-894-4012

Abbas Ourmazd
University of Wisconsin
1900 E Kenwood Blvd.
Milwaukee, WI 53211
Phone: 414-229-2610

Enrique Parra
Air Force Office of Scientific Research
875 N. Randolph Street, Suite 325
Arlington, VA 22203
Phone: 703-696-8571

Herschel Rabitz
Princeton University
Frick Chemistry Building
Princeton, NJ 8544
Phone: 609-258-3917

David Reis
SLAC National Accelerator Laboratory
2575 Sand Hill Rd
Menlo Park, CA 94025
Phone: 972-926-4192

Thomas Rescigno
Lawrence Berkeley National Laboratory
One Cyclotron Road
Berkeley, CA 94720
Phone: 510-486-8652

Francis Robicheaux
Purdue University
525 Northwestern Ave
West Lafayette, IN 47907
Phone: 765-494-3029

Jorge Rocca
Colorado State University
942 Driftwood Drive
Fort Collins, CO 80525
Phone: 970-491-8371

Daniel Rolles
Kansas State University
Physics Department
Manhattan, KS
Phone:

Christoph Rose-Petruck
Brown University
324 Brook Street
Providence, RI 2912
Phone: 401-863-1533

Artem Rudenko
Kansas State University
116 Cardwell Hall
Manhattan, KS 66506
Phone: 785-532-4470

Kenneth Schafer
Louisiana State University
Dept. of Physics & Astronomy
Baton Rouge, LA 70803
Phone: 225-578-0466

H. Bernhard Schlegel
Wayne State University
375 Chemistry
Detroit, MI 48202
Phone: 313-577-2562

Robert Schoenlein
Lawrence Berkeley National Laboratory
One Cyclotron Road, MS: 2-300
Berkeley, CA 94720
Phone: 510-486-6557

Tamar Seideman
Northwestern University
2145 Sheridan Road
Evanston, IL
Phone: 847-467-4979

Thomas Settersten
Sandia National Laboratories/DOE BES
19901 Germantown Road
Germantown, MD 20874
Phone: 301-903-8428

Daniel Slaughter
Lawrence Berkeley National Laboratory
One Cyclotron Road
Berkeley, CA 94720
Phone: 510-486-4847

Stephen Southworth
Argonne National Laboratory
Bldg. 401
Argonne, IL 60439
Phone: 630-252-3894

Anthony Starace
University of Nebraska
855 North 16th St., 208 JH
Lincoln, NE 0
Phone: 402-47-22795

Mark Stockman
Georgia State University
29 Peachtree Center Ave.
Atlanta, GA 30302
Phone: 678-457-4739

Carlos Trallero
Kansas State University
116 Cardwell Hall
Manhattan, KS 66506
Phone: 785-532-0846

Donald Umstadter
University of Nebraska
500 Stadium Dr. Rm. 257
Lincoln, NE 0
Phone: 402-472-8115

Uwe Thumm
Kansas State University
Department of Physics
Manhattan, KS 66506
Phone: 785-532-1613

Thorsten Weber
Lawrence Berkeley National Laboratory
One Cyclotron Road
Berkeley, CA 94720
Phone: 510-486-5588

Thomas Weinacht
Stony Brook University
Dept. of Physics and Astronomy
Stony Brook, NY 11794
Phone: 631-632-8163

Jun Ye
University of Colorado
UCB 440
Boulder, CO 80309
Phone: 303-735-3171

Linda Young
Argonne National Laboratory
9700 S. Cass Avenue
Argonne, IL 60439
Phone: 630-252-8878